UNIVERSITY OF CALIFORNIA, SAN DIEGO

Synthetic Studies Toward the Pladienolide and Spirohexenolide Natural Products

A dissertation submitted in partial satisfaction of the
requirements for the degree

Doctor of Philosophy

in

Chemistry

by

Brian D. Jones

Committee in charge:

Professor Michael Burkart, Chair
Professor Partho Ghosh
Professor Thomas Hermann
Professor Randall Johnson
Professor Charles Perrin

2010

The dissertation of Brian D. Jones is approved, and it is acceptable in quality and form for publication on microfilm and electronically:

_____

_____

_____

_____

_____

Chair

University of California, San Diego

2010

TABLE OF CONTENTS

LIST OF ABBREVIATIONS

Å	angstrom
Ac	acetyl
Ac_2O	acetic anhydride
AcOH	acetic acid
$AsPh_3$	triphenylarsine
$BaSO_4$	barium sulfate
BnBr	benzyl bromide
BF_3	boron trifluoride
BOM	benzyloxymethyl
BORSM	based on recovered starting material
br	broad NMR peak
Bu or *n*-Bu	butyl
t-Bu	*tert*-butyl
Bu_4NI	tetrabutylammonium iodide
t-BuOK	potassium *tert*-butoxide
Bu_2SnCl_2	dibutyltin dichloride
Bu_2SnH_2	dibutylstannane
Bu_3SnH	tributyltin hydride
Bz	benzoyl
c	concentration in g/dL

calcd	calculated
CCDC	Cambridge Crystallographic Data Center
C_6D_6	deuterated benzene
$CDCl_3$	deuterated chloroform
$CHCl_3$	chloroform
CH_2Cl_2	dichloromethane
C_6H_6	benzene
cm^{-1}	wave number (frequency, IR)
COSY	correlation spectroscopy
CSA	camphorsulfonic acid
$CuBr*SMe_2$	copper (I) bromide, methyl sulfide complex
CuI	copper (I) iodide
$CuSO_4*xH_2O$	copper (II) sulfate hydrate
d	doublet (NMR)
DBU	1,8-diazabicyclo[5.4.0]undec-7-ene
DCC	1,3-dicyclohexylcarbodiimide
DDQ	2,3-dichloro-5,6-dicyano-1,4-benzoquinone
d.e.	diastereomeric excess
DHP	3,4-dihydro-2*H*-pyran
DIAD	diisopropyl azodicarboxylate
DIBAL-H	diisobutylaluminum hydride
DIPEA	diisopropylethylamine – Hünig's base
dm	decimeters

DMAP	4-dimethylaminopyridine
DMF	*N*,*N*-dimethylformamide
DMP	Dess-Martin periodinane or 3,4-dimethoxyphenyl
DNP	dinitrophenylhydrazine
DMSO	dimethylsulfoxide
DMSO-*d*6	deuterated dimethylsulfoxide
EDC	1-ethyl-3-(3-dimethylaminopropyl) carbodiimide hydrochloride
e.e.	enantiomeric excess
EI	electron impact ionization
eq.	equivalents (molar)
ESI	electrospray ionization
Et	ethyl
Et_3N	triethylamine
Et_2O	diethyl ether
EtOAc	ethyl acetate
EtOH	ethanol
EtSH	ethanethiol
FAB	fast atom bombardment
FT-IR	fourier transform infrared spectroscopy
g	grams
GI_{50}	concentration required for 50% growth inhibition
h	hours
HCl	hydrogen chloride

HF-py	pyridine hydrofluoride
HMPA	hexamethylphosphoramide
HOBt	hydroxybenzotriazole
HRMS	high-resolution mass spectrometry
H_2SO_4	sulfuric acid
HWE	Horner-Wadsworth-Emmons olefination
Hz	hertz
IBX	*o*-iodoxybenzoic acid
IC_{50}	half-maximal inhibitory concentration
(-)-Ipc_2BOMe	(-)-*B*-methoxydiisopinylcampheylborane
IR	infrared spectroscopy
J	coupling constant (NMR)
KCN	potassium cyanide
KHMDS	potassium bis(trimethylsilyl)amide
KF	potassium fluoride
$KMnO_4$	potassium permanganate
KOH	potassium hydroxide
L	liters
LC_{50}	median lethal dose
LDA	lithium diisopropylamide
$LiAlH_4$	lithium aluminum hydride
$LiBF_4$	lithium tetrafluoroborate
LiCl	lithium chloride

LiHMDS	lithium bis(trimethylsilyl)amide
LiOH	lithium hydroxide
m	multiplet (NMR)
M	concentration in molarity (mol/L)
$[M]^+$	molecular ion (found in EI/MS)
m/z	mass per charge ratio of detected ion (mass spectrometry)
$[M+H]^+$	protonated molecular ion (found in ESI/MS)
$[M+Na]^+$	sodium molecular ion (found in ESI/MS)
$[M+NH_4]^+$	ammonium molecular ion (found in ESI/MS)
$[M+K]^+$	potassium molecular ion (found in ESI/MS)
Me	methyl
$MeAlCl_2$	methylaluminum dichloride
MeI	iodomethane
MeLi	methyllithium
MeOH	methanol
$(MeO)_2SO_2$	dimethyl sulfate
mg	milligrams
$MgBr_2$	magnesium bromide
$MgSO_4$	magnesium sulfate
MHz	megahertz
μg	micrograms
μL	microliters
μmol	micromoles

MeCN	acetonitrile
mL	milliliters
mM	millimolar
mmol	millimoles
mol	moles
Ms	methanesulfonyl
MS	mass spectrometry
$NaBO_3$	sodium perborate
NaCl	sodium chloride
NaH	sodium hydride
$NaHCO_3$	sodium bicarbonate
Na_2SO_3	sodium sulfite
Na_2SO_4	sodium sulfate
NH_4Cl	ammonium chloride
$(NH_4)_6Mo_7O_{24}*4H_2O$	ammonium molybdate tetrahydrate
nM	nanomolar
NMO	4-methylmorpholine N-oxide
NMP	1-methyl-2-pyrrolidinone
NMR	nuclear magnetic resonance
NOE	nuclear overhauser effect
NOESY	nuclear overhauser effect spectroscopy
ORTEP	Oak Ridge thermal ellipsoid plot
p	pentet (NMR)

Pd_2dba_3	tris(dibenzylideneacetone)dipalladium(0)
$Pd(PPh_3)_4$	tetrakis(triphenylphosphine)palladium(0)
PG	protecting group
Ph	phenyl
PhMe	toluene (methylbenzene)
$(Ph_3P)_2PdCl_2$	bis(triphenylphosphine)palladium(II)dichloride
PMB	*para*-methoxybenzyl
PMP	*para*-methoxyphenyl
PPh_3	triphenylphosphine
ppm	parts per million
PPTS	pyridinium p-toluenesulfonate
PT	1-phenyl-1*H*-tetrazol-5-yl
py	pyridine
PyBOP	(benzotriazol-1-yloxy)tripyrrolidinophosphonium hexafluorophosphate
q	quartet (NMR)
RCM	ring-closing metathesis
R_f	retention factor (TLC)
rt	room temperature (20-25 °C)
s	singlet (NMR)
SAR	structure - activity relationship
$Sc(OTf)_3$	scandium (III) trifluoromethanesulfonate
SEM	2-(trimethylsilyl)ethoxymethyl

t	triplet (NMR)
TBAF	tetrabutylammonium fluoride
TBDPS	*tert*-butyldiphenylsilyl
TBS	*tert*-butyldimethylsilyl
TBDMS	*tert*-butyldimethylsilyl (same as TBS, above)
TES	triethylsilyl
Tf	trifluoromethanesulfonyl
TFA	trifluoroacetic acid
THF	tetrahydrofuran
THP	2-tetrahydropyranyl
TIPS	triisopropylsilyl
TLC	thin layer chromatography
TMS	trimethylsilyl
$TMSCHN_2$	(trimethylsilyl)diazomethane
TPAP	tetrapropylammonium perruthenate
Ts	*p*-toluenesulfonyl
UV	ultraviolet
$ZnCl_2$	zinc chloride
$[\alpha]_D$	optical rotation, sodium D line (589 nm), rt (20-25 °C)
°C	degrees celsius
δ	chemical shift in ppm (NMR)

LIST OF FIGURES

LIST OF SCHEMES

LIST OF SPECTRA

LIST OF TABLES

ACKNOWLEDGEMENTS

I wish to extend my gratitude to Professor Michael Burkart and Dr. James La Clair, who provided me the opportunity to conduct the research described herein. In addition to providing support and direction in this research, they allowed me to work together with Dr. Alexander Mandel on the project described in the first chapter. Alex is an outstanding chemist who served as a continuous source of inspiration and knowledge, and was instrumental in my growth as a synthetic chemist. I wish to thank Dr. Matthew Alexander, a postdoctoral researcher in the Burkart group who provided me with useful advice and assistance during my first two years in the laboratory. Dr. Min Jin Kang brought her expertise in microbiology to the Burkart group and deserves special thanks for her tireless work in culturing *Streptomyces platensis* for the isolation studies described in the second chapter.

I would like to thank Professor Donoghue and everyone on the Growth Regulation and Oncogenesis training grant at UCSD for support during my fourth and fifth years. Being on the training grant allowed me to focus on my thesis project during this time period, and also gave me the opportunity to hear about cutting edge research in cancer biology.

I would like to thank Dr. Anthony Mrse at the NMR facilities in Pacific Hall for keeping the instruments well maintained and helping me troubleshoot many of the problems I had with obtaining quality spectra. Professor Rheingold operates the fantastic small molecule X-Ray facility at UCSD, where all of the crystal structures described herein were obtained. The service of all my committee members is

acknowledged and appreciated. I wish to thank all past and present Burkart group members who assisted me during my time in graduate school. I also thank all the students and postdocs in the organic division at UCSD from other laboratories who helped me with advice, chemicals, solvents or anything else.

Chapter 1 contains some material that was published in *Bioorg Med Chem Lett.*, 17, 18, pp. 5159-5164, 2007. The dissertation author was the second author of this paper.

Section 2.1, in full, is a reprint of the material as it appears in *J Org Chem.*, 74, 23, pp. 9094-9061, 2009. The compound and reference numbering, and some of the formatting were changed to fit the requirements for the dissertation. The dissertation author was the second author of this paper.

Section 2.4.2 describes material being prepared for publication entitled "Total Synthesis of (±) – Spirohexenolide B", Jones B.D., La Clair J.J., Burkart M.D. The dissertation author is the primary author of the manuscript.

VITA

2002 Bachelor of Arts, Chemistry. University of Colorado, Boulder.

2006 Master of Science, Chemistry. University of California, San Diego.

2010 Doctor of Philosophy, Chemistry. University of California, San Diego.

PUBLICATIONS

Mandel, A. L.; Jones, B. D.; La Clair, J. J.; Burkart, M. D., A Synthetic Entry to Pladienolide B and FD-895. *Bioorg. Med. Chem. Lett.* **2007,** 17, (18), 5159-5164.

Kang, M. J.; Jones, B. D.; Mandel, A. L.; Hammons, J. C.; DiPasquale, A. G.; Rheingold, A. L.; La Clair, J. J.; Burkart, M. D., Isolation, Structure Elucidation, and Antitumor Activity of Spirohexenolides A and B. *J. Org. Chem.* **2009,** 74, (23), 9054-9061.

Jones, B.D., La Clair, J.J., Burkart, M.D., Total Synthesis of (±)-Spirohexenolide B, *in preparation*

ABSTRACT OF THE DISSERTATION

Synthetic Studies Toward the Pladienolide and Spirohexenolide Natural Products

by

Brian D. Jones

Doctor of Philosophy in Chemistry

University of California, San Diego, 2010

Professor Michael Burkart, Chair

Actinomycetes are microbes found in terrestrial soil and marine sediment that produce a rich variety of secondary metabolites. These natural products have diverse biological activity including antifungal, insecticidal, antibacterial, and antitumor activities. Although in most cases we can only speculate why the producer microbes make these natural products, they have been in use throughout human history. Some of these secondary metabolites and their semi-synthetic derivatives have proven to be indispensible to modern medicine, and others are highly desirable for non-essential uses such as food additives, fragrances and dyes.

Our laboratory became interested in the actinomycetes produced pladienolide natural products when they were originally reported due to their potent antitumor activity and unique cell-cycle arrest profile. The novel assay used in their discovery,

and the reported biological data indicated that these natural products probably had a unique mechanism of action against tumor cells.

Herein is described research toward the synthesis and structural elucidation of the pladienolides and their close structural relative FD-895. This research was accompanied by efforts to isolate authentic samples of the pladienolides from their producer organism, *Streptomyces platensis* MER 11107. These efforts led to the isolation and structural elucidation of novel spirotetronate polyketides from this organism, the spirohexenolides. Chapter 1 describes attempts toward the synthesis of the core macrolactone ring of the pladienolides and FD-895, the synthesis of the sidechain of FD-895, and the synthesis of two models of FD-895 which demonstrate the feasibility of our end-game strategy toward this family of natural products. Chapter 2 describes the isolation efforts directed toward the pladienolides, and the isolation and structural elucidation of the spirohexenolides. An intramolecular Diels-Alder (IMDA) approach to (±) – spirohexenolide A, and a Lewis-acid catalyzed Diels-Alder approach to (±) – spirohexenolide B are described.

Chapter 1

Studies toward the pladienolides and FD-895

1.1 Introduction to the pladienolides and FD-895

The first member of a new family of polyketide natural products, FD-895 (**1**), was discovered in 1994 at the Taisho Corporation in Japan, through efforts to discover antitumor agents active against drug resistant cell lines.[1] It was isolated from the culture broth of a soil microbe collected in Japan, later determined to be *Streptomyces hygroscopicus* A-9561. The planar structure of **1** was elucidated through NMR, IR, UV and mass spectrometric analyses, which revealed an unusual twelve-membered macrolide attached to a long lipophilic, epoxide containing sidechain (Figure 1.1). Because it was discovered by activity guided fractionation using adriamycin resistant HL-60 cells, it was not surprising that **1** showed low nanomolar IC_{50} values against a variety of other drug resistant and non resistant tumor cell lines *in vitro*. The original report describes that **1** was shown to block biosynthesis of nucleic acids and protein but had no activity against V-ATPases, a common target of cytotoxic polyketides with related structures. Compound **1** had no discernable antibacterial or antifungal activity, and was shown not to prolong the survival time of mice transplanted with P388 leukemia cells, a cell line that it had been shown to be very active against *in vitro*. The Taisho Corporation published no further reports on **1**, suggesting that the poor result in the mouse xenograft study and possibly other discouraging biological activity data forced them to cancel the project.

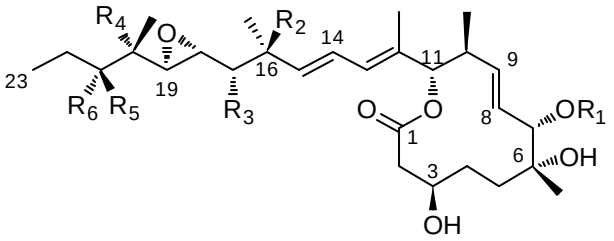

		R_1	R_2	R_3	R_4	R_5	R_6
FD-895	**1**	Ac	H	OH	H	OCH_3	H
pladienolide A	**2a**	H	H	H	H	OH	H
pladienolide B	**2b**	Ac	H	H	H	OH	H
pladienolide C	**2c**	Ac	H	H	H	=O	
pladienolide D	**2d**	Ac	OH	H	H	OH	H
pladienolide E	**2e**	Ac	H	H	OH	OH	H
pladienolide F	**2f**	H	OH	H	H	OH	H
pladienolide G	**2g**	H	H	H	OH	OH	H

Figure 1.1 FD-895 (**1**) and pladienolides A-G (**2a-2g**)

Seven pladienolides (**2a-2g**) were reported in 2004 by the Eisai Corporation (Figure 1.1).[2] Their discovery was the result of the development of a cell-based assay designed to identify small molecules that block the hypoxia inducible factor (HIF-1) transcription factor pathway and thus expression of vascular endothelial growth factor (VEGF) genes. This pathway is critical to the growth of tumors in their common low oxygen (hypoxic) environment, because VEGF stimulates the recruitment of new blood vessels to the tumors, a process known as angiogenesis.[3] A high-throughput screening assay was developed that allowed the Eisai Corporation to rapidly examine thousands of crude bacterial culture broths for this activity, and one of the hits resulted in the isolation of **2a-2g**. Their producer organism was determined by taxonomic

methods to be *Streptomyces platensis* and the strain was designated MER 11107. Standard spectroscopic structural elucidation methods revealed their planar structures to be almost identical to **1** (Figure 1.1).[4]

In addition to powerful anti-VEGF activity, the pladienolides displayed a broad range of *in vitro* cytotoxicity against a panel of 39 tumor cell lines. Exposure of WiDr cells to **2a-2g** resulted in cell cycle arrest at the G1 and G2/M phases, and the cell cycle arrest profile of **2a-2g** did not correlate well with 5-fluorouracil, vincristine, or taxol. Additionally, COMPARE analysis[5, 6] of the *in vitro* activity profile data of **2b** did not identify a standard antitumor drug with a high correlation coefficient. Thus, the cellular target of these angiogenesis inhibitors was thought to be new for antitumor agent development. Initial *in vivo* activity results were promising; in particular, **2b** demonstrated potent activity in six mouse xenograft models, slowing tumor growth in five and causing complete regression in one.[7] The most important structure-activity relationship result from the isolation of the pladienolides was that the acetate at C-7 (as in **1** and **2b-2e**) is critical for anti-VEGF activity; the non-acetylated congeners are much less active. Much of the subsequent semi-synthetic medicinal chemistry work on the pladienolides by the Eisai Corporation was done by making various esters and carbamates at C-7 of **2b** and **2d**. Eventually a urethane derivative of **2d**, with 7-(4-cycloheptylpiperazin-1-yl) substituted for 7-Ac was identified with complete retention of anti-VEGF activity and in vitro antitumor activity.[8, 9] This derivative with enhanced *in vivo* potency and pharmacokinetic properties was denoted E7107 (compound **3**, Figure 1.2), and entered phase I clinical trials for cancer treatment in 2007. Several chemical biology experiments at the Eisai Corporation were conducted

to identify the molecular target of **2a-2g** and **3**. Three 'chemical probes', semisynthetic derivatives of **2b** were developed for this purpose (compounds **4-6**, Figure 1.2).[10]

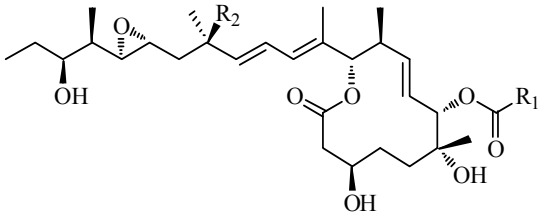

		R_1	R_2
pladienolide B	**2b**	CH_3	H
pladienolide D	**2d**	CH_3	OH
E7107	**3**	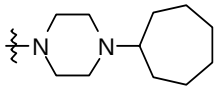	OH
^3H probe	**4**	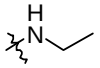 [w / ^3H on ethyl group]	H
fluorescent probe	**5**	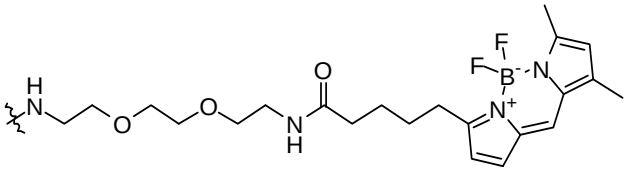	H
biotin-tethered probe with photocrosslinking agent	**6**	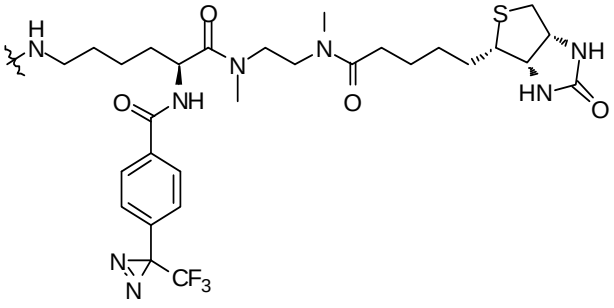	H

Figure 1.2 Semisynthetic analogs of pladienolides B and D (**2b** and **2d**)

^{3}H probe **4** was incubated with HeLa cells and subsequent cell fractionation and scintillation counting indicated that the target was most likely a nuclear protein. Fluorescent probe **5** was incubated with the same cells and fluorescence microscopy indicated probe localization on the nuclear speckles. Cells incubated with **4** were thus fractionated and the nuclear fraction subjected to co-precipitation experiments with antibodies against nuclear speckle proteins. Antibodies against the U2 small nuclear ribonucleoprotein (U2 snRNP) proteins, components of the spliceosome, precipitated most efficiently with the probe. The antibody against the spliceosome associated protein SAP155 precipitated 40-60% of the ^{3}H signal. Biotin linked analog of **6** with a photocrosslinking agent was developed and incubated with the HeLa cells, precipitated with the anti-SAP155 antibody, and irradiated to form a covalent conjugate with the target protein. Immunoblotting experiments identified two candidates, both components of splicing factor SF3b. Additional immunoblotting experiments with green fluorescent protein fused SF3b subunit 3 (SAP 130) indicated a direct interaction with probe **6**. Other experiments revealed that the target protein must be incorporated into the SF3b complex for probe binding. Finally, it was shown that **2b** inhibits *in vivo* mRNA splicing in HeLa cells in a dose-dependent fashion and causes enlargement of the nuclear speckles, most likely due to the accumulation of unspliced pre-mRNA.

These results suggest that the pladienolides are part of a new class of spliceosome targeting antitumor agents including FR901464 (**7b**) and its methyl ketal derivative spliceostatin A (**7a**).[11-13] Although the pladienolides are very different structurally (Figure 1.3), it is possible that they share an identical mechanism of

action. Spliceostatin A was also demonstrated to target SF3b, and displays a similar cell cycle arrest profile to the pladienolides.[11] The total synthesis of FR901464 by the Jacobsen group revealed that both the epoxide and acetate groups are required for activity.[14] The independent synthetic efforts from the Jacobsen and Kitihara groups toward **7b** resulted in the discovery that replacement of the 1-hemiketal moiety with more stable alkyl or alkoxy groups improved compound stability and potency *in vitro*. This discovery led to the development of semisynthetic probes used in the discovery of the target protein of these compounds. The methyl ketal **7a** was named spliceostatin A and was used for further biological studies by the Kitihara group (IC_{50} values for comparison were not reported but it is stated that activity of **7a** in the assay used was greater than **7b**).[15] The 1-deoxy analog **7c** was prepared by the Jacobsen group in their synthetic efforts and demonstrated enhanced potency, and the 1-methyl analog **7d** was later prepared by the Koide group and shown to have low picomolar activity.[16]

It is unknown whether **2a-2g** bind to the same site of SF3b as **7a-7d**, or interact with it in the same way. It is also not known exactly how interfering with mRNA splicing confers cytotoxicity, but it is likely that truncated proteins resulting from the translation of unspliced pre-mRNA translation such as p27 CDK may play a role. It has not been proven that inhibition of SF3b by **2a-2g** is the reason VEGF genes are not expressed in cells exposed to these compounds. There may be additional cellular targets of **2a-2g** responsible for the observed cytotoxicity effects. Because structure-activity studies have demonstrated that the epoxide and distal acyloxy groups are essential for cytotoxicity for both natural product types, medicinal chemistry work was

done to try to identify a minimal pharmacophore.[17] The minimal analogs that were made had much reduced potency, and were not proven to bind to SF3b, so more work needs to be done to validate this approach.

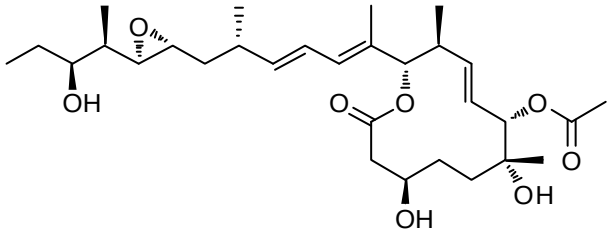

pladienolide B (**2b**)

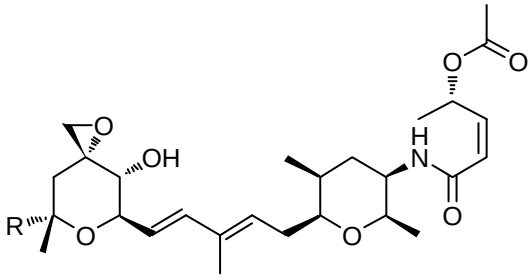

		R	Activity
spliceostatin A	**7a**	OCH_3	N/A
FR901464	**7b**	OH	IC_{50} = 2 nM (Tag Jurkat cells)
1-deoxy analog	**7c**	H	IC_{50} = 1.8 nM (Tag Jurkat cells)
1-methyl analog	**7d**	CH_3	GI_{50} = 10.2 pM, MCF-7 cells

Figure 1.3 Spliceosome targeting natural products

1.2 Synthetic approaches to the pladienolides and FD-895

1.2.1 Eisai Corp.'s total syntheses of pladienolides B and D

The primary objective of the first synthetic studies toward **2b** and **2d** was to elucidate their relative and absolute stereochemistry, because the isolation studies on **1** and **2a-2g** provided only planar structures. Material supply of the natural products was not the motivation, since high production titers of **2b** are consistent when the patented optimized procedures are used.[18, 19] Researchers at the Eisai Corporation employed a flexible four-component strategy to synthesize **2b** and **2d**, with all of the components generated using reagent-controlled asymmetric synthesis (Scheme 1.1).[9, 20] The work was done concurrently with traditional structural elucidation studies involving degredation and derivitization of **2b**.[21] If, during the synthesis, the working stereochemical model was changed, they could adjust the stereochemistry of each fragment by altering the reagents.

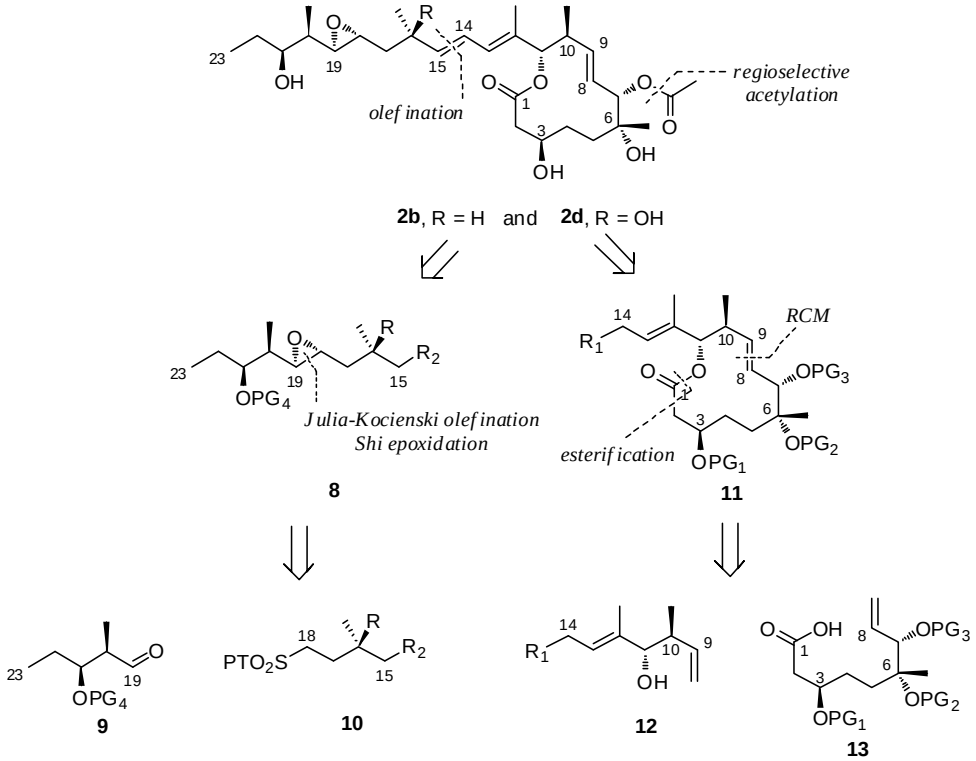

Scheme 1.1 Eisai Corp.'s retrosynthetic analysis of **2b** and **2d**

The synthetic group made the first retrosynthetic disconnection of **2b** and **2d** at the *E*-1,2-disubstituted $\Delta^{14,15}$ olefin, which they reasoned could be efficiently generated (in the case of **2b**) by a Julia-Kocienski olefination between a terminal sulfone sidechain fragment **8** (R_2 = SO_2PT) and aldehyde core component **11** (R_1 : =O). For **2d**, hinderance at C-16 (R = OPG) prevented the required C-15 sulfone nucleophile from adding to aldehydes in model studies. Therefore, this bond was installed by cross metathesis between terminal olefins of these advanced fragments.

The C-15 to C-23 sidechain fragment **8** was disconnected at the C-18/C-19 *trans* epoxide, which was installed by asymmetric epoxidation of a precursor *E*-1,2-disubstituted $\Delta^{18.19}$ olefin. The necessary olefin came from a Julia-Kocienski coupling of C-15 to C-18 sulfone subunit **10** and C-19 to C-23 aldehyde **9**. The C-20/C-21 syn stereodiad of aldehyde **9** was the result of Evans' asymmetric aldol chemistry. The isolated C-16 stereocenter of **2b** was acquired from methyl (*R*)-3-hydroxy isobutyrate; both enantiomers of this starting material are commercially available for the same price. The C-16 tertiary alcohol of **2d** had to be installed by Sharpless' asymmetric epoxidation of an appropriate allylic alcohol precursor, and iodination followed by reduction using Luche's conditions[22] afforded the desired fragment.

An esterification / ring-closing metathesis strategy was chosen for the synthesis of the core fragment **11**, an increasingly common approach to propionate-derived macrolactone natural products.[23, 24] A multifunctional fragment **12** was prepared, in addition to the acid-olefin component **13**. The C-9 to C-14 fragment **12** was generated using Paterson's *anti*-aldol addition[25] of a reported aldehyde and a lactate-derived chiral ketone, and 4 subsequent steps to install the terminal olefin. The

C-1 to C-8 acid olefin component **13** was prepared in 10 steps from the commercially available terpene nerol. The C-3 hydroxyl group was set by an auxiliary driven asymmetric Reformatsky reaction.[26] The C-6/C-7 diol was prepared using Sharpless' asymmetric dihydroxylation which proceeded in modest (76%) d.e., and the diastereomers could not be separated. After 2 protecting group manipulations on the diol mixture, a crystalline intermediate was formed, which after a single recrystallization gave a single pure diastereomer.

To complete the synthesis of **2b**, esterification of alcohol **12** and acid **13** was effected in 92% yield under Yamaguchi's conditions to form the RCM precursor. The precursor was treated with the Hoveyda-Grubbs catalyst in refluxing toluene to afford the core component **11** in modest (46%) yield. The core component was converted to an aldehyde in 2 steps, which coupled to the C-15 to C-23 sidechain sulfone fragment **8** in 64% yield. After 5 protecting group steps, the tetraol pladienolide A (**2a**) was formed. The researchers knew from their semisynthetic work on the natural products that **2a** could be regioselectively acetylated at the C-7 hydroxyl group, so this was the last step to produce **2b**.

To synthesize **2d**, the aldehyde of the core component **11** was converted to a terminal olefin with the Tebbe reagent, the protecting groups were removed and the C-7 acetate was regioselectively installed. The fully deprotected C-15 to C-23 terminal olefin sidechain fragment **8** (R = OH, PG = H, R_2 : $=CH_2$) was prepared for the final cross metathesis reaction. A 2:1 mole ratio mixture of **8**:**11** was refluxed in CH_2Cl_2 in the presence of Grubbs' second generation olefin metathesis catalyst, and **2d** was formed in 64% yield based on the limiting component **11**.

In summary, **2b** and **2d** were synthesized in 22 and 19 steps respectively, and 2.1% and 2.2% overall yields, respectively. **2a** was also synthesized as a target of opportunity *en route* to **2b**. Included in the synthetic work was a degredation experiment done on **2d** (Scheme 1.2) to elucidate the absolute stereochemistry at C-16 which was confirmed by the synthesis. The synthesis of **2b** confirmed the results of the degredation and structural elucidation studies described in the next section.

1.2.2 Structural elucidation of pladienolides B and D

The relative stereochemistry of the core macrolactone of pladienolide B was elucidated by 1D selective TOCSY and homonuclear-decoupling experiments.[20, 21] The NMR data obtained allowed the researchers at the Eisai Corporation to accurately determine coupling constants for every proton on the molecule, which allowed them to make a conformational model. This model was supported by observation of all the expected 2D-NOESY correlations in the core structure.

It follows from the vicinal coupling constant $^{3}J_{\text{H-18/H-19}}$ = 2.4 Hz that the C-18/C19 epoxide is *trans* in **1** and **2a**-**2g**.[4] The rest of the relative stereochemistry of the sidechain of **2b** and **2d** was determined by degredation and NMR analysis of derivatives as shown (Scheme 1.2). The C-3 and C-21 hydroxyl groups of **2b** were silylated, and exhaustive olefin dihydroxylation was carried out with OsO_4. Subsequent cleavage with $NaIO_4$ provided aldehyde **14**, which was then reduced to the primary alcohol with $NaBH_4$. The alcohol was converted to the corresponding tetrahydrofuran compound **15** by treatment with *t*-BuOK, which promoted the favorable 5-*exo*-tet epoxide ring opening at C-18. After removal of the silyl group, the

resultant C-21/C-19 1,3-diol was protected as the *p*-bromobenzylidene acetal, which formed as a 2:1 α:β mixture of diastereomers **16(α/β)**, which were separable on silica gel. NOESY interactions then revealed the relative stereochemistry of the sidechain of **2b** (Figure 1.4).

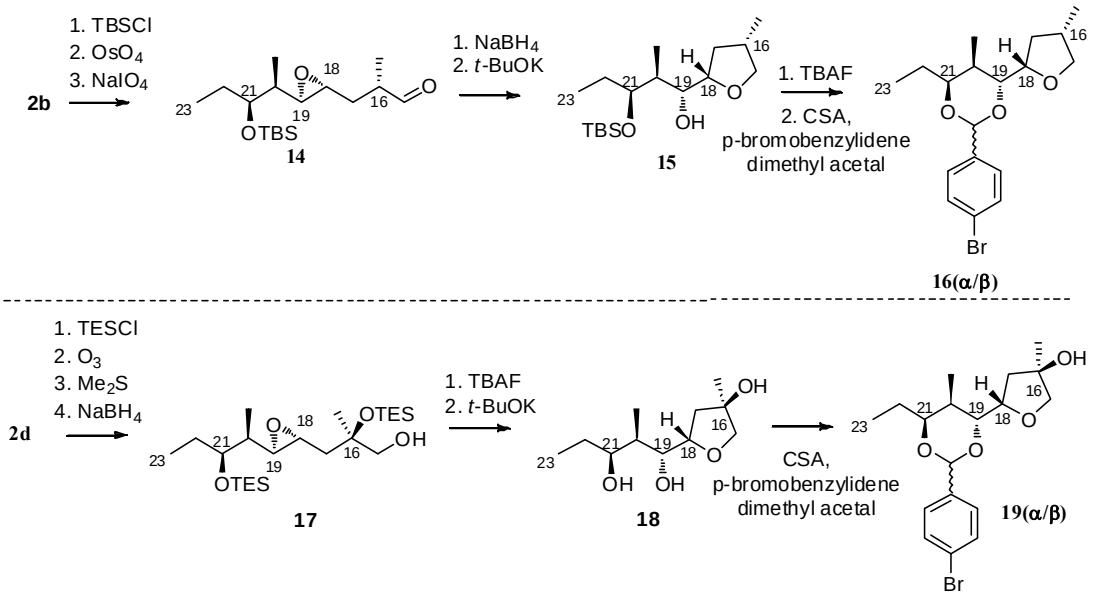

Scheme 1.2 Degredation experiments on **2b** and **2d**

The C-16 hydroxyl group of **2d** prevented this method from being employed for its derivatization. **2d** was thus silylated and subjected to reductive ozonolysis to afford alcohol **17**, which formed the corresponding tetrahydrofuran **18** upon deprotection and treatment with *t*-BuOK. The *p*-bromobenzylidene acetal **19** also formed as a mixture of separable diastereomers, and NOESY interactions confirmed that the C-16 methyl group of **2d** had the same relative configuration as **2b**, as expected.

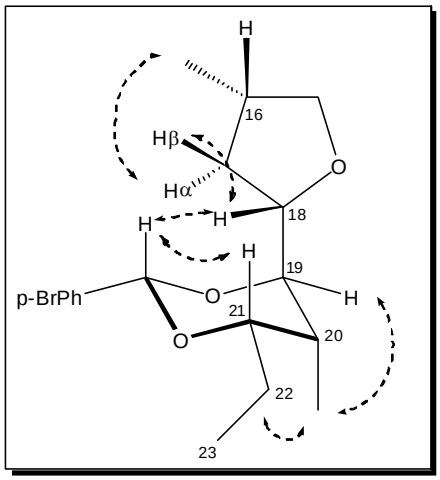

Figure 1.4 NOESY interactions observed on **16α**

Finally, preparation of the (*R*)- and (*S*)- C-3/C-21 bis-MTPA esters of **2b** allowed the researchers to unambiguously assign absolute stereochemistry by the modified Mosher method.[27]

1.2.3 Skaanderup's approach to the pladienolide core

A more efficient route to the pladienolide core was reported by Skaanderup and Jensen's group a year after Eisai's completed total synthesis report (Scheme 1.3).[28] The work was begun before the absolute stereochemistry of the pladienolides was published and they prepared the incorrect enantiomer, but it is clear that they had correctly deduced the relative stereochemistry of the core. The researchers mentioned an interest in studying the structural basis for the interaction of the pladienolides with the spliceosome, and intend to explore this by developing novel sidechain analogs to be tethered to the core for SAR studies.

The core macrolide **20** was disconnected at the C-1/C-11 lactone linkage and the *E* 1,2-disubstituted $\Delta^{8,9}$ olefin as in the Eisai route, and the sidechain was left out to focus efforts on improving the synthesis of the C-1 to C-8 ester olefin fragment **22**. This fragment was generated in 9 steps and 38% overall yield from the commercially available neryl acetate (Scheme 1.3), a substantial improvement in comparison to the Eisai route. An asymmetric acetate aldol reaction was used to set the C-3 hydroxyl group in 89% yield but a moderate 4:1 d.r. The diastereomers were separable on a single column, so the material was taken forward to evaluate the installation of the C-6/C-7 stereodiad by Sharpless' asymmetric dihydroxylation. Surprisingly, the researchers report that the substrate **23** reacted with AD-mix-β in 95% yield and > 20:1 d.r., much higher selectivity for essentially the same reaction that had been run by the Eisai group. Eisai was using AD-mix-α to form the correct stereoisomer, but it has been observed that the selectivity difference between the AD-mix ligands (DHQ-PHAL for AD-mix-α *vs* DHQD-PHAL for AD-mix-β) is negligible in general[29], so the observed disparity in selectivity is most likely due to the substrate used. The Skaanderup group left the chiral auxiliary from the aldol reaction on substrate **23** for the AD-mix reaction, whereas the Eisai group had cleaved the auxiliary from their Reformatsky reaction prior to the dihydroxylation step.

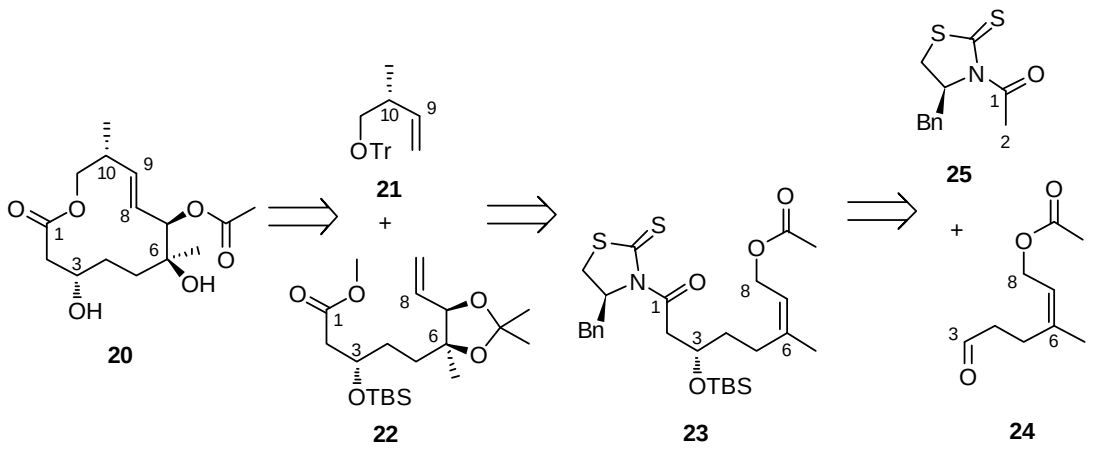

Scheme 1.3 Skaanderup's approach to the pladienolide core **20**

Skaanderup's group converted the diol product of the dihydroxylation reaction to the ester olefin fragment **22** in 4 steps and 71% overall yield. Compound **21** was prepared in 4 steps and 84% overall yield from the Roche ester, a commonly employed chiral precursor. After some optimization effort, it was observed that **21** and **22** reacted efficiently under cross-metathesis conditions using the Hoveyda-Grubbs catalyst to afford the *E*-1,2-disubstituted $\Delta^{8,9}$ olefin in 76% yield. The core structure **20** was then prepared in 5 steps from the cross-metathesis product.

In summary, the Skaanderup synthesis demonstrated some improvements in the synthesis of the C-1 to C-8 fragment, and increased the efficiency of the formation of the $\Delta^{8,9}$ olefin by opting for cross-metathesis instead of RCM. It is not clear from these studies how they intend to install the C-10/C-11 stereodiad, or how they intend to couple their sidechain analogs to the core as there is no functionality available on compound **20** for this purpose.

1.2.4 Retrosynthetic analysis of the pladienolides and FD-895

We became engaged in similar synthetic efforts during roughly the same time period as Skaanderup / Jensen's group.[30-33] It is likely that the Eisai Corporation began their synthetic efforts before their report of the isolation of **2a-2g**, because they applied for a patent on the syntheses of **2b** and **2d** in October 2005.[20] Unfortunately, authentic samples of **2a-2g** were not available to us. To circumvent this issue, we sought to acquire the producer strains of **2a-2g** from Japanese culture collections. After many repetitions of the published isolation protocols[2], both of the strains delivered to us failed to produce **2a-2g** in detectable quantities. The only secondary metabolites that could be identified and reproducibly detected from these efforts are the subject of chapter 2.

We were eventually provided an authentic sample of **1**, which was used to conduct 2D NMR experiments in attempts to deduce its relative configuration. The spectra obtained on this sample indicated very good agreement between **1** and the reported data for its closest pladienolide congener **2b** for many of the δ_C and δ_H values and $^3J_{HH}$ vicinal proton coupling constants. It was thus proposed that **1** probably has the same relative configuration as **2b** and **2d**, although **1** has the additional C-17 stereocenter such that its sidechain has six contiguous stereogenic centers.

Due to the limited amount of **1** provided to us we were hesitant to conduct extensive degredation studies on it, instead focusing on NMR studies combined with a few attempts to crystallize it or make crystalline derivatives (such as p-bromobenzoates or 3,5-dinitrobenzoates). Our NMR instruments were not set up to

run *J*-resolved HMBC or HETLOC experiments, which are necessary to measure the $^{2,3}J_{CH}$ values needed to conduct *J*-based configurational analyses (JBCA)[34, 35], so we assigned as many $^{3}J_{HH}$ vicinal coupling constants as possible, comparing them with similar fragments from the literature, and NOESY experiments to get relative information between separate spin systems.

At the same time, strategies toward stereodivergent fragment synthesis were devised to make models of the possible diastereomers, and hopefully start ruling out some of the possibilities in this way. Additionally, it was desired that these fragments should incorporate useful handles for couplings to complete the molecule. Our retrosynthetic analysis for **2b** was similar to the one used successfully by the Eisai researchers, with the major difference being the method of attachment of the sidechain to the core (Scheme 1.4). We proposed disconnection at the C-13/C-14 bond of the diene on the sidechain, reasoning that a Stille coupling would be the mildest method to achieve late stage fragment assembly.

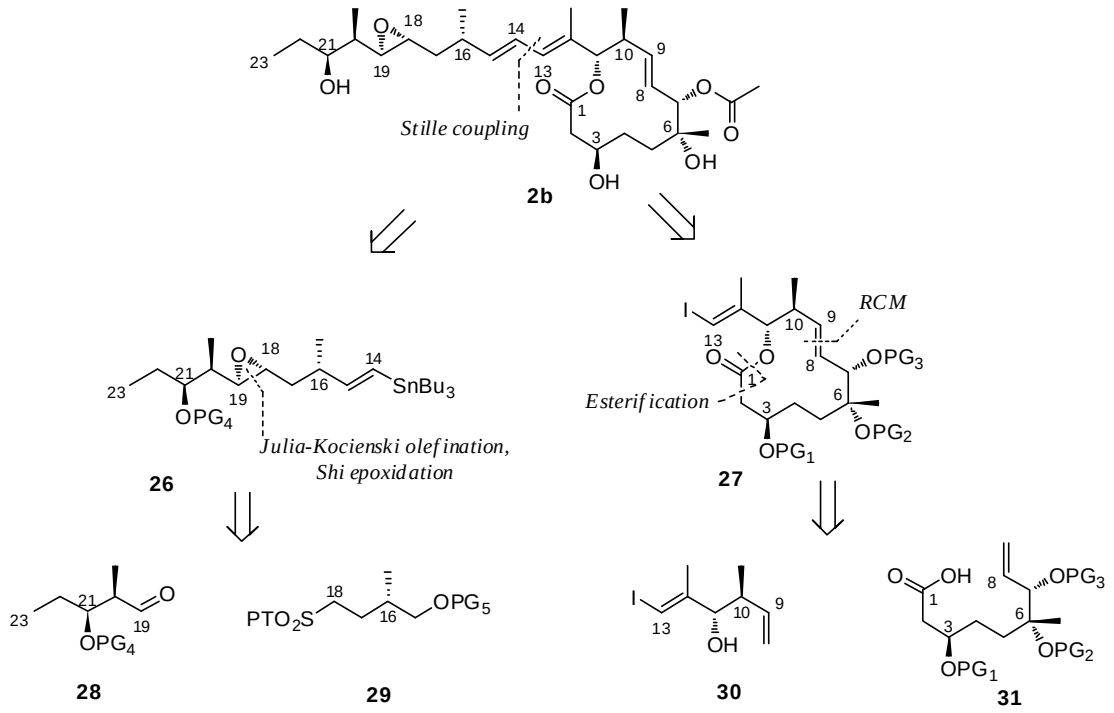

Scheme 1.4 Retrosynthetic analysis of pladienolide B (**2b**)

Disconnecting the core vinyl iodide fragment **27** at the C-1/C-11 lactone and the *E* 1,2-disubstituted $\Delta^{8,9}$ olefin required the production of **31**, the same C-1 to C-8 acid olefin fragment synthesized in the Eisai route (compound **13**) (Scheme 1.1). Because no synthesis of such a fragment existed at the time our studies began, many routes were examined involving asymmetric synthesis and also chiral pool approaches. The multifunctional fragment **30** was also needed, for which a three-step synthesis from propargyl alcohol was devised, using crotylboration to set the C-10/C-11 stereocenters. This was chosen because both stereocenters were set in a single step, and all 4 stereoisomers were accessible. The crotylboration product also had the appropriate handles for fragment assembly. It was thought that because $^{3}J_{\text{H-10/H-11}}$ = 9.8 Hz in **1** and **2b** that C-10/C-11 had the *anti* configuration.

Disconnection of stannane **26** at the C-18/C-19 *E* olefin precursor to the epoxide was also the same strategy employed by the Eisai route. This left us to synthesize sulfone **29**, easily accessible from 2-methyl 1,4-butanediol, both enantiomers of which are commercially available. Aldehyde **28** was prepared by asymmetric aldol methodology. All that remained was to couple the fragments and find a suitable asymmetric epoxidation to form the C-18/C-19 epoxide, which proved more difficult than expected.

Because we had an authentic sample of **1**, we sought to develop a stereodivergent route to its sidechain. For this aspect of the project, the major disconnection of the Stille coupling to core component **27** was retained, and thus required a different stannane fragment **32** to be produced by reagent controlled methods that could provide either stereochemistry of the C-17 alcohol (Scheme 1.5). Crotylation or aldol addition to aldehyde **34** was envisioned for this purpose, because both *syn* and *anti* methods are available with high levels of reagent control. Sharpless' method was used to set the epoxide of the sidechain of **1**, since the precursor would be an allylic alcohol. This required the preparation of allylic alcohol **35**, which was accomplished by Horner-Wadsworth-Emmons homologation of aldol-derived aldehyde **36**.

Having developed flexible strategies to **1** and **2b**, several attempts to generate the C-1 to C-8 acid olefin fragment **31** were initiated. It was soon realized that **31** is the most intractable piece of the molecule, requiring the most synthetic operations in any route yet devised toward **1** and **2a-2g**.

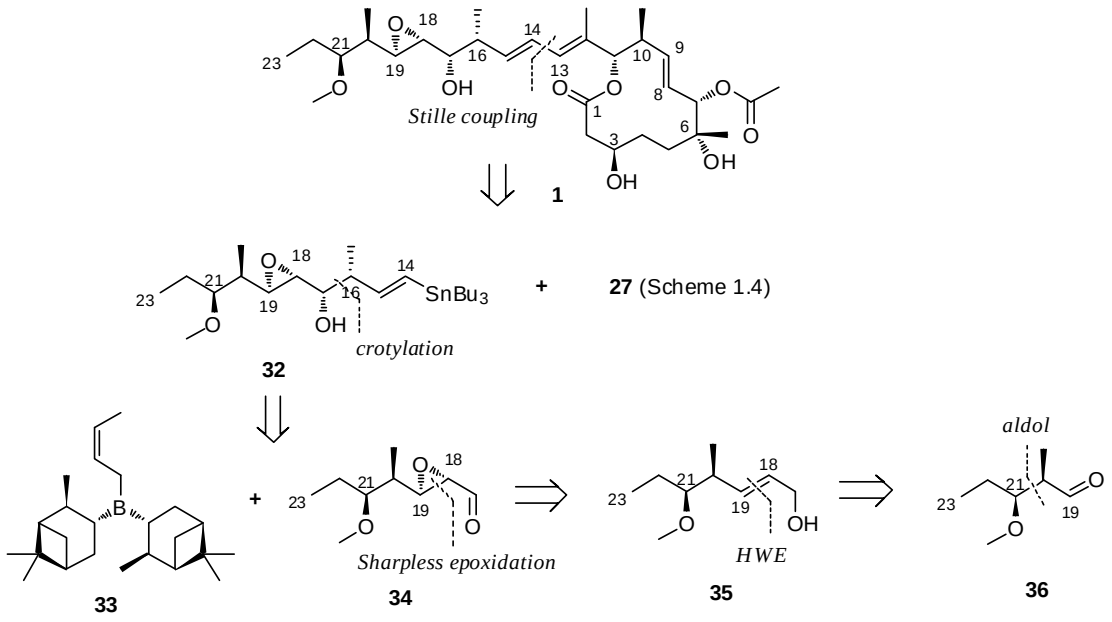

Scheme 1.5 Retrosynthetic analysis of FD-895 (**1**)

1.2.5 A chiral pool approach to the C-1 to C-8 acid olefin of 1

At the outset, it was suspected that the relative configuration of the C-6/C-7 stereodiad of **1** was as shown in fragment **31** (Scheme 1.4) due to NOE correlation between the C-6 methyl substituent and methine proton H-7. The relative configuration of the isolated C-3 stereocenter to the C-6/C-7 diol could not be definitively assigned from the NOESY spectra. Fragment **37**, a diastereomer of **31**, was arbitrarily chosen as the synthetic target for the C-1 to C-8 segment of the core. One of the initial forays toward **37** was a chiral pool approach using a carbohydrate derived scaffold to provide the C-3 stereocenter (Scheme 1.6). Precursor **38** was targeted to achieve this goal because it was apparently simple to prepare.

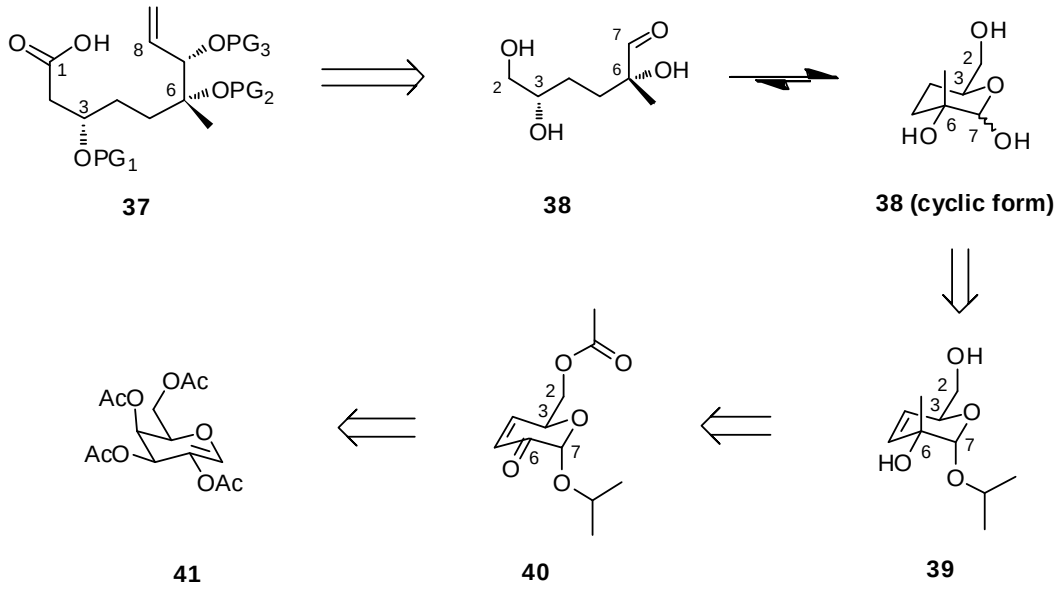

Scheme 1.6 A chiral pool retrosynthetic approach to **37**

A report of high levels of substrate control in the addition of methylcerium dichloride to carbohydrate derived chiral ketones **42** and **43** to give axial addition products **44** and **45**, respectively, was thought to be particularly suitable for this type of fragment (Scheme 1.7).[36] Substrate controlled methylation of known enone **40** (similar to **42**), would thus provide **39**.

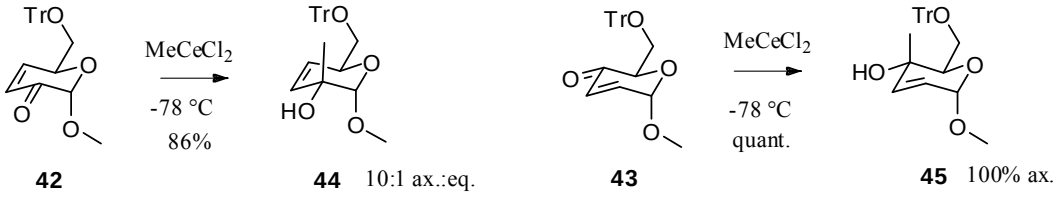

Scheme 1.7 Substrate-controlled methylations of chiral ketones

A survey of the literature revealed numerous methods for the preparation of enones such as **40**. A one-step high yielding method developed by De Fina starting with the widely used galactose-derived glycal **41** (Scheme 1.6) was chosen for our

first attempt.[37] It was thought that if an efficient method to open the acetal of **39** to a manipulable acyclic form could be found, this route could provide rapid access to the scaffold needed for **37**. Two techniques were considered for this transformation (Scheme 1.8). Hydrogenation of **39** would provide **46**, and several conditions have been reported for converting acetals directly to 1,3-dithianes such as **47**, or similarly to acyclic dithioacetals.[38, 39] Alternatively, acid catalyzed hydrolysis of **46** would give the triol **38**. A number of methods exist for converting hemiacetals of this type to oximes (**48**, R = Me or Bn), for which there is a spectrum of oxidative cleavage conditions.[40]

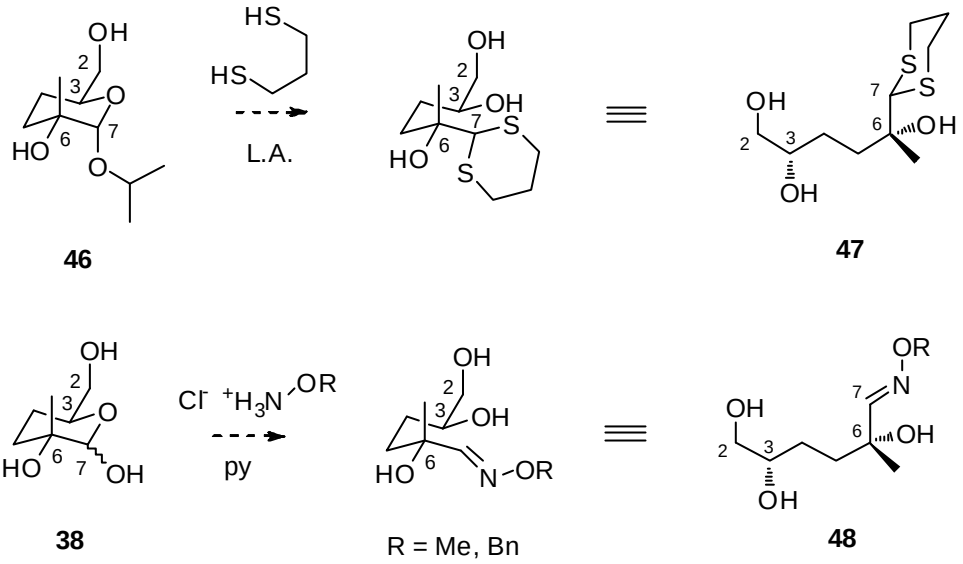

Scheme 1.8 Methods for opening the C-7 acetal to an acyclic intermediate

Two homologations of acyclic intermediates such as **47** or **48** would be necessary to reach **37** (Scheme 1.6), the first being introduction of the C-1 carbon which could be accomplished by cyanide or 2-lithio-1,3-dithiane displacement of the corresponding C-2 tosylate or iodide.[41, 42] Additionally, the C-8 carbon needed to be

introduced preferably as the terminal olefin for the RCM step, with concurrent installation of the C-7 stereocenter. Chelate-controlled addition of vinylmagnesium bromide to the C-7 aldehyde from this route would give the wrong diastereomer, so protection of the C-6 hydroxyl with a bulky, non-chelating silyl group such as TES would favor the Felkin-Anh type addition product.[43] For example, if cyanide displacement were used to install C-1, a bis-TES protected open chain aldehyde such as compound **49** would be generated upon cleavage of the C-7 dithioacetal or oxime. A projection of **49** is shown on the top right in Scheme 1.9, which predicts generation of product **50**, which has the correct stereochemistry to form **37** (see Scheme 1.6).

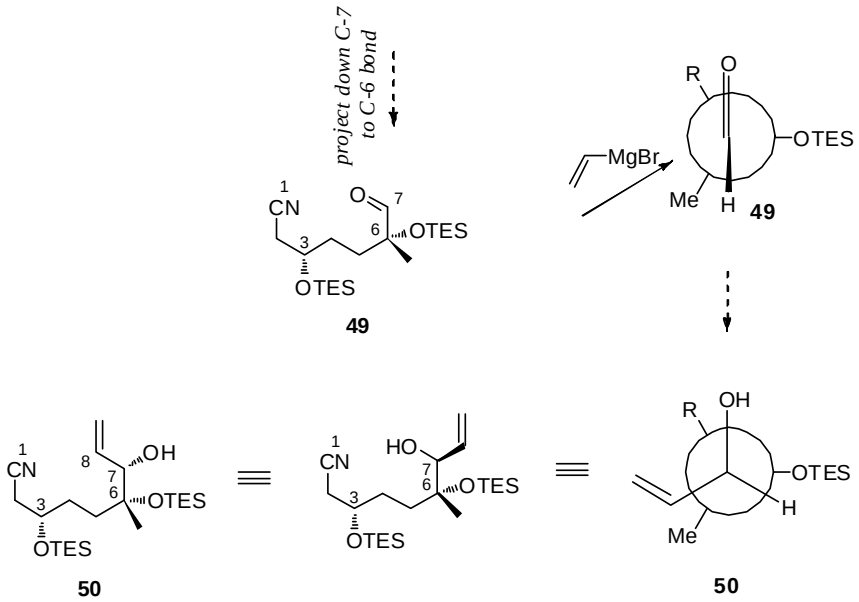

Scheme 1.9 Predicted mode of addition to intermediate **49**

Once this outline was developed, it was thought to be flexible enough that it would be worthwhile to attempt the synthesis of compounds **39** and **38** to test our hypotheses.

1.2.6 Exploration of the chiral pool approach to the C-1 to C-8 fragment

De Fina's preparation of enone **40** proceeded as reported, provided that the purity of the starting material was high, that freshly distilled isopropanol was used, and that anhydrous conditions were strictly maintained.[37] Temperature control was also important; if the reaction was allowed to warm to room temperature before quenching, more of the reported byproduct 5-acetoxymethyl-2-furaldehyde was observed.

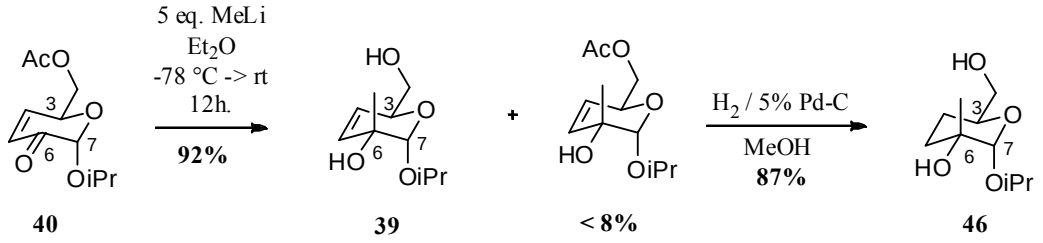

Scheme 1.10 Synthesis of acetal **46**

During examination of the methylation of enone **40**, it was discovered that transmetallation of methyllithium to cerium was unnecessary to achieve selectivity for this substrate. The first method used for this addition (Scheme 1.7) described similar substrates to **40**, but they were methyl glycosides.[36] It was thought that the bulkiness of the 7-OiPr group blocked equatorial attack of methyllithium, such that product **39** was exclusively observed in excellent yield, with some of the C-2 acetate side-product (Scheme 1.10). Hydrogenation of **39** provided compound **46** in good yield, upon which 1D selective NOESY experiments were conducted to confirm the axial mode of addition of MeLi to enone **40**, and a strong interaction was observed between the isolated C-6 methyl group and the H-7 anomeric proton (Spectrum 1.7). Efforts then

commenced to open the acetal of **46** to an acyclic dithioacetal, or a cyclic dithiane such as **47** (Scheme 1.8). When acetal **46** was subjected to the thioacetalization conditions reported by Frejd, clean 62% conversion to trimercaptan **51** was observed (Scheme 1.11).[39] It was originally thought that this product was dithioacetal **52**, although there seemed to be an additional ethanethiol unit in the NMR spectrum (Spectrum 1.8). Product **51** was converted to acetonide **53** with the intention of protecting the C-6 hydroxyl group such that various dithioacetal cleavage methods could be examined to obtain a C-7 aldehyde. All attempts to protect **53** returned starting material, and the NMR spectrum of **53** appeared to still have the extra ethanethiol unit (Spectrum 1.10).

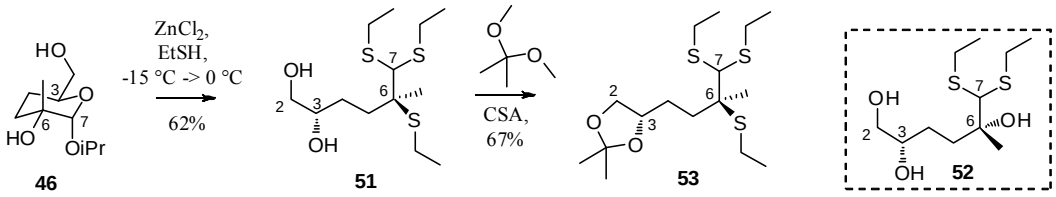

Scheme 1.11 Attempted thioacetalization of **46**

Re-evaluation of the NMR spectra of **53** and HRMS analysis led to its identification, which provided the explanation for why attempts to install a C-6 protecting group were not working. This type of overreaction of a dithioacetal was postulated by Horton *et. al.* to proceed via an episulfonium ion intermediate, resulting in inversion at C-6 of compound **46**.[44] It is thought that the desired product **52** forms under the reaction conditions, undergoes Lewis-acid assisted episulfonium ion formation, and this intermediate is then converted to **51** by substitution of ethanethiol at C-7 (Scheme 1.12).

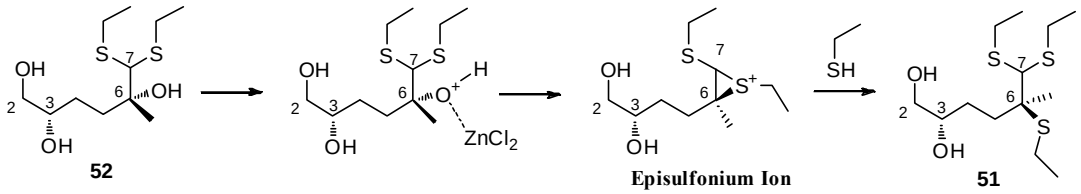

Scheme 1.12 Possible mechanism of formation of trimercaptan **51**

The thioacetalization conditions were altered to avoid the overreaction of **46**. Experiments included lowering the temperature, controlling stoichiometry (not using an excess of ethanethiol), use of different solvents and Lewis-acids, and the similar reaction with 1,3-propanedithiol to form the cyclic dithiane **47** as in Scheme 1.8. Lack of success with these modifications led to the idea that if the C-6 hydroxyl group was appended with an acid-stable protecting group before thioacetalization, maybe the episulfonium ion formation would not be as favorable. Acetal **46** was silylated at the C-2 hydroxyl group, and the C-6 hydroxyl group was protected as benzyl ether **55** (Scheme 1.13).

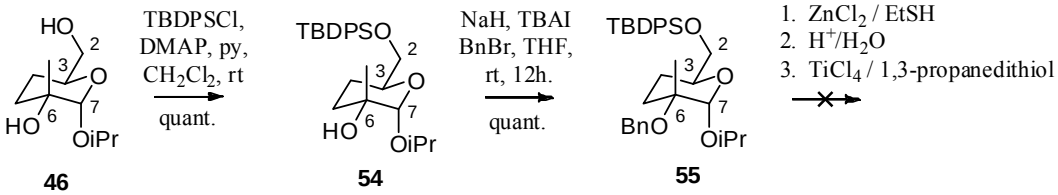

Scheme 1.13 Preparation of compound **55**

Reaction of acetal **55** under $ZnCl_2$ catalyzed thioacetalization conditions again resulted in trimercaptan formation. All attempts at acidic aqueous hydrolysis of **55** to the hemiacetal returned starting material. $TiCl_4$ catalyzed 1,3-dithiane formation with

1,3-propanedithiol also resulted in overreaction, either by trimercaptan formation or the alternative 7-membered thioether ring.

An unexpected result was observed in an attempt to generate dibenzoate **56** from acetal **46** (Scheme 1.14).

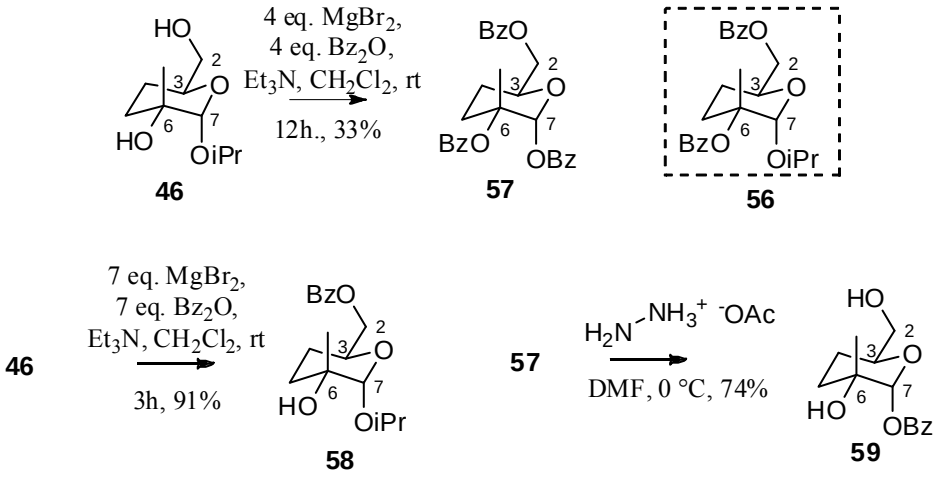

Scheme 1.14 An alternate method to break the –OiPr acetal of **46**

Under conditions reported to benzoylate tertiary hydroxyl groups[45], the Lewis acid used to activate benzoic anhydride cleaved the –OiPr acetal of **46** and afforded tribenzoate **57** as the only product. This constituted another method for the preparation of **38** by a two-step sequence, if it could be optimized. Unfortunately the reaction proved difficult to monitor because the intermediates had similar R_f to the product. Because of this difficulty, in a later optimization attempt, monobenzoate **58** was recovered as the sole product. Additionally, an attempt to selectively cleave the anomeric benzoate of **57** with hydrazine acetate[46] resulted in cleavage of the primary and tertiary benzoates to give **59** as the sole product. A different strategy was adopted, conversion of **46** to oximes as in **48** (Scheme 1.8).

Acidic hydrolysis of **46** proved to be problematic, and the only conditions that provided **38** reproducibly were heating to 80 °C overnight in 2N HCl (Scheme 1.15). Any more mild conditions than this returned starting material, and harsher conditions resulted in decomposition. Although the consistently low yields of **38** were frustrating, it was decided that the route should be continued under the rationale that if the subsequent steps succeeded, the acetal hydrolysis step could be optimized.

Alternatively, it might be possible to generate a more labile acetal from De Fina's rearrangement reaction on glycal **41** to form enone **40**, by clever choice of the substituting alcohol (Figure 1.5). The rearrangement reaction was attempted with benzyl and p-methoxybenzyl alcohol, 2-trimethylsilylethanol, and methanol. Unfortunately the reaction only seems to work well on secondary aliphatic alcohols without much functionality. Of all the alcohols tried, only the methanol variation provided any product, and it was an inseparable mixture of anomers, which would not confer the axial selectivity of methyllithium addition that was achieved using enone **40**. Manipulations on oximes from **38** were continued.

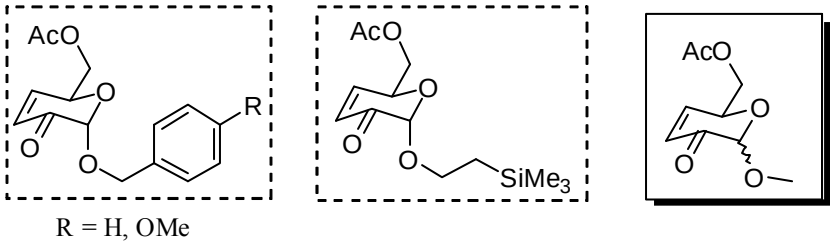

Figure 1.5 Alternate enones to **40** targeted

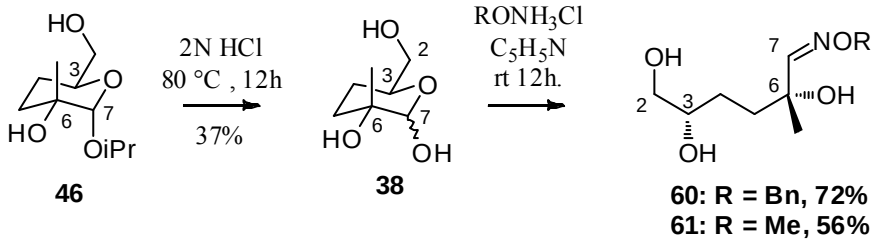

Scheme 1.15 Synthesis of oximes **60** and **61**

Compound **38** was converted to the benzyl (**60**) and methyl (**61**) oximes in moderate yields (Scheme 1.15). Some of the *Z*-isomer of the methyl oxime was observed in the ^{1}H NMR spectrum of **61** (Spectrum 1.22), but only the *E*-isomer was observed in **60** (Spectrum 1.20). The original plan was to homologate at C-7 prior to the C-2 homologation, so these oximes were first protected as the C-2/C-3 acetonides **62** and **63** (Scheme 1.16).

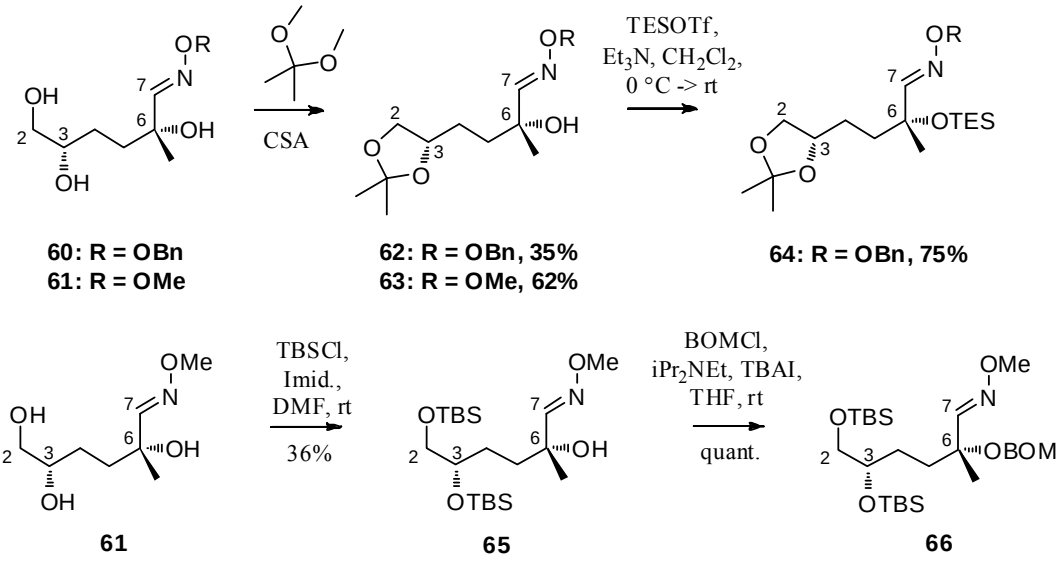

Scheme 1.16 Early protecting group manipulations on **60** and **61**

The benzyl oxime acetonide **62** was protected as its C-6 OTES ether **64**, and subjected to ozonolytic cleavage in an attempt to generate a C-7 aldehyde. Although the ^{1}H NMR indicated product formation, the reaction was done on too small of a scale to confirm that it was the correct product aldehyde. Additionally, it was decided that the C2/C3 diol of oximes **60** and **61** should be differentially protected to retain the option of homologation at C-2 prior to installation of the C-7 stereocenter. Methyl oxime **61** was protected as the C-2/C-3 bis-TBS ether **65** and the C-6 hydroxyl group protected as the BOM ether **66**. Compound **66** was subjected to an oxime exchange reaction with paraformaldehyde, and acetone, catalyzed by the cation exchange resin amberlyst 15.[47] Decomposition of starting material was observed.

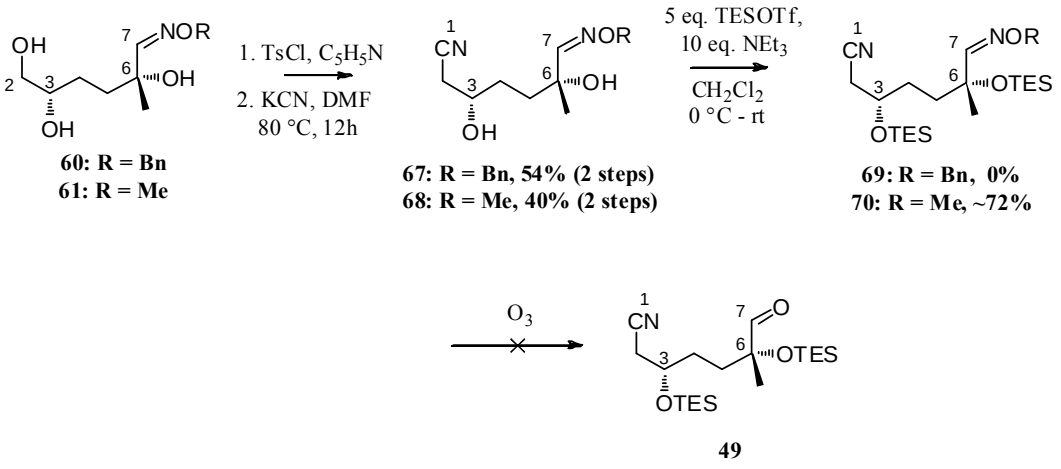

Scheme 1.17 Additional manipulations on oximes **60** and **61**

The C-2 primary hydroxyl group of oximes **60** and **61** were selectively activated as the tosylates, and displaced with cyanide in moderate yields over 2 steps to afford the nitriles **67** and **68** (Scheme 1.17). Silylation of the methyl oxime **68** with excess TESOTf provided **70** in moderate yield, but a complex mixture resulted from

the same attempted protection of the benzyl oxime **67** on the second repetition. It is not obvious why this result was observed, since the reaction apparently worked the first time on smaller scale, and also worked on the corresponding acetonide substrate **62** to produce **64** (Scheme 1.16). The methyl oxime **70** could not be converted to the aldehyde **49** (see Scheme 1.9) by ozonolysis followed by standing overnight at -78 °C in unquenched ozone.

Failure of both strategies to efficiently produce useful acyclic intermediates as illustrated in Scheme 1.8, and the realization that the chiral pool strategy was forcing excessive protecting group manipulation steps left us to consider strategic changes. The chiral pool approach was abandoned in favor of an asymmetric dihydroxylation strategy to provide the C-6/C-7 diol.

It should be noted that the chiral pool strategy may have been more successful by starting with enone **43** (Scheme 1.7), as the tertiary alcohol would be remote from the acetal to be opened. Further, there are efficient syntheses of enone **43** that could be used to incorporate various primary alcohols at the anomeric position that would be more hydrolytically labile than the bulky –OiPr acetal of **46**.[48] This strategy would be used to develop the enantiomer of **37**, because the positions of enone **43** as they map to the product are reversed relative to **46**, but at this point the absolute stereochemistry of the target natural products was unknown to us. Reagent controlled methods would have to be used to install C-3 in this route, as well.

A dihydroxylation strategy seemed more promising and flexible, being able to afford all possible stereoisomers of the C-6/C-7 diol from readily available starting materials. As seen in sections 1.2.1 and 1.2.3, synthetic efforts from other groups

toward these natural products have used dihydroxylation effectively to generate the retron **31** (Scheme 1.4). In general, it is not advisable to use chiral pool synthetic strategies unless both the relative and absolute stereochemistry of the target have been unambiguously determined.

1.2.7 Asymmetric dihydroxylation approaches to fragment 37

Our first retrosynthetic scheme under this new approach to **37** involved the use of an asymmetric acetate aldol reaction on aldehyde **71** to install the C-3 stereocenter. Aldehyde **71** could be derived from alcohol **72**, which could be generated by substrate-controlled Felkin addition of vinylmagnesium bromide to the chiral aldehyde **73** to provide the C-7 stereocenter.

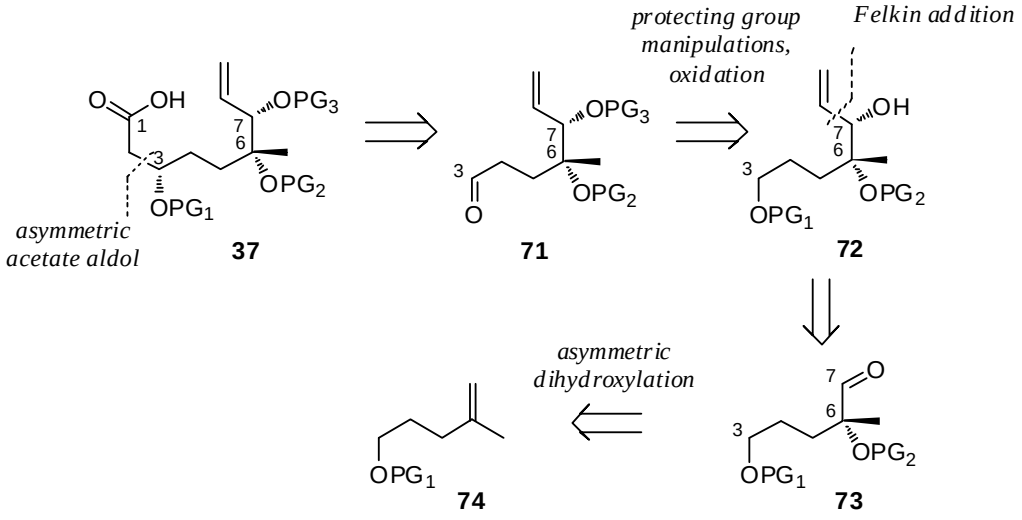

Scheme 1.18 Initial asymmetric dihydroxylation retrosynthetic scheme

The C-6 tertiary alcohol of aldehyde **73** would result from asymmetric dihydroxylation of the readily available 4-methylpent-4-en-1-ol derivative **74**. High

levels of enantioselectivity had been recently reported for dihydroxylation of **74** (PG_1 = Bn).[49] In the course of preparation of **74**, the precursor ester **75** was prepared by the previously described Claisen orthoester rearrangement of β-methallyl alcohol and triethyl orthoacetate. Dihydroxylation of **75** unexpectedly provided lactone **76** in 97% yield (Scheme 1.19), which was thought to be potentially useful. The only previously reported preparation of lactone **76** was accomplished in racemic form by hydroxylactonization of the corresponding acid of **75** using MTO / H_2O_2.[50]

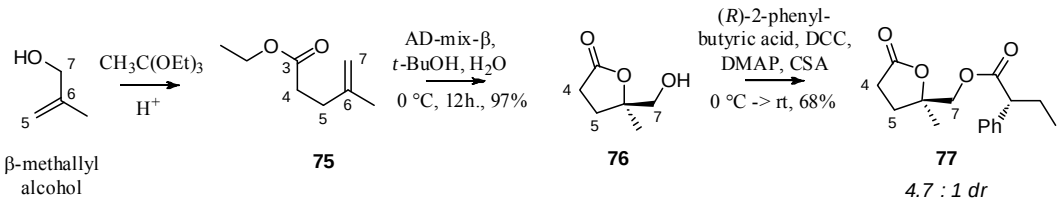

Scheme 1.19 Dihydroxylation of ester **75**

We were interested in oxidizing the C-7 primary alcohol of **76** to the aldehyde and examining the selectivity of the addition of vinylmagnesium bromide to it. It is not obvious which diastereomer would be preferred in this addition, or if the α-oxygen in the lactone ring would cause chelation control to predominate. Alternatively, the C-7 hydroxyl group could be protected, and the lactone opened and homologated at C-3 first. Most importantly, the selectivity of the AD-mix reaction in its formation needed evaluation. Derivitization of **76** as its (*R*)-2-phenylbutyrate ester[51, 52] **77** revealed that the dihydroxylation step had proceeded in a disappointing 65% e.e.

The selectivity of asymmetric dihydroxylation is substrate dependent, so ester **75** was reduced and protected as in **78-79**, and the reaction was repeated according to

the published procedure. Although the dihydroxylations proceeded in good yield as described, derivitization of the product diols **80-81** as their (*R*)-2-phenylbutyrate esters **82-83** indicated only 42-60% e.e. for the AD-mix reactions (Scheme 1.20).

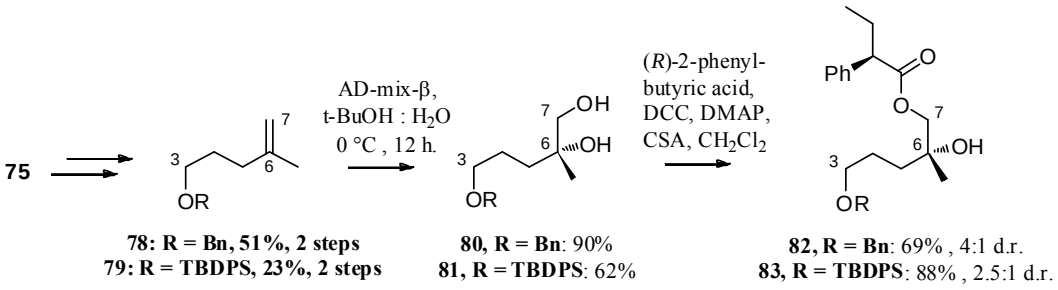

Scheme 1.20 Dihydroxylation of 4-methylpent-4-en-1-ol derivatives

These results were confusing in light of the reported selectivity for **74**, and could not be improved by altering the protecting group at the C-3 OH. It should be noted that the derivitization reagent used, 2-phenylbutyric acid, was judged to be enantiomerically pure by reaction with control chiral alcohols under the same esterification conditions used for derivitization. In any event, it was decided that a trisubstituted olefin would be a better choice for the substrate, such that the C-6/C-7 stereodiad would be set in a single step.

The trisubstituted olefin approach necessitated a small change in the retrosynthetic strategy, being installation of the C-8 terminal olefin handle on intermediate **71** (Scheme 1.18) by means of Wittig homologation of a terminal C-8 aldehyde. This type of aldehyde could derive from an intermediate such as **84** (Scheme 1.21), which in turn could come from the dihydroxylation product of an appropriate *Z*-trisubstituted olefin such as **85**, after protecting group manipulations and reduction.

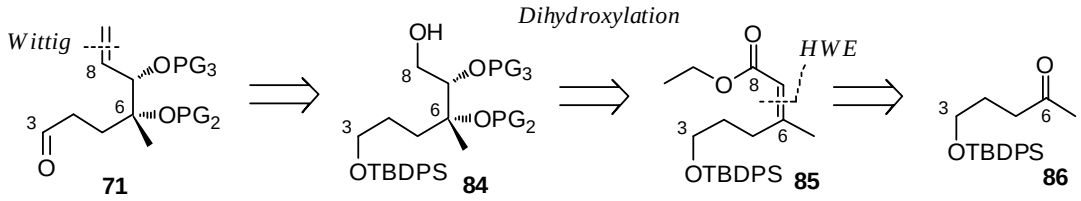

Scheme 1.21 Modified dihydroxylation retrosynthesis of **71**

There was a recent report of generating **85** with its *E*-isomer **87** by using Horner-Wadsworth-Emmons (HWE) homologation of ketone **86**.[53] HWE reactions are known not to show high selectivity on ketone substrates, and the report did not mention the isomer ratio as it was unimportant for the authors' purposes. If the isomers could be generated in a roughly equal ratio and chromatographically separated, this would constitute a stereo-divergent route to the fragment, being able to develop diol **84** from the *Z*-trisubstituted olefin **85** and the alternatetively configured C-6/C-7 diol from the *E*-trisubstituted olefin **87**.

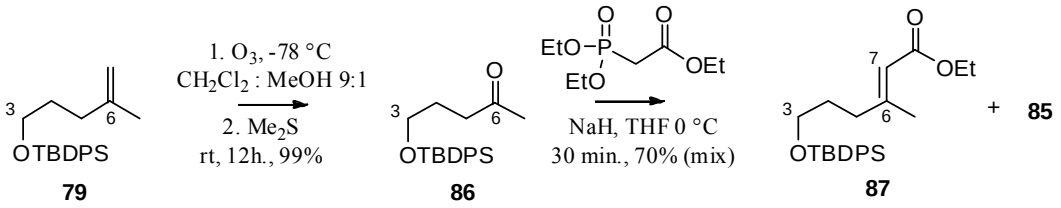

Scheme 1.22 HWE homologation of ketone **86**

Ketone **86** was generated by ozonolysis of the 1,1-disubstituted olefin **79**, and reacted with the triethylphosphonoacetate anion. The quantitative yield of the α,β-unsaturated esters **85** and **87** observed in the first report was not observed in our experiment. A moderate yield of a roughly 4:1 mixture of **87:85** was produced, and

with some experimentation it was found that the isomers were separable on silica gel. Selective 1D NOESY experiments confirmed that the reaction proceeded with modest *E*-selectivity, such that more pure **87** (Spectrum 1.44, Spectrum 1.45) was obtained than **85** (Spectrum 1.42, Spectrum 1.43). Although this did not bode well for the synthesis of the C-6/C-7 diol with the predicted configuration, both isomers were obtained so that their reactivity with AD-mix could be evaluated. There are a few *Z*-selective variations of the HWE reaction that could be explored if the dihydroxylation results were promising.[54, 55]

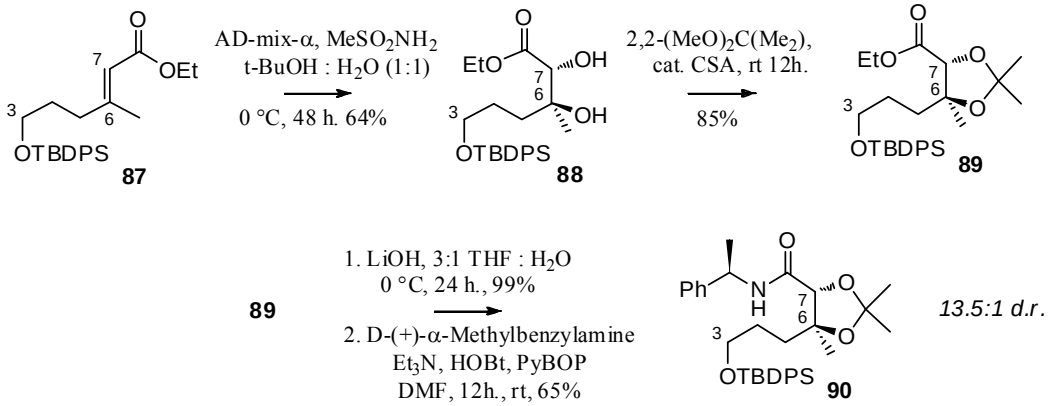

Scheme 1.23 Dihydroxylation of substrate **87**

The *E*-isomer **87** reacted sluggishly with AD-mix-α and in moderate yield to form diol **88**, but a three-step derivitization with a chiral amine (Scheme 1.23) showed that the reaction had proceeded in > 86% e.e., the highest yet observed selectivity. We sought to carry out the same sequence on the pure sample of **85** that we had obtained, but failed to find a set of conditions under which **85** would react with AD-mix. Starting material was returned even under the most forcing conditions. Although the electron-deficiency of the olefin in **85** may have been remediated by reducing the ester

and protecting the resulting alcohol, the problem of how to generate the *Z*-isomer selectively remained. Instead of opting for a *Z*-selective phosphonate type homologation, two medium-ring lactones were targeted, in a slightly modified retrosynthetic scheme.

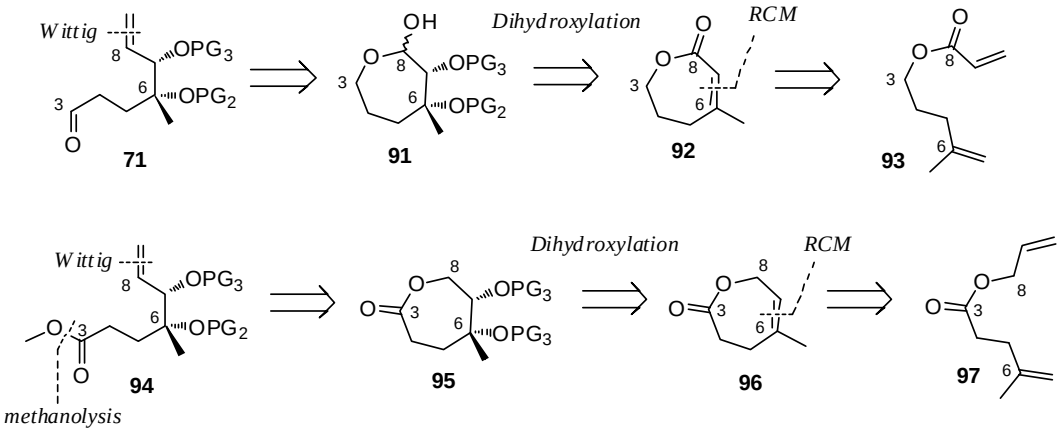

Scheme 1.24 Dihydroxylation of 7-membered lactones

Intermediate **71** (Scheme 1.18) was targeted again, and it was realized that its precursor could be derived from a C-8 aldehyde/lactol such as **91** (Scheme 1.24). It has been observed in our own laboratory and by others that such hemiacetals/lactols can be homologated in the presence of excess ylide.[56, 57] Hemiacetal **91** would be the result of dihydroxylation of medium-ring lactone **92** after protecting group manipulations and careful reduction with DIBAL-H. Lactone **92** is a known compound, but its reported synthesis is inefficient and involves thermal fragmentation of a diastereomeric mixture of chlorocyclopropanes to force ring expansion.[58] Since the report of lactone **92**, several catalysts and conditions have become available for the formation of medium rings by RCM.[59-61] The ease of preparation of the precursor **93**

(Scheme 1.24), combined with the possibility of an intramolecular HWE to form this lactone, was interesting enough to prompt experimentation.

Alternatively, the unknown lactone **96** (Scheme 1.24) could provide intermediate **94** which is analogous to **71**. Lactone **96** should be more reactive to AD-mix than **92**, since the olefin is not conjugated to the lactone carbonyl, but its formation would have to occur through RCM; there would be no intramolecular HWE option.

Diene **98**, the cinnamate ester (surrogates for acrylate esters in RCM reactions) of 4-methylpent-4-en-1-ol was prepared to evaluate whether it could form lactone **92**, but none of the desired product was observed in reactions using Grubbs' 2nd generation catalyst (Scheme 1.25).

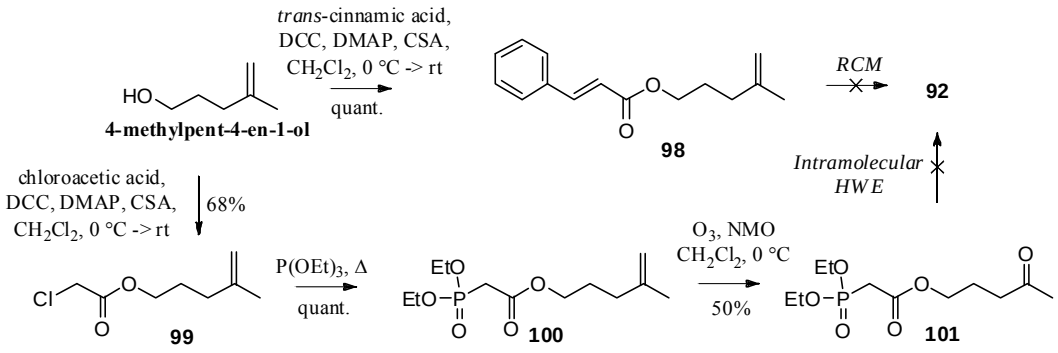

Scheme 1.25 Attempts at forming lactone **92**

The HWE alternative was examined by forming chloroacetate ester **99** and the subsequent Arbuzov reaction to form phosphonate **100** (Scheme 1.25). Ketone **101** was cleanly afforded by ozonolysis, and this substrate was subjected four different sets of HWE conditions. K_2CO_3 in the presence of 18-Crown-6, NaH in THF, Et_3N in refluxing THF, and DBU in refluxing THF all of which failed to effect cyclization of

101 to lactone **92**. The reactivity of lactone **92** under dihydroxylation conditions is still unknown, and lactone **96** has not yet been prepared. These studies were abandoned before a thorough investigation could be made. At this time, the project shifted focus to the preparation of the sidechain of FD-895 (**1**) as well as fragment assembly and model studies, the remaining sections of Chapter 1.

It should be noted that there is the possibility that lactone **92** could be synthesized from the previously reported saturated lactone **102**. Several methods exist to convert the readily available and inexpensive 3-methylcyclohexanone to lactone **102** by Baeyer-Villager oxidation.[62-64] Conversion of **102** to **92** could then proceed via oxidation of the α-phenylselenide.

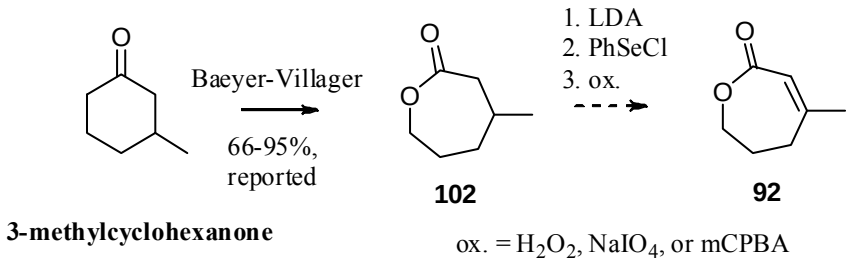

Scheme 1.26 Another method to form lactone **92**

1.2.8 Preparation of the sidechain of FD-895

As outlined in Scheme 1.5, we sought to develop the sidechain of FD-895 (**1**), in a linear fashion with stannane fragment **32** as the target. We planned to introduce the six continguous stereocenters in three asymmetric reactions.[31, 33] Aldehyde **36** was prepared in 4 steps and 48% overall yield from propionaldehyde, and the propionylated thiazolidinethione auxiliary (prepared in 3 steps from L-Phe) described

by Crimmins *et. al.*[65] Aldehyde **36** could be converted to allylic alcohol **35** in 2 steps and 74% yield by HWE homologation, which proceeds with complete *E*-selectivity, and reduction of the ester with DIBAL-H.

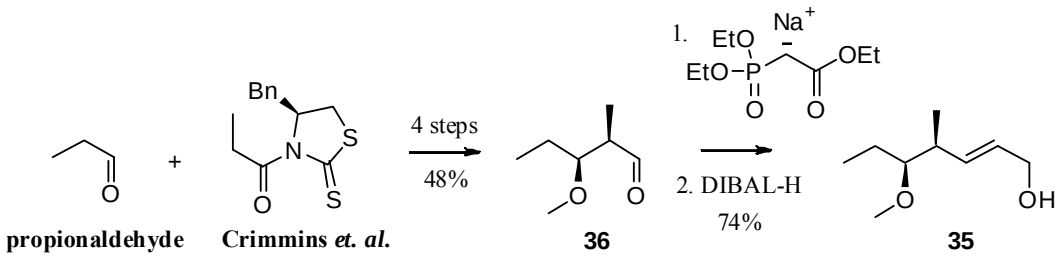

Scheme 1.27 Preparation of allylic alcohol **35**

Selectivity issues were encountered with asymmetric epoxidation on substrate **35**. The catalytic asymmetric epoxidation proceeded in high yield (typically 90-95%), but the 9:1 d.r. was not reproducible. Several careful repetitions of the standard catalytic procedure[66] gave inseparable mixtures of epoxides **103** and **104** in unacceptable d.r. of 2:1 - 4:1 (Scheme 1.28).

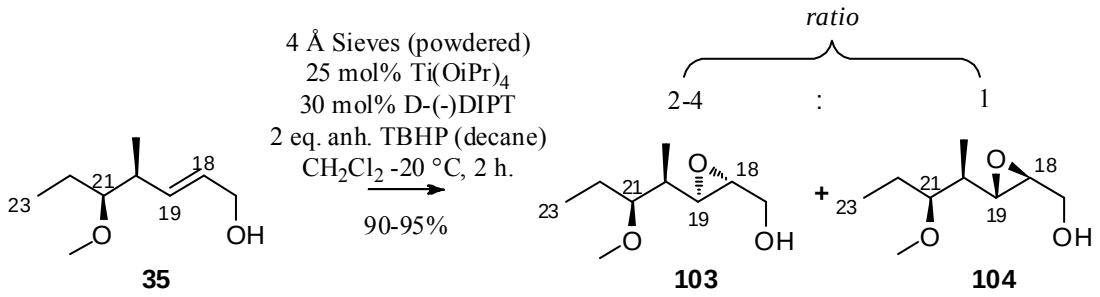

Scheme 1.28 Catalytic Sharpless epoxidation of allylic alcohol **35**

This result was confusing in light of published reports of high levels of reagent control on similar substrates, and a satisfactory explanation for the low observed d.r.'s under these conditions was not obtained.

Yamamoto *et. al.* had recently reported the use of chiral bishydroxamic acid ligands in complexation with vanadium isopropoxide and *t*-BuOOH as a new method for the asymmetric synthesis of epoxides from allylic alcohols.[67] Evaluation of this method for the epoxidation of **35** resulted in modest improvement with one of the ligands reported; a 7.5:1 d.r. was obtained favoring the desired epoxide **103**, but the reaction did not proceed to completion and a 65% yield was observed. Yamamoto's methodology was deemed unsatisfactory due to the long reaction times (3-5 days), and the need to synthesize the ligands over 6 steps not including the resolution of (±)-*trans*-1,2-diaminocyclohexane.

Re-evaluation of Sharpless' asymmetric epoxidation at stoichiometric reagent levels and low concentration ([substrate] ≤ 0.02 M) provided reproducible high yields (94%) of **103:104** in 6:1 or higher d.r., which was accepted and further exploration of the route was continued.

A more serious problem was encountered once the α,β-epoxy alcohol **103** was converted to aldehyde **34** (IBX was discovered to be the preferred oxidizing agent for this transformation). A *syn*-crotylation using $^{d}Ipc_2B$-(*Z*)-crotyl reagent **33** (Scheme 1.5) was required to obtain the necessary *syn*-C-16/C-17 fragment **105**. We assigned the relative stereochemistry of C-17 from the NOE interactions of methine H-17 with the epoxide protons H-18 and H-19, and H-16, all of which corresponds most closely with H-17β for **2b** as tabulated in Eisai's published and patented NMR data.[20, 21]

Several repetitions of the reaction of **34** with **33** afforded only decomposition of starting material and trace amounts of **105** (Scheme 1.29). This result was confusing because reports in the literature indicate that in most cases, with almost any relative configuration of the precursor aldehyde, Brown's crotylation methodology should provide the product in at least moderate yield and typically high selectivity.[68, 69] It had also been observed that **34** reacts with the $^{l}Ipc_2B$-(*Z*)-crotyl antipode **106** in low to moderate yield to afford diastereomer **107**. The little amount of **105** obtained was a single diastereomer and its ^{1}H NMR spectrum appeared similar to the sidechain of **1**, but it was clear that an alternate method was needed to install these stereocenters.

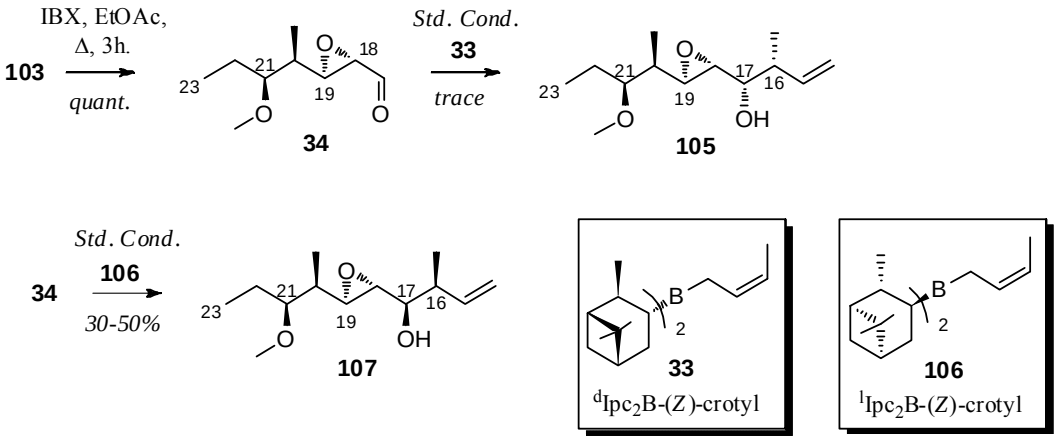

Scheme 1.29 Attempted crotylation of aldehyde **34**

A few attempts were made at using the same asymmetric aldol methodology for C-16/C-17 that had been used to install the C-20/C-21 stereodiad as in **36** (Scheme 1.27). The results indicated that the Lewis acids used to generate the enolates in these types of reactions were too harsh for the epoxide of aldehyde **34**.

The Marshall group developed methodology to deliver the type of stereochemistry needed for fragment **105** with high selectivity using chiral allenic stannanes.[70-72] These reagents add in S_E' fashion to aldehydes, with the selectivity being governed by a combination of reagent and substrate control. (*P*)-allenic stannane **108** was prepared in two steps from (*R*)-(+)-3-butyn-2-ol which was predicted to generate homopropargylic alcohol **109** upon Lewis acid catalyzed addition to **34** (Scheme 1.30). This method appeared to be particularly useful for our synthesis because **109** could be directly hydrostannylated to the desired stannane fragment **32** (Scheme 1.5), thus reducing the number of linear steps.

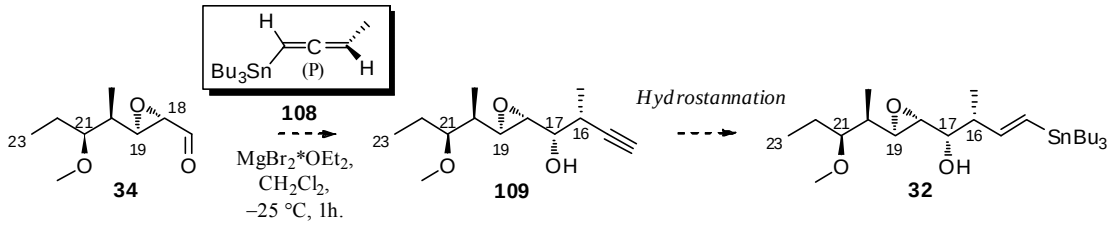

Scheme 1.30 A new approach to fragment **32** using Marshall's methodology

It was thought that the chelation-controlled result observed for the addition of **108** to (*S*)-lactic aldehyde benzyl ether **110** to provide the all *syn*-**111** (Scheme 1.31) should work similarly on aldehyde **34**, the transition state involving chelation of the Lewis acid to the α-epoxide unit.[72] In the event, **108** reacted with **34** under $MgBr_2$*OEt_2 catalysis to provide bromohydrin **112** in modest yield (Scheme 1.32). The structure of the product bromohydrin **112** was not clear upon inspection of its ^{1}H NMR spectrum, but it could be immediately seen that the C-18/C-19 epoxide had been

opened. The structure of **112** was confirmed by mass spectrometric, NMR, and X-ray crystallographic analyses.

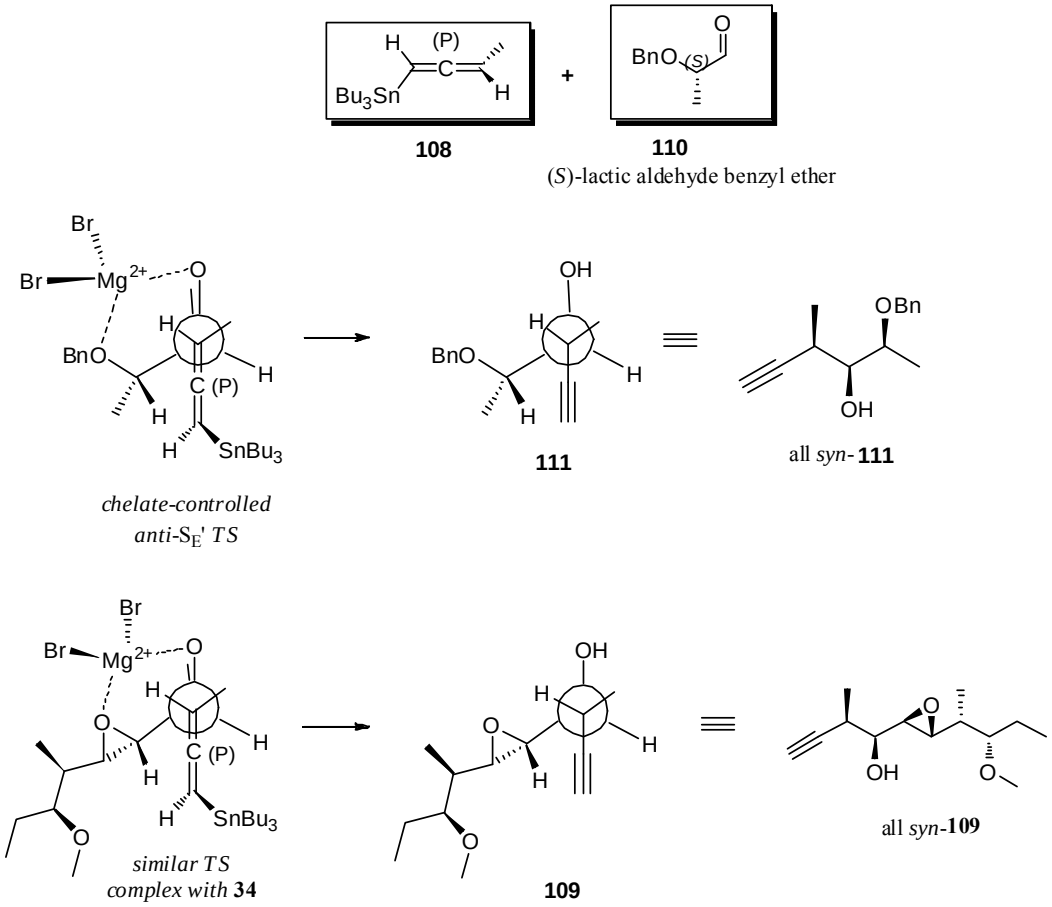

Scheme 1.31 Predicted mode of addition of stannane **108** to aldehyde **34**

The reaction of *trans*-α,β-epoxy aldehydes with $MgBr_2$ to form bromohydrins has been reported by several groups in the literature and it appears that epoxide opening occurs regioselectively adjacent to the carbonyl group in almost all cases.[73, 74] Conversion of **112** to **109** by treatment with base was not explored because it would most likely result in an inseparable mixture of epoxides, and there were still other options available to us using Marshall's methodology. Although there is no clear

consensus on whether or not the ring opening occurs by magnesium chelation of the oxirane and the carbonyl, the observed relative stereochemistry of **112** seems to preclude the possibility that the epoxide opening occurs prior to the S_E' addition of **108**. If the bromohydrin formed first, a different chelation model would ensue from the resulting β-alkoxide and the aldehyde,[70] and the opposite relative configuration between the C-17 alcohol and the C-18 bromide would have been observed.

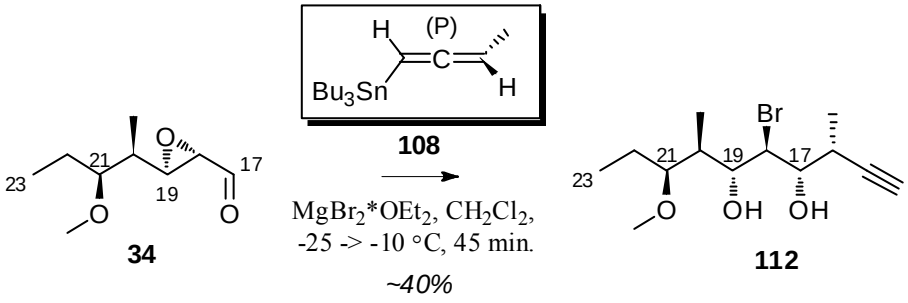

Scheme 1.32 $MgBr_2$ catalyzed addition of **108** to aldehyde **34**

However, the questionability raised by others about the potential for $MgBr_2$ to actually chelate this type of epoxy aldehyde leaves open the question of whether the TS shown in Scheme 1.31 is correct, or if a Felkin-Anh type model would be more appropriate, as both would lead to the predicted product **109**. These ambiguities lead to uncertainty as to which model to apply to our system, which is unique in the context of this methodology. We were left with the need to explore two alternatives to obtain **109**.

It was clear that we could not use $MgBr_2$ to promote the addition of these allenic stannanes, so it was necessary to examine the addition of both **108** and its (*M*)-antipode **113** with aldehyde **34** under catalysis with the monodentate Lewis acid

BF_3*OEt_2, one of which should provide the correct all *syn* configuration for C-16-C-19 in products **109** and **114** (Scheme 1.33). Also, **109** would form **112** upon treatment with $MgBr_2$*OEt_2, if our theory about the formation of **112** was correct.

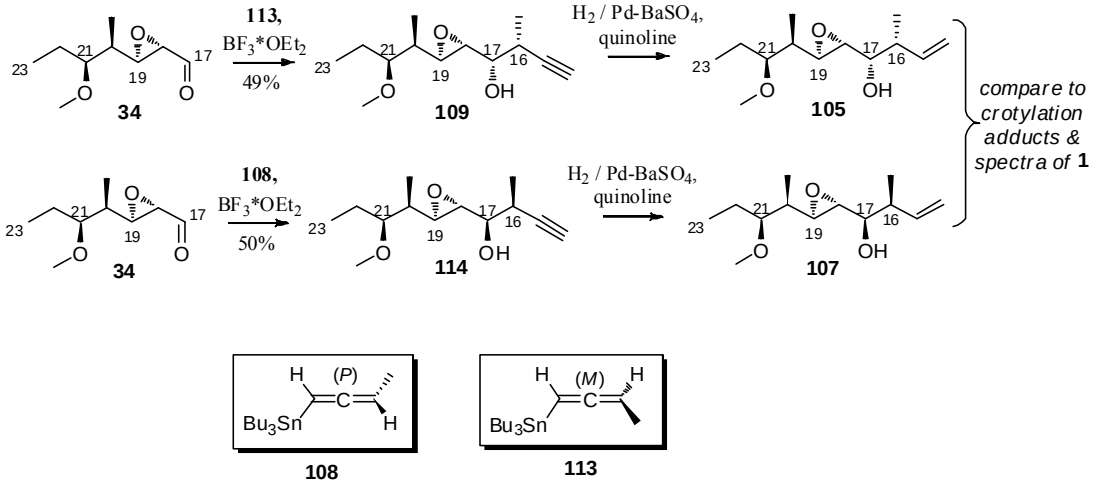

Scheme 1.33 Experiment to determine the correct reagent to form **109**

Aldehyde **34** reacted with both **108** and **113** in moderate yields with BF_3*OEt_2 catalysis, and the epoxides stayed intact in both of the products recovered, **109** and **114** (Scheme 1.33). Both were subjected to hydrogenation with Rosenmund's Pd-$BaSO_4$ catalyst in the presence of quinoline. Although the spectra obtained from the reduction experiments are crude and complicated by some overreduction to the alkane in both cases, neither product **105** or **107** appears to match the spectrum obtained for the putative **105** from the crotylboration experiment. Most disconcerting in each spectrum is the chemical shift of the H-17 methine, which is too far downfield in each as compared to the putative **105** from crotylboration and the spectrum of authentic **1** (see section 1.5 for overlays of these intermediates with **1**). Additionally, the epoxide protons H-18 and H-19 do not agree well in terms of chemical shift or $^3J_{H\text{-}H}$ values.

These results indicate that more experimentation needs to be done to acquire a fragment with C-16/C-17 stereochemistry corresponding to **1**. It is likely that the target **109** was generated in one of the addition reactions, but that the all *syn* relative configuration of C-16 to C-19 is not the relative configuration of the sidechain of **1**. Additionally, the products **109** and **114** should each be treated with $MgBr_2$*OEt_2 to see if they form crystalline bromohydrins as in **112**. It may be coincidental that the small amount of putative **105** obtained from the crotylboration experiment appears very similar to the sidechain of authentic **1**. The trace amount obtained could have been the result of 1,3-sigmatropic isomerization of the crotylborane species *in situ* prior to addition (a process known to normally happen in trace amounts),[75] and that the relative stereochemistry of the fragment generated is not as shown.

If the relative configuration of the C-16/C-17 stereodiad in **1** is *anti*, then the allenic stannane methodology would need to be replaced, because these additions are always *syn* between the newly formed stereocenters when BF_3*OEt_2 is used as the catalyst. Fortunately, Marshall's group has developed allenylzinc and allenylindium reagents to deliver the *anti* configuration if this adjustment needs to be made.[76, 77] Crotylboration with the (*E*)-crotyl species to give the *anti* stereochemistry may also be more efficient with **34** than the *syn* crotylboration attempt described in Scheme 1.29. Also, when exploring this system, it would be advisable to generate bromohydrins from as many of the synthetically prepared isomers as possible and check if they are also crystalline like **112**, as this is a convenient method to confirm stereochemistry. Because there are ample techniques to deliver the homopropargylic and homoallylic alcohols **109** and **105**, and a good method was obtained to produce two of the potential

diastereomers with great selectivity, the putative **109** was carried through the final stages of model assembly, and its stereochemistry while tentative will continue to be shown as in Scheme 1.33.

The final step in assembly of the sidechain of **1** was hydrostannation of alkyne **109**, which provided the desired (*E*)-vinylstannane **32** (see Scheme 1.5) in moderate yield (Scheme 1.34).

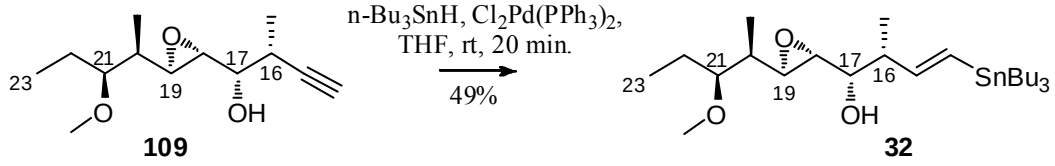

109 **32**

Scheme 1.34 Hydrostannation of alkyne **109**

1.2.9 Model studies of the endgame fragment assembly of FD-895

The preparation of **32** allowed the late-stage fragment assembly steps toward a total synthesis of **1** to be examined, because we had already developed an efficient synthesis of the multifunctional fragment **30** (Scheme 1.4) for our model studies on **2b**.[31, 33] In these model studies, 8-nonenoic acid served as as a surrogate for C-1 to C-8 acid olefin fragment **31**. At this stage of the project, all of the devised schemes (such as Scheme 1.18) toward **31** required a reagent-controlled installation of C-3. A new surrogate **115** including the C-3 stereocenter was devised so that methods could be evaluated for its installation (Scheme 1.35). A recently described acetate aldol methodology using an L-*tert*-leucine derived thiazolidinethione auxiliary **116** was employed, so that 6-heptenal **117** would be the substrate for the aldol reaction.[78]

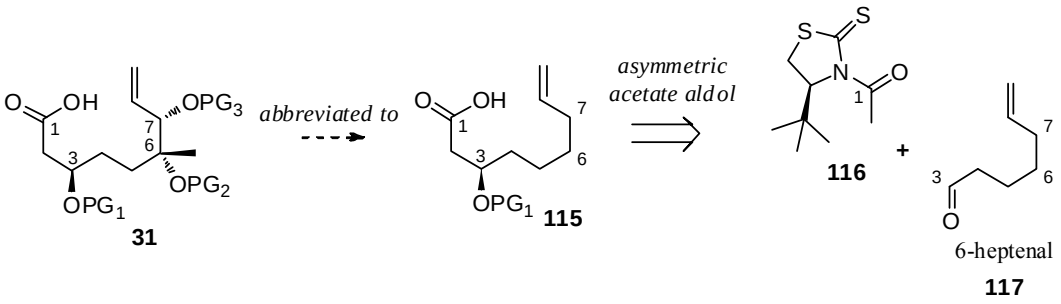

Scheme 1.35 A new C-1 to C-8 acid olefin fragment model **115**

The aldol reaction between the acetylated thiazolidinethione **116** and aldehyde **117** proceeded in high yield and selectivity to afford adduct **118** (Scheme 1.36). Because these adducts were reportedly prone to hydrolysis in aqueous workups, we chose to remove it immediately by treatment with methanol and imidazole, and the methyl ester **119** was protected as its C-3 -OTBS ether **120** in a low, unoptimized yield, probably owing to the remaining cleaved auxiliary, which had not been entirely removed in the purification of **119**. More than enough silylated material was obtained to continue through the remaining steps of saponification to afford acid **121**, which was then esterified to fragment **30** in nearly quantitative yield to provide RCM precursor diene **122**. The ring-closing event proceeded uneventfully to form the model core **123** in less than 2 hours' reaction time, as the single *E*- $\Delta^{8,9}$ olefin isomer.

Because the sidechain fragment **32** had been prepared in ~ 20 mg quantity (see the previous section), we were in position to evaluate its coupling to the new model core **123** as well as the older model **124**, of which we still had a few milligrams left over from our studies on **2b**. For these couplings, the Stille conditions employed by the Marshall group in their synthesis of Bafilomycin V_1 were used, and we were

pleased to observe the couplings proceed to completion in both cases, in moderate yields to afford models **125** and **126**, respectively (Scheme 1.37).[79]

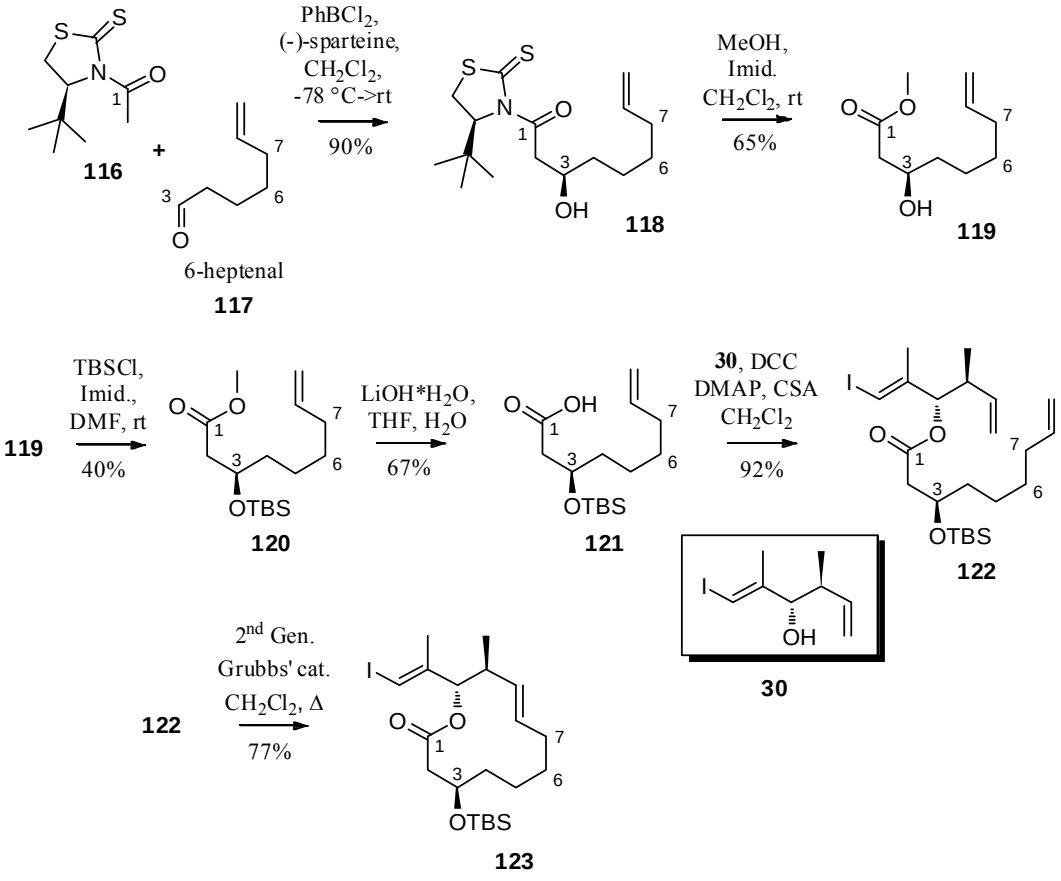

Scheme 1.36 Synthesis of the model core system **123**

For the sake of completeness, the C-3 OTBS ether was removed on model **125** to provide model **127**, which proved that the C-18/C-19 epoxide is stable to unbuffered HF-pyridine in acetonitrile, as observed in the model studies of **2b**. The dissertation author then turned to a new project, which was conceived during isolation efforts toward obtaining authentic samples of **2a**-**2g** (see Chapter 2).

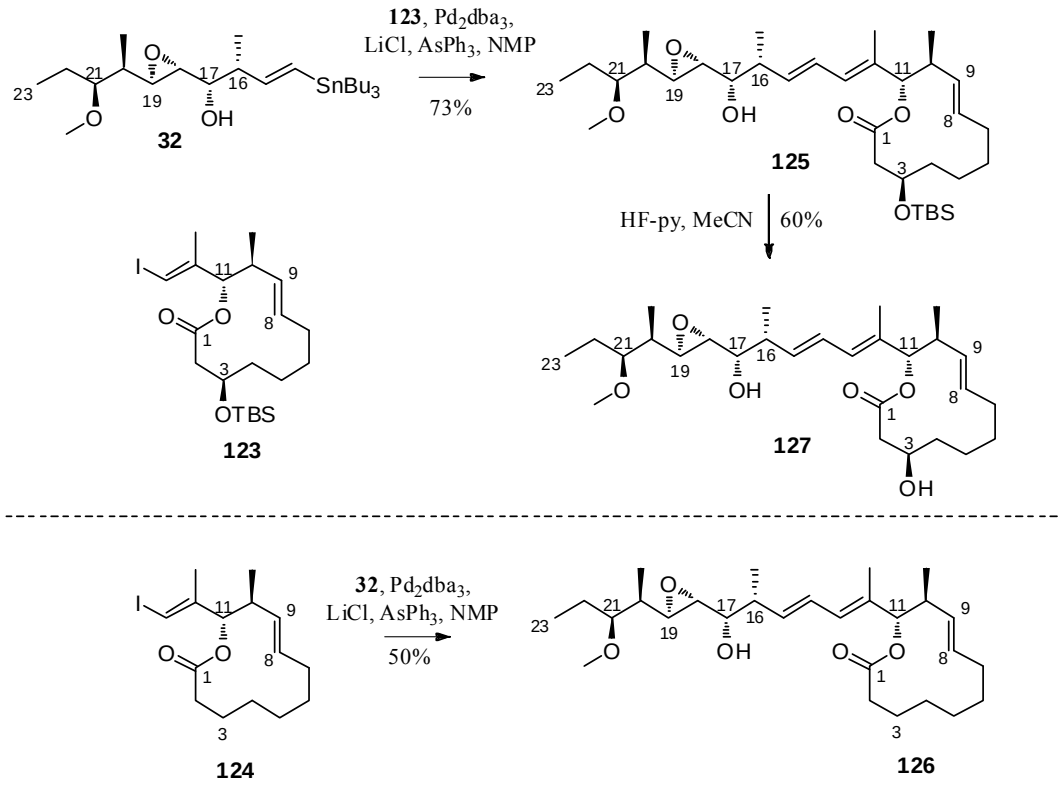

Scheme 1.37 Synthesis of model compounds **125-127**

1.3 Concluding remarks

Two approaches to the C-1 to C-8 acid-olefin fragment **31** as shown in Scheme 1.4 were described. The chiral pool approach was unsuccessful due to difficulties in cleavage of the acetal of intermediate **46** by the methods outlined in Scheme 1.8, and the need for two homologations, which forced the use of excessive protecting group manipulations. The asymmetric dihydroxylation approach was unsuccessful on the few substrates that were tried, but the viability of this approach was later demonstrated by the research published by others on similar fragments.

The synthesis of the sidechain of **1**, stannane fragment **32**, was achieved in an efficient manner without the use of protecting groups (Section 1.2.8). This fragment was then coupled to models of the FD-895 core to evaluate the end-game assembly steps (Section 1.2.9). The success of these studies demonstrates the feasibility of our strategy toward **1**.

Remaining obstacles to the synthesis of **1** are the synthesis of the core component **31** and subsequent assembly of the complete molecule. Modification of the stannane fragment **32** may also be necessary pending future revision of the relative configuration of **1**. Efforts continue in the laboratory to address these issues and complete the synthesis of **1**. This work could provide analogs of **1** unaccessible by fermentation or semisynthetic manipulations, which should be evaluated for antitumor activity in comparison to **1**.

1.4 Acknowledgements

Dr. Alexander Mandel was the first to design and synthesize aldehyde **34** as summarized in Scheme 1.27 - Scheme 1.29, the "keystone" fragment **30** and the first model core compound **124**, and this work is described in *Bioorg Med Chem Lett.*, 17, 18, pp. 5159-5164, 2007. The dissertation author was the second author of this paper. Dr. James La Clair procured the authentic sample of FD-895 (**1**).

1.5 NMR spectra of intermediates compared to authentic FD-895 (1)

This section consists of spectral overlays of selected synthetic intermediates from the sidechain and model studies described in sections 1.2.8 and 1.2.9, with authentic FD-895 (**1**). The region of the spectra chosen for comparison is δ_H 4.5 – 2.7 ppm, which includes the C-17 to C-19 stereotriad, and the C-21 center of **1**.

The experimental methods, characterization data, and full spectra for each of these intermediates are in sections 1.6 and 1.7, respectively. The full ^{1}H spectrum of authentic **1** is shown as Figure 1.6, and assignments were made on the basis of gHMQC, gHMBC, and gCOSY experiments.

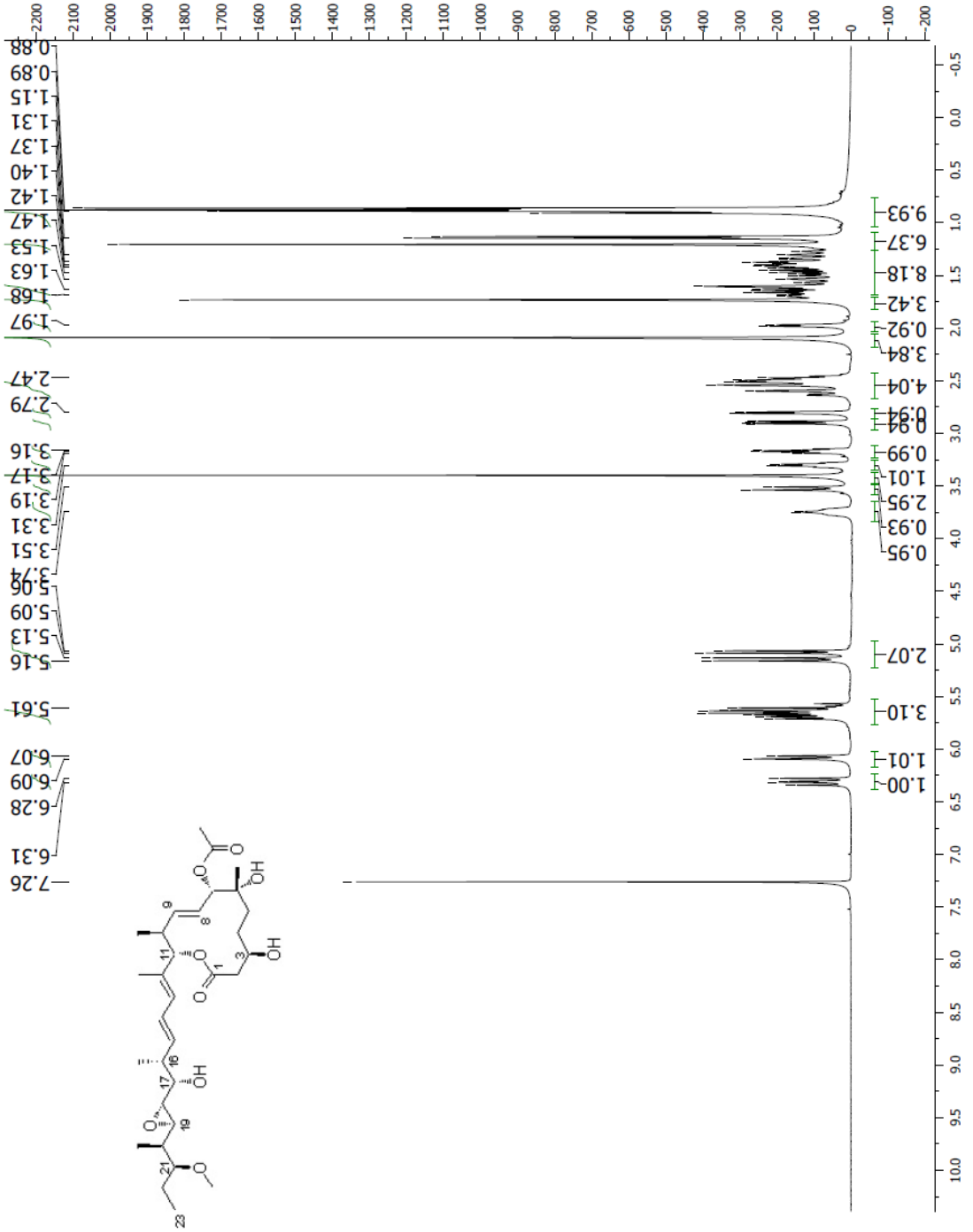

Figure 1.6 ^{1}H NMR ($CDCl_3$, 400 MHz) of compound **1**

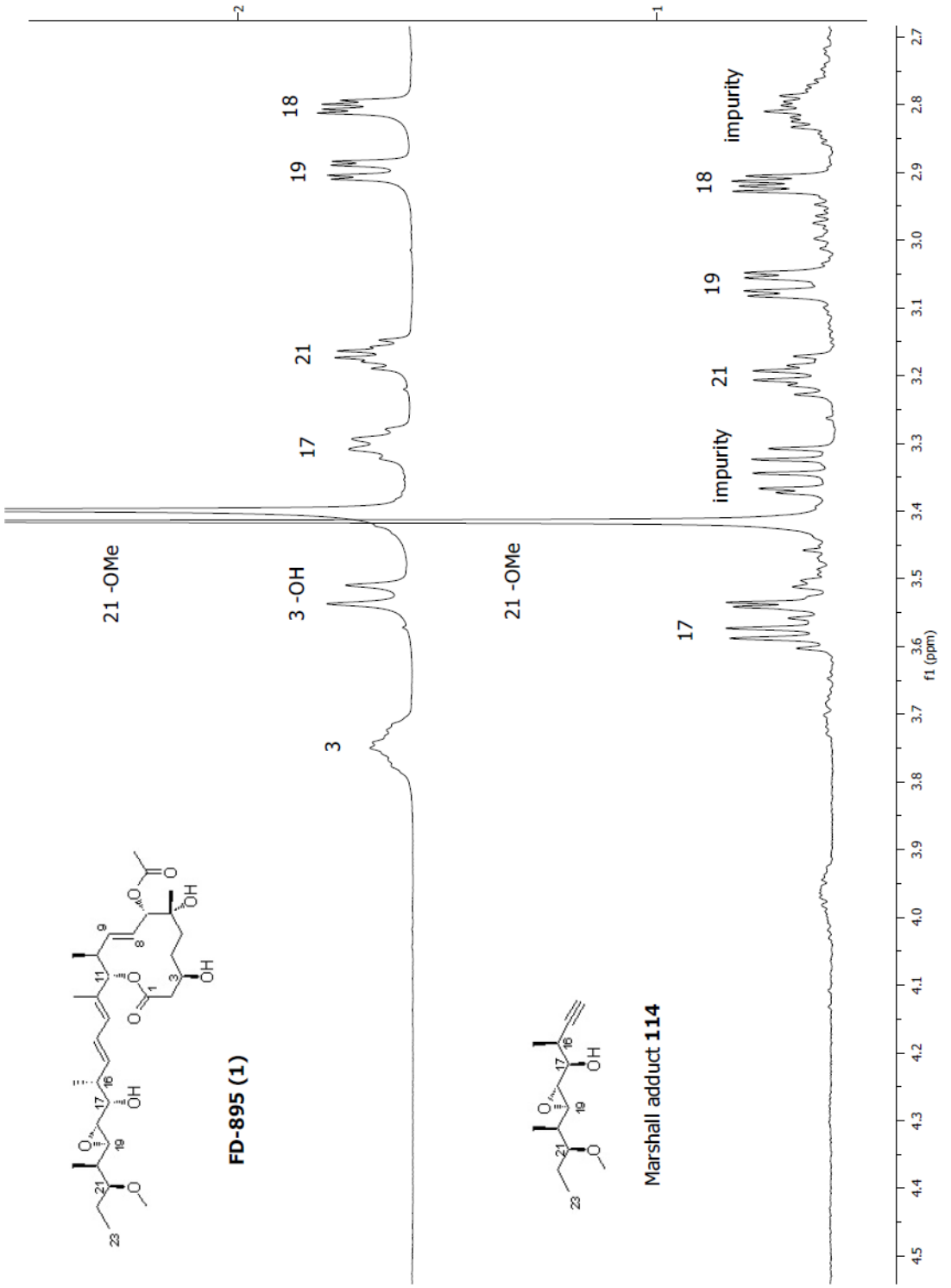

Figure 1.7 Comparison of adduct **114** to **1**

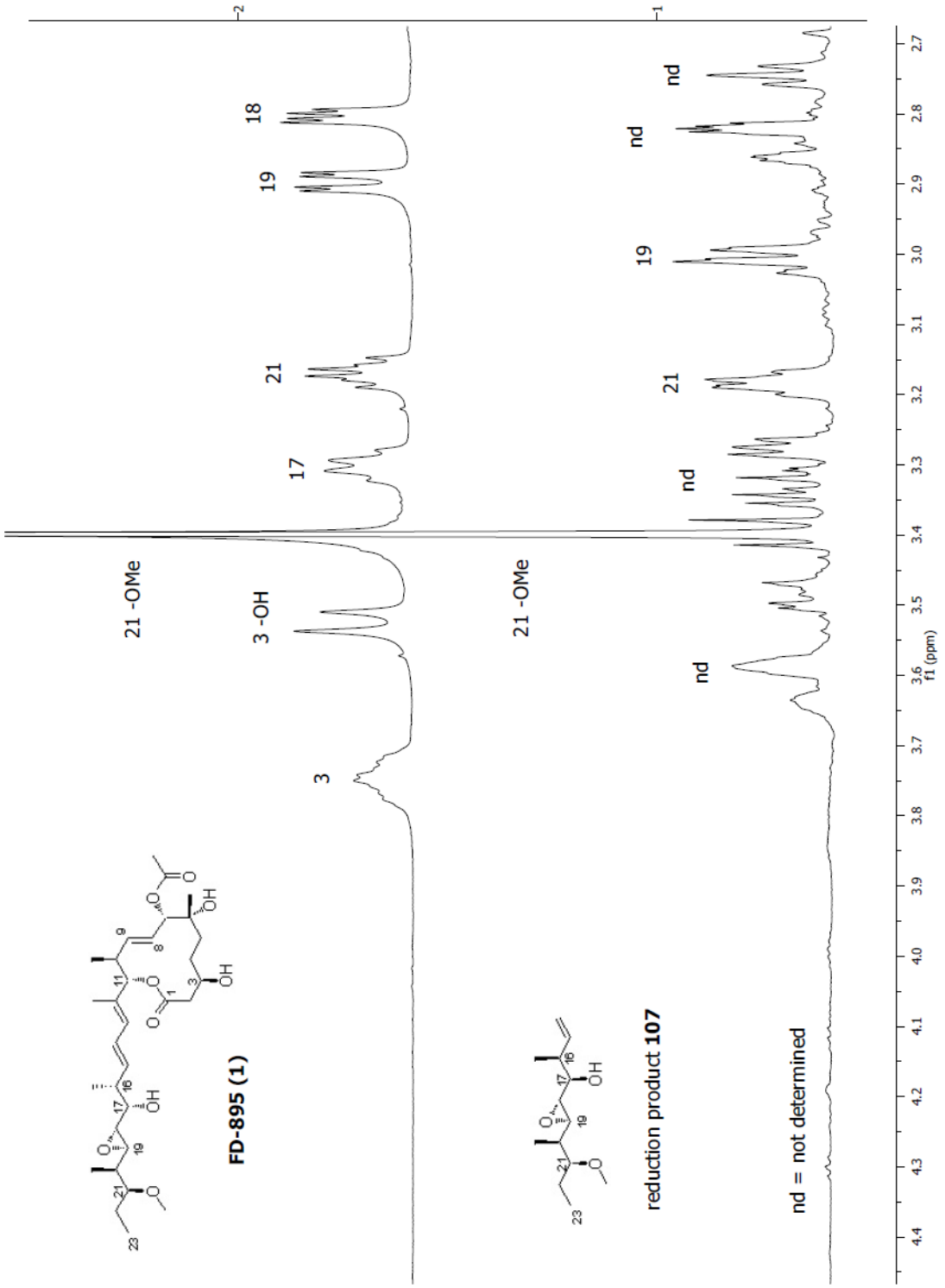

Figure 1.8 Comparison of hydrogenation product **107** to **1**

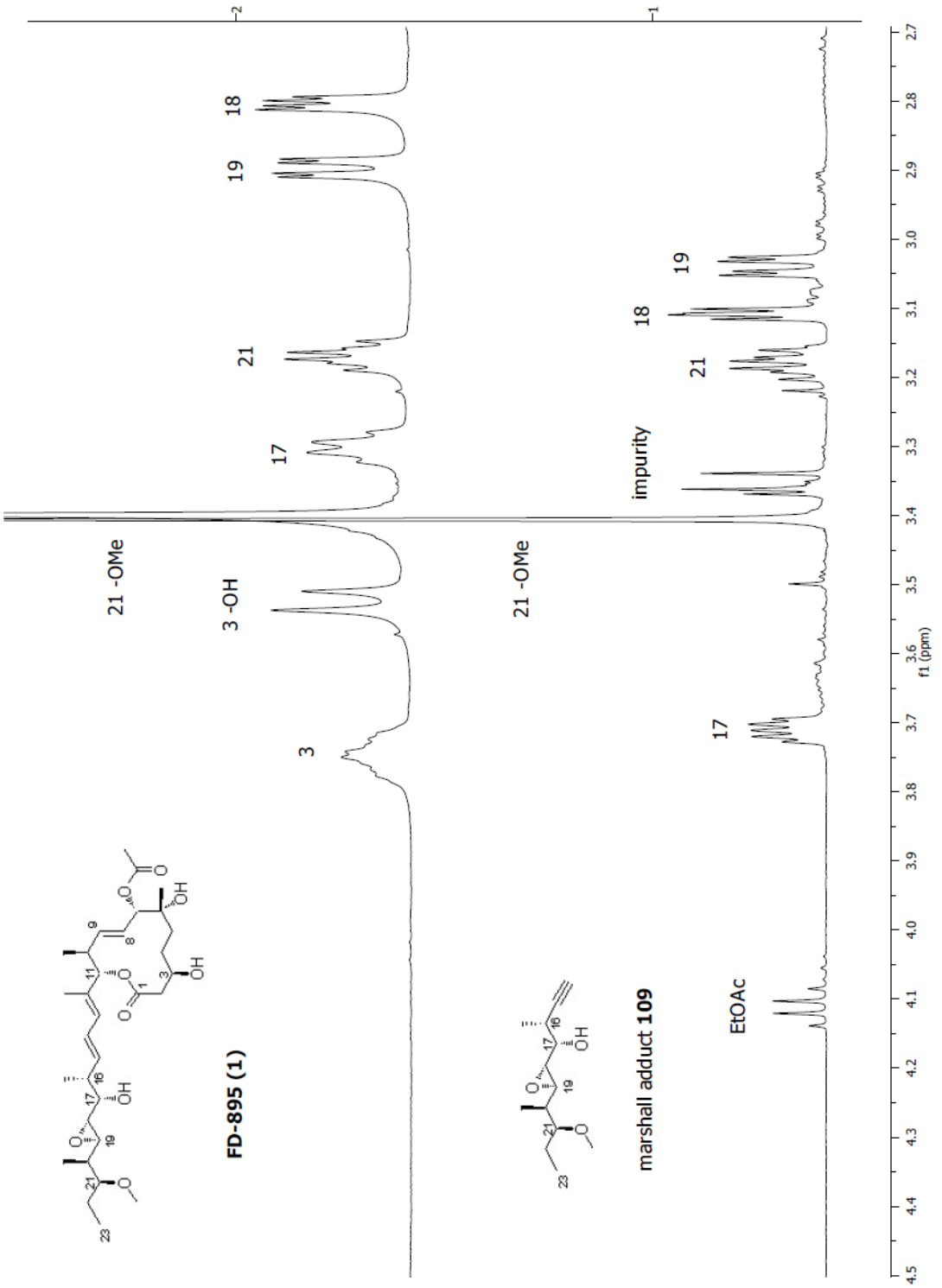

Figure 1.9 Comparison of adduct **109** to **1**

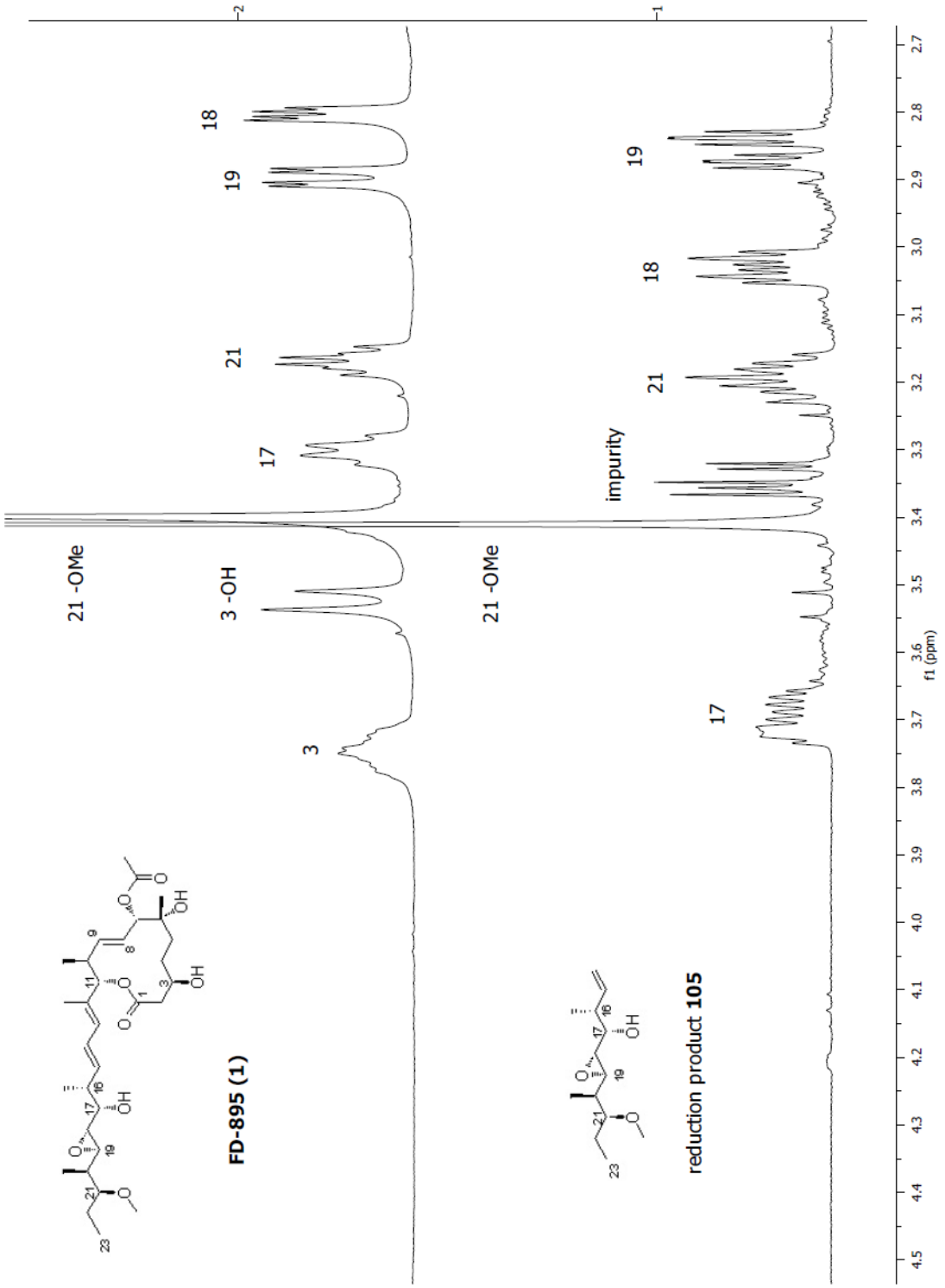

Figure 1.10 Comparison of hydrogenation product **105** to **1**

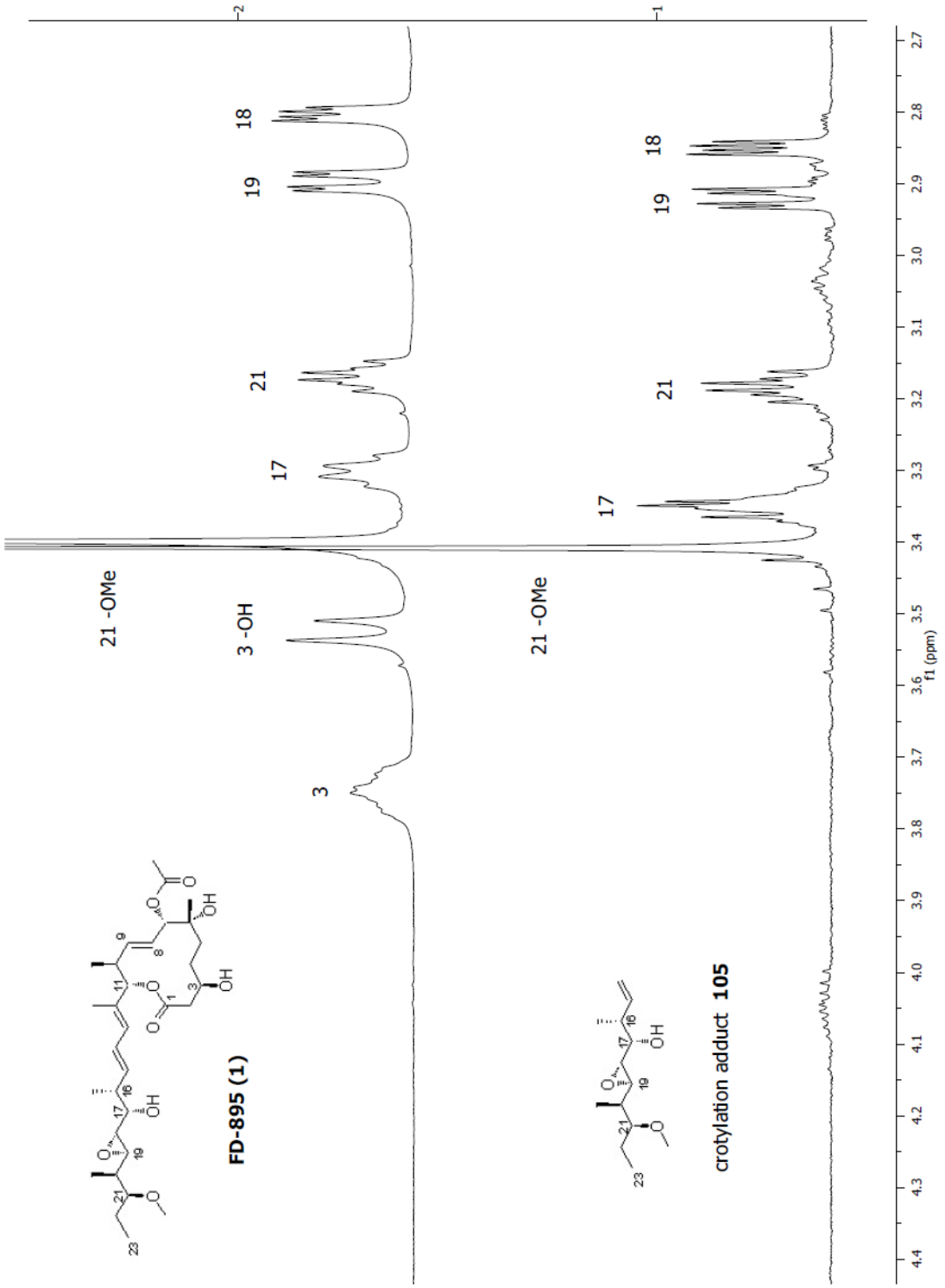

Figure 1.11 Comparison of crotylboration adduct **105** to **1**

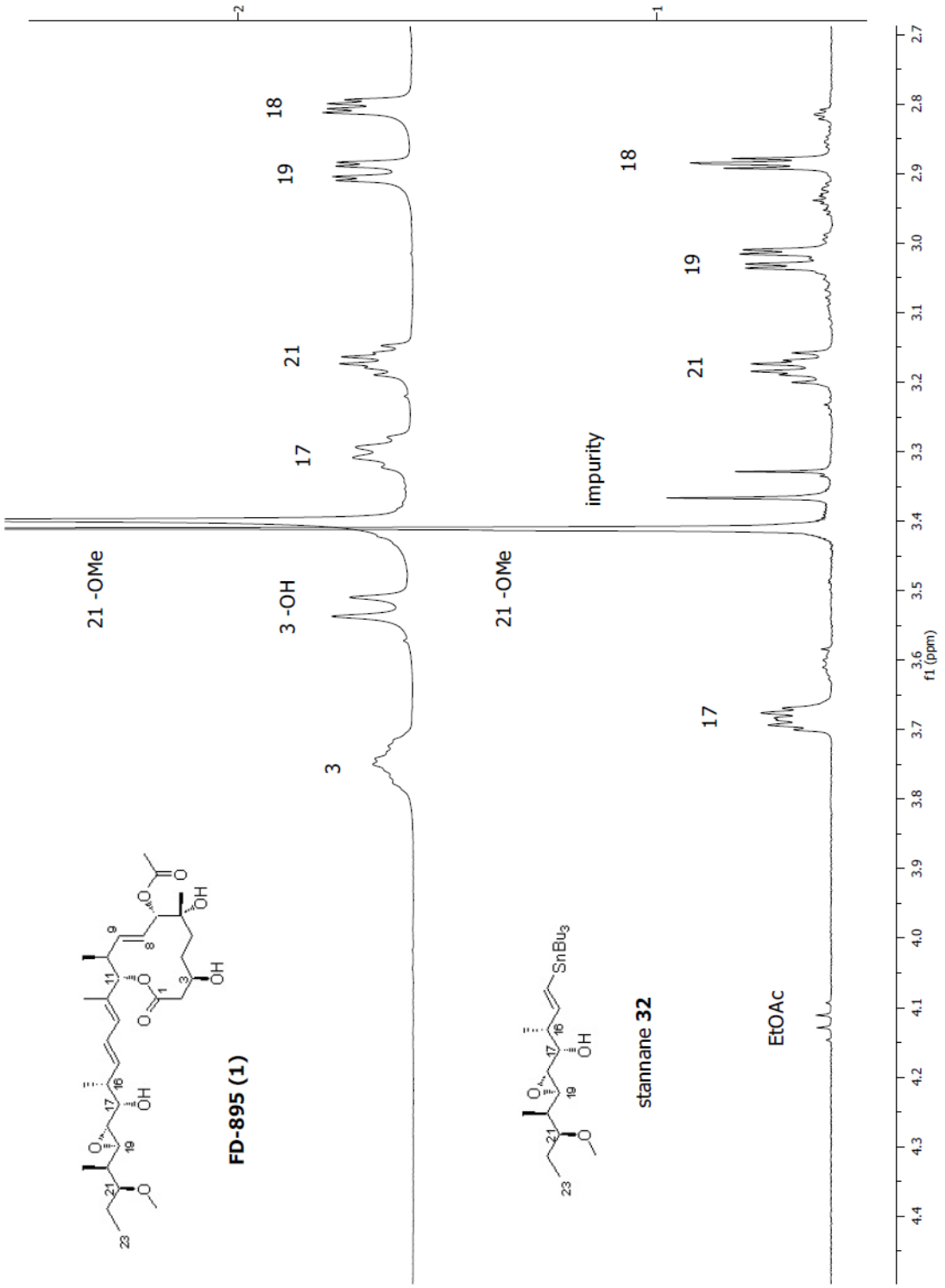

Figure 1.12 Comparison of stannane **32** to **1**

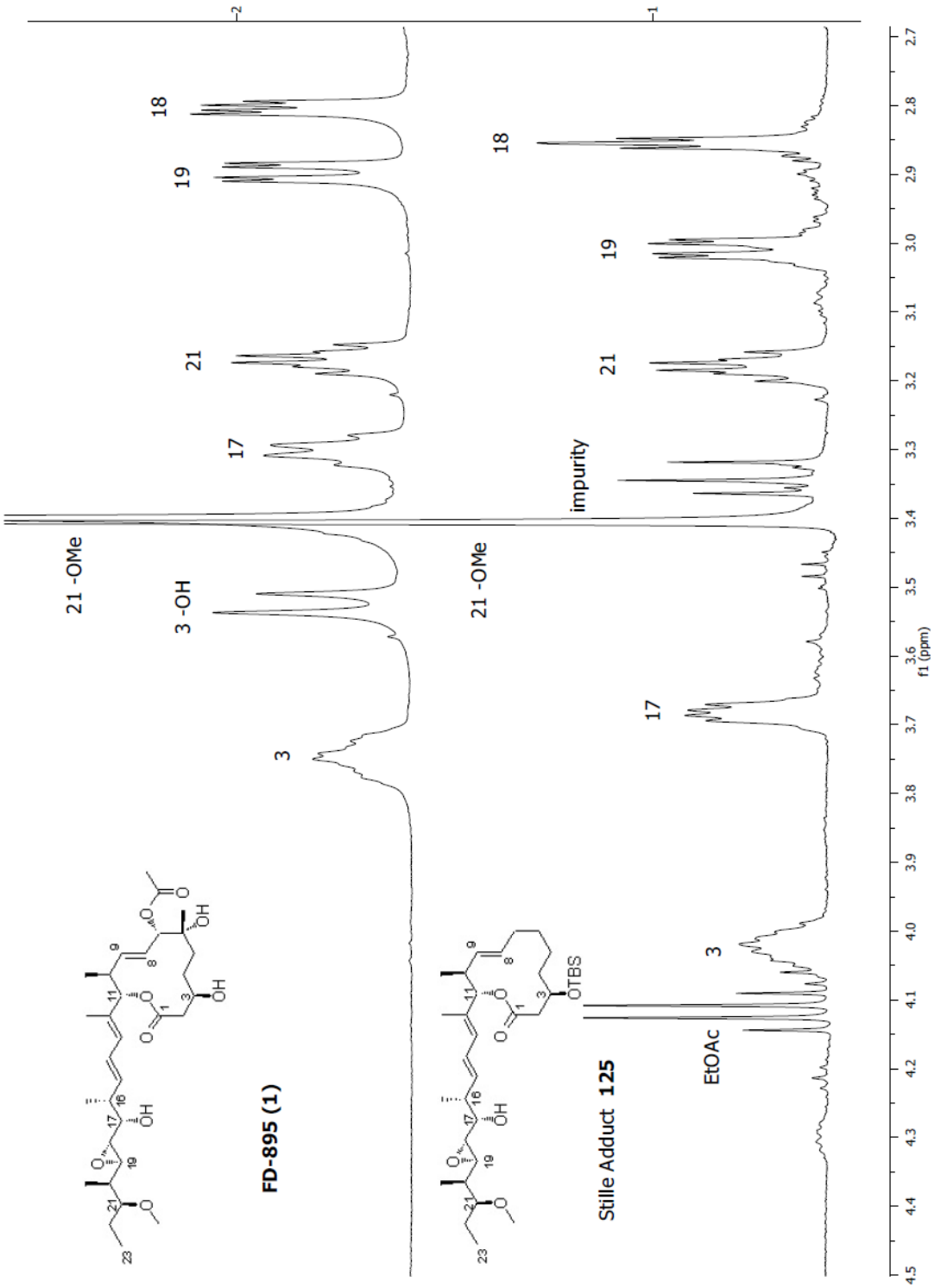

Figure 1.13 Comparison of adduct **125** to **1**

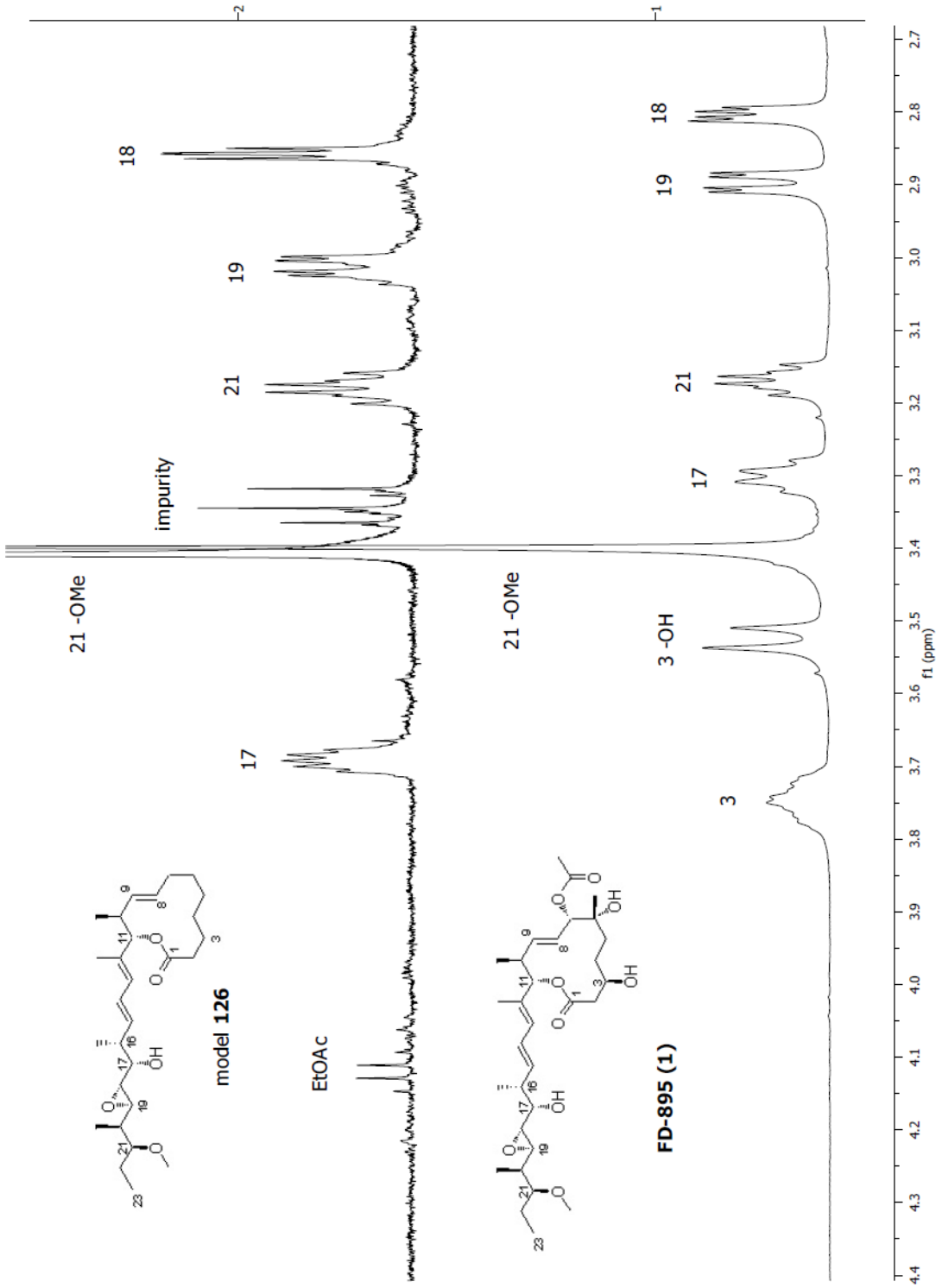

Figure 1.14 Comparison of model **126** to **1**

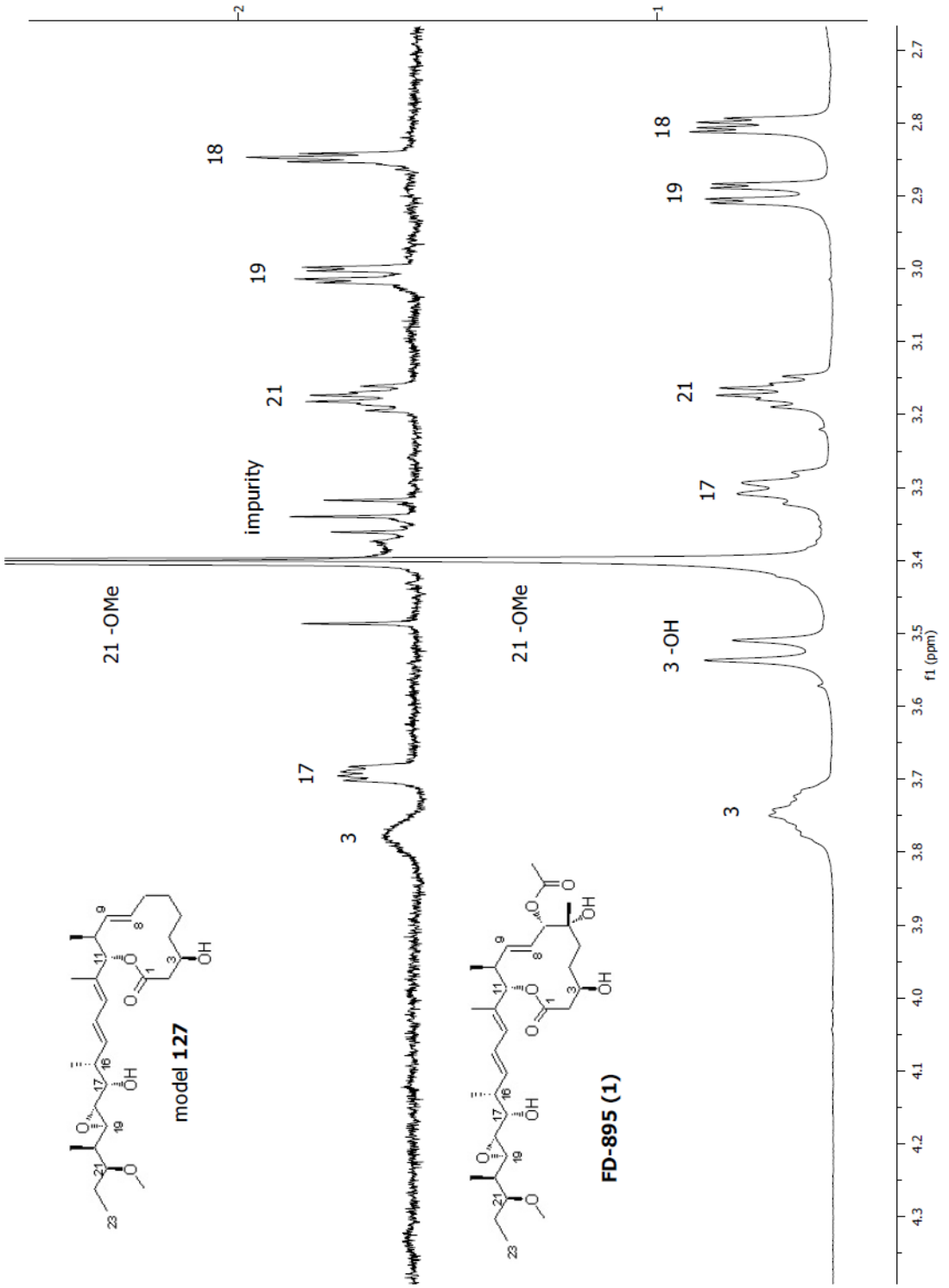

Figure 1.15 Comparison of model **127** to **1**

1.6 Experimental techniques and characterization data

General experimental methods:

Unless otherwise noted, all reagents and chemical compounds were purchased from commercial sources and used without further purification. High purity anhydrous solvents (tetrahydrofuran, dichloromethane, diethyl ether, and toluene) were obtained by passing through a solvent column composed of activated A-1 alumina.[80] Anhydrous *N*,*N*-dimethylformamide was obtained by passage over activated molecular sieves and a subsequent sodium isocyanate column to remove traces of dimethylamine. Triethylamine (Et_3N) was dried over sodium and freshly distilled. Ethyl-*N*,*N*-diisopropylamine (*i*-Pr_2NEt) was distilled from ninhydrin, then from potassium hydroxide. All air or moisture sensitive reactions were performed under positive pressure of dry argon in oven-dried glassware sealed with septa. Reactions were magnetically stirred with Teflon coated stir bars. Flash chromatography was performed on EMD Geduran Silica Gel 60 (40-63 mesh) according to the method of Still.[81] Analytical TLC was performed on Silica Gel 60 F254 pre-coated glass plates. Visualization was achieved with UV light and/or an appropriate stain (I_2 on SiO_2, $KMnO_4$, bromocresol green, dinitrophenylhydrazine, ninhydrin, and ceric ammonium molybdate). Yields and characterization data correspond to isolated, chromatographically and spectroscopically homogeneous materials unless otherwise noted. ^1H NMR spectra were recorded on Varian Mercury 300 MHz or 400 MHz spectrometers, or a Varian Mercury Plus 400 MHz

spectrometer, or on a Varian Unity spectrometer at 500 MHz. ^{13}C NMR spectra were recorded at 100 MHz on either a Varian Mercury or the Mercury Plus instrument, or at 75 MHz on a Varian Mercury spectrometer. Chemical shifts for ^{1}H NMR and ^{13}C NMR analyses were referenced to the reported values of Gottlieb *et. al.*, using the signal from the residual protonated solvent for ^{1}H spectra, or to the ^{13}C signal from the deuterated solvent.[82] Chemical shift δ values for ^{1}H and ^{13}C spectra are reported in parts per million (ppm) relative to these referenced values, and multiplicities are abbreviated as s = singlet, d = doublet, t = triplet, q = quartet, m = multiplet, br = broad. All ^{13}C NMR spectra were recorded with complete proton decoupling. FID files were processed using MestReNova software version 5.3.0-4399. Electrospray (ESI) mass spectrometric analyses were performed using a ThermoFinnigan LCQdeca mass spectrometer, and high resolution analyses were conducted using a ThermoFinnigan MAT900XL mass spectrometer with electron impact (EI) ionization. Optical rotations were measured on a Perkin-Elmer polarimeter (Model 241) using a 1 mL quartz cell with a 10 cm path length.

Stannane 32

A solution of alkyne **109** (28 mg, 0.124 mmol) in 5 mL of THF was added to solid $(PPh_3)_2PdCl_2$ (4 mg, 0.0062 mmol) and the suspension was stirred at room temperature. Stirring continued as Bu_3SnH (42 μL, 0.155 mmol) was added dropwise via syringe. The solution darkened and was stirred for 20 min at room temperature, then concentrated under reduced pressure. The residue was purified by column chromatography (hexanes / ethyl acetate gradient) to provide 19 mg (30%) of stannane

32 as a clear oil, and 13 mg (20%) of a mixture of **32** and unidentified regioisomers. $[\alpha]^{22}_{D}$ +16.4 (*c* 0.077, CH_2Cl_2); ^{1}H NMR ($CDCl_3$, 400 MHz) δ 6.18-5.79 (m, 2H), 3.71-3.65 (m, 1H), 3.41 (s, 3H), 3.22-3.15 (m, 1H), 3.02 (dd, *J* = 2.4, 8.1 Hz, 1H), 2.88 (m, 1H), 2.42-2.31 (m, 1H), 1.87 (d, *J* = 2.3 Hz, 1H), 1.73-1.60 (m, 1H), 1.59-1.37 (m, 7H), 1.36-1.22 (m, 6H), 1.14 (d, *J* = 8 Hz, 3H), 1.00-0.82 (m, 21H); ^{13}C NMR ($CDCl_3$, 100 MHz) δ 149.9, 129.8, 83.9, 71.3, 59.4, 58.3, 57.0, 46.1, 39.0, 29.3, 27.4, 24.0, 16.1, 13.9, 10.8, 10.1, 9.6; ESI-MS *m/z* 541.14 $[M+Na]^+$, 519.02 $[M+H]^+$.

Lactol 38

To the clear oil acetal **46** (60 mg, 0.296 mmol) was added aqueous HCl (4 mL of a 2N solution, 9 mmol), and the stirred solution was heated to 80 °C for 12 hours. After this time period, the reaction mixture was cooled to room temperature and quenched with saturated aqueous $NaHCO_3$ solution. The quenched solution was concentrated under reduced pressure, and the residue was triturated several times with EtOAc. The EtOAc was filtered and concentrated under reduced pressure, and the residue was purified by column chromatography to afford the lactol **38** (15 mg, 31%) as a clear oil. TLC (EtOAc): R_f = 0.03; ^{1}H NMR (D_2O, 400 MHz) δ 4.61 (br, 1H), 3.96 (d, *J* = 7.5 Hz, 1H), 3.75 (t, *J* = 5.5 Hz, 1H), 3.64-3.50 (m, 1H), 2.07-1.46 (m, 4H), 1.11 (s, 3H).

Diol 39

A solution of enone **40** (1.88 g, 8.24 mmol) in 75 mL Et_2O was stirred, and cooled to -78 °C. Stirring continued as MeLi (25.7 mL of a 1.6 M solution in Et_2O,

41.2 mmol) was added slowly via syringe. The solution continued to stir, and was allowed to slowly warm to room temperature over 12 h. The reaction mixture was then cooled to 0 °C and quenched with MeOH, then saturated NH_4Cl. The mixture was diluted with H_2O and ethyl acetate, and the layers were separated. The aqueous layer was extracted with ethyl acetate (2x), and the combined organic layers were washed with brine and dried over Na_2SO_4. The solution was filtered and concentrated under reduced pressure, and the residue was purified by column chromatography (5:1 to 1:1 hexanes / ethyl acetate gradient) to provide 0.95 g (57%) of diol **39** as a colorless oil. TLC (1:1 hexanes / ethyl acetate): R_f = 0.1; ^{1}H NMR ($CDCl_3$, 400 MHz) δ 5.78 (dt, *J* = 10.3, 2.1 Hz, 1H), 5.57 (dd, *J* = 10.5, 1.7 Hz, 1H), 4.76 (s, 1H), 4.26-4.22 (m, 1H), 4.00 (septet, *J* = 6.2 Hz, 1H), 3.72 (dd, *J* = 3.1, 11.4 Hz, 1H), 3.58 (dd, *J* = 6.4, 11.4 Hz, 1H), 1.32 (s, 3H), 1.25 (d, *J* = 6.2 Hz, 3H), 1.21 (d, *J* = 6.2 Hz, 3H); ^{13}C NMR ($CDCl_3$, 100 MHz) δ 133.0, 124.3, 100.1, 70.8, 69.7, 67.1, 65.1, 26.1, 23.5, 22.0; ESI-MS *m/z* 225.01 $[M+Na]^+$, 219.86 $[M+NH_4]^+$.

Acetal 46

To a solution of diol **39** (950 mg, 4.7 mmol) in 10 mL of MeOH was added 5% Pd on carbon (400 mg, 0.188 mmol), and the mixture was stirred at room temperature. A balloon of H_2 was attached to a 6" needle, the tip of which was submerged below the solution surface. A vent needle was inserted through the septum, so that the H_2 gas bubbled through the solution. Three repetitions with fresh balloons of H_2 were conducted, and then the reaction mixture was filtered through celite, which was washed with EtOAc. The filtrate was concentrated under reduced pressure, and the

residue was filtered through a short silica gel plug with ethyl acetate to provide 0.86 g (90%) of acetal **46** as a colorless oil. ^{1}H NMR ($CDCl_3$, 400 MHz) δ 4.47 (s, 1H), 3.91 (septet, *J* = 6.2 Hz, 1H), 3.83 (m, 1H), 3.58 (dd, *J* = 11.6, 3.1 Hz, 1H), 3.48 (dd, *J* = 11.5, 6.6 Hz, 1H), 3.43 (s, 1H), 1.88-1.77 (m, 1H), 1.66-1.58 (m, 1H), 1.52-1.44 (m, 2H), 1.24 (s, 3H), 1.22 (d, *J* = 6.2 Hz, 3H), 1.15 (d, *J* = 6.2 Hz, 3H); ^{13}C NMR ($CDCl_3$, 100 MHz) δ 100.5, 69.8, 69.0, 68.6, 65.6, 32.8, 25.5, 23.6, 22.8, 21.9; ESI-MS *m/z* 227.02 $[M+Na]^+$, 221.89 $[M+NH_4]^+$, 204.84 $[M+H]^+$; HR-EI-MS: *m/z* calcd. for $C_{10}H_{20}O_4$ $[M]^+$: 204.1356, found 204.1354.

Trimercaptan 51

Acetal **46** (96 mg, 0.471 mmol) was dissolved in 700 μL EtSH (9.42 mmol), and the stirred solution was cooled to -15 °C in an ethylene glycol / CO_2 bath. Solid $ZnCl_2$ (385 mg, 2.82 mmol) was added to the cooled solution in one portion, and the suspension was stirred at -15 °C for 30 min, then at 0 °C for an additional 15 min. The EtSH was removed under high vacuum, and a saturated solution of $NaHCO_3$ (10 mL) was poured onto the residue, causing the precipitation of insoluble zinc salts. EtOAc (20 mL) was added to the suspension, and the biphasic mixture was filtered through celite, which was washed with additional ethyl acetate. The layers of the filtrate were separated, and the aqueous layer was extracted with ethyl acetate (3 x 10 mL). The combined organic layers were dried over Na_2SO_4, filtered and concentrated under reduced pressure. The residue was purified by column chromatography (10:1 to 1:1 hexanes / ethyl acetate gradient) to provide 59 mg (40%) of trimercaptan **51** as a colorless oil. TLC (1:1 hexanes / ethyl acetate): R_f = 0.1; ^{1}H NMR ($CDCl_3$, 400 MHz)

δ 3.83 (s, 1H), 3.71-3.64 (m, 1H), 3.68-3.62 (m, 1H), 3.46 (dd, *J* = 11.4, 3.7 Hz, 1H), 2.82-2.65 (m, 4H), 2.64-2.50 (m, 2H), 2.58-2.44 (br, 2H), 2.02-1.91 (m, 1H), 1.88-1.77 (m, 1H), 1.68-1.51 (m, 2H), 1.40 (s, 3H), 1.26 (t, *J* = 7.4 Hz, 3H), 1.26 (t, *J* = 7.4 Hz, 3H), 1.19 (t, *J* = 7.5 Hz, 3H); ^{13}C NMR ($CDCl_3$, 100 MHz) δ 72.6, 66.8, 63.9, 55.3, 34.8, 28.2, 28.2, 27.7, 24.4, 23.1, 14.5, 14.0.

Acetonide 53

Trimercaptan **51** (47 mg, 0.175 mmol) was dissolved in 2,2-dimethoxypropane (430 μL, 3.5 mmol), and to the stirring solution was added (±)-10-camphorsulfonic acid (6 mg, 0.0027 mmol). After the solution had stirred for 12 h at room temperature, a saturated aqueous solution of $NaHCO_3$ (10 mL) and EtOAc (10 mL) were added, and the layers were separated. The aqueous layer was extracted with additional EtOAc (2 x 5 mL), and the combined organic layers were washed with brine, dried over Na_2SO_4, filtered and concentrated under reduced pressure. Column chromatography (1:1 hexanes / ethyl acetate) provided acetonide **53** (37 mg, 67%) as a clear oil. ^{1}H NMR ($CDCl_3$, 300 MHz) δ 4.15-4.00 (m, 1H), 4.11-4.01 (m, 1H), 3.84 (s, 1H), 3.63-3.50 (m, 1H), 2.87-2.65 (m, 4H), 2.66-2.49 (m, 2H), 2.01-1.57 (m, 4H), 1.41 (s, 6H), 1.35 (s, 3H), 1.28 (t, *J* = 9.9 Hz, 3H), 1.27 (t, *J* = 9.9 Hz, 3H), 1.21 (t, *J* = 9.9 Hz, 3H); ^{13}C NMR ($CDCl_3$, 75 MHz) δ 108.9, 76.2, 69.5, 63.7, 55.3, 34.7, 28.2, 27.8, 27.1, 25.8, 24.3, 23.0, 14.6, 13.9; ESI-MS *m/z* 290.82 $[M\text{-}EtS]^+$; HR-EI-MS: *m/z* calcd. for $C_{16}H_{32}O_2S_3$ $[M]^+$: 352.1559, found 352.1563.

Silyl ether 54

To a solution of acetal **46** (75 mg, 0.369 mmol) in CH_2Cl_2 (5 mL) was added pyridine (33 μL, 0.41 mmol) and 4-dimethylaminopyridine (2 mg, 0.016 mmol), and the solution was stirred at room temperature. To this solution was added TBDPSCl (106 μL, 0.41 mmol) via syringe, and the reaction mixture was stirred for 24 h, after which it was diluted with CH_2Cl_2 (15 mL), and washed sequentially with 2% HCl, deionized H_2O, sat'd aqueous $NaHCO_3$, and brine. The organic layer was dried over Na_2SO_4, filtered, and concentrated under reduced pressure. Column chromatography (10:1 to 4:1 hexanes / ethyl acetate) provided silyl ether **54** (164 mg, 99%) as a clear oil. TLC (1:1 hexanes / ethyl acetate): R_f = 0.6; ^{1}H NMR ($CDCl_3$, 400 MHz) δ 7.70-7.65 (m, 4H), 7.45-7.34 (m, 6H), 4.49 (s, 1H), 3.94 (septet, *J* = 6.2 Hz, 1H), 3.89-3.80 (m, 1H), 3.66 (dd, *J* = 10.5, 5.7 Hz, 1H), 3.58 (dd, *J* = 10.5, 4.8 Hz, 1H), 1.82 (td, *J* = 13.0, 4.5 Hz), 1.68-1.39 (m, 3H), 1.27 (s, 3H), 1.22 (d, *J* = 6.2 Hz, 3H), 1.17 (d, *J* = 6.2 Hz, 3H), 1.05 (s, 9H).

Benzyl ether 55

To a solution of silyl ether **54** (118 mg, 0.267 mmol) in THF (500 μL) was added NaH (60% dispersion in oil, 11 mg, 0.28 mmol) and n-Bu_4NI (1 mg, 0.0027 mmol), and the solution was stirred at room temperature. To this solution was added BnBr (33 μL, 0.28 mmol), and the solution was stirred for 3 hours. At this time, TLC analysis indicated the presence of starting material, so an additional 5 mg of the catalyst n-Bu_4NI was added to the solution, which was allowed to stir for an additional 12 hours. The reaction mixture was then diluted with H_2O and ethyl acetate and the layers were separated. The aqueous layer was extracted with additional ethyl acetate,

and the combined organic layers were washed with brine, dried over Na_2SO_4, filtered and concentrated under reduced pressure. The residue was purified by column chromatography (10:1 hexanes / ethyl acetate) to provide the starting material silyl ether **54** (69 mg) and benzyl ether **55** (68 mg, > 100% BORSM) which was contaminated with oil from the sodium hydride dispersion and the benzyl bromide reagent. TLC (10:1 hexanes / ethyl acetate): R_f = 0.5; ^{1}H NMR ($CDCl_3$, 500 MHz) δ 7.74-7.67 (m, 4H), 7.46-7.28 (m, 11H), 4.78 (s, 1H), 4.59 (d, *J* = 11.1 Hz, 1H), 4.51 (d, *J* = 11.1 Hz, 1H), 3.99 (septet, *J* = 6.2 Hz, 1H), 3.96-3.90 (m, 1H), 3.69 (dd, *J* = 10.5, 5.7 Hz, 1H), 3.60 (dd, *J* = 10.5, 4.7 Hz, 1H), 2.12 (td, *J* = 13.1, 5.1 Hz, 1H), 1.66-1.49 (m, 3H), 1.38 (s, 3H), 1.26 (d, *J* = 6.2 Hz, 3H), 1.20 (d, *J* = 6.2 Hz, 3H), 1.06 (s, 9H).

Tribenzoate 57

To a solution of benzoic anhydride (1.29 g, 5.7 mmol) in CH_2Cl_2 (5 mL) was added $MgBr_2$ (1.06 g, 5.7 mmol) and Et_3N (1.4 mL, 10 mmol). To this stirring suspension was added a solution of acetal **46** (292 mg, 1.43 mmol) in CH_2Cl_2 (5 mL), and the reaction was stirred at room temperature and monitored by TLC. Once the majority of the starting material had been consumed, the reaction mixture was diluted with CH_2Cl_2 and H_2O, and the layers were separated. The aqueous layer was extracted with additional CH_2Cl_2, and the combined organic layers were washed with brine, dried over Na_2SO_4, filtered, and concentrated under reduced pressure. Column chromatography (hexanes / ethyl acetate gradient) provided the starting material acetal **46** (53 mg) and tribenzoate **57** (186 mg, 33% BORSM). ^{1}H NMR ($CDCl_3$, 400 MHz)

δ 8.20-8.14 (m, 4H), 8.06-8.01 (m, 2H), 7.72-7.65 (m, 2H), 7.58-7.50 (m, 5H), 7.47-7.40 (m, 2H), 5.87 (s, 1H), 4.57-4.51 (m, 1H), 3.89 (dd, *J* = 7.1, 0.5 Hz), 3.85-3.80 (m, 1H), 2.27-2.08 (m, 2H), 1.89-1.78 (m, 1H), 1.57 (s, 3H), 1.52-1.43 (m, 1H); ^{13}C NMR ($CDCl_3$, 100 MHz) δ 165.8, 162.5, 134.7, 132.9, 130.7, 129.8, 129.0, 129.0, 128.4, 102.4, 80.1, 73.0, 67.6, 28.0, 25.7, 21.6.

O-benzyl oxime 60

To a solution of the lactol **38** (64 mg, 0.395 mmol) in pyridine (1 mL) was added $BnONH_2$*HCl (95 mg, 0.593 mmol) as a solid, and the solution was stirred for 12 h at room temperature. After this time period, the pyridine was evaporated under reduced pressure, and the residue was purified by column chromatography (100% ethyl acetate) to afford the O-benzyl oxime **60** (76 mg, 72%) as a clear oil. TLC (ethyl acetate): R_f = 0.2; ^{1}H NMR ($CDCl_3$, 400 MHz) δ 7.44 (s, 1H), 7.39-7.31 (m, 5H), 5.08 (s, 2H), 3.71-3.62 (m, 1H), 3.63-3.56 (m, 1H), 3.44-3.35 (m, 1H), 3.23 (br, 1H), 2.62 (d, *J* = 4.1 Hz, 1H), 1.92-1.66 (m, 3H), 1.52-1.43 (m, 2H), 1.35 (s, 3H); ^{13}C NMR ($CDCl_3$, 100 MHz) δ 154.6, 137.3, 128.6, 128.5, 128.2, 76.4, 72.3, 72.1, 66.9, 36.7, 27.3, 27.2.

O-methyl oxime 61

To a solution of the lactol **38** (20 mg, 0.123 mmol) in pyridine (600 μL) was added $MeONH_2$*HCl (12 mg, 0.147 mmol) as a solid, and the solution was stirred for 12 h at room temperature. After this time period, the pyridine was evaporated under reduced pressure, and the residue was purified by column chromatography (100%

ethyl acetate) to afford the O-methyl oxime **61** (12 mg, 50%) as a clear oil. TLC (ethyl acetate): R_f = 0.1; ^{1}H NMR ($CDCl_3$, 400 MHz) δ 7.37 (s, 1H), 3.84 (s, 3H), 3.74-3.66 (m, 1H), 3.63 (dd, *J* = 11.1, 3.1 Hz, 1H), 3.45 (dd, *J* = 11.1, 7.2 Hz, 1H), 3.06 (br, 3H), 1.87-1.67 (m, 2H), 1.60-1.49 (m, 2H), 1.35 (s, 3H); ^{13}C NMR ($CDCl_3$, 100 MHz) δ 154.1, 72.3, 72.0, 66.8, 62.0, 36.8, 27.2, 27.2; ESI-MS *m/z* 214.02 $[M+Na]^+$, 191.70 $[M+H]^+$; HR-FAB-MS *m/z* calcd. for $C_8H_{18}O_4N_1$ $[M+H]^+$: 192.1230, found 192.1234.

Acetonide 62

The O-benzyl oxime **60** (15 mg, 0.0561 mmol) was dissolved in 2,2-dimethoxypropane (2 mL) and the solution was stirred at room temperature. A catalytic amount of (±)-10-camphorsulfonic acid was added in one portion, and the solution was stirred for 12 h. After this time period, a few drops of Et_3N were added, and the solution was concentrated. The residue was purified by column chromatography to provide the acetonide **62** (6 mg, 35%). ^{1}H NMR ($CDCl_3$, 400 MHz) δ 7.44 (s, 1H), 7.39-7.28 (m, 5H), 5.08 (s, 2H), 4.11-3.97 (m, 1H), 4.02 (dd, *J* = 13.4, 6.0 Hz, 1H), 3.53-3.44 (m, 1H), 3.09 (s, 1H), 1.83-1.73 (m, 1H), 1.72-1.60 (m, 2H), 1.56-1.47 (m, 1H), 1.39 (s, 3H), 1.34 (s, 3H), 1.34 (s, 3H); ^{13}C NMR ($CDCl_3$, 100 MHz) δ 154.6, 128.6, 128.5, 128.2, 109.1, 76.4, 76.1, 71.8, 69.5, 37.0, 27.8, 27.1, 27.0, 25.8.

Acetonide 63

To a solution of the lactol **38** (15 mg, 0.0926 mmol) in pyridine (440 μL, 5.4 mmol) was added $MeONH_2$*HCl (9 mg, 0.111 mmol) in one portion. The solution was stirred for 12 h at room temperature, and then concentrated under reduced pressure. The residue was dissolved in 2,2-dimethoxypropane, and (±)-10-camphorsulfonic acid (4 mg, 0.018 mmol) was added. This solution was stirred for 12 h, and then quenched with a few drops of Et_3N. The solution was concentrated under reduced pressure, and the residue was purified by column chromatography (100% ethyl acetate) to provide the acetonide **63** (13 mg, 62% over 2 steps) as a clear oil. ^1H NMR ($CDCl_3$, 400 MHz) δ 7.37 (s, 1H), 4.13-4.02 (m, 1H), 4.08-4.01 (m, 1H), 3.84 (s, 3H), 3.56-3.47 (m, 1H), 1.83-1.66 (m, 2H), 1.66-1.53 (m, 2H), 1.41 (s, 3H), 1.34 (s, 3H), 1.34 (s, 3H); ^{13}C NMR ($CDCl_3$, 100 MHz) δ 154.0, 109.1, 76.1, 71.7, 69.5, 62.0, 37.0, 27.8, 27.0, 25.8; ESI-MS *m/z* 254.06 $[M+Na]^+$; HR-EI-MS *m/z* calcd. for $C_{11}H_{21}O_4N_1$ $[M]^+$: 231.1465, found 231.1470.

Silyl ether 64

To a solution of acetonide **62** (6 mg, 0.0195 mmol) in CH_2Cl_2 was added Et_3N (15 μL, 0.098 mmol) via syringe, and the solution was stirred and cooled to 0 °C. To the cooled solution was added TESOTf (11 μL, 0.049 mmol) via syringe, and the solution was allowed to warm to room temperature, and stirred for 12 h. After this time period, the reaction mixture was diluted with saturated aqueous $NaHCO_3$ and CH_2Cl_2, and the layers were separated. The aqueous layer was extracted with additional CH_2Cl_2, and the combined organic layers were washed with brine, dried

over Na_2SO_4, filtered and concentrated under reduced pressure. The residue was purified by column chromatography (20:1 to 10:1 hexanes / ethyl acetate gradient) to provide the silyl ether **64** (6 mg, 75%) as a colorless oil. ^{1}H NMR ($CDCl_3$, 400 MHz) δ 7.41-7.27 (m, 6H), 5.05 (s, 2H), 4.08-3.97 (m, 2H), 3.61-3.33 (m, 1H), 1.80-1.60 (m, 2H), 1.61-1.44 (m, 2H), 1.40 (s, 3H), 1.35 (s, 3H), 1.35 (s, 3H), 0.96 (t, *J* = 7.9 Hz, 3H), 0.90 (t, *J* = 7.8 Hz, 6H), 0.61 (q, *J* = 7.9 Hz, 2H), 0.52 (q, *J* = 8.0 Hz, 4H); ^{13}C NMR ($CDCl_3$, 100 MHz) δ 155.3, 128.5, 128.5, 128.0, 108.9, 76.3, 76.0, 74.1, 72.2, 69.6, 67.0, 38.6, 28.0, 27.1, 25.9, 25.6, 7.1, 6.6, 4.5.

Bis TBS ether 65

DMF (50 μL) was added to a mixture of O-methyl oxime **61** (11 mg, 0.060 mmol) and imidazole (20 mg, 0.30 mmol), and the solution was stirred at room temperature. To this solution was quickly added TBSCl (22 mg, 0.144 mmol) in one portion. The solution was stirred at room temperature for 2 days, and then the reaction mixture was partitioned between hexanes / Et_2O (1:1) and H_2O. The layers were separated, and the aqueous layer was extracted with an additional portion of hexanes / Et_2O. The combined organic layers were washed with brine, dried over Na_2SO_4, filtered and concentrated under reduced pressure. The residue was purified by column chromatography (10:1 to 1:1 hexanes / ethyl acetate gradient) to provide the bis-TBS ether **65** (9 mg, 36%) as a colorless oil. ^{1}H NMR ($CDCl_3$, 400 MHz) δ 7.36 (s, 1H), 3.84 (s, 3H), 3.73-3.65 (m, 1H), 3.52 (dd, *J* = 10.0, 5.5 Hz, 1H), 3.41 (dd, *J* = 10.0, 6.7 Hz, 1H), 1.80-1.45 (m, 4H), 1.33 (s, 3H), 0.89 (s, 9H), 0.88 (s, 9H), 0.06 (s, 6H), 0.05 (s, 3H), 0.04 (s, 3H); ^{13}C NMR ($CDCl_3$, 100 MHz) δ 154.1, 79.2, 73.0, 67.0, 61.9,

36.1, 28.2, 26.8, 26.2, 26.2, 18.4, -4.0, -4.4, -5.0; ESI-MS *m/z* 442.15 $[M+Na]^+$, 419.94 $[M+H]^+$, 402.03 $[M-H_2O+H]^+$.

BOM ether 66

To a solution of bis-TBS ether **65** (3 mg, 0.007 mmol) in THF (200 μL) was added a single crystal of n-Bu_4NI, and iPr_2NEt (5 μL, 0.021 mmol) via syringe. The solution was stirred as BOMCl (2 μL, 0.014 mmol) was added via syringe, and the reaction was stirred for 12 h at room temperature. The reaction mixture was applied directly to a preparatory TLC plate, which was eluted with 9:1 hexanes / ethyl acetate to provide the BOM ether **66** (3 mg, 100%) as a colorless oil. TLC (9:1 hexanes / ethyl acetate): R_f = 0.2; ^1H NMR ($CDCl_3$, 400 MHz) δ 7.39-7.29 (m, 6H), 4.79 (s, 2H), 4.63 (d, *J* = 11.8 Hz, 1H), 4.59 (d, *J* = 11.8 Hz, 1H), 3.83 (s, 3H), 3.70-3.62 (m, 1H), 3.52 (dd, *J* = 10.0, 5.5 Hz, 1H), 3.40 (dd, *J* = 10.0, 6.5 Hz, 1H), 1.86-1.58 (m, 3H), 1.50-1.36 (m, 1H), 1.39 (s, 3H), 0.89 (s, 9H), 0.88 (s, 9H), 0.06 (s, 3H), 0.06 (s, 3H), 0.04 (s, 3H), 0.04 (s, 3H); ^{13}C NMR ($CDCl_3$, 100 MHz) δ 153.4, 128.4, 127.9, 127.6, 89.8, 76.6, 73.2, 69.6, 67.3, 35.0, 28.2, 26.2, 26.2, 21.8, -5.3; ESI-MS *m/z* 562.22 $[M+Na]^+$, 539.83 $[M+H]^+$.

Nitrile 67

To a solution of O-benzyl oxime **60** (15 mg, 0.056 mmol) in pyridine (1.5 mL) was added TsCl (13 mg, 0.067 mmol) in one portion, and the solution was stirred at room temperature for 12 h. The solution was then diluted with EtOAc and washed successively with 1% aqueous HCl and brine. The organic layer was dried over

Na_2SO_4, filtered and concentrated under reduced pressure. The residue was dissolved in DMF (1 mL) and KCN (36 mg, 0.056 mmol) was added in one portion. The suspension was heated to 80 °C, and was stirred for 12 h. The suspension was filtered through a short silica gel plug which was washed with ethyl acetate, and the filtered solution was concentrated under reduced pressure, and high vacuum. The residue was purified by column chromatography (1:1 hexanes / ethyl acetate) to provide nitrile **67** (11 mg, 75%) as a colorless oil. TLC (1:1 hexanes / ethyl acetate): $R_f = 0.2$; ^{1}H NMR ($CDCl_3$, 400 MHz) δ 7.43 (s, 1H), 7.41-7.29 (m, 5H), 5.09 (s, 2H), 3.98-3.84 (m, 1H), 3.20-3.11 (m, 2H), 2.46 (d, *J* = 5.9 Hz, 2H), 1.85-1.62 (m, 3H), 1.61-1.50 (m, 1H), 1.36 (s, 3H).

Nitrile 68

To a solution of O-methyl oxime **61** (43 mg, 0.225 mmol) in pyridine (2 mL, 24.7 mmol) was added TsCl (52 mg, 0.270 mmol) in one portion, and the reaction mixture was stirred for 12 h at room temperature. The mixture was diluted with EtOAc, and extracted with 2N HCl, and then washed with brine. The organic layer was dried over Na_2SO_4, filtered and concentrated under reduced pressure to afford 62 mg of crude tosylate that was dissolved in DMF (2 mL). This solution was stirred, and KCN (116 mg, 1.79 mmol) was added in one portion, and the suspension was heated to 80 °C for 12 h. After this period of time, the reaction mixture was cooled to ambient temperature and filtered through a short silica gel plug, which was rinsed with EtOAc. The filtrate was concentrated under reduced pressure, and the residue was purified by column chromatography (100% EtOAc) to afford nitrile **68** (18 mg, 51%, 2

steps) as a colorless oil. TLC (EtOAc): R_f = 0.4; ^{1}H NMR ($CDCl_3$, 400 MHz) δ 7.36 (s, 1H), 4.02-3.91 (m, 1H), 3.87 (s, 3H), 3.30 (br, 1H), 3.17 (br, 1H), 2.53 (dd, *J* = 5.8, 1.0 Hz, 2H), 1.86-1.60 (m, 4H), 1.37 (s, 3H); ^{13}C NMR ($CDCl_3$, 100 MHz) δ 153.0, 117.7, 72.0, 67.9, 62.2, 36.2, 30.7, 27.4, 26.3.

Bis-TES ether 70

To a solution of nitrile **68** (18 mg, 0.088 mmol) in CH_2Cl_2 (3 mL) was added Et_3N (122 μL, 0.88 mmol) via syringe, and the solution was stirred and cooled to 0 °C. To the cooled solution was added TESOTf (100 μL, 0.44 mmol) via syringe, and the reaction was monitored by TLC. When the starting material (R_f < 0.1 in 2:1 hexanes / ethyl acetate) had been consumed and a single product (R_f = 0.6 in 2:1 hexanes / ethyl acetate) was observed, the reaction was quenched by the addition of saturated aqueous $NaHCO_3$, and diluted with CH_2Cl_2. The layers were separated and the aqueous layer was extracted with additional CH_2Cl_2. The combined organic layers were dried over Na_2SO_4, filtered and concentrated under reduced pressure. The residue was purified by preparative TLC (10:1 hexanes / ethyl acetate) to afford bis-TES ether **70** (28 mg, 76%) as a clear oil. TLC (10:1 hexanes / ethyl acetate): R_f = 0.4; ^{1}H NMR ($CDCl_3$, 400 MHz) δ 7.30 (s, 1H), 4.00-3.90 (m, 1H), 3.82 (s, 3H), 2.46 (dd, *J* = 5.6, 3.7 Hz, 2H), 1.77-1.50 (m, 4H), 1.37 (s, 3H), 0.97 (t, *J* = 8.0 Hz, 9H), 0.93 (t, *J* = 8.0 Hz, 9H), 0.63 (q, *J* = 8.0 Hz, 6H), 0.57 (q, *J* = 8.0 Hz, 6H); ^{13}C NMR ($CDCl_3$, 100 MHz) δ 154.6, 117.9, 73.9, 68.7, 61.7, 37.8, 31.4, 26.3, 25.8, 7.1, 6.9, 6.6, 5.0.

2-phenylbutyrate ester 77

To a solution of the lactone alcohol **76** (72 mg, 0.554 mmol) in CH_2Cl_2 (2 mL) was added DMAP (67 mg, 0.554 mmol), CSA (122 mg, 0.526 mmol), and (*R*)-2-phenylbutyric acid (94 μL, 0.61 mmol) via syringe, and the solution was cooled to 0 °C as it stirred. To the cooled solution was added DCC (183 mg, 0.886 mmol) in one portion, and the solution was stirred at 0 °C for 1 h before being allowed to warm to room temperature over 12 h. After this period of time, the suspension (due to precipitation of dicyclohexylurea during the course of the reaction) was diluted with CH_2Cl_2 and washed with 10% aqueous citric acid solution, followed by saturated aqueous $NaHCO_3$, and brine. The organic layer was dried over Na_2SO_4 and concentrated under reduced pressure. The residue was purified by column chromatography (5:1 to 1:1 hexanes / ethyl acetate gradient) to afford the 2-phenylbutyrate ester **77** (105 mg, 69%) as a 4.7:1 mixture of diastereomers as judged by ^{1}H NMR integration. ^{1}H NMR ($CDCl_3$, 400 MHz) *major diastereomer* δ 7.38-7.22 (m, 5H), 4.13 (d, *J* = 11.7 Hz, 1H), 4.08 (d, *J* = 11.7 Hz, 1H), 3.46 (t, *J* = 7.7 Hz, 1H), 2.43-2.31 (m, 1H), 2.24-2.06 (m, 2H), 1.96-1.76 (m, 3H), 1.35 (s, 3H), 0.88 (t, *J* = 7.4 Hz, 3H).

Diol 80

To a stirred mixture of 1.5 mL H_2O : 1.5 mL *t*-BuOH was added AD-mix-β (442 mg), and the mixture was stirred until the AD-mix dissolved. The stirred mixture was cooled to 0 °C, and benzyl ether **78** (60 mg, 0.316 mmol) was added via syringe. The reaction mixture was stirred at 0 °C for 12 h before being quenched by the

addition of Na_2SO_3 (500 mg), and warmed to room temperature over 1 h with stirring. The reaction mixture was diluted with H_2O and CH_2Cl_2, and the layers were separated. The aqueous layer was extracted with additional CH_2Cl_2, and the combined organic layers were dried over Na_2SO_4, filtered, and concentrated under reduced pressure. Column chromatography of the residue (1:1 to 2:1 ethyl acetate / hexanes) provided the diol **80** (64 mg, 90%) as a colorless oil. TLC (1:1 hexanes / ethyl acetate): R_f < 0.1; ^{1}H NMR ($CDCl_3$, 400 MHz) δ 7.38-7.27 (m, 5H), 4.52 (s, 2H), 3.55-3.47 (m, 2H), 3.44 (dd, *J* = 11.0, 5.9 Hz, 1H), 3.38 (dd, *J* = 10.9, 6.3 Hz, 1H), 2.81 (s, 1H), 2.30 (t, 6.1 Hz), 1.79-1.51 (m, 4H), 1.15 (s, 3H).

Diol 81

To a mixture of H_2O (3 mL) and *t*-BuOH (3 mL) was added AD-mix-β (827 mg) and the mixture was stirred until the AD-mix dissolved, and continued to stir as it was cooled to 0 °C. To the cooled reaction mixture was added TBDPS ether **79** (200 mg, 0.590 mmol), and the reaction was stirred for 12 h at 0 °C. After this period of time, the reaction was quenched by the addition of Na_2SO_3 (900 mg), and was allowed to slowly warm to room temperature over 1 h with stirring. The mixture was diluted with H_2O and CH_2Cl_2, and the layers were separated. The aqueous layer was extracted with additional CH_2Cl_2, and the combined organic layers were dried over Na_2SO_4, filtered, and concentrated under reduced pressure. The residue was purified by column chromatography (ethyl acetate / hexanes gradient) to provide diol **81** (135 mg, 62%) as a colorless oil. ^{1}H NMR ($CDCl_3$, 400 MHz) δ 7.70-7.64 (m, 4H), 7.47-

7.36 (m, 6H), 3.75-3.61 (m, 2H), 3.51-3.37 (m, 2H), 2.61 (br, 1H), 1.91 (t, *J* = 5.8 Hz, 1H), 1.72-1.53 (m, 4H), 1.18 (s, 3H), 1.05 (s, 9H).

(*Z*) – olefin 85 and (*E*) – olefin 87

To a reaction flask containing THF (2 mL) was added NaH (94 mg of a 60% dispersion in oil, 2.36 mmol), and the suspension was cooled to 0 °C. To the suspension was added triethylphosphonoacetate (485 μL, 2.44 mmol) via syringe, and the solution stirred for 30 min. To the solution was added ketone **86** (277 mg, 0.815 mmol) as a solution in THF (3 mL) via cannula, and the reaction stirred at 0 °C with occasional monitoring by TLC. When the starting material ketone **86** was no longer visible, the reaction mixture was partitioned between saturated aqueous NH_4Cl and EtOAc, and the layers were separated. The aqueous layer was extracted with additional EtOAc, and the combined organic layers were washed with brine, dried over Na_2SO_4, filtered and concentrated under reduced pressure. The residue was purified by column chromatography using a 3 component solvent system to effect separation of the product mixture (40:10:1 to 20:10:1 hexanes / toluene / diethyl ether) and in this way (*Z*) – olefin **85** (17 mg, 5%) was obtained, and (*E*) – olefin **87** (59 mg, 18%) with the remaining mixed fractions (155 mg, 46%) being a mixture of **87:85** in an approximately 4:1 ratio. TLC (4:1 hexanes / ethyl acetate): R_f = 0.5 (**85** and **87** not distinguishable by TLC); **Compound 85**: ^{1}H NMR ($CDCl_3$, 500 MHz) δ 7.74-7.61 (m, 4H), 7.46-7.33 (m, 6H), 5.64 (s, 1H), 4.11 (q, *J* = 7.1 Hz, 2H), 3.70 (t, *J* = 6.5 Hz, 2H), 2.72-2.65 (m, 2H), 1.86 (s, 3H), 1.77-1.69 (m, 2H), 1.24 (t, *J* = 7.1 Hz, 3H), 1.05 (s, 9H). **Compound 87**: ^{1}H NMR ($CDCl_3$, 400 MHz) δ 7.72-7.61 (m, 4H), 7.49-7.31 (m,

6H), 5.67 (s, 1H), 4.15 (q, *J* = 7.1 Hz, 2H), 3.56 (t, *J* = 6.2 Hz, 2H), 2.27-2.20 (m, 2H), 2.14 (s, 3H), 1.78-1.66 (m, 2H), 1.28 (t, *J* = 7.1 Hz, 3H), 1.05 (s, 9H).

Diol 88

To a mixture of H_2O (730 μL) and *t*-BuOH (730 μL) was added AD-mix-α (202 mg) and the mixture was stirred until the AD-mix dissolved, and then was cooled to 0 °C. To the cooled solution was added $MeSO_2NH_2$ (14 mg, 0.145 mmol), and then a solution of (*E*) – olefin **87** (59 mg, 0.145 mmol) in *t*-BuOH (100 μL). H_2O (100 μL) was added to maintain the 1:1 solvent ratio, and the reaction mixture was stirred at 0 °C for 2 days, at which point starting material (R_f = 0.5 in 4:1 hexanes / ethyl acetate) was still observed by TLC, so additional portions of AD-mix-α (100 mg) and $MeSO_2NH_2$ (15 mg, 0.145 mmol) were added. After an additional day of stirring at 0 °C, the reaction mixture was quenched by the addition of Na_2SO_3, and diluted with CH_2Cl_2 and H_2O. The layers were separated, and the aqueous layer was extracted with additional CH_2Cl_2. The combined organic layers were dried over Na_2SO_4, filtered and concentrated under reduced pressure. The residue was purified by column chromatography (hexanes / ethyl acetate gradient) to provide diol **88** (41 mg, 64%) as a clear oil. TLC (4:1 hexanes / ethyl acetate): R_f = 0.; ^{1}H NMR ($CDCl_3$, 400 MHz) δ 7.71-7.61 (m, 4H), 7.49-7.33 (m, 6H), 4.27 (q, *J* = 7.1 Hz, 2H), 4.01 (d, *J* = 6.6 Hz, 1H), 3.68 (t, *J* = 5.5 Hz, 2H), 3.12 (d, *J* = 6.6 Hz, 1H), 2.75 (s, 1H), 1.77-1.60 (m, 4H), 1.30 (t, *J* = 7.1 Hz, 3H), 1.17 (s, 3H), 1.04 (s, 9H).

Acetonide 89

The diol **88** (19 mg, 0.042 mmol) was dissolved in 2,2-dimethoxypropane (3 mL, 24 mmol), and to the stirred solution was added a catalytic amount of CSA. The solution was stirred for 2 days at room temperature, and TLC analysis indicated the consumption of starting material (R_f = 0 in 4:1 hexanes / ethyl acetate) and the formation of the product (R_f = 0.3 in 4:1 hexanes / ethyl acetate). A few drops of Et_3N were added to quench the reaction, and the mixture was concentrated. The residue was purified by column chromatography (4:1 hexanes / ethyl acetate) to provide the acetonide **89** (17 mg, 85%) as a clear oil. TLC (4:1 hexanes / ethyl acetate): R_f = 0.3; ^{1}H NMR ($CDCl_3$, 500 MHz) δ 7.70-7.63 (m, 4H), 7.46-7.34 (m, 6H), 4.36 (s, 1H), 4.25 (q, *J* = 7.1 Hz, 2H), 3.70 (t, *J* = 6.0 Hz, 2H), 1.88-1.65 (m, 4H), 1.54 (s, 3H), 1.34 (s, 3H), 1.29 (t, *J* = 7.1 Hz, 3H), 1.15 (s, 3H), 1.05 (s, 9H).

Derivative 90

To the acetonide **89** (17 mg, 0.034 mmol) was added THF (300 μL) and aqueous LiOH (100 μL of a 1N solution, 0.103 mmol), and the solution was stirred at 0 °C for 24 hours. After this period of time, TLC analysis indicated that the reaction mixture consisted mostly of unreacted **89**. The mixture continued stirring at 0 °C, and solid LiOH*H_2O was added in 5 mg (0.083 mmol) portions with occasional TLC monitoring until the starting material was consumed. After the reaction was complete, acetic acid was added dropwise until the reaction mixture was slightly acidic according to pH paper. The reaction mixture was applied to a silica gel column, which was eluted with a 3 component eluent system (95:4:1 CH_2Cl_2 / MeOH / acetic acid) to provide the intermediate carboxylic acid (16 mg, 100%). The purified carboxylic acid

was dissolved in DMF (350 μL), and to this solution was added D-(+)-α-methylbenzylamine (9 μL, 0.069 mmol), HOBt (7 mg, 0.052 mmol), PyBOP (27 mg, 0.052 mmol), and Et_3N (20 μL, 0.138 mmol). The reaction mixture was stirred at room temperature for 12 h, then diluted with H_2O and EtOAc. The aqueous layer was extracted with additional EtOAc, and the combined organic layers were washed with brine, dried over Na_2SO_4, filtered and concentrated under reduced pressure. Column chromatography (4:1 hexanes / ethyl acetate) provided the derivative **90** (12 mg, 63%) which contained impurities as noted by TLC and NMR. Preparative TLC (4:1 hexanes / ethyl acetate) of this material provided a more pure sample of derivative **90** (9 mg, 47%), which was a 13.5:1 mixture of diastereomers as judged by ^{1}H NMR integration. TLC (4:1 hexanes ethyl acetate): R_f = 0.3; ^{1}H NMR ($CDCl_3$, 400 MHz) *major diastereomer* δ 7.70-7.63 (m, 4H), 7.45-7.29 (m, 11H), 6.81 (d, *J* = 8.2 Hz, 1H), 5.17 (dq, *J* = 8.2, 6.9 Hz, 1H), 4.21 (s, 1H), 3.68 (t, *J* = 6.2 Hz, 2H), 1.92-1.66 (m, 4H), 1.52 (d, *J* = 6.9 Hz, 3H), 1.50 (s, 3H), 1.32 (s, 3H), 1.16 (s, 3H), 1.04 (s, 9H); ^{13}C NMR ($CDCl_3$, 100 MHz) δ 142.8, 135.7, 134.2, 129.6, 128.9, 127.7, 127.6, 126.4, 108.7, 83.4, 81.5, 64.2, 48.1, 36.5, 27.2, 27.2, 27.0, 21.9, 21.8, 19.4.

Cinnamate ester 98

Into a round bottom flask were added *trans*-cinnamic acid (489 mg, 3.3 mmol), DMAP (366 mg, 3.0 mmol), CSA (661 mg, 2.85 mmol), and 4-methylpent-4-en-1-ol (300 mg, 3.0 mmol). The mixture was dissolved in CH_2Cl_2 (50 mL) and cooled to 0 °C with stirring. To the cooled solution was added DCC (988 mg, 4.8 mmol) in one portion, and the ice-water bath was allowed to slowly melt, and the reaction mixture

stirred for 24 h. The reaction mixture became cloudy due to precipitation of dicyclohexylurea during the course of the reaction, and the suspension was diluted with CH_2Cl_2 and extracted sequentially with 10% aqueous citric acid, deionized H_2O, saturated aqueous $NaHCO_3$, and brine. The organic layer was dried over Na_2SO_4, filtered, and concentrated under reduced pressure. The residue was purified by column chromatography (10:1 hexanes / ethyl acetate) to provide the cinnamate ester **98** (880 mg, >100%) which contained a small amount of unreacted DCC, and the mass of the recovered product indicated inaccurate measurements of the starting materials. ^{1}H NMR ($CDCl_3$, 400 MHz) δ 7.69 (d, *J* = 16.0 Hz, 1H), 7.57-7.49 (m, 2H), 7.42-7.35 (m, 3H), 6.45 (d, *J* = 16.0 Hz, 1H), 4.75 (br, 1H), 4.72 (br, 1H), 4.21 (t, *J* = 6.7 Hz, 2H), 2.17-2.10 (m, 2H), 1.97-1.80 (m, 2H), 1.75 (s, 3H).

Chloroacetate ester 99

To a reaction flask were added chloroacetic acid (423 mg, 4.47 mmol), 4-methylpent-4-en-1-ol (407 mg, 4.07 mmol), DMAP (496 mg, 4.07 mmol), and CSA (896 mg, 3.87 mmol). The mixture was dissolved in CH_2Cl_2 (50 mL) and cooled to 0 °C with stirring. To the cooled solution was added DCC (1.34 g, 6.51 mmol) in one portion, and the ice-bath was allowed to melt as the reaction mixture stirred for 24 h. The reaction mixture became cloudy with precipitated dicyclohexylurea, and was diluted with CH_2Cl_2, and extracted sequentially with 10% aqueous citric acid, deionized H_2O, saturated aqueous $NaHCO_3$, and brine. The organic layer was dried over Na_2SO_4, filtered and concentrated under reduced pressure. The residue was purified by column chromatography (10:1 hexanes / ethyl acetate) to provide the

chloroacetate ester **99** (479 mg, 67%). ^{1}H NMR ($CDCl_3$, 500 MHz) δ 4.75 (br, 1H), 4.70 (br, 1H), 4.20 (t, J = 6.7 Hz, 2H), 4.06 (s, 2H), 2.09 (t, J = 7.6 Hz, 2H), 1.87-1.78 (m, 2H), 1.73 (s, 3H).

Phosphonate 100

The chloroacetate ester **99** (479 mg, 2.71 mmol) was dissolved in triethylphosphite (1.4 mL, 8.1 mmol) and the solution was stirred and heated to reflux for 12 h. The excess triethylphosphite was distilled from the reaction mixture under high vacuum, and the residue was purified by column chromatography (hexanes / ethyl acetate gradient) to provide the phosphonate **100** (1.26 g, <100%) which was contaminated with triethylphosphite derived impurities. ^{1}H NMR ($CDCl_3$, 400 MHz) δ 4.74 (br, 1H), 4.69 (br, 1H), 4.22-4.06 (m, 6H), 2.97 (d, $^{2}J_{H,P}$ = 21.5 Hz, 2H), 2.09 (t, J = 7.6 Hz, 2H), 1.84-1.75 (m, 2H), 1.72 (s, 3H), 1.34 (td, J = 6.0, 0.6 Hz, 6H); ^{13}C NMR ($CDCl_3$, 100 MHz) δ 144.5, 110.7, 65.3, 62.8 (d, $^{2}J_{CP}$ = 6.0 Hz), 34.5 (d, $^{1}J_{CP}$ = 133.2 Hz), 33.9, 26.5, 22.5, 16.5 (d, $^{3}J_{CP}$ = 6.4 Hz).

Ketone 101

The crude phosphonate **100** (1.26 g of material, theoretical 754 mg, 2.71 mmol) was dissolved in CH_2Cl_2 (50 mL), and NMO (949 mg, 8.1 mmol) was added to the solution. The solution was cooled to 0 °C, and ozone was bubbled through a pipet for 10 min with stirring. The solution was purged with N_2, and concentrated under reduced pressure. Column chromatography of the residue (hexanes / ethyl acetate gradient) provided ketone **101** (372 mg, 49%). ^{1}H NMR ($CDCl_3$, 400 MHz) δ 4.23-

4.08 (m, 6H), 2.96 (d, $^{2}J_{HP}$ = 21.6 Hz, 2H), 2.56 (t, J = 7.2 Hz, 2H), 2.16 (s, 3H), 1.97-1.88 (m, 2H), 1.35 (td, J = 7.1, 0.5 Hz, 6H); ^{13}C NMR ($CDCl_3$, 100 MHz) δ 207.7, 64.7, 62.8 (d, $^{2}J_{CP}$ = 6.5 Hz), 39.7, 34.4 (d, $^{1}J_{CP}$ = 133.2 Hz), 30.2, 22.7, 16.5 (d, $^{3}J_{CP}$ = 6.1 Hz).

Crotylation adduct 105

A reaction flask was charged with *t*-BuOK (127 mg, 1.13 mmol) and heated to 110 °C with a sand bath under high vacuum (0.1 mm Hg) for 12 h, then backfilled with Ar, and allowed to cool to ambient temperature under positive pressure of Ar. A dry 10 mL graduated cylinder under Ar was partially submerged in a -78 °C dewar bath in order to condense *cis*-2-butene (3.0 mL) which was transferred from a lecture bottle via cannula. To the condensed *cis*-2-butene was added THF (5.0 mL) via syringe, and the graduated cylinder indicated a total mixed volume of 7.6 mL. A portion of this solution (700 μL, corresponding to 276 μL of *cis*-2-butene) was transferred via syringe to the reaction flask containing the *t*-BuOK and THF (5 mL). The suspension was cooled to -78 °C, and n-BuLi (420 μL of a 2.7 M solution in hexanes, 1.13 mmol) was added, and the solution turned yellow. The solution was allowed to warm to -45 °C for 10 minutes, and then recooled to -78 °C. To the solution was added (-)-Ipc_2BOMe (393 mg, 1.24 mmol) as a solution in THF (1 mL) via cannula, causing the yellow color to fade. The solution was stirred for 0.5 h before BF_3*OEt_2 (190 μL, 1.50 mmol) was added, followed by a solution of aldehyde **34** as a solution in THF (1 mL) via syringe. The reaction mixture stirred for 8 h at -78 °C before a saturated aqueous solution of $NaBO_3$ was added to quench the reaction. The

solution was allowed to warm to room temperature and was stirred for 12 hours, and then it was diluted with ether and the layers were separated. The aqueous layer was extracted with additional ether, and the combined organic layers were washed with brine, dried over Na_2SO_4, filtered and concentrated under reduced pressure. The residue was purified by column chromatography (10:1 to 1:1 hexane / diethyl ether gradient) to provide crotylation adduct **105** (6 mg, 2%). TLC (1:1 hexanes / diethyl ether): R_f = 0.4; $[\alpha]_D^{22}$ = +10.0 (*c* 0.10, $CHCl_3$); ^{1}H NMR ($CDCl_3$, 400 MHz) δ 5.81 (ddd, *J* = 17.2, 10.3, 8.0 Hz, 1H), 5.14 (d, *J* = 17.2 Hz, 1H), 5.10 (d, *J* = 10.3 Hz, 1H), 3.41 (s, 3H), 3.39-3.31 (m, 1H), 3.18 (td, *J* = 6.5, 4.1 Hz, 1H), 2.92 (dd, *J* = 8.1, 2.3 Hz, 1H), 2.85 (dd, *J* = 4.8, 2.3 Hz, 1H), 2.43 (dd, *J* = 14.1, 7.1 Hz, 1H), 1.91 (d, *J* = 6.5 Hz, 1H), 1.72-1.57 (m, 1H), 1.56-1.38 (m, 2H), 1.13 (d, *J* = 9.0 Hz, 3H), 0.92 (d, *J* = 7.0 Hz, 3H), 0.90 (t, *J* = 7.3 Hz, 3H); ^{13}C NMR ($CDCl_3$, 100 MHz) δ 139.8, 116.2, 83.8, 74.1, 59.7, 59.1, 58.3, 42.9, 39.0, 23.9, 15.9, 10.4, 10.2; ESI-MS *m/z* 245.94 $[M+NH_4]^+$, 229.02 $[M+H]^+$; HR-EI-MS *m/z* calcd. for $C_{13}H_{23}O_3$ $[M-H]^+$: 227.1642, found 227.1638.

Reduction product 105

To a solution of alkyne **109** (6 mg, 0.027 mmol) in EtOAc (4 mL) were added a few drops of quinoline via Pasteur pipet, and a catalytic amount of Pd-$BaSO_4$. Two balloons of H_2 were bubbled through the solution with stirring, by the use of a 6" needle and a vent needle. The solution was filtered and stirred over solid $CuSO_4$*xH_2O for 10 min to remove quinoline, filtered through a short plug of silica with EtOAc, and concentrated under reduced pressure. The residue was analyzed by

^{1}H NMR to compare with the crotylation adduct **105**, and it appeared to be a roughly 1:1 mixture of the desired olefin **105** and the overreduction product (alkane). ^{1}H NMR ($CDCl_3$, 300 MHz) δ 5.84 (ddd, *J* = 17.2, 10.3, 7.8 Hz, 1H), 5.13 (d, *J* = 17.2 Hz, 1H), 5.11 (d, *J* = 10.3 Hz, 1H), 3.76-3.62 (m, 1H), 3.41 (s, 3H), 3.26-3.14 (m, 1H), 3.04 (t, *J* = 2.8 Hz, 1H), 2.87 (dd, *J* = 2.5, 3.2 Hz, 1H), 2.39 (dd, *J* = 14.5, 7.8 Hz, 1H), 1.88 (d, *J* = 2.4 Hz, 1H), 1.75-1.38 (m, 3H), 1.14 (d, 6.8 Hz, 3H), 1.01-0.87 (m, 5H, obscured because of the 2 compounds).

Reduction product 107

To a solution of the alkyne **114** (3 mg, 0.013 mmol) in EtOAc (2 mL) was added a drop of quinoline and a catalytic amount of Pd-$BaSO_4$. Two balloons of H_2 were bubbled through the stirring solution, by the use of a 6" needle connected to the balloon, and a vent needle through the septum. The reaction mixture was directly applied to a silica column packed with hexanes, and was eluted off with a hexanes / ethyl acetate gradient. The product alkene **107** was contaminated with quinoline and overreduction product as seen in the ^{1}H NMR spectrum. ^{1}H NMR ($CDCl_3$, 500 MHz) *crude* δ 5.88 (ddd, *J* = 15.9, 10.3, 8.0 Hz, 1H), 5.14 (d, *J* = 15.9 Hz, 1H), 5.12 (d, *J* = 10.3 Hz, 1H), 3.64-3.54 (m, 1H), 3.40 (s, 3H), 3.22-3.14 (m, 1H), 3.05-2.96 (m, 1H), 2.87-2.80 (m, 1H), 2.52-2.37 (m, 1H), 1.74-1.35 (m, 3H), 1.14 (d, *J* = 6.9 Hz, 3H), 0.97-0.86 (m, 5H).

Alkyne 109

To a stirred solution of aldehyde **34** (35 mg, 0.205 mmol) and (*M*)-allenylstannane **113** (100 mg, 0.287 mmol) in CH_2Cl_2 (5 mL) at -78 °C was added BF_3*OEt_2 (63 μL, 0.513 mmol) via syringe. The solution was stirred at -78 °C for 1 h, and then quenched by the addition of a saturated $NaHCO_3$ solution. The mixture was allowed to warm to ambient temperature, and the layers were separated. The aqueous layer was extracted with additional CH_2Cl_2, and the combined organic layers were stirred over solid KF on Celite for 2 h at room temperature. The solution was filtered and concentrated under reduced pressure, and the residue was purified by column chromatography (4:1 to 1:1 hexanes / ethyl acetate gradient) to provide alkyne **109** as a clear oil. TLC (1:1 hexanes / ethyl acetate): $R_f \sim 0.5$; ^{1}H NMR ($CDCl_3$, 400 MHz) δ 3.74-3.68 (m, 1H), 3.41 (s, 3H), 3.18 (td, *J* = 6.4, 4.2 Hz, 1H), 3.11 (dd, *J* = 3.4, 2.5 Hz, 1H), 3.04 (dd, *J* = 8.1, 2.5 Hz, 1H), 2.60 (pentet of doublets, *J* = 7.0, 2.4 Hz, 1H), 2.15 (d, *J* = 2.5 Hz, 1H), 2.13 (d, *J* = 2.7 Hz, 1H), 1.72-1.43 (m, 3H), 1.31 (d, *J* = 7.0 Hz, 3H), 0.96 (d, *J* = 7.1 Hz, 3H), 0.91 (t, *J* = 7.1 Hz, 3H); ^{13}C NMR ($CDCl_3$, 100 MHz) δ 84.9, 83.9, 71.2, 71.1, 58.5, 58.2, 57.0, 38.8, 30.6, 23.9, 17.0, 10.6, 10.1; ESI-MS *m/z* 249.09 $[M+Na]^+$, 243.96 $[M+NH_4]^+$, 227.02 $[M+H]^+$; HR-EI-MS *m/z* calcd. for $C_{13}H_{23}O_3$ $[M]^+$: 226.1563, found 226.1562; *m/z* calcd. for $C_{13}H_{23}O_3$ $[M+H]^+$: 227.1642, found 227.1641.

Bromohydrin 112

To a stirred solution of aldehyde **34** (38 mg, 0.221 mmol) in CH_2Cl_2 (3 mL) at -25 °C was added $MgBr_2$*OEt_2 (114 mg, 0.442 mmol) in one portion, and stirring continued for 5 minutes before the (*P*)-allenylstannane **108** (85 mg, 0.243 mmol) in 2

mL of CH_2Cl_2 was added. Stirring continued for 45 minutes at -25 °C at which point the reaction was quenched by the addition of saturated aqueous $NaHCO_3$, and the mixture was allowed to warm to room temperature. The aqueous layer was extracted with additional CH_2Cl_2, and the combined organic layers were stirred over KF on Celite for 2 h at room temperature. The solution was filtered and concentrated under reduced pressure, and the residue was purified by column chromatography (3:1 to 1:1 hexanes / ethyl acetate gradient) to provide the bromohydrin **112** (27 mg, 40% based on the MW of the actual product). Diffraction quality crystals were obtained by perfusion of hexanes into diethyl ether at 4 °C. $[\alpha]_D^{22}$ +21.7 (*c* 0.75, $CHCl_3$); ^{1}H NMR ($CDCl_3$, 400 MHz) δ 4.87 (d, *J* = 7.8 Hz, 1H), 4.11 (s, 3H), 3.99 (td, *J* = 8.8, 3.2 Hz, 1H), 3.52 (ddd, *J* = 9.6, 4.7, 2.3 Hz, 1H), 3.26-3.14 (m, 1H), 2.46-2.35 (m, 1H), 2.16 (d, *J* = 2.5 Hz, 1H), 1.89-1.74 (m, 1H), 1.49-1.36 (m, 2H), 1.28 (d, *J* = 6.9 Hz, 3H), 1.06 (d, *J* = 7.3 Hz, 3H), 0.88 (t, *J* = 7.5 Hz, 3H); ^{13}C NMR ($CDCl_3$, 100 MHz) δ 87.0, 83.1, 79.8, 78.6, 69.9, 56.3, 55.4, 34.8, 31.7, 31.1, 22.0, 15.3, 11.0, 9.9; IR (film) νmax: 3441, 2969, 2934, 2873, 1650, 1457, 1431, 1380, 1235, 1082, 933, 636; ESI-MS *m/z* 329.01 $[M+Na]^+$, 306.93 $[M+H]^+$; HR-EI-MS *m/z* calcd. for $C_{13}H_{24}O_3Br_1$ $[M+H]^+$: 307.0903, found 307.0902.

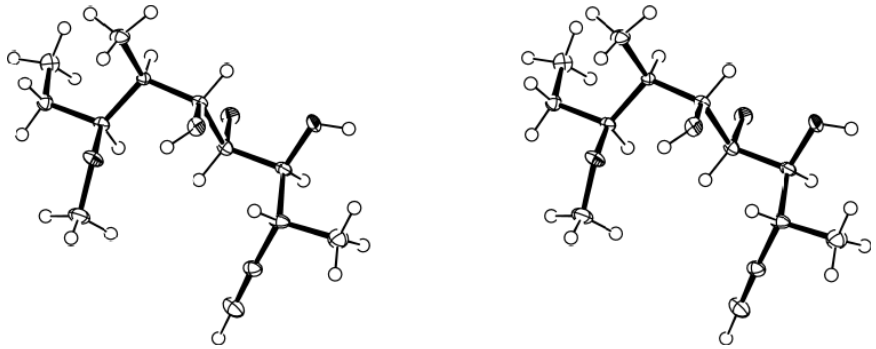

Figure 1.16 ORTEP stereopair drawing of the X-ray crystal structure of bromohydrin **112**, ellipsoids drawn at the 50% probability level.

Structure report for bromohydrin 112 (burk05):

A colorless block 0.12 x 0.10 x 0.10 mm in size was mounted on a Cryoloop with Paratone oil. Data were collected in a nitrogen gas stream at 100(2) K using phi and omega scans. Crystal-to-detector distance was 60 mm and exposure time was 5 seconds per frame using a scan width of 0.3°. Data collection was 97.0% complete to 25.00° in θ. A total of 8399 reflections were collected covering the indices, -9<=*h*<=9, -10<=*k*<=5, -31<=*l*<=30. 3113 reflections were found to be symmetry independent, with an R_{int} of 0.0351. Indexing and unit cell refinement indicated a primitive, orthorhombic lattice. The space group was found to be P2(1)2(1)2(1) (No. 19). The data were integrated using the Bruker SAINT software program and scaled using the SADABS software program. Solution by direct methods (SIR-2004) produced a complete heavy-atom phasing model consistent with the proposed structure. All non-hydrogen atoms were refined anisotropically by full-matrix least-squares (SHELXL-97). All hydrogen atoms were placed using a riding model. Their

positions were constrained relative to their parent atom using the appropriate HFIX command in SHELXL-97.

Absolute Configuration of C3	...	R
Absolute Configuration of C4	...	S
Absolute Configuration of C6	...	R
Absolute Configuration of C8	...	S

Table 1.1 Crystal data and structure refinement for burk05.

X-ray ID	burk05	
Sample/notebook ID	BDJ4-139-1	
Empirical formula	C13 H23 Br O3	
Formula weight	307.22	
Temperature	100(2) K	
Wavelength	0.71073 Å	
Crystal system	Orthorhombic	
Space group	P2(1)2(1)2(1)	
Unit cell dimensions	a = 7.5546(6) Å	α= 90°.
	b = 8.0599(7) Å	β= 90°.
	c = 23.4853(18) Å	γ = 90°.
Volume	1430.0(2) $Å^3$	
Z	4	
Density (calculated)	1.427 Mg/m^3	
Absorption coefficient	2.870 mm^{-1}	
F(000)	640	
Crystal size	0.12 x 0.10 x 0.10 mm^3	
Crystal color/habit	colorless block	
Theta range for data collection	1.73 to 28.19°.	
Index ranges	-9<=h<=9, -10<=k<=5, -31<=l<=30	
Reflections collected	8399	
Independent reflections	3113 [R(int) = 0.0351]	

Table 1.1 Crystal data and structure refinement for burk05, continued.

Completeness to theta = 25.00°	97.0 %
Absorption correction	Semi-empirical from equivalents
Max. and min. transmission	0.7623 and 0.7245
Refinement method	Full-matrix least-squares on F^2
Data / restraints / parameters	3113 / 0 / 161
Goodness-of-fit on F^2	1.169
Final R indices [I>2sigma(I)]	R1 = 0.0325, wR2 = 0.0929
R indices (all data)	R1 = 0.0409, wR2 = 0.1190
Absolute structure parameter	0.020(15)
Extinction coefficient	0.014(2)
Largest diff. peak and hole	0.716 and -1.048 e.$Å^{-3}$

Table 1.2 Atomic coordinates (x 10^4) and equivalent isotropic displacement parameters ($Å^2$x 10^3) for burk05. U(eq) is defined as one third of the trace of the orthogonalized U^{ij} tensor.

	x	y	z	U(eq)
C(1)	4572(6)	-3577(6)	9708(2)	24(1)
C(2)	4366(6)	-2160(5)	9822(2)	18(1)
C(3)	4124(5)	-418(5)	9990(2)	18(1)
C(4)	5436(5)	710(5)	9656(2)	15(1)
C(5)	5024(5)	697(5)	9018(2)	14(1)
C(6)	3687(5)	2015(5)	8816(2)	14(1)
C(7)	3325(5)	2087(5)	8176(2)	11(1)
C(8)	2921(5)	375(5)	7927(2)	13(1)
C(9)	2565(5)	358(5)	7285(2)	16(1)
C(10)	4051(6)	1117(6)	6931(2)	22(1)
C(11)	4389(6)	-233(6)	10630(2)	24(1)
C(12)	1853(6)	3355(5)	8048(2)	18(1)

Table 1.2 Atomic coordinates (x 10^4) and equivalent isotropic displacement parameters ($Å^2$x 10^3) for burk05. U(eq) is defined as one third of the trace of the orthogonalized U^{ij} tensor., continued.

C(13)	1342(7)	-2020(5)	8260(2)	23(1)
O(1)	5367(4)	2382(4)	9847(1)	20(1)
O(2)	2077(4)	1756(4)	9133(1)	17(1)
O(3)	1387(4)	-245(4)	8226(1)	18(1)
Br(1)	7274(1)	998(1)	8594(1)	18(1)

Table 1.3 Bond lengths [Å] and angles [°] for burk05.

C(1)-C(2)	1.183(6)	C(8)-H(8)	1.0000
C(1)-H(1)	0.9500	C(9)-C(10)	1.525(6)
C(2)-C(3)	1.469(6)	C(9)-H(9A)	0.9900
C(3)-C(11)	1.524(7)	C(9)-H(9B)	0.9900
C(3)-C(4)	1.557(6)	C(10)-H(10A)	0.9800
C(3)-H(3)	1.0000	C(10)-H(10B)	0.9800
C(4)-O(1)	1.421(5)	C(10)-H(10C)	0.9800
C(4)-C(5)	1.531(6)	C(11)-H(11A)	0.9800
C(4)-H(4)	1.0000	C(11)-H(11B)	0.9800
C(5)-C(6)	1.540(5)	C(11)-H(11C)	0.9800
C(5)-Br(1)	1.985(4)	C(12)-H(12A)	0.9800
C(5)-H(5)	1.0000	C(12)-H(12B)	0.9800
C(6)-O(2)	1.441(5)	C(12)-H(12C)	0.9800
C(6)-C(7)	1.529(6)	C(13)-O(3)	1.433(5)
C(6)-H(6)	1.0000	C(13)-H(13A)	0.9800
C(7)-C(8)	1.530(5)	C(13)-H(13B)	0.9800
C(7)-C(12)	1.541(6)	C(13)-H(13C)	0.9800
C(7)-H(7)	1.0000	O(1)-H(1A)	0.8400
C(8)-O(3)	1.444(5)	O(2)-H(2)	0.8400
C(8)-C(9)	1.530(6)		

C(2)-C(1)-H(1)	180.0	C(3)-C(4)-H(4)	108.7
C(1)-C(2)-C(3)	177.5(5)	C(4)-C(5)-C(6)	115.5(3)
C(2)-C(3)-C(11)	110.0(4)	C(4)-C(5)-Br(1)	108.4(3)
C(2)-C(3)-C(4)	110.1(4)	C(6)-C(5)-Br(1)	108.8(3)
C(11)-C(3)-C(4)	110.8(4)	C(4)-C(5)-H(5)	108.0
C(2)-C(3)-H(3)	108.6	C(6)-C(5)-H(5)	108.0
C(11)-C(3)-H(3)	108.6	Br(1)-C(5)-H(5)	108.0

Table 1.3 Bond lengths [Å] and angles [°] for burk05, continued.

C(4)-C(3)-H(3)	108.6	O(2)-C(6)-C(7)	111.2(3)
O(1)-C(4)-C(5)	107.9(3)	O(2)-C(6)-C(5)	107.1(3)
O(1)-C(4)-C(3)	111.8(3)	C(7)-C(6)-C(5)	116.5(3)
C(5)-C(4)-C(3)	111.0(3)	O(2)-C(6)-H(6)	107.2
O(1)-C(4)-H(4)	108.7	C(7)-C(6)-H(6)	107.2
C(5)-C(4)-H(4)	108.7	C(5)-C(6)-H(6)	107.2
C(6)-C(7)-C(8)	112.2(3)	H(10B)-C(10)-H(10C)	109.5
C(6)-C(7)-C(12)	110.3(3)	C(3)-C(11)-H(11A)	109.5
C(8)-C(7)-C(12)	112.3(3)	C(3)-C(11)-H(11B)	109.5
C(6)-C(7)-H(7)	107.2	H(11A)-C(11)-H(11B)	109.5
C(8)-C(7)-H(7)	107.2	C(3)-C(11)-H(11C)	109.5
C(12)-C(7)-H(7)	107.2	H(11A)-C(11)-H(11C)	109.5
O(3)-C(8)-C(7)	106.6(3)	H(11B)-C(11)-H(11C)	109.5
O(3)-C(8)-C(9)	109.6(3)	C(7)-C(12)-H(12A)	109.5
C(7)-C(8)-C(9)	114.8(3)	C(7)-C(12)-H(12B)	109.5
O(3)-C(8)-H(8)	108.6	H(12A)-C(12)-H(12B)	109.5
C(7)-C(8)-H(8)	108.6	C(7)-C(12)-H(12C)	109.5
C(9)-C(8)-H(8)	108.6	H(12A)-C(12)-H(12C)	109.5
C(10)-C(9)-C(8)	113.8(4)	H(12B)-C(12)-H(12C)	109.5
C(10)-C(9)-H(9A)	108.8	O(3)-C(13)-H(13A)	109.5
C(8)-C(9)-H(9A)	108.8	O(3)-C(13)-H(13B)	109.5
C(10)-C(9)-H(9B)	108.8	H(13A)-C(13)-H(13B)	109.5
C(8)-C(9)-H(9B)	108.8	O(3)-C(13)-H(13C)	109.5
H(9A)-C(9)-H(9B)	107.7	H(13A)-C(13)-H(13C)	109.5
C(9)-C(10)-H(10A)	109.5	H(13B)-C(13)-H(13C)	109.5
C(9)-C(10)-H(10B)	109.5	C(4)-O(1)-H(1A)	109.5
H(10A)-C(10)-H(10B)	109.5	C(6)-O(2)-H(2)	109.5
C(9)-C(10)-H(10C)	109.5	C(13)-O(3)-C(8)	113.1(4)
H(10A)-C(10)-H(10C)	109.5		

Symmetry transformations used to generate equivalent atoms:

Table 1.4 Anisotropic displacement parameters ($Å^2 x\ 10^3$)for burk05. The anisotropic displacement factor exponent takes the form: $-2\pi^2[\ h^2 a^{*2} U^{11} + ... + 2\ h\ k\ a^*\ b^*\ U^{12}\ ]$

	U^{11}	U^{22}	U^{33}	U^{23}	U^{13}	U^{12}
C(1)	18(2)	18(2)	37(3)	-3(2)	-2(2)	-1(2)
C(2)	13(2)	16(2)	25(3)	4(2)	-1(2)	-3(2)
C(3)	11(2)	12(2)	30(3)	5(2)	2(2)	0(2)
C(4)	13(2)	10(2)	21(2)	1(2)	-2(2)	-2(2)
C(5)	8(2)	14(2)	19(2)	-2(2)	1(2)	-1(1)
C(6)	11(2)	12(2)	18(2)	-1(2)	2(2)	1(2)
C(7)	12(2)	9(2)	12(2)	0(2)	0(2)	1(1)
C(8)	7(2)	11(2)	19(2)	2(2)	0(2)	0(1)
C(9)	16(2)	15(2)	16(2)	-2(2)	0(2)	1(2)
C(10)	21(2)	24(2)	21(2)	-2(2)	2(2)	1(2)
C(11)	29(2)	20(2)	22(3)	-1(2)	1(2)	1(2)
C(12)	16(2)	14(2)	25(2)	3(2)	-1(2)	3(2)
C(13)	25(2)	15(2)	30(3)	3(2)	0(2)	-6(2)
O(1)	25(2)	13(1)	22(2)	-4(1)	-10(1)	-2(1)
O(2)	12(1)	19(1)	20(2)	-2(1)	3(1)	2(1)
O(3)	15(2)	13(1)	25(2)	-1(1)	4(1)	-4(1)
Br(1)	10(1)	22(1)	23(1)	3(1)	1(1)	-1(1)

Table 1.5 Hydrogen coordinates (x 10^4) and isotropic displacement parameters ($Å^2$x 10^3) for burk05.

	x	y	z	U(eq)
H(1)	4738	-4714	9617	29
H(3)	2887	-76	9893	21
H(4)	6665	280	9714	18
H(5)	4537	-420	8919	16
H(6)	4166	3123	8931	16
H(7)	4430	2497	7989	13
H(8)	3945	-375	8008	15
H(9A)	2381	-803	7162	19
H(9B)	1457	976	7209	19
H(10A)	4054	2323	6982	33
H(10B)	3864	853	6529	33
H(10C)	5190	661	7056	33
H(11A)	3615	-1013	10831	35
H(11B)	4098	904	10745	35
H(11C)	5626	-470	10726	35
H(12A)	700	2875	8146	27
H(12B)	1872	3636	7642	27
H(12C)	2049	4361	8274	27
H(13A)	1409	-2490	7875	35
H(13B)	237	-2372	8442	35
H(13C)	2350	-2412	8485	35
H(1A)	5997	2489	10139	30
H(2)	1479	1004	8977	26

Alkyne 114

To a stirred solution of aldehyde **34** (27 mg, 0.157 mmol) and (*P*)-allenylstannane **108** (78 mg, 0.220 mmol) in CH_2Cl_2 (3 mL) at -78 °C was added BF_3*OEt_2 (48 μL, 0.393 mmol) via syringe. The reaction was stirred for 1 h at this temperature and then quenched by the addition of a saturated solution of $NaHCO_3$, and warmed to room temperature. The layers were separated and the aqueous layer was extracted with additional CH_2Cl_2, and the combined organic layers were stirred over KF on Celite for 2 h at room temperature. The solution was filtered and concentrated under reduced pressure, and the residue was purified by column chromatography (4:1 to 1:1 hexanes / ethyl acetate gradient) to provide alkyne **114** (18 mg, 50%). ^{1}H NMR ($CDCl_3$, 300 MHz) δ 3.58 (q, *J* = 4.5 Hz, 1H), 3.42 (s, 3H), 3.20 (td, *J* = 6.5, 4.1 Hz, 1H), 3.07 (dd, *J* = 8.0, 2.3 Hz, 1H), 2.92 (dd, *J* = 4.5, 2.3 Hz, 1H), 2.86-2.74 (m, 1H), 2.17 (d, *J* = 2.4 Hz, 1H), 2.02 (d, *J* = 4.7 Hz, 1H), 1.76-1.56 (m, 1H), 1.56-1.40 (m, 2H), 1.31 (d, *J* = 7.1 Hz, 3H), 0.97 (d, *J* = 7.1 Hz, 3H), 0.91 (t, *J* = 7.4 Hz, 3H).

Aldol adduct 118

To a stirred solution of acetylated auxiliary **116** (290 mg, 1.34 mmol) in CH_2Cl_2 (10 mL) was added $PhBCl_2$ (174 μL, 1.34 mmol) at room temperature. The mixture was stirred for 10 minutes and then (-)-sparteine (616 μL, 2.68 mmol) was added. The mixture was stirred for 30 minutes at room temperature and then was cooled to -78 °C, and then 6-heptenal **117** (141 μL, 1.03 mmol) was added dropwise. The reaction mixture was stirred at -78 °C for 5 h, then allowed to warm slowly to ambient temperature over a period of 2 h. The mixture was stirred at ambient

temperature for 30 min, then quenched by the addition of 30% H_2O_2 (3 mL) and was stirred for 3 min before being diluted with H_2O and CH_2Cl_2. The layers were separated and the organic layer was washed with deionized H_2O and then brine. The organic layer was dried over Na_2SO_4, filtered, and concentrated under reduced pressure. The residue was purified by column chromatography on neutral silica gel (4:1 hexanes / ethyl acetate isocratic) to provide aldol adduct **118** (305 mg, 90%) as a yellow oil. TLC (4:1 hexanes / ethyl acetate) $R_f = 0.2$; ^{1}H NMR ($CDCl_3$, 400 MHz) δ 5.81 (ddt, *J* = 17.0, 10.2, 6.7 Hz, 1H), 5.36 (d, *J* = 8.3 Hz, 1H), 5.00 (d, *J* = 17.0 Hz, 1H), 4.94 (d, *J* = 10.2 Hz, 1H), 4.08-3.97 (m, 1H), 3.54 (dd, *J* = 8.3, 11.8 Hz, 1H), 3.46 (dd, *J* = 9.4, 17.5 Hz, 1H), 3.33 (dd, *J* = 17.5, 2.7 Hz, 1H), 3.22 (d, *J* = 4.3, 1H), 3.12 (d, *J* = 11.8 Hz, 1H), 2.11-2.02 (m, 2H), 1.67-1.30 (m, 6H), 1.04 (s, 9H); ^{13}C NMR ($CDCl_3$, 100 MHz) δ 205.4, 173.3, 139.0, 114.6, 72.2, 68.4, 45.1, 38.1, 36.5, 33.8, 30.7, 29.0, 27.0, 25.2; ESI-MS *m/z* 352.06 $[M+Na]^+$, 330.02 $[M+H]^+$; HR-EI-MS *m/z* calcd. for $C_{16}H_{27}O_2N_1S_2$ $[M]^+$: 329.1478, found 329.1480.

Methyl ester 119

To a solution of aldol adduct **118** (204 mg, 0.619 mmol) in CH_2Cl_2 (2 mL) was added MeOH (40 μL, 0.929 mmol) via syringe. To the stirring solution was added imidazole (126 mg, 1.86 mmol), and the solution stirred at room temperature for 12 hours as the yellow color slowly faded. The reaction mixture was concentrated under reduced pressure and purified by column chromatography to provide the methyl ester **119** (75 mg, 65%) which was contaminated with the deacetylated thiazolidinethione auxiliary. ^{1}H NMR *crude* ($CDCl_3$, 400 MHz) δ 5.80 (ddt, *J* = 17.1, 10.2, 6.8 Hz, 1H),

4.99 (d, *J* = 17.1 Hz, 1H), 4.94 (d, *J* = 10.2 Hz, 1H), 4.05-3.95 (m, 1H), 3.71 (s, 3H), 2.89 (d, *J* = 4.0 Hz, 1H), 2.51 (dd, *J* = 16.5, 3.1 Hz, 1H), 2.41 (dd, *J* = 16.5, 9.0 Hz, 1H), 2.11-1.98 (m, 2H), 1.59-1.26 (m, 6H); ^{13}C ($CDCl_3$, 100 MHz) δ 173.7, 138.9, 114.6, 68.1, 51.9, 41.2, 33.8, 28.9, 26.0, 25.1.

TBS ether 120

To a solution of the methyl ester **119** (75 mg, 0.400 mmol) in DMF (2 mL) was added imidazole (136 mg, 2 mmol) and TBSCl (96 mg, 0.64 mmol) and the solution was stirred for 12 h. at room temperature. The reaction mixture was partitioned between H_2O and a 1:1 mixture of diethyl ether / hexanes. The aqueous layer was extracted with additional portions of the mixture, and the combined organic layers were washed with brine, dried over Na_2SO_4, filtered and concentrated under reduced pressure. The residue was purified by column chromatography to provide the TBS ether **120** (47 mg, 39%). ^{1}H NMR ($CDCl_3$, 400 MHz) δ 5.79 (ddt, *J* = 17.1, 10.2, 6.6 Hz, 1H), 4.99 (d, *J* = 17.1 Hz, 1H), 4.94 (d, *J* = 10.2 Hz, 1H), 4.17-4.06 (m, 1H), 3.66 (s, 3H), 2.46 (dd, *J* = 12.6, 5.0 Hz, 1H), 2.41 (dd, *J* = 12.6, 3.8 Hz, 1H), 2.10-1.98 (m, 2H), 1.53-1.26 (m, 6H), 0.86 (s, 9H), 0.05 (s, 3H), 0.03 (s, 3H); ^{13}C NMR ($CDCl_3$, 100 MHz) δ 139.0, 114.6, 69.6, 51.6, 42.7, 37.6, 31.1, 29.0, 25.9, 24.6, 18.1, -4.4, -4.7.

Carboxylic acid 121

To a solution of methyl ester **120** (48 mg, 0.16 mmol) in THF (1.5 mL) was added a solution of LiOH*H_2O (20 mg, 0.48 mmol) in H_2O (500 μL). The solution was stirred for 24 h at room temperature, and after this period of time TLC analysis

indicated almost no reaction. An additional portion of LiOH*H_2O (82 mg, 1.95 mmol) was added, and the mixture was stirred for an additional 12 h at room temperature. After this period of time, acetic acid was added dropwise to the reaction mixture until it was slightly acidic according to pH paper, and the mixture was partitioned between H_2O and EtOAc. The layers were separated and the aqueous layer was extracted with two additional portions of EtOAc. The combined organic layers were dried over Na_2SO_4, filtered, and concentrated under reduced pressure. The residue was purified by column chromatography to provide the carboxylic acid **121** (31 mg, 67%). ^{1}H NMR ($CDCl_3$, 400 MHz) δ 5.79 (ddt, *J* = 17.1, 10.0, 6.7 Hz, 1H), 4.99 (d, *J* = 17.1 Hz, 1H), 4.94 (d, 10.0 Hz, 1H), 4.15-4.05 (m, 1H), 2.51 (dd, *J* = 13.3, 3.7 Hz, 1H), 2.47 (dd, *J* = 13.3, 4.7 Hz, 1H), 2.10-1.98 (m, 2H), 1.62-1.18 (m, 6H), 0.87 (s, 9H), 0.08 (s, 3H), 0.06 (s, 3H); ^{13}C NMR ($CDCl_3$, 100 MHz) δ 177.1, 138.8, 114.7, 69.5, 42.2, 33.8, 25.9, 24.7, 18.1, -4.4, -4.7; ESI-MS *m/z* 285.10 $[M-H]^-$; HR-EI-MS *m/z* calcd. for $C_{15}H_{29}O_3Si_1$ $[M-H]^+$: 285.1880, found 285.1883.

Diene-ester 122

A solution of carboxylic acid **121** (31 mg, 0.108 mmol), alcohol **30** (24 mg, 0.095 mmol), DMAP (13 mg, 0.108 mmol), and CSA (12 mg, 0.054 mmol) in CH_2Cl_2 (3 mL) was stirred, and cooled to 0 °C. To the cooled solution was added DCC (33 mg, 0.162 mmol) in one portion, and the ice-bath was allowed to melt as the reaction stirred for 12 h. The reaction mixture became cloudy with precipitated dicyclohexylurea, and the suspension was diluted with CH_2Cl_2 and extracted sequentially with 10% aqueous citric acid, deionized H_2O, brine, and then the organic

layer was dried over Na_2SO_4, filtered and concentrated under reduced pressure. The residue was purified by column chromatography (10:1 hexanes / ethyl acetate) to provide the diene-ester **122** (46 mg, 92%) as a clear oil. ^{1}H NMR ($CDCl_3$, 400 MHz) δ 6.32 (s, 1H), 5.87-5.73 (m, 1H), 5.72-5.60 (m, 1H), 5.18-4.89 (m, 4H), 4.12-4.01 (m, 1H), 2.56-2.33 (m, 3H), 2.11-1.98 (m, 2H), 1.81 (s, 3H), 1.51-1.21 (m, 6H), 0.92 (d, *J* = 6.9 Hz, 3H), 0.87 (s, 9H), 0.052 (s, 3H), 0.033 (s, 3H); ^{13}C NMR ($CDCl_3$, 100 MHz) δ 170.6, 144.5, 139.4, 139.0, 116.0, 114.6, 81.8, 80.5, 69.3, 42.9, 40.3, 37.3, 33.9, 26.0, 24.7, 20.3, 18.2, 16.6, -4.5, -4.5; ESI-MS *m/z* 543.04 $[M+Na]^+$, 520.74 $[M+H]^+$; HR-EI-MS *m/z* calcd. for $C_{23}H_{41}O_3I_1Si_1$ $[M]^+$: 520.1864, found 520.1851.

Vinyl iodide lactone 123

A solution of the diene-ester **122** (45 mg, 0.0864 mmol) in CH_2Cl_2 (9 mL) was stirred, and a catalytic amount of the second generation Grubbs catalyst was quickly added under a blanket of Ar. A condenser was attached, and the solution was heated to reflux for 2 h, at which point the color had changed from pink to brown. An additional portion (catalytic amount) of the catalyst was added, and the solution was refluxed for an additional 2 h. At this time, TLC of the reaction mixture (100% hexanes) indicated the formation of a lower R_f spot, and the disappearance of **122** (higher in R_f). The solution was filtered through a silica gel plug (washed with CH_2Cl_2) and concentrated under reduced pressure. The residue was purified by column chromatography to provide the vinyl iodide lactone **123** (33 mg, 77%) as a clear oil. $[\alpha]_D^{22}$ -3.2 (*c* 0.0625, CH_2Cl_2); ^{1}H NMR ($CDCl_3$, 300 MHz) δ 6.42 (s, 1H), 5.37 (ddd, *J* = 14.6, 11.0, 3.3 Hz, 1H), 5.14-5.02 (m, 1H), 5.07 (d, *J* = 10.7 Hz, 1H),

4.09-3.93 (m, 1H), 2.58 (dd, *J* = 12.9, 4.1 Hz, 1H), 2.49-2.35 (m, 1H), 2.33-2.18 (m, 1H), 2.27 (dd, *J* = 12.9, 8.1 Hz, 1H), 1.97-1.77 (m, 1H), 1.81 (s, 3H), 1.74-1.47 (m, 2H), 1.36-1.19 (m, 2H), 0.89 (s, 9H), 0.84 (d, *J* = 6.8 Hz, 3H), 0.08 (s, 3H), 0.08 (s, 3H); ^{13}C NMR ($CDCl_3$, 75 MHz) δ 169.5, 144.4, 134.3, 131.9, 83.5, 80.1, 68.2, 43.6, 40.8, 32.9, 31.2, 25.9, 24.4, 24.2, 19.2, 18.2, 16.9, -4.3, -4.6; ESI-MS *m/z* 515.06 $[M+Na]^+$, 492.92 $[M+H]^+$; HR-EI-MS *m/z* calcd. for $C_{21}H_{37}O_3I_1Si_1$ $[M]^+$: 492.1551, found 492.1553.

Stille adduct 125

A mixture of the stannane **32** (16 mg, 0.0313 mmol) and vinyl iodide lactone **123** (15 mg, 0.0313 mmol) was prepared in a 5 mL conical shaped flask and the mixture was dried by toluene azeotrope. A reaction flask was charged with LiCl (4 mg, 0.094 mmol) which had been dried under high vacuum with a heat gun, Pd_2dba_3 (7 mg, 0.008 mmol), and $AsPh_3$ (19 mg, 0.063 mmol) under an argon atmosphere. The mixture of the stannane **32** and vinyl iodide lactone **123** was then dissolved in freshly distilled NMP (0.4 mL), and the solution was transferred to the reaction flask containing the solid reagents. The green suspension was then stirred for 6 h at room temperature, which over the course of the reaction turned to black. The reaction mixture was then diluted with Et_2O and H_2O, and the aqueous layer was extracted with additional Et_2O. The combined organic layers were washed with brine, dried over Na_2SO_4, filtered and concentrated under reduced pressure. The residue was purified by column chromatography (10:1 to 4:1 hexanes / ethyl acetate gradient) to provide the Stille adduct **125** (14 mg, 73%) as an oil which contained an orange colored

impurity. TLC (4:1 hexanes / ethyl acetate): R_f = 0.2; ^{1}H NMR ($CDCl_3$, 400 MHz) δ 6.30 (dd, *J* = 14.5, 10.8 Hz, 1H), 6.08 (d, *J* = 10.8 Hz, 1H), 5.70 (dd, *J* = 15.1, 8.2 Hz), 5.35 (ddd, *J* = 14.5, 10.9, 3.3 Hz, 1H), 5.21-5.02 (m, 1H), 4.93 (d, *J* = 10.6 Hz, 1H), 4.09-3.96 (m, 1H), 3.73-3.63 (m, 1H), 3.41 (s, 3H), 3.18 (td, *J* = 6.3, 4.4 Hz, 1H), 3.01 (dd, *J* = 8.1, 2.3 Hz), 2.85 (dd, *J* = 3.0, 2.8 Hz, 1H), 2.58 (dd, *J* = 12.8, 4.1 Hz, 1H), 2.52-2.36 (m, 3H), 2.30-2.21 (m, 1H), 2.25 (dd, *J* = 12.8, 8.2 Hz, 1H), 1.78-1.38 (m, 8H), 1.71 (s, 3H), 1.16 (d, *J* = 6.8 Hz, 3H), 0.96-0.78 (m, 9H), 0.88 (s, 9H), 0.81 (s, 6H); ^{13}C NMR ($CDCl_3$, 100 MHz) δ 169.7, 136.4, 133.8, 132.9, 132.6, 130.1, 126.6, 83.9, 82.3, 71.8, 68.2, 59.1, 58.2, 57.1, 44.0, 41.4, 40.8, 38.9, 33.0, 31.3, 26.0, 24.5, 24.3, 23.9, 18.3, 17.1, 16.1, 12.0, 10.7, 10.1, -4.3, -4.6; ESI-MS *m/z* 615.37 $[M+Na]^+$; HR-EI-MS *m/z* calcd. for $C_{34}H_{60}O_6Si_1$ $[M]^+$: 592.4154, found 592.4160.

Stille adduct 126

A mixture of the stannane **32** (5 mg, 0.0097 mmol) and vinyl iodide lactone **124** (3 mg, 0.0091 mmol) was prepared in a 5 mL conical shaped flask and the mixture was dried by toluene azeotrope. A reaction flask was charged with LiCl (1 mg, 0.027 mmol) which had been dried under high vacuum with a heat gun, Pd_2dba_3 (2 mg, 0.002 mmol), and $AsPh_3$ (6 mg, 0.018 mmol) under an argon atmosphere. The mixture of the stannane **32** and vinyl iodide lactone **124** was then dissolved in freshly distilled NMP (0.2 mL), and the solution was transferred to the reaction flask containing the solid reagents. The green suspension was then stirred for 6 h at room temperature, which over the course of the reaction turned to black. The reaction mixture was then diluted with Et_2O and H_2O, and the aqueous layer was extracted with

additional Et_2O. The combined organic layers were washed with brine, dried over Na_2SO_4, filtered and concentrated under reduced pressure. The residue was purified by column chromatography (10:1 to 4:1 hexanes / ethyl acetate gradient) to provide the Stille adduct **126** (2 mg, ~50%) as an oil which contained an orange colored impurity. ^{1}H NMR ($CDCl_3$, 400 MHz) δ 6.32 (dd, *J* = 15.2, 10.9 Hz, 1H), 6.09 (d, *J* = 10.9 Hz, 1H), 5.71 (dd, *J* = 15.2, 8.1 Hz, 1H), 5.37-5.26 (m, 1H), 5.11 (dd, *J* = 14.9, 9.7 Hz, 1H), 5.03 (d, *J* = 10.6 Hz, 1H), 3.73-3.65 (m, 1H), 3.41 (s, 3H), 3.18 (td, *J* = 6.3, 4.4 Hz, 1H), 3.01 (dd, *J* = 8.1, 2.1 Hz, 1H), 2.86 (dd, *J* = 3.3, 2.5 Hz, 1H), 2.51-2.34 (m, 2H), 2.25-2.11 (m, 1H), 2.01-1.33 (m, 12H), 1.74 (s, 3H), 1.16 (d, *J* = 6.9 Hz, 3H), 0.92 (d, *J* = 7.0 Hz, 3H), 0.90 (t, *J* = 7.5 Hz), 0.84 (d, *J* = 6.8 Hz).

Model 127

A solution of the Stille adduct **125** (2.6 mg, 0.00436 mmol) was prepared in MeCN (200 μL), and was stirred as HF-py (100 μL of a 70% w/w solution) was added, and the reaction was monitored by TLC (1:1 hexanes / ethyl acetate). When the starting material adduct **125** (R_f = 0.5 in 1:1 hexanes / ethyl acetate) was consumed, the reaction was quenched by the addition of Et_3N (100 μL), and the suspension was filtered through a short silica gel plug which was washed with EtOAc. The solution was concentrated under reduced pressure, and the residue was purified by column chromatography (1:1 to 2:1 ethyl acetate / hexanes gradient) to provide the model **127** (1.2 mg, 60%) as a clear oil. ^{1}H NMR ($CDCl_3$, 500 MHz) δ 6.31 (dd, *J* = 15.5, 11.3 Hz, 1H), 6.08 (d, *J* = 11.3 Hz, 1H), 5.73 (dd, *J* = 15.5, 8.2 Hz, 1H), 5.31-5.24 (m, 1H), 5.18-5.10 (m, 1H), 5.13 (d, *J* = 10.6 Hz, 1H), 3.84-3.73 (m, 1H), 3.73-

3.66 (m, 1H), 3.40 (s, 3H), 3.18 (td, J = 6.2, 4.4 Hz, 1H), 3.00 (dd, J = 8.1, 2.5 Hz, 1H), 2.85 (dd, J = 3.2, 2.2 Hz, 1H), 2.56 (d, J = 3.7 Hz, 1H), 2.51-2.40 (m, 2H), 2.24-1.34 (m, 10H), 1.74 (s, 3H), 1.16 (d, J = 6.8 Hz, 3H), 0.92 (d, J = 6.9 Hz, 3H), 0.90 (t, J = 7.5 Hz, 3H), 0.86 (d, J = 6.8 Hz, 3H).

1.7 Selected NMR Spectra

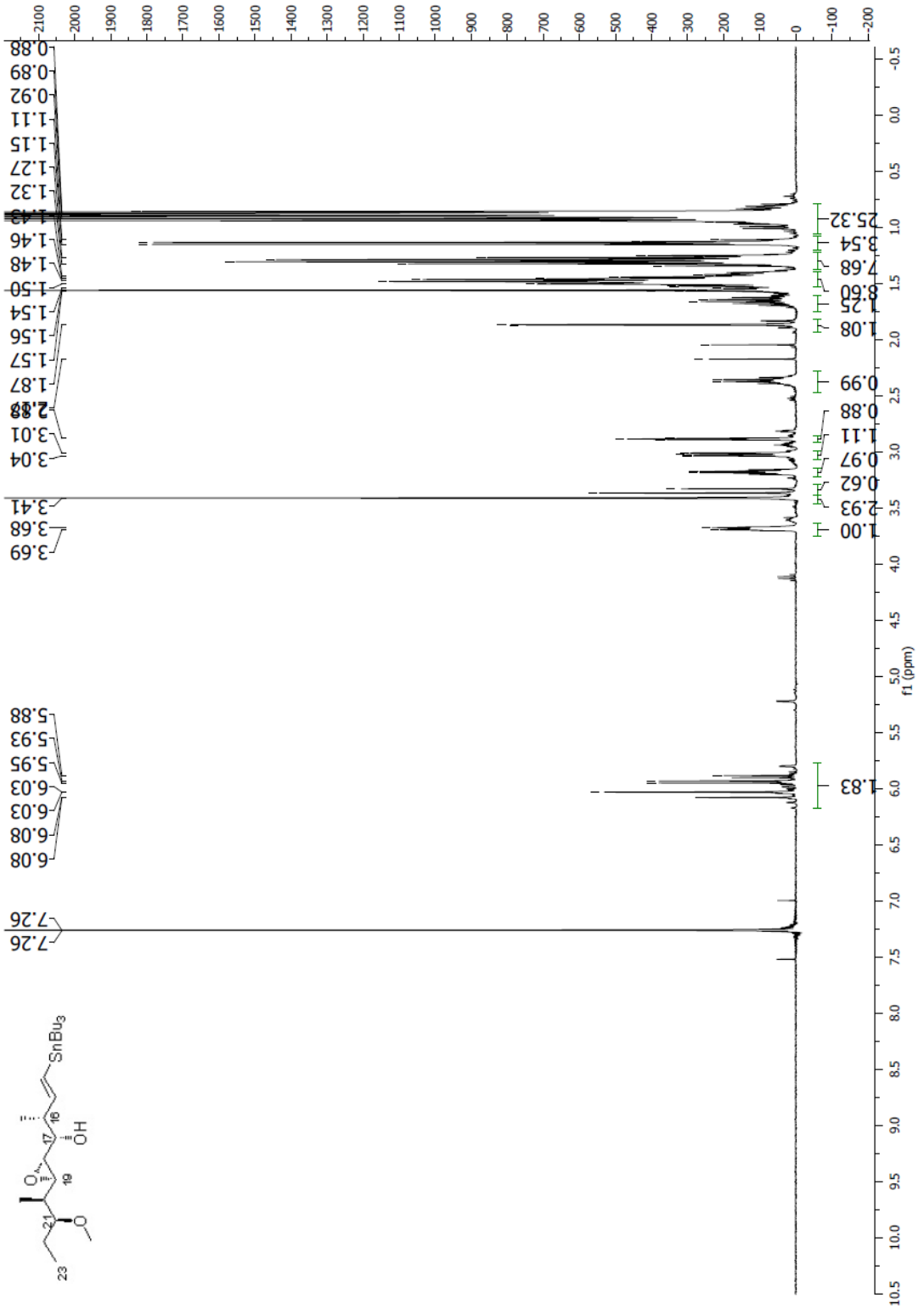

Spectrum 1.1 ^{1}H NMR ($CDCl_3$, 400 MHz) of compound **32**

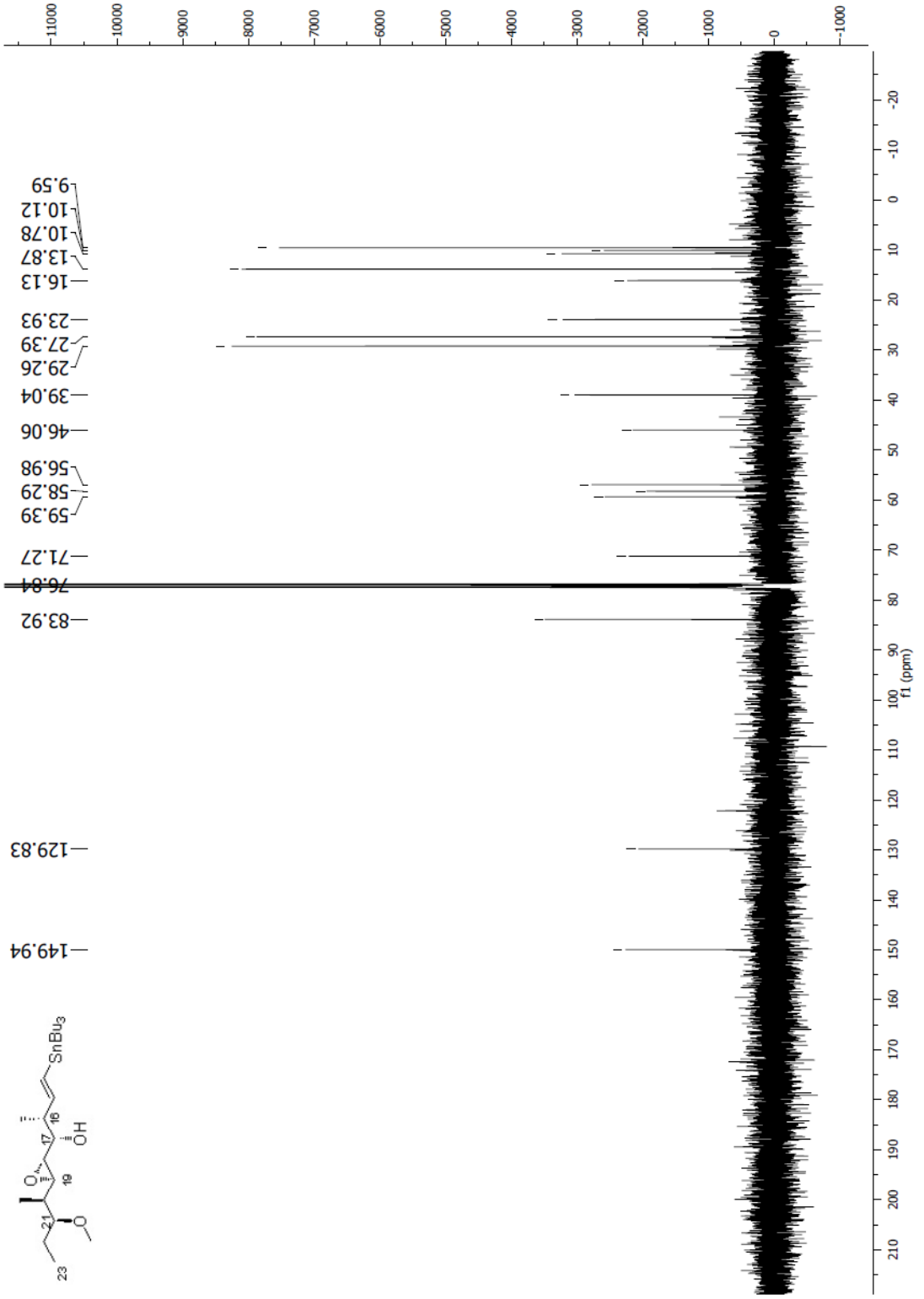

Spectrum 1.2 ^{13}C NMR ($CDCl_3$, 100 MHz) of compound **32**

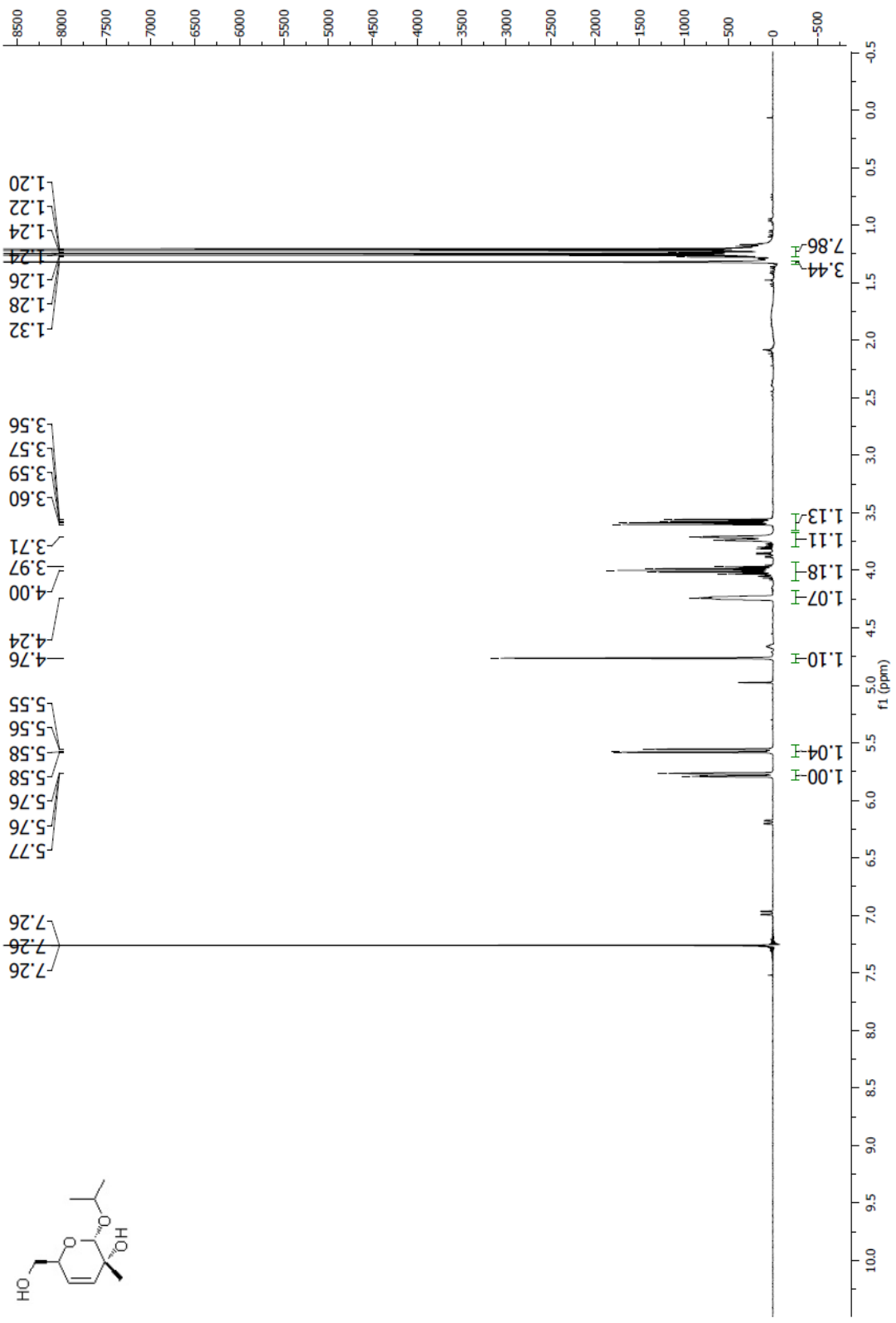

Spectrum 1.3 ^{1}H NMR ($CDCl_3$, 400 MHz) of compound **39**

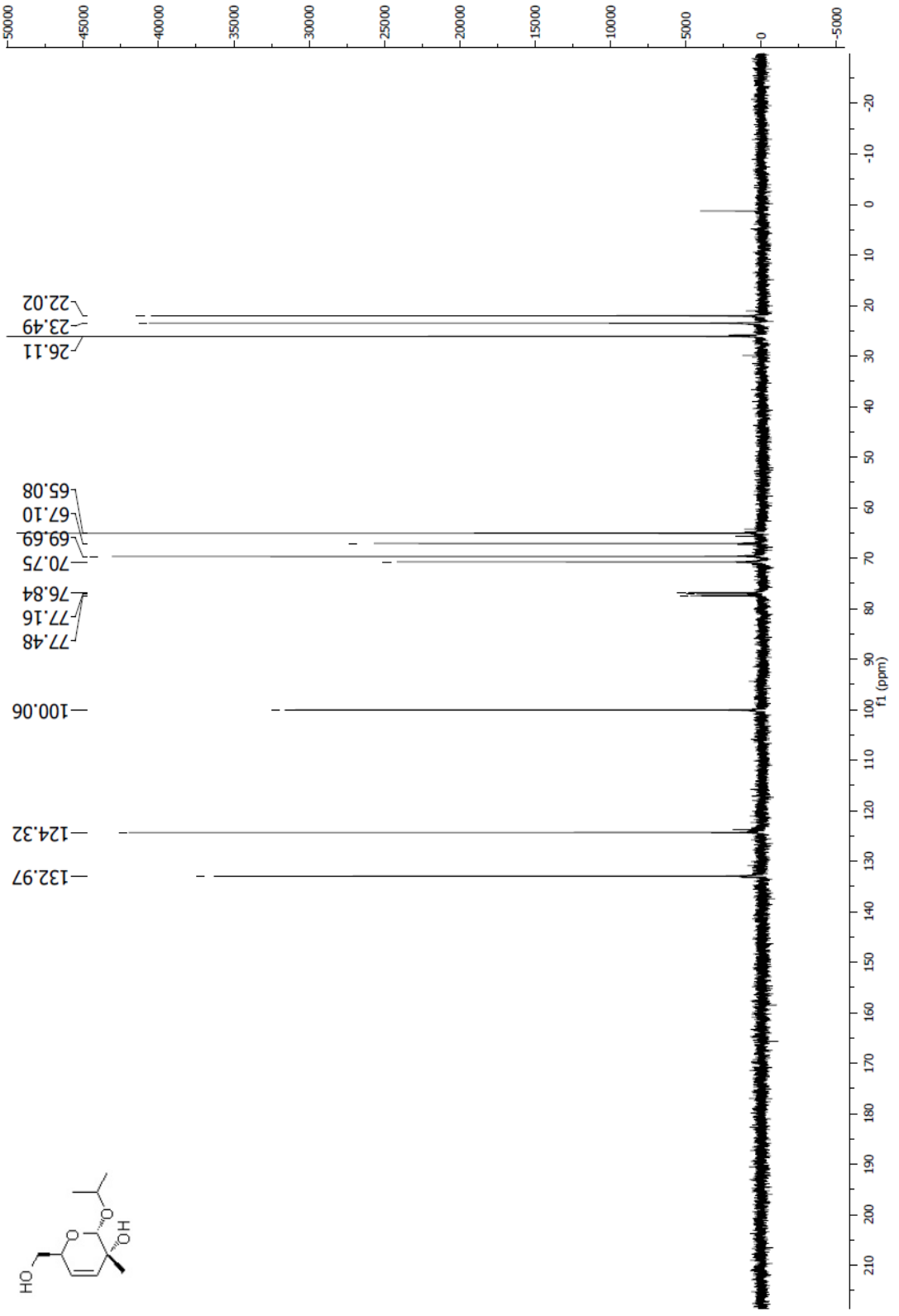

Spectrum 1.4 ^{13}C NMR ($CDCl_3$, 100 MHz) of compound **39**

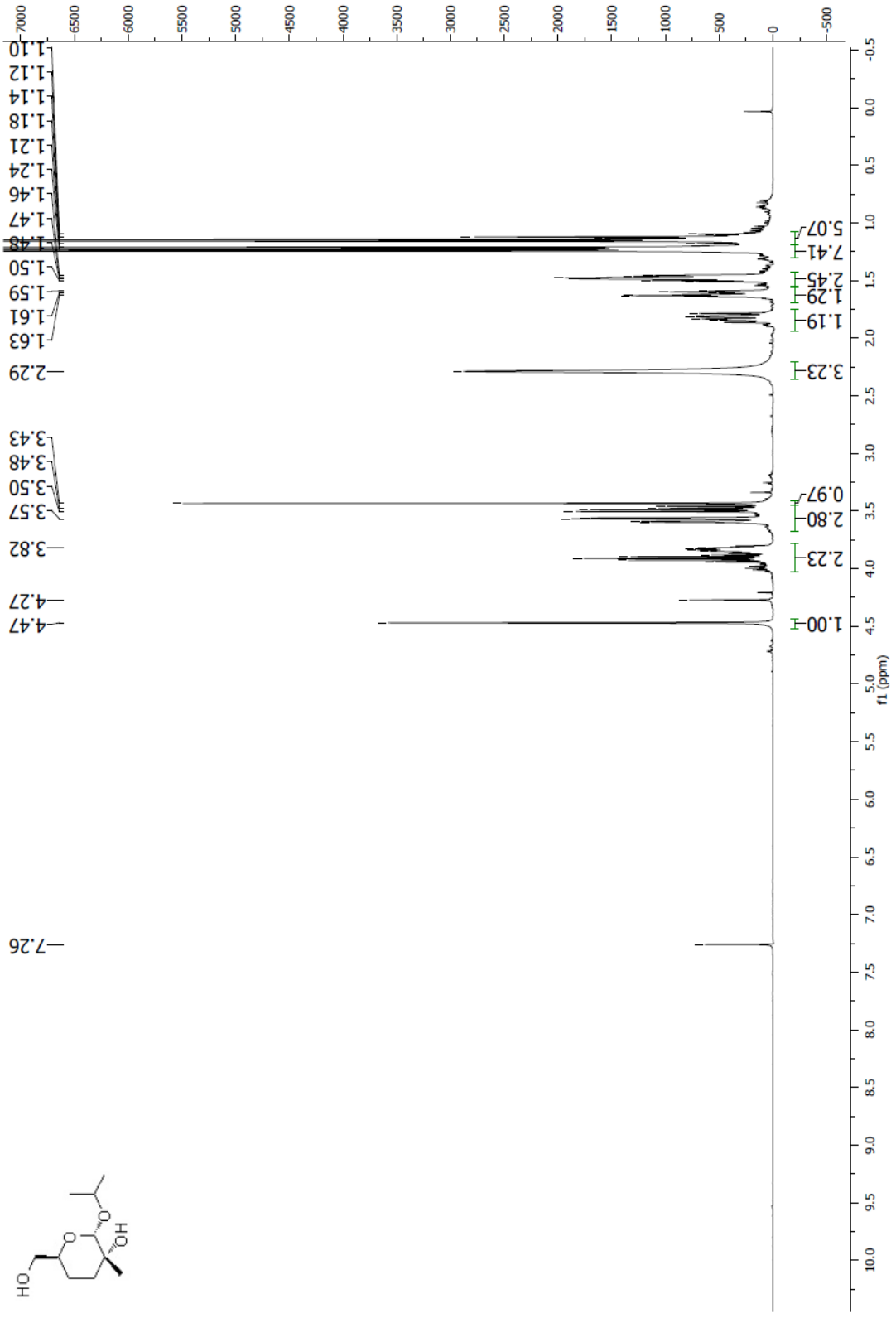

Spectrum 1.5 ^{1}H NMR ($CDCl_3$, 400 MHz) of compound **46**

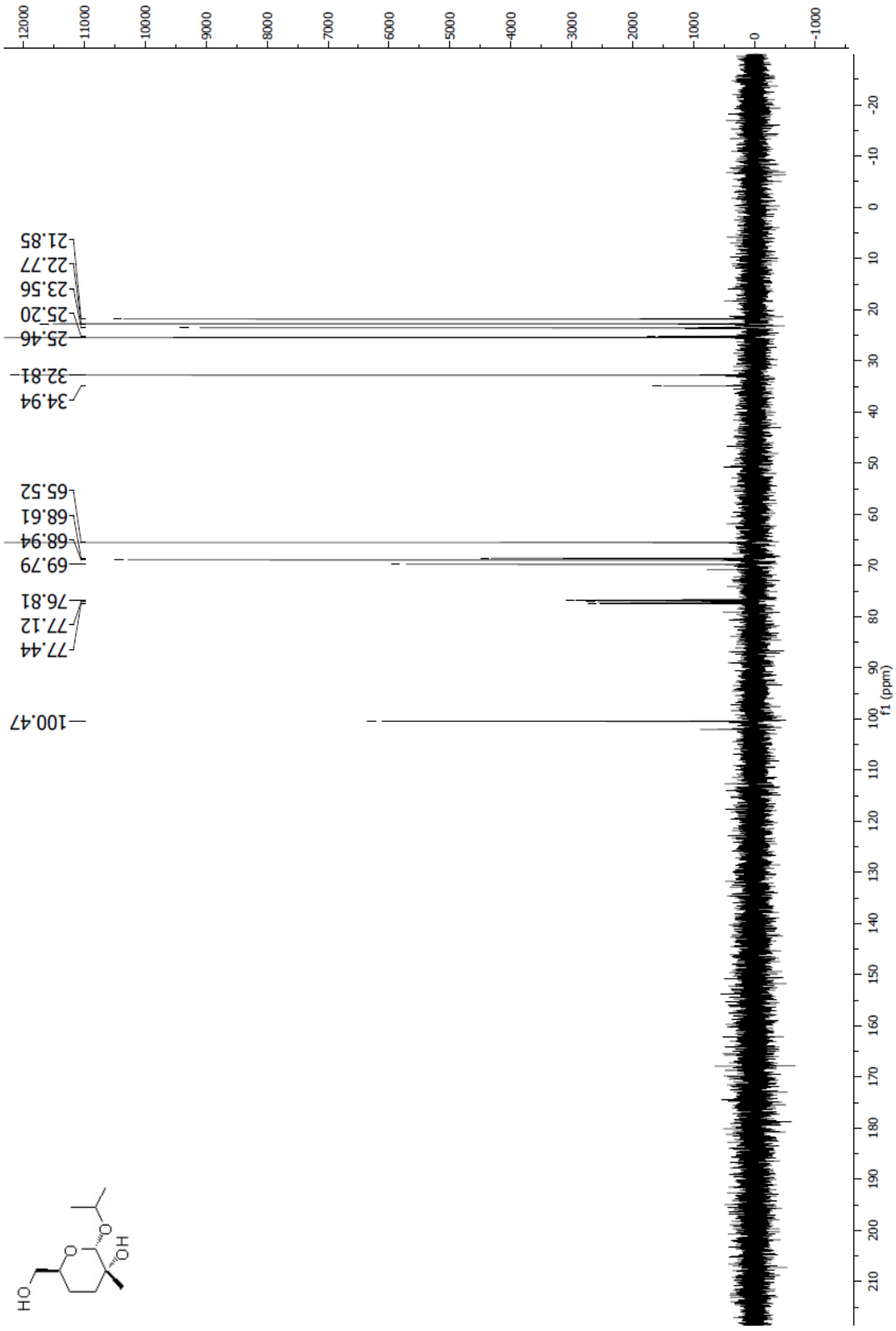

Spectrum 1.6 ^{13}C NMR ($CDCl_3$, 100 MHz) of compound **46**

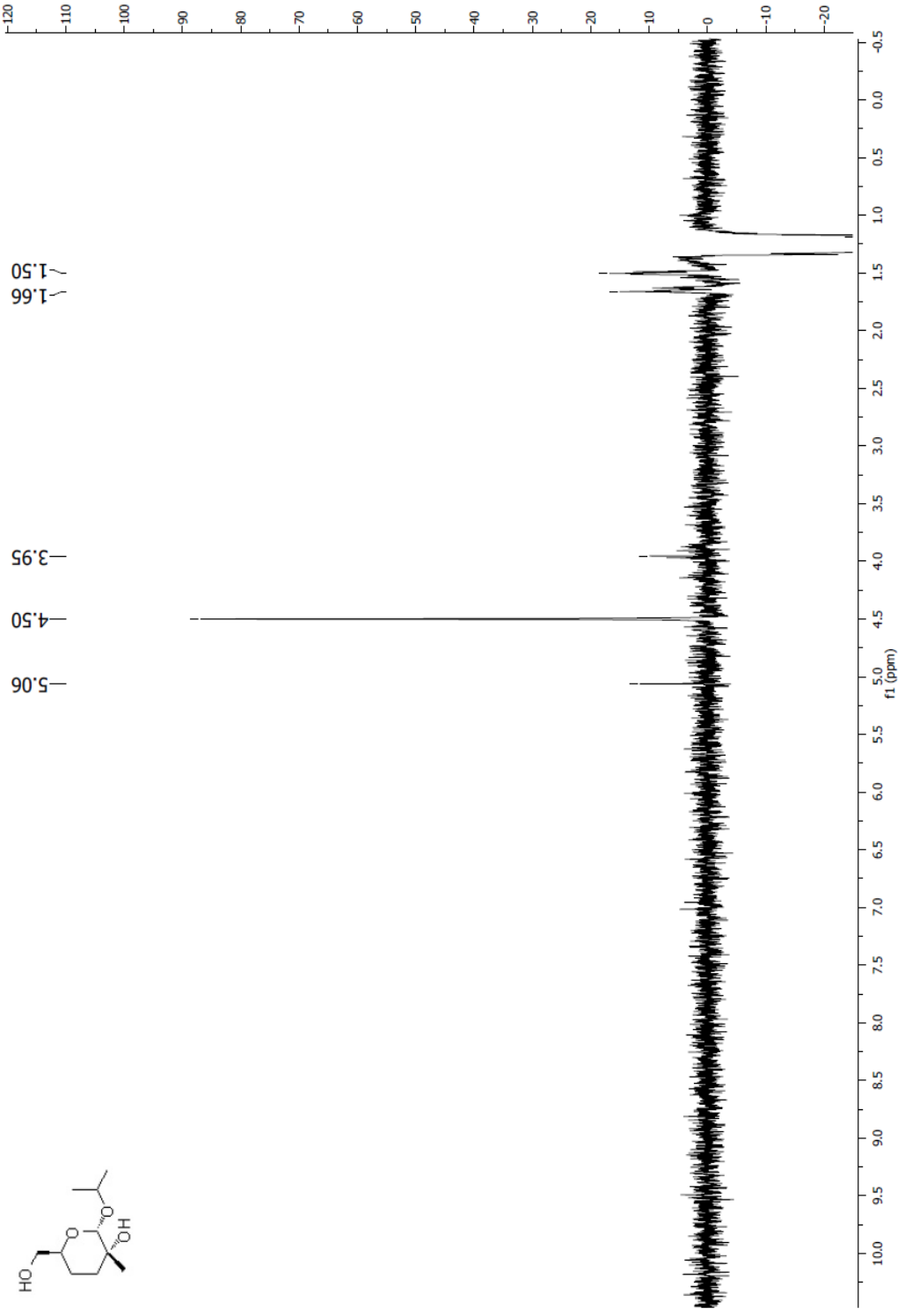

Spectrum 1.7 NOESY1D NMR ($CDCl_3$, 400 MHz) of compound **46**, irradiation at 1.24 ppm, the C-6 methyl singlet

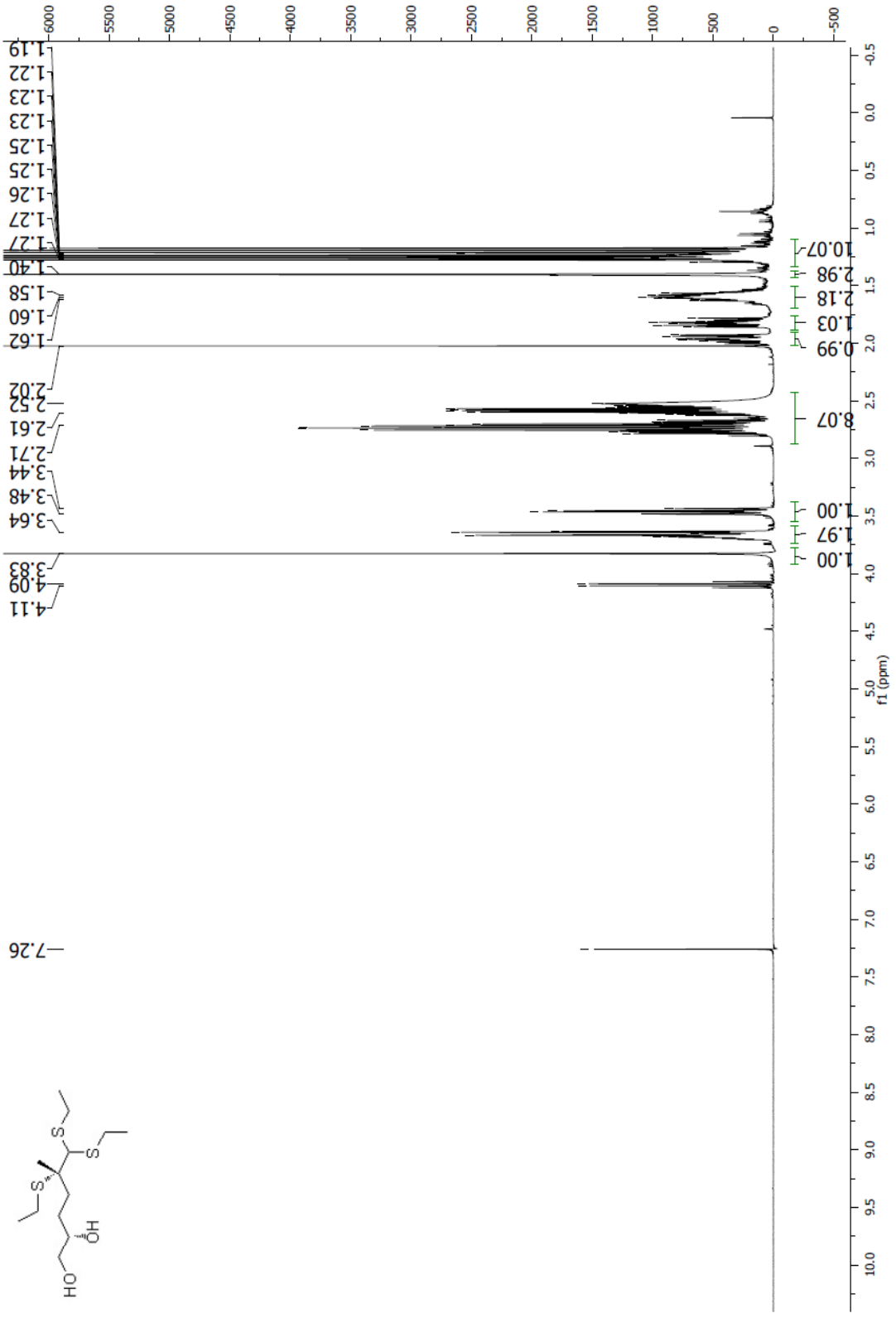

Spectrum 1.8 ^{1}H NMR ($CDCl_3$, 400 MHz) of compound **51**

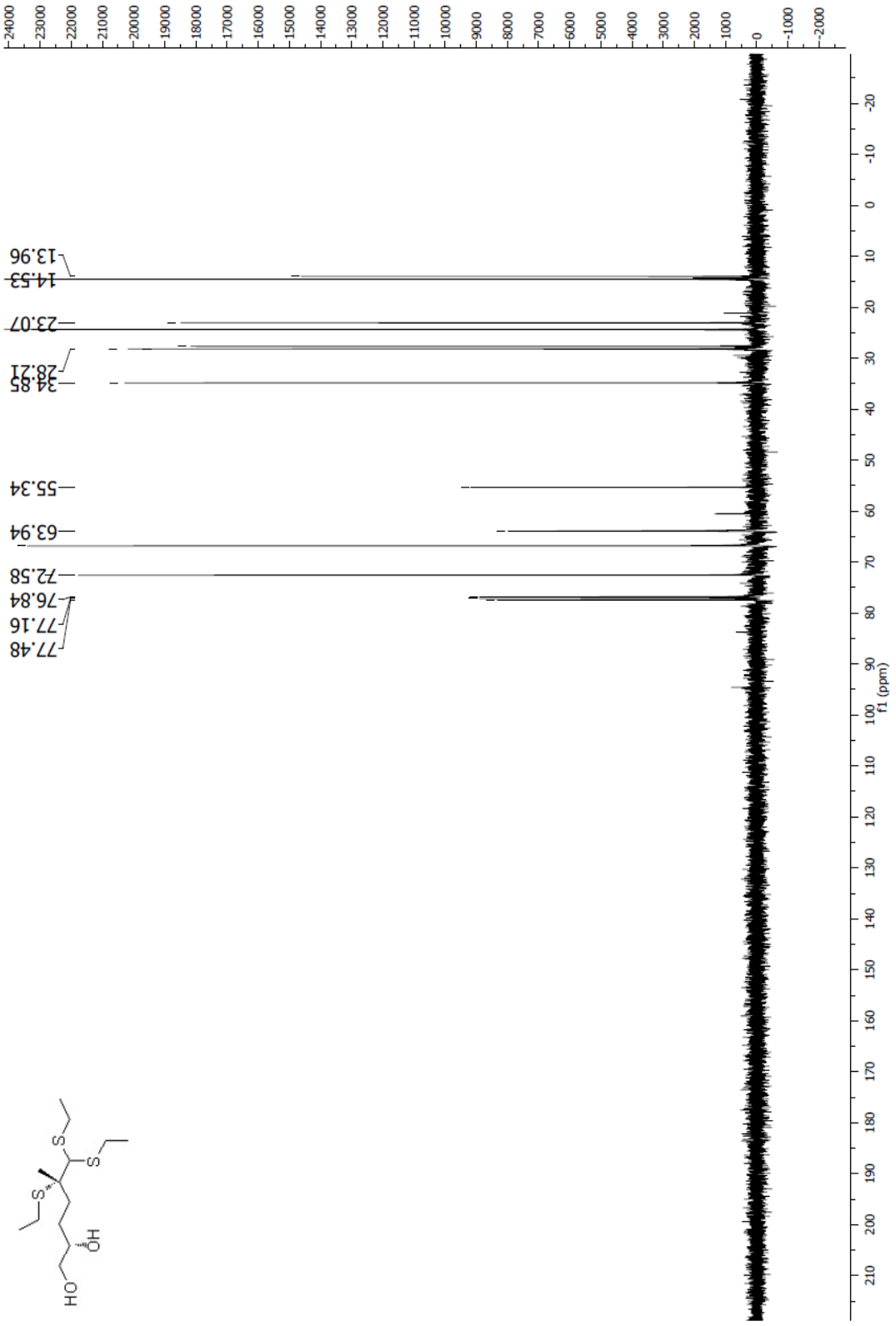

Spectrum 1.9 ^{13}C NMR ($CDCl_3$, 100 MHz) of compound **51**

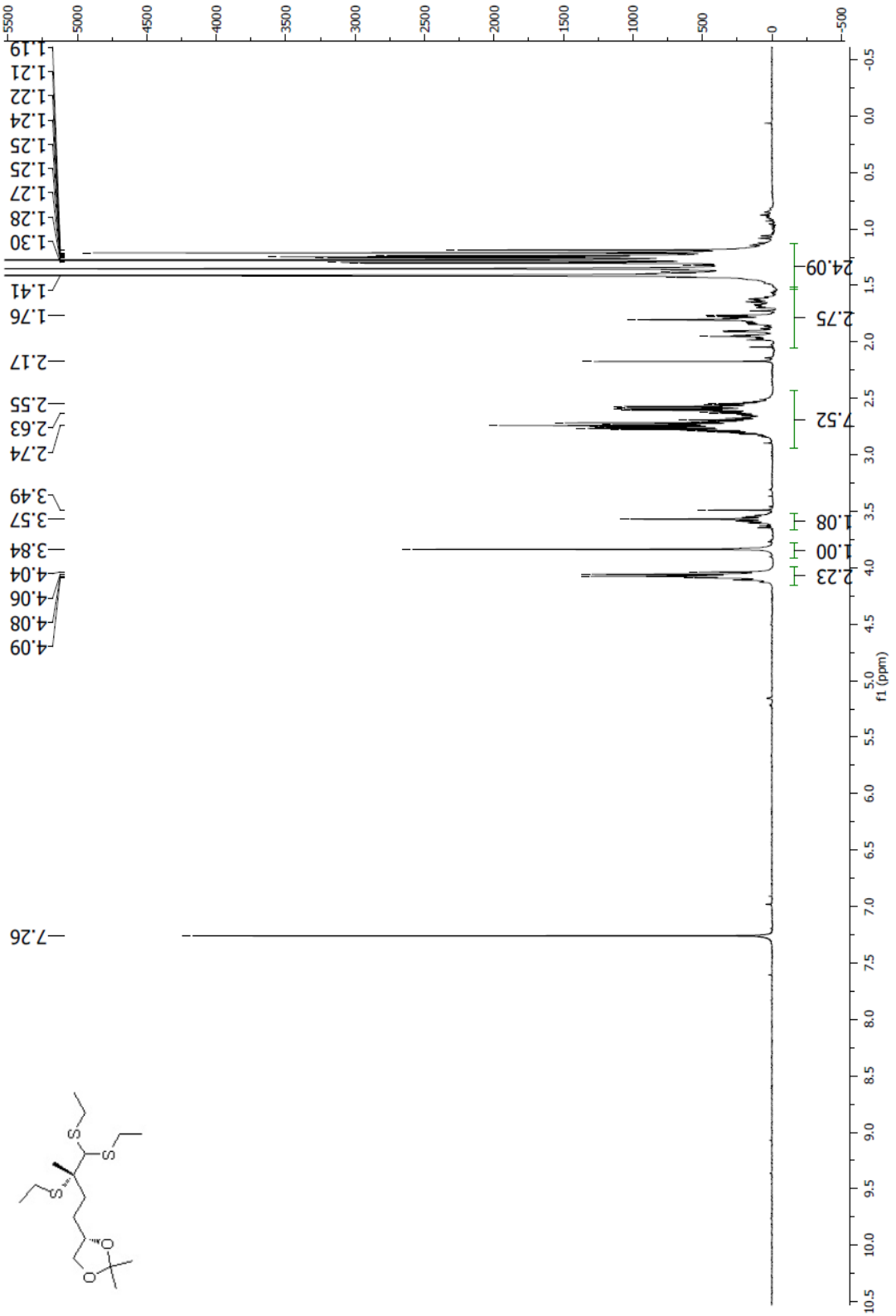

Spectrum 1.10 ^{1}H NMR ($CDCl_3$, 400 MHz) of compound **53**

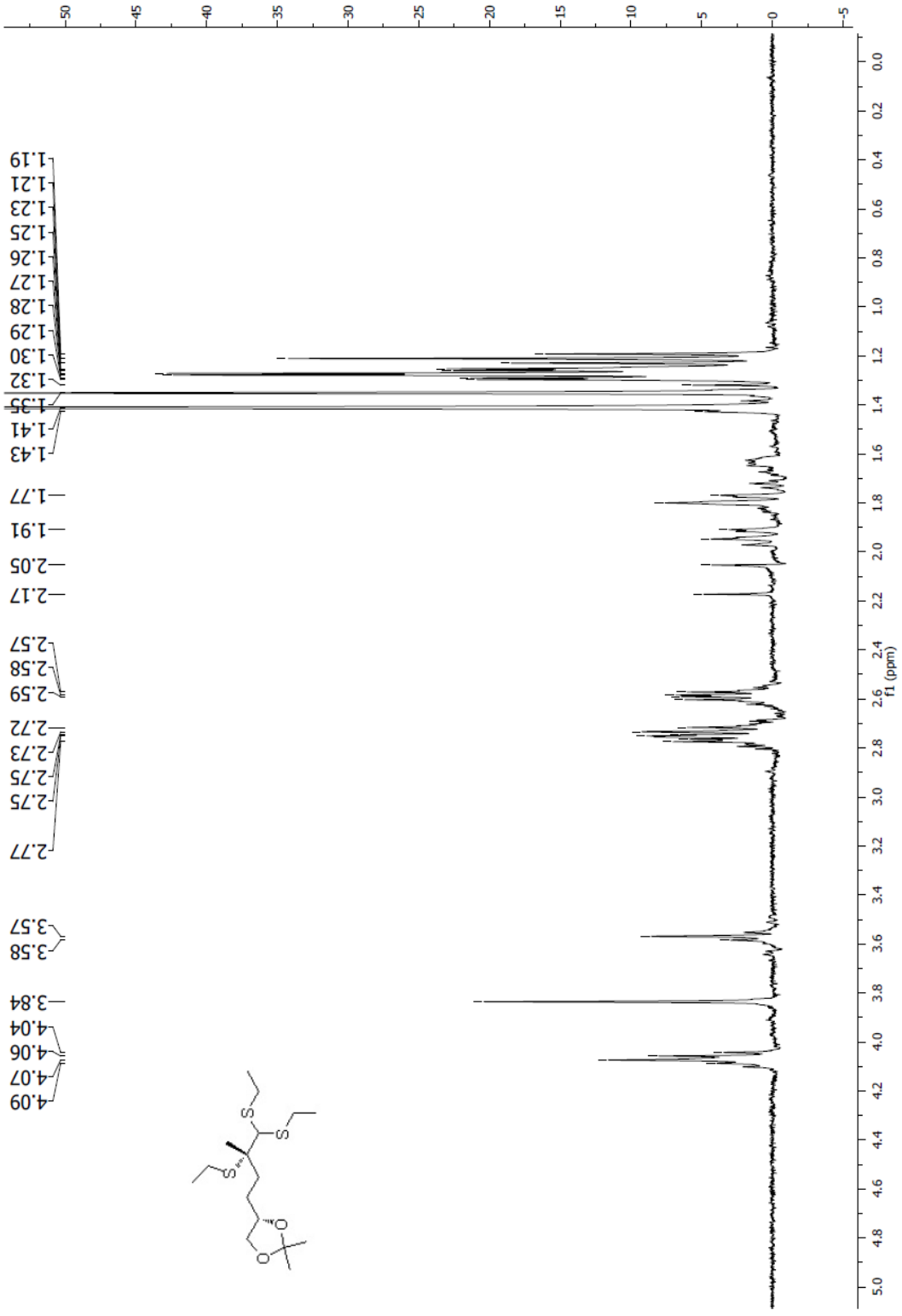

Spectrum 1.11 ^{1}H NMR ($CDCl_3$, 400 MHz) of compound **53**

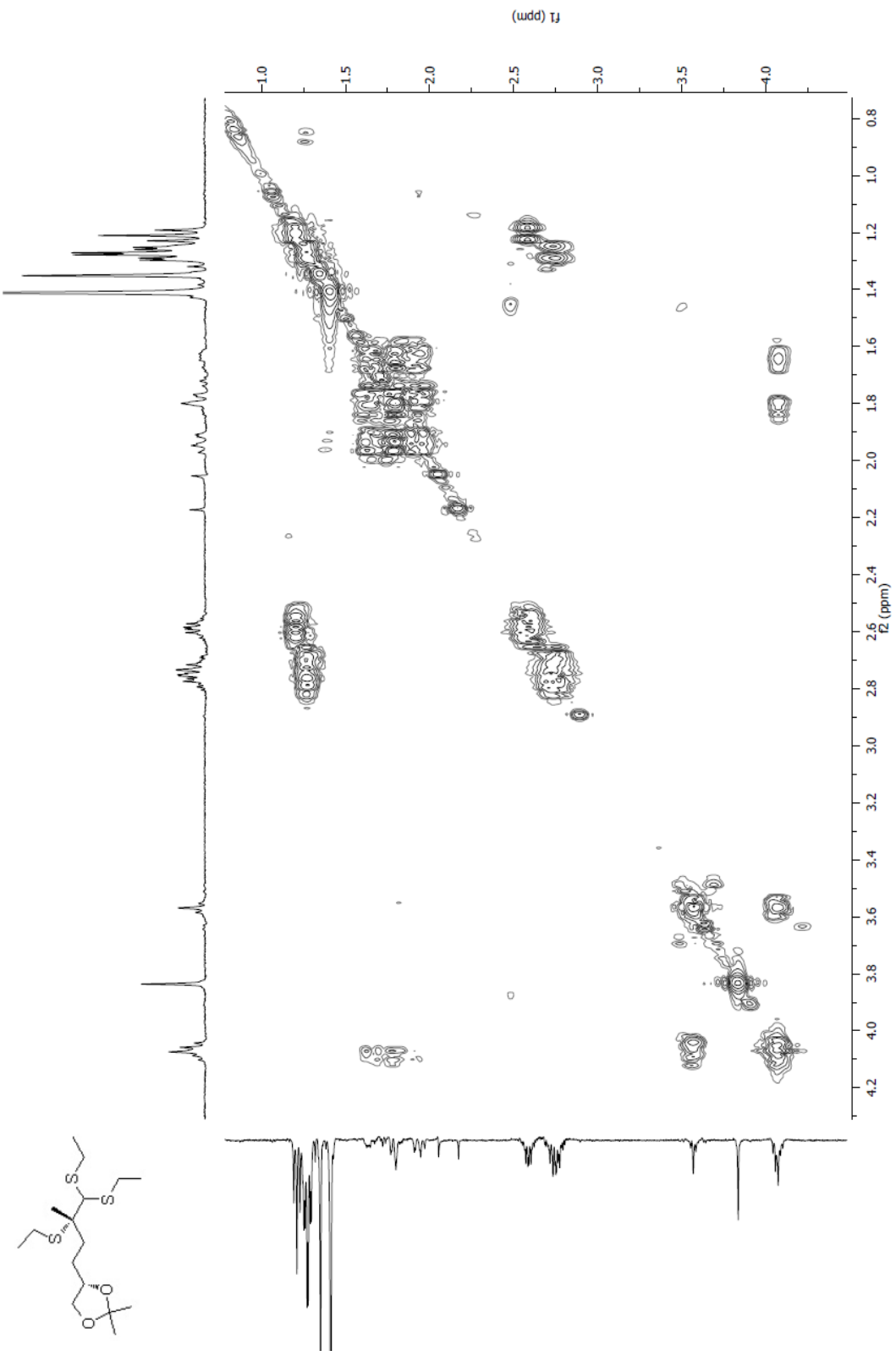

Spectrum 1.12 ^{1}H-^{1}H gCOSY NMR ($CDCl_3$, 400 MHz) of compound **53**

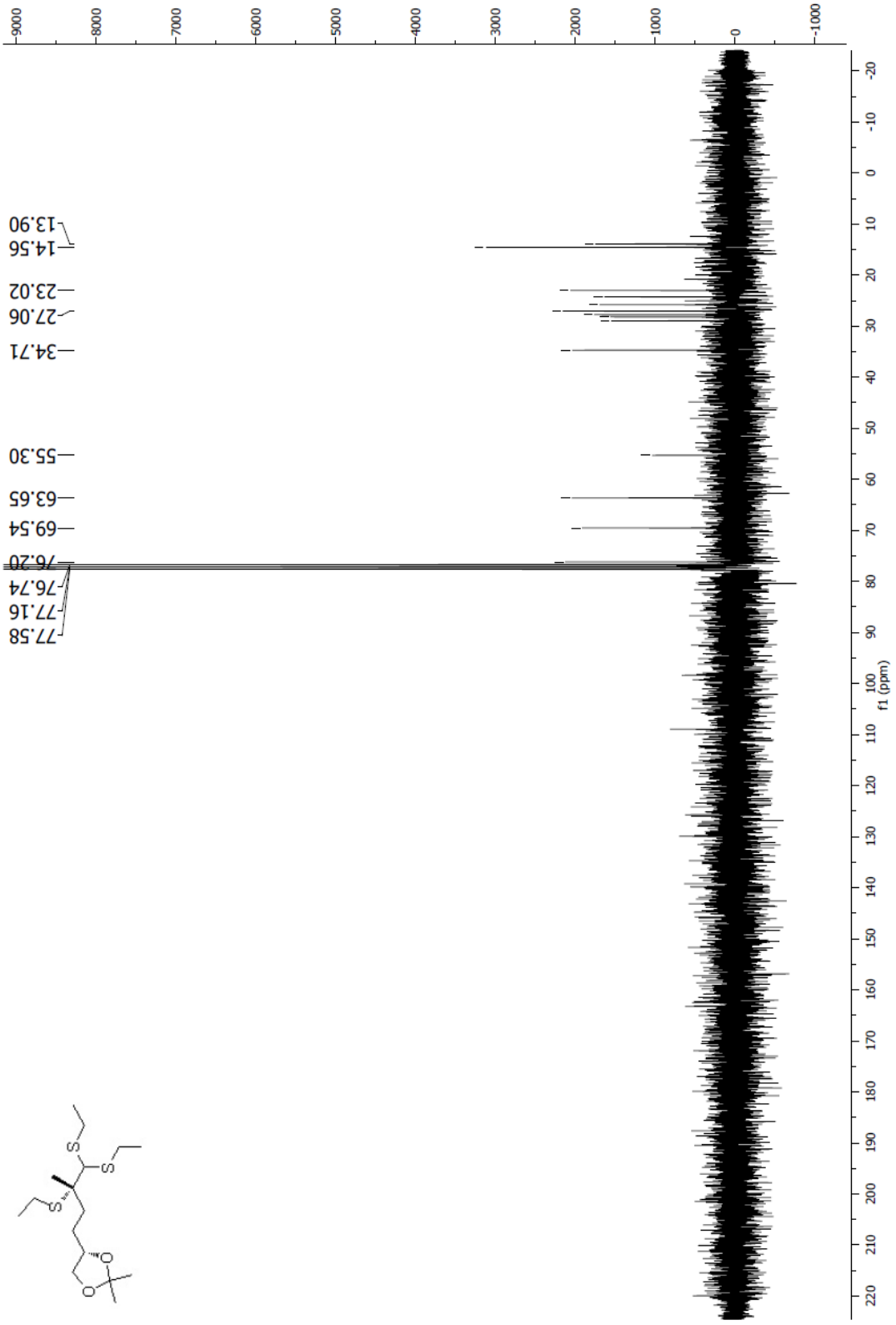

Spectrum 1.13 ^{13}C NMR ($CDCl_3$, 100 MHz) of compound **53**

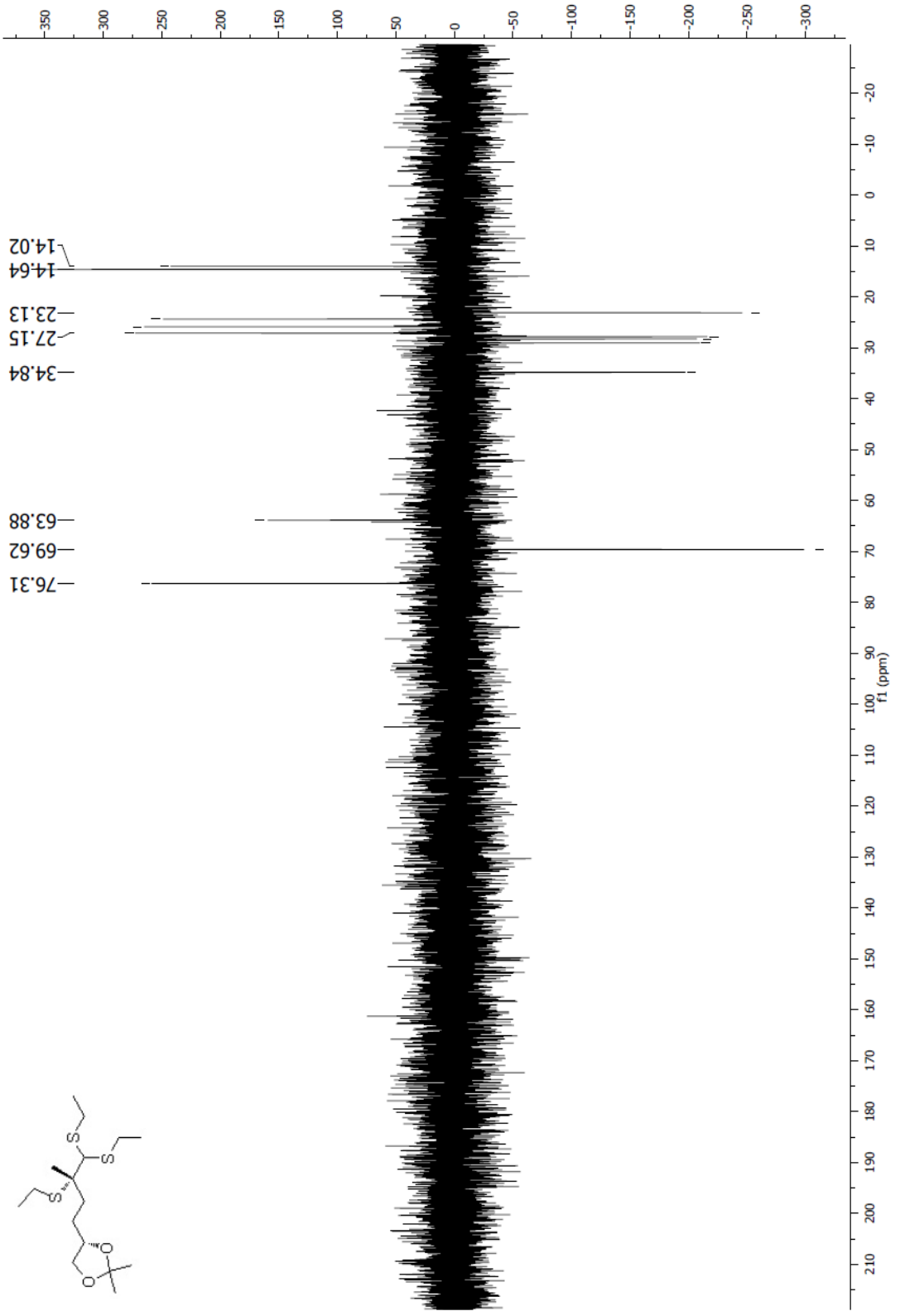

Spectrum 1.14 DEPT135 NMR ($CDCl_3$, 100 MHz) of compound **53**

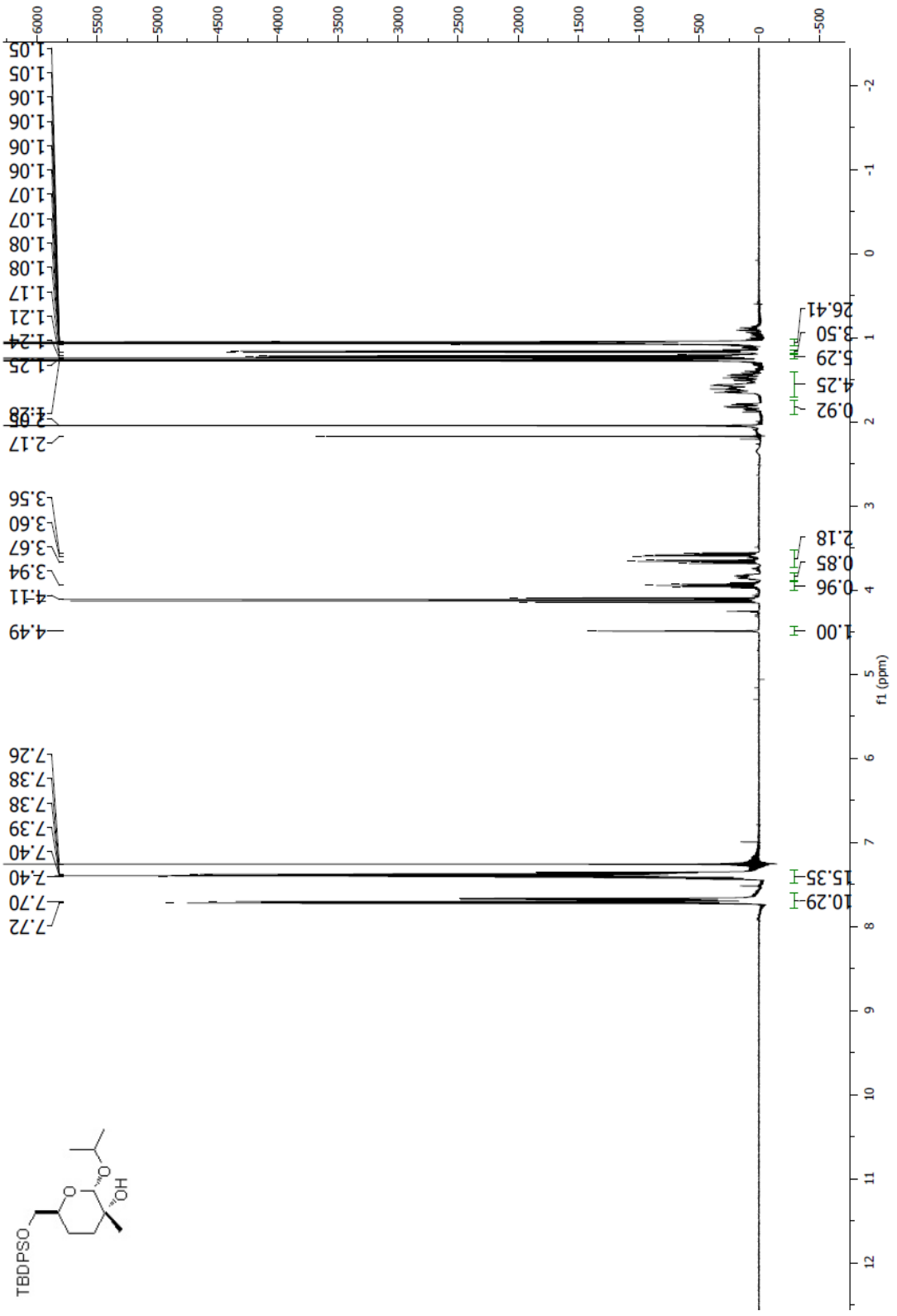

Spectrum 1.15 ^{1}H NMR ($CDCl_3$, 400 MHz) of compound **54**

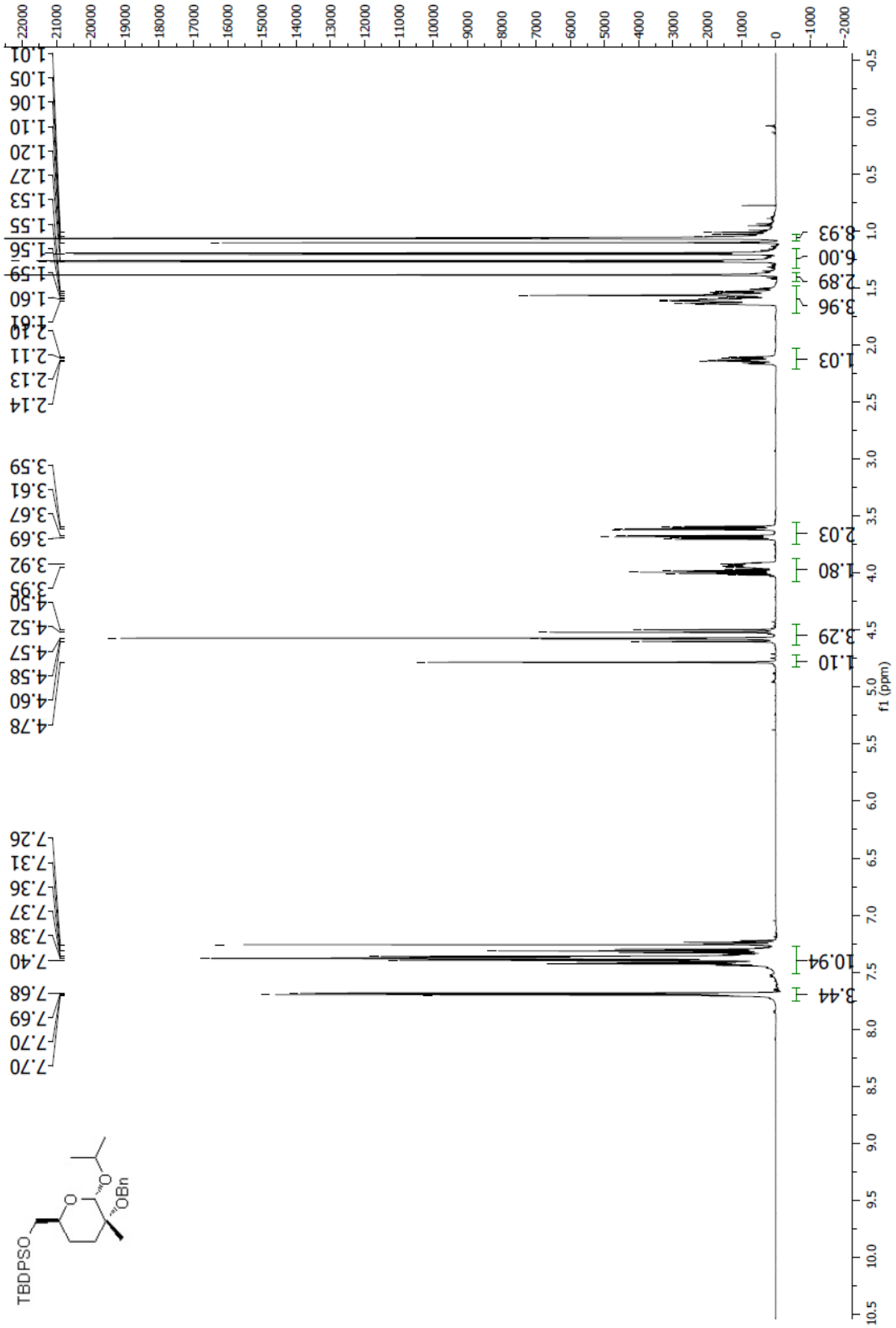

Spectrum 1.16 ^{1}H NMR ($CDCl_3$, 500 MHz) of compound **55**

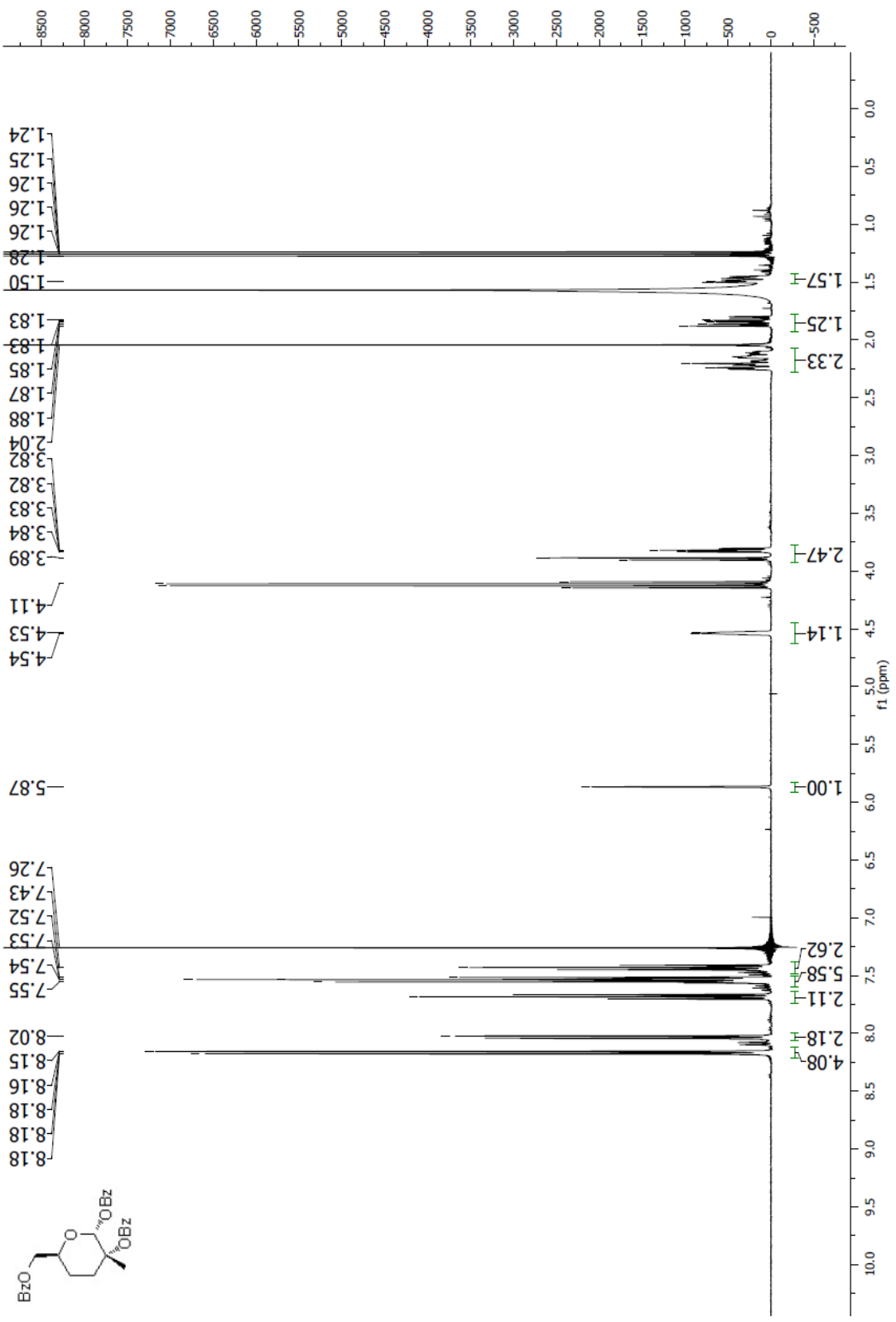

Spectrum 1.17 ^{1}H NMR ($CDCl_3$, 400 MHz) of compound **57**

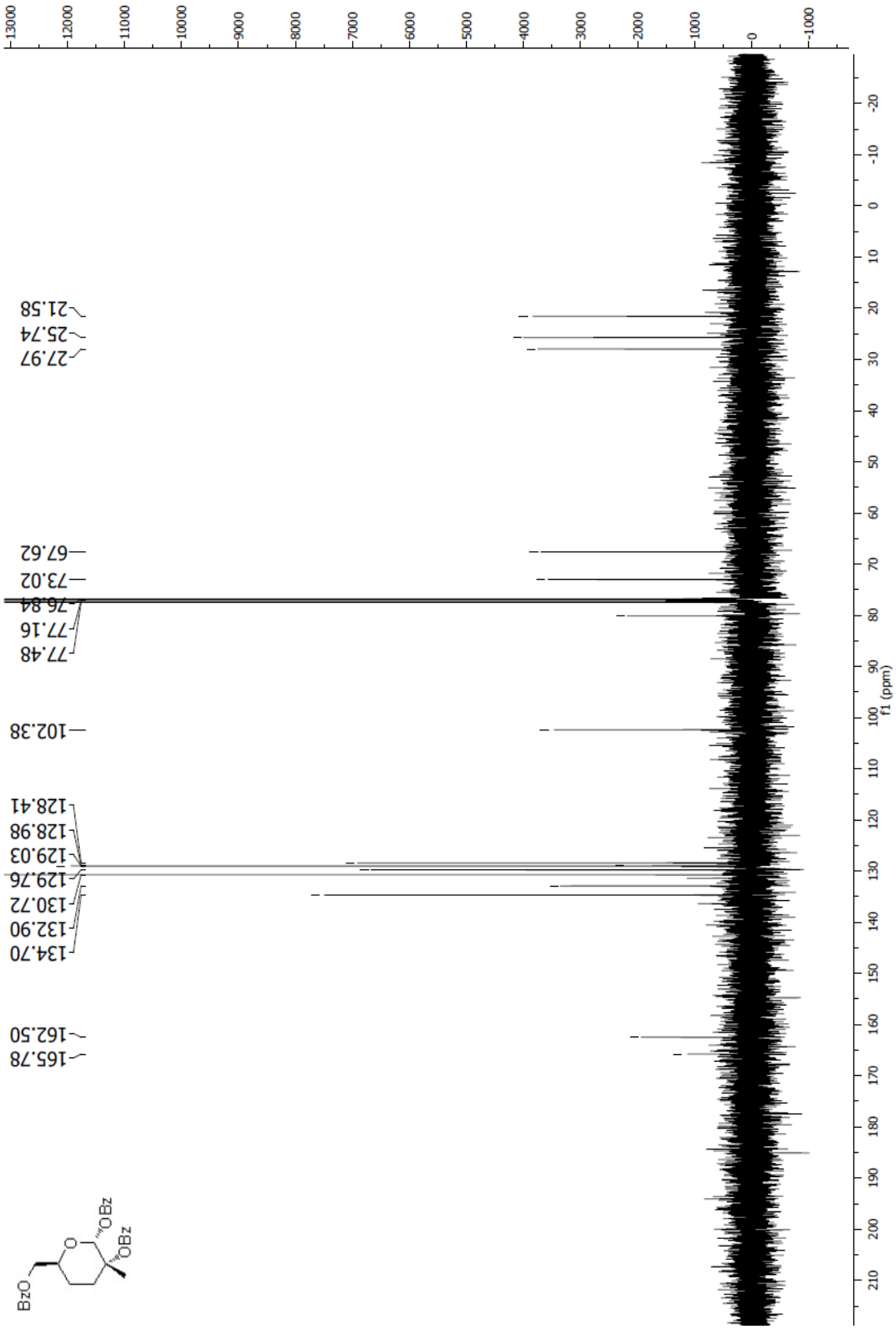

Spectrum 1.18 ^{13}C NMR ($CDCl_3$, 100 MHz) of compound **57**

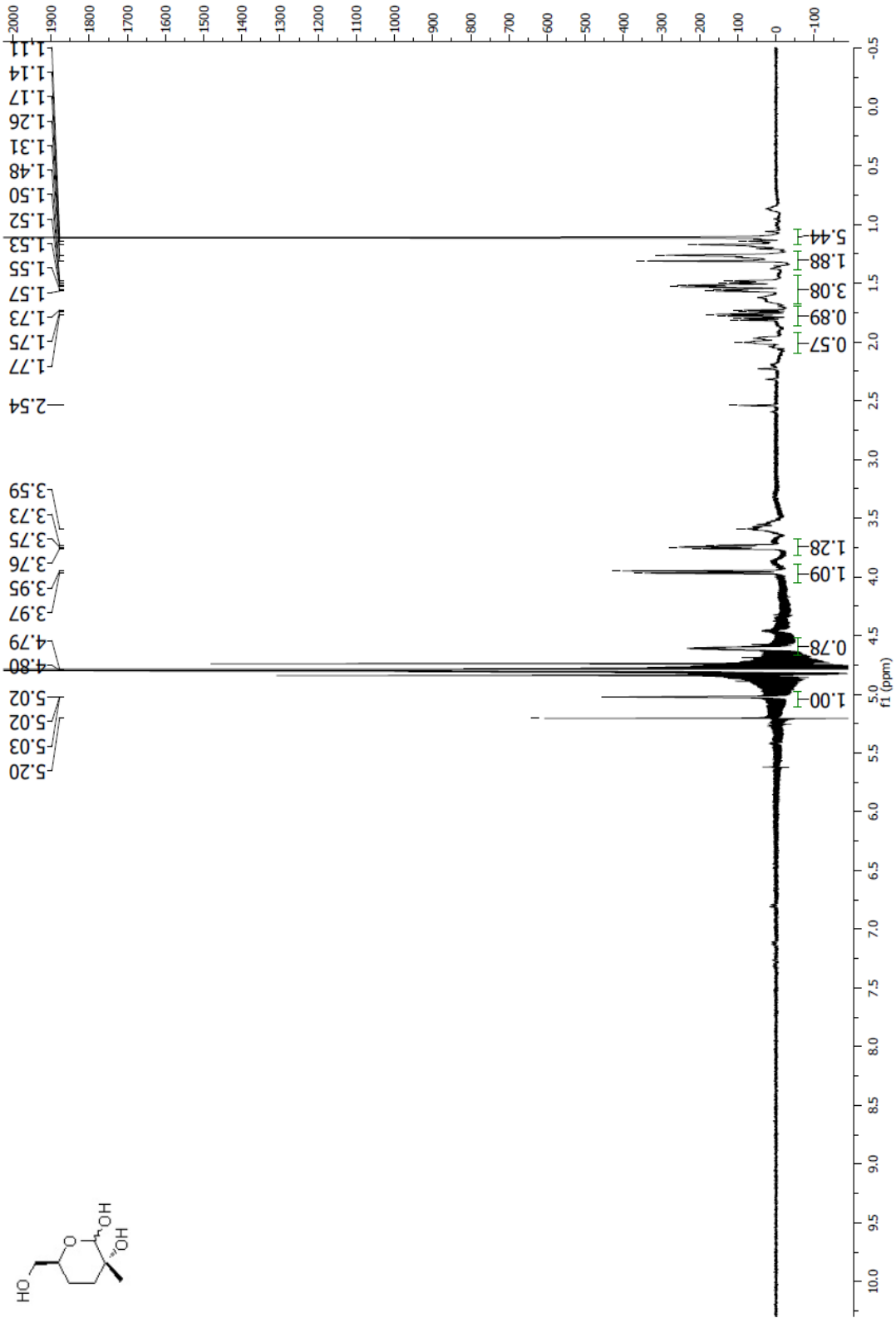

Spectrum 1.19 ^{1}H NMR (D_2O, 400 MHz) of compound **38**

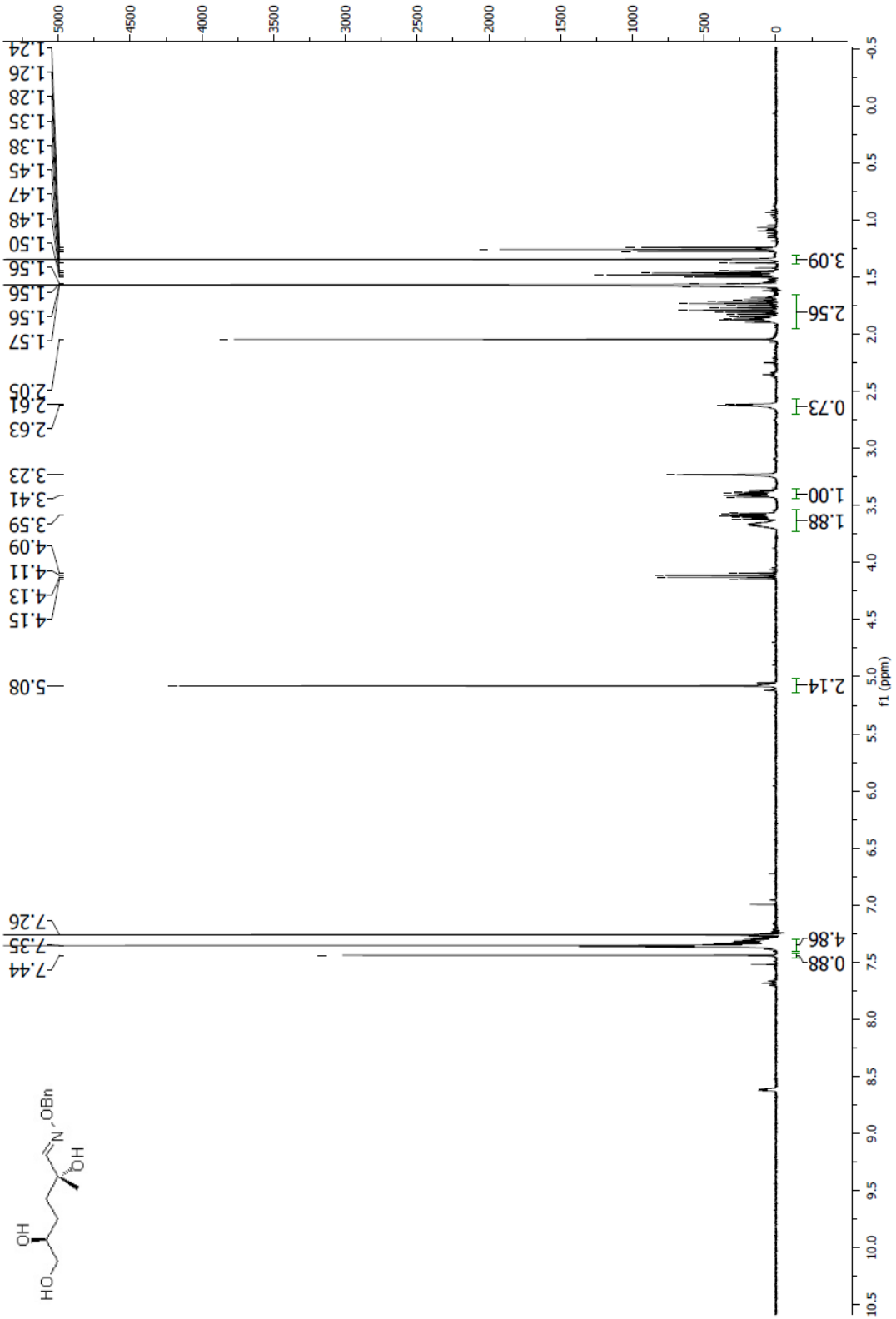

Spectrum 1.20 ^{1}H NMR ($CDCl_3$, 400 MHz) of compound **60**

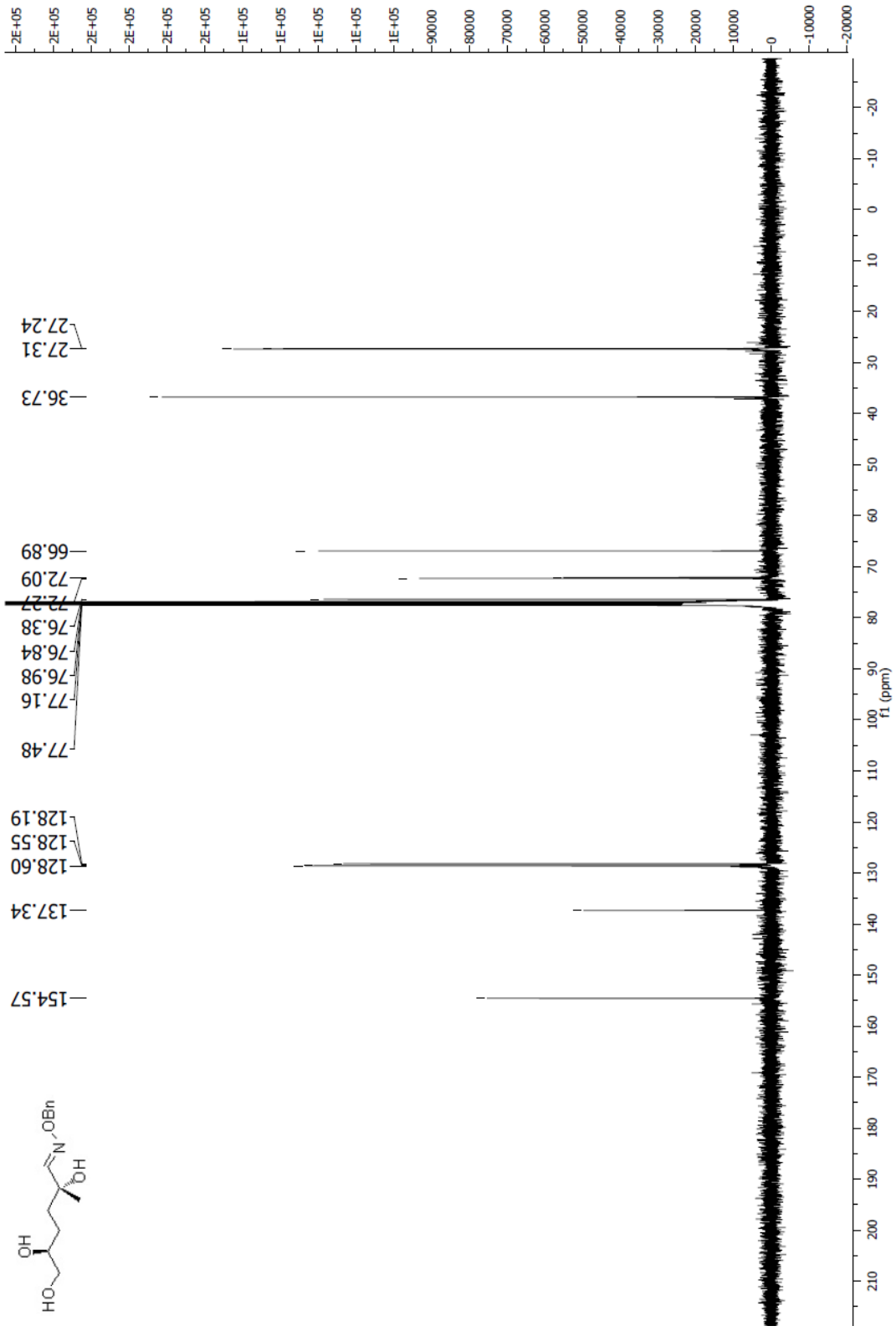

Spectrum 1.21 ^{13}C NMR ($CDCl_3$, 100 MHz) of compound **60**

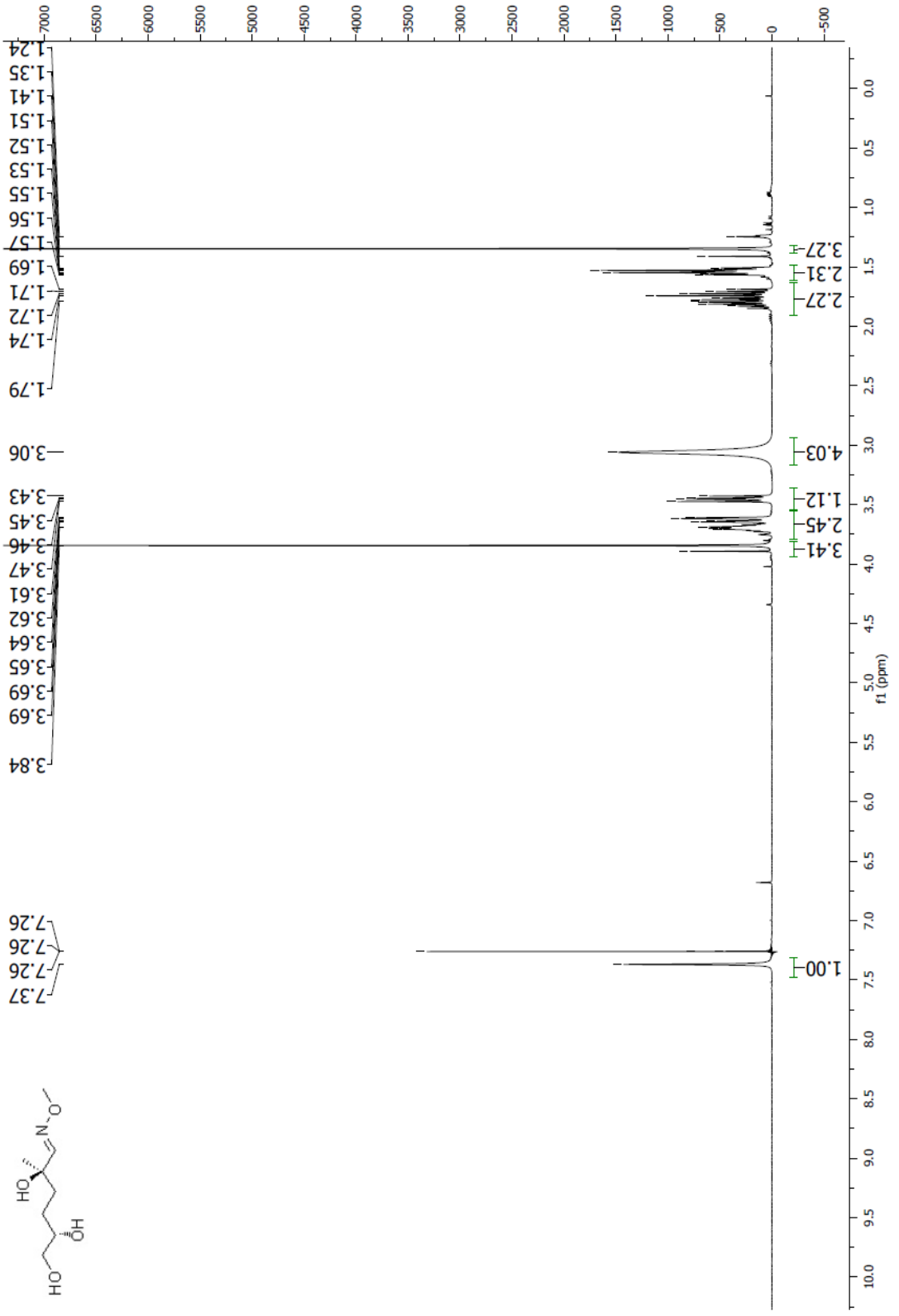

Spectrum 1.22 ^{1}H NMR ($CDCl_3$, 400 MHz) of compound **61**

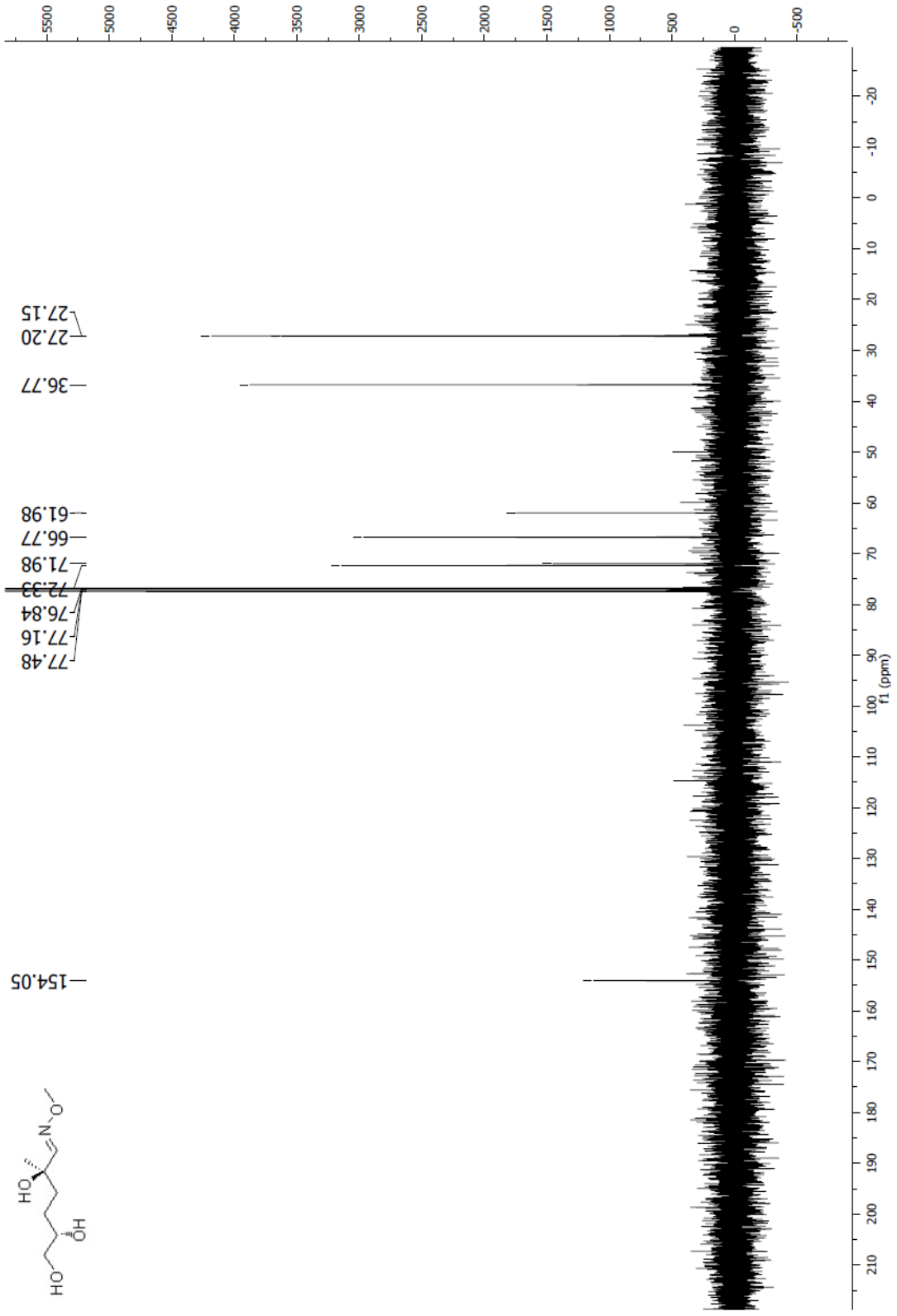

Spectrum 1.23 ^{13}C NMR ($CDCl_3$, 100 MHz) of compound **61**

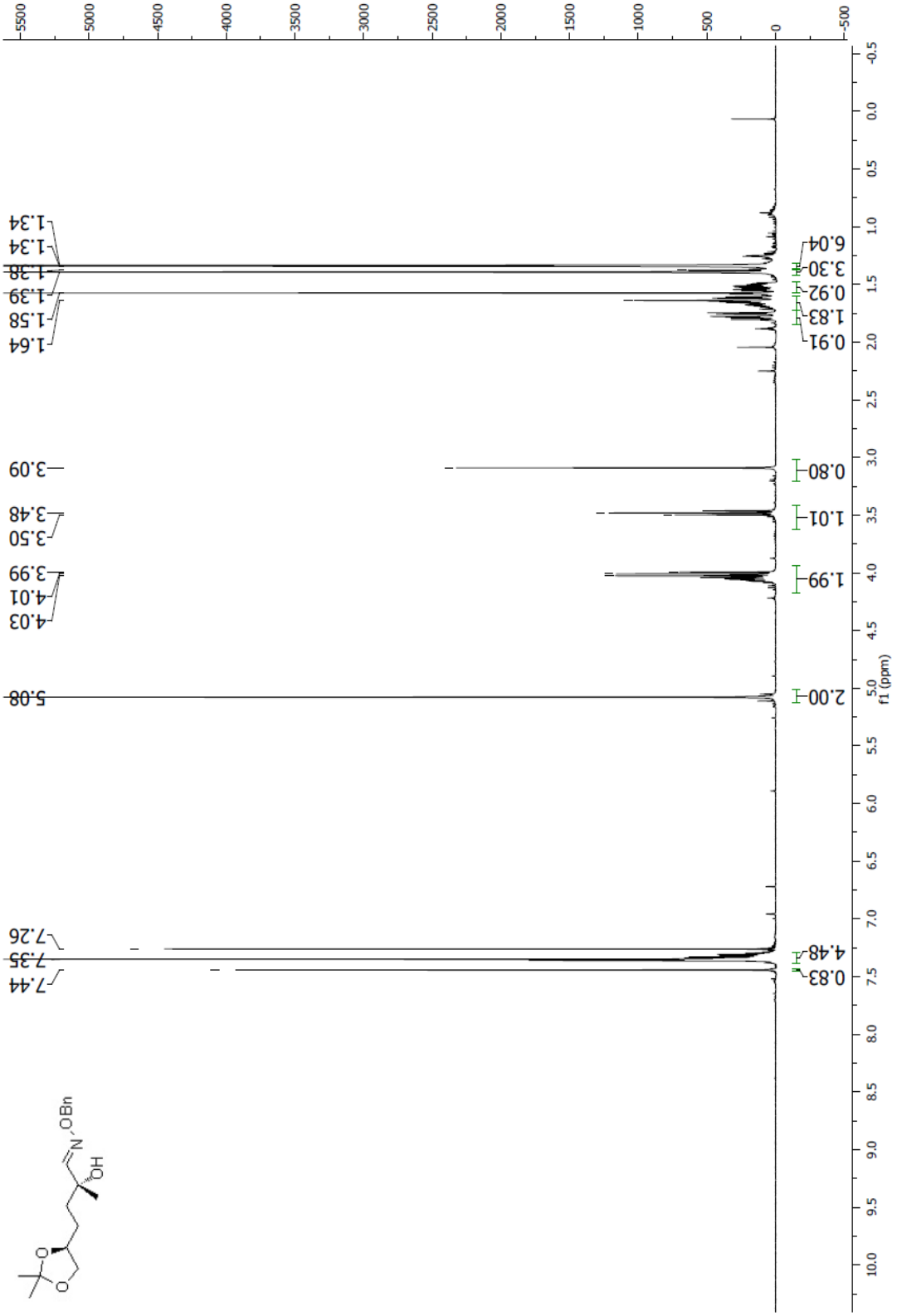

Spectrum 1.24 ^{1}H NMR ($CDCl_3$, 400 MHz) of compound **62**

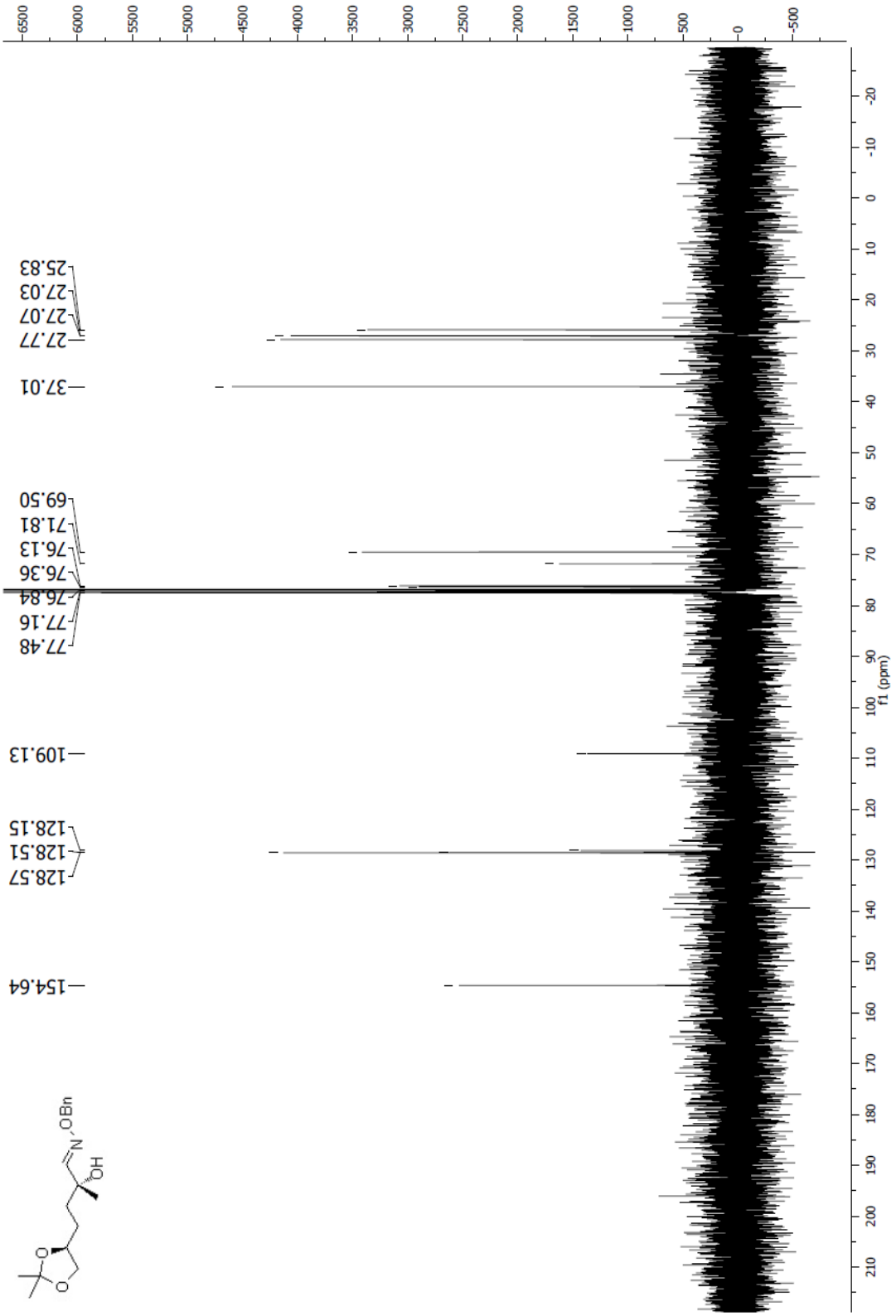

Spectrum 1.25 ^{13}C NMR ($CDCl_3$, 100 MHz) of compound **62**

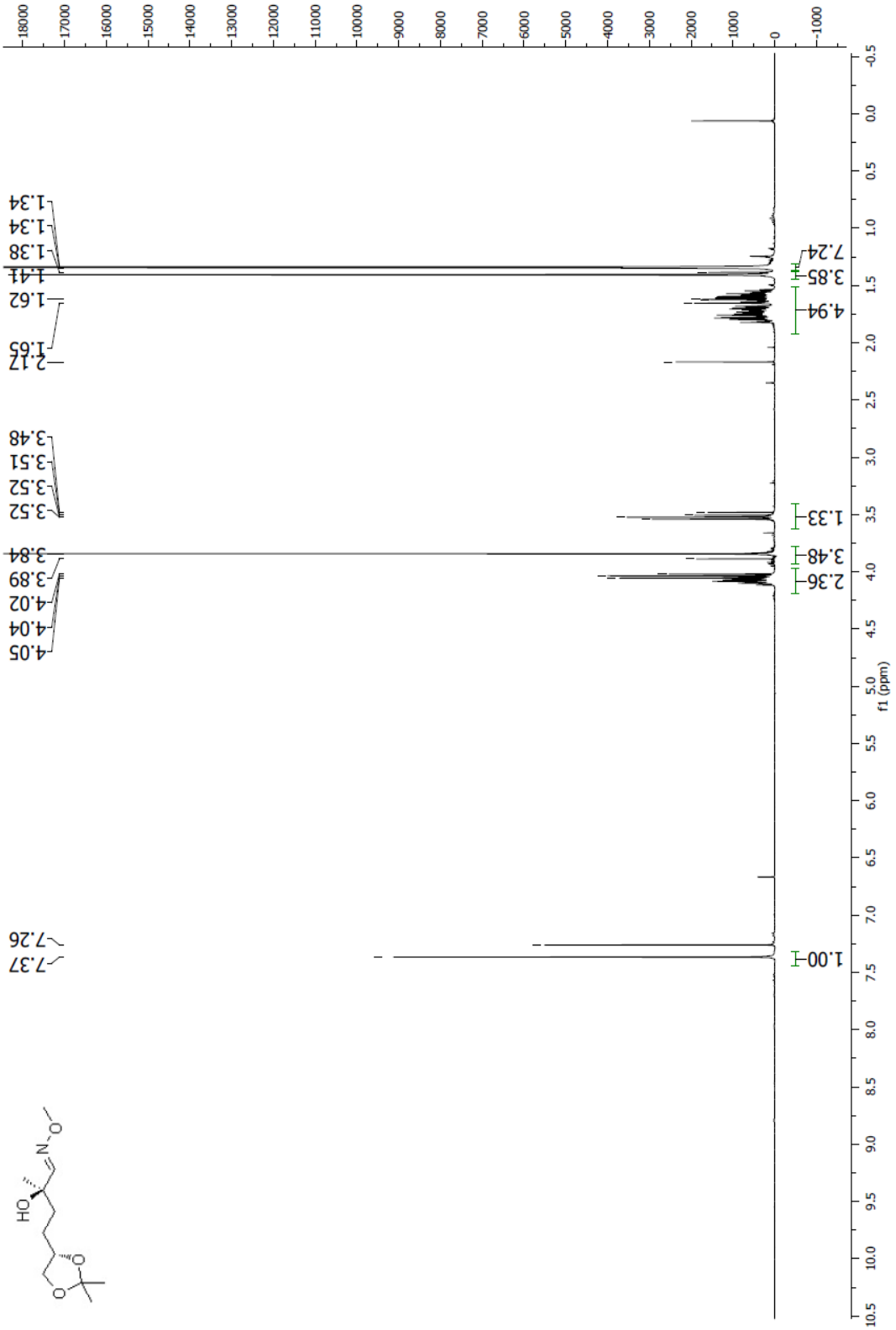

Spectrum 1.26 ^{1}H NMR ($CDCl_3$, 400 MHz) of compound **63**

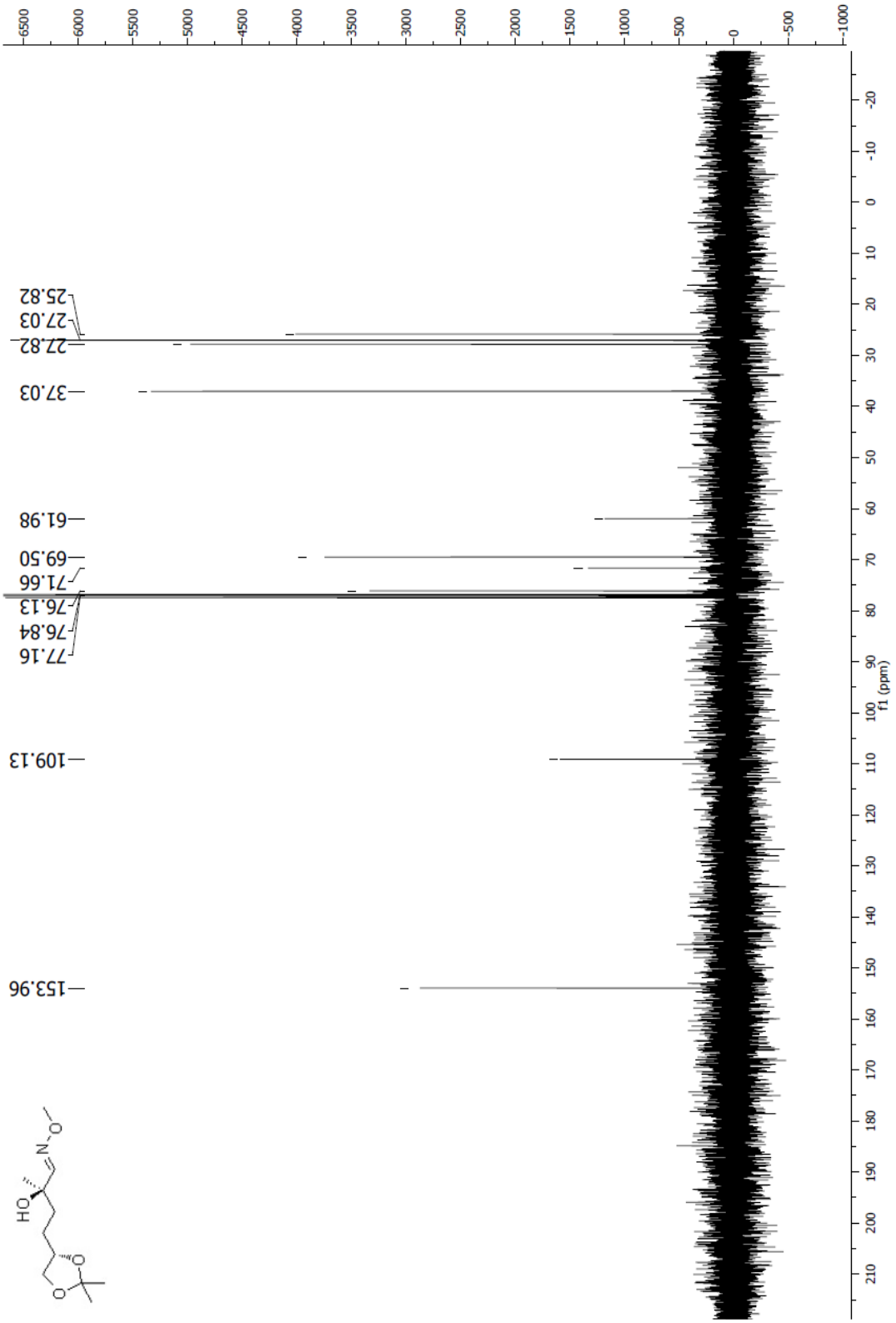

Spectrum 1.27 ^{13}C NMR ($CDCl_3$, 100 MHz) of compound **63**

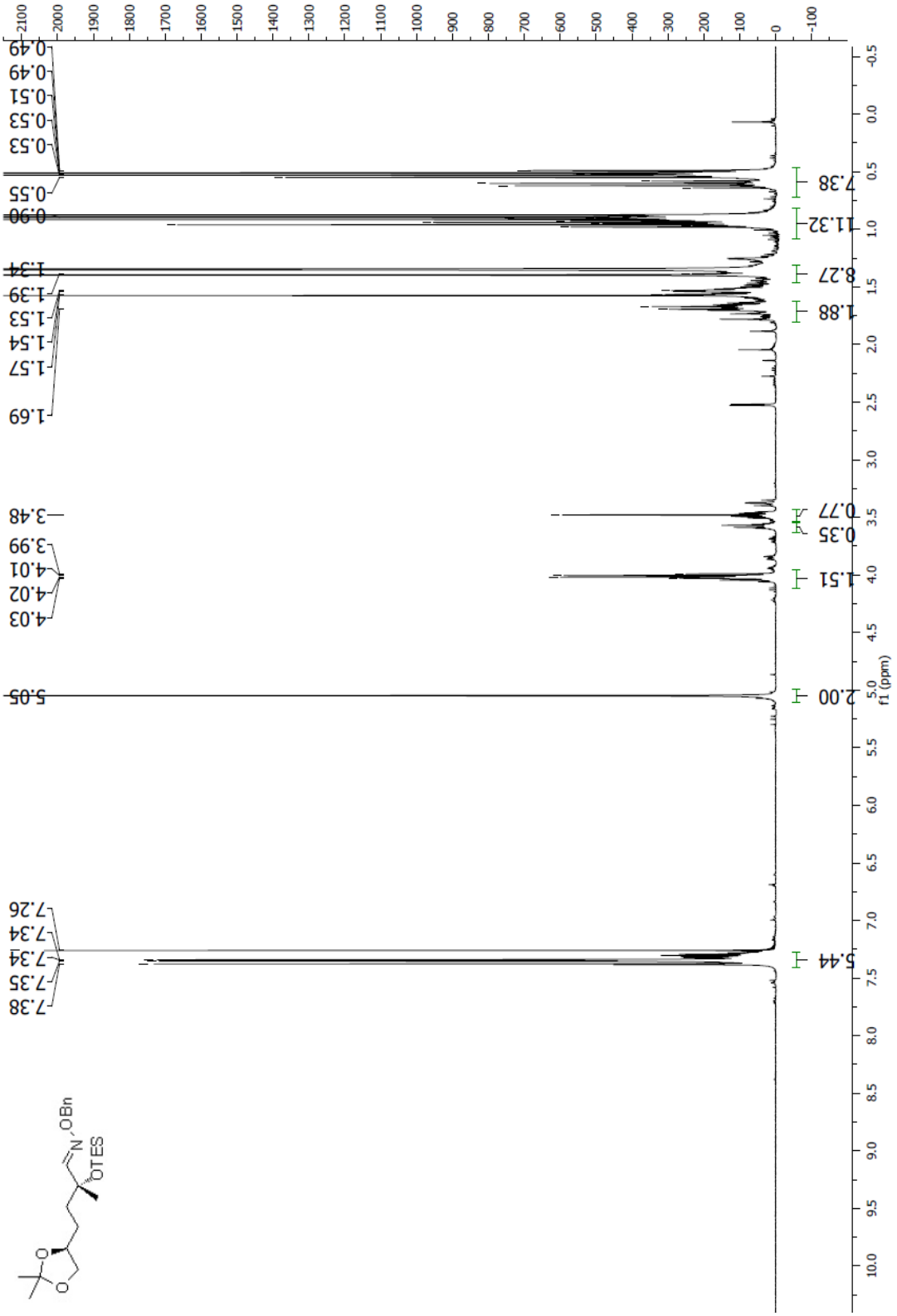

Spectrum 1.28 ^{1}H NMR ($CDCl_3$, 400 MHz) of compound **64**

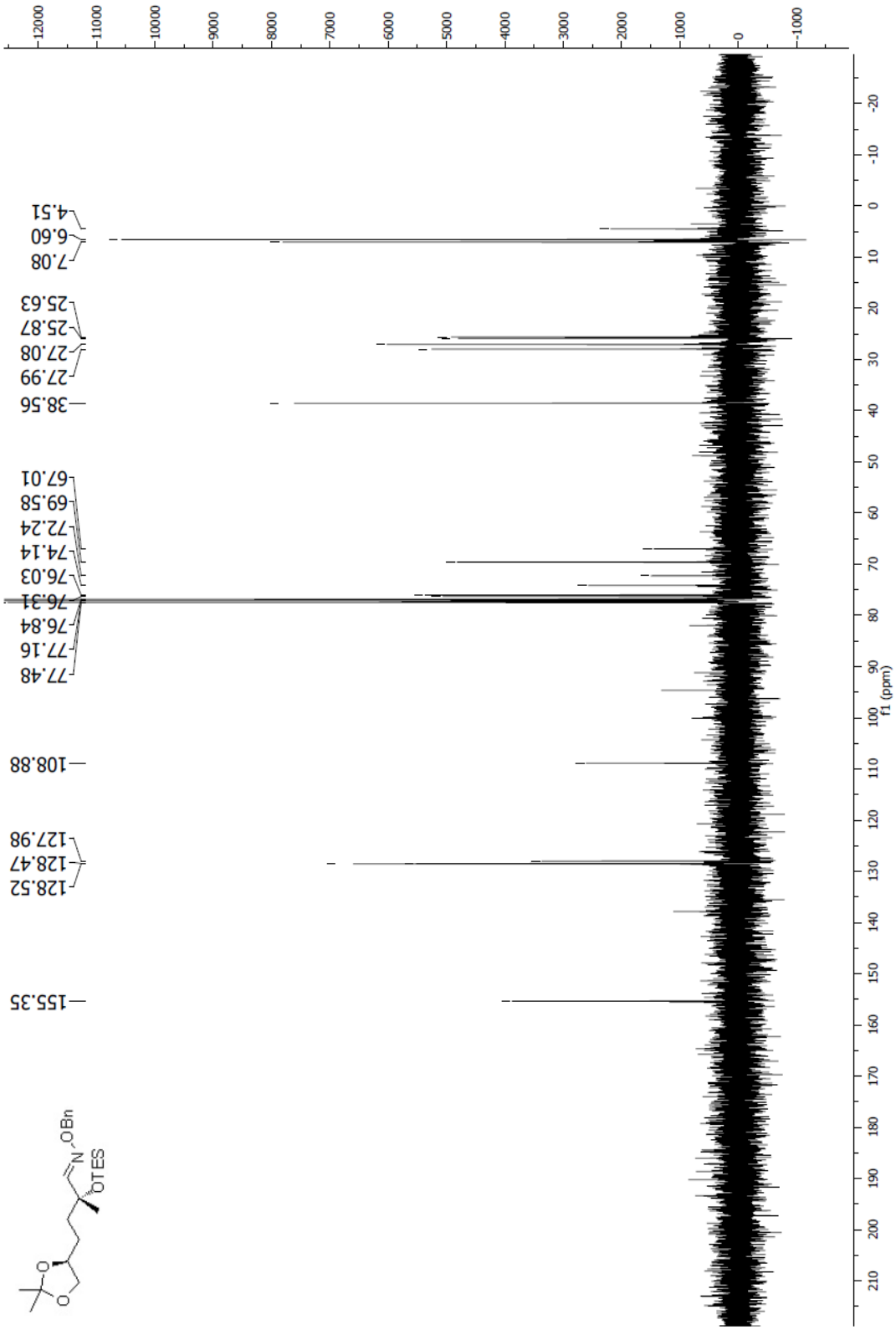

Spectrum 1.29 ^{13}C NMR ($CDCl_3$, 100 MHz) of compound **64**

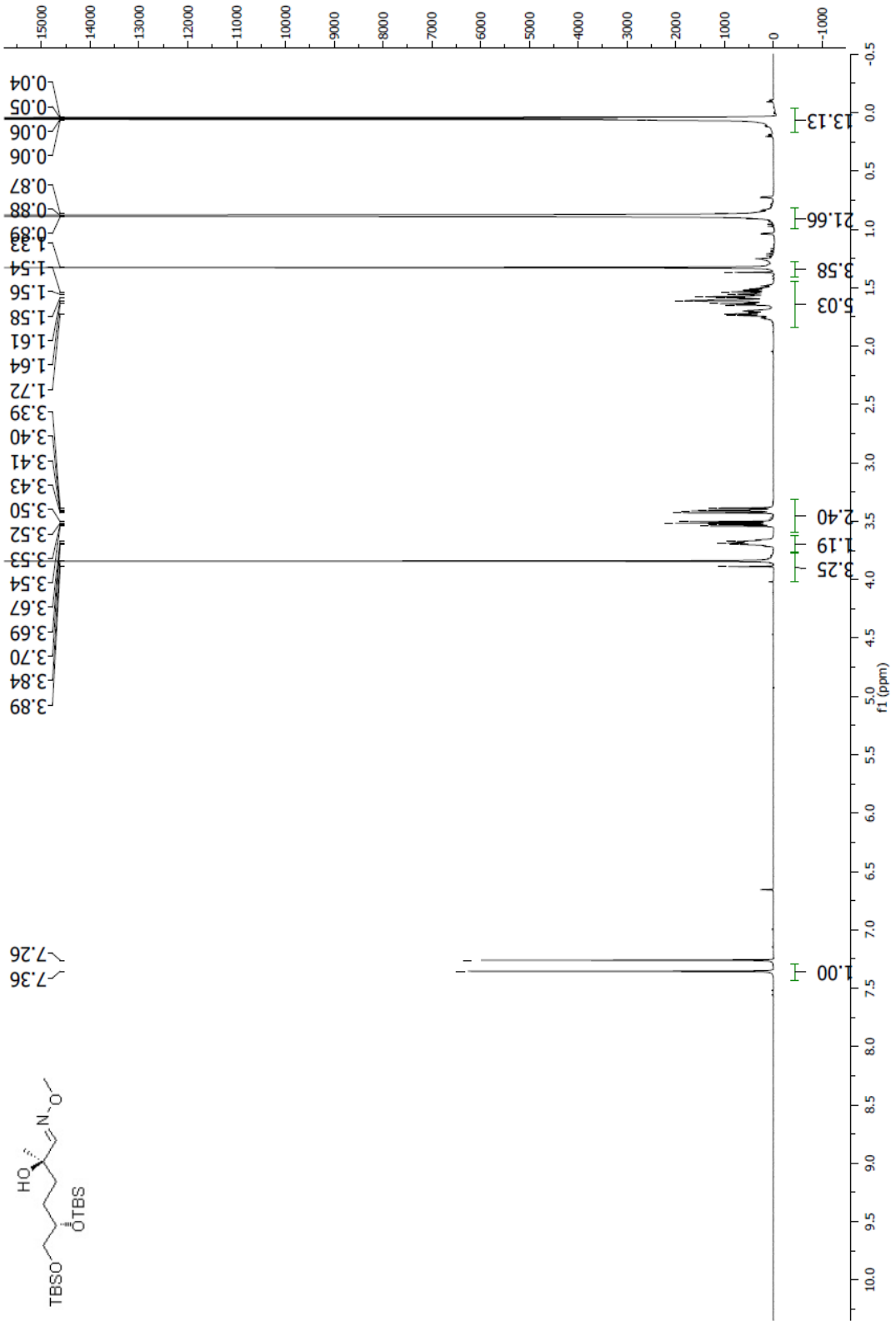

Spectrum 1.30 ^{1}H NMR ($CDCl_3$, 400 MHz) of compound **65**

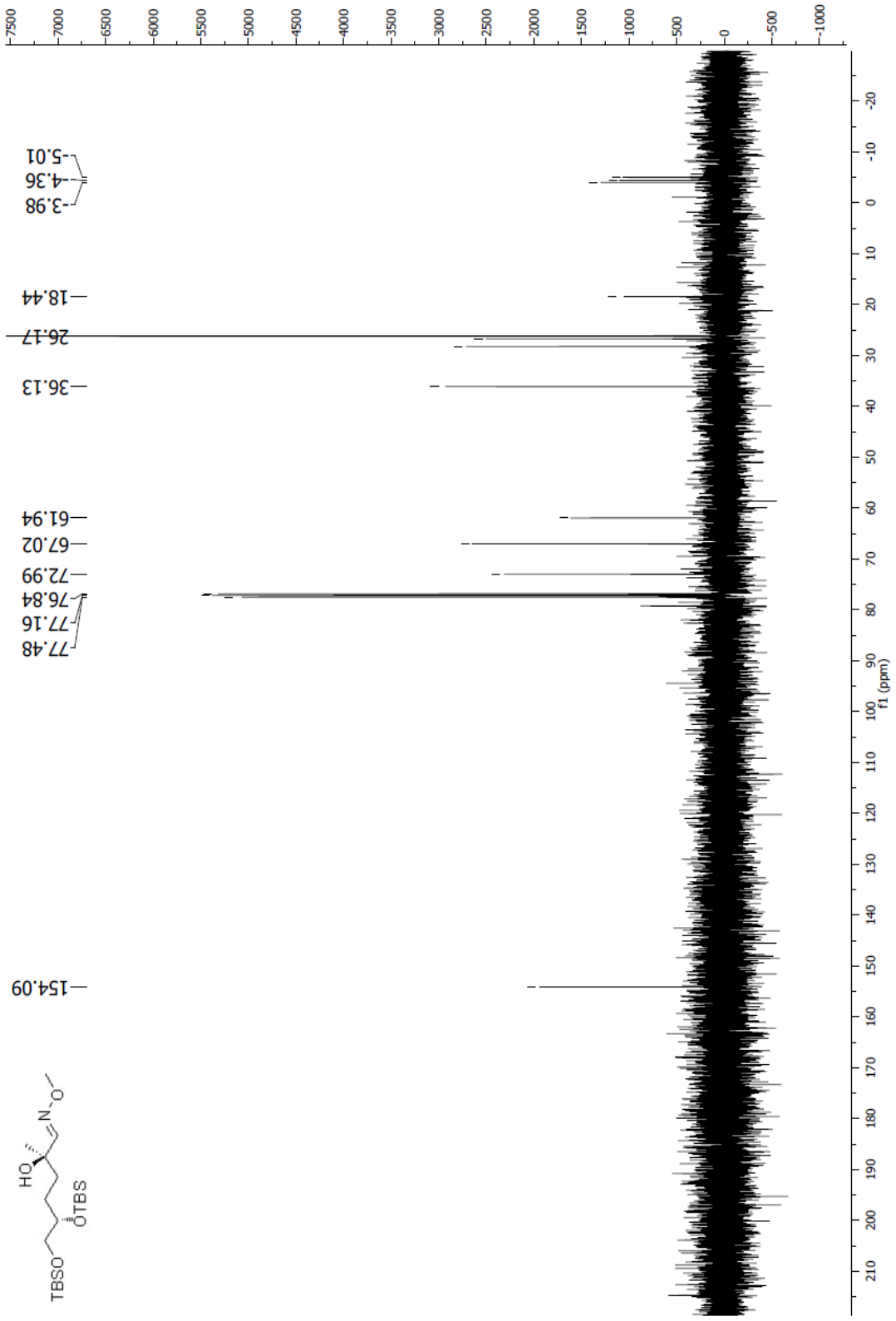

Spectrum 1.31 ^{13}C NMR ($CDCl_3$, 100 MHz) of compound **65**

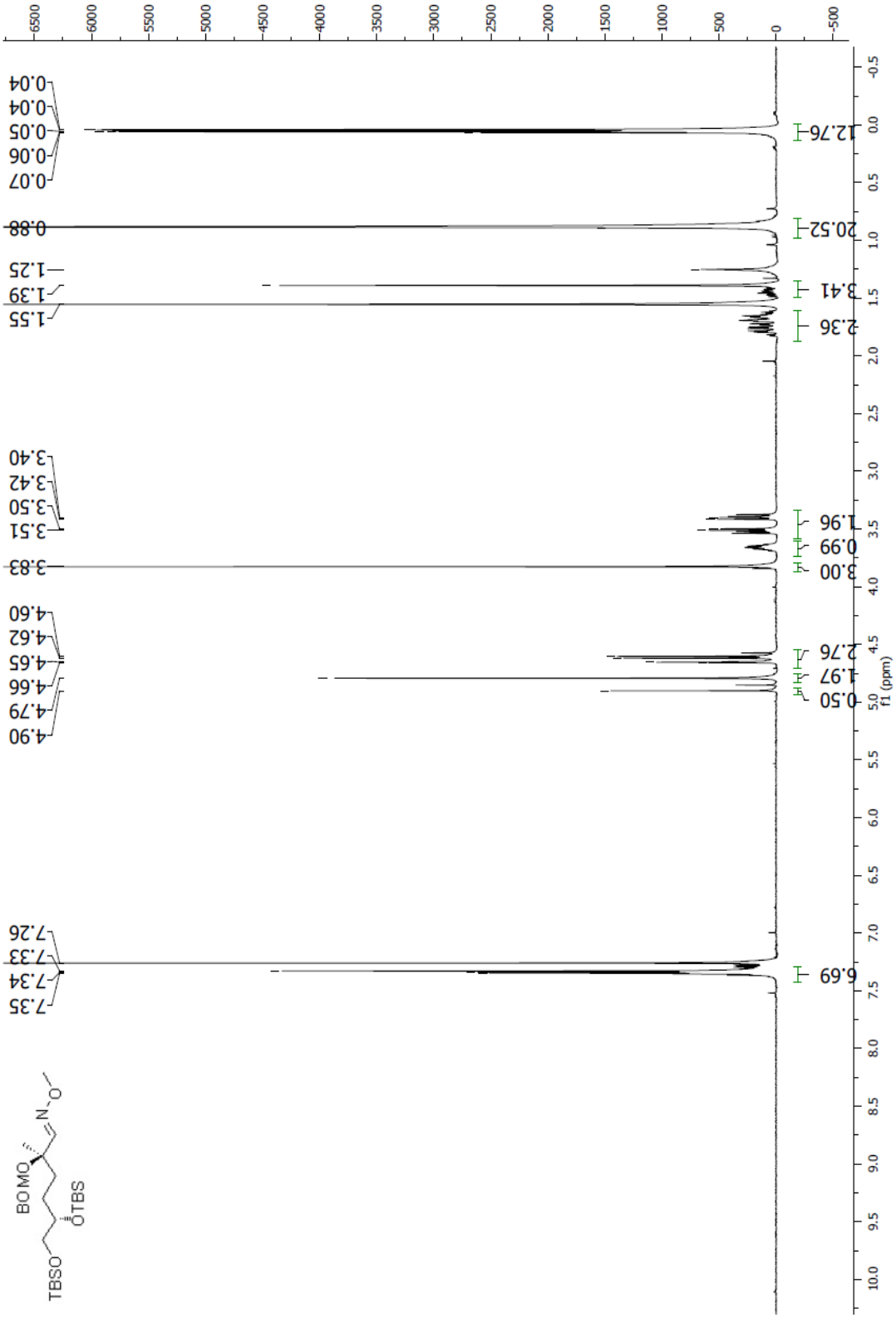

Spectrum 1.32 ^{1}H NMR ($CDCl_3$, 400 MHz) of compound **66**

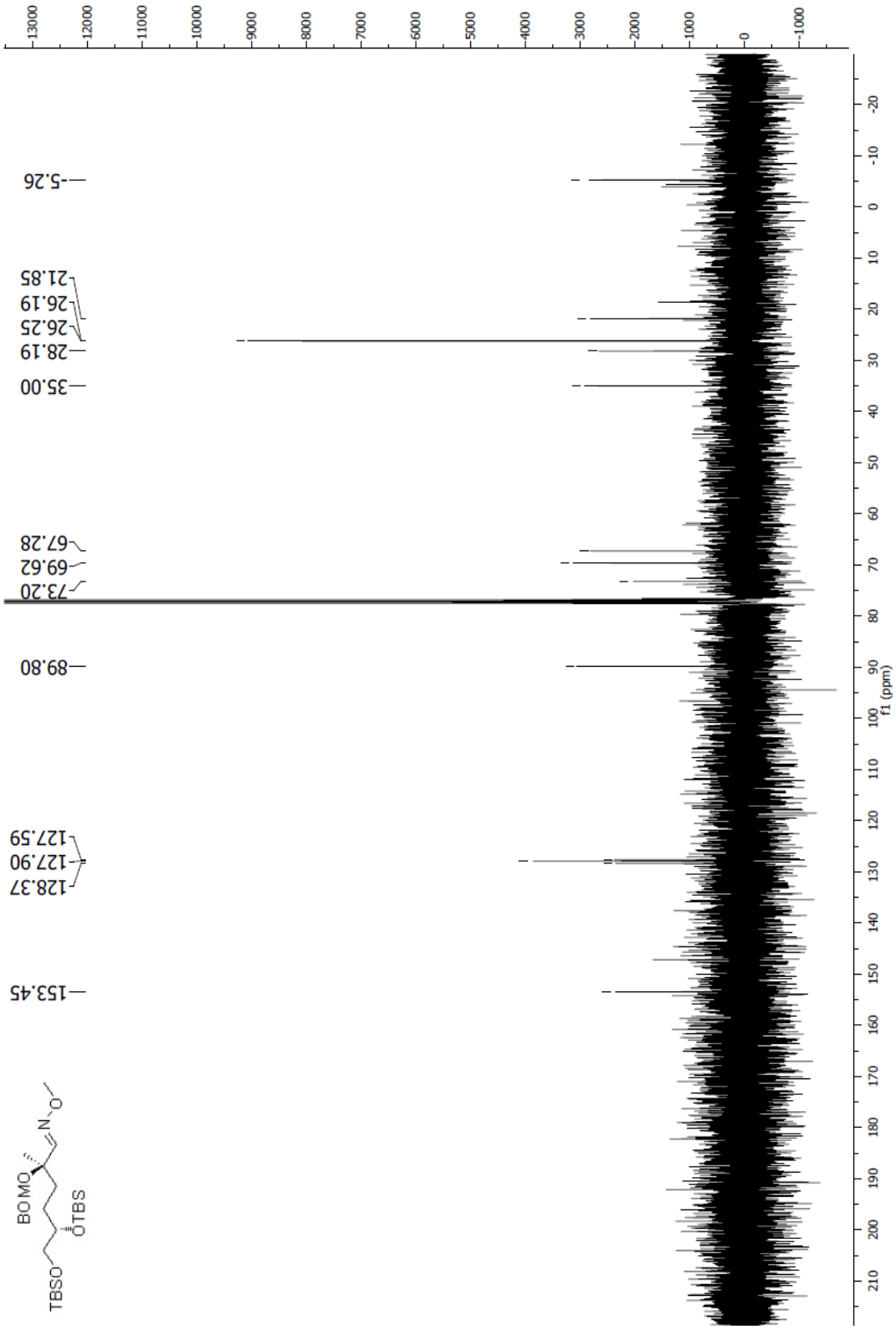

Spectrum 1.33 ^{13}C NMR ($CDCl_3$, 100 MHz) of compound **66**

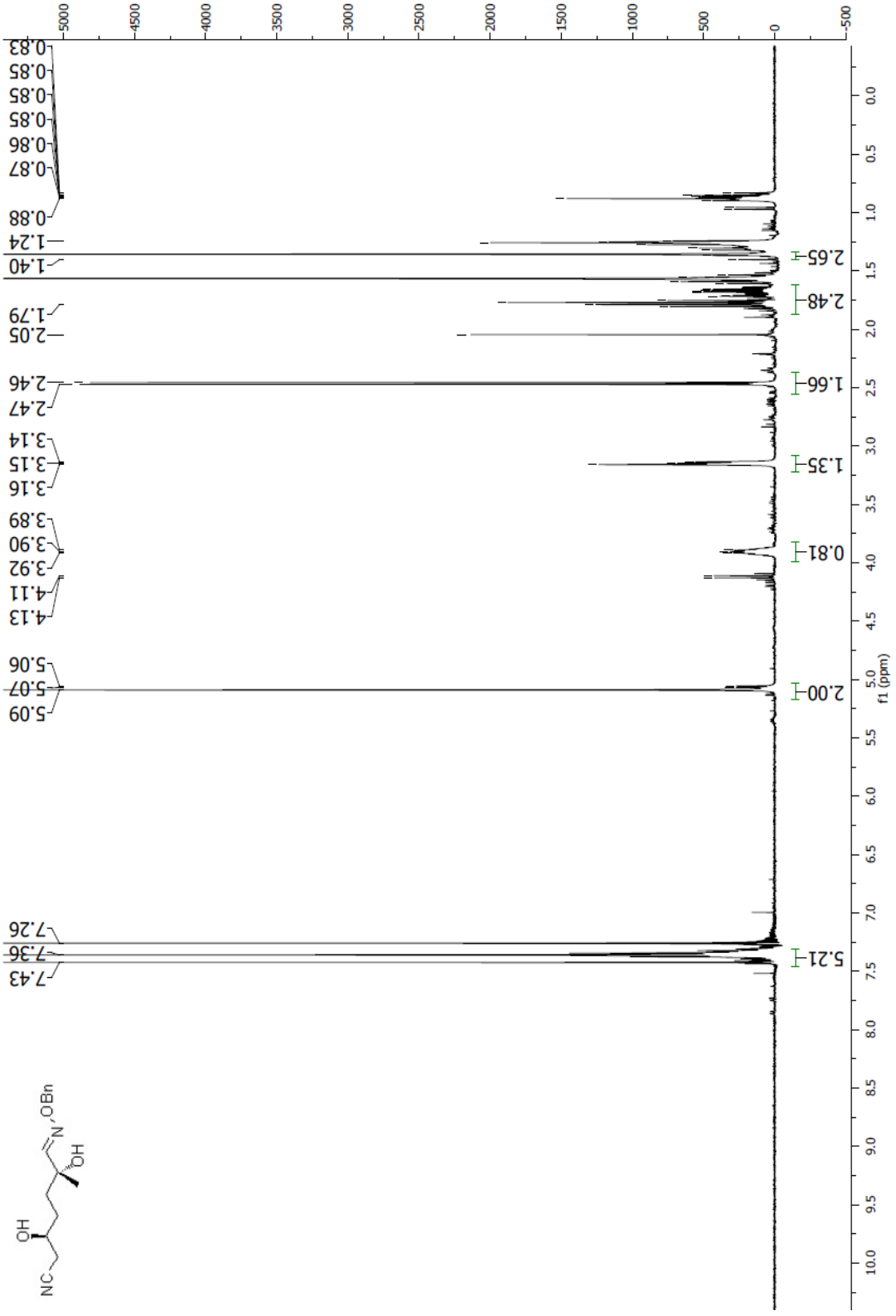

Spectrum 1.34 ^{1}H NMR ($CDCl_3$, 400 MHz) of compound **67**

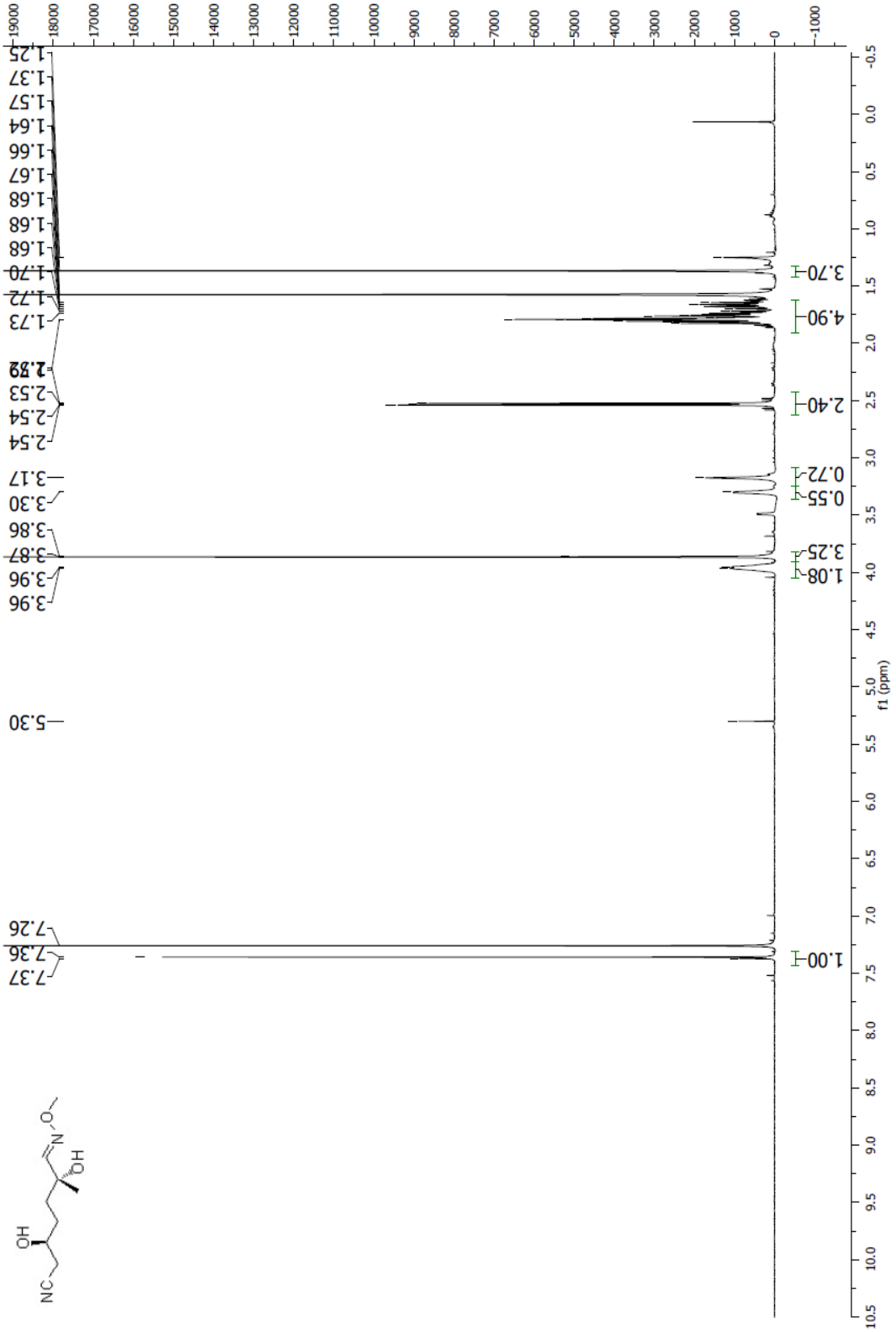

Spectrum 1.35 ^{1}H NMR ($CDCl_3$, 400 MHz) of compound **68**

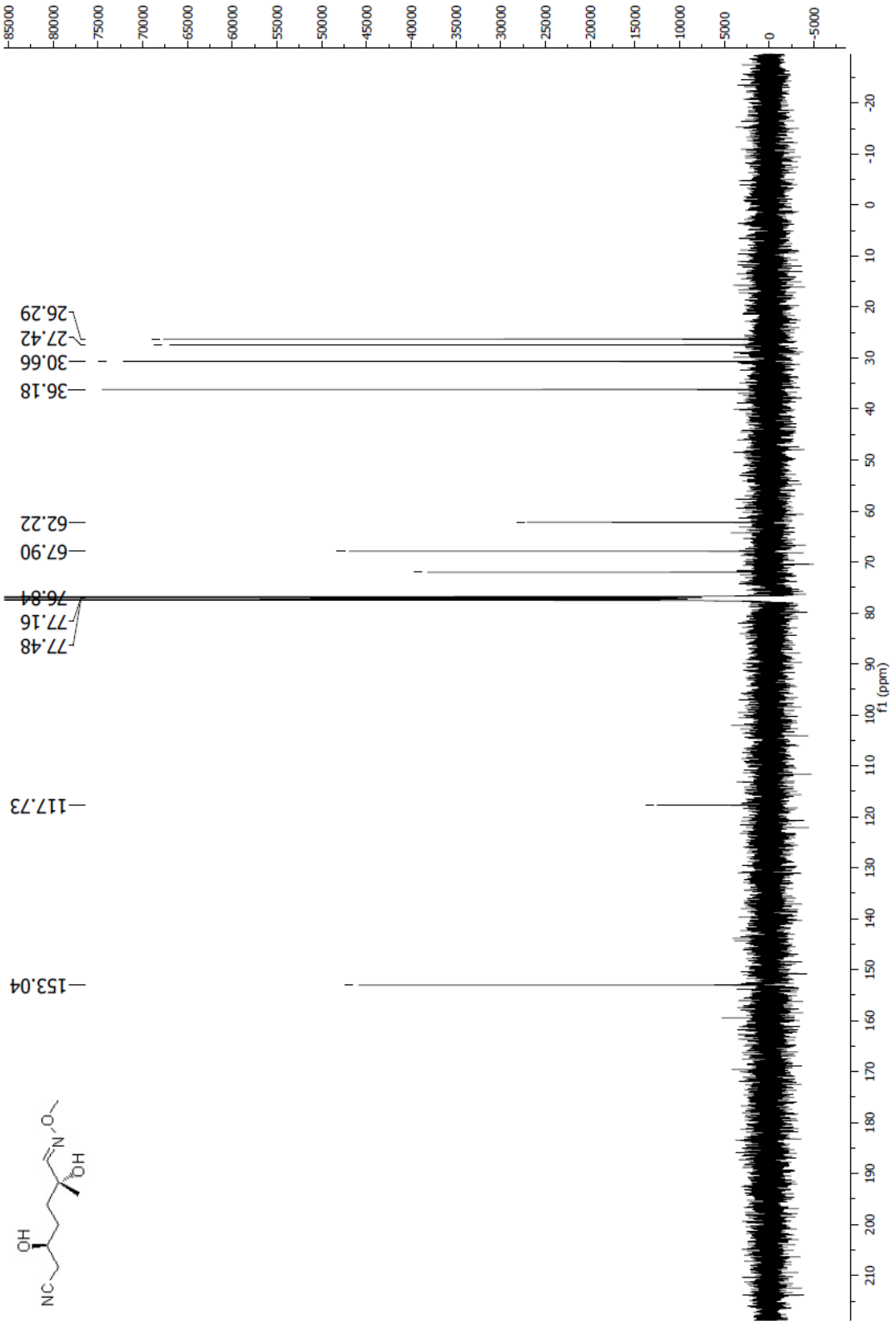

Spectrum 1.36 ^{13}C NMR ($CDCl_3$, 100 MHz) of compound **68**

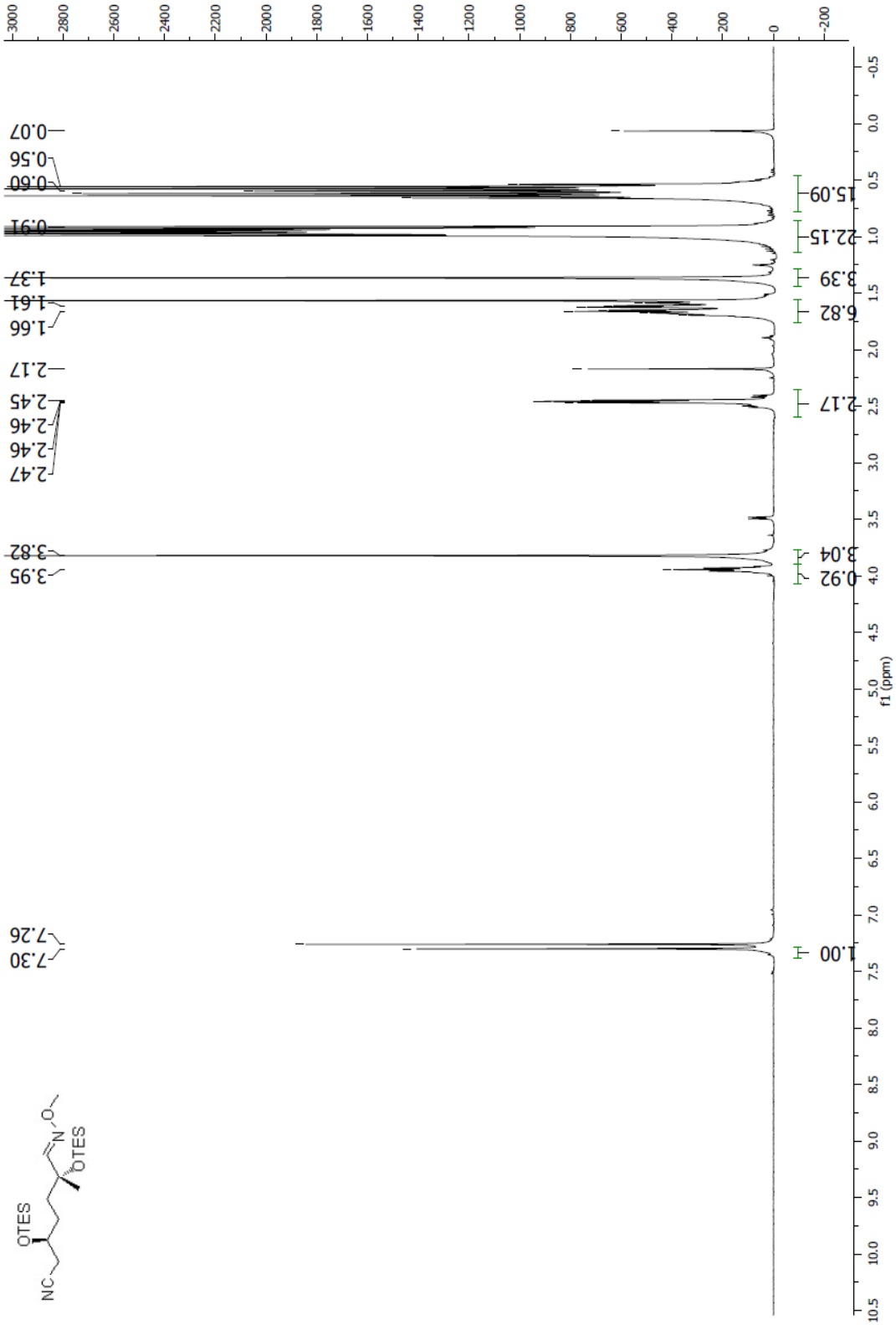

Spectrum 1.37 ^{1}H NMR ($CDCl_3$, 400 MHz) of compound **70**

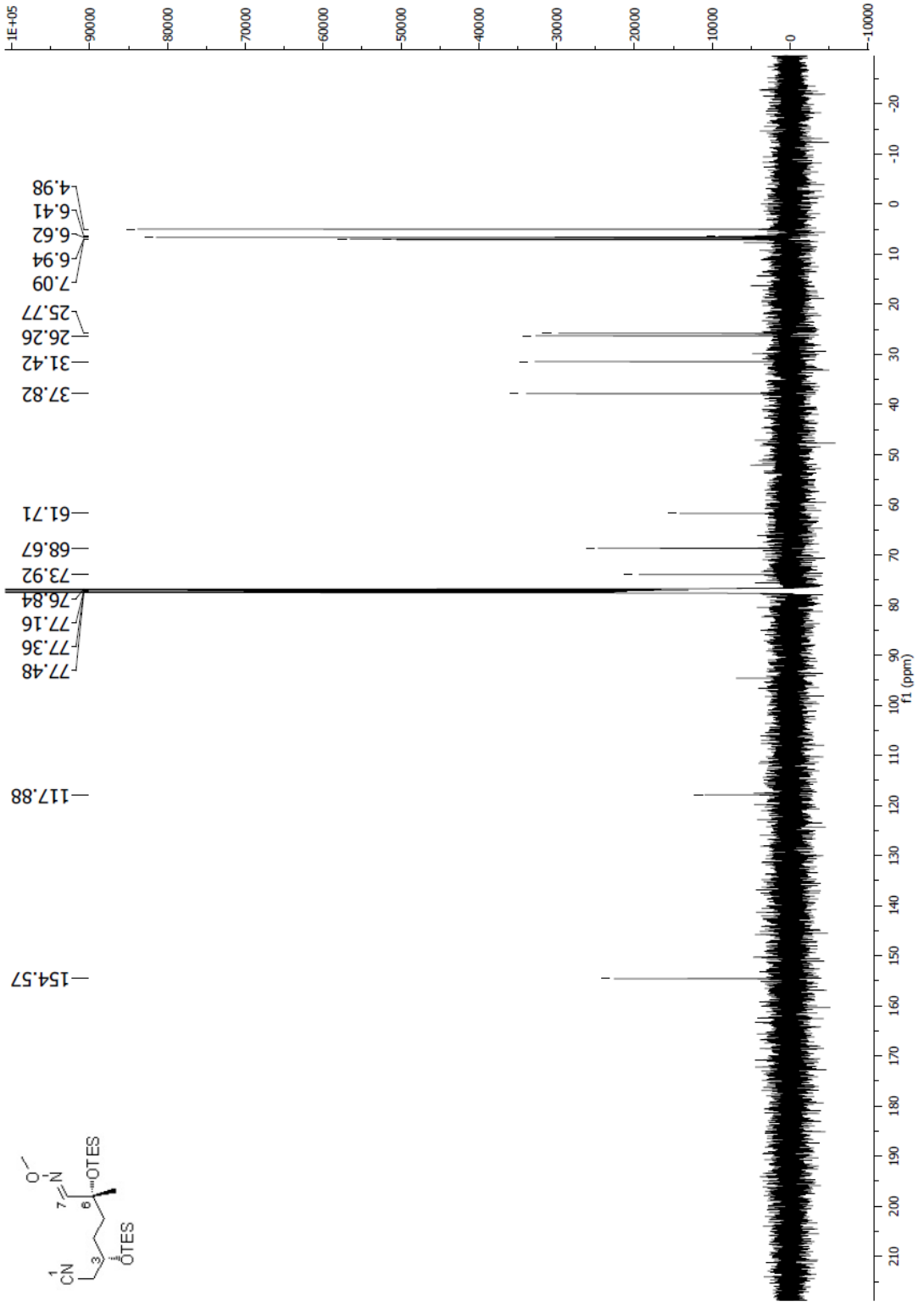

Spectrum 1.38 ^{13}C NMR ($CDCl_3$, 100 MHz) of compound **70**

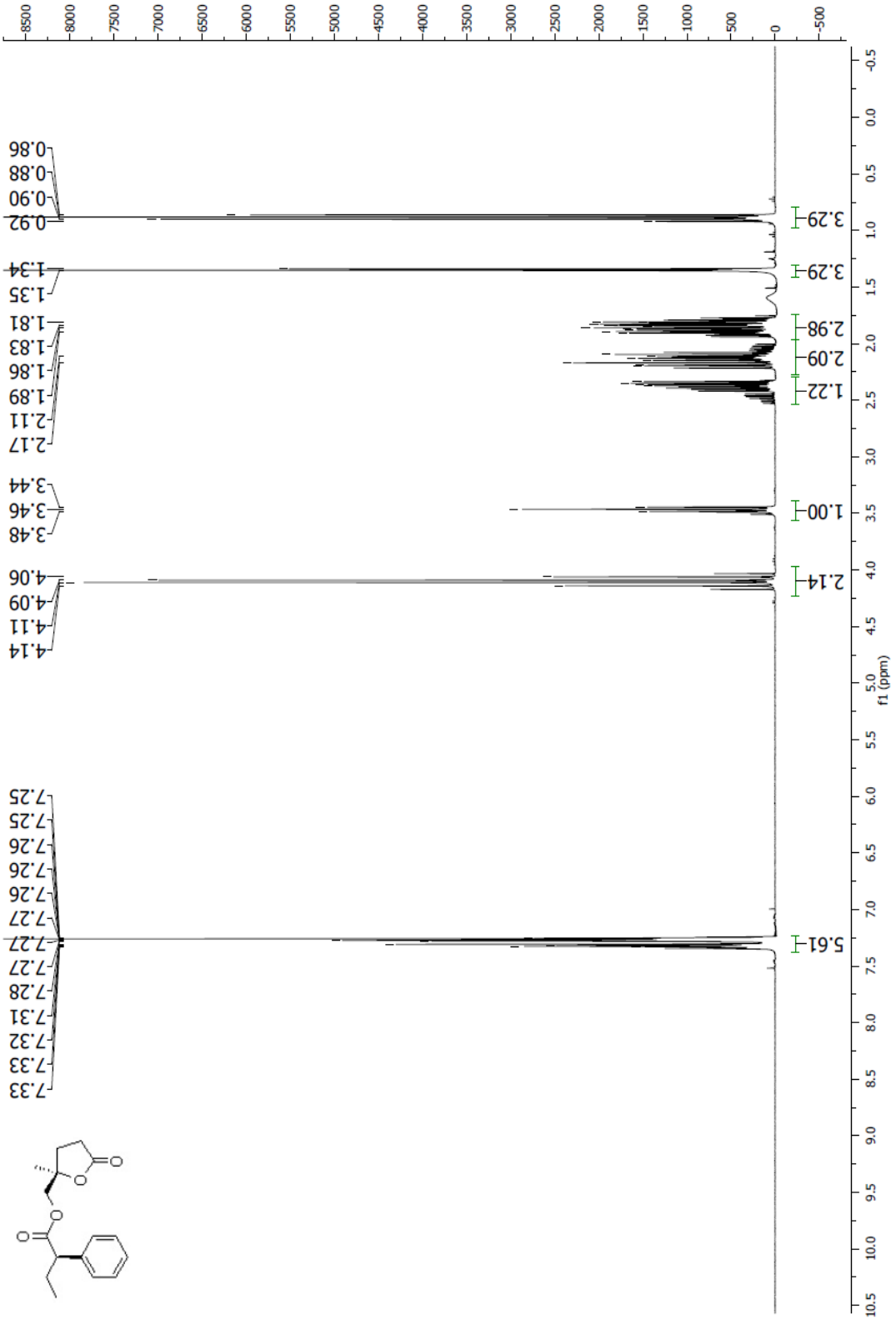

Spectrum 1.39 ^{1}H NMR ($CDCl_3$, 400 MHz) of compound **77**

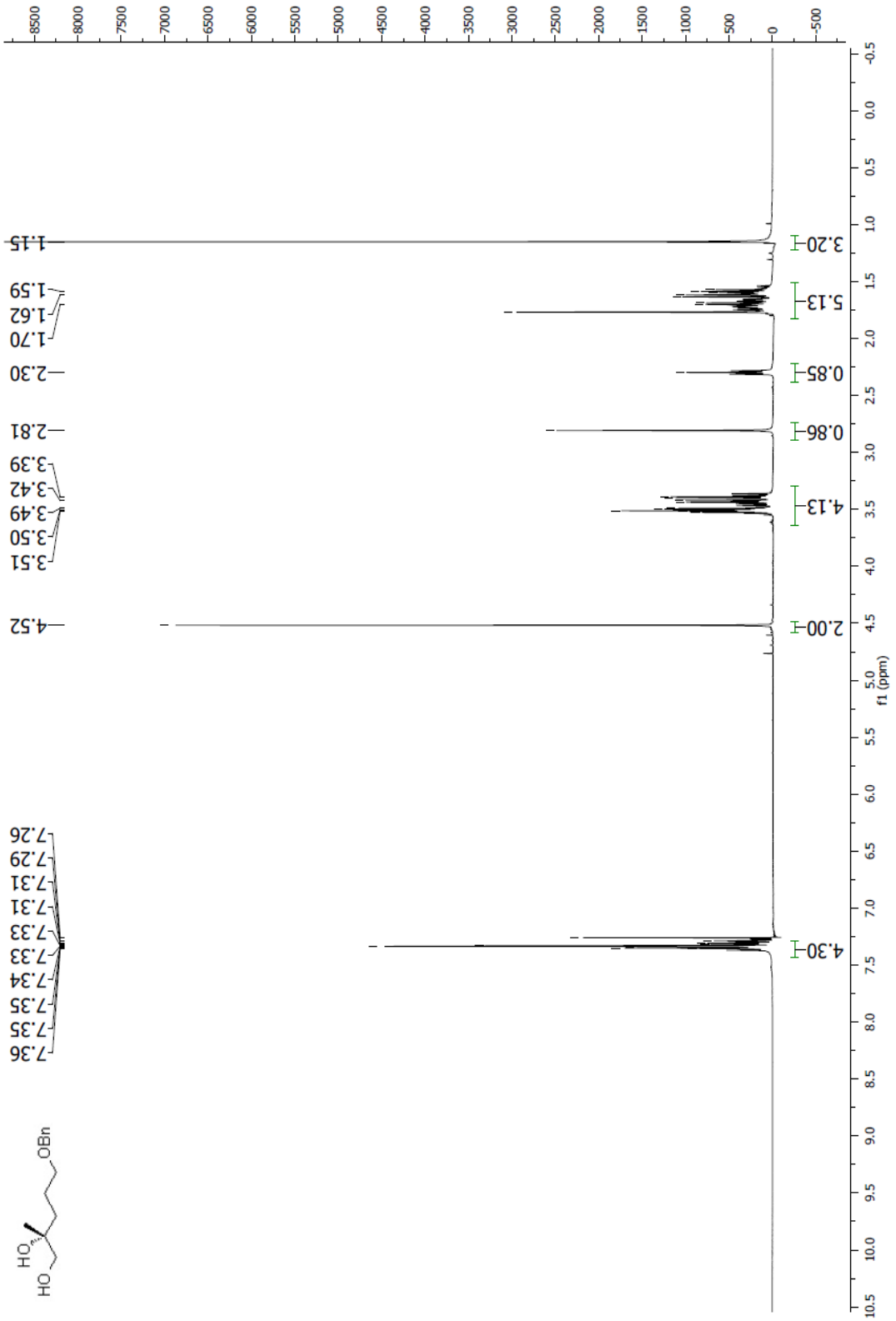

Spectrum 1.40 ^{1}H NMR ($CDCl_3$, 400 MHz) of compound **80**

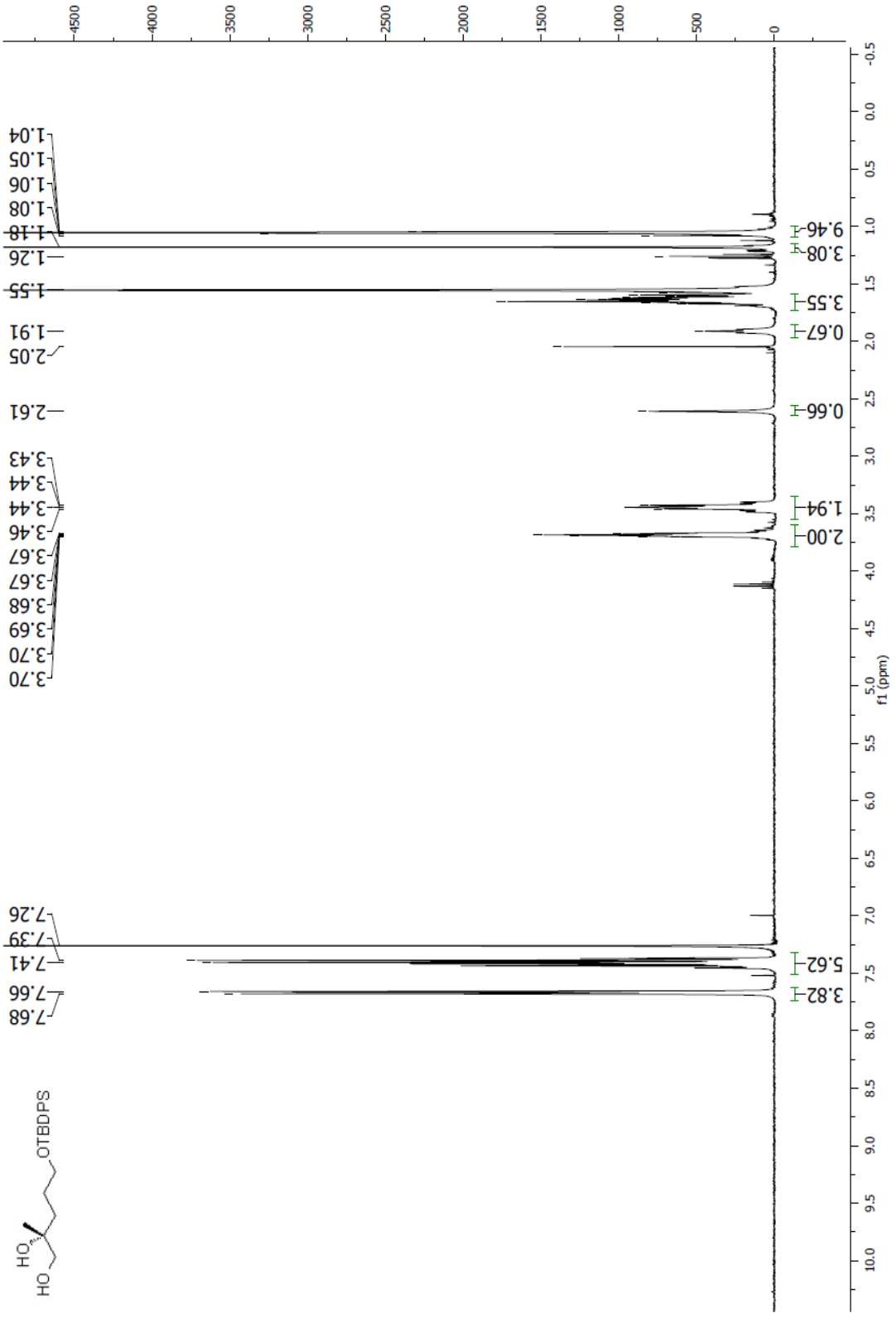

Spectrum 1.41 ^{1}H NMR ($CDCl_3$, 400 MHz) of compound **81**

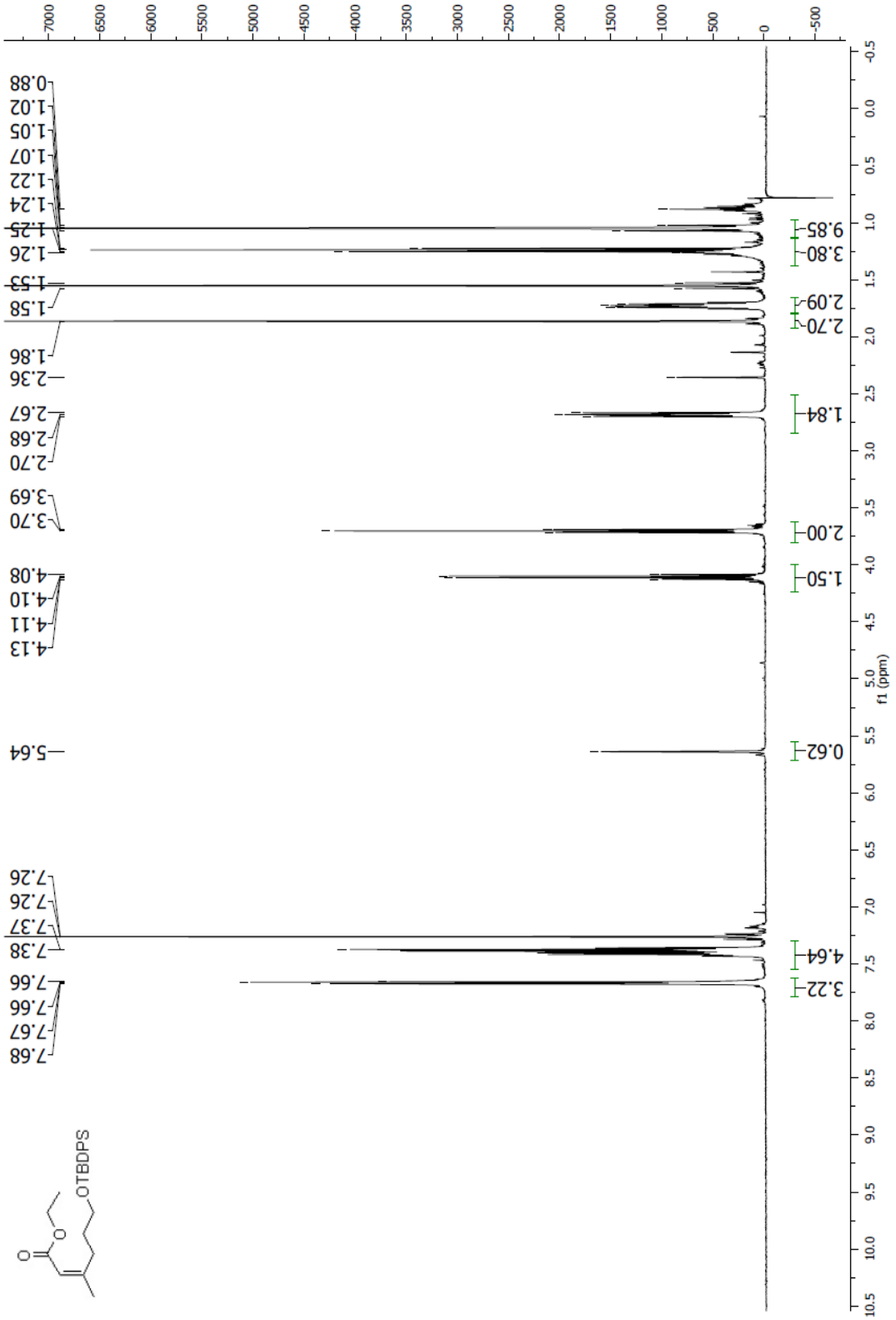

Spectrum 1.42 ^{1}H NMR ($CDCl_3$, 500 MHz) of compound **85**

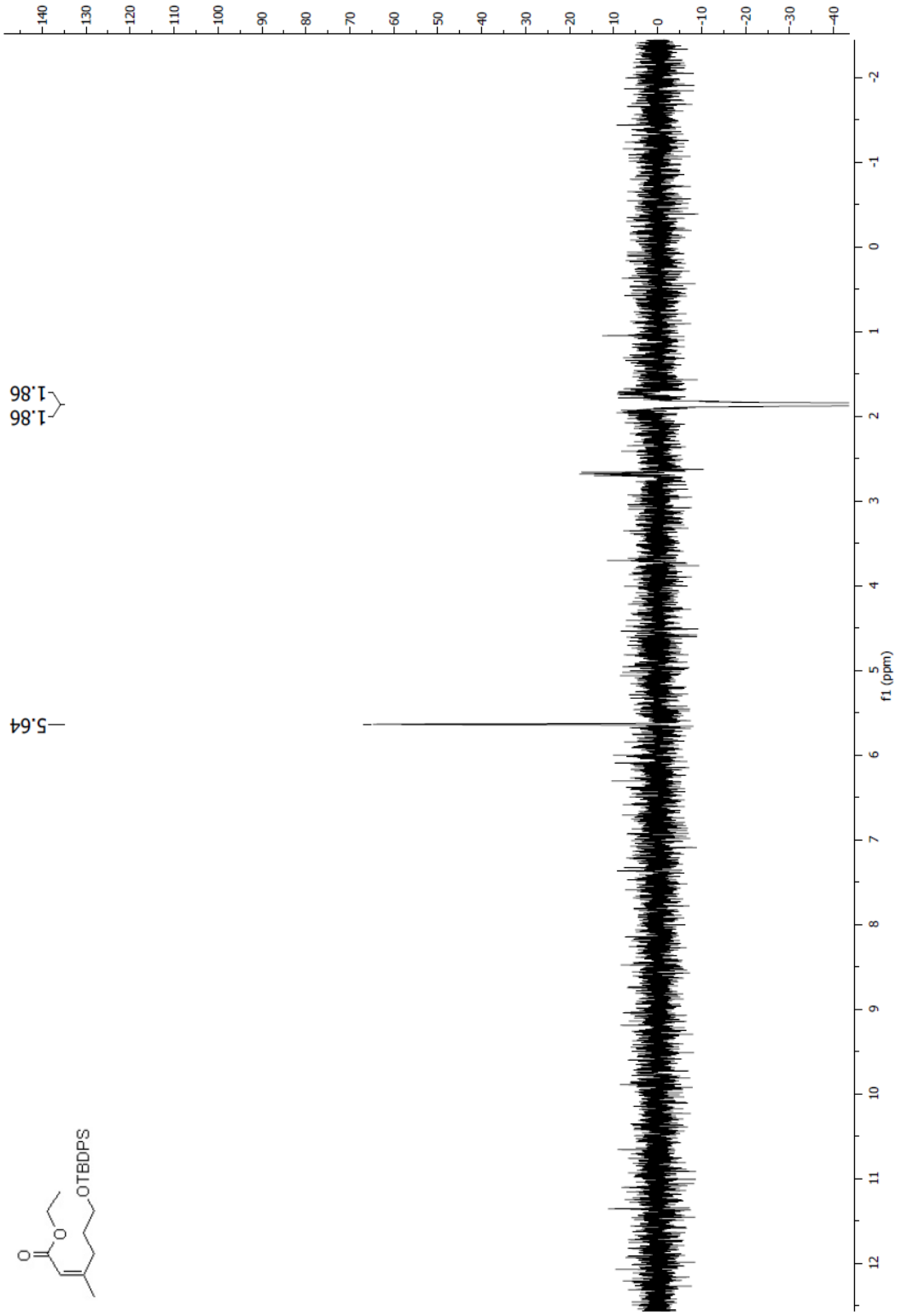

Spectrum 1.43 NOESY1D NMR ($CDCl_3$, 400 MHz) of compound **85**, irradiation at 1.86 ppm, the C-6 methyl, mixing time = 0.5 sec.

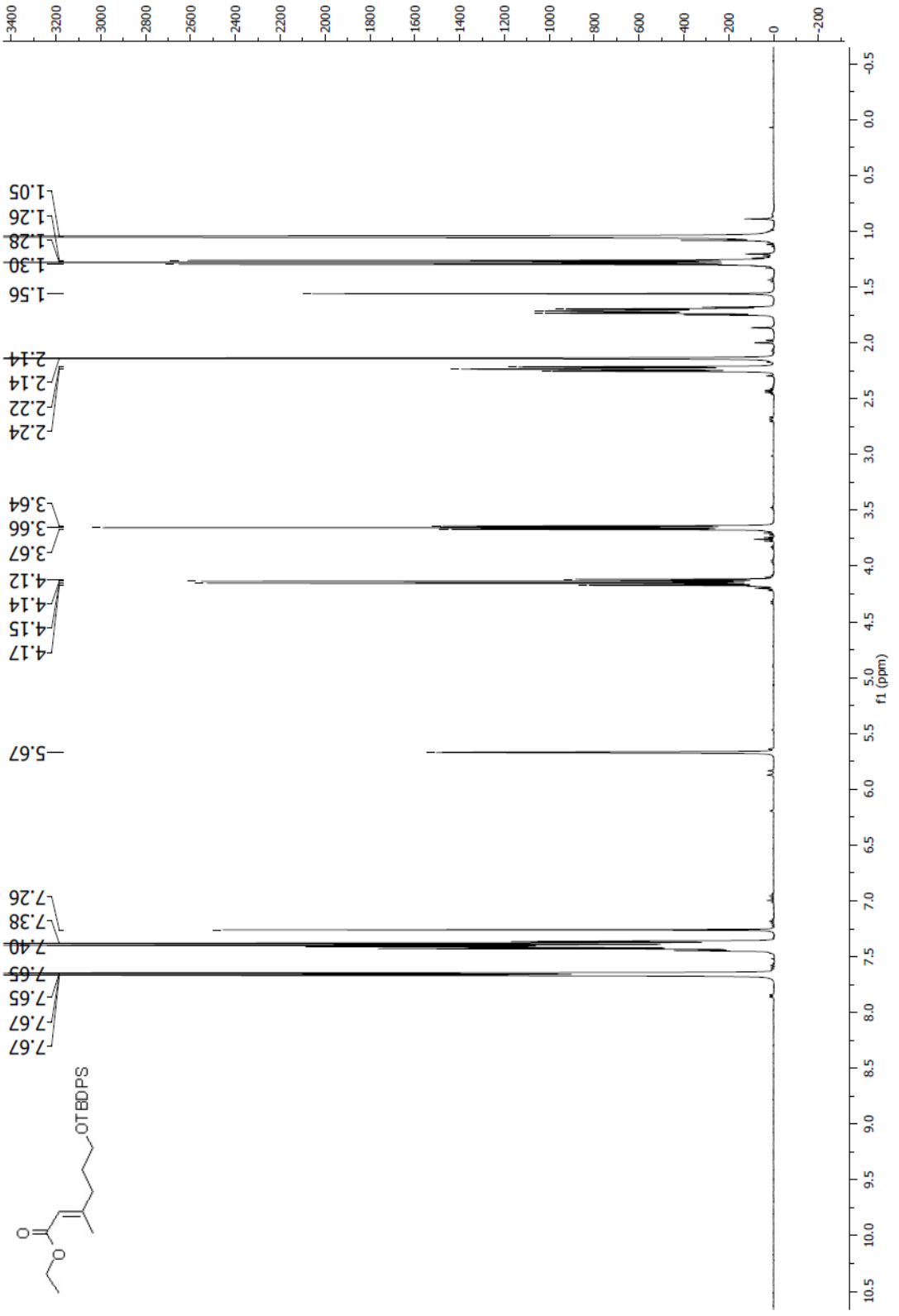

Spectrum 1.44 ^{1}H NMR ($CDCl_3$, 400 MHz) of compound **87**

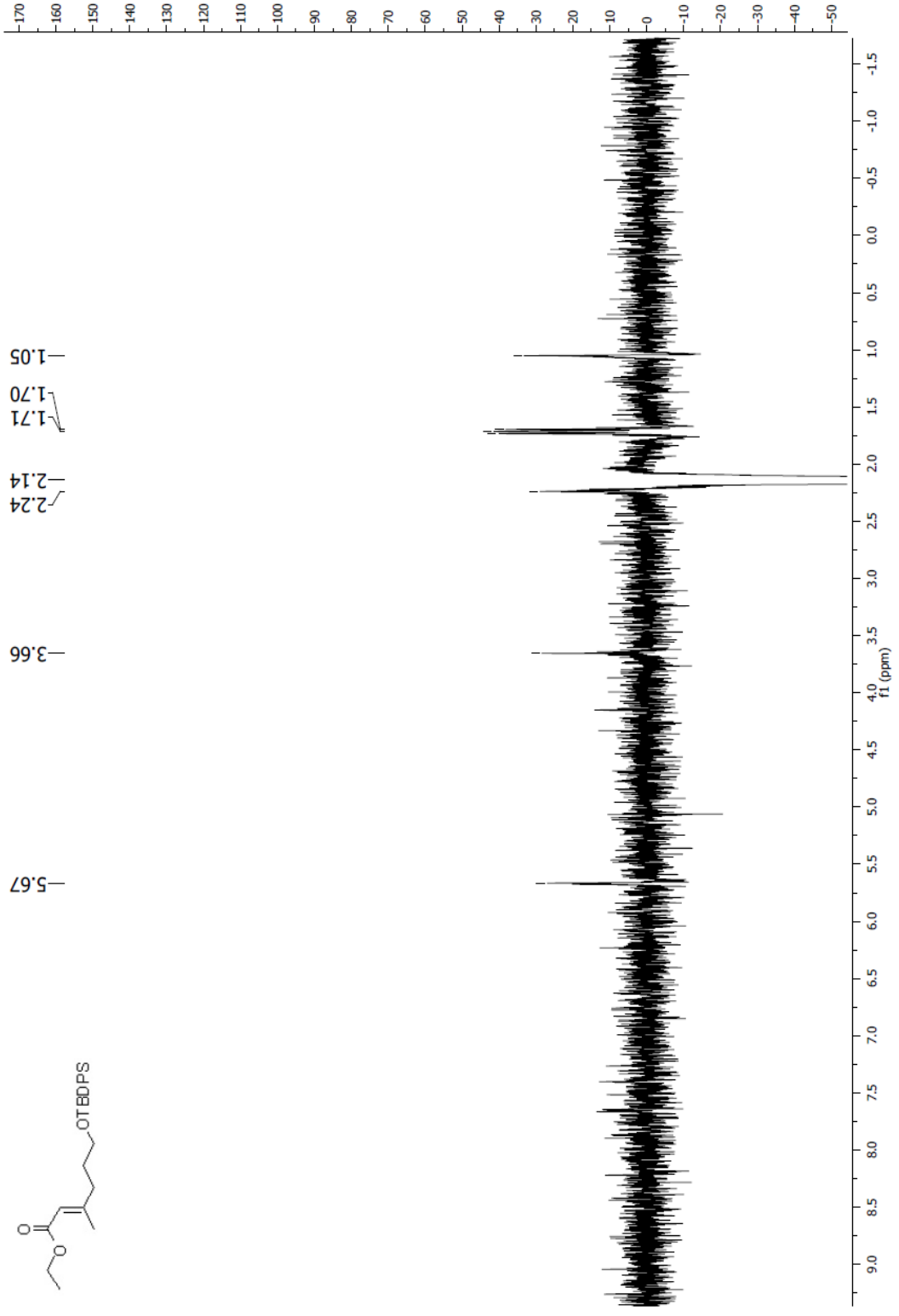

Spectrum 1.45 NOESY1D NMR ($CDCl_3$, 400 MHz) of compound **87**, irradiation at 2.14 ppm, the C-6 methyl

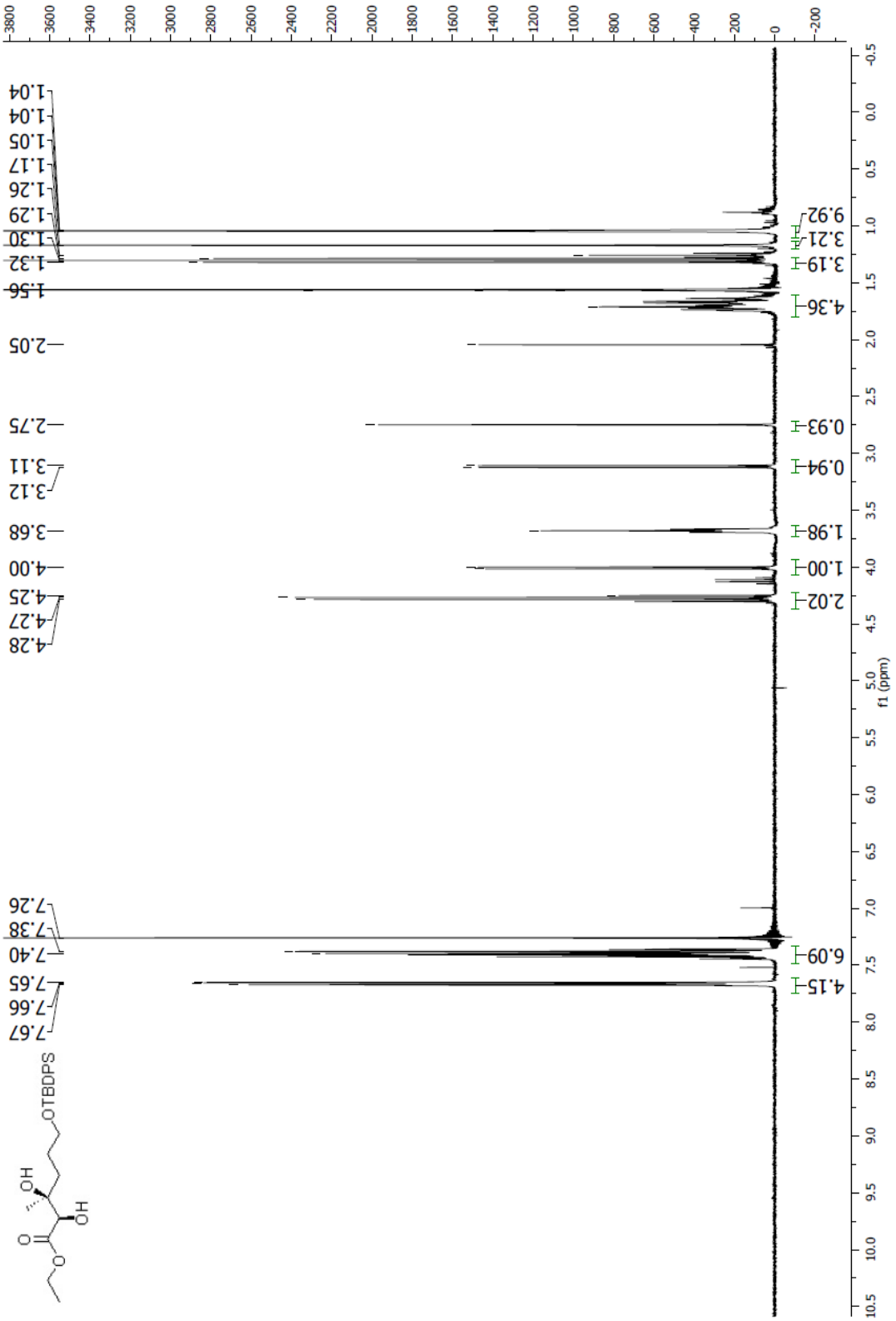

Spectrum 1.46 ^{1}H NMR ($CDCl_3$, 400 MHz) of compound **88**

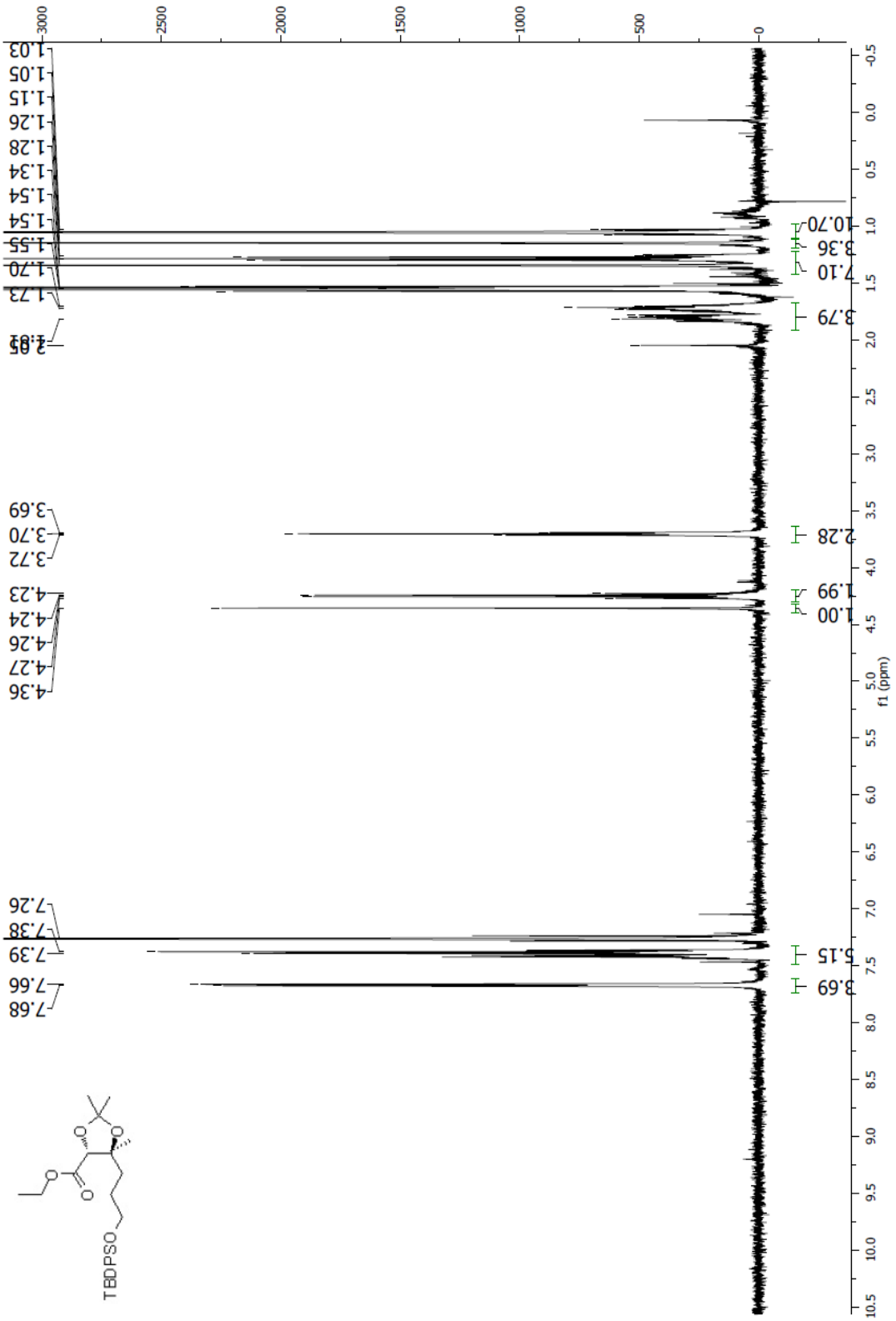

Spectrum 1.47 ^{1}H NMR ($CDCl_3$, 500 MHz) of compound **89**

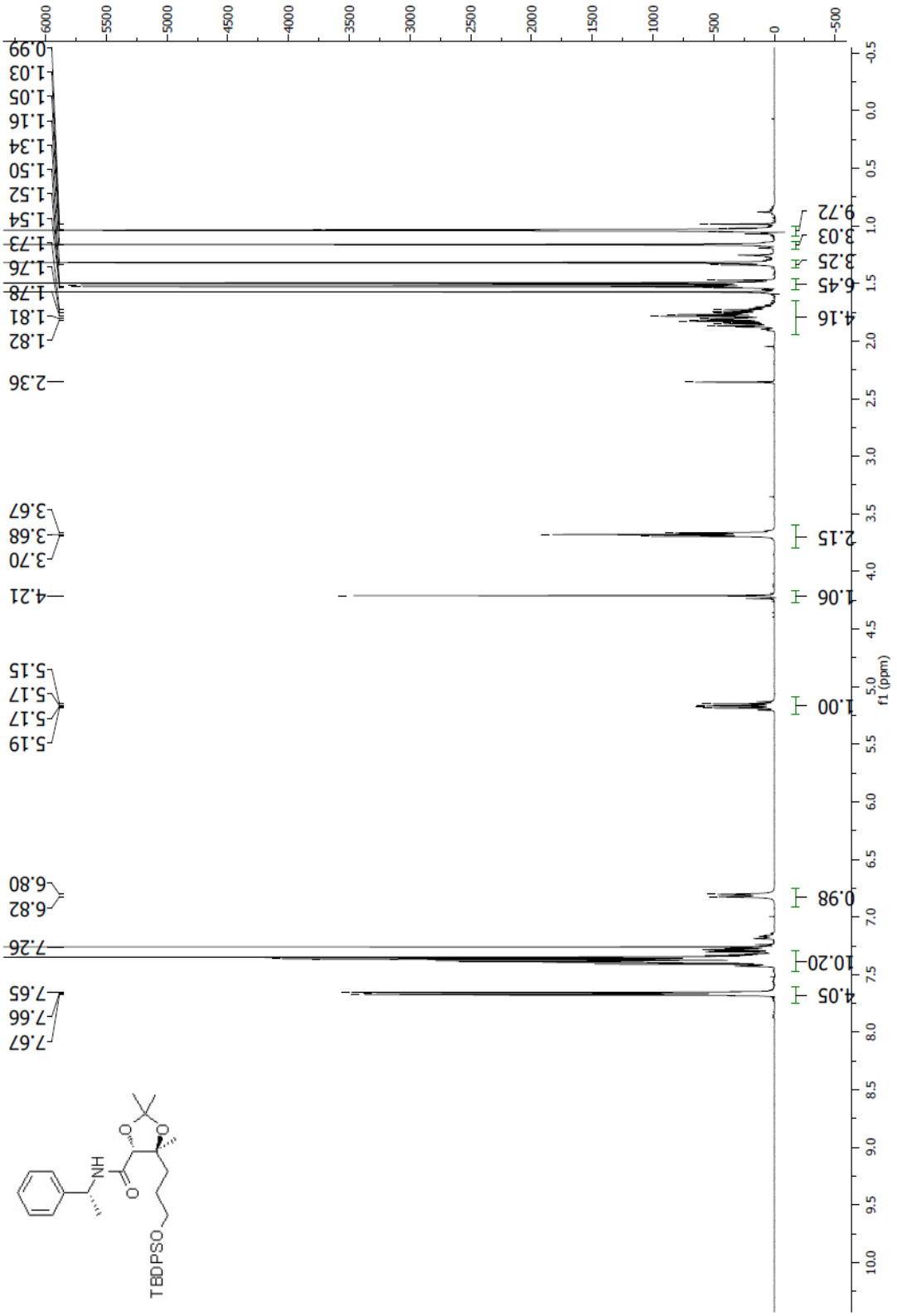

Spectrum 1.48 ^{1}H NMR ($CDCl_3$, 400 MHz) of compound **90**

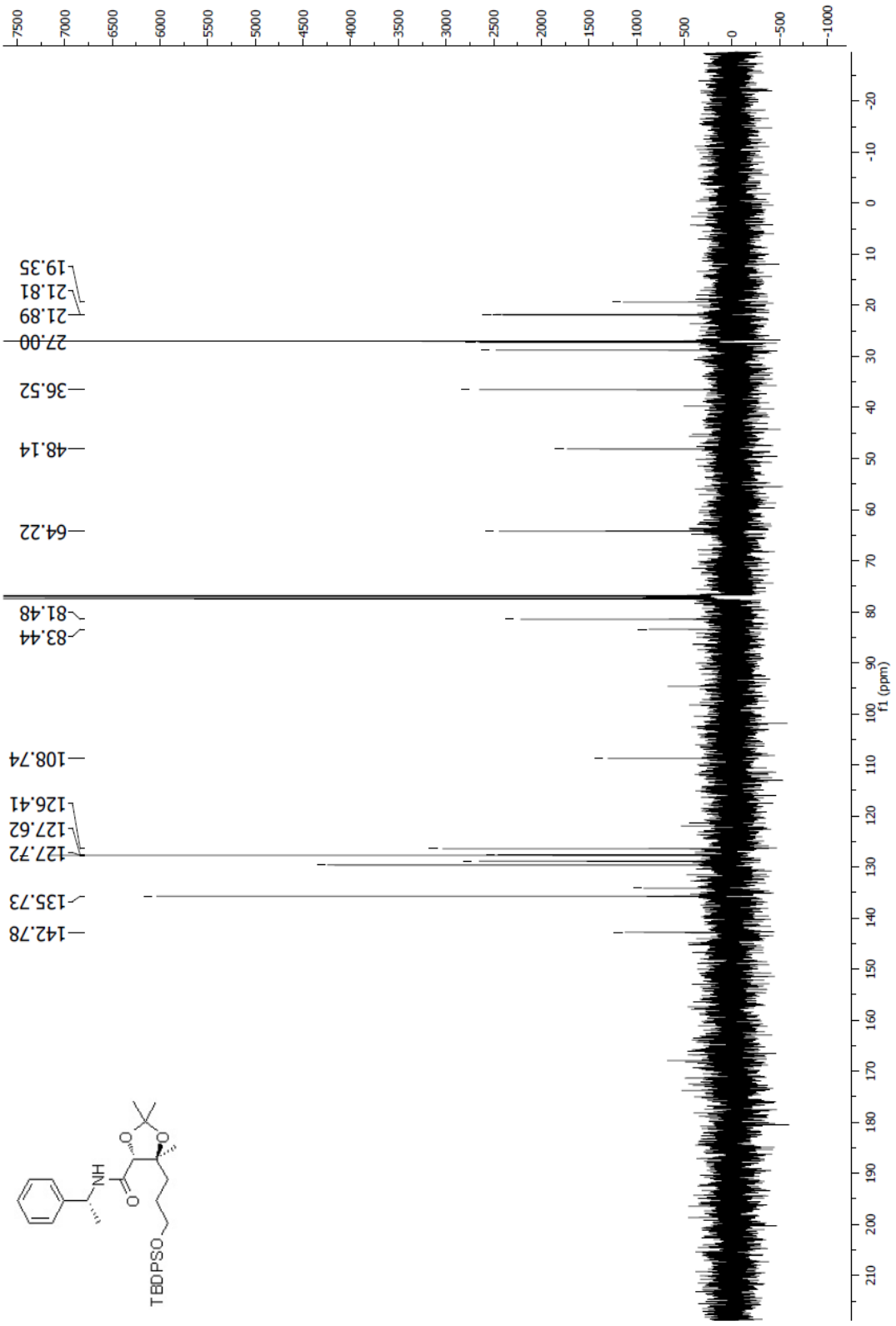

Spectrum 1.49 ^{13}C NMR ($CDCl_3$, 100 MHz) of compound **90**

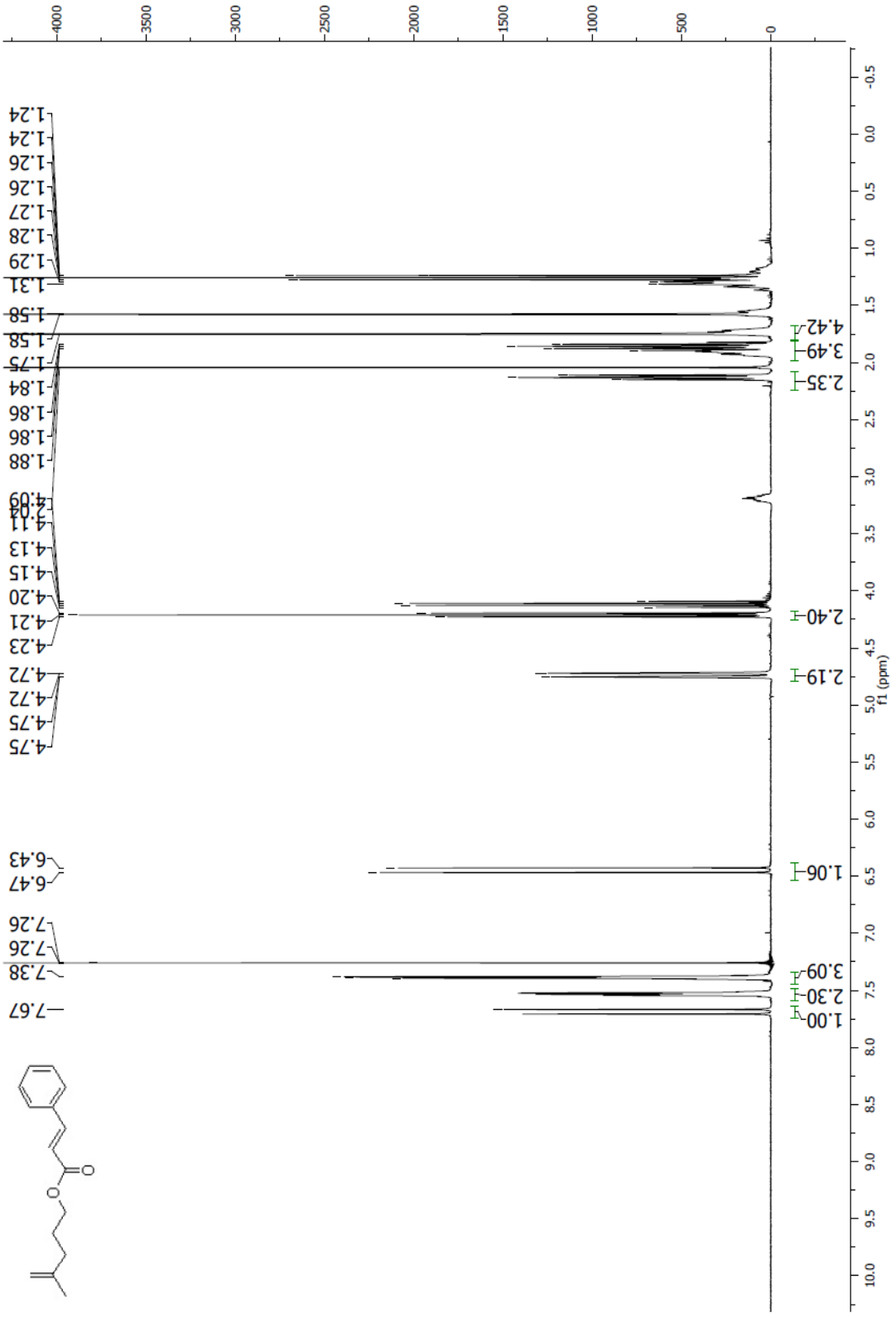

Spectrum 1.50 ^{1}H NMR ($CDCl_3$, 400 MHz) of compound **98**

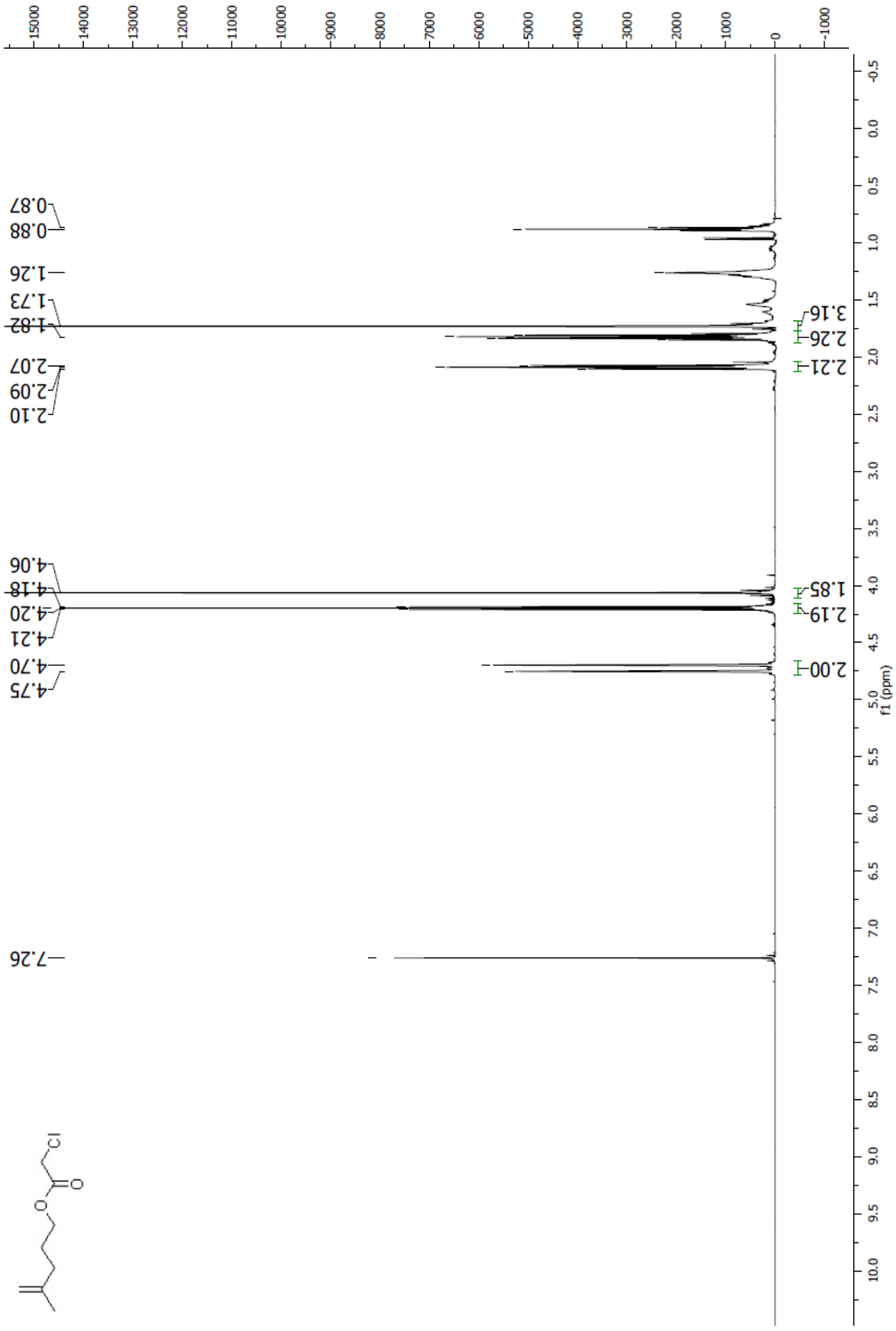

Spectrum 1.51 ^{1}H NMR ($CDCl_3$, 500 MHz) of compound **99**

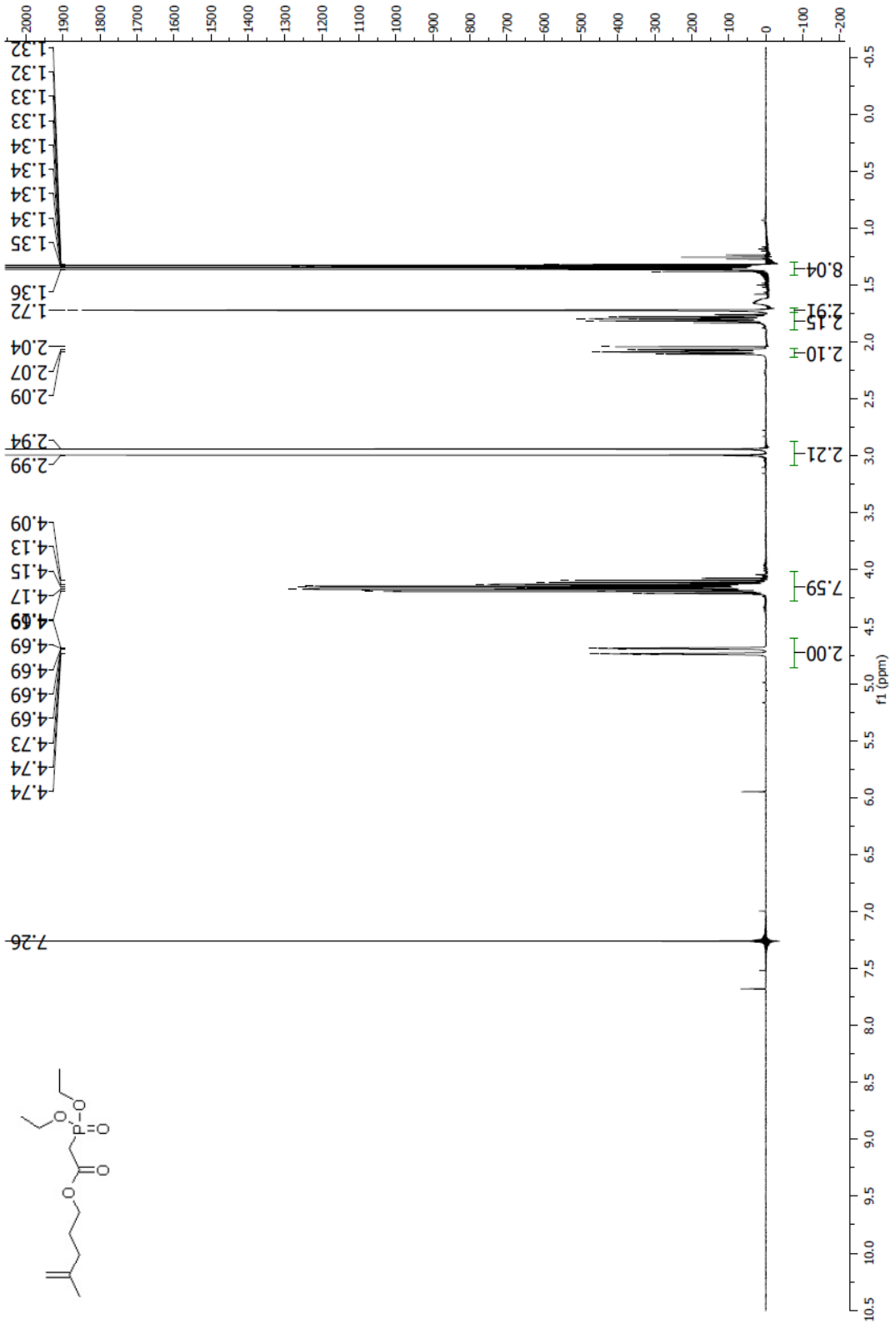

Spectrum 1.52 ^{1}H NMR ($CDCl_3$, 400 MHz) of compound **100**

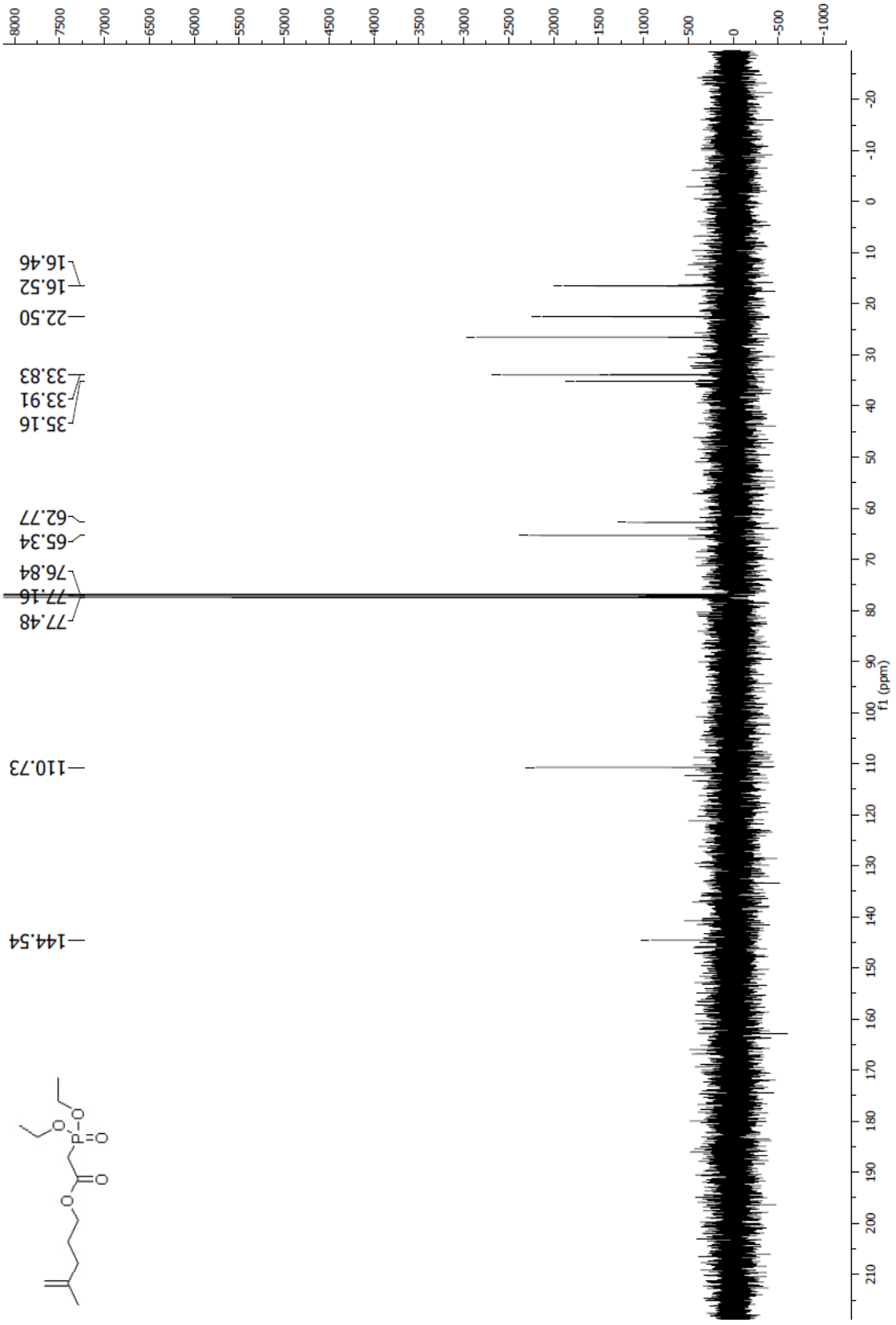

Spectrum 1.53 ^{13}C NMR ($CDCl_3$, 100 MHz) of compound **100**

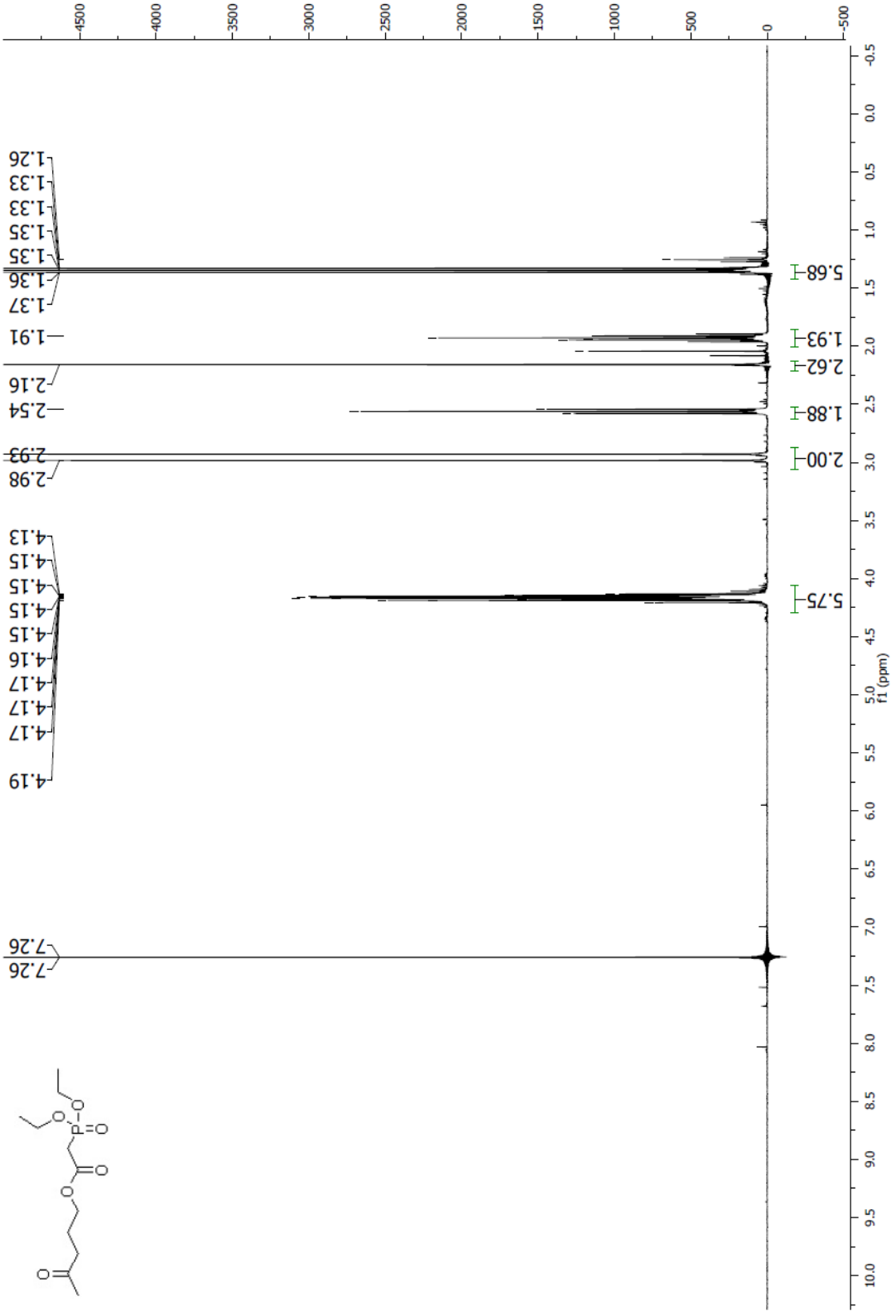

Spectrum 1.54 ^{1}H NMR ($CDCl_3$, 400 MHz) of compound **101**

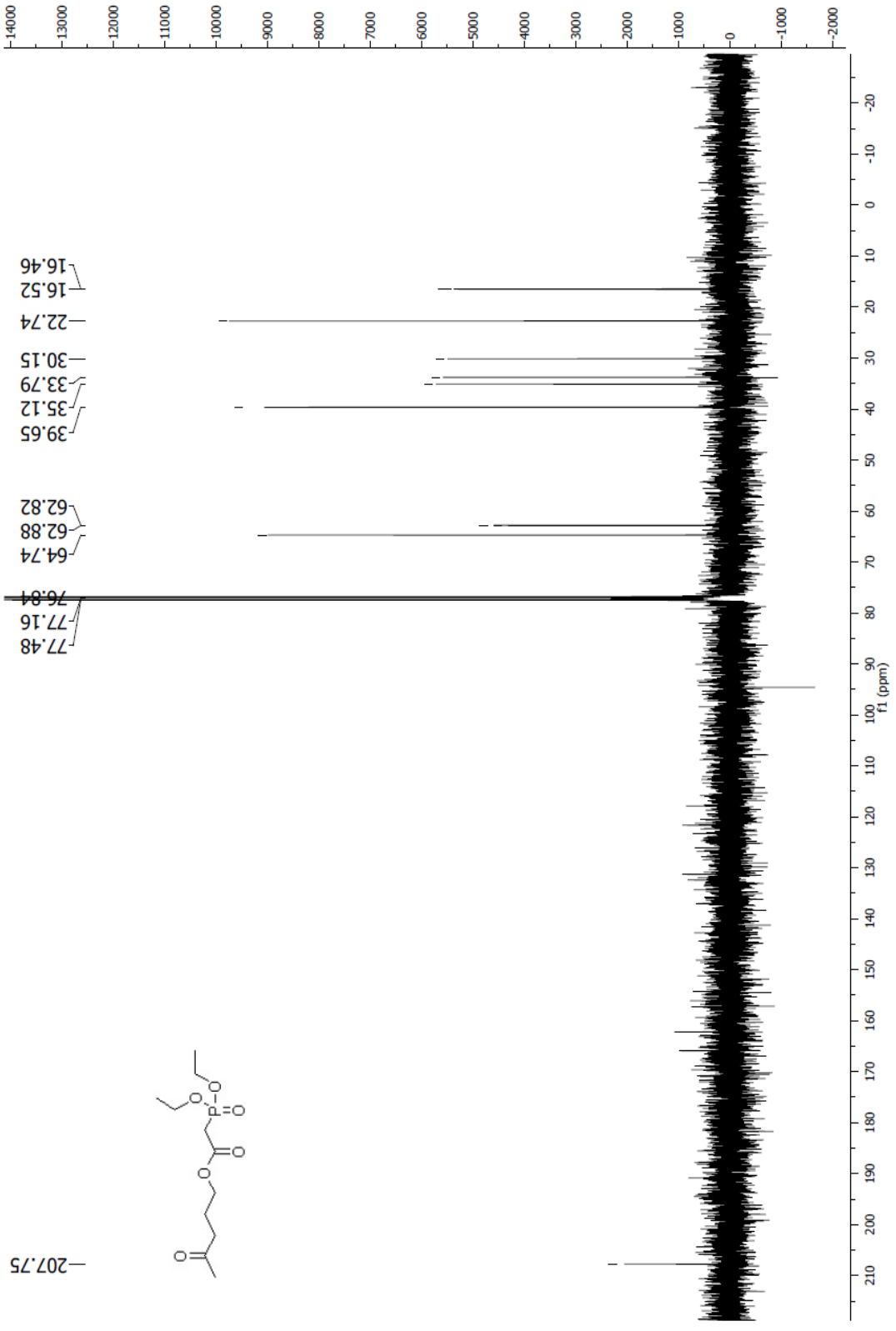

Spectrum 1.55 ^{13}C NMR ($CDCl_3$, 100 MHz) of compound **101**

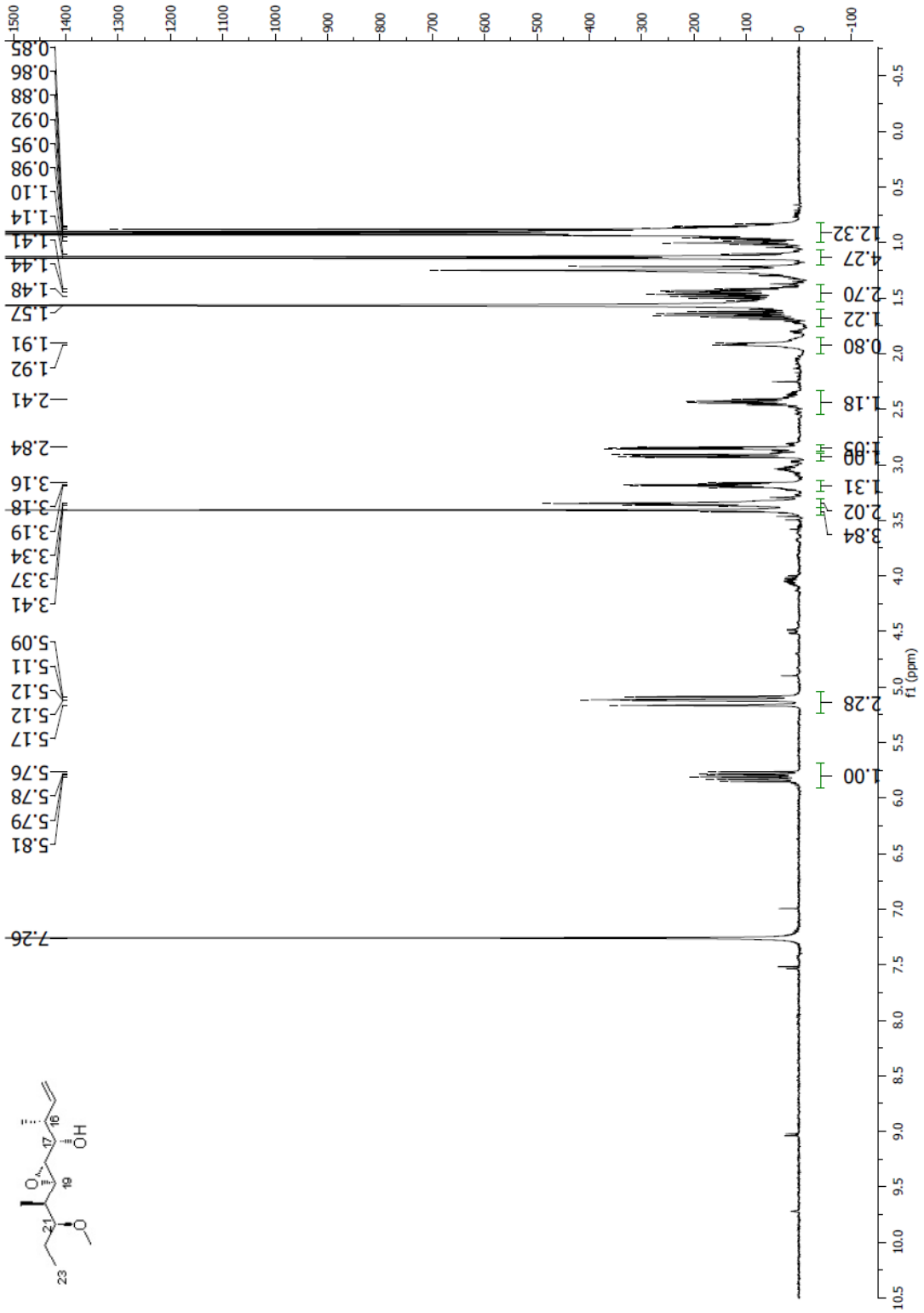

Spectrum 1.56 ^{1}H NMR ($CDCl_3$, 400 MHz) of crotylboration product **105**

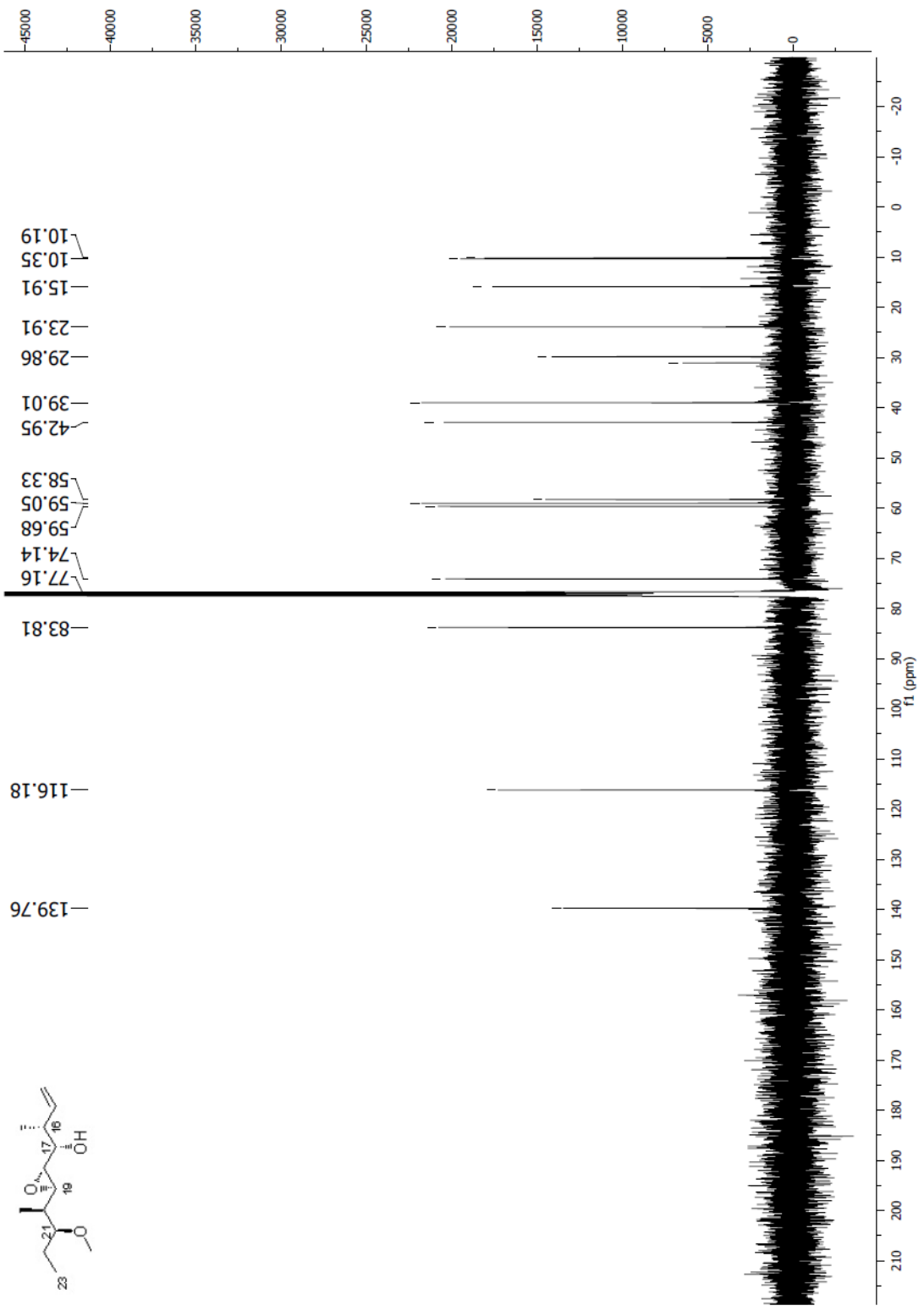

Spectrum 1.57 ^{13}C NMR ($CDCl_3$, 100 MHz) of crotylboration product **105**

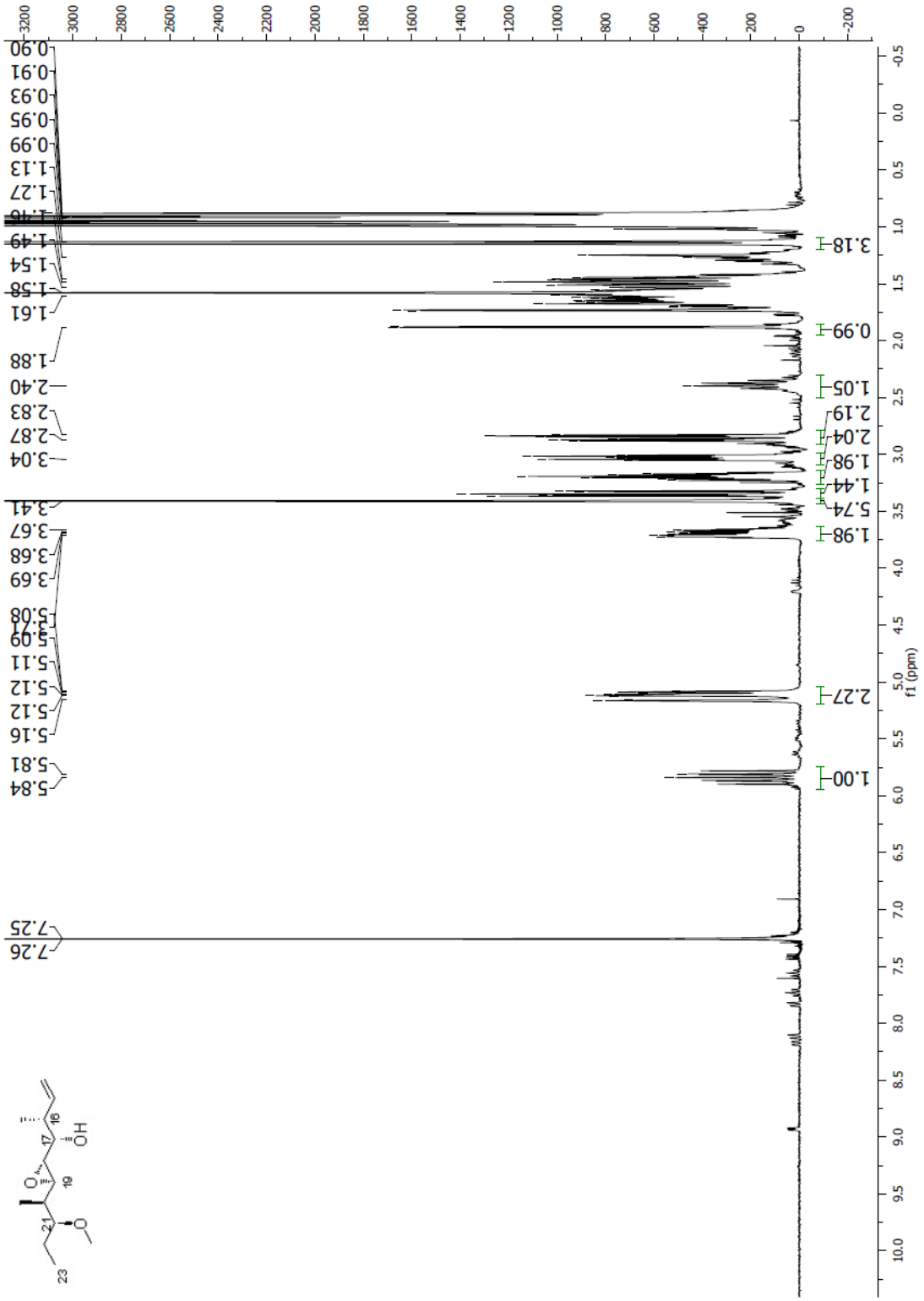

Spectrum 1.58 ^{1}H NMR ($CDCl_3$, 300 MHz) of reduction product **105**

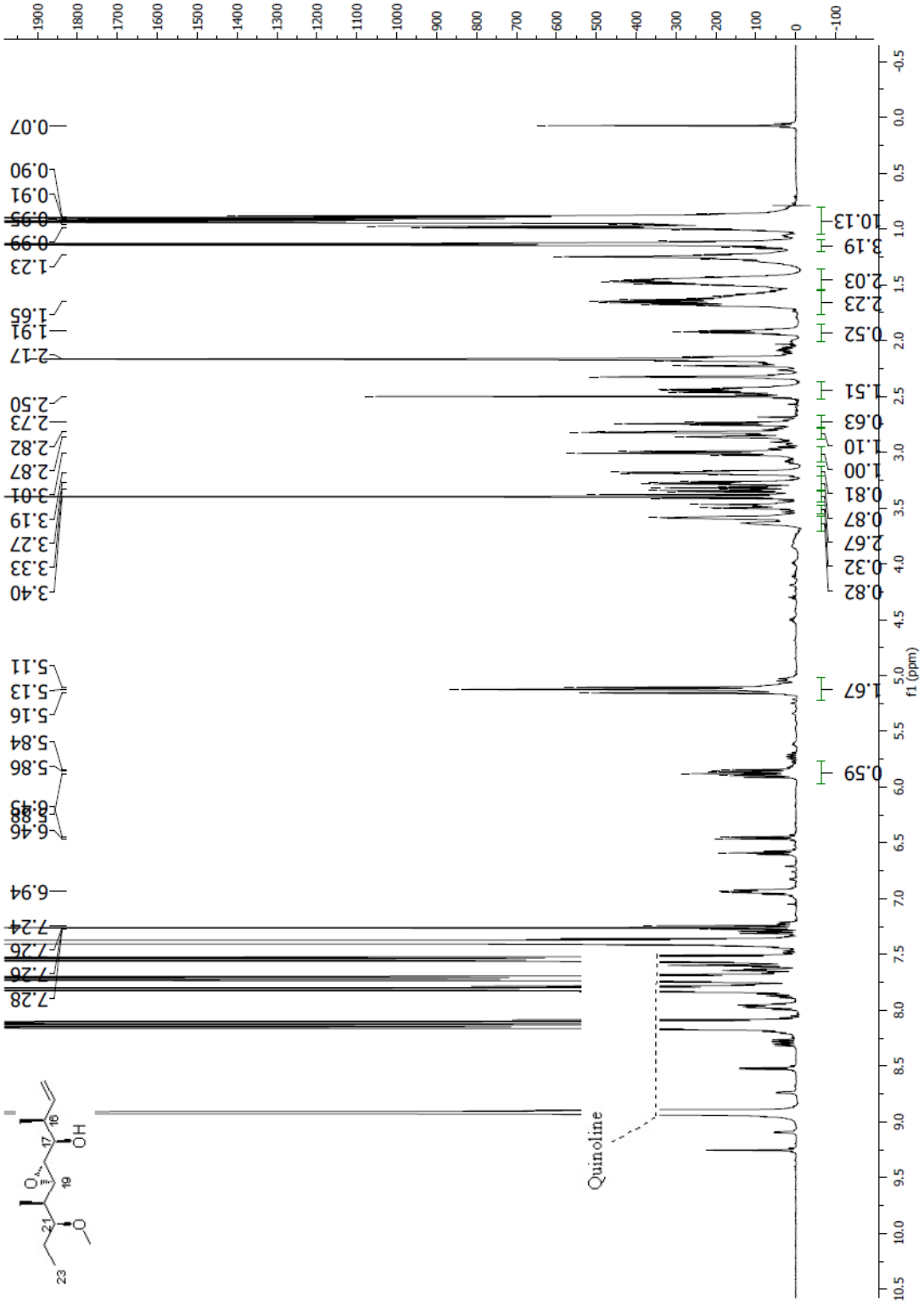

Spectrum 1.59 ^{1}H NMR ($CDCl_3$, 500 MHz) of compound **107**

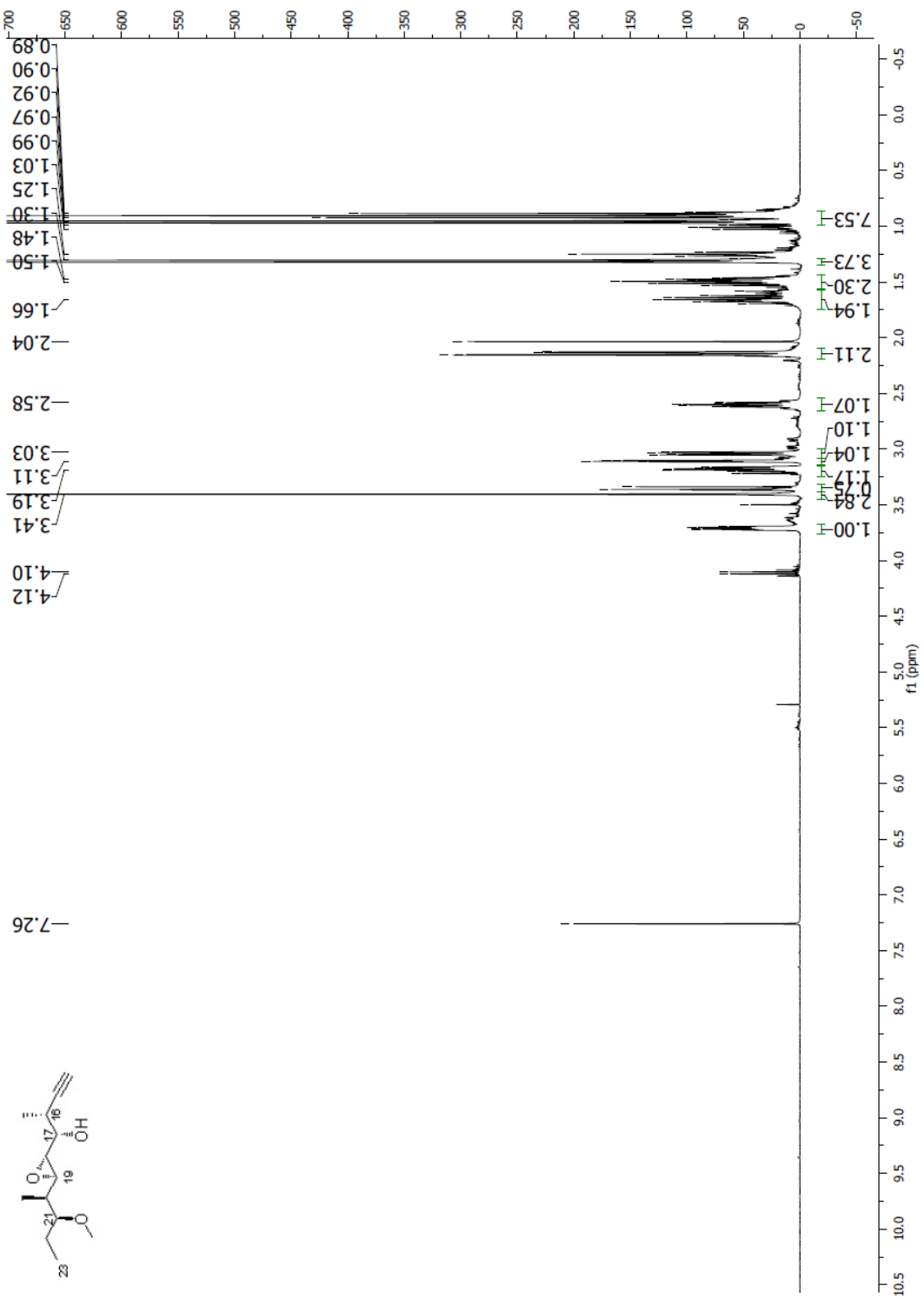

Spectrum 1.60 ^{1}H NMR ($CDCl_3$, 400 MHz) of compound **109**

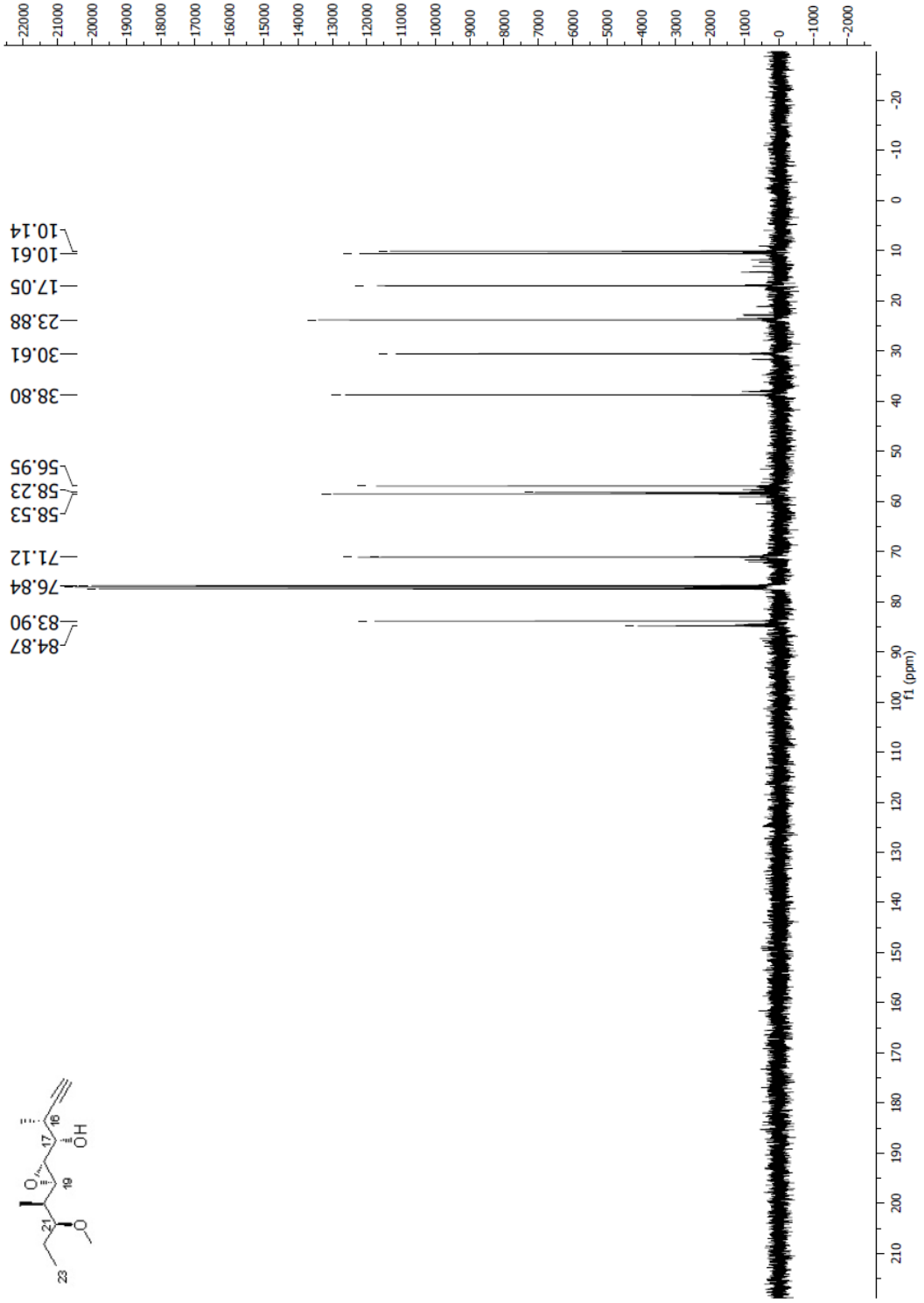

Spectrum 1.61 ^{13}C NMR ($CDCl_3$, 100 MHz) of compound **109**

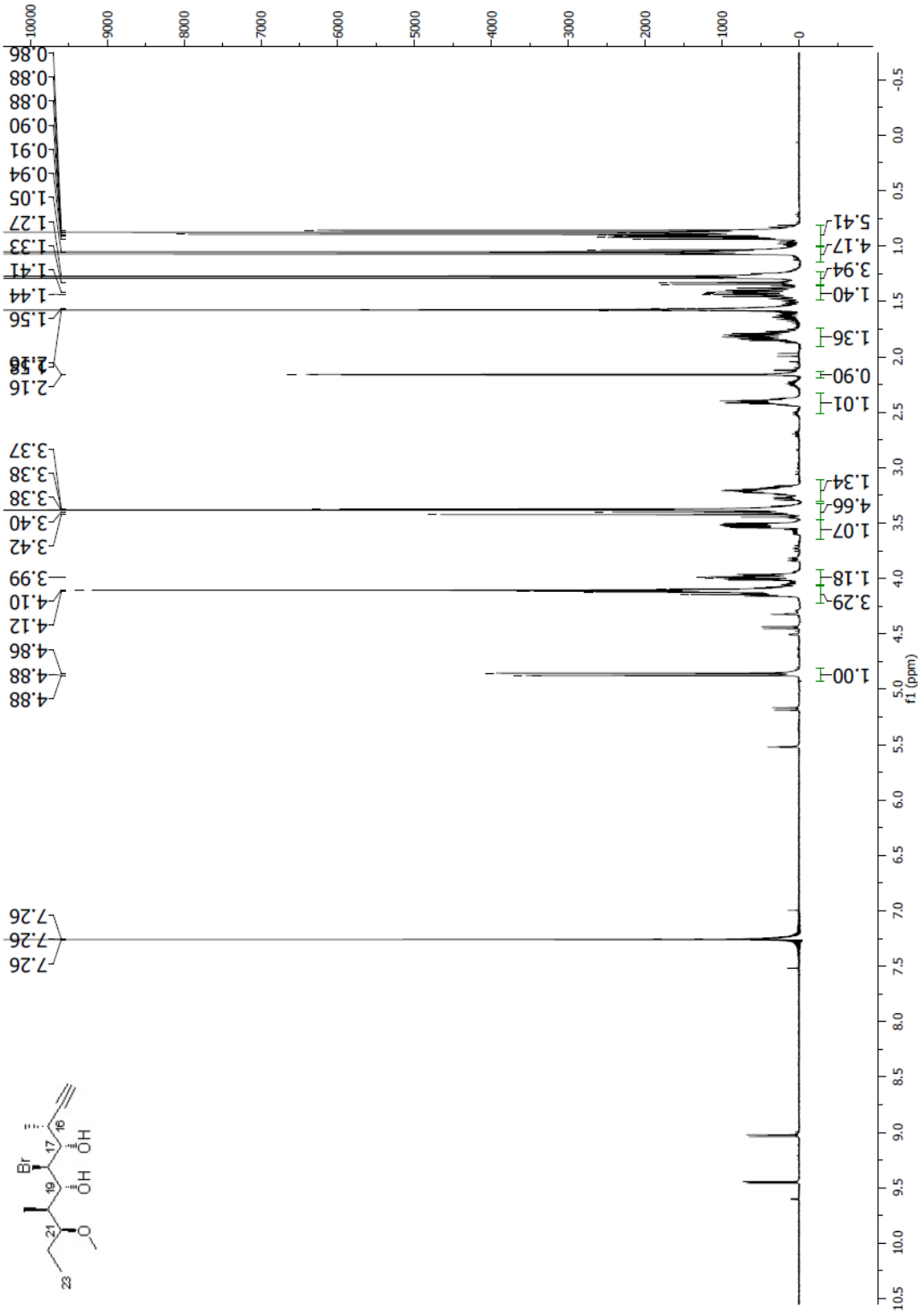

Spectrum 1.62 ^{1}H NMR ($CDCl_3$, 400 MHz) of compound **112**

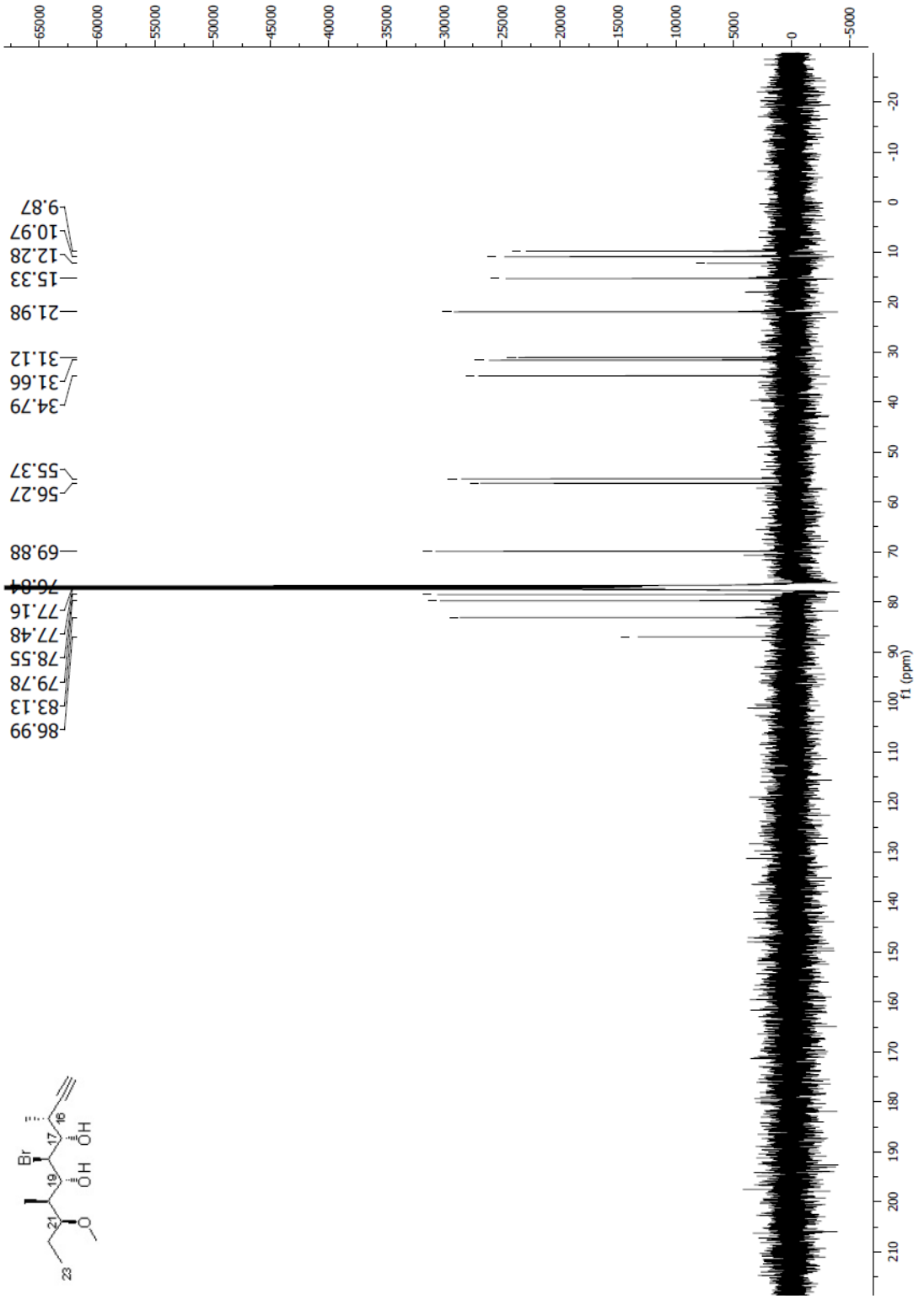

Spectrum 1.63 ^{13}C NMR ($CDCl_3$, 100 MHz) of compound **112**

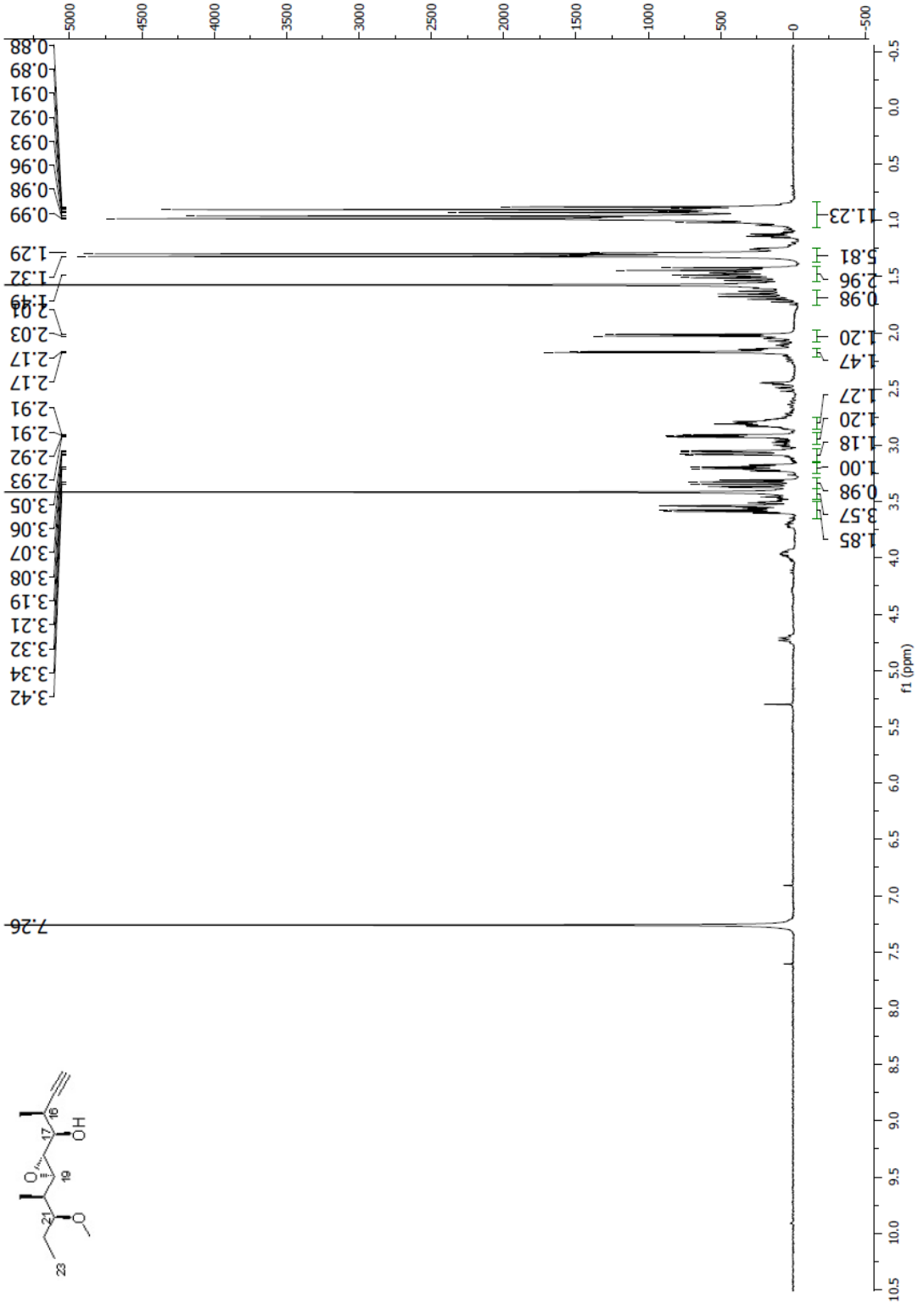

Spectrum 1.64 ^{1}H NMR ($CDCl_3$, 300 MHz) of compound **114**

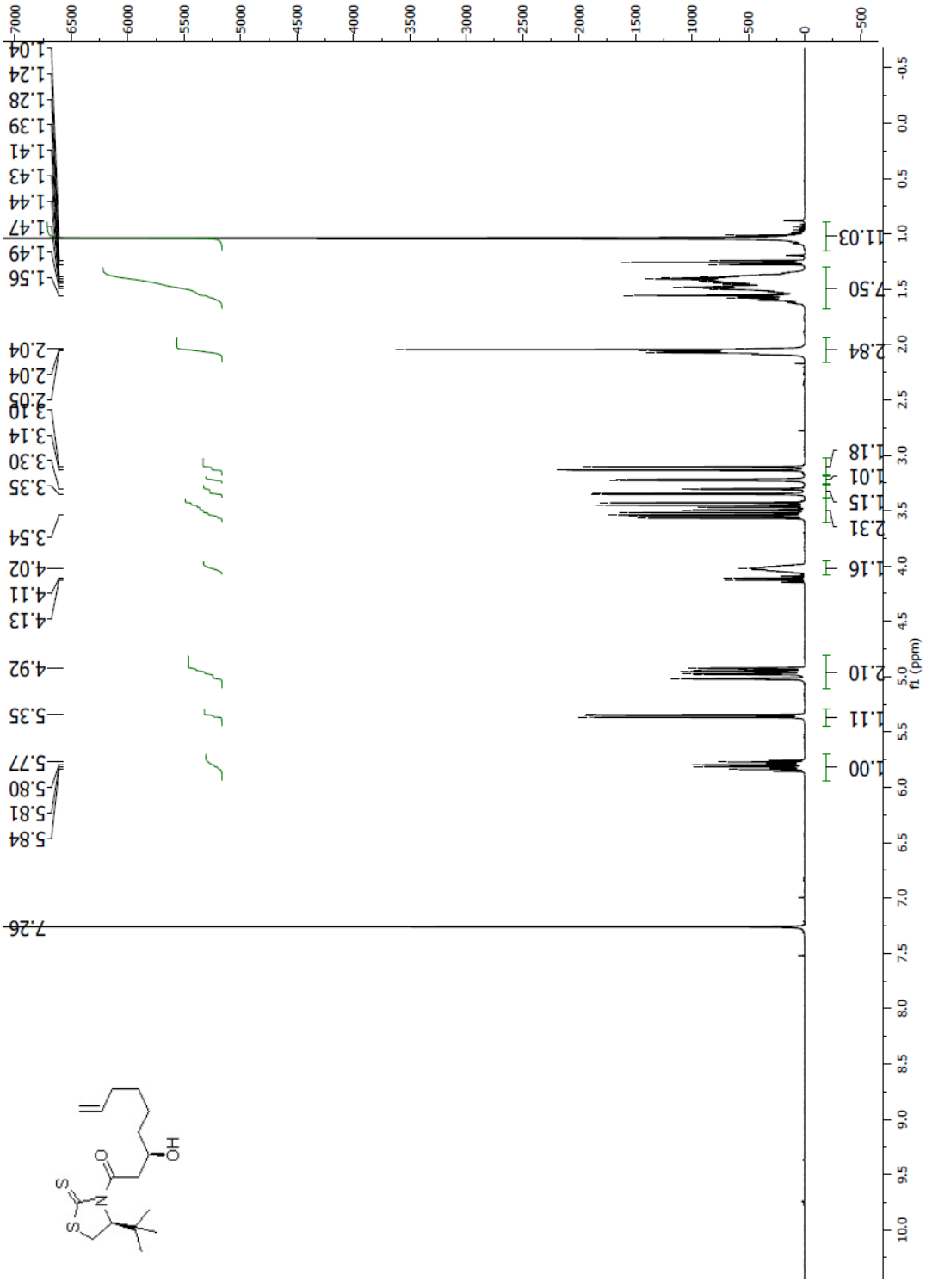

Spectrum 1.65 ^{1}H NMR ($CDCl_3$, 400 MHz) of compound **118**

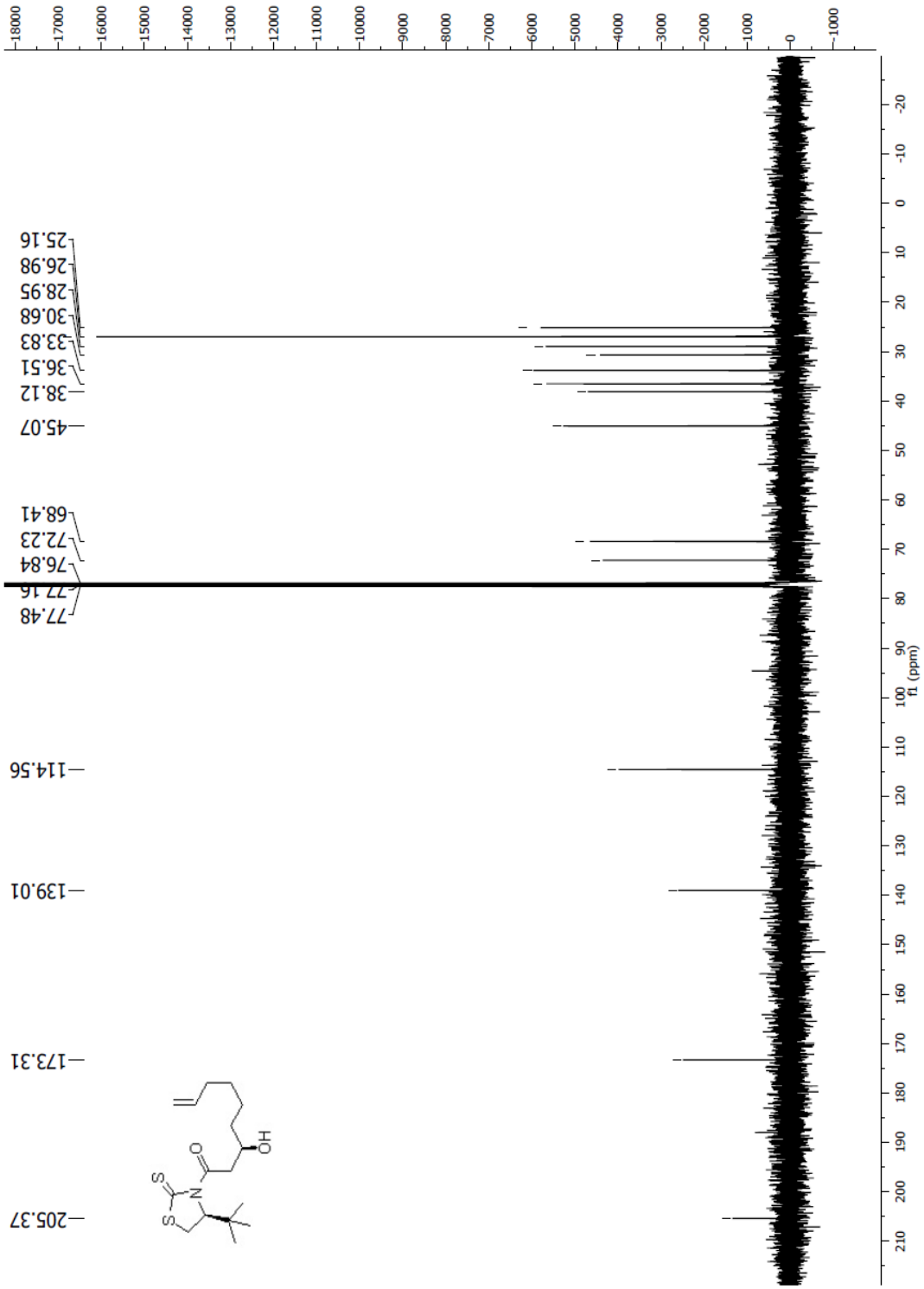

Spectrum 1.66 ^{13}C NMR ($CDCl_3$, 100 MHz) of compound **118**

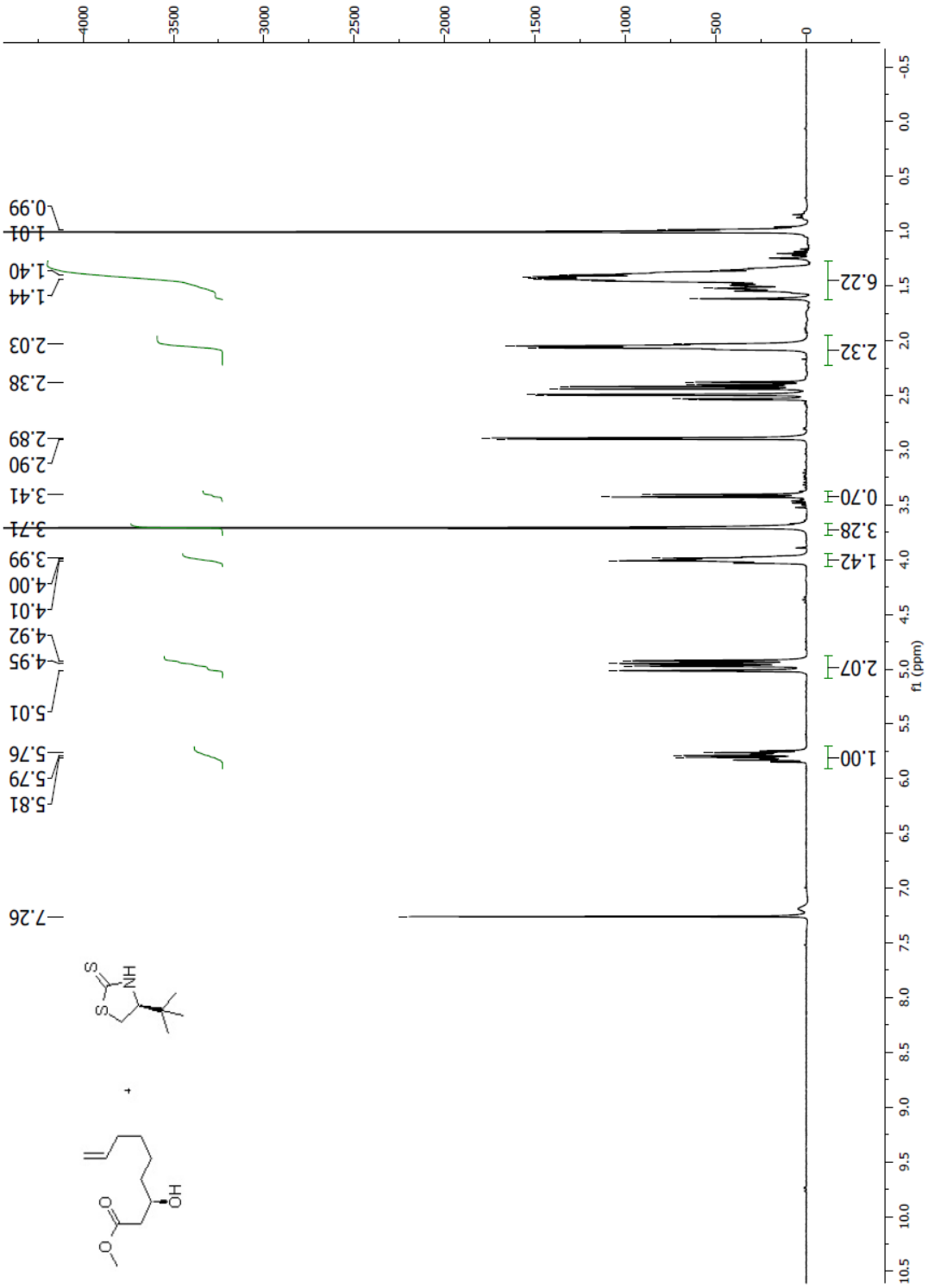

Spectrum 1.67 ^{1}H NMR ($CDCl_3$, 400 MHz) of compound **119**

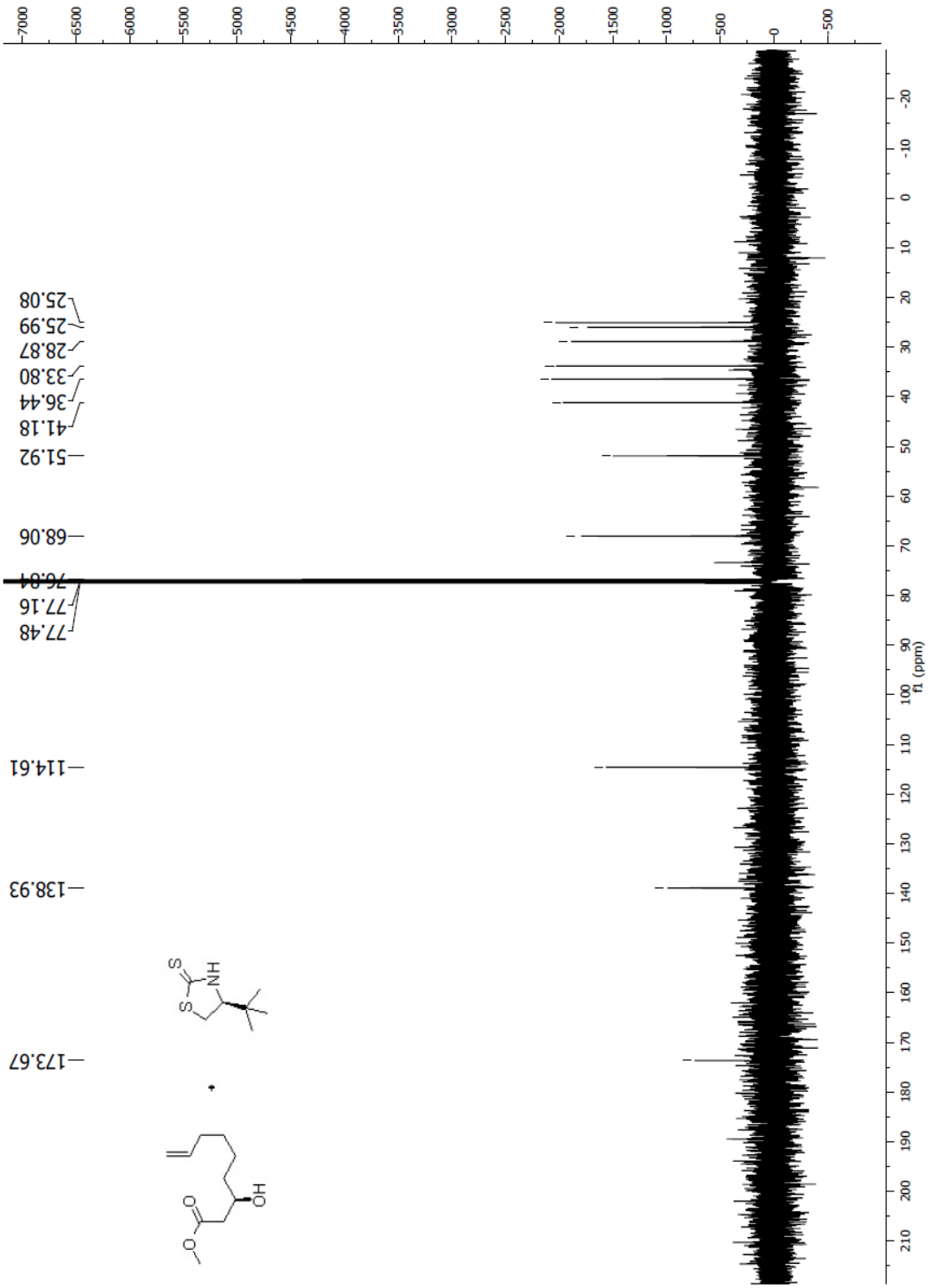

Spectrum 1.68 ^{13}C NMR ($CDCl_3$, 100 MHz) of compound **119**

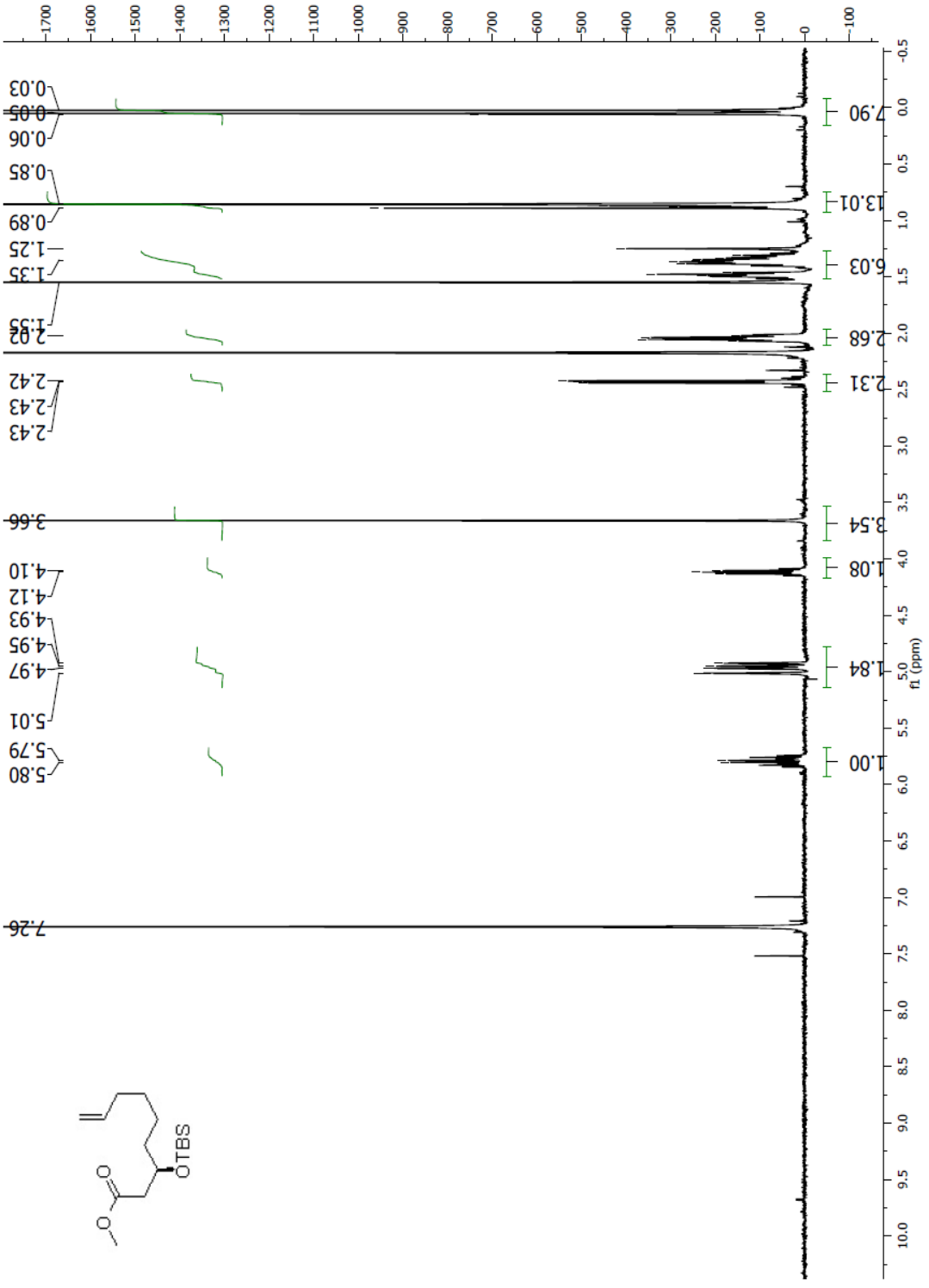

Spectrum 1.69 ^{1}H NMR ($CDCl_3$, 400 MHz) of compound **120**

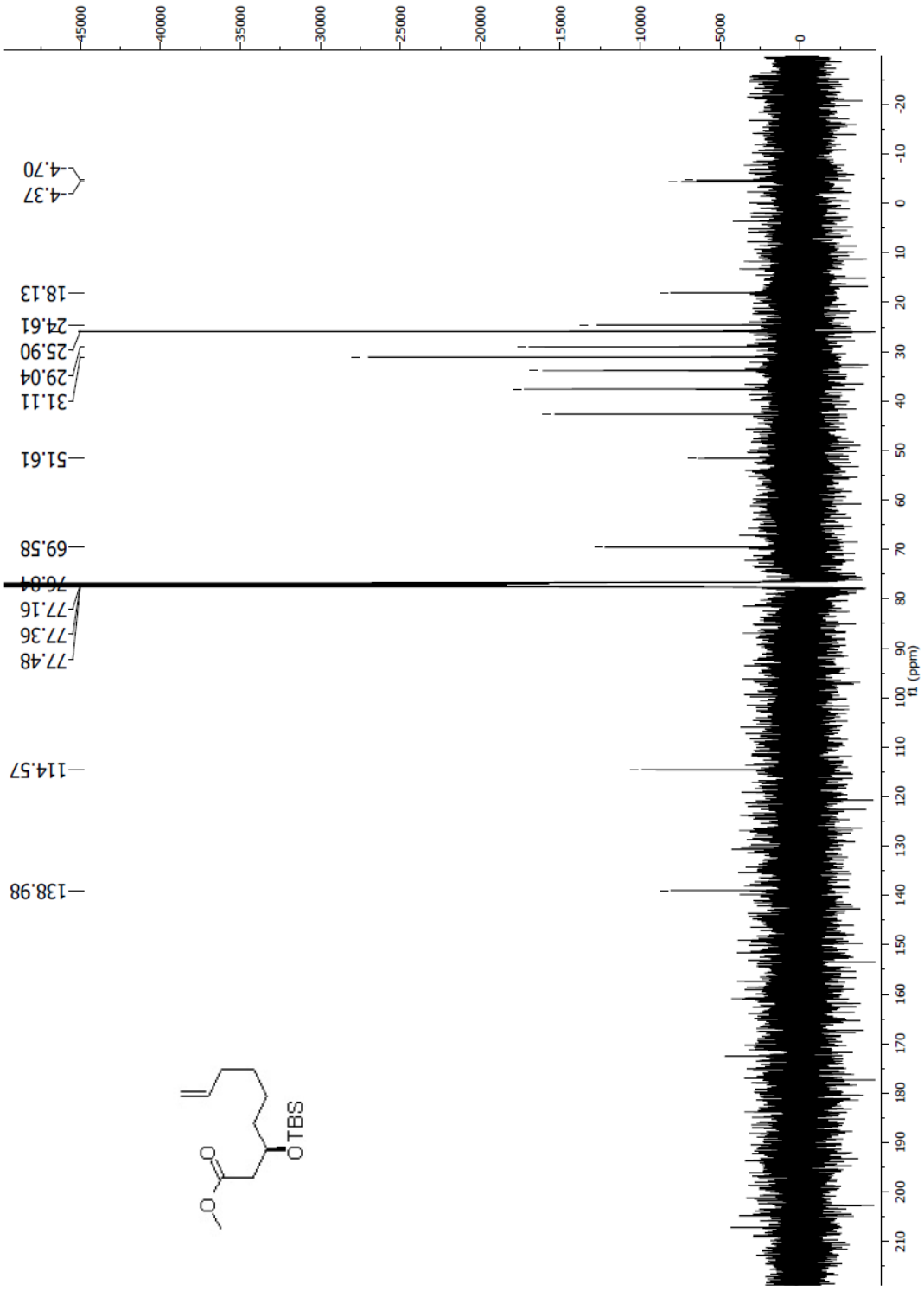

Spectrum 1.70 ^{13}C NMR ($CDCl_3$, 100 MHz) of compound **120**

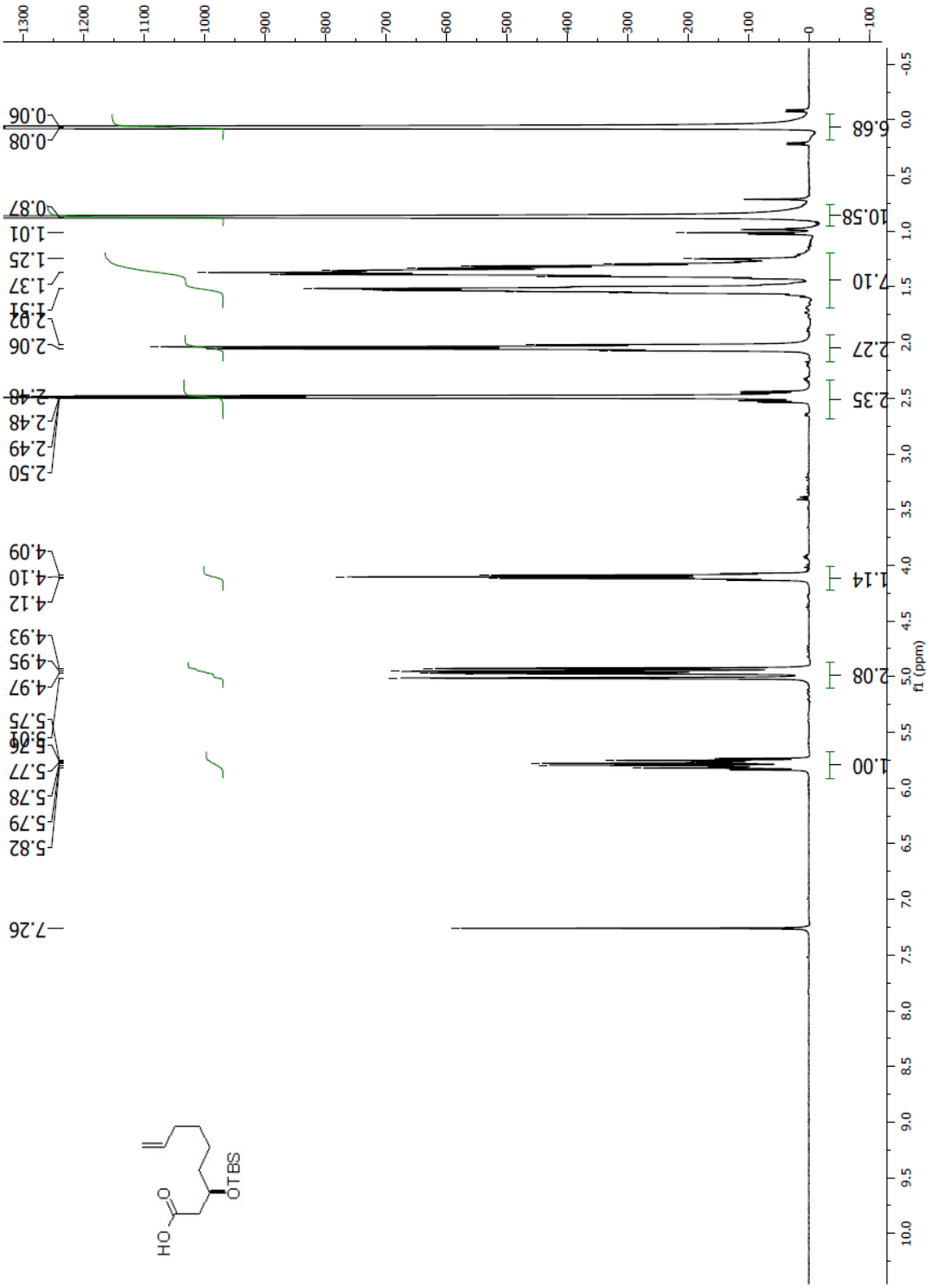

Spectrum 1.71 ^{1}H NMR ($CDCl_3$, 400 MHz) of compound **121**

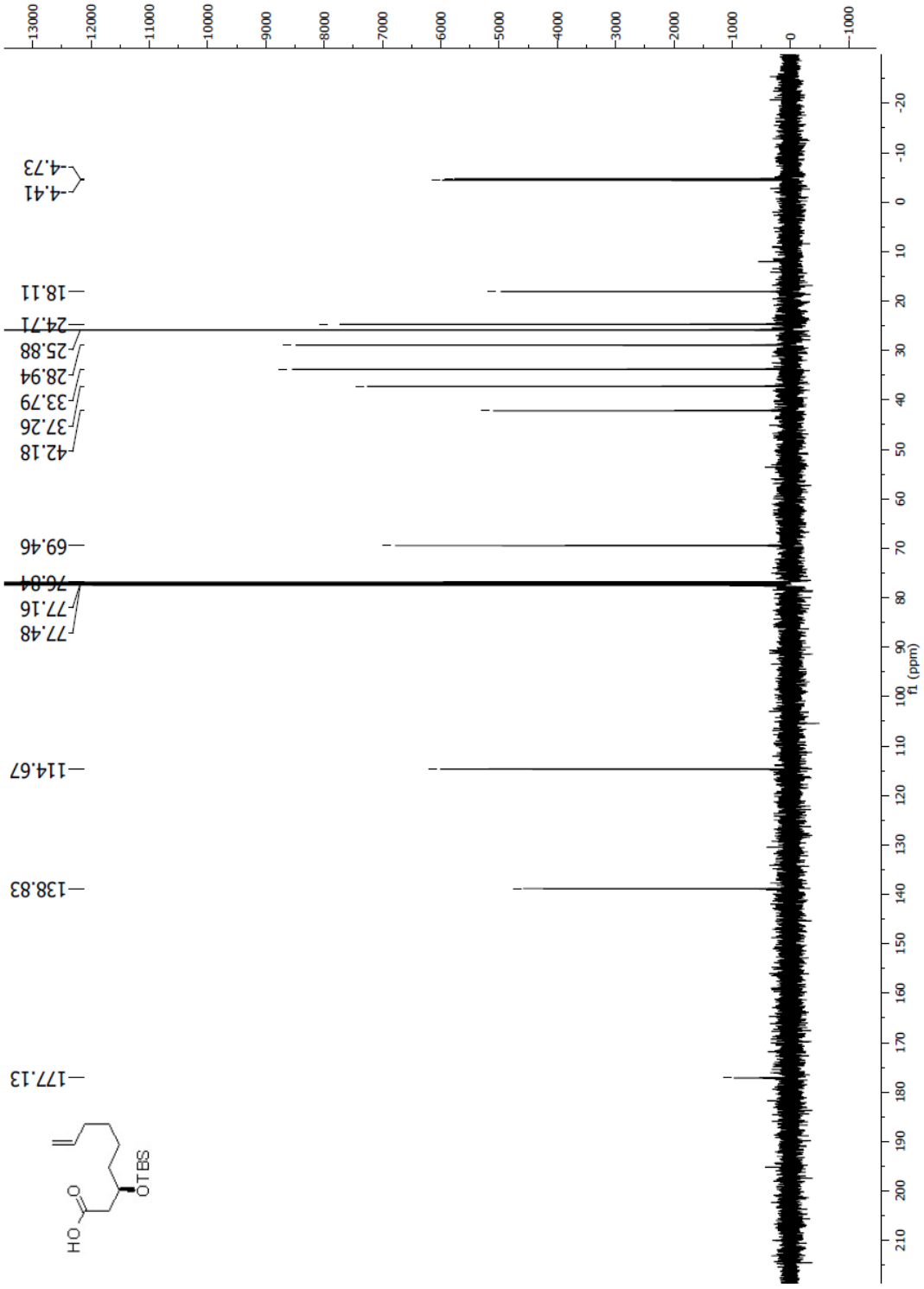

Spectrum 1.72 ^{13}C NMR ($CDCl_3$, 100 MHz) of compound **121**

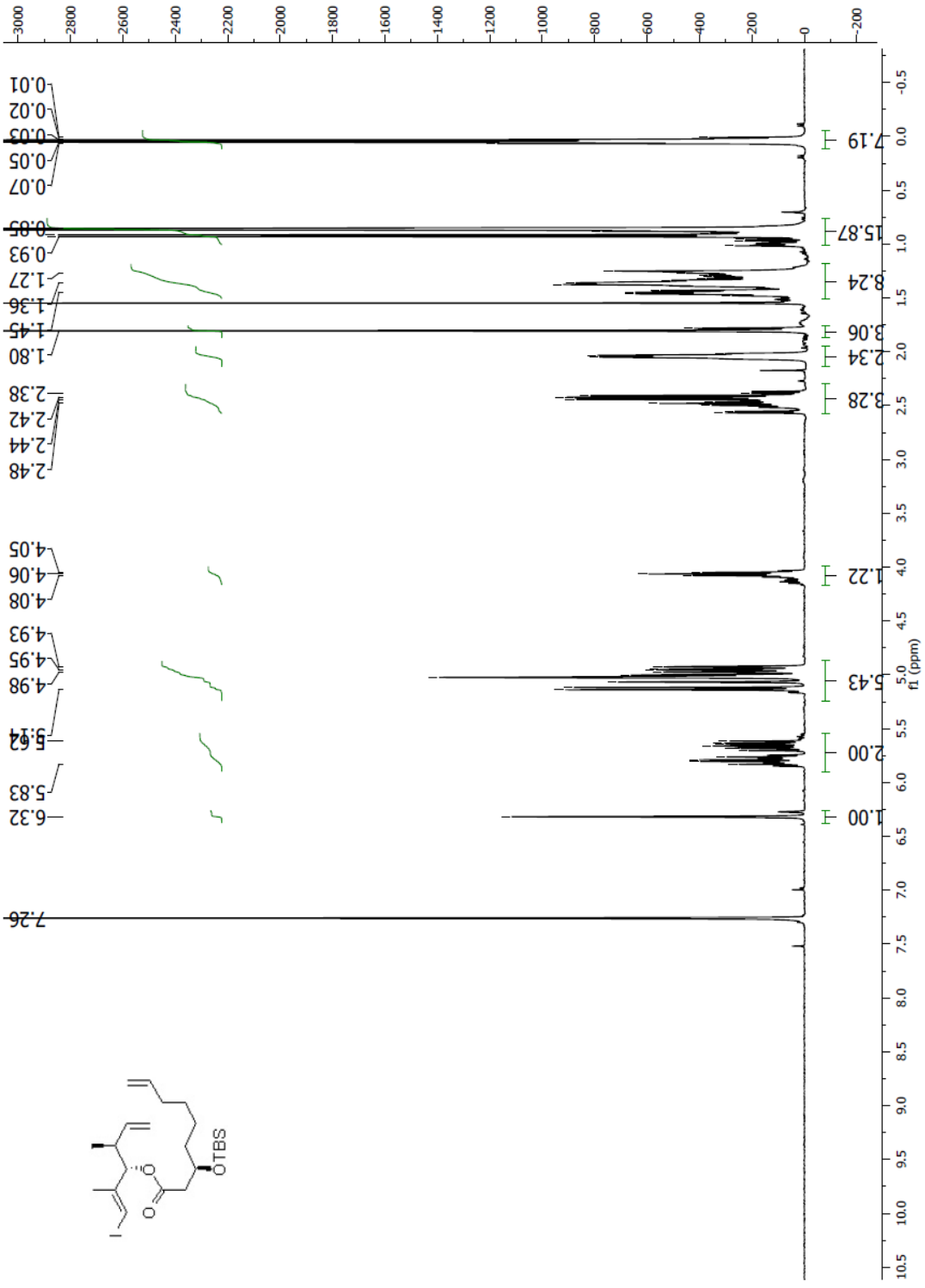

Spectrum 1.73 ^{1}H NMR ($CDCl_3$, 400 MHz) of compound **122**

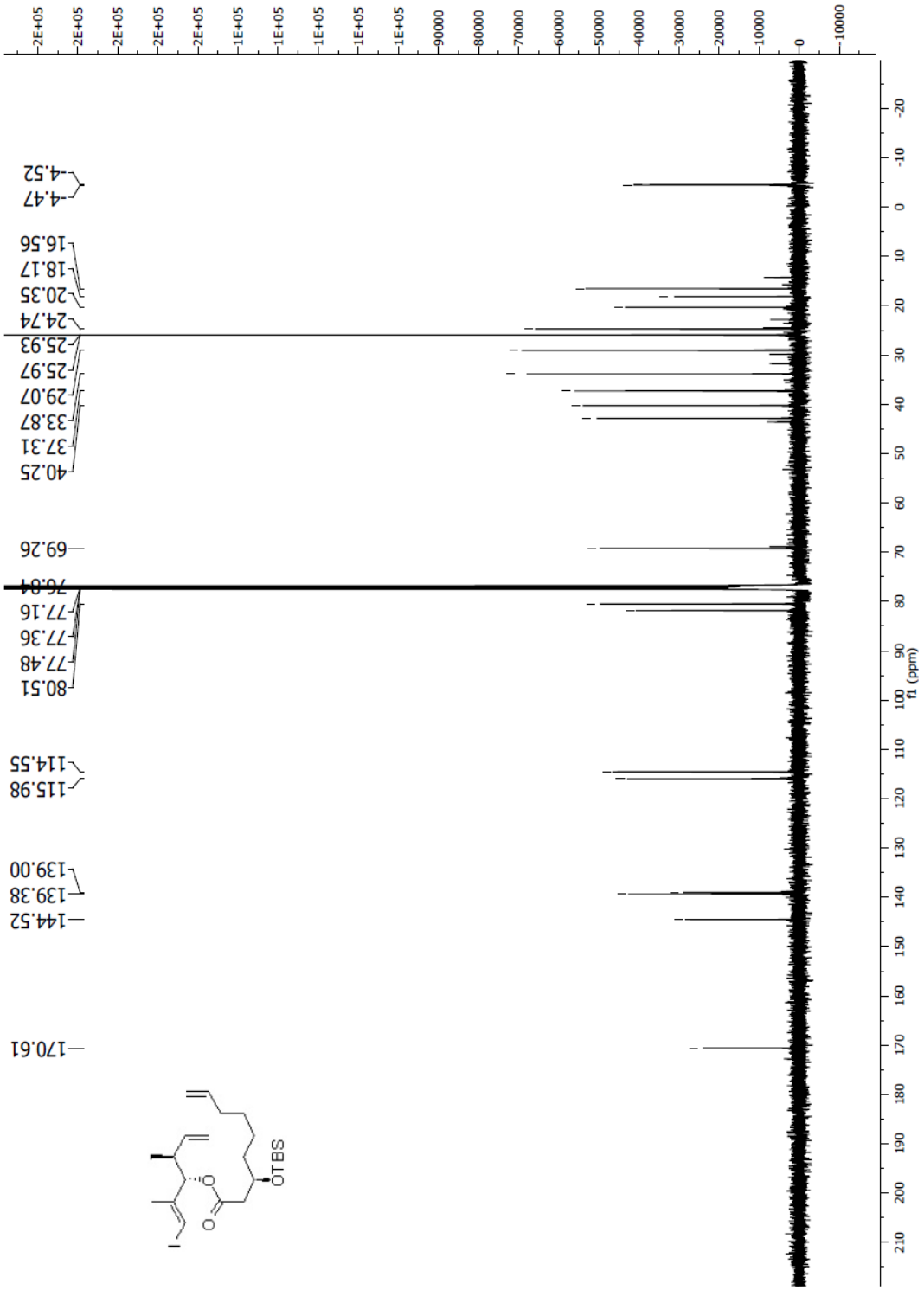

Spectrum 1.74 ^{13}C NMR ($CDCl_3$, 100 MHz) of compound **122**

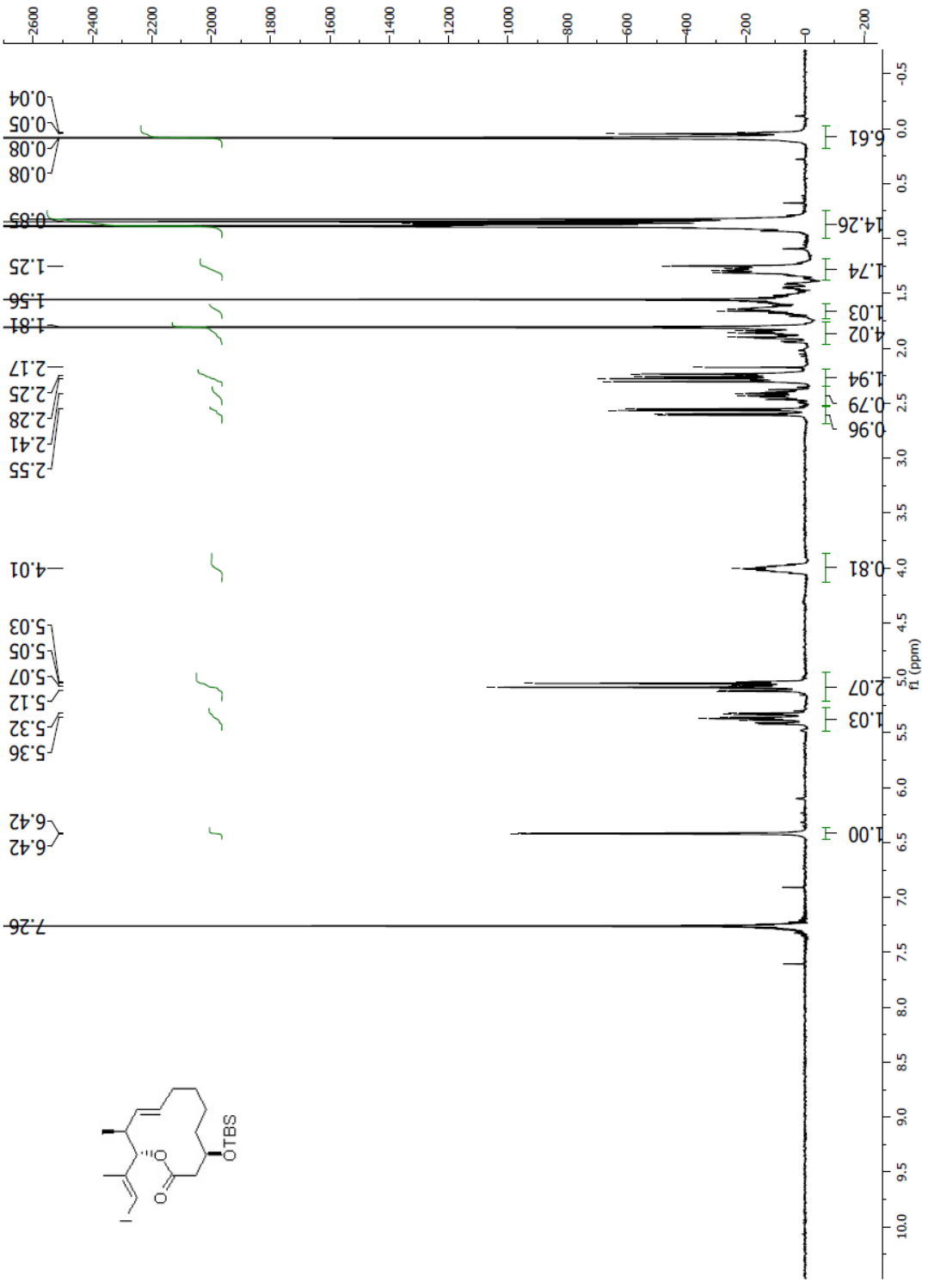

Spectrum 1.75 ^{1}H NMR ($CDCl_3$, 300 MHz) of compound **123**

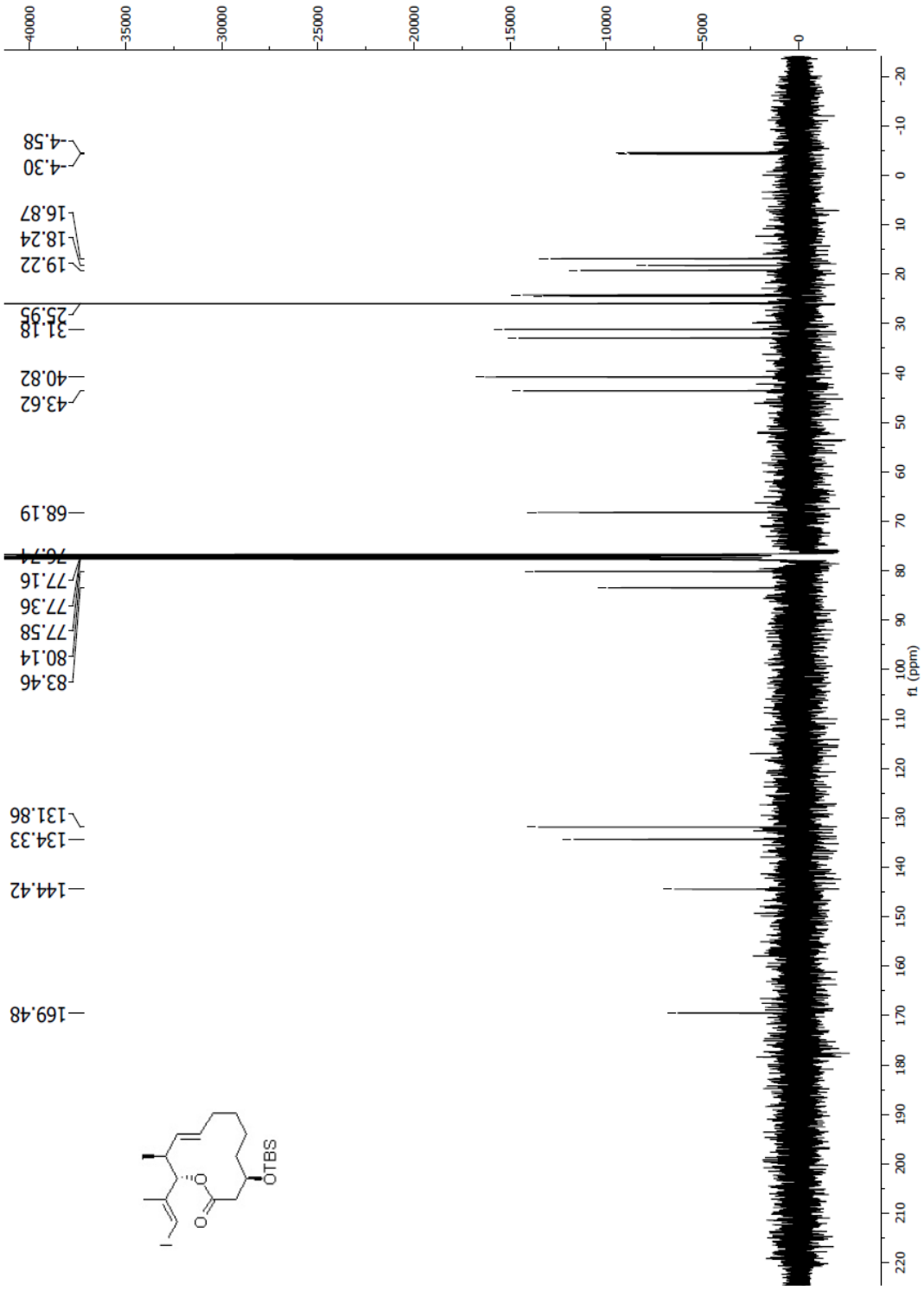

Spectrum 1.76 ^{13}C NMR ($CDCl_3$, 75 MHz) of compound **123**

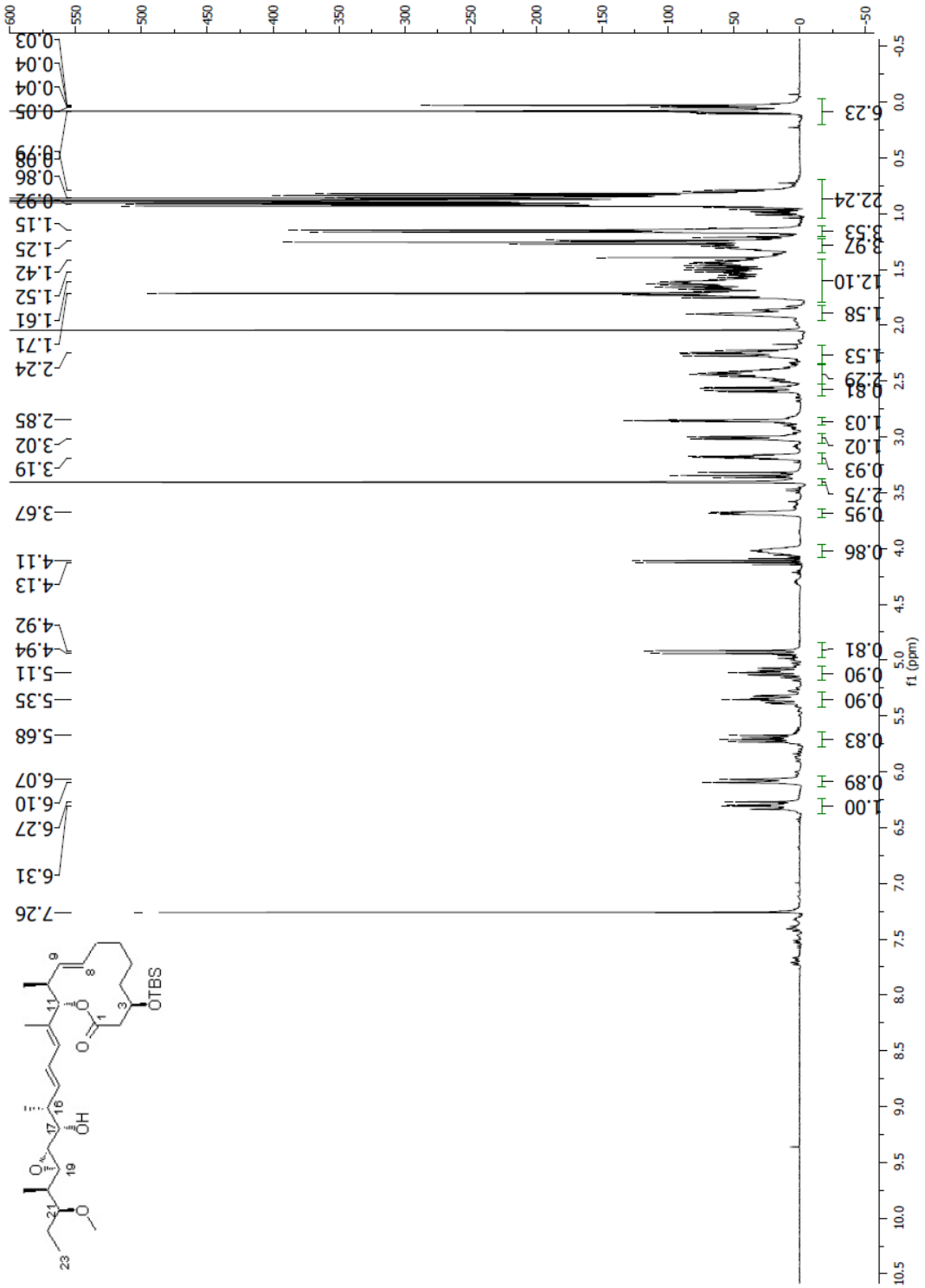

Spectrum 1.77 ^{1}H NMR ($CDCl_3$, 400 MHz) of compound **125**

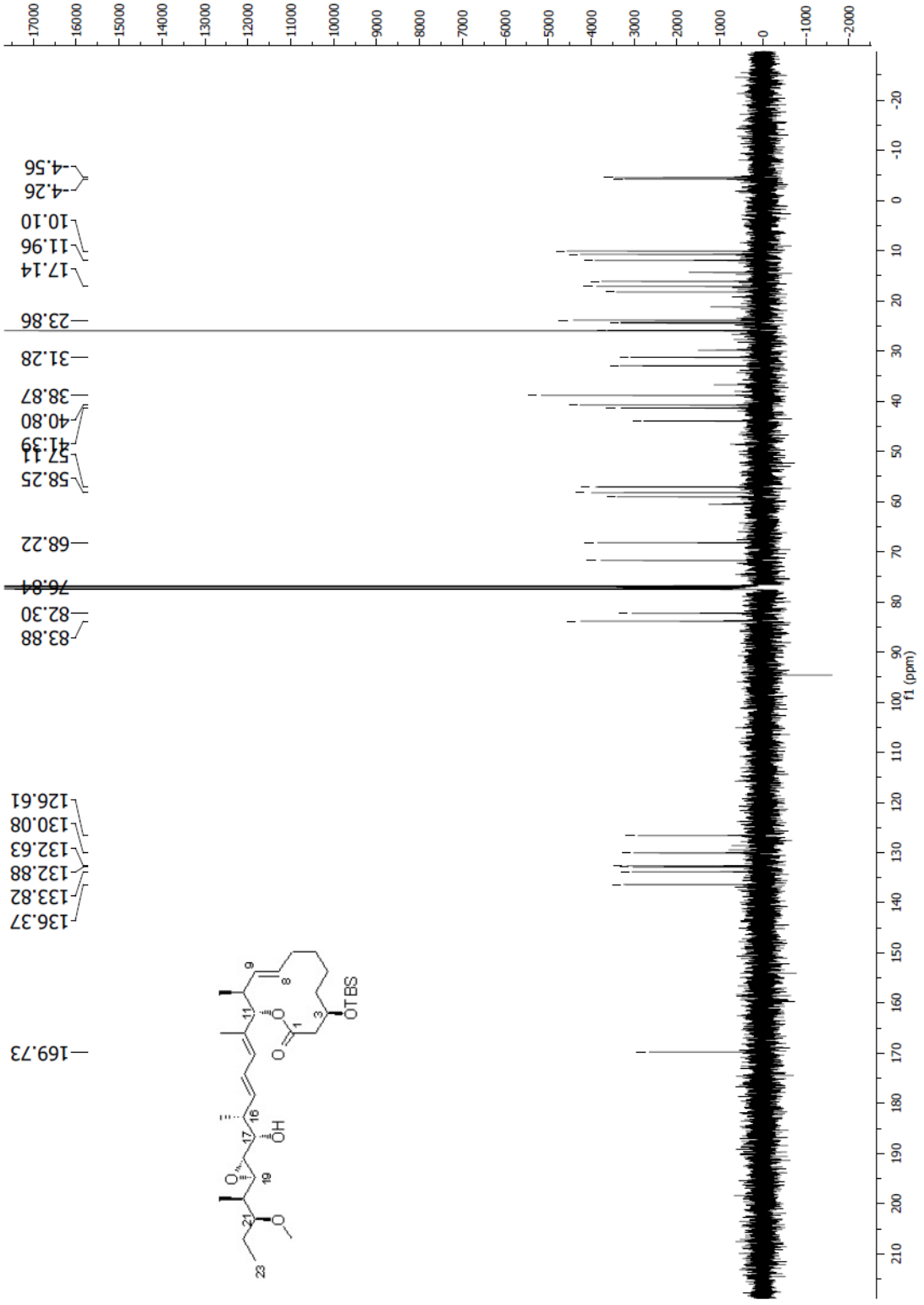

Spectrum 1.78 ^{13}C NMR ($CDCl_3$, 100 MHz) of compound **125**

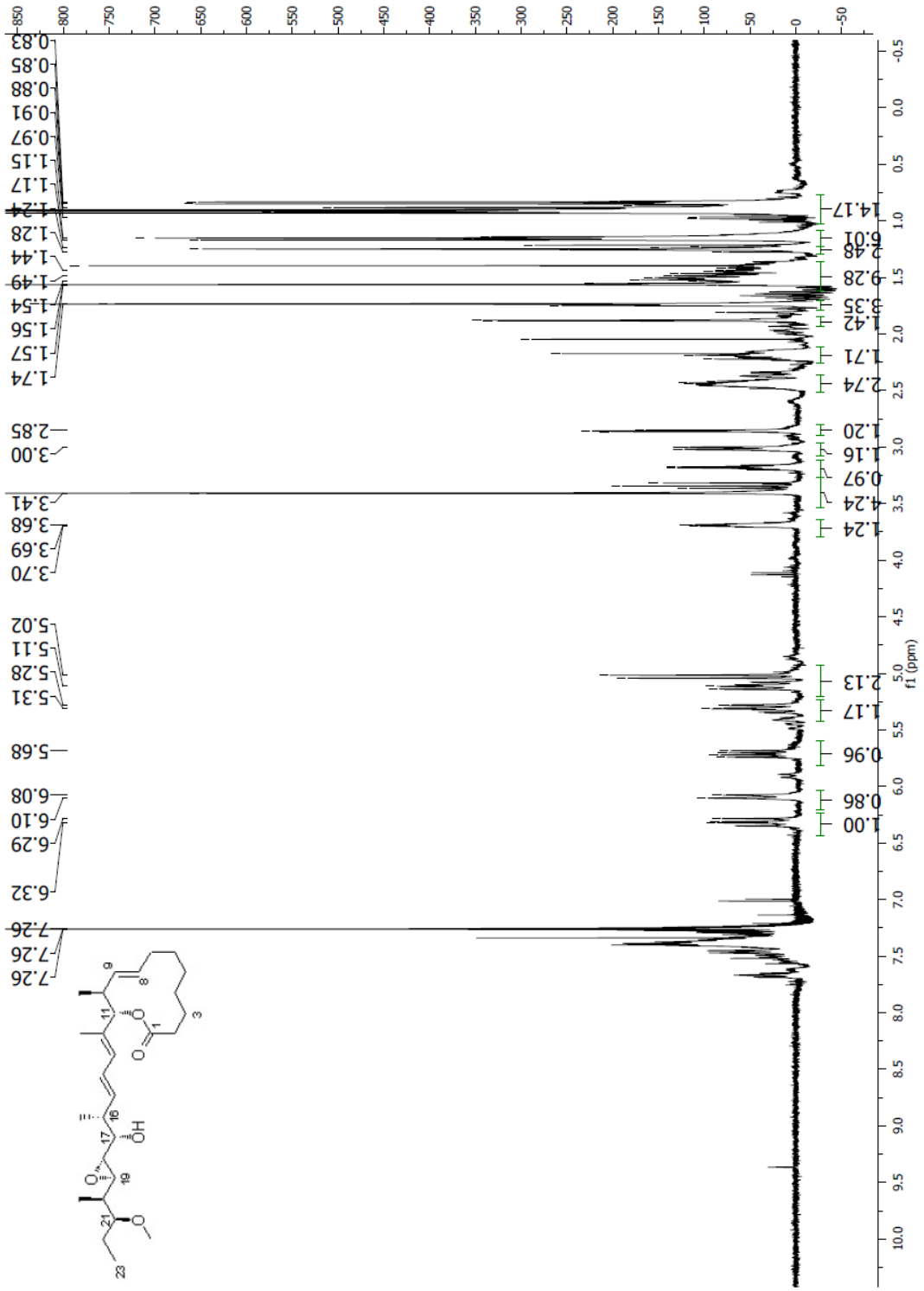

Spectrum 1.79 ^{1}H NMR ($CDCl_3$, 400 MHz) of compound **126**

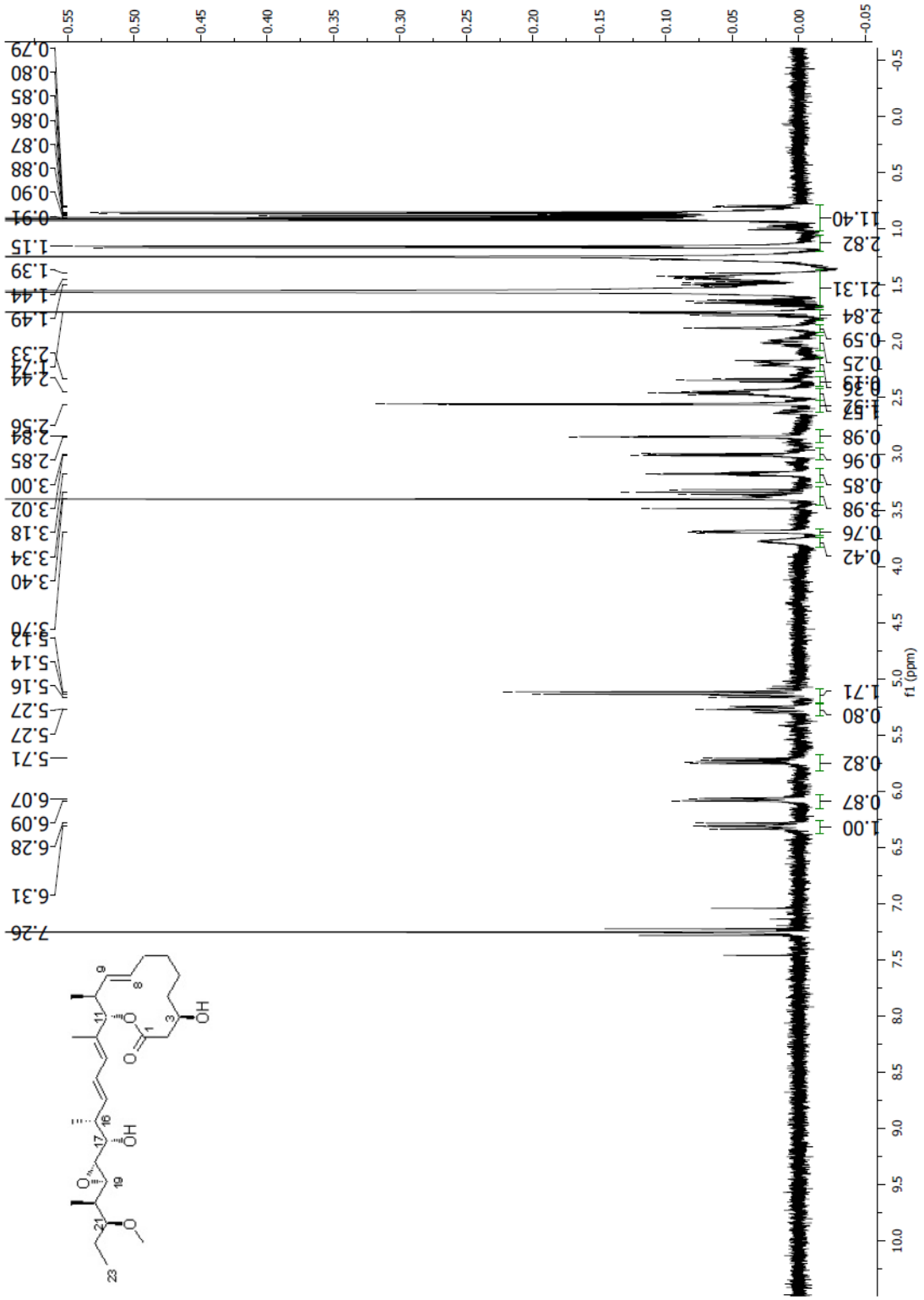

Spectrum 1.80 ^{1}H NMR ($CDCl_3$, 500 MHz) of compound **127**

Chapter 2

Studies on the spirohexenolides

2.1 Isolation of spirohexenolides A and B

2.1.1 Abstract

In this report, we describe the discovery of a pair of bioactive spirotetronates, spirohexenolides A (**128**) and B (**129**) that arose from the application of mutagenesis, clonal selection techniques and media optimization to strains of *Streptomyces platensis*. The structures of spirohexenolides A (**128**) and B (**129**) were elucidated through X-ray crystallography and confirmed by 1D and 2D NMR studies. Under all examined culture conditions, spirohexenolide A (**128**) was the major metabolite with traces of spirohexenolide B (**129**) arising in cultures containing increased loads of adsorbent resins. Spirohexenolide A (**128**) inhibited tumor cell growth with a GI_{50} values spanning from 0.1 to 17 μM across the NCI 60 cell line panel. An increased activity was observed in leukemia (GI_{50} value of 254 nM in RPMI-8226 cells), lung cancer (GI_{50} value of 191 nM in HOP-92 cells) and colon cancer (GI_{50} value of 565 nM in SW-620 cells) tumor cells. Metabolite **128** was fluorescent and could be examined on a confocal fluorescent microscope using conventional laser excitation and filter sets. Time lapse imaging studies indicated that spirohexenolide A (**128**) was readily taken up by tumor cells, appearing through the cell immediately after dosing and subcellularly localizing in the lysosomes. This activity, combined with a unique

selectivity in NCI 60 cancer cell line screening, indicates that **128** warrants further chemotherapeutic evaluation.

2.1.2 Introduction

Since its classification in 1956,[83] *Streptomyces platensis* has demonstrated a remarkable ability to produce biologically active polyketides including the dorrigocins,[84, 85] the migrastatins,[86-88] the pladienolides,[9, 21, 31] leustroducin B,[89] TPU-0037,[90] platensimide A,[91] and platensimycin.[92] Many of these compounds,[93] including synthetic analogs,[94] have demonstrated potent activity against tumor progression, and an analog of pladienolide D, E7107, has recently entered clinical trials.[10] Given this track record, we were interested in evaluating associated strains of *S. platensis* for the production of yet undiscovered polyketides.

Recently, genome sequencing studies suggest that the bacterial secondary metabolomes are far more complicated than previously recognized by evaluation of their natural product content.[95-98] This, combined with further genetic screening programs, suggests that only a fraction of the potential natural products produced in bacteria have been identified.[99, 100] The cause for this lack in production is complex. First, media and environmental stimuli can contribute to bacterial secondary metabolism either up- or down- regulating the production of specific metabolites based on external cues or morphological reponses.[101] Second, evolutionary pressures are often key in regulating a microbe's ability to access secondary metabolism.[102-104] Mutagenesis offers a strong potential to circumvent the lack in production,[105-111] as mutant strains can be directed, through associated screening efforts, to enhance

production. In this study, we demonstrate how applications of such strain improvement techniques can be used to access the production of new metabolites.

2.1.3 Results

Our studies began by evaluating a panel of *S. platensis* strains from available culture collections. An antibiotic assay using the inhibition of *Bacillus subtilis* growth was eventually chosen (comparable methods have been used in the discovery of spirotetronate natural products).[112-114] Due to the presence of only traces of compound **128** from the parent strain (often less than 1 mg/L), we applied both UV irradiation and NTG (*N*-methyl-*N*'-nitrosoguanidine) chemical mutagenesis for strain improvement. From UV irradiation analysis, we identified three mutant strains, MJ1A (1A, Figure 2.1a), MJ2B (2B, Figure 2.1a), and MJ6 (6, Figure 2.1a) that displayed an increased zone of inhibition over their parent *S. platensis* strain MJ (wt, Figure 2.1a). Subsequent efforts led to the production of two stable morphologies of MJ1A noted as strains MJ1A1 and MJ1A2.[115] 16S rRNA gene sequence data indicated that MJ1A strain showed high sequence identity to *S. platensis* NBRC12901 (99%),[116] *S. hygroscopicus* subsp. *glebosus* LMG 19950 (99%),[117] *S. libani* subsp. *rufus* NBRC 15424 (99%),[118] and *S. caniferus* NBRC 15389 (99%).[119]

Figure 2.1 Production of metabolite **128** from *Streptomyces platensis* strains MJ1A1 and MJ1A2.

a) Ultraviolet light mutagenesis provided mutants with an increased ability to inhibit the growth of *Bacllius subtilis* 6633. An enhanced zone of growth inhibition was observed from mutant strains MJ1A, MJ2B, and MJ6 as compared to their parent strain (wt). b) TLC analysis of extracts from *S. platensis* strains cultures. A direct comparison of crude extracts from these cultures indicates that metabolite **128** (lane 1) was enhanced in *S. platensis* strain MJ1A1 (lane 2) and strain MJ1A2 (lane 3), as compared to their parental strain (lane 4) or two morphologically different colonies of *S. platensis* FERM BP-8442 (lanes 5-6). An arrow denotes position of metabolite **128** and stars denote the position of lipids and acylglycerides. The TLC observations were confirmed by preparative isolation, which after multiple repeats failed to return traces of **128** from cultures of the strains in lanes 5-6. c) HPLC traces collected with UV detection at 254 nm confirmed the presence of **128** in both parent *S. platensis* MJ and mutant *S. platensis* MJ1A2 strains while not in *S. platensis* FERM BP-8442. The MIC of pure **128** against *Bacillus subtilis* was determined to be 12.25 μM (see Experimental section), therein supporting the viability of the screening procedure.

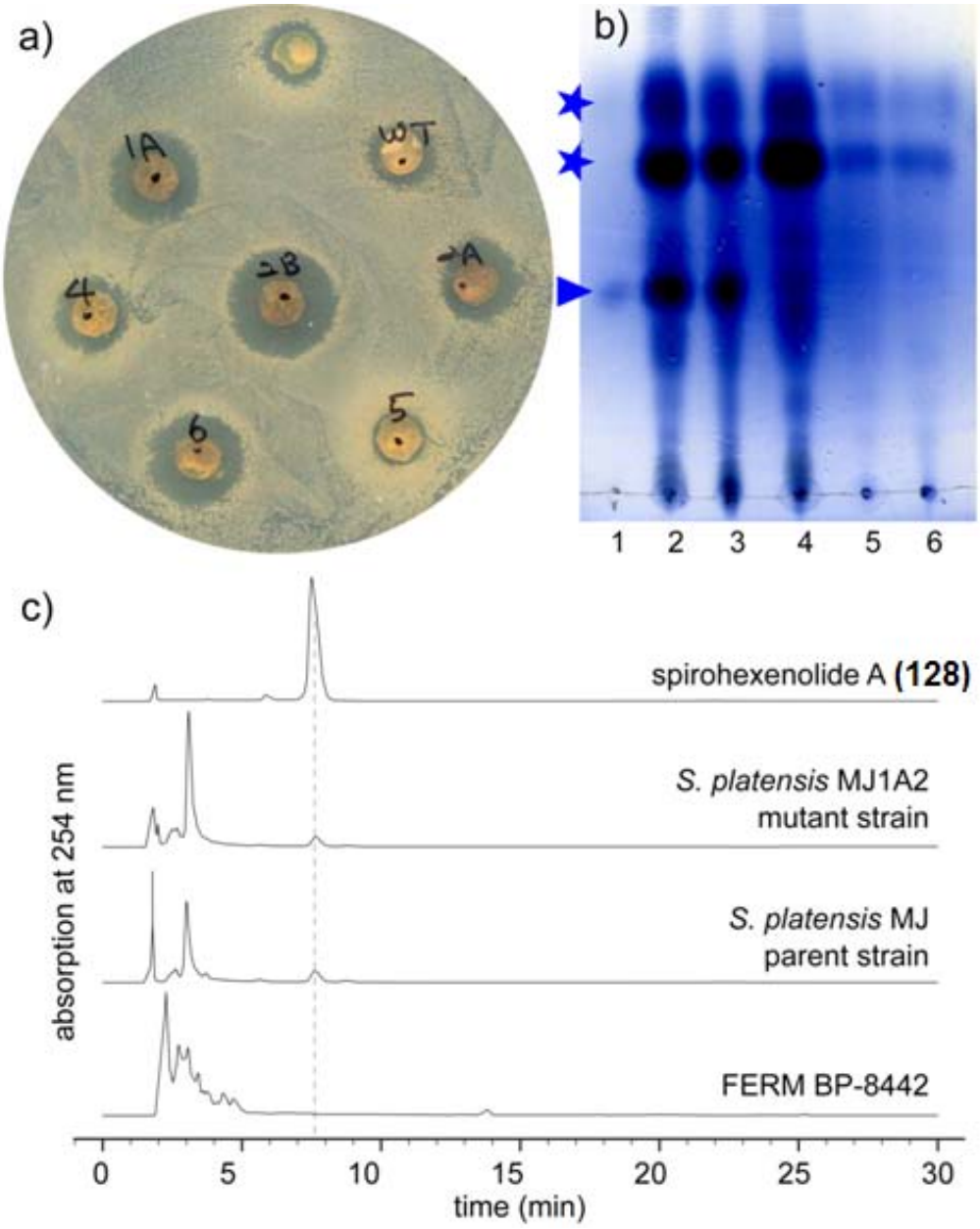
a)
1A
WT
2B
2A
4
6
5
b)
1 2 3 4 5 6
c)
spirohexenolide A (128)
S. platensis MJ1A2
mutant strain
S. platensis MJ
parent strain
FERM BP-8442
absorption at 254 nm
0 5 10 15 20 25 30
time (min)

^{1}H NMR-guided fractionation was applied to extracts from cultures of the *S. platensis* MJ1A1 and *S. platensis* MJ1A2. Metabolite **128**, with a unique signature of olefinic protons in the NMR spectrum, was identified in the ethyl acetate (EtOAc) extract from both cultures. TLC analysis indicated that metabolite **128** (lane 1, Figure 2.1b) was more abundant in extracts from strains MJ1A1 (lane 2, Figure 2.1b) and MJ1A2 (lane 3, Figure 2.1b) than their parent strain *S. platensis* MJ (lane 4, Figure 2.1b). Control experimentation indicated that **128** also did not appear in related strains such as FERM BP-8442 (lanes 5-6, Figure 2.1b), indicating that the production of **128** was restricted to strains MJ1A1 and MJ1A2. Similarly, HPLC analyses using UV detection at 254 nm confirmed the presence of **128** in both parent (*S. platensis* strain MJ) and mutant strains but not in other strains of *S. platensis* (Figure 2.1c). While **128** was observed in parent (traces) and mutant extracts, TLC evidence (Figure 2.1b) indicates that the mutants offered a significant increase in production of **128** relative to their lipid content (lipids could not be detected under our HPLC methods).

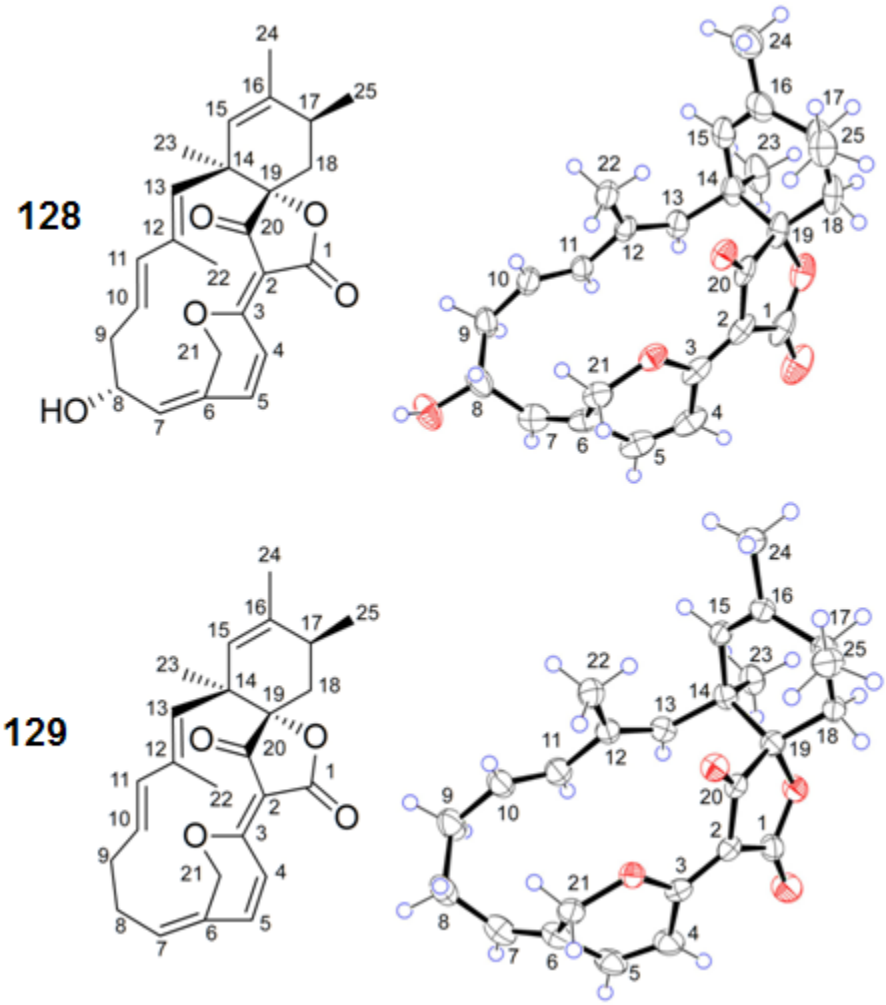

Figure 2.2 Structures of spirohexenolides A (**128**) and B (**129**)

Structures of spirohexenolides A (**128**) and B (**129**), and corresponding ORTEP drawings of their X-ray crystal structures with ellipsoids drawn at the 50% probability level. The drawings represent absolute configuration as the Flack x parameter was 0.0(3).[120]

After identification by ^{1}H NMR and MS analyses, small yellow needles of compound **128** were obtained by perfusion of a chloroform solution of **129** with benzene. Yellow plates were more effectively obtained by recrystallization from ethanol, mp = 280-285 °C (dec). Samples of these crystals were then evaluated by X-ray crystallography. The structure of **128** was refined to a final R1 of 4.6%. Using

anomalous copper dispersion effects,[121] absolute stereochemical information was obtained as depicted in Figure 2.2.

Spectroscopic methods confirmed the crystal structure as follows. A molecular formula for **128** of $C_{25}H_{28}O_5$ was determined from high resolution EI-MS analysis (*m/z* = 408.1947, M^+, Δ 3.7 ppm). Strong absorption bands at 1754 cm^{-1} and 1702 cm^{-1} in the FT-IR spectrum confirmed the presence of both ester and ketone groups, respectively.

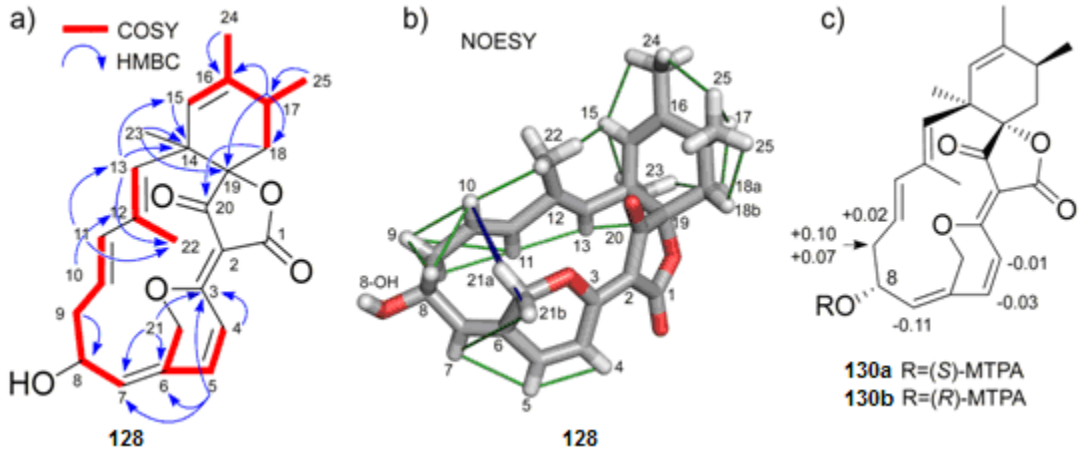

Figure 2.3 Select NMR data.

a) Key gCOSY and HMBC correlations for spirohexenolide A (**128**) and b) Nuclear Overhauser effects identified through analysis of a NOESY spectrum as mapped on the X-ray crystal structure of **128**. Both proximal (green) and transannluar (blue) NOEs are shown. c) $\Delta\delta_{S-R}$ values for the Mosher esters **130a** and **130b**.

An NMR data set including ^1H, ^{13}C, gCOSY, TOCSY, NOESY, ROESY, HMQC, HSQC, DEPT, and HMBC spectra was collected for spirohexenolide A (**128**) in $CDCl_3$ (Table 2.1). Twenty-five resonances were observed in the ^{13}C spectrum as expected from the HRMS data. The DEPT spectrum indicated sixteen protonated carbons including four methyl carbons, an oxymethylene, two aliphatic methylene

carbons, an aliphatic methine, an oxymethine, and seven olefin methine carbons. Three of the nine quaternary carbons were observed in the olefin region for a total of ten olefinic carbon resonances, indicating five double bonds.

Table 2.1 ^{1}H, ^{13}C, gCOSY, NOESY and HMBC NMR data for spirohexenolide A (**128**) in $CDCl_3$.

Spectra were collected at 296 K in $CDCl_3$.[a] ^{1}H NMR data was collected at 500 MHz. [b] ^{13}C NMR data was collected at 100 MHz. ^{13}C NMR multiplicities were determined by the DEPT spectrum. [c] gCOSY, HMBC, and NOESY spectra were collected at 800 MHz. [d] Overlapping signals detected [e] A weak crosspeak was detected. [f] HMBC data was collected with an evolution delay optimized for $^{2,3}J_{CH}$ = 8 Hz.

C/H no.	δ_H mult. (J , Hz)[a]	δ_C (mult.)[b]	COSY[c]	NOESY[c]	HMBC[c,f]
1		169.3 (C)			
2		100.8 (C)			
3		165.7 (C)			
4	7.44 d (10.0)	120.3 (CH)	5	5	3,6
5	7.02 d (10.0, <1)	142.1 (CH)	4,21a	4,7	3,6,7,21
6		126.7 (C)			
7	5.72 d (8.4)	139.3 (CH)	8	5,21b	5,21
8	4.60 m	69.3 (CH)	7,9a,9b	9a,9b,10	9
9a	2.60 m		8,9b,10	8,9b,10,11[e]	8,10,11
9b	2.17 dt (10.6, 12.3)	42.6 (CH_2)	8,9a,10	8,9a,10,11	8,10,11
10	5.55 ddd (5.4, 10.6, 15.5)	120.8 (CH)	9a,9b,11	8[d],9a,9b,13[e],21a,21b[d],22[d]	9,11,12
11	5.69 d (15.5)	140.9 (CH)	9a,10	9b,13	9,10,13,22
12		136.2 (C)			
13	5.07 s	134.8 (CH)	22	10,11,15[e],23[e]	11,14,15,22,23
14		44.3 (C)			

Table 2.1 ^{1}H, ^{13}C, gCOSY, NOESY and HMBC NMR data for spirohexenolide A (**128**) in $CDCl_3$, continued.

C/H no.	δ_H mult. (J , Hz)[a]	δ_C (mult.)[b]	COSY[c]	NOESY[c]	HMBC[c,f]
15	5.29 s	128.0 (CH)	17,24	13,23,24	13,14,17,19,24
16		133.4 (C)			
17	2.39 m	33.5 (CH)	15,18a,18b,25	18a,25	15,16,18,19,25
18a	2.35 m		17,18b	17,18b,23	14,17,19,20,25
18b	1.71 d (13.6)	33.3 (CH_2)	17,18a	18a,25	14,16,17,19,20,25
19		89.2 (C)			
20		196.0 (C)			
21a	4.73 d (12.5)		5,21b	10,21b[d]	3,5,6,7
21b	4.57 d (12.5)	64.8 (CH_2)	21a	7,10,21a	5,6,7
22	1.76 s	14.1 (CH_3)	13	10	11,12
23	1.19 s	27.2 (CH_3)		13,15,18a	13,14,15,19
24	1.76 s	22.0 (CH_3)	15	15,25	15,16,17,18
25	1.34 d (7.2)	19.6 (CH_3)	17	17,18b,24[d]	16,17,18

Three of the six remaining quaternary carbons appeared in the carbonyl region of the spectrum, one of which was the conjugated ketone at δ_C 196.0 and two of which appeared in the ester/lactone region at δ_C 169.3 and δ_C 165.7; this was supported by the carbonyl peaks in the FT-IR spectrum. The fourth was thought to be a quaternary center due to its upfield shift at δ_C 44.3. The two quaternary carbons at δ_C 100.8 and δ_C 89.2 remained ambiguous.

Analysis of the ^{1}H and gCOSY spectra of **128** (Figure 2.3a) revealed four spin systems. The first system began with the two downfield olefin methine protons H-4 (δ_H 7.44, d, 10.0 Hz) and H-5 (δ_H 7.02, d, 10.0 Hz). H-5 showed allylic coupling to oxymethylene proton H-21a (δ_H 4.73, d, 12.5 Hz), implicating a four-carbon subunit

for this spin system with a junction at quaternary olefinic C-6. The J = 10.0 Hz coupling constant between H-4 and H-5 was consistent with a *cis*-olefin.

The second spin system comprised a linear subunit including olefinic methine H-7 (δ_H 5.72, d, 8.4 Hz), oxymethine H-8 (δ_H 4.60, m), aliphatic methylene pair H_2-9 ($\delta_{H\text{-}9a}$ 2.60, m, $\delta_{H\text{-}9b}$ 2.17, dt, 12.3, 10.6 Hz), olefinic methine H-10 (δ_H 5.55, ddd, 5.4, 10.6, 15.5 Hz), and olefinic methine H-11 (δ_H 5.69, d, 15.5 Hz). The J = 15.5 Hz coupling constant between H-10 and H-11 established the *E* configuration for the $\Delta^{10,11}$ olefin. The third spin system was an isolated two-resonance spin system including olefinic methine H-13 (δ_H 5.07, s) and vinyl methyl H_3-22 (δ_H 1.76, s), presumably connected via quaternary olefinic C-12.

The fourth spin system was a branched subunit beginning with olefinic methine H-15 (δ_H 5.29, s), which displayed allylic coupling to vinyl methyl H_3-24 (δ_H 1.76, s) and to aliphatic methine H-17 (δ_H 2.39, m). H-17 also coupled to methyl H_3-25 (δ_H 1.34, d, 7.2 Hz) and methylene pair H_2-18 ($\delta_{H\text{-}18a}$ 2.35, m, $\delta_{H\text{-}18b}$ 1.71, d, 13.6 Hz). The C-23 methyl group was not in any of the spin systems, indicating that it was attached to a quaternary center.

Figure 2.3a depicts several of the key HMBC correlations that validated the structure. The HMBC data confirmed the assignments of the C-3 and C-6 ^{13}C signals at δ_C 165.7 and δ_C 126.7, respectively, based on the correlations from H-4, H-5 and H-21a, all in the first spin system. Tethering of the first and second spin systems hinged on the HMBC correlation from H-5 and H-21b to olefinic methine C-7, suggesting quaternary C-6 as the junction. This C-3 to C-11 segment could be extended to include the CH-13/CH_3-22 system based on reciprocal HMBC correlations between olefinic

H-11 and H-13 and their respective carbons. Quaternary olefinic C-12 (δ_C 136.2) was assigned as the link due to correlations from H-10 and H_3-22. Mutual HMBC correlations between olefinic H-13 and H-15 and their respective carbons combined with their additional correlation to the upfield quaternary center C-14 (δ_C 44.3), indicated that C-14 was the link to the fourth spin system. Correlation from the isolated CH_3-23 methyl group to C-14 established its position. Quaternary C-16 (δ_C 133.4) was assigned due to HMBC correlations from H-17, H-18b, H_3-24 and H_3-25. Fourth spin system protons H-15, H-17, H_2-18 and the isolated methyl H_3-23 correlated to the downfield quaternary carbon C-19 (δ_C 89.2), placing it adjacent to CH_2-18, indicating a bond to quaternary C-14 and thus a cyclohexene ring. The ketone carbonyl at C-20 (δ_C 196.0) was assigned adjacent to C-19 due to correlations from CH_2-18. The chemical shift of C-19 suggested oxidation, which implicated it as the quaternary center of a spirotetronate system due to its inclusion in the cyclohexene ring. C-1 (δ_C 169.3) and C-2 (δ_C 100.8) were assigned based on their chemical shifts since no protons were within HMBC correlation distance to them.

The NOESY spectrum (Table 2.1, Figure 2.3b) revealed an NOE correlation between methylene proton H-18a and the H_3-23 isolated methyl group, providing additional support for the presence of the cyclohexene ring. The transannular NOE correlation between olefinic methine H-10 and oxymethylene H_2-21 was indicative of the macrocycle in **128**. Key NOESY interactions are shown in Figure 2.3b. Taken together, the NMR data was consistent the X-ray crystal structure. The absolute configuration of **128** was confirmed by preparing (*S*)-MTPA (**130a**) and (*R*)-MTPA (**130b**) esters (Figure 2.3c).[27, 122]

With structure elucidation studies complete, we returned to culturing to produce additional quantities of compound **128** for biological studies. Using our optimized strains, we screened for media that provided an optimal yield of **128**. After evaluating over 50 different liquid cultures, we found that culturing *S. platensis* MJ1A in a rich media (6% w/v soluble starch, 1% w/v dry yeast, 1% w/v β-cyclodextrin) containing 2% of Amberlite XAD-16 resin provided **128** at up to 325 mg/L (see Experimental section for further details). By increasing the resin content to 10%, we were able to obtain 15-20 mg/L of a second metabolite spirohexenolide B (**129**) from these cultures. The structure of **129** was characterized by X-ray crystallography (Figure 2.2) and subsequent NMR analyses (Table 2.2) indicating that **129** failed to undergo oxidation at C-8, suggesting that **129** is a biosynthetic precursor to **128**.

Table 2.2 ^{1}H, ^{13}C, gCOSY, and HMBC data for spirohexenolide B (**129**) in C_6D_6.

Spectra were collected at 296 K in C_6D_6. Due to a slow decomposition of **129** in $CDCl_3$, C_6D_6 was required for extended times required to collect ^{13}C NMR, HMBC and HSQC data. [a] ^{1}H NMR data was collected at 500 MHz. [b] ^{13}C NMR data was collected at 125 MHz. [c] gCOSY and HMBC spectra were collected at 800 MHz. [d] The HMBC spectrum was collected with an evolution delay of $^{2,3}J_{CH} = 6$ Hz.

C/H no.	δ_H mult. (J , Hz)[a]	δ_C (mult.)[b]	COSY[c]	HMBC[c,d]
1		168.9 (C)		
2		101.1 (C)		
3		165.5 (C)		
4	7.59 d (10.0)	119.3 (CH)	5	3,6
5	6.20 d (10.0)	142.2 (CH)	4,21b	3,6,7,21

Table 2.2 ^{1}H, ^{13}C, gCOSY, and HMBC data for spirohexenolide B (**129**) in C_6D_6, continued.

C/H no.	δ_H mult. (J , Hz)[a]	δ_C (mult.)[b]	COSY[c]	HMBC[c,d]
6		128.8 (C)		
7	4.97 t (8.5)	135.4 (CH)	8,21a	
8	1.53 m	27.8 (CH_2)	7,9a,9b	
9a	1.92 m		8,9b,10	
9b	1.40 m	32.3 (CH_2)	8,9a,10	
10	5.16 ddd (4.9, 10.9, 15.4)	125.3 (CH)	9a,9b,11	12
11	5.46 d (15.4)	139.7 (CH)	10	13,22
12		135.5 (C)		
13	5.13 s	134.8 (CH)	22	11,14,15,22,23
14		44.5 (C)		
15	5.33 s	129.0 (CH)	17,24	17,19,24
16		133.3 (C)		
17	2.10 m	33.9 (CH)	15,18a,18b,25	16,25
18a	2.30 dd (8.6, 14.6)		17,18b	14,17,19,20,25
18b	1.62 d (14.6)	33.7 (CH_2)	18a	14,16,17,19,20,25
19		88.4 (C)		
20		195.3 (C)		
21a	4.13 d (12.6)		5,21b	3,5,6,7
21b	3.72 d (12.6)	63.4 (CH_2)	7,21a	6,7
22	1.96 s	14.6 (CH_3)	13	11,12
23	1.30 s	27.4 (CH_3)		13,14,15,19
24	1.65 s	22.0 (CH_3)	15	15,16,17
25	1.43 d (6.9)	19.9 (CH_3)	17	16,17

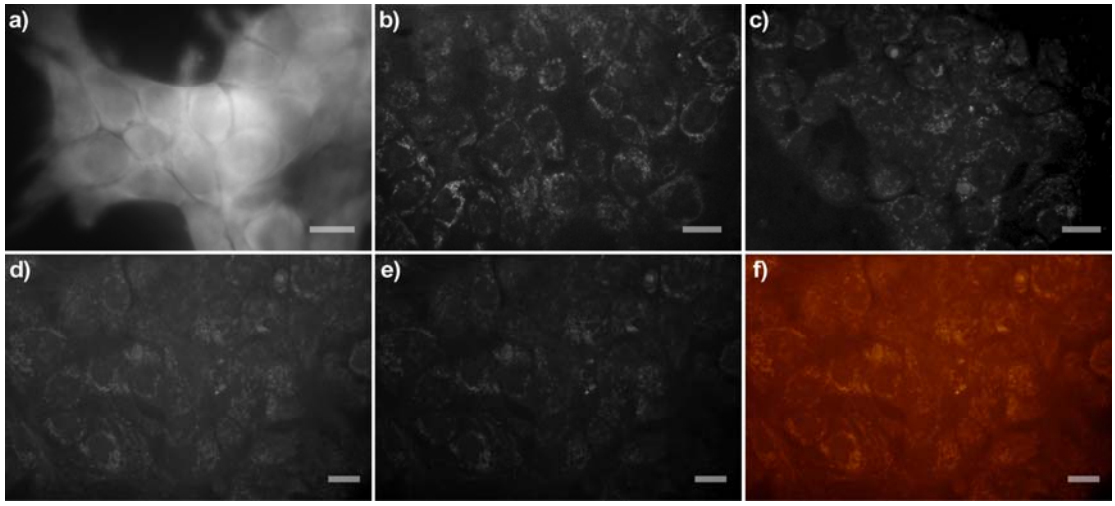

Figure 2.4 Uptake and subcellular localization of spirohexenolide A (**128**) in HCT-116 cells.

Confocal fluorescent images from HCT-116 cells treated with 10 μM **128** for a) 1 h, b) 6 h and c) 12 h. Cells were washed twice with media prior to imaging. Live cell images were collected with excitation from a laser at 488 nm (emission filtered at 524±40 nm). Co-staining with LysoTracker Red DND-99 indicates that compound **128** localizes within the lysosomes. HCT-116 cells were treated with 10 μM **128** for 6 h and washed before staining with 10 μM LysoTracker Red DND-99[23] for 20 min. d) Fluorescence from **128** collected with excitation from a laser at 488 nm (emission filtered at 524±40 nm); e) Fluorescence from LysoTracker Red DND-99 collected with excitation from a laser at 568 nm (emission filtered at 624±40 nm). f) Two-color overlap depicting the fluorescence from **128** (red) and LysoTracker Red DND-99 (green). Yellow color denotes overlap of both probes. Bars denote 10 μm.

With access to the natural product, we were able to characterize its biological activity. While we identified **128** using an antibiotic screen, the activity of **128** was more significant in tumor cell lines. Initial activity studies used the human colon tumor HCT-116 cell line, and **128** displayed cytotoxicity activity with a GI_{50} value of 36.0±5.1 μM using the MTT assay. Submission of **128** to the single and multiple dose screens NCI-60 human tumor cell line screen[6] identified the enhanced activity as given by lower GI_{50} values in leukemia (CCRF-CEM, MOLT-4 and RPMI-8226), lung

cancer (HOP-92), and colon cancer (SW-629) cell lines. Subsequent COMPARE analysis failed to provide a match to a known compound and any associated mechanism of action, suggesting a novel anticancer action for **128**. *In vivo* studies in athymic nude mice produced toxicity after a single dose of **128** (6-10 mg/kg), indicating the threshold for further *in vivo* applications.

We then turned to evaluate the cellular uptake and localization of **128** in HCT-116 tumor cells using fluorescence microscopy. Fortunately, spirohexenolide A (**128**) was natively fluorescent, with an excitation maximum λ_{max} = 435 nm and emission maximum at λ_{max} = 466 nm. HCT-116 cells were treated with 10 μM **128** in DMEM containing 10% FCS, 100 U/mL penicillin-G and 100 μg/mL streptomycin and analyzed by fluorescence microscopy. Spirohexenolide A (**128**) was readily uptaken and appeared within minutes throughout the cell (Figure 2.4a). Within 6-12 h, fluorescence from **128** concentrated within vesicles surrounding the nucleus and remained in these structures (Figure 2.4b). This staining could not be washed from the cells by repetitive incubation with media and remained consistent thereafter (Figure 2.4c). Co-staining experiments using a panel of organelle probes provided a direct correlation with LysoTracker Red DND-99[123] (Figure 2.4d-e) indicating that the localization occurred in the lysosomes.

2.1.4 Discussion

Spirohexenolide A (**128**) belongs to a large class of spirotetronate natural products that includes A88696F,[124] abyssomicins,[125] chlorothricin,[126] decatromicins,[127]

pyrrolosporin A,[128] PA-46101-A,[129] tetronomycin[130] and versipelostatin.[131] While structural similarities exist, spirohexenolide A (**128**) contains a unique and functionally compact carbon framework and offers a new carbon skeleton. Its salient features include a unique pyran, a high degree of unsaturation, and a tetrasubstituted olefin juncture between its tetronic acid and the adjacent pyran. This juncture may be the result of an intramolecular dehydration reaction of an appropriately spaced distal alcohol onto the 3-keto portion of the spirotetronate, such as in carolic acid.[132]

The biosynthesis of **128** may be derived through a late-stage intramolecular Diels-Alder (IMDA) cycloaddition. Application of IMDA reactions to the syntheses of spirotetronate natural products is well established, such as in the total synthesis of abyssomicin C by Sorensen[133] and an approach to chlorothricolide by Yoshii.[134] To date, the biosynthetic gene clusters of four metabolites of this family (chlorothricin,[135] kijanimicin,[136] tetronomycin,[137] and tetrocarcin A[138]) have been elucidated and several of these pathways include a putative IMDA biogenesis. The isolation of spirohexenolide B (**129**) suggests that oxidation at C-8 arose at a late stage by oxidation via a cytochrome P450 or related enzyme.[139-141]

In conclusion, we have discovered two new spirotetronate polyketides, spirohexenolide A (**128**) and B (**129**), from *S. platensis*. We have elucidated their structures through spectroscopic and X-ray crystallographic analyses. We have shown that mutagenesis can be used in conjunction with culture optimization to provide viable quantities of trace metabolites.[142] Activity analyses indicated that **128** displayed significant activity against tumor cell growth with a unique specificity to select tumor cell lines (cf. NCI-60 cell line screening data in the Supporting Information). The fact

that **129** (GI_{50} value of 61.2±7.8 μM in HCT116 cells) also displayed comparable activity to **128** (GI_{50} value of 36.0±5.1 μM in HCT116 cells) when screened in house using the MTT assay indicates that the C-8 hydroxyl group may serve as a site for reporter attachment for identifying its cellular targets.[143-145] The combination of the unique structure and activity of these spirohexenolides serve as the starting point for the development of both chemical synthesis and mechanism of action studies.

2.1.5 Experimental methods

Mutagenesis of *S. platensis*. Spore suspensions were prepared from glycerol stocks of *S. platensis* MJ. While a series of strains were examined, we have only obtained compounds **128** and **129** from this parent strain and its mutants. A 1 μL aliquot of these suspensions was added to 1 mL in sterilized water and further diluted by addition of 10 μL of this solution into 10 mL of water to yield a solution containing approximately $6x10^5$ spores/mL. This solution was then poured onto a sterile 9 cm glass Petri dish and UV irradiated (Stratalinker 1800) at 8000 μJ at 12 cm distance while being stirred. Samples were taken every 6 seconds over a 3 min period. After serial dilution of UV-irradiated spore suspension in deionized H_2O, the sample was spread onto Bennett's agar (1.0% w/v glucose, 0.2% w/v pancreatic digest of casein, 0.1 w/v of yeast extract, 0.1% w/v beef extract, 1.5% w/v of agar in deionized H_2O at pH 7.0), YEMED agar (0.4% w/v yeast extract, 1.0% w/v malt extract, 0.4% w/v glucose, 1.5% w/v agar in deionized H_2O at pH 7.2) and ISP4 agar (1.0% w/v soluble starch, 0.2% w/v $CaCO_3$, 0.1% w/v K_2HPO_4, 0.1% w/v $MgSO_4 \cdot 7H_2O$, 0.1% w/v

NaCl, 0.2% w/v $(NH_4)_2SO_4$, 0.001% w/v $FeSO_4•7H_2O$, 0.001% w/v $MnCl_2•4H_2O$ and 0.001% w/v of $ZnSO_4•7H_2O$ in deionized H_2O at pH 7.2) for examining the morphologically differentiating colonies. In order to prevent photoreactivation, the plates were wrapped with foil for 24 h and then incubated at 30°C for 15 days.

Mutant screening identifies producer strains *S. platensis* MJ1A1 and MJ1A2. After 15 days of incubation, survival colonies were transferred onto R2YE media (10.3 % w/v sucrose, 0.5% w/v yeast extract (Difco), 0.01% w/v casaminoacids (Difco), 0.025% w/v K_2SO_4, 1.01% w/v $MgCl_2 • 6H_2O$, 1% w/v glucose, 0.025% w/v KH_2PO_4, 0.29 % w/v $CaCl_2 • 2 H_2O$, 0.0008% w/v $ZnCl_2$, 0.004% w/v $FeCl_3 • 6 H_2O$, 0.0004% w/v $CuCl_2 • 2 H_2O$, 0.0004% w/v $MnCl_2 • 4 H_2O$, 0.0004% w/v $Na_2B_4O_7 • 10 H_2O$, 0.0004% w/v $(NH_4)_5Mo_7O_{24} • 4 H_2O$ 0.3% w/v L-proline, 0.573% w/v N-tris(hydroxymethyl)methyl-2-aminoethane-sulfonic acid (TES), 0.005 % v/v 1 N NaOH to provide a pH 7.2). Once the mutants had sporulated, agar cones (3 mm OD x 5 mm height) were excised containing a single colony and stamped on top of a glucose basal salt (1% g of glucose, 0.01% yeast extract, 1.5% agar, 0.02% $MgSO_4 • 7 H_2O$, 0.001% NaCl, 0.001% $FeSO_4 • 7 H_2O$, 0.001% MnSO • 4 H_2O 0.2% NH_4Cl, 0.465% K_2HPO_4, 0.09% of KH_2PO_4 at pH 7.0) agar seeded with ~$8x10^7$ of *Bacillus subtilis* 6633 per cm^2. After incubation at 37 °C for 24 h, colonies showing a zone of inhibition were compared against their parent strain. Using this method, strains MJ1A, MJ2B and MJ6 (Figure 1a) were obtained.

Minimum Inhibitory Concentration (MIC) assay of spirohexenolide A (128) using *Bacillus subtilis* 6633. Spirohexenolide A (**128**) in dimethyl sulfoxide (DMSO) was diluted to 10, 15, 30, 60, 120, 250, 500 and 1000 µg/ml stocks in tryptic

soy broth with a final concentration of 1% DMSO. *B. subtilis*, cultured for 18 h at 37 °C in tryptic soy broth, was inoculated at 1/10,000 to a final volume of 200 μL per well on 96 well plate and then treated with 2 μL of a stock solution of **128** (10, 15, 30, 60, 120, 250, 500 and 1000 μg/ml in tryptic soy broth containing 1% DMSO). The plate was incubated in 37 °C for 18 hours indicating that pure **128** had an MIC value of 12.25 μM (no visible bacterial growth). The compound was tested in duplicates. Negative control comprised of DMSO solvent did not show any effect on the bacterial growth.

Culturing of spirohexenolide A (128) from *S. platensis* strain MJ1A1. A single colony of *S. platensis* MJ1A1 grown on yeast extract-malt extract-dextrose (YEMED) agar was resuspended in 50 μl of sterilized water using a sterilized pellet pestle and inoculated into 3 mL of tryptic soy broth (BD Biosciences) and shaken at 220 rpm at 28 °C for 40 hours. An aliquot (2 mL) of this starter culture was transferred into a 250 mL baffled Erlenmeyer flask containing 100 mL of seed medium containing 1% w/v glucose, 2.4% w/v soluble starch, 0.3% w/v beef extract, 0.5% w/v tryptone, 0.5% w/v yeast extract and 2.0% w/v $CaCO_3$ adjusted to pH 7.2. After shaking the seed medium for 48 h at 220 rpm and 28 °C, a 50 mL aliquot was transferred to 2.8 L baffled Erlenmeyer flask containing 500 mL of fermentation media (6% w/v soluble starch, 1% w/v dry yeast, 1% w/v β-cyclodextrin, 0.2% w/v $CaCO_3$ adjusted to pH 6.8 prior to sterilization) and 2% w/v of Amberlite XAD-16 resin (Alfa Aesar) that was washed repetitively with deionized water prior to sterilization. The fermentation media was shaken for 72 h at 220 rpm at 28 °C. The cultures were filtered through cheesecloth to collect the resin. The resin was then

returned to the baffled flask and acetone (250 mL) and EtOAc (250 mL) were added. The flask was shaken for 2 h at 220 rpm. The resin was filtered again through cheesecloth, and the filtrate was concentrated on a rotary evaporator until only insoluble solids and water remained. EtOAc was added until most of the solids were dissolved, and the mixture was poured into a separatory funnel. The aqueous layer was extracted with additional EtOAc (2x100 mL), and the combined organic layers were concentrated to provide a crude extract. Crude extract was dissolved in a minimum amount of 1:1 hexanes:EtOAc (sonication was used to facilitate dissolution). A 2 inch ID column containing silica gel (EM Sciences) was packed with 1:1 hexanes:EtOAc, and the solution of the crude extract was loaded. The column was run with 1:1 hexanes:EtOAc for at least two column volumes before EtOAc was used to elute **128** with an R_f = 0.29 (EtOAc). Compounds **128** and **129** could be visualized by ceric ammonium molybdate, 2,4-dinitrophenylhydrazine, iodine, and potassium permanganate stains, and short wave UV (excitation at 254 nm). Pure spirohexenolide A (**128**) was obtained after a second flash column using a gradient from hexanes to EtOAc or trituration with small amounts of absolute ethanol.

Isolation of spirohexenolide B (129) from cultures of *S. platensis* strain MJ1A1. *S. platensis* strain MJ1A1 was cultured in the same manner on the same scale used to produce spirohexenolide A (**128**), (above), but the fermentation media was supplemented with 10% w/v of Amberlite XAD-16 resin (Alfa Aesar) that was washed repetitively with deionized water prior to sterilization. The fermentation media was shaken for 72 h at in 220 rpm at 28 °C. The crude extract of the resin was processed in the same manner as used for the isolation of spirohexenolide A (**128**), as

described in the preceding paragraph. A 2 inch ID column containing silica gel (EM Sciences) was packed with 1:1 hexanes:EtOAc, and the solution of the crude extract was loaded. The column was run with 1:1 hexanes:EtOAc for two column volumes, and spirohexenolide B (**129**) was obtained from the eluted and concentrated material by subjecting it to a second Flash purification on a 2 inch ID column with a gradient from hexanes to 1:1 hexanes:EtOAc with elution of **129** in 1:1 hexanes:EtOAc with an R_f = 0.68 (EtOAc), followed by crystallization from either EtOH or a mixture of CH_2Cl_2 and hexanes to obtain yellow crystals.

Synthesis of Mosher esters 130a and 130b. The (*S*)- and (*R*)-MTPA derivatives **130a** and **130b** were prepared using a slight modification of the standard procedure.[21] (*S*)-MTPA ester **130a**: To a sample of compound **128** (30.3 mg, 0.0743 mmol) in a dry 25 mL round bottom flask with a teflon-coated magnetic stirbar, were added a few crystals of 4-dimethylaminopyridine and the flask was sealed with a rubber septum and flushed with argon. CH_2Cl_2 (3 mL), and pyridine (0.120 mL, 1.5 mmol) were added at rt, and the mixture was stirred until a yellow solution was achieved. Stirring was then continued as 70 μL of (*R*)-MTPA-Cl (0.374 mmol) was added via syringe at rt. After 30 minutes the solution turned dark green. After 50 min, TLC indicated a new compound had formed with an R_f = 0.76 (EtOAc), and that compound **128** had been consumed. The reaction mixture was then poured into a separatory funnel containing half-saturated $NaHCO_3$ (30 mL), and CH_2Cl_2 (20 mL), and the organic layer became yellow again upon shaking. The aqueous layer was extracted with another 20 mL of CH_2Cl_2 and the combined organic layers were dried over Na_2SO_4 and concentrated under reduced pressure. The residue was dissolved in

3:1 Hexanes:EtOAc (5 mL), and standard flash chromatography with 3:1 Hexanes:EtOAc provided pure **130a** (16.3 mg, 35%). The same procedure was used on **128** and (*S*)-MTPA-Cl to make the (*R*)-MTPA ester **130b** (13.5 mg, 40%).

Spirohexenolide A (128): yellow needles, mp = 280-285 °C (dec.); $[\alpha]_{25}^{D}$ = +551.3 (*c* 0.4, $CHCl_3$); UV λ_{max} (MeOH): 339 (ε = 8650), 236 (ε = 25583) nm; IR (film) ν_{max} 3469, 1754, 1702, 1582, 1550, 1059, 1043, 988, and 968 cm^{-1}; ESIMS *m/z* 409.03 $[M+H]^+$, 431.03, $[M+Na]^+$; HR-EI-MS *m/z* 408.1947, $[M]^+$ (calcd for $C_{25}H_{28}O_5$ $[M]^+$, 408.1931); ^1H and ^{13}C NMR (Table 2.1).

Spirohexenolide B (129): yellow rhomboid crystals recrystallized from CH_2Cl_2 and hexanes, mp = 219-221 °C (dec); IR (film) ν_{max} 2922, 2852, 1735, 1707, 1587, 1551, 1466, 1410 cm^{-1}; ESIMS *m/z* 392.91 $[M+H]^+$; HR-ESI-MS *m/z* 415.1888, $[M+Na]^+$ (calcd for $C_{25}H_{28}O_4Na$ $[M+Na]^+$, 415.1885); ^1H and ^{13}C NMR (Table 2.2).

Spirohexenolide A (*S*)-MTPA derivative (130a): yellow solid, mp = 208-211 °C (dec.); $\alpha]_{23}^{D}$ = +159.3 (*c* 1, CH_2Cl_2); IR (film) ν_{max} 2936, 1750, 1709, 1594, 1554, 1252, 1168, 1056, 1014, and 722 cm^{-1}; ESI-MS *m/z*: 624.92 [M + H]+, 647.04 $[M+Na]^+$; HR-ESI-FT-MS (Orbit-trap-MS) *m/z* calcd for $C_{35}H_{35}F_3O_7Na$ $[M+Na]^+$ 647.2227, found 647.2218; See Section 2.6 for ^1H and ^{13}C NMR spectra.

Spirohexenolide A (*R*)-MTPA derivative (130b): yellow solid, mp = 246-250 °C (dec.); $[\alpha]_{23}^{D}$ = +223.5 (*c* 1, CH_2Cl_2); IR (film) ν_{max} 2936, 1750, 1709, 1594, 1554, 1252, 1169, 1056, and 1014 cm^{-1}; ESI-MS *m/z*: 625.18 [M + H]+, 647.21 $[M+Na]^+$; HR-ESI-FT-MS (Orbit-trap-MS) *m/z* calcd for $C_{35}H_{36}F_3O_7$ $[M+H]^+$ 625.2408, found 625.2419; See Section 2.6 for ^1H and ^{13}C NMR spectra.

Uptake and localization in HeLa cells. HCT-116 cells (ATCC CCL-247) were cultured in Dulbecco's modification of Eagle's medium (DMEM) with 4.5 g L^{-1} glucose, 4.5 g L^{-1} L-glutamine and 5% heat inactivated fetal calf serum (FCS) in glass-bottom dishes. Fluorescent images were collected on a Leica (Wetzlar, Germany) DMI6000 inverted confocal microscope with a Yokogawa (Tokyo, Japan) spinning disk confocal head, Orca ER High Resolution B&W Cooled CCD camera (6.45 μm/pixel at 1X) (Hamamatsu, Sewickley, PA), Plan Apochromat 40x/1.25 na and 63x/1.4 na objective, and a Melles Griot (Carlsbad, CA) Argon/Krypton 100 mW air-cooled laser for 488, 568, and 647 nm excitations. Confocal z-stacks were acquired in all experiments. Co-staining was conducted by treating cells exposed to **128** to either Syto-60 (nucleus), LysoTracker Red DND-99 (lysosomes), BODIPY TR glibenclamide (endoplasmic reticulum), or MitoTracker Red 580 (mitochondria) for 20 min and washing the cells three times with media and collecting images in two colors.

X-ray crystallography. A yellow needle of compound **128** 0.25 x 0.10 x 0.10 mm in size was mounted on a Cryoloop with Paratone oil. Data were collected in a nitrogen gas stream at 100(2) K using phi and omega scans. Crystal-to-detector distance was 50 mm and exposure time was 10 seconds per frame using a scan width of 0.5°. Data collection was 99.3% complete to 67.00° in θ. A total of 7195 reflections were collected covering the indices, -8<=h<=8, -15<=k<=14, -13<=l<=13. 3065 reflections were found to be symmetry independent, with a R_{int} of 0.0366. Indexing and unit cell refinement indicated a primitive, monoclinic lattice. The space group was found to be P2(1) (No. 4). The data were integrated using the Bruker SAINT software

program and scaled using the SADABS software program. Solution by direct methods (SIR-2004) produced a complete heavy-atom phasing model consistent with the proposed structure. All non-hydrogen atoms were refined anisotropically by full-matrix least squares (SHELXL-97). All hydrogen atoms were placed using a riding model. Their positions were constrained relative to their parent atom using the appropriate HFIX command in SHELXL-97.

A colorless plate of compound **129** 0.33 x 0.28 x 0.08 mm^3 in size was mounted on a Cryoloop with Paratone oil. Data were collected in a nitrogen gas stream at 100(2) K using phi and omega scans. Crystal-to-detector distance was 50 mm and exposure time was 10 seconds per frame using a scan width of 0.5°. Data collection was 99.9% complete to 25.00° in θ. A total of 24117 reflections were collected covering the indices, -8<=h<=8, -15<=k<=15, -27<=l<=27. 7549 reflections were found to be symmetry independent, with a R_{int} of 0.0363. Indexing and unit cell refinement indicated a primitive, monoclinic lattice. The space group was found to be P2(1). The data were integrated using the Bruker SAINT software program and scaled using the SADABS software program. Solution by direct methods (SIR-2004) produced a complete heavy-atom phasing model consistent with the proposed structure. All non-hydrogen atoms were refined anisotropically by full-matrix least squares (SHELXL-97). All hydrogen atoms were placed using a riding model. Their positions were constrained relative to their parent atom using the appropriate HFIX command in SHELXL-97.

2.1.6 Acknowledgements

Financial support from the American Cancer Society (RSG-06-011-01-CDD) is gratefully acknowledged. We thank Dr. Yongxuan Su (UC San Diego) for mass spectrometric analyses, and Drs. Anthony Mrse and Xuemei Huang (UC San Diego) for assistance with acquiring NMR data.

2.2 Spirotetronate biosynthesis

Spirotetronate natural products such as spirohexenolide A (**128**) consist of a polyketide chain tied into a macrocycle by a tetronic acid moiety (Figure 2.5) spiro fused at the 5 position to a cyclohexene ring. A few months prior to the discovery of **128**, the research groups of Tang and Liu reported the characterization of the biosynthetic gene cluster for the spirotetronate chlorothricin (**135**).[135] These studies confirmed previous feeding studies which had suggested that spirotetronates are of polyketide origin.[146-148]

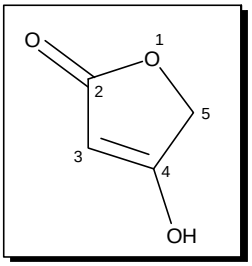

4-hydroxyfuran-2(5*H*)-one
(Tetronic acid)

Figure 2.5 Tetronic acid numbering scheme

They showed that after chain elongation, the β-keto thioester intermediate **131** is condensed with an enzyme bound glycerate derived three-carbon unit **132** resulting in release of the chain from the polyketide synthase and formation of the tetronate ring

(Scheme 2.1). Tetronates biosynthesized in this way form intermediates such as **133** which have a 5-exo methylene unit (see Figure 2.5 for tetronate numbering) that is sufficiently activated by the 3-acyl group to serve as a dienophile in intramolecular Diels-Alder reactions, provided there is an available diene.

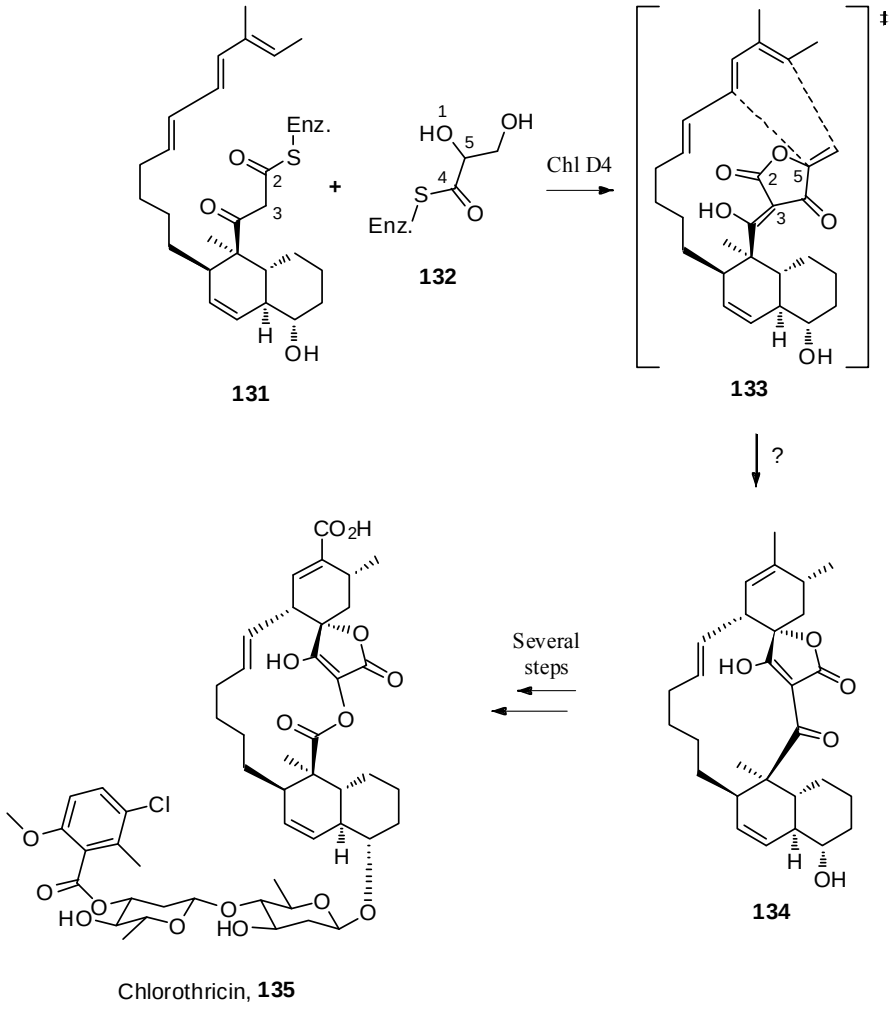

Scheme 2.1 Biosynthesis of chlorothricin (**135**)

One notable exception is the antibiotic ionophore tetronasin, which is thought to be constructed in the same way, but loses this carbon at some point after tetronate closure to form a 5-unsubstituted tetronate.[149] Candidate "Diels-Alderase" enzymes[150]

have not yet been proposed in the context of spirotetronates, but the Liu group hypothesized (in their report of the characterization of the kijanimicin gene cluster) that one or more of the synthetase's domains with other assigned functionality may either catalyze the reaction or assist it by guiding the substrate via proximity effects.[136] In the case of chlorothricin, the product of cycloaddition is pre-chlorothricolide **134**, which is processed by several post-synthase enzymes to the fully functionalized natural product **135** (Scheme 2.1). To date, there is no evidence to show whether the biosynthesis of these natural products occurs by the concerted Diels-Alder mechanism, or a stepwise Michael-aldol type mechanism.[151]

2.3 IMDA approaches to spirotetronate natural products

Confirmation of this biosynthetic pathway prompted us to consider the use of an intramolecular Diels-Alder approach in a synthetic route to **128**. Examination of spirotetronate syntheses in the literature provided some encouraging precedent. The Sorensen group had recently utilized this type of approach with great success in their elegant synthesis of abyssomicin C (**138**, Scheme 2.2).[133] They prepared the biosynthetic precursor of **138**, trienone **136** in 12 steps from *meso*-2,4-dimethylglutaric anhydride. They also found that **136** could be generated from a dienone intermediate *in-situ* during the thermal Diels-Alder reaction. They observed that the cyclization of **136** proceeded in moderate to good yield (50-79%) depending on the conditions used, and total diastereoselectivity to provide the desired *endo*-

IMDA adduct spirotetronate **137**. It was then shown that substrate-controlled epoxidation of the cyclohexene ring of **137** and demethylation of the tetronate provided the oxabicyclo[2.2.2]octane core of **138**, as a 1:1 mixture together with what was later determined by the Nicolaou group to be its atropisomer (about the enone moiety in the macrocycle), under acid-catalyzed conditions. Atrop-abyssomicin C was shown to equilibrate to abyssomicin C upon standing at room temperature in unstabilized $CDCl_3$.[152]

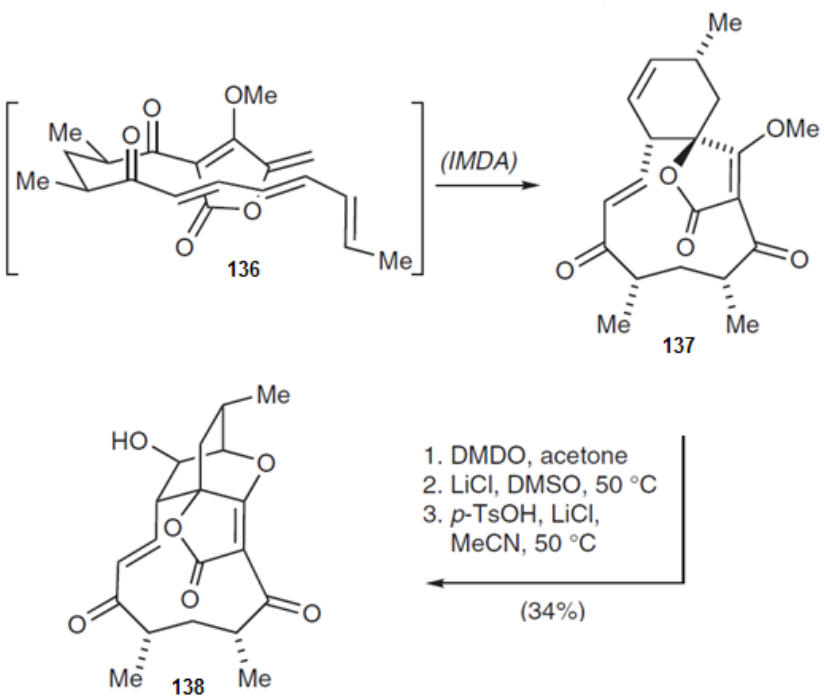

Scheme 2.2 The Sorensen group's synthesis of abyssomicin C (**138**)

Prior to Sorensen's studies, Takeda and Yoshii described an IMDA approach applied to chlorothricolide, which required the precursor triene / tetronate intermediate **139** (Scheme 2.3).[134] The synthesis of **139** involved an IMDA cyclization of a precursor triene to form the octalin system, which proceeded in 87% yield as a mixture

of four separable diastereomers, and the desired stereoisomer comprised 47% of the product mixture. The route to **139** totalled 17 linear steps in 2.82% overall yield, but enough product was obtained to examine the IMDA reaction. The thermal conditions employed for cyclization resulted in complete conversion of the mixed terminal olefin to the *E* isomer, and the reaction provided a 51% combined yield of four diastereomers. The desired *exo* cycloadduct **140** was isolated in a 9% yield after MPLC of the mixture, and its stereochemistry was confirmed by X-ray crystallographic analysis after it had been converted to the methyl ester of chlorothricolide.

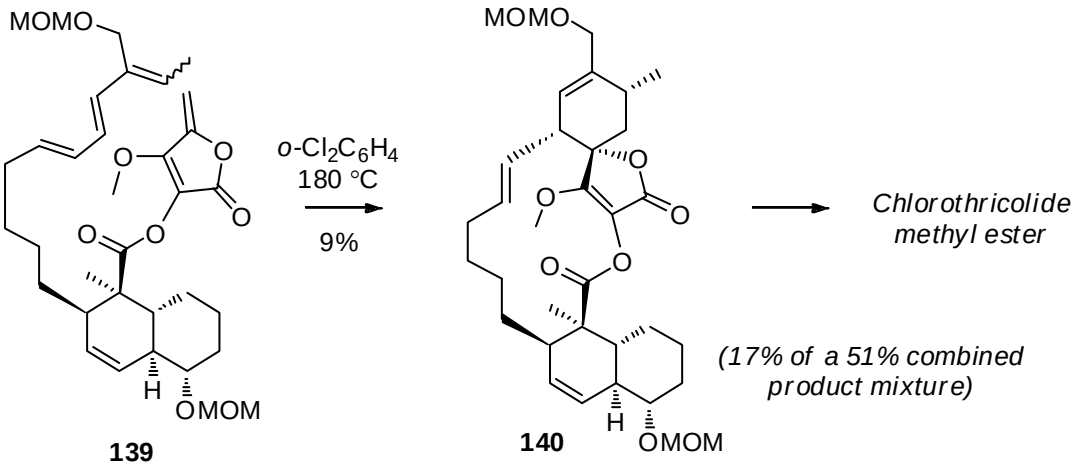

Scheme 2.3 Yoshii's IMDA approach to chlorothricolide

The modest result obtained by the Yoshii group may have been partially due to substituent effects on the tetronate ring. As illustrated in Scheme 2.1, the true biosynthetic precursor to chlorothricolide is 3-acyl tetronate **133**, and the cyclization product pre-chlorothricolide **134** is processed to the natural product by the action of several post-synthetase modification enzymes, including a Baeyer-Villagerase that

installs the oxygenation on the tetronate ring. It is thought that the 3-acyl group plays a significant role in the reactivity of the tetronate dienophile in these IMDA reactions. A computational study on substrate **136** in Sorensen's synthesis of abyssomicin C indicated that the *anti* relationship between the two carbonyl groups on the acyl tetronate dictates the preferred conformation, leading to the stereochemical outcome.[133] The other existing stereochemistry in the IMDA precursors also contributes to the result, and it should be noted that in contrast to the complicated octalin system of chlorothricolide precursor **139**, the abyssomicin C precursor **136** has only two pre-existing stereocenters, but they were enough to influence the outcome such that a single product was observed.

2.4 Synthetic approaches to the spirohexenolides

2.4.1 An IMDA approach to spirohexenolide A

Spirohexenolide A (**128**) is unique among the spirotetronates, in that the C-8 hydroxyl group is the only stereocenter that is not part of the spirotetronate system. When we discovered **128**, a standard bioretrosynthetic analysis indicated that it was likely that both the C-8 hydroxyl group and the C-21 oxygen of the pyran system were installed by the action of post-synthetase enzymes, such that the IMDA precursor would be achiral. An IMDA approach to **128** would thus be a racemic synthesis, unless some other method could be devised of setting the stereochemistry during the

reaction. We set out to construct the linear IMDA precursor to **128** with the understanding that if the penultimate cyclization step was difficult or unsuccessful, there are ample asymmetric methods available for the construction of spirotetronate systems that do not involve IMDA reactions.[153]

The first strategy involved the preparation of linear precursor **141**, which would form **128** upon IMDA and deprotection of the C-8 –OPMB ether (Scheme 2.4). An HWE coupling of phosphonate **142** and aldehyde **143** would provide the C-10/C-11 *E*-olefin, a strategy that was used with good results in Yoshii's chlorothricolide synthesis.

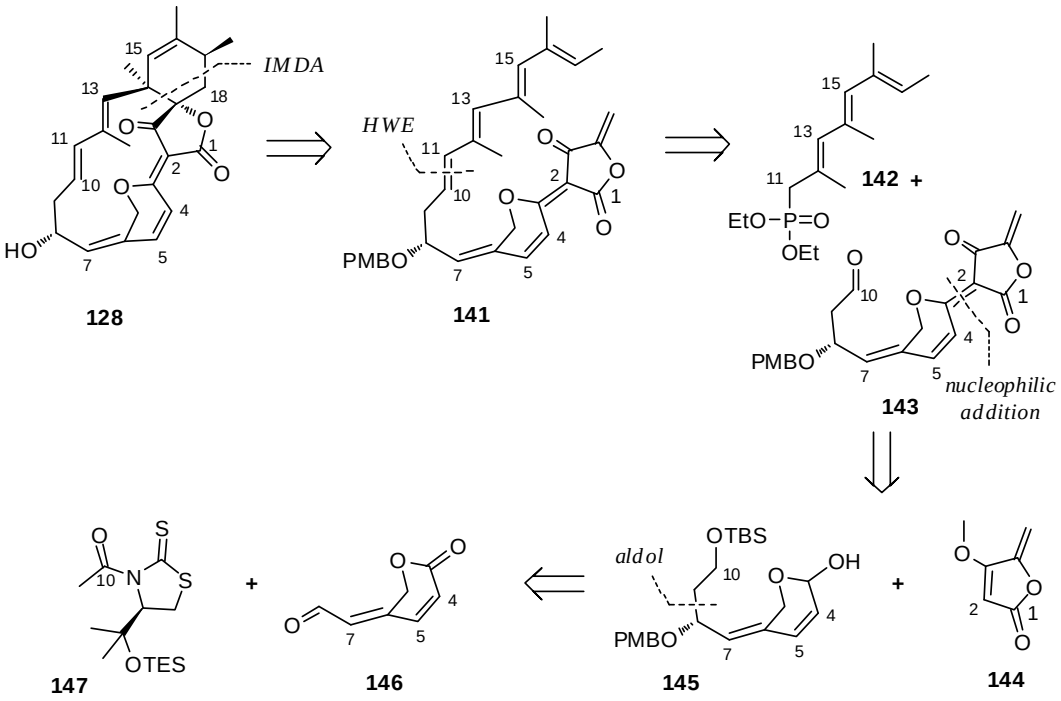

Scheme 2.4 First generation IMDA approach to **128**

The known tetronate fragment **144**,[154] which has been used in several spirotetronate syntheses, can be lithiated at the C-2 position with LDA and added to

aldehydes. We thought it could be possible to add tetronate **144** to lactol **145** (or alternatively, the ring opened aldehyde form if this proved to not be feasible). In turn, lactol **145** could be derived from an asymmetric aldol reaction on the unreported aldehyde **146**, and the acetylated thiazolidinethione **147** developed by the Sammakia group.[155] Although aldehyde **146** had not been reported, there were reports of the corresponding C-8 acid in the older literature. The acetylated auxiliary **147** is the "pseudo-enantiomer" of **116** (Scheme 1.36) that we planned to use in our synthesis of the core of FD-895 (**1**), prepared in a slightly different way due to the prohibitive cost of D-*tert*-leucine, the required enantiomer of the starting material for **116**. There have not been reports of switching the selectivity of **116** by changing the aldol reaction conditions, as there have been for the versatile propionylated thiazolidinethiones (see Scheme 1.27) described by Crimmins.[156]

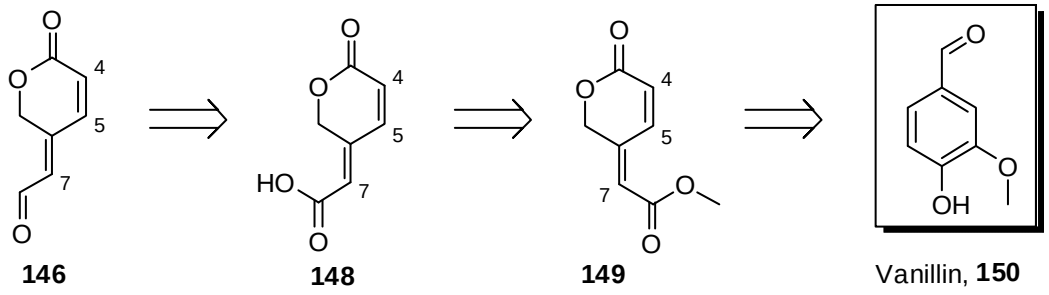

Scheme 2.5 Retrosynthetic analysis of aldehyde **146**

The plan for the generation of aldehyde **146** was based on a report that described isomerization about the C-6/C-7 trisubstituted olefin of ester **149** under saponification conditions to form the acid, such that the *Z*-trisubstituted olefin was observed in the product **148**.[157] The older reports on these muconic acid derivatives

described the formation of **149** by oxidation of vanillin **150** with chlorous acid.[158, 159] The characterization of the stereochemistry about the C-6/C-7 trisubstituted olefin in **148**/**149** was based on long-range coupling constants between the H-7 methine and the H-4/H-5 methines. These compounds had not been used in the last 20 years, so we sought to determine if ester **149** could be easily prepared as described, and if the isomerization proceeded as described. If an efficient route to **148** could be secured, a method for the selective reduction of the acid in the presence of the olefins and the lactone would need to be found.

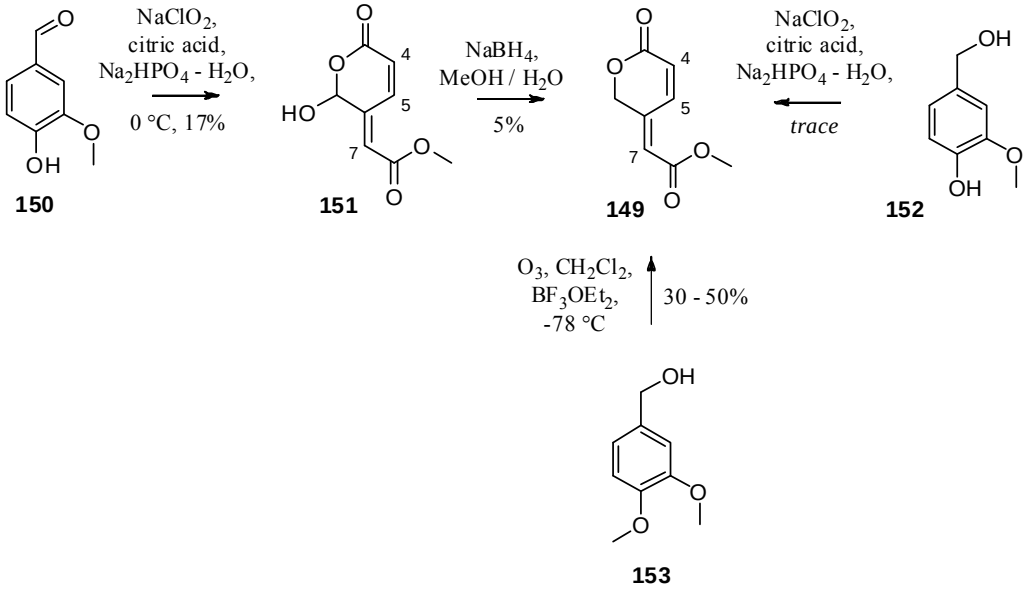

Scheme 2.6 Preparation of lactone ester **149**

Efforts commenced with the oxidation of vanillin **150**, but after a few repetitions, it was observed that various undesired quinones were the major products, and it was difficult to purify the desired lactol product **151**, which still needed to be reduced with sodium borohydride to obtain lactone **149**. The first report on these

compounds described the direct formation of **149** by the oxidation of vanillyl alcohol **152** under similar conditions, but again quinones were observed as the major product and purification was difficult.[160] A more efficient method was found, the BF_3*OEt_2 mediated ozonolysis of 3,4-dimethoxybenzyl alcohol **153**.[161] This reaction proceeded in reproducible moderate yields to provide **149** in gram quantities (Scheme 2.6).

In the original report of the saponification of **149**, the reaction was run in an NMR tube to monitor the formation of the intermediates, and it was found that the first step is the opening of the lactone as evidenced by the dramatic upfield shift of the hydroxymethylene unit almost immediately upon treatment with base (Scheme 2.7).

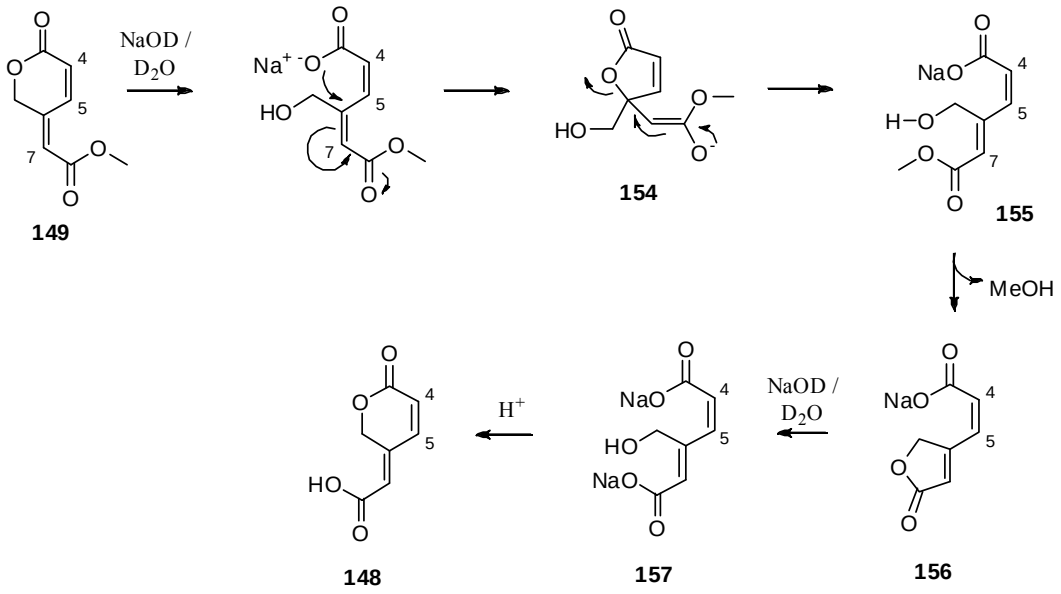

Scheme 2.7 Saponification of ester **149**

The C-6/C-7 double bond is thought to isomerize by formation of the intermediate γ-lactone **154**, and any formation of the *cis*, *cis* diene intermediate **155** is immediately trapped by the favorable 5-*exo*-trig lactonization to form lactone **156** with

loss of methanol. Lactone **156** can be isolated by acidification of the reaction mixture after brief exposure of **149** to 1 equivalent of sodium hydroxide. The addition of a second equivalent of sodium hydroxide is thought to generate the double salt **157**, which is converted to the δ-lactone **148** upon acidification of the reaction mixture.

We were able to generate **148** in this way, and X-ray crystallographic analysis showed that the olefin isomerization occurred as reported. Unfortunately, the yields were consistently poor (*ca*. 5-15% range), and could not be improved by altering the concentration, reaction times, or temperature. However, because this essentially constituted a 2 step synthesis of **148** from the readily available 3,4-dimethoxybenzyl alcohol **153**, we looked for methods to reduce the acid.

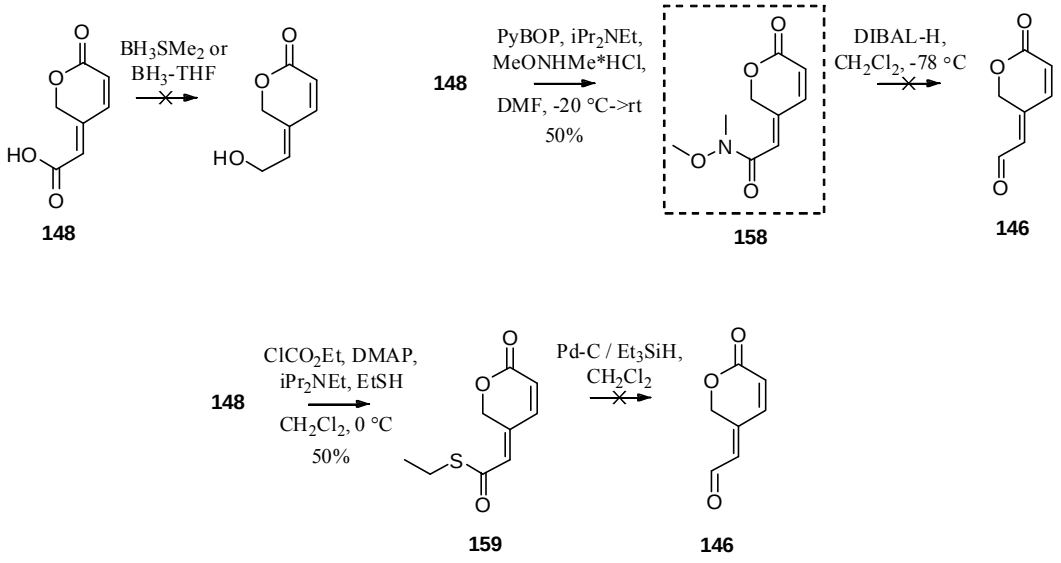

Scheme 2.8 Attempts to convert acid **148** to aldehyde **146**

It was quickly discovered that neither BH_3*SMe_2 or BH_3*THF would be viable, because concurrent reduction of one or both of the double bonds always took place (Scheme 2.8). Conversion to the S-ethyl thioester **159** was effected in modest

yield, but the reduction under Fukuyama's conditions failed to provide any detectable aldehyde **146**.[162] Coupling of N,O-dimethylhydroxylamine formed a single pure product with a mass spectrum consistent with **158**, but the ^{13}C NMR spectrum appeared to be missing the oxymethylene peak, which also did not appear in its usual location in the ^{1}H spectrum, suggesting the product obtained was not Weinreb amide **158**. These disappointments combined with the inefficient saponification step to form **148** caused us to turn to the intermediate γ-lactone **156**. This lactone had the correct geometry for both olefins and could be produced in reproducible good yields (> 70%) quickly from treatment of **149** with a single equivalent of NaOH. We sought to protect the carboxylic acid of **156** and then find a method to homologate at C-8, the lactone carbonyl.

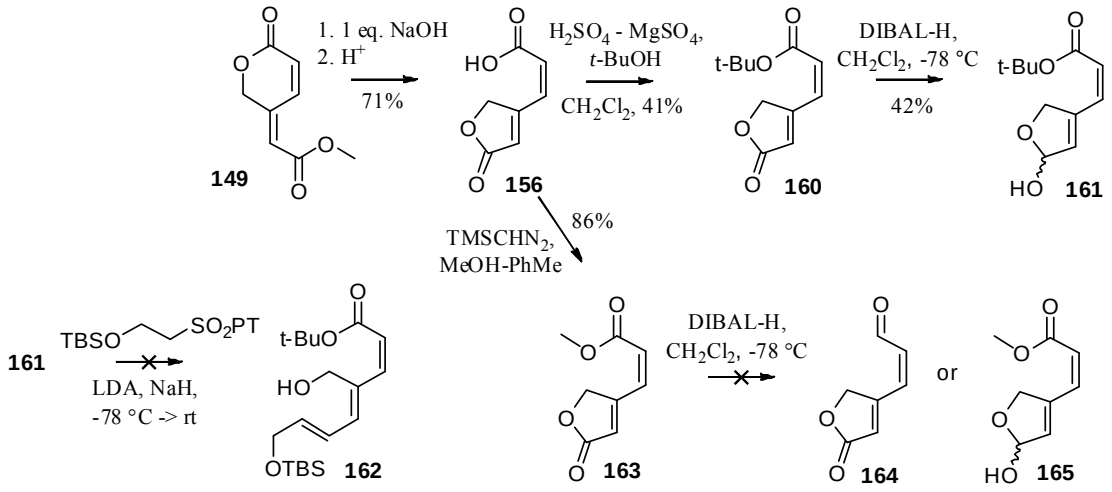

Scheme 2.9 Attempts to homologate lactone **156**

The carboxylic acid of **156** could be protected as its methyl ester **163** in good yield with $TMSCHN_2$, but attempted DIBAL-H reduction of **163** resulted in a complex mixture, apparently due to the roughly equal reactivity of the ester and the lactone. On

the other hand, the *t*-butyl ester **160** could be formed in low yield under acid-catalyzed conditions.[163] Several alterations were made to the reaction conditions to try to push the esterification reaction to completion without success, and no other esterification technique could be found to produce **160**. Interestingly, the bulk of the *t*-butyl ester does in fact block the approach of DIBAL-H to this carbonyl at low temperature such that selective reduction to the lactol **161** is favored, although the recovered yield was low. It was found that lactol **161** was unstable, tending to spontaneously aromatize to the furan, presumably by acid catalysis from unstabilized $CDCl_3$. It was envisioned that **161** might be homologated to an allylic alcohol precursor such as **162**, which might then allow installation of the C-8 hydroxyl group by asymmetric epoxidation. Unfortunately, standard alcohol/aldehyde lactols are not reactive to Julia-Kocienski olefination reagents in the same fashion as acid/aldehyde lactols, a strategy used in the synthesis of cassiol.[164]

At this point it was realized that too much effort was being spent on obtaining the C-6/C-7 trisubstituted olefin by known intermediates from lactone **149** without substantial progress. We turned to a different aspect of the project, installation of the C-10/C-11 *E*-olefin by Julia-Kocienski methods, which was thought to be a better approach than the HWE method for this coupling (Scheme 2.10). In addition, it was thought that we could acquire the C-8 hydroxyl group from the chiral pool thus eliminating the need for asymmetric synthesis.

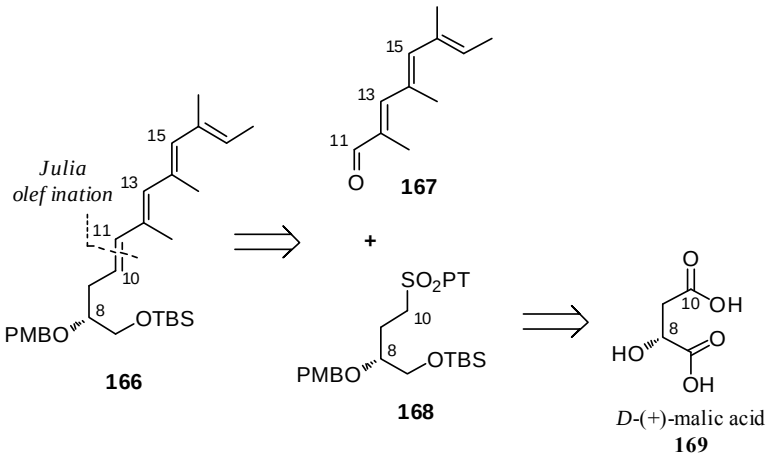

Scheme 2.10 The Julia method applied to the C-10/C-11 olefin

We reasoned that a sulfone should be easy to install at C-10 of the lower-portion fragment, and to explore this method we targeted the four-carbon subunit **168**, which could be prepared by manipulations on D-(+)-malic acid **169**. Aldehyde **167**, which had been prepared by the Baldwin group during their studies on polyene natural products,[165] seemed to be a better choice for the upper-portion fragment than phosphonate **142** (Scheme 2.4). The preparation of **142** would presumably have involved Arbuzov displacement of the corresponding volatile and unstable halide, most likely resulting in scrambling at the terminal olefin which had been observed in similar cases.[166] If this route could provide access to **166**, a C-7 aldehyde could be generated upon which HWE-type homologations could be examined for the installation of the C-6/C-7 trisubstituted olefin.

It was found that reduction of malic acid **169** to (*R*)-1,2,4-butanetriol proceeded as reported, which favors the formation of the 6 membered *p*-methoxybenzylidene acetal **170** (Scheme 2.11).[167] The primary hydroxyl group at C-7

was silylated, and product **171** was converted to sulfone **168** by reduction of the PMP acetal, conversion of the C-10 hydroxyl group to the mesylate, substitution of the phenyltetrazolyl sulfide nucleophile, and oxidation. It was observed that sulfone **168** coupled to aldehyde **167** with complete *E*-selectivity about the C-10/C-11 olefin in 67% yield. Unfortunately the polyene product **166** was not very stable, and was deemed unsuitable for the examination of a long linear sequence to install the right-hand portion of the molecule. While the coupling result was promising, our judgement was that fragment **167** should be installed closer to the end of the IMDA route to avoid multiple steps handling polyene intermediates.

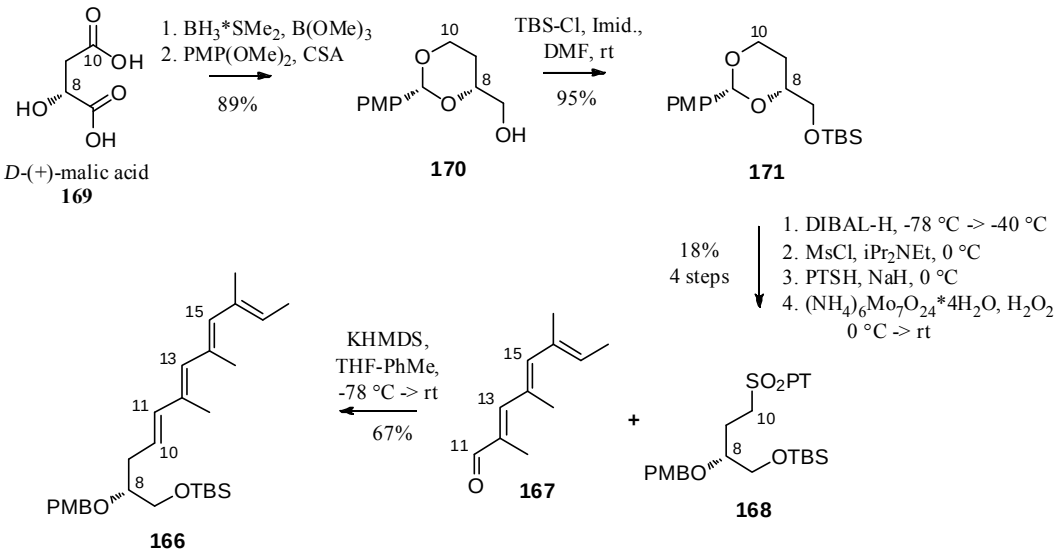

Scheme 2.11 Testing the Julia method for the C-10/C-11 olefination

We searched for a phosphorane or phosphonate reagent that could deliver the required C-6/C-7 *E*-olefin on various aldehydes derived from **170**, without success. The solution to this problem came from a method developed by the Marshall group involving the hydrostannation of propargylic alcohols.[168]

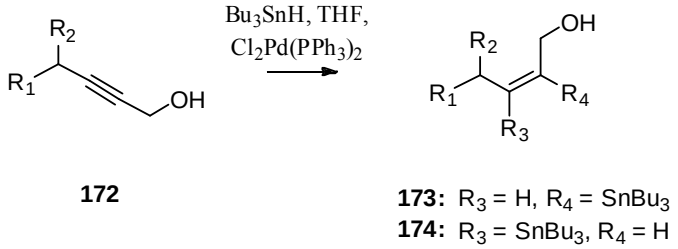

Scheme 2.12 Hydrostannation regioselectivity influenced by propargylic alcohols

When propargylic alcohols such as **172** were hydrostannylated under the standard conditions, regioselectivity of **173:174** > 20:1 was observed on several substrates, especially with substituents at R_1 and R_2. Stannanes such as **173** represent the regioisomer required for the C-6/C-7 trisubstituted olefin of **128**, and could be suitable for Stille couplings.

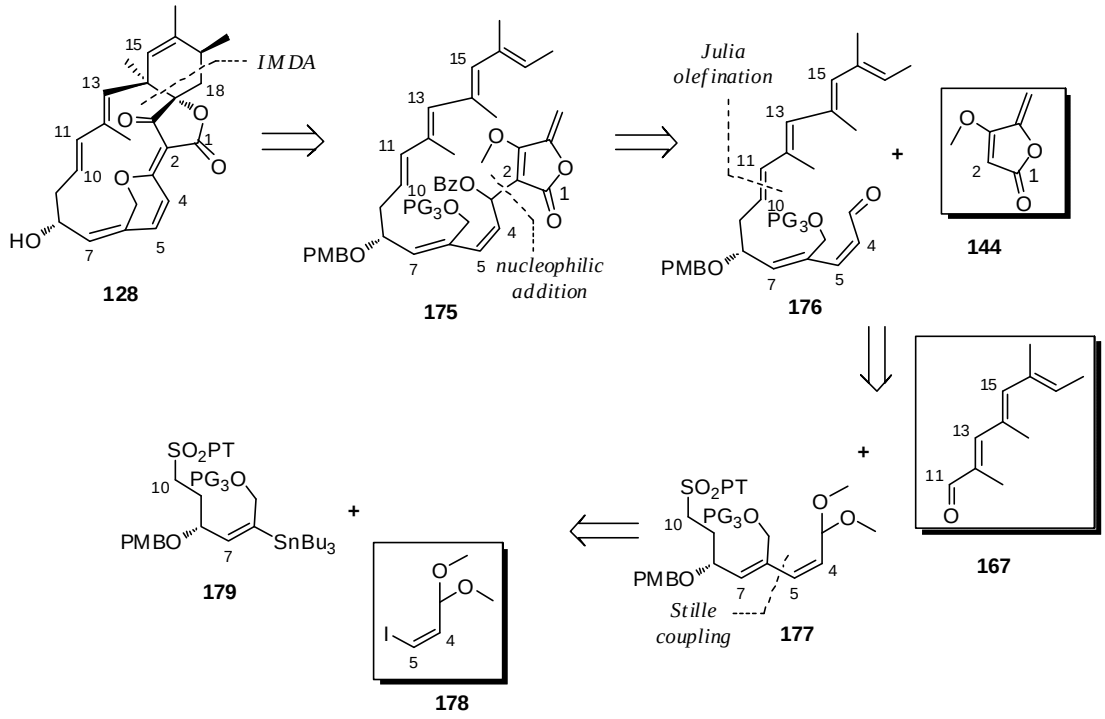

Scheme 2.13 Second generation IMDA approach to spirohexenolide A

The retrosynthetic scheme was modified to accommodate Marshall's method. A fragment such as **179** (Scheme 2.13) should thus be accessible from a precursor propargylic alcohol, and we envisioned coupling it to acetal **178**, which can be prepared in good yield from the commercially available ethyl *cis*-3-iodoacrylate. The development of the necessary propargylic alcohol began with malic acid, but C-10 was left as a protected alcohol to focus efforts on homologation at C-7.

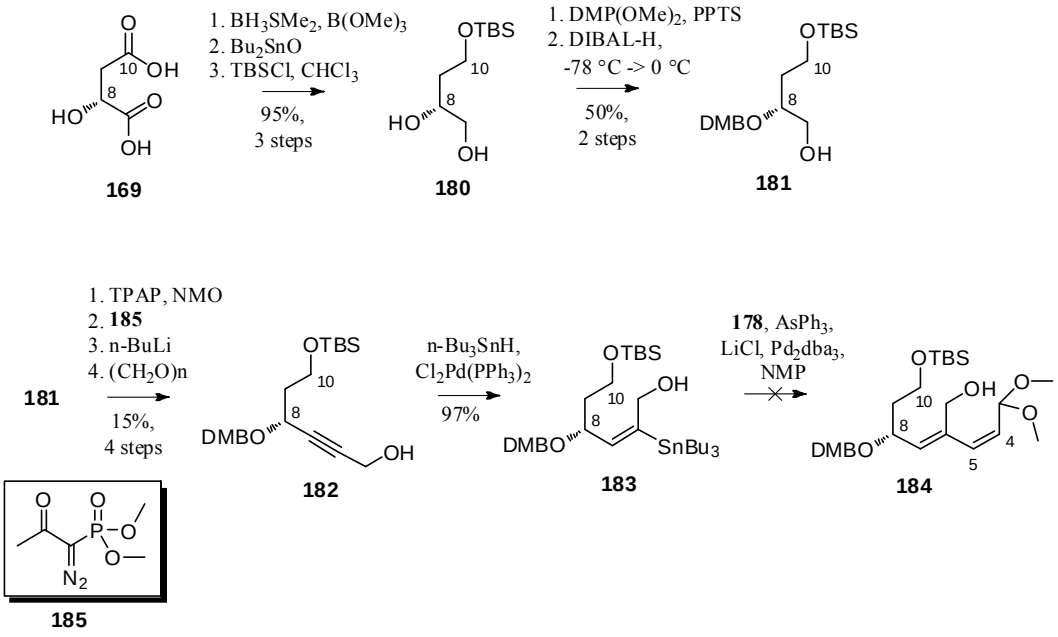

Scheme 2.14 Preparation of stannane **183**

(*R*)-1,2,4-butanetriol was prepared by the reduction of malic acid, and regioselectively silylated at the less hindered primary hydroxyl group via the dibutylstannanediyl acetal. The 1,2-diol of **180** was converted to the 3,4-dimethoxybenzylidene acetal which was reduced to form the secondary –ODMB ether **181**. With position 7 available for homologation, the primary alcohol was oxidized and converted to the terminal alkyne using the modified Ohira-Bestmann protocol in

which the diazophosphonate reagent **185** is generated by a mixture of tosyl azide and the commercially available phosphonate.[169] The terminal alkyne was then converted to the propargylic alcohol **182** in poor yield over the 4 step homologation sequence, mostly due to the unoptimized 30% yield at the Ohira-Bestmann step. Marshall's methodology provided stannane **183** as the only detectable regioisomer, which gave us confidence in this approach to the C-6/C-7 olefin, but attempted coupling to acetal **178** (Scheme 2.13) only returned unreacted **183**.

The sequence shown in Scheme 2.14 to **183** was lengthy, and even if it could be optimized it suffered from the major drawback that it begins with the unnatural and expensive D-(+)-malic acid. A better approach to fragments such as **182** would be the addition of a propargyl alcohol equivalent such as **187** to a protected 3-hydroxypropionaldehyde unit **186**, for which an asymmetric method utilizing N-methylephedrine **188** was developed by the Carreira group.[170]

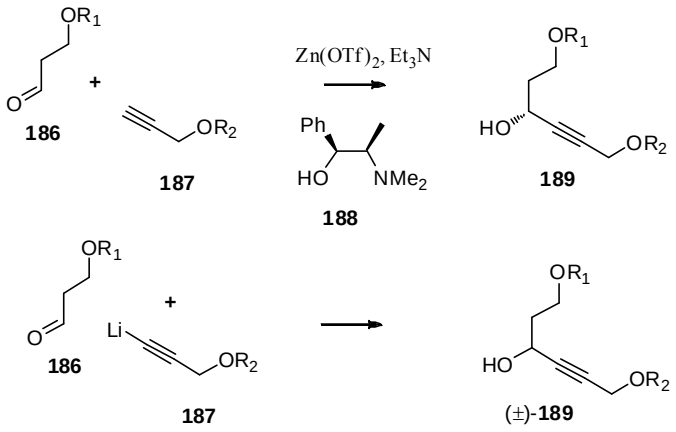

Scheme 2.15 A different approach to the propargylic alcohol fragment

A few attempts at the Carreira reaction indicated that it would require some troubleshooting to get the reaction conditions right for the addition to work, time that

would be better spent evaluating the later stage fragment couplings. The racemic approach shown in the bottom portion of Scheme 2.15 was adopted due to its expediency and high efficiency, and a few modifications were made to the protecting group scheme used in Scheme 2.14.

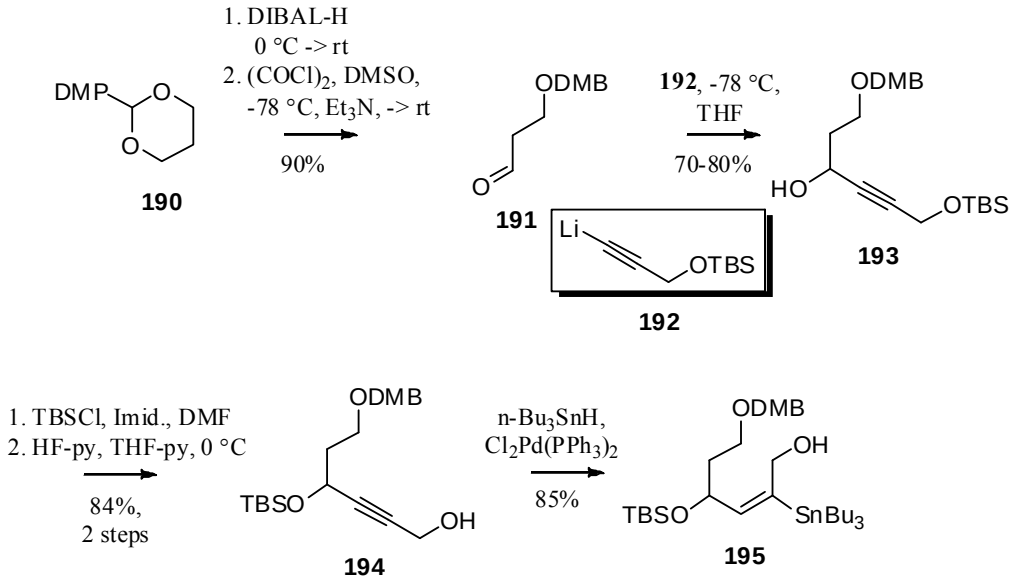

Scheme 2.16 Synthesis of stannane **195**

An efficient 6 step linear route to stannane **195** was developed (Scheme 2.16), and material throughput was good enough to allow the evaluation of its coupling to **178** and other vinyl iodides. Every Stille coupling attempted using stannane **195** either failed to produce adduct, or did so in very low yields even under forcing conditions. This may be due to hinderance of the stannane, and it is known that terminal stannanes are more reactive than internal ones such as **195**.[171]

As an alternative to using stannane **195**, the corresponding vinyl iodide **196** was prepared by tin-halogen exchange after hydrostannation of **194** (Scheme 2.17).

Vinyl iodides are highly reactive under Sonogashira conditions, and we envisioned that if an enyne could be formed at this position, the C-4/C-5 *cis*-olefin could be obtained by Lindlar hydrogenation.

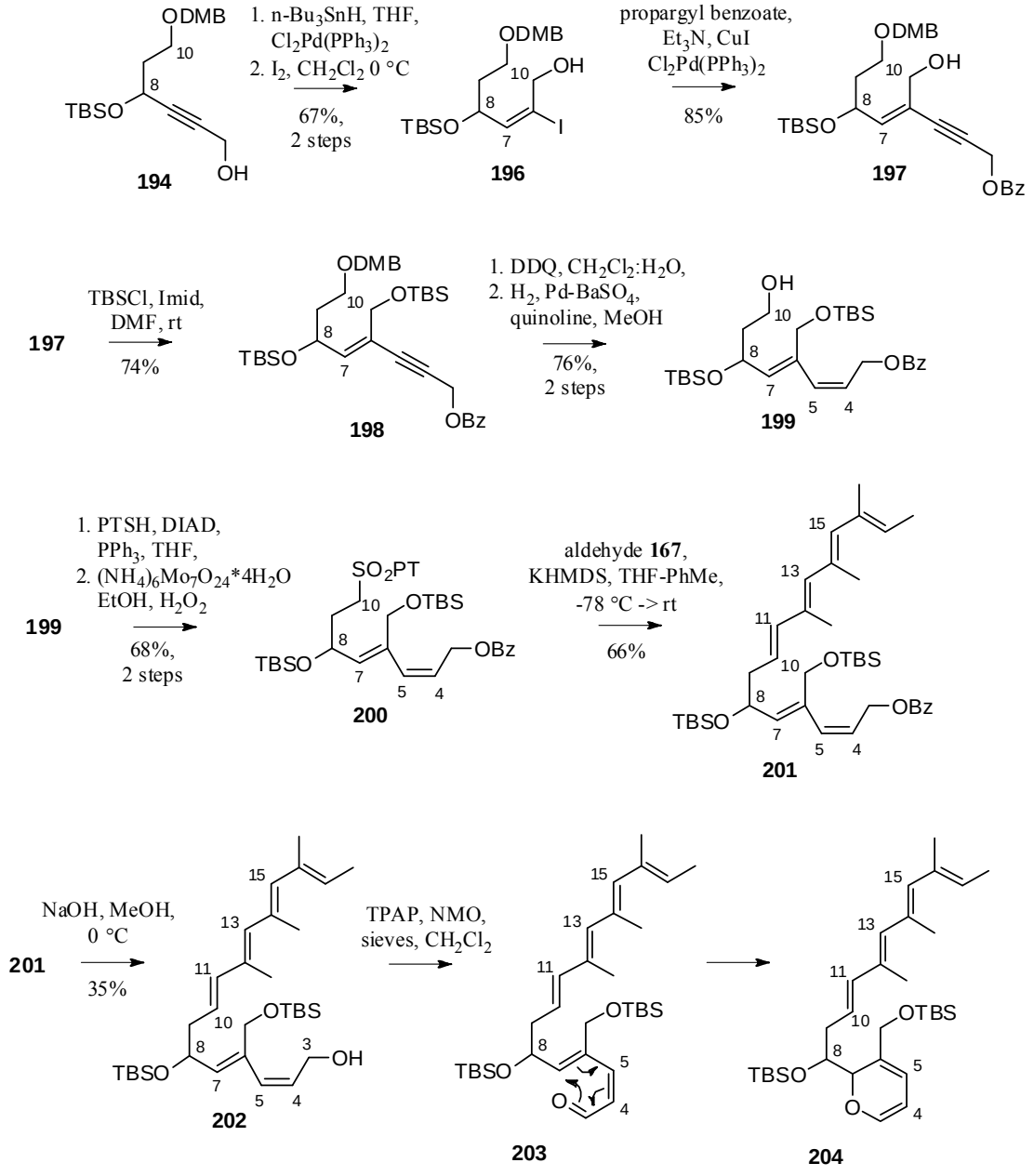

Scheme 2.17 Preparation of polyene **202**

Iodide **196** was observed to couple with propargyl benzoate in good yield to afford Sonogashira adduct **197**. Silylation of the primary hydroxyl group and deprotection of the C-10 –ODMB ether with DDQ provided the desired enyne substrate to test hydrogenation, and it was found that Rosenmund's Pd-$BaSO_4$ catalyst in the presence of quinoline was the preferred set of conditions to afford the diene **199**. Installation of the PT-sulfide under Mitsunobu conditions and oxidation provided sulfone **200**, which coupled in moderate yield to Baldwin's aldehyde **167** to provide the polyene product **201**. Deprotection of the benzoate proceeded in low yield, but we neglected to optimize this step due to the unfortunate 6π electrocyclic rearrangement of the intermediate aldehyde **203** to form the undesired pyran **204**, effectively bringing the route to its demise because we had no way of adding the tetronate to the rest of the molecule.

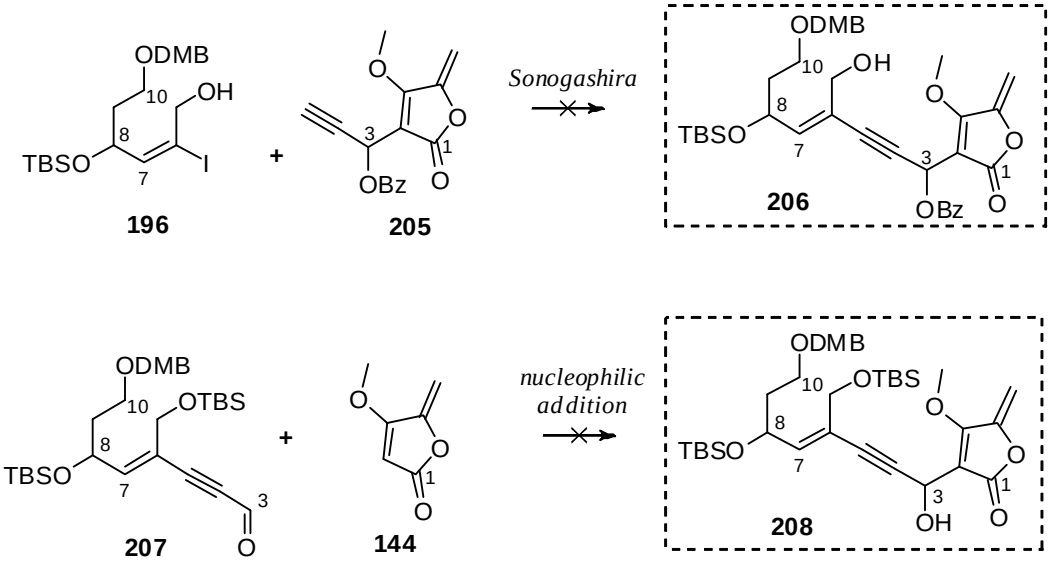

Scheme 2.18 Attempts to install the tetronate earlier in the route

We thought that including the tetronate ring on the alkyne partner as in **205** might provide a solution to this problem, because the C-3 carbonyl would not need to be generated in the presence of the adjacent diene (Scheme 2.18). Although we were able to prepare alkyne **205** in 3 steps from **144**, it was not stable under the Sonogashira coupling conditions with vinyl iodide **196**. None of the desired enyne **206** was detected, and **205** was not recovered from the reaction mixture. As an alternative to this method, we generated ene-yn-al **207** in 3 steps from **196** to see if we could access adduct **208**, essentially the same idea as with the Sonogashira strategy. The failure of this approach brought us to the realization that it would be prudent to examine Stille couplings using iodide **196**.

In particular, a literature search showed that aldehyde **209** was available in 2 steps from propargyl alcohol.[172] It was found that the lithiated tetronate fragment **144** added in good yield to this aldehyde to provide racemic stannane **210**, which was exactly the coupling piece we needed for a Stille reaction with iodide **196**. Before coupling, iodide **196** was silylated to compound **211** in order to differentiate the hydroxyl groups. In contrast to the reversed-partner situation with stannane **195**, the coupling of **210** and **211** proceeded in excellent yield to give Stille adduct **212** as a 1:1 mixture of separable diastereomers (Scheme 2.19). At this point, it was discovered that protecting the C-3 hydroxyl group was going to be difficult. A protecting group orthogonal to the DMB group at C-10 (oxidative cleavage conditions) and the silyl groups was needed, which led us to consider esters. The benzoate ester was chosen because of its lability under mild alkaline conditions, and non-enolizability, which was desired because the Julia-Kocienski coupling uses the strong base KHMDS.

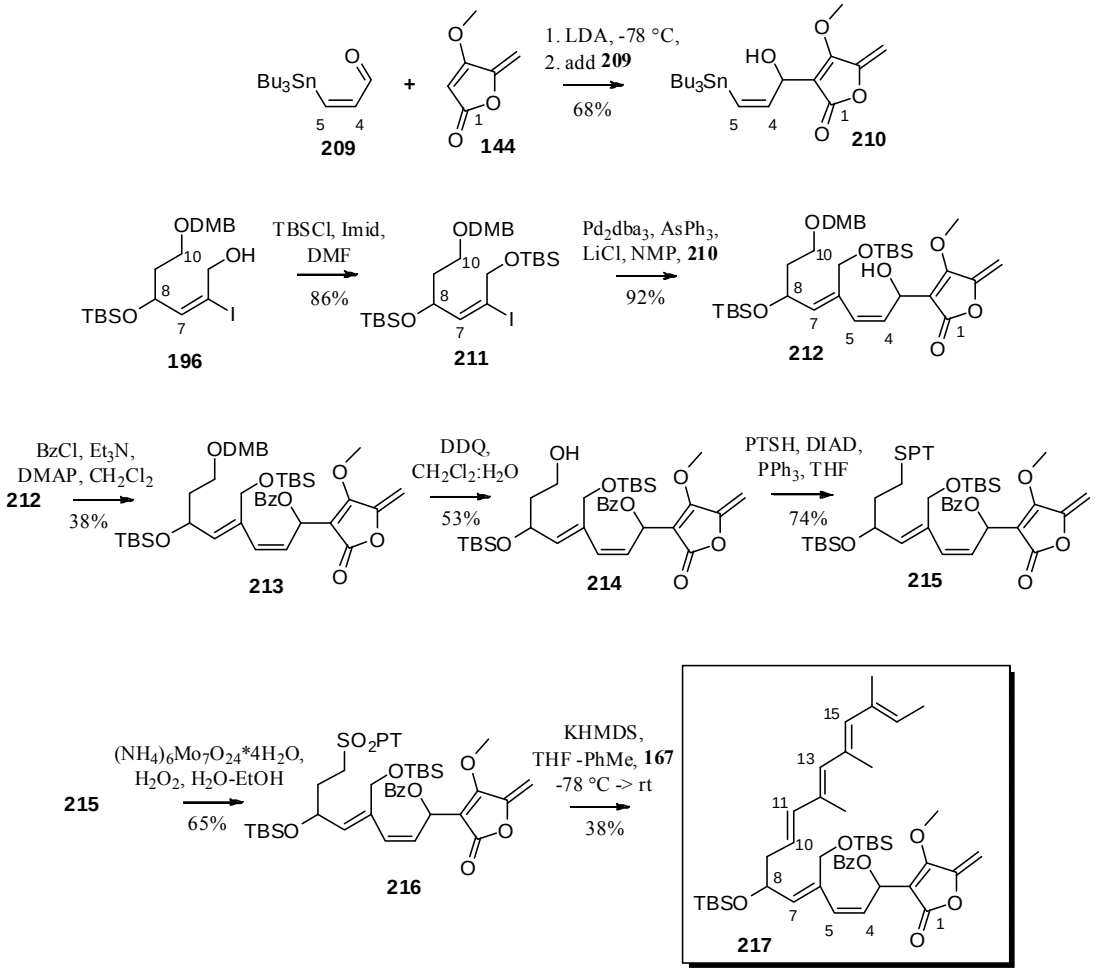

Scheme 2.19 Preparation of IMDA precursor **217**

Strangely, installation of the benzoate proved to be quite difficult, and only one of the **212** diastereomers gave any product **213**, and in poor yield. No other conditions were found to produce **213**, but since we had a good route to **212**, it was decided that we could optimize the protecting group steps later, after the fragment coupling steps had been examined. Removal of the C-10 ODMB ether also proved to be difficult, possibly due to the instability of product **214** under the mildly acidic conditions of the deprotection, as the hydroquinone byproducts may catalyze the S_E2' elimination of the

benzoate at C-3, by the 5-*exo*-trig formation of a tetrahydrofuran byproduct. This byproduct was not fully characterized. If **214** was quickly subjected to the Mitsunobu conditions to install the PT-sulfide at C-10, enough material throughput was possible to carry on with the route, and the sulfide product **215** and sulfone **216** were both stable intermediates. Coupling of Baldwin's aldehyde **167** occurred in low yield, but on a larger scale campaign through the route (Scheme 2.19), we were able to secure over 10 mg of the IMDA precursor **217**. The precursor polyene was thought to be delicate, and was immediately subjected to mild IMDA conditions (Toluene, 110 °C, 12h.) in a sealed tube, in the presence of the radical inhibitor BHT. There were two potential products analyzed after chromatography of the crude reaction mixture, but in both of these products the clearly distinguishable 5-exo methylene unit of the tetronate dienophile had not reacted (section **2.8** – see Figure 2.11 and Figure 2.12).

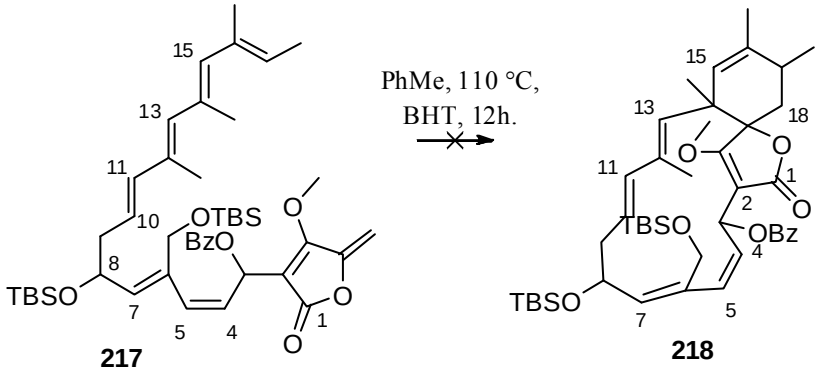

Scheme 2.20 Attempted IMDA cyclization of **217**

In addition to the lack of observation of any cyclized product **218** in the reaction mixture, there were several problems with the route to precursor **217** shown in Scheme 2.19. The fact that only one of the diastereomers could be carried forward

from the Stille coupling, combined with the poor yields in the protecting group steps did not bode well for this being a viable route to complete the synthesis of **128**. It was unknown which diastereomer (relative stereochemistry about C-3 and C-8) was being carried forward, and what influence if any this relative stereochemistry would play in the cycloaddition step. Further, the previous studies on abyssomicin and chlorothricolide (Section 2.3) had shown that the substituent at the 3-position of the tetronate ring (acyl in abyssomicin precursor **136**, oxygen in chlorothricolide precursor **139**) plays an influential role on the reactivity of the tetronate in the IMDA step. During the synthesis of **217**, we tested the oxidation of the C-3 hydroxyl group on Stille adduct **212**, and pyran **219** was the only isolated product as a single diastereomer, which had formed presumably by the same type of rearrangement that we had observed in the Sonogashira route (Scheme 2.17) **203** -> **204**.

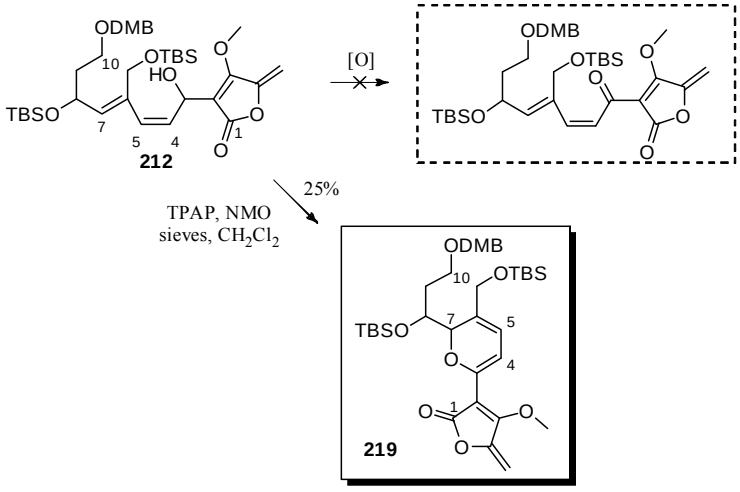

Scheme 2.21 Oxidation of Stille adduct **212**

It is likely that a 3-acyl tetronate IMDA precursor would have had better success than **217** under thermal conditions, but this rearrangement chemistry

prevented us from preparing such a precursor. We were forced to leave a protected oxymethine group at this position, which is presumably less reactive. Also, the precursors for abyssomicin (**136**) and chlorothricolide (**139**) had only 4 and 5 total olefins, respectively, whereas spirohexenolide precursor **217** has 7, all in a compact framework. A number of side reactions and dimerization / polymerization reactions could be possible in such a system. A lower risk approach to the spirotetronate system was needed.

2.4.2 A Lewis acid catalyzed Diels-Alder approach to (±)-spirohexenolide B

During roughly the same time period these disappointing results were being observed in our synthetic studies on **128**, its biosynthetic precursor **129** was discovered during efforts to increase production titers of **128** for bioactivity studies (see Section 2.1). To our knowledge, **129** is the only known spirotetronate where the only stereocenters are in the spirotetronate system, and its existence proves that the linear precursor to the spirohexenolides is achiral. Because the stereocenters in the spirotetronate system are installed in the Diels-Alder reaction, a diastereoselective route to the spirotetronate fragment would secure a synthesis of (±)-**129**, if the rest of the molecule could be built around it. To implement this strategy, we retained the retrosynthetic disconnections used in our synthesis of **217**, but substituted fragment **224** for the tetronate **144**, and the simplified vinyl iodide **222** would substitute for fragment **211** (Scheme 2.22).

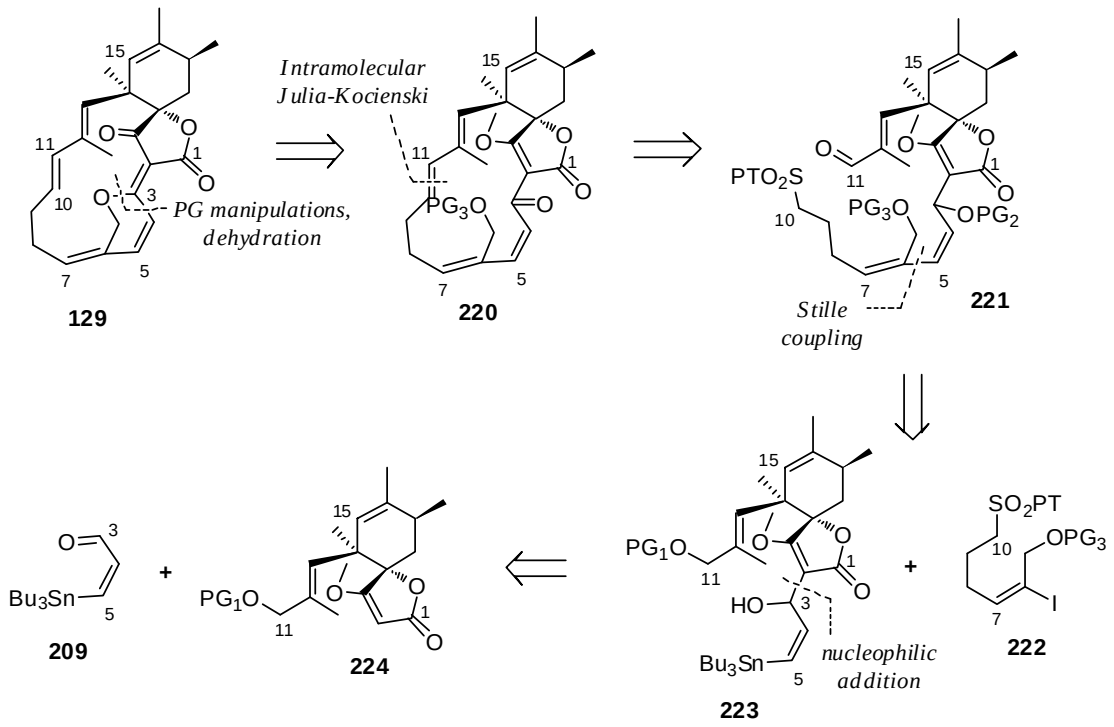

Scheme 2.22 Retrosynthetic analysis of spirohexenolide B

We had already prepared fragment **209** for our synthesis of **217**, and fragment **222** could be prepared in an analogous way to fragment **211**. A diastereoselective route to **224** was needed, and for this we turned to methodology developed for the spiroteteronate systems of abyssomicin C (**138**), and quartromicin.[173, 174] Although they appeared to be very similar to the system that we needed, serious problems were encountered in attempts to mimic these syntheses.

The first option explored was the use of an Al(III) tethered Lewis acid catalyzed Diels-Alder reaction, which had been reported to proceed with complete *endo* selectivity in the construction of the abyssomicin core.[173] This reaction is a modification of methodology developed by the Roush group for the diastereoselective construction of the spirotetronate systems of the quartromicins.[175] This reaction

utilizes the same Lewis acid and dienophile (α-acetoxy acrolein **226**), but the tethered reaction involves an unprotected diene-alcohol **225**, which is thought to promote a rigid, highly ordered transition state **227**.

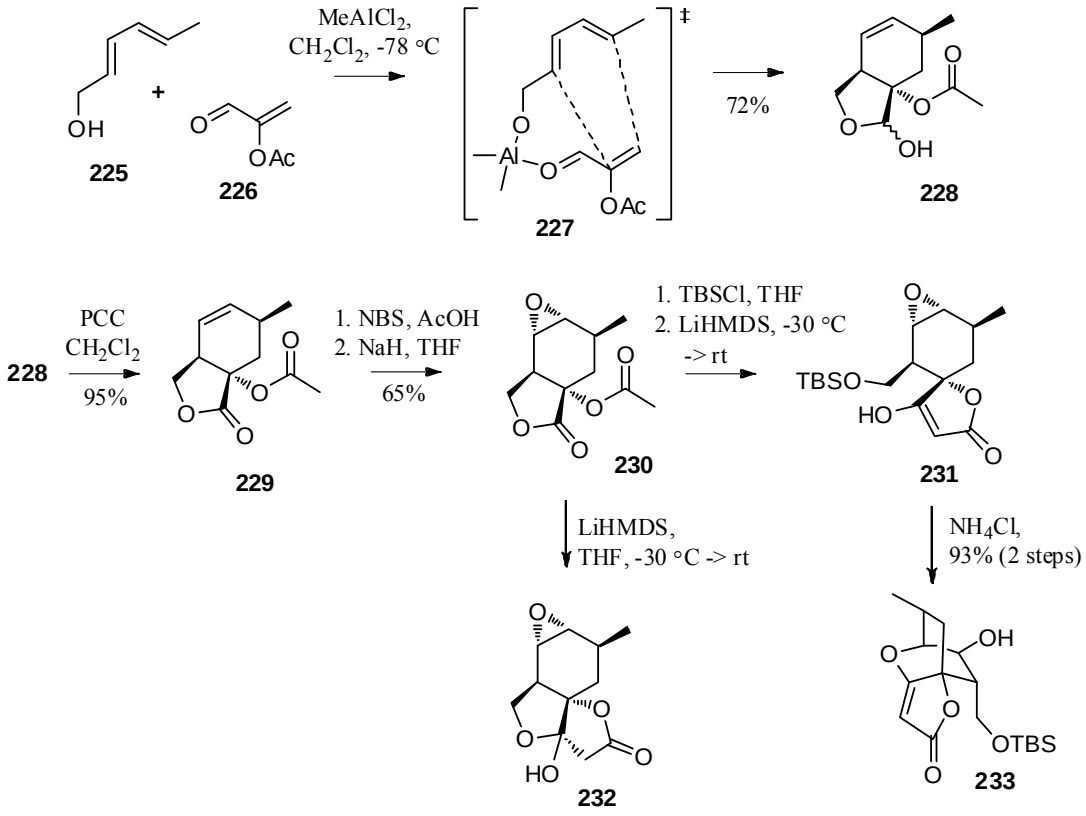

Scheme 2.23 Zografos' route to the abyssomicin core

Scheme 2.23 illustrates the efficient route to the oxabicyclo[2.2.2]octane core of the abyssomicins, modeled by (±)-**233**, developed by the Zografos group using this methodology. The *endo* Diels-Alder adduct **228** was oxidized to the lactone **229** and the cyclohexene ring was epoxidized in a two step sequence through the intermediate bromohydrin to form **230**. Dieckmann cyclization was effective in forming the tetronate ring, but it is especially noteworthy that if the resulting alkoxide was not

trapped *in situ* as its silyl ether, formation of the tricyclic lactol **232** was the only observed product. Lactol **232** was very stable and proved recalcitrant to all attempts to open it to an intermediate such as spirotetronate **231**.

Adaptation of this strategy to the spirohexenolides began with the reaction of dienol **234** with α-acetoxy acrolein **226** to provide the Diels Alder adduct (±)-**235** in good yield as a mixture of epimers (Scheme 2.24).

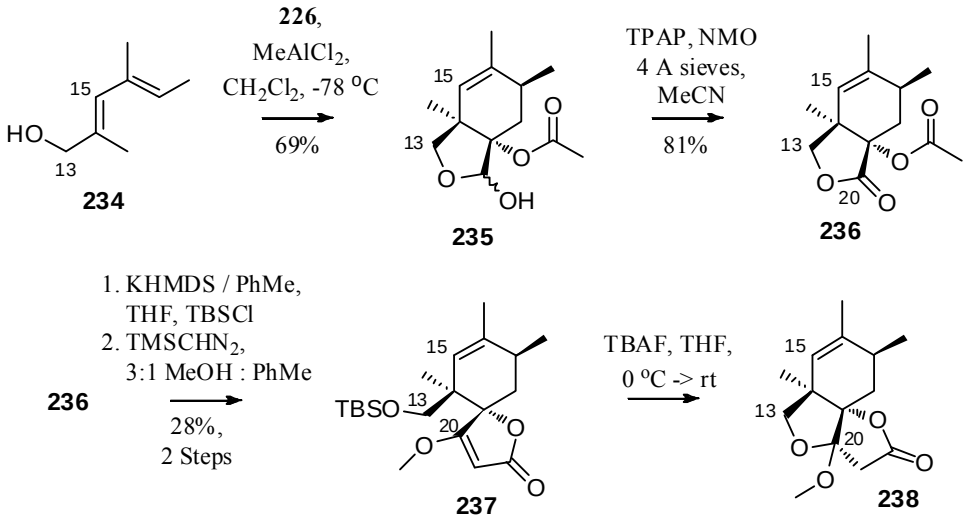

Scheme 2.24 First Lewis acid catalyzed Diels-Alder approach

Oxidation of adduct **235** to the lactone **236** proceeded in good yield, and the complete *endo* selectivity of the Diels-Alder reaction was confirmed by X-ray crystallographic analysis of **236**. The Dieckmann cyclization and trapping of the C-13 alkoxide as its silyl ether proceeded as in the Zografos route, and the tetronic acid moiety was protected as its methyl ether. It was not entirely unexpected that deprotection of the C-13 hydroxyl group, which was necessary for homologation at that position, resulted in Michael addition to the tetronate ring to form acetal **238**.

This represented a dead end to the route, unless a method of blocking addition to C-20 could be devised. We thought it could be possible to convert the Diels-Alder adduct **235** to a protected aldehyde form, generate the necessary C-12/C-13 trisubstituted olefin by HWE/Wittig type methods, and then deprotect and form the tetronate afterward. The corresponding dithiane was generated and the 5-membered dithiolane. Unfortunately, both of these reactions proceeded in poor yields (35% and 34% respectively) and both occurred with cleavage of the acetate. These yields could not be improved by altering the Lewis acids, temperatures, stoichiometry, or other reaction parameters despite much effort. No other method was found to be successful in protecting the C-20 lactol, and so it was clear that new dienes for the Diels-Alder reaction needed to be explored.

It was thought that if the aldol adduct **241** could act as the diene in the Diels-Alder reaction, it might be possible to activate the lactol of the adduct **243** (as its triflate, tosylate, or halide, for example), and eliminate to form the C-12/C-13 olefin. A racemic *syn* selective aldol was carried out between the dibutylboron enolate of ethyl propionate **239** and aldehyde **240** to provide the aldol product **241** in modest yield.[176] Use of **241** as the diene in the Diels-Alder reaction with α-acetoxy acrolein **226** provided the adduct **243** in low yield together with unreacted starting material. Oxidation of **243** to the lactone **244** showed that the Diels-Alder reaction had proceeded in a disappointing 1.7:1 d.r. We reduced the ester of aldol adduct **241** and protected the primary alcohol as the silyl ether **242**, and tried the Diels-Alder reaction with this substrate. Oxidation of the product **245** indicated similar results to those obtained using the ester substrate.

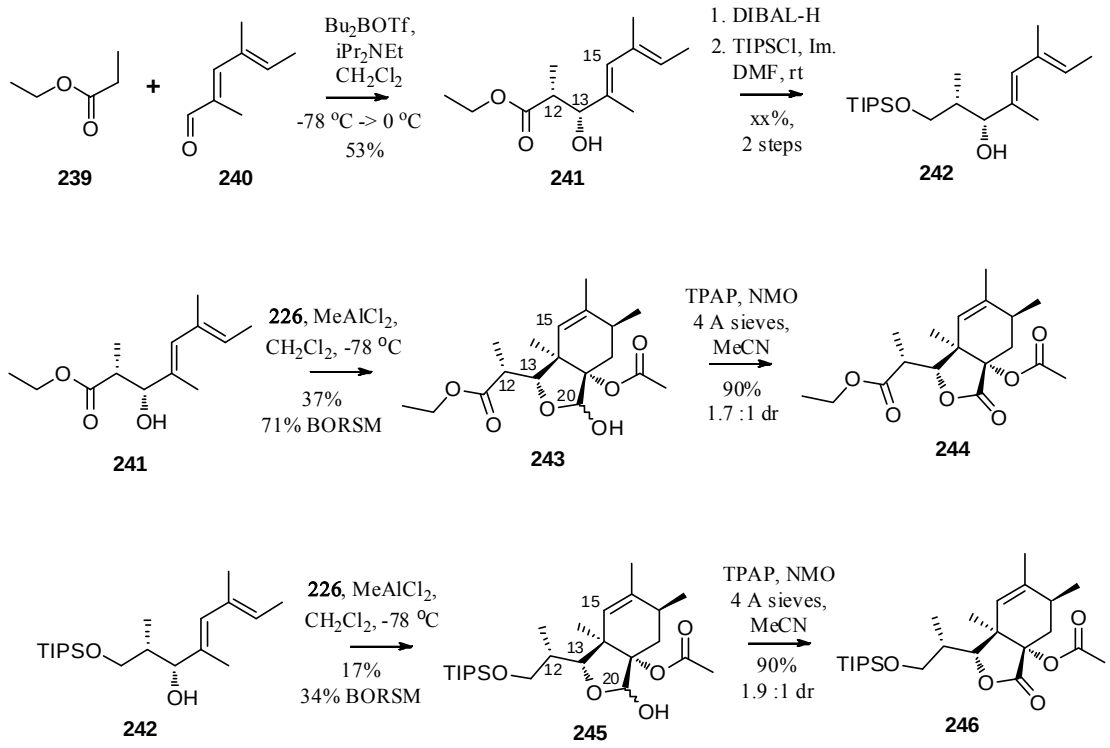

Scheme 2.25 Use of aldol adduct derived dienes in the Diels-Alder reaction

Because low diastereoselectivity was observed with these dienes, but total diastereoselectivity was observed with diene **234**, it seemed reasonable that we could achieve better results by removing either the C-13 hydroxyl group or the C-12 methyl group of **241** or **242**. One of these functional groups had to be responsible for the poor results obtained with the aldol derived dienes, and based on previous studies from the Roush laboratory on the *endo* (galacto) quartromicin subunit, it seemed more likely that it was the C-13 hydroxyl group.[174]

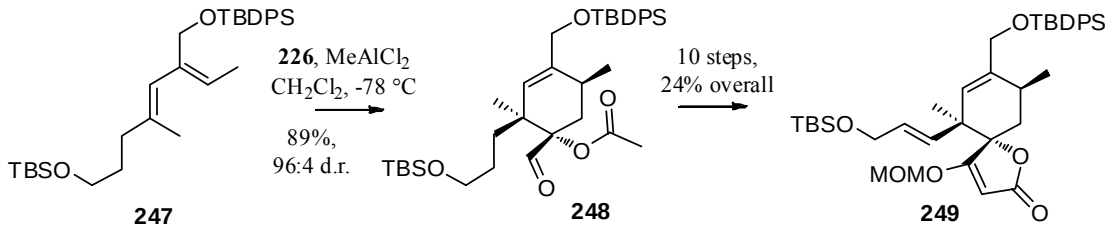

Scheme 2.26 The Roush group's synthesis of *endo*-spirotetronate **249**

The Roush group had used diene **247** in a comparable reaction with α-acetoxy acrolein **226** and achieved almost complete diastereoselectivity in the formation of Diels-Alder adduct **248**. Adduct **248** was then processed to the spirotetronate fragment **249** in a 10 step linear sequence that involved generation of the *E*-disubstituted olefin through the intermediate aldehyde, which was converted to its α-phenylselenide via the enamine (by the Williams procedure).[177]

The analogous route to the spirohexenolide subunit **224** began with the dieneol **234**, which was converted to the mesylate and LiBr was added, generating a mixture of the mesylate and bromide **250**, which was then added to a solution of the lithium enolate of ethyl propionate **239** to form the adduct **251**.[178] The adduct **251** was reduced and silylated to form **252**, which was subjected to the Diels-Alder reaction with α-acetoxy acrolein **226**, and the adduct **253** was observed as a 1.6:1 mixture of diastereomers. It was thought that these diastereomers were probably the α/β C-12 methyl isomers, which would not be an issue if the unsaturation reaction proceeded as planned later. The adduct **253** was prepared for the Dieckmann reaction by oxidation and conversion to the methyl ether **254**.

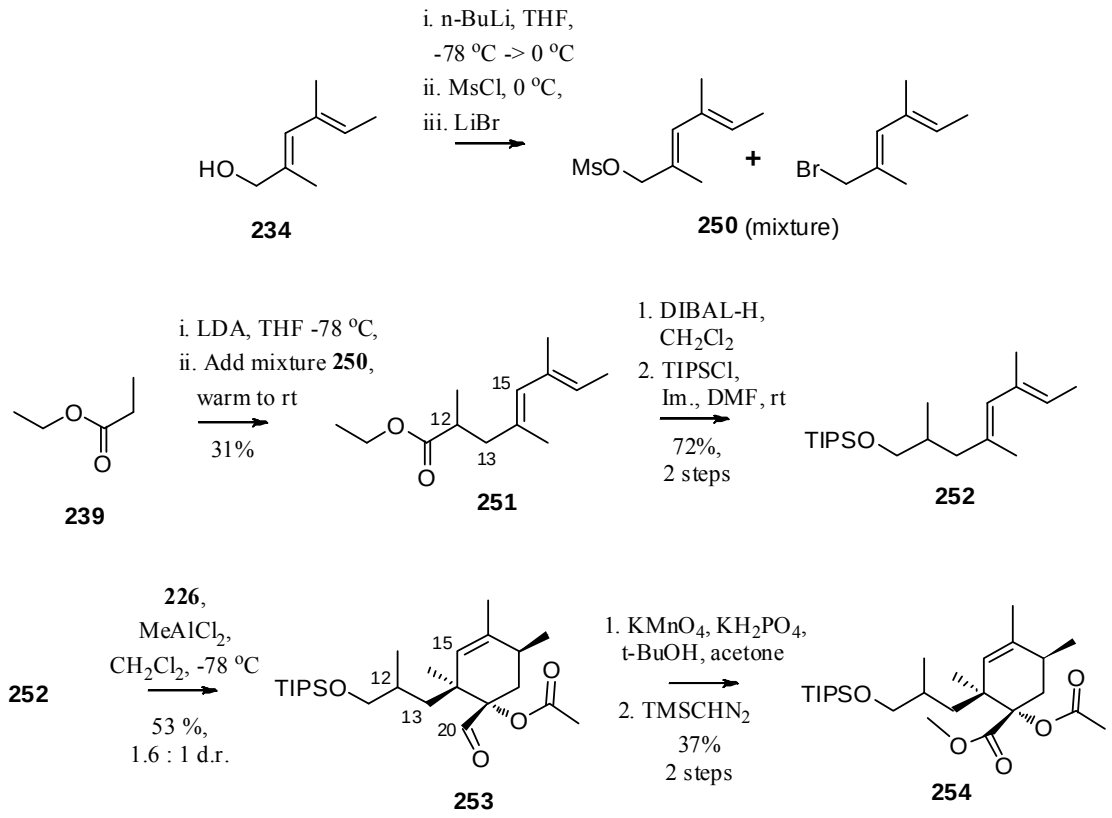

Scheme 2.27 Use of diene **251** and processing to the spirotetronate fragment

It was discovered that introduction of unsaturation by the Williams procedure resulted in formation of the undesired regioisomer **256**, likely due to the greater accessibility of the methyl protons to the selenoxide that forms in the reaction mixture.

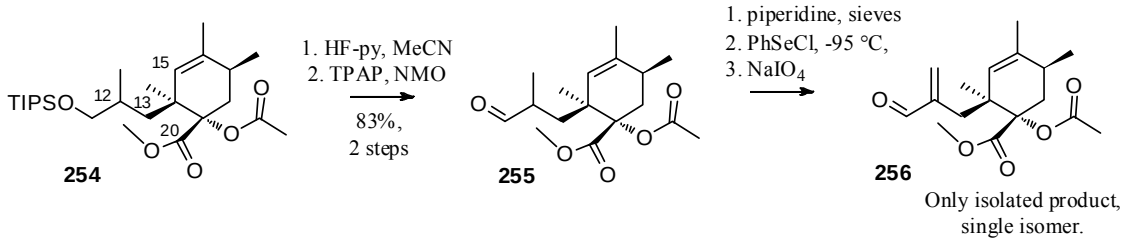

Scheme 2.28 Attempt to introduce unsaturation to aldehyde **255**

The isolation of **256** as a single diastereomer showed that the Diels-Alder reaction had proceeded with complete *endo* selectivity, but the result from the unsaturation procedure was troubling. After a survey of a number of literature examples, it was discovered that this is the usual outcome for α-methylated aldehydes, and so it became clear that this method could not be used to form the C-12/C-13 trisubstituted olefin.

A synthesis of the spirotetronate subunit of kijanolide described by the Marshall group showed that a triene substrate could be used in Lewis acid catalyzed Diels-Alder reactions with α-bromoacrolein as the dienophile. They had used Corey's tryptophan derived oxazaborolidine Lewis acid catalyst, and observed complete regioselectivity for the desired spirotetronate, and 72% e.e. in the reaction.[179]

It had been observed earlier by the Roush group that α-acetoxy acrolein **226** behaves the same way in the Diels-Alder reactions as α-bromoacrolein,[175] so based on these observations we reasoned that reaction of a triene substrate such as **257** might provide adduct **258** directly by reaction with **226**.

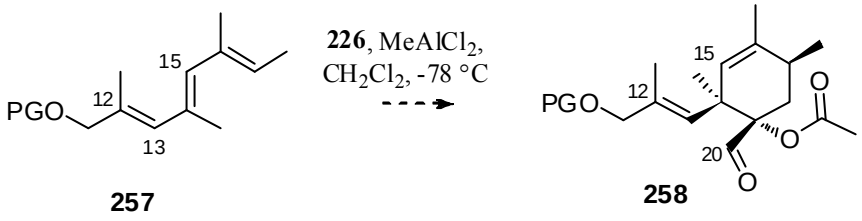

Scheme 2.29 The triene substrate Diels-Alder strategy

The triene ester **259** was reduced and protected as its benzoate ester **260**, and its reaction with α-acetoxy acrolein **226** provided the adduct **261** in reproducible

moderate yields; 60% is typical for the reaction, which has been performed on 100 mg – 10 g scale. It should be noted that use of the TBS protecting group instead of the benzoate **260** did not affect the reaction, but it was impossible to separate the desired adduct from the other isomers either from the reaction or in subsequent steps. In contrast, **261** can be recovered as a single isomer from the Diels-Alder reaction.

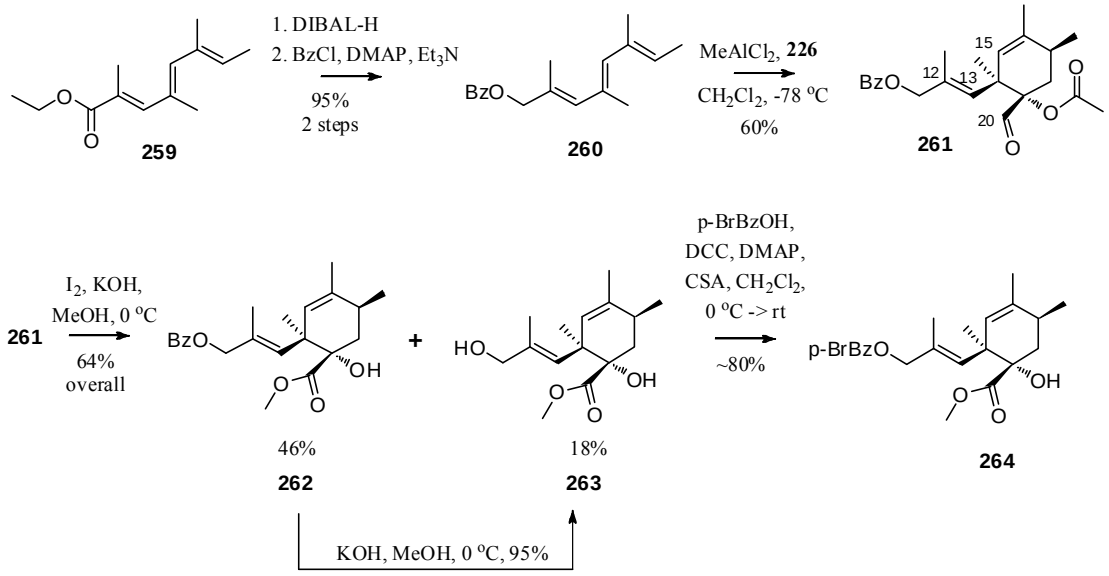

Scheme 2.30 Implementation of the triene Diels-Alder strategy

A number of oxidations were attempted to provide either **262** or the corresponding acid from **261**. None of the chromium methods, oxone, $KMnO_4$, or $NaClO_2$ were satisfactory. Only the alkaline iodine method provided sufficient yields of the oxidized products, and only with complete deprotection of the acetate, and partial deprotection of the benzoate.[180] After further exploration of the route it was discovered that the diol **263** would be used as the intermediate; in practice, after workup of the reaction, **262** is methanolyzed to **263**. The diol **263** was derivatized as its *p*-bromobenzoate ester **264**, which confirmed the regio- and diastereoselectivity of

the Diels-Alder reaction by X-ray crystallographic analysis. The diol **263** could be converted to the bis-acetate **265** and selectively reduced to the mono-acetate **266**. Further exploration of the route demonstrated that the TBS protecting group was needed at C-11, so **266** was silylated to **267**, and converted to the spirotetronate system by Dieckmann cyclization and methylation to form **268**.

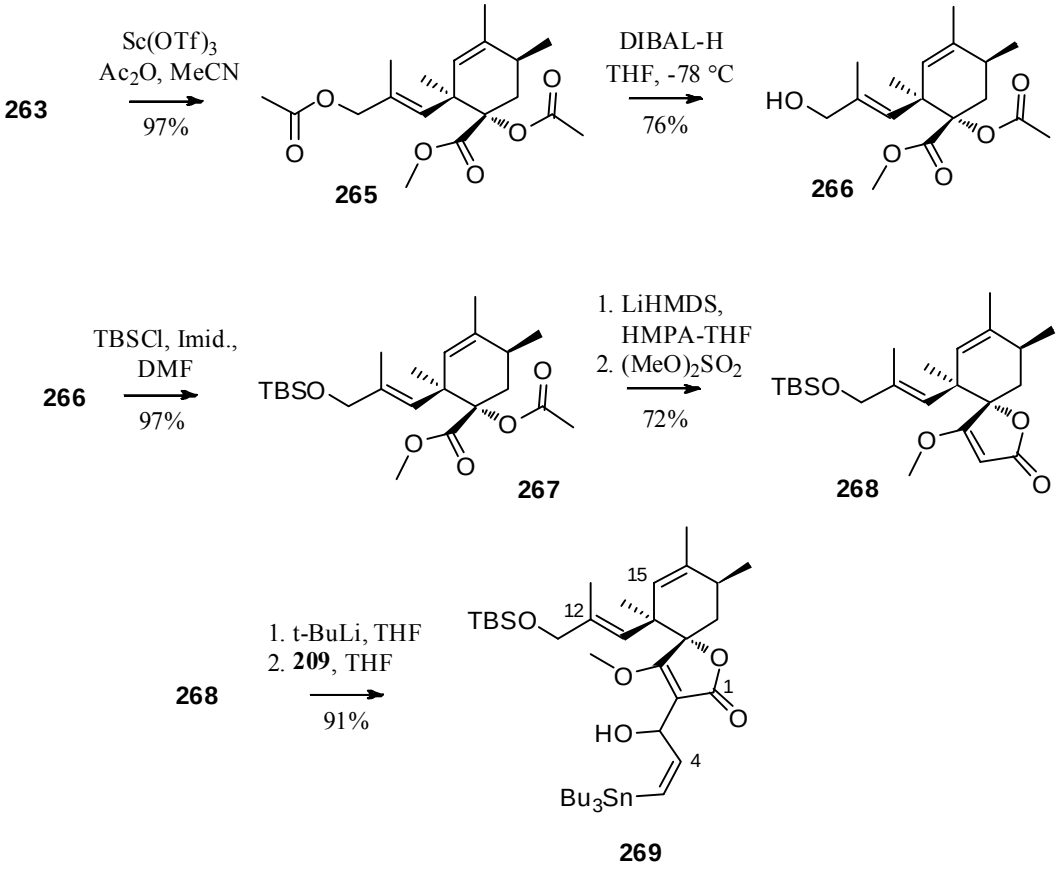

Scheme 2.31 Generation of the spirotetronate fragment **268**

Although variable reactivity of *endo*-spirotetronate subunits similar to **268** has been reported,[181] we were pleased to observe that **268** can be directly lithiated with *t*-BuLi and added in high efficiency to the aldehyde **209**, to provide the required stannane partner **269** for the Stille coupling.

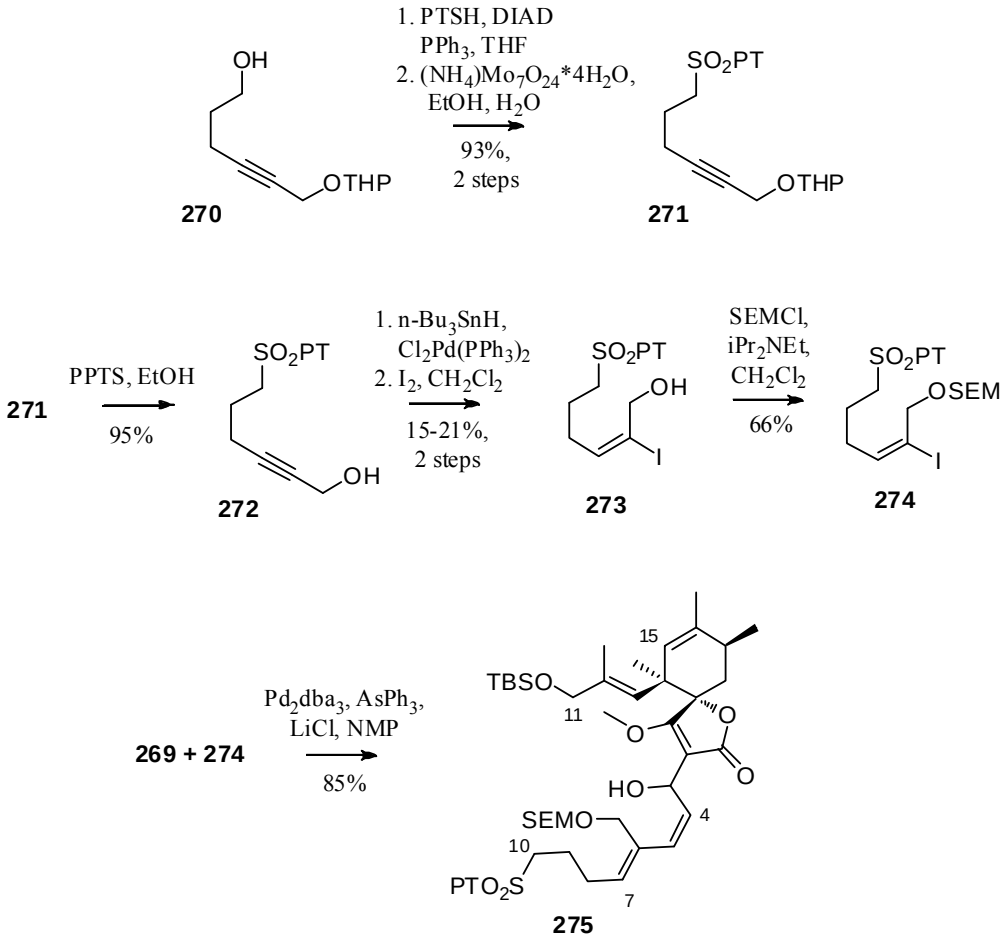

Scheme 2.32 Synthesis of the iodide **274** and Stille coupling with **269**

A route to an iodide such as **222** (Scheme 2.22) was still needed, and for this fragment a survey of the literature revealed a convenient starting material **270**, available from a ring opening reaction of oxetane.[182] Installation of the PT-sulfide, oxidation, and removal of the THP group provided propargylic alcohol **272**, which after hydrostannation and tin-iodine exchange provided vinyl iodide **273** in low yield with other regioisomers. We identified **273** as the desired isomer from this mixture based on the ^{1}H NMR spectrum and selective NOESY1D spectra. We selected the SEM protecting group for fragment **274** as it would be orthogonal to the C-11 OTBS

group as well as a C-3 OTBS group, in our later schemes. Coupling of the stannane **269** to **274** proceeded in good yield to the Stille adduct **275** using the conditions from Marshall's synthesis of Bafilomycin V_1.[79]

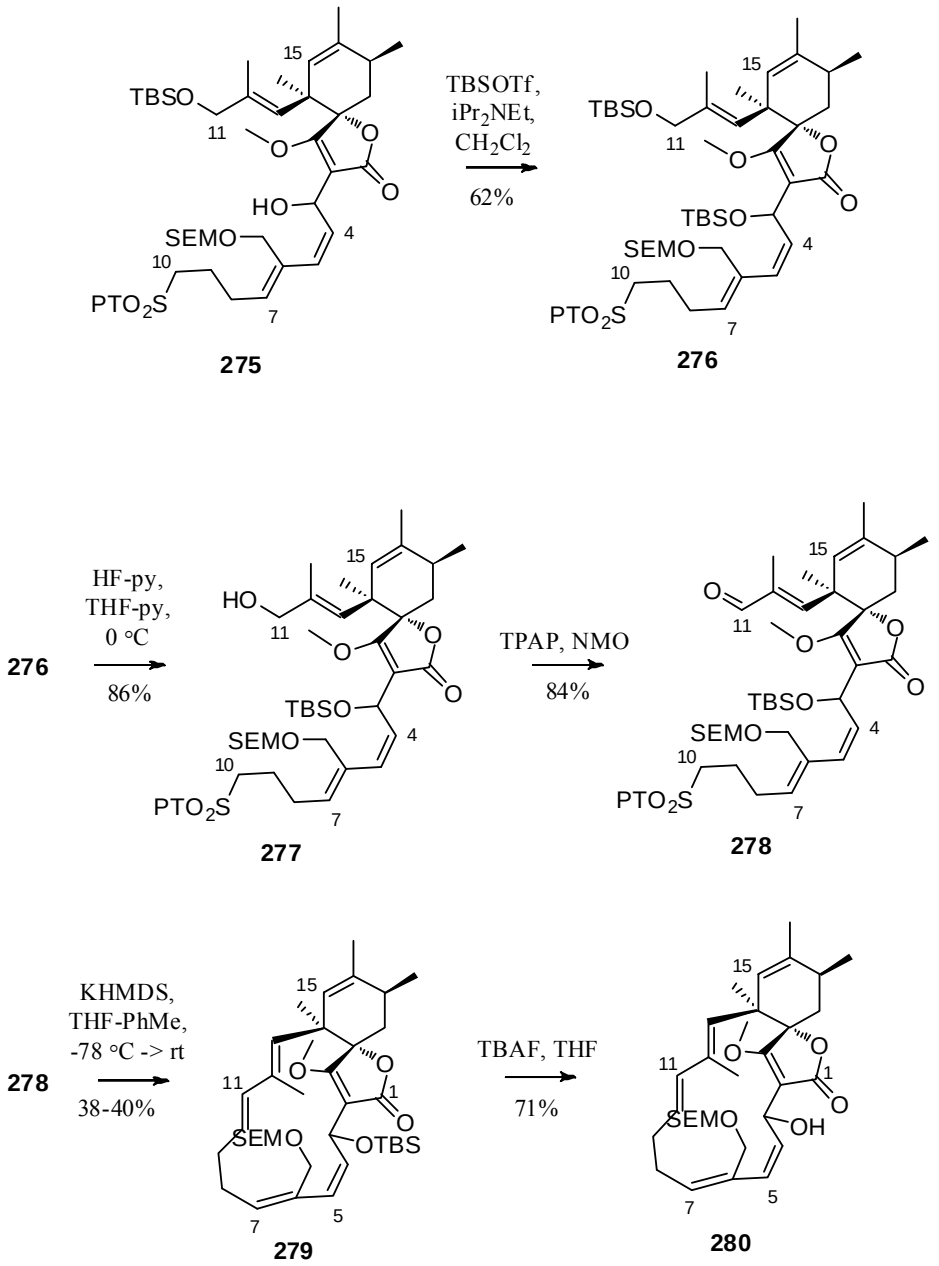

Scheme 2.33 Processing of Stille adduct **275** through Julia adduct **279**

It was discovered that the more active silylating reagent TBSOTf was needed to protect the hindered secondary C-3 hydroxyl group as **276**, and that removal of the primary C-11 OTBS ether proceeded in good yield and selectivity to provide **277**. Oxidation to **278** allowed the critical intramolecular Julia-Kocienski reaction to be tested. The reaction has only been run twice, and both times the yield of **279** appears to be less than 50%. The ^{1}H NMR spectrum indicates the presence of impurities, but the ^{13}C NMR shows what appears to be a single diastereomer, indicating that only one of the α/β C-3 OTBS diastereomers cyclizes under the reaction conditions. The rest of the material has not yet been identified. Removal of the C-3 OTBS group with TBAF provides **280**, which has a better but still not completely pure ^{1}H NMR spectrum. At this stage, the characteristic ddd of H-10 in the ^{1}H spectrum of **280** can be matched to the natural **129** (section **2.9** - Figure 2.13). Efforts are in progress to convert **280** to (±)-**129**.

2.5 Concluding remarks

The spirohexenolides are a new, biologically active class of spirotetronate natural products that have shown moderate antitumor and antibiotic activity. Their structures were elucidated by NMR and X-ray crystallographic methods, and to further study and understand the chemistry of these structures, a synthetic campaign toward **128** and **129** was begun. A route toward (±)-**128** culminated in the synthesis of the linear IMDA precursor **217**, which failed to cyclize in the desired way under thermal

conditions. A route toward (±)-**129** which is still ongoing, has progressed to intermediate **280**, which has the complete carbon skeleton of **129**, and a method needs to be developed to form the fused pyran-tetronate system in order to complete the molecule.

2.6 Acknowledgements

I wish to thank Professor Michael Burkart and Dr. James La Clair for useful guidance and assistance on this project. All of the culturing work described in section 2.1 and manipulations of the *S. Platensis* strains was done by Dr. Min Jin Kang.

Section 2.1, in full, is a reprint of the material as it appears in *J Org Chem*., 74, 23, pp. 9054-9061, 2009. The dissertation author was the second author of this paper.

2.7 Experimental techniques and characterization data

General experimental methods:

Unless otherwise noted, all reagents and chemical compounds were purchased from commercial sources and used without further purification. High purity anhydrous solvents (tetrahydrofuran, dichloromethane, diethyl ether, and toluene) were obtained by passing through a solvent column composed of activated A-1 alumina.[80] Anhydrous *N*,*N*-dimethylformamide was obtained by passage over activated molecular sieves and a subsequent sodium isocyanate column to remove

traces of dimethylamine. Triethylamine (Et_3N) was dried over sodium and freshly distilled. Ethyl-*N*,*N*-diisopropylamine (*i*-Pr_2NEt) was distilled from ninhydrin, then from potassium hydroxide. All air or moisture sensitive reactions were performed under positive pressure of dry argon in oven-dried glassware sealed with septa. Reactions were magnetically stirred with Teflon coated stir bars. Flash chromatography was performed on EMD Geduran Silica Gel 60 (40-63 mesh) according to the method of Still.[81] Analytical TLC was performed on Silica Gel 60 F254 pre-coated glass plates. Visualization was achieved with UV light and/or an appropriate stain (I_2 on SiO_2, $KMnO_4$, bromocresol green, dinitrophenylhydrazine, ninhydrin, and ceric ammonium molybdate). Yields and characterization data correspond to isolated, chromatographically and spectroscopically homogeneous materials unless otherwise noted. ^1H NMR spectra were recorded on Varian Mercury 300 MHz or 400 MHz spectrometers, or a Varian Mercury Plus 400 MHz spectrometer, or a JEOL ECA 500 MHz spectrometer, or a Varian VX 500 MHz spectrometer. ^{13}C NMR spectra were recorded at 125 MHz on the JEOL ECA 500 instrument or the Varian VX 500 spectrometer, or at 100 MHz on either a Varian Mercury or the Mercury Plus instrument, or at 75 MHz on a Varian Mercury spectrometer. Chemical shifts for ^1H NMR and ^{13}C NMR analyses were referenced to the reported values of Gottlieb *et. al.*, using the signal from the residual protonated solvent for ^1H spectra, or to the ^{13}C signal from the deuterated solvent.[82] Chemical shift δ values for ^1H and ^{13}C spectra are reported in parts per million (ppm) relative to these referenced values, and multiplicities are abbreviated as s = singlet, d = doublet, t = triplet, q = quartet, m = multiplet, br = broad. All ^{13}C NMR spectra were recorded

with complete proton decoupling. FID files were processed using MestReNova software version 5.3.0-4399. Electrospray (ESI) mass spectrometric analyses were performed using a ThermoFinnigan LCQdeca mass spectrometer, and high resolution analyses were conducted using a ThermoFinnigan MAT900XL mass spectrometer with electron impact (EI) ionization. A Thermo Scientific LTQ Orbitrap XL mass spectrometer was used for high resolution electrospray ionization mass spectrometry analysis (HR-ESI-MS). Optical rotations were measured on a Perkin-Elmer polarimeter (Model 241) using a 1 mL quartz cell with a 10 cm path length. FTIR spectra were obtained on a Nicolet magna-550 series II spectrometer with samples prepared as thin films on either KBr or NaCl discs, and peaks are reported in wavenumbers (cm^{-1}).

Structure report for spirohexenolide A (128) (burk03)

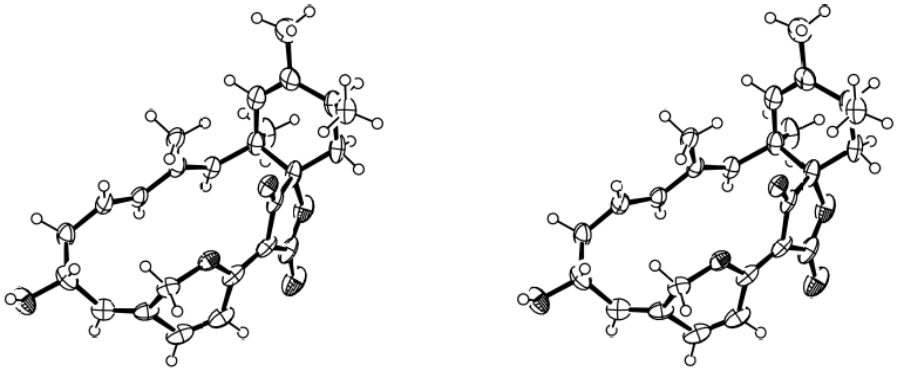

Figure 2.6 ORTEP stereopair drawing of the X-ray crystal structure of compound 128 with ellipsoids drawn at the 50% probability level

A yellow needle 0.25 x 0.10 x 0.10 mm in size was mounted on a Cryoloop with Paratone oil. Data were collected in a nitrogen gas stream at 100(2) K using phi

and omega scans. Crystal-to-detector distance was 50 mm and exposure time was 10 seconds per frame using a scan width of 0.5°. Data collection was 99.3% complete to 67.00° in θ. A total of 7195 reflections were collected covering the indices, -8<=*h*<=8, -15<=*k*<=14, -13<=*l*<=13. 3065 reflections were found to be symmetry independent, with an R_{int} of 0.0366. Indexing and unit cell refinement indicated a primitive, monoclinic lattice. The space group was found to be P2(1) (No. 4). The data were integrated using the Bruker SAINT software program and scaled using the SADABS software program. Solution by direct methods (SIR-2004) produced a complete heavy-atom phasing model consistent with the proposed structure. All non-hydrogen atoms were refined anisotropically by full-matrix least-squares (SHELXL-97). All hydrogen atoms were placed using a riding model. Their positions were constrained relative to their parent atom using the appropriate HFIX command in SHELXL-97.

Table 2.3 Crystal data and structure refinement for burk03.

X-ray ID	burk03	
Sample/notebook ID	ESMedin_cmpd1	
Empirical formula	C25 H28 O5	
Formula weight	408.47	
Temperature	100(2) K	
Wavelength	1.54178 Å	
Crystal system	Monoclinic	
Space group	P2(1)	
Unit cell dimensions	a = 7.0073(4) Å	α= 90°.
	b = 13.0187(9) Å	β= 105.946(4)°.
	c = 12.0229(7) Å	γ = 90°.

Table 2.3 Crystal data and structure refinement for burk03, continued

Volume	1054.60(11) $Å^3$
Z	2
Density (calculated)	1.286 Mg/m^3
Absorption coefficient	0.718 mm^{-1}
F(000)	436
Crystal size	0.25 x 0.10 x 0.10 mm^3
Crystal color/habit	yellow needle
Theta range for data collection	5.12 to 67.00°.
Index ranges	-8<=h<=8, -15<=k<=14, -13<=l<=13
Reflections collected	7195
Independent reflections	3065 [R(int) = 0.0366]
Completeness to theta = 67.00°	99.3 %
Absorption correction	Semi-empirical from equivalents
Max. and min. transmission	0.9317 and 0.8409
Refinement method	Full-matrix least-squares on F^2
Data / restraints / parameters	3065 / 1 / 276
Goodness-of-fit on F^2	1.048
Final R indices [I>2sigma(I)]	R1 = 0.0460, wR2 = 0.1062
R indices (all data)	R1 = 0.0570, wR2 = 0.1114
Absolute structure parameter	0.0(3)
Largest diff. peak and hole	0.248 and -0.171 $e.Å^{-3}$

Table 2.4 Atomic coordinates (x 10^4) and equivalent isotropic displacement parameters ($Å^2$x 10^3) for burk03. U(eq) is defined as one third of the trace of the orthogonalized U^{ij} tensor.

	x	y	z	U(eq)
C(1)	8990(4)	4153(3)	3792(3)	38(1)
C(2)	7680(5)	3370(3)	3022(3)	40(1)
C(3)	8162(5)	2424(3)	2767(3)	43(1)

Table 2.4 Atomic coordinates (x 10^4) and equivalent isotropic displacement parameters ($Å^2$x 10^3) for burk03. U(eq) is defined as one third of the trace of the orthogonalized U^{ij} tensor, continued.

	x	y	z	U(eq)
C(4)	10243(5)	2013(3)	3206(3)	44(1)
C(5)	11618(5)	2723(3)	4092(3)	47(1)
C(6)	11209(5)	3876(3)	3927(2)	39(1)
C(7)	8546(6)	4092(3)	4978(3)	54(1)
C(8)	6633(5)	1698(3)	2054(3)	54(1)
C(9)	11157(5)	1684(3)	2239(3)	47(1)
C(10)	8605(4)	5245(3)	3357(3)	33(1)
C(11)	7932(4)	5643(3)	2289(3)	32(1)
C(12)	7280(5)	5043(3)	1174(3)	39(1)
C(13)	7826(4)	6758(3)	2163(3)	34(1)
C(14)	7316(4)	7280(3)	1180(3)	39(1)
C(15)	7267(5)	8425(3)	1064(3)	42(1)
C(16)	8970(5)	8832(3)	611(3)	42(1)
C(17)	10857(5)	8798(3)	1589(3)	42(1)
C(18)	12153(4)	8032(3)	1844(3)	39(1)
C(19)	12228(4)	7109(3)	1115(2)	36(1)
C(20)	13624(5)	7981(3)	2971(3)	44(1)
C(21)	14163(4)	7083(3)	3454(3)	43(1)
C(22)	13250(4)	6161(3)	2895(2)	34(1)
C(23)	13064(4)	5274(3)	3468(2)	36(1)
C(24)	11885(4)	4391(3)	2962(2)	31(1)
C(25)	13514(5)	5180(3)	4719(3)	45(1)
O(1)	8581(4)	9867(2)	223(2)	50(1)
O(2)	12343(3)	6157(2)	1763(2)	35(1)
O(3)	12460(3)	4370(2)	4971(2)	47(1)
O(4)	11460(3)	4092(2)	1963(2)	34(1)
O(5)	14569(4)	5668(2)	5494(2)	59(1)

Table 2.5 Bond lengths [Å] and angles [°] for burk03.

C(1)-C(2)	1.508(5)	C(12)-H(12C)	0.9800
C(1)-C(10)	1.513(5)	C(13)-C(14)	1.325(4)
C(1)-C(7)	1.542(4)	C(13)-H(13)	0.9500
C(1)-C(6)	1.561(4)	C(14)-C(15)	1.496(5)
C(2)-C(3)	1.335(5)	C(14)-H(14)	0.9500
C(2)-H(2)	0.9500	C(15)-C(16)	1.536(5)
C(3)-C(4)	1.506(4)	C(15)-H(15A)	0.9900
C(3)-C(8)	1.507(5)	C(15)-H(15B)	0.9900
C(4)-C(5)	1.534(5)	C(16)-O(1)	1.427(4)
C(4)-C(9)	1.534(5)	C(16)-C(17)	1.509(4)
C(4)-H(4)	1.0000	C(16)-H(16)	1.0000
C(5)-C(6)	1.531(5)	C(17)-C(18)	1.327(5)
C(5)-H(5A)	0.9900	C(17)-H(17)	0.9500
C(5)-H(5B)	0.9900	C(18)-C(20)	1.461(4)
C(6)-O(3)	1.468(4)	C(18)-C(19)	1.496(5)
C(6)-C(24)	1.523(4)	C(19)-O(2)	1.454(4)
C(7)-H(7A)	0.9800	C(19)-H(19A)	0.9900
C(7)-H(7B)	0.9800	C(19)-H(19B)	0.9900
C(7)-H(7C)	0.9800	C(20)-C(21)	1.314(6)
C(8)-H(8A)	0.9800	C(20)-H(20)	0.9500
C(8)-H(8B)	0.9800	C(21)-C(22)	1.437(5)
C(8)-H(8C)	0.9800	C(21)-H(21)	0.9500
C(9)-H(9A)	0.9800	C(22)-O(2)	1.334(3)
C(9)-H(9B)	0.9800	C(22)-C(23)	1.369(5)
C(9)-H(9C)	0.9800	C(23)-C(24)	1.448(5)
C(10)-C(11)	1.345(4)	C(23)-C(25)	1.454(4)
C(10)-H(10)	0.9500	C(24)-O(4)	1.220(3)
C(11)-C(13)	1.459(4)	C(25)-O(5)	1.200(4)
C(11)-C(12)	1.510(5)	C(25)-O(3)	1.368(5)
C(12)-H(12A)	0.9800	O(1)-H(1)	0.8400
C(12)-H(12B)	0.9800		

C(2)-C(1)-C(10)	113.7(3)	C(10)-C(1)-C(7)	107.8(3)
C(2)-C(1)-C(7)	106.8(3)	C(2)-C(1)-C(6)	109.1(3)
C(10)-C(1)-C(6)	109.3(3)	H(8A)-C(8)-H(8C)	109.5
C(7)-C(1)-C(6)	109.9(2)	H(8B)-C(8)-H(8C)	109.5
C(3)-C(2)-C(1)	128.0(3)	C(4)-C(9)-H(9A)	109.5
C(3)-C(2)-H(2)	116.0	C(4)-C(9)-H(9B)	109.5
C(1)-C(2)-H(2)	116.0	H(9A)-C(9)-H(9B)	109.5
C(2)-C(3)-C(4)	121.9(3)	C(4)-C(9)-H(9C)	109.5
C(2)-C(3)-C(8)	121.6(3)	H(9A)-C(9)-H(9C)	109.5
C(4)-C(3)-C(8)	116.5(3)	H(9B)-C(9)-H(9C)	109.5
C(3)-C(4)-C(5)	113.1(3)	C(11)-C(10)-C(1)	132.4(3)

Table 2.5 Bond lengths [Å] and angles [°] for burk03, continued.

C(3)-C(4)-C(9)	113.5(3)	C(11)-C(10)-H(10)	113.8
C(5)-C(4)-C(9)	112.3(3)	C(1)-C(10)-H(10)	113.8
C(3)-C(4)-H(4)	105.7	C(10)-C(11)-C(13)	118.5(3)
C(5)-C(4)-H(4)	105.7	C(10)-C(11)-C(12)	126.1(3)
C(9)-C(4)-H(4)	105.7	C(13)-C(11)-C(12)	115.4(3)
C(4)-C(5)-C(6)	116.2(3)	C(11)-C(12)-H(12A)	109.5
C(4)-C(5)-H(5A)	108.2	C(11)-C(12)-H(12B)	109.5
C(6)-C(5)-H(5A)	108.2	H(12A)-C(12)-H(12B)	109.5
C(4)-C(5)-H(5B)	108.2	C(11)-C(12)-H(12C)	109.5
C(6)-C(5)-H(5B)	108.2	H(12A)-C(12)-H(12C)	109.5
H(5A)-C(5)-H(5B)	107.4	H(12B)-C(12)-H(12C)	109.5
O(3)-C(6)-C(24)	102.7(3)	C(14)-C(13)-C(11)	126.6(3)
O(3)-C(6)-C(5)	105.8(2)	C(14)-C(13)-H(13)	116.7
C(24)-C(6)-C(5)	116.4(3)	C(11)-C(13)-H(13)	116.7
O(3)-C(6)-C(1)	109.3(2)	C(13)-C(14)-C(15)	126.0(3)
C(24)-C(6)-C(1)	109.2(2)	C(13)-C(14)-H(14)	117.0
C(5)-C(6)-C(1)	112.7(3)	C(15)-C(14)-H(14)	117.0
C(1)-C(7)-H(7A)	109.5	C(14)-C(15)-C(16)	112.1(3)
C(1)-C(7)-H(7B)	109.5	C(14)-C(15)-H(15A)	109.2
H(7A)-C(7)-H(7B)	109.5	C(16)-C(15)-H(15A)	109.2
C(1)-C(7)-H(7C)	109.5	C(14)-C(15)-H(15B)	109.2
H(7A)-C(7)-H(7C)	109.5	C(16)-C(15)-H(15B)	109.2
H(7B)-C(7)-H(7C)	109.5	H(15A)-C(15)-H(15B)	107.9
C(3)-C(8)-H(8A)	109.5	O(1)-C(16)-C(17)	109.2(3)
C(3)-C(8)-H(8B)	109.5	O(1)-C(16)-C(15)	110.1(3)
H(8A)-C(8)-H(8B)	109.5	C(17)-C(16)-C(15)	108.3(3)
C(3)-C(8)-H(8C)	109.5	O(1)-C(16)-H(16)	109.7
C(17)-C(16)-H(16)	109.7	C(20)-C(21)-H(21)	120.0
C(15)-C(16)-H(16)	109.7	C(22)-C(21)-H(21)	120.0
C(18)-C(17)-C(16)	126.8(3)	O(2)-C(22)-C(23)	115.2(3)
C(18)-C(17)-H(17)	116.6	O(2)-C(22)-C(21)	120.4(3)
C(16)-C(17)-H(17)	116.6	C(23)-C(22)-C(21)	124.1(3)
C(17)-C(18)-C(20)	120.8(3)	C(22)-C(23)-C(24)	125.4(3)
C(17)-C(18)-C(19)	126.8(3)	C(22)-C(23)-C(25)	124.6(3)
C(20)-C(18)-C(19)	112.2(3)	C(24)-C(23)-C(25)	107.7(3)
O(2)-C(19)-C(18)	112.1(2)	O(4)-C(24)-C(23)	128.6(3)
O(2)-C(19)-H(19A)	109.2	O(4)-C(24)-C(6)	124.5(3)
C(18)-C(19)-H(19A)	109.2	C(23)-C(24)-C(6)	106.9(3)
O(2)-C(19)-H(19B)	109.2	O(5)-C(25)-O(3)	119.4(3)
C(18)-C(19)-H(19B)	109.2	O(5)-C(25)-C(23)	132.1(4)
H(19A)-C(19)-H(19B)	107.9	O(3)-C(25)-C(23)	108.5(3)
C(21)-C(20)-C(18)	119.6(3)	C(16)-O(1)-H(1)	109.5
C(21)-C(20)-H(20)	120.2	C(22)-O(2)-C(19)	118.9(3)
C(18)-C(20)-H(20)	120.2	C(25)-O(3)-C(6)	112.3(2)
C(20)-C(21)-C(22)	120.0(3)		

Table 2.6 Anisotropic displacement parameters ($Å^2 x\ 10^3$)for burk03. The anisotropic displacement factor exponent takes the form: $-2\pi^2[\ h^2 a^{*2} U^{11} + ... + 2\ h\ k\ a^*\ b^*\ U^{12}\ ]$

	U^{11}	U^{22}	U^{33}	U^{23}	U^{13}	U^{12}
C(1)	39(2)	44(2)	34(2)	12(2)	16(1)	12(2)
C(2)	36(2)	53(2)	36(2)	20(2)	18(1)	10(2)
C(3)	48(2)	46(2)	38(2)	16(2)	20(2)	0(2)
C(4)	55(2)	45(2)	33(2)	13(2)	13(1)	11(2)
C(5)	52(2)	55(2)	31(2)	15(2)	6(1)	25(2)
C(6)	41(2)	57(2)	19(1)	6(1)	6(1)	19(2)
C(7)	68(2)	59(3)	44(2)	22(2)	33(2)	27(2)
C(8)	53(2)	57(2)	54(2)	17(2)	21(2)	-2(2)
C(9)	51(2)	47(2)	43(2)	4(2)	13(2)	14(2)
C(10)	31(2)	45(2)	28(2)	10(2)	14(1)	7(1)
C(11)	21(1)	46(2)	31(2)	10(2)	9(1)	5(1)
C(12)	32(2)	46(2)	34(2)	10(2)	2(1)	4(2)
C(13)	24(1)	44(2)	36(2)	12(2)	11(1)	4(1)
C(14)	29(2)	50(2)	36(2)	12(2)	7(1)	5(2)
C(15)	42(2)	47(2)	35(2)	15(2)	10(1)	9(2)
C(16)	66(2)	35(2)	26(2)	3(2)	14(2)	-1(2)
C(17)	46(2)	48(2)	34(2)	-7(2)	17(1)	-7(2)
C(18)	31(2)	49(2)	42(2)	-10(2)	19(1)	-10(2)
C(19)	36(2)	45(2)	28(1)	-5(2)	9(1)	-5(2)
C(20)	35(2)	61(3)	38(2)	-22(2)	13(1)	-10(2)
C(21)	30(2)	66(3)	33(2)	-19(2)	8(1)	-4(2)
C(22)	22(1)	55(2)	26(2)	-13(2)	6(1)	2(2)
C(23)	22(1)	59(2)	24(1)	-10(2)	2(1)	7(2)
C(24)	24(1)	51(2)	17(1)	3(1)	2(1)	12(1)
C(25)	35(2)	70(3)	24(2)	-8(2)	-2(1)	16(2)
O(1)	81(2)	44(2)	28(1)	7(1)	18(1)	0(1)
O(2)	30(1)	47(1)	26(1)	-6(1)	5(1)	-3(1)
O(3)	51(1)	67(2)	19(1)	1(1)	1(1)	17(1)
O(4)	32(1)	47(1)	22(1)	-1(1)	5(1)	4(1)

Table 2.6 Anisotropic displacement parameters ($Å^2 x\ 10^3$)for burk03. The anisotropic displacement factor exponent takes the form: $-2\pi^2[\ h^2 a^{*2} U^{11} + ... + 2\ h\ k\ a^*\ b^*\ U^{12}\ ]$, continued.

	U^{11}	U^{22}	U^{33}	U^{23}	U^{13}	U^{12}
O(5)	52(1)	87(2)	29(1)	-18(1)	-6(1)	11(1)

Table 2.7 Hydrogen coordinates ($x\ 10^4$) and isotropic displacement parameters ($Å^2 x\ 10^3$) for burk03.

	x	y	z	U(eq)
H(2)	6348	3575	2676	47
H(4)	10126	1369	3637	53
H(5A)	13001	2594	4071	56
H(5B)	11527	2530	4872	56
H(7A)	8861	3402	5301	80
H(7B)	7138	4238	4882	80
H(7C)	9358	4599	5504	80
H(8A)	5347	2048	1805	80
H(8B)	6518	1096	2521	80
H(8C)	7039	1479	1374	80
H(9A)	11358	2291	1802	70
H(9B)	10261	1204	1719	70
H(9C)	12436	1348	2579	70
H(10)	8894	5746	3954	40
H(12A)	7573	4313	1332	59
H(12B)	7993	5293	632	59
H(12C)	5849	5133	834	59
H(13)	8157	7149	2857	41

Table 2.7 Hydrogen coordinates (x 10^4) and isotropic displacement parameters ($Å^2$x 10^3) for burk03, continued.

	x	y	z	U(eq)
H(14)	6947	6892	485	47
H(15A)	7358	8737	1828	50
H(15B)	5984	8635	528	50
H(16)	9116	8391	-42	51
H(17)	11148	9388	2071	50
H(19A)	11027	7097	449	43
H(19B)	13399	7162	809	43
H(20)	14187	8593	3353	53
H(21)	15156	7042	4173	52
H(1)	8377	9890	-498	75

Structure report for spirohexenolide B (129) (burk08)

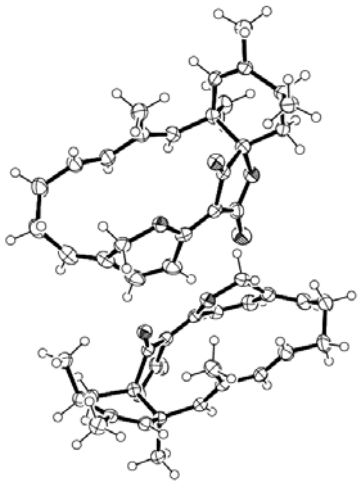

Figure 2.7 ORTEP drawing of the X-ray crystal structure of compound **129** with ellipsoids drawn at the 50% probability level

Table 2.8 Crystal data and structure refinement for burk08.

Identification code	burk08	
Empirical formula	C25 H28 O4	
Formula weight	392.47	
Temperature	100(2) K	
Wavelength	1.54178 Å	
Crystal system	Monoclinic	
Space group	P2(1)	
Unit cell dimensions	a = 6.9077(3) Å	⟨= 90°
	b = 13.0543(6) Å	®= 93.289(3)°
	c = 23.0708(10) Å	© = 90°
Volume	2076.99(16) $Å^3$	
Z	4	
Density (calculated)	1.255 g/cm^3	
Absorption coefficient	0.671 mm^{-1}	
F(000)	840	
Crystal size	0.37 x 0.34 x 0.14 mm^3	
Crystal color, habit	Pale yellow plate	
Theta range for data collection	5.12 to 68.37°	
Index ranges	-7<=h<=8, -15<=k<=15, -27<=l<=27	
Reflections collected	12003	
Independent reflections	6245 [R(int) = 0.0346]	
Completeness to theta = 55.00°	97.7 %	
Absorption correction	Multi-scan	
Max. and min. transmission	0.9120 and 0.7895	
Refinement method	Full-matrix least-squares on F^2	
Data / restraints / parameters	6245 / 1 / 523	
Goodness-of-fit on F^2	1.011	
Final R indices [I>2sigma(I)]	R1 = 0.0398, wR2 = 0.0970	
R indices (all data)	R1 = 0.0493, wR2 = 0.1039	
Absolute structure parameter	0.12(16)	
Largest diff. peak and hole	0.175 and -0.171 e $Å^{-3}$	

Table 2.9 Atomic coordinates (x 10^4) and equivalent isotropic displacement parameters ($Å^2$x 10^3)for burk08. U(eq) is defined as one third of the trace of the orthogonalized U^{ij} tensor.

	x	y	z	U(eq)
O(1')	447(3)	2307(1)	841(1)	28(1)
O(1)	4626(3)	7013(1)	4048(1)	30(1)
O(2')	2334(3)	1184(1)	1325(1)	37(1)
O(2)	2742(3)	6013(1)	3478(1)	45(1)
O(3')	1417(3)	4729(1)	1463(1)	28(1)
O(3)	3575(2)	9556(1)	3649(1)	29(1)
O(4)	2532(2)	8890(1)	2511(1)	28(1)
O(4')	2350(3)	3748(1)	2539(1)	28(1)
C(1')	230(4)	3786(2)	242(1)	27(1)
C(2')	-506(4)	4877(2)	114(1)	27(1)
C(3')	-2293(4)	5127(2)	426(1)	28(1)
C(4')	-3035(3)	4520(2)	822(1)	28(1)
C(5')	-2264(4)	3483(2)	1014(1)	25(1)
C(6')	-2397(3)	3260(2)	1661(1)	27(1)
C(7')	-2408(4)	3874(2)	2125(1)	28(1)
C(8')	-2457(4)	3380(2)	2701(1)	33(1)
C(9')	-2349(4)	3852(3)	3212(1)	39(1)
C(10')	-2390(4)	3326(3)	3791(1)	46(1)
C(11')	-362(4)	3318(3)	4120(1)	44(1)
C(12')	885(4)	2543(2)	3853(1)	39(1)
C(13')	2026(4)	2701(2)	3409(1)	33(1)
C(14')	2799(4)	1839(2)	3094(1)	34(1)
C(15')	3130(4)	1954(2)	2535(1)	31(1)
C(16')	2597(3)	2895(2)	2236(1)	26(1)
C(17')	2562(4)	3710(2)	3169(1)	30(1)
C(18')	2091(3)	2946(2)	1655(1)	25(1)
C(19')	1721(4)	2053(2)	1291(1)	28(1)
C(20')	1215(3)	3821(2)	1352(1)	23(1)

Table 2.9 Atomic coordinates (x 10^4) and equivalent isotropic displacement parameters ($Å^2$x 10^3)for burk08. U(eq) is defined as one third of the trace of the orthogonalized U^{ij} tensor, continued.

	x	y	z	U(eq)
C(21')	-110(4)	3389(2)	853(1)	24(1)
C(22')	1105(4)	5677(2)	211(1)	32(1)
C(23')	-3284(4)	6119(2)	252(1)	36(1)
C(24')	-3522(4)	2670(2)	683(1)	31(1)
C(25')	-2335(4)	5034(2)	2126(1)	37(1)
C(1)	4851(4)	8331(2)	4757(1)	27(1)
C(2)	5579(4)	9381(2)	4974(1)	29(1)
C(3)	7381(4)	9712(2)	4686(1)	27(1)
C(4)	8104(4)	9213(2)	4245(1)	27(1)
C(5)	7314(4)	8244(2)	3963(1)	27(1)
C(6)	7413(4)	8228(2)	3304(1)	29(1)
C(7)	7372(3)	8976(2)	2905(1)	29(1)
C(8)	7371(4)	8684(2)	2291(1)	35(1)
C(9)	7181(4)	9322(3)	1837(1)	39(1)
C(10)	7177(4)	9013(3)	1210(1)	46(1)
C(11)	5129(4)	9057(2)	901(1)	40(1)
C(12)	3961(5)	8173(2)	1093(1)	43(1)
C(13)	2858(4)	8141(2)	1549(1)	34(1)
C(14)	2165(4)	7177(2)	1782(1)	42(1)
C(15)	1877(4)	7102(2)	2346(1)	39(1)
C(16)	2372(4)	7954(2)	2729(1)	28(1)
C(17)	2276(4)	9046(2)	1892(1)	31(1)
C(18)	2928(4)	7841(2)	3305(1)	27(1)
C(19)	3338(4)	6860(2)	3585(1)	32(1)
C(20)	3800(3)	8632(2)	3675(1)	23(1)
C(21)	5159(4)	8089(2)	4122(1)	27(1)
C(22)	3978(4)	10203(2)	4947(1)	35(1)

Table 2.9 Atomic coordinates (x 10^4) and equivalent isotropic displacement parameters ($Å^2$x 10^3)for burk08. U(eq) is defined as one third of the trace of the orthogonalized U^{ij} tensor, continued.

	x	y	z	U(eq)
C(23)	8343(4)	10664(2)	4927(1)	35(1)
C(24)	8571(4)	7343(2)	4211(1)	34(1)
C(25)	7311(4)	10107(2)	3031(1)	35(1)

Table 2.10 Bond lengths [Å] and angles [°] for burk08.

O(1')-C(19')	1.363(3)
O(1')-C(21')	1.465(3)
O(1)-C(19)	1.365(3)
O(1)-C(21)	1.460(3)
O(2')-C(19')	1.211(3)
O(2)-C(19)	1.201(3)
O(3')-C(20')	1.219(3)
O(3)-C(20)	1.217(3)
O(4)-C(16)	1.329(3)
O(4)-C(17)	1.444(3)
O(4')-C(16')	1.330(3)
O(4')-C(17')	1.453(3)
C(1')-C(21')	1.533(3)
C(1')-C(2')	1.535(3)
C(2')-C(3')	1.500(3)
C(2')-C(22')	1.534(3)
C(3')-C(4')	1.333(3)
C(3')-C(23')	1.508(3)
C(4')-C(5')	1.512(3)

Table 2.10 Bond lengths [Å] and angles [°] for burk08, continued.

C(5')-C(6')	1.530(3)
C(5')-C(24')	1.545(3)
C(5')-C(21')	1.558(3)
C(6')-C(7')	1.337(3)
C(7')-C(8')	1.480(3)
C(7')-C(25')	1.515(4)
C(8')-C(9')	1.329(4)
C(9')-C(10')	1.502(4)
C(10')-C(11')	1.554(4)
C(11')-C(12')	1.485(4)
C(12')-C(13')	1.343(4)
C(13')-C(14')	1.457(4)
C(13')-C(17')	1.485(4)
C(14')-C(15')	1.330(4)
C(15')-C(16')	1.447(3)
C(16')-C(18')	1.369(3)
C(18')-C(19')	1.450(3)
C(18')-C(20')	1.452(3)
C(20')-C(21')	1.536(3)
C(1)-C(21)	1.526(3)
C(1)-C(2)	1.535(3)
C(2)-C(3)	1.508(3)
C(2)-C(22)	1.540(3)
C(3)-C(4)	1.329(3)
C(3)-C(23)	1.500(3)
C(4)-C(5)	1.510(3)
C(5)-C(6)	1.525(3)
C(5)-C(24)	1.551(3)
C(5)-C(21)	1.567(3)
C(6)-C(7)	1.341(4)
C(7)-C(8)	1.468(3)
C(7)-C(25)	1.505(4)
C(8)-C(9)	1.339(4)
C(9)-C(10)	1.502(4)

Table 2.10 Bond lengths [Å] and angles [°] for burk08, continued.

C(10)-C(11)	1.548(4)
C(11)-C(12)	1.489(4)
C(12)-C(13)	1.336(4)
C(13)-C(14)	1.460(4)
C(13)-C(17)	1.490(4)
C(14)-C(15)	1.331(4)
C(15)-C(16)	1.449(4)
C(16)-C(18)	1.369(3)
C(18)-C(20)	1.449(3)
C(18)-C(19)	1.455(3)
C(20)-C(21)	1.527(3)

C(19')-O(1')-C(21')	112.29(18)
C(19)-O(1)-C(21)	112.34(18)
C(16)-O(4)-C(17)	119.78(19)
C(16')-O(4')-C(17')	119.12(18)
C(21')-C(1')-C(2')	115.04(19)
C(3')-C(2')-C(22')	113.1(2)
C(3')-C(2')-C(1')	112.5(2)
C(22')-C(2')-C(1')	112.0(2)
C(4')-C(3')-C(2')	123.9(2)
C(4')-C(3')-C(23')	120.4(2)
C(2')-C(3')-C(23')	115.7(2)
C(3')-C(4')-C(5')	126.2(2)
C(4')-C(5')-C(6')	114.6(2)
C(4')-C(5')-C(24')	106.9(2)
C(6')-C(5')-C(24')	106.75(19)
C(4')-C(5')-C(21')	109.02(19)
C(6')-C(5')-C(21')	109.20(19)
C(24')-C(5')-C(21')	110.29(19)
C(7')-C(6')-C(5')	132.1(2)
C(6')-C(7')-C(8')	117.3(2)
C(6')-C(7')-C(25')	126.7(2)
C(8')-C(7')-C(25')	115.9(2)

Table 2.10 Bond lengths [Å] and angles [°] for burk08, continued.

C(9')-C(8')-C(7')	126.3(3)
C(8')-C(9')-C(10')	125.0(3)
C(9')-C(10')-C(11')	112.0(3)
C(12')-C(11')-C(10')	109.3(2)
C(13')-C(12')-C(11')	126.2(3)
C(12')-C(13')-C(14')	120.7(3)
C(12')-C(13')-C(17')	126.2(3)
C(14')-C(13')-C(17')	113.0(2)
C(15')-C(14')-C(13')	119.1(2)
C(14')-C(15')-C(16')	120.3(2)
O(4')-C(16')-C(18')	116.1(2)
O(4')-C(16')-C(15')	119.9(2)
C(18')-C(16')-C(15')	123.5(2)
O(4')-C(17')-C(13')	113.1(2)
C(16')-C(18')-C(19')	123.7(2)
C(16')-C(18')-C(20')	125.8(2)
C(19')-C(18')-C(20')	107.4(2)
O(2')-C(19')-O(1')	119.0(2)
O(2')-C(19')-C(18')	131.8(2)
O(1')-C(19')-C(18')	109.2(2)
O(3')-C(20')-C(18')	128.7(2)
O(3')-C(20')-C(21')	124.7(2)
C(18')-C(20')-C(21')	106.61(19)
O(1')-C(21')-C(1')	104.72(18)
O(1')-C(21')-C(20')	102.81(18)
C(1')-C(21')-C(20')	116.7(2)
O(1')-C(21')-C(5')	109.58(18)
C(1')-C(21')-C(5')	113.01(19)
C(20')-C(21')-C(5')	109.23(17)
C(21)-C(1)-C(2)	115.9(2)
C(3)-C(2)-C(1)	112.1(2)
C(3)-C(2)-C(22)	113.1(2)
C(1)-C(2)-C(22)	112.9(2)
C(4)-C(3)-C(23)	120.8(2)

Table 2.10 Bond lengths [Å] and angles [°] for burk08, continued.

C(4)-C(3)-C(2)	123.6(2)
C(23)-C(3)-C(2)	115.7(2)
C(3)-C(4)-C(5)	126.8(2)
C(4)-C(5)-C(6)	114.0(2)
C(4)-C(5)-C(24)	107.1(2)
C(6)-C(5)-C(24)	107.53(19)
C(4)-C(5)-C(21)	109.38(19)
C(6)-C(5)-C(21)	109.17(19)
C(24)-C(5)-C(21)	109.6(2)
C(7)-C(6)-C(5)	132.3(2)
C(6)-C(7)-C(8)	118.1(2)
C(6)-C(7)-C(25)	125.6(2)
C(8)-C(7)-C(25)	116.3(2)
C(9)-C(8)-C(7)	126.0(3)
C(8)-C(9)-C(10)	125.5(3)
C(9)-C(10)-C(11)	112.6(2)
C(12)-C(11)-C(10)	109.3(2)
C(13)-C(12)-C(11)	127.0(3)
C(12)-C(13)-C(14)	122.1(3)
C(12)-C(13)-C(17)	125.2(3)
C(14)-C(13)-C(17)	112.6(2)
C(15)-C(14)-C(13)	119.6(3)
C(14)-C(15)-C(16)	119.8(3)
O(4)-C(16)-C(18)	116.2(2)
O(4)-C(16)-C(15)	119.8(2)
C(18)-C(16)-C(15)	123.6(2)
O(4)-C(17)-C(13)	113.1(2)
C(16)-C(18)-C(20)	125.4(2)
C(16)-C(18)-C(19)	124.2(2)
C(20)-C(18)-C(19)	107.5(2)
O(2)-C(19)-O(1)	119.8(2)
O(2)-C(19)-C(18)	131.5(2)
O(1)-C(19)-C(18)	108.7(2)
O(3)-C(20)-C(18)	129.0(2)

Table 2.10 Bond lengths [Å] and angles [°] for burk08, continued.

O(3)-C(20)-C(21)	124.4(2)
C(18)-C(20)-C(21)	106.58(19)
O(1)-C(21)-C(1)	105.19(19)
O(1)-C(21)-C(20)	103.15(19)
C(1)-C(21)-C(20)	115.9(2)
O(1)-C(21)-C(5)	109.48(19)
C(1)-C(21)-C(5)	112.6(2)
C(20)-C(21)-C(5)	109.76(18)

Table 2.11 Anisotropic displacement parameters ($Å^2 x\ 10^3$) for burk08. The anisotropic displacement factor exponent takes the form: $-2\pi^2[h^2 a^{*2} U^{11} + ... + 2 h k a^* b^* U^{12}]$

	U^{11}	U^{22}	U^{33}	U^{23}	U^{13}	U^{12}
O(1')	35(1)	21(1)	28(1)	-2(1)	2(1)	3(1)
O(1)	41(1)	21(1)	29(1)	4(1)	-1(1)	-2(1)
O(2')	53(1)	25(1)	34(1)	-1(1)	3(1)	11(1)
O(2)	68(2)	24(1)	43(1)	2(1)	-6(1)	-13(1)
O(3')	31(1)	24(1)	30(1)	2(1)	-1(1)	-3(1)
O(3)	32(1)	23(1)	32(1)	-1(1)	2(1)	2(1)
O(4)	29(1)	25(1)	28(1)	2(1)	-1(1)	0(1)
O(4')	32(1)	24(1)	28(1)	1(1)	-2(1)	2(1)
C(1')	25(1)	30(1)	25(1)	1(1)	5(1)	3(1)
C(2')	28(1)	28(1)	26(1)	4(1)	0(1)	3(1)
C(3')	26(1)	30(1)	27(1)	0(1)	-2(1)	3(1)
C(4')	22(1)	33(1)	28(1)	-5(1)	1(1)	3(1)
C(5')	25(1)	26(1)	25(1)	-2(1)	1(1)	-3(1)
C(6')	23(1)	30(1)	28(1)	0(1)	3(1)	-3(1)
C(7')	22(1)	34(1)	29(1)	-1(1)	3(1)	-1(1)
C(8')	20(1)	48(2)	31(1)	-1(1)	5(1)	0(1)

Table 2.11 Anisotropic displacement parameters ($Å^2 x\ 10^3$) for burk08. The anisotropic displacement factor exponent takes the form: $-2\pi^2[h^2 a^{*2} U^{11} + ... + 2 h k a^* b^* U^{12}]$, continued.

	U^{11}	U^{22}	U^{33}	U^{23}	U^{13}	U^{12}
C(9')	29(2)	58(2)	30(1)	-5(1)	3(1)	3(1)
C(10')	34(2)	80(2)	25(1)	-1(1)	6(1)	4(2)
C(11')	38(2)	68(2)	28(1)	-1(1)	2(1)	1(1)
C(12')	41(2)	45(2)	31(1)	8(1)	-3(1)	-2(1)
C(13')	29(1)	38(2)	32(1)	6(1)	-6(1)	0(1)
C(14')	37(2)	28(1)	38(1)	6(1)	-4(1)	2(1)
C(15')	33(1)	26(1)	35(1)	1(1)	-3(1)	5(1)
C(16')	19(1)	26(1)	33(1)	1(1)	4(1)	1(1)
C(17')	29(1)	32(1)	30(1)	-5(1)	-2(1)	0(1)
C(18')	23(1)	24(1)	30(1)	1(1)	4(1)	2(1)
C(19')	32(1)	26(1)	26(1)	0(1)	8(1)	4(1)
C(20')	23(1)	22(1)	26(1)	1(1)	3(1)	1(1)
C(21')	28(1)	19(1)	26(1)	0(1)	2(1)	1(1)
C(22')	32(2)	31(1)	33(1)	7(1)	1(1)	-2(1)
C(23')	34(2)	34(2)	41(1)	5(1)	2(1)	8(1)
C(24')	31(1)	34(1)	28(1)	-2(1)	3(1)	-9(1)
C(25')	43(2)	36(2)	31(1)	-7(1)	1(1)	1(1)
C(1)	26(1)	30(1)	25(1)	2(1)	3(1)	-1(1)
C(2)	26(1)	34(1)	26(1)	-5(1)	1(1)	-2(1)
C(3)	26(1)	30(1)	26(1)	1(1)	-2(1)	0(1)
C(4)	23(1)	33(1)	26(1)	6(1)	1(1)	-3(1)
C(5)	25(1)	30(1)	26(1)	3(1)	1(1)	6(1)
C(6)	27(1)	30(1)	29(1)	-4(1)	2(1)	4(1)
C(7)	20(1)	39(2)	28(1)	3(1)	1(1)	2(1)
C(8)	23(2)	49(2)	33(1)	1(1)	5(1)	3(1)
C(9)	30(2)	60(2)	28(1)	3(1)	0(1)	0(1)
C(10)	32(2)	75(2)	31(1)	4(1)	5(1)	5(1)

Table 2.11 Anisotropic displacement parameters ($Å^2 x\ 10^3$) for burk08. The anisotropic displacement factor exponent takes the form: $-2\pi^2[h^2 a^{*2} U^{11} + ... + 2 h k a^* b^* U^{12}]$, continued.

	U^{11}	U^{22}	U^{33}	U^{23}	U^{13}	U^{12}
C(11)	38(2)	58(2)	25(1)	2(1)	0(1)	8(1)
C(12)	52(2)	44(2)	32(1)	-6(1)	-6(1)	8(1)
C(13)	38(2)	34(1)	30(1)	-3(1)	-6(1)	3(1)
C(14)	54(2)	34(2)	37(1)	-10(1)	-10(1)	-5(1)
C(15)	49(2)	27(1)	40(1)	-1(1)	-8(1)	-10(1)
C(16)	24(1)	25(1)	35(1)	-1(1)	0(1)	-4(1)
C(17)	26(1)	33(1)	32(1)	3(1)	-1(1)	2(1)
C(18)	25(1)	24(1)	31(1)	1(1)	5(1)	-4(1)
C(19)	39(2)	29(1)	26(1)	2(1)	3(1)	-3(1)
C(20)	22(1)	23(1)	26(1)	2(1)	4(1)	0(1)
C(21)	31(2)	21(1)	29(1)	1(1)	1(1)	-1(1)
C(22)	29(2)	36(2)	39(1)	-10(1)	5(1)	1(1)
C(23)	32(2)	38(2)	34(1)	-5(1)	2(1)	-7(1)
C(24)	34(2)	36(2)	32(1)	7(1)	2(1)	10(1)
C(25)	37(2)	35(1)	33(1)	8(1)	0(1)	-2(1)

Table 2.12 Hydrogen coordinates ($x\ 10^4$) and isotropic displacement parameters ($Å^2 x\ 10^3$) for burk08.

	x	y	z	U(eq)
H(1'A)	-415	3314	-45	32
H(1'B)	1638	3765	184	32
H(2'A)	-899	4896	-310	33
H(4'A)	-4155	4761	999	33

Table 2.12 Hydrogen coordinates (x 10^4) and isotropic displacement parameters ($Å^2$ x 10^3) for burk08, continued.

	x	y	z	U(eq)
H(6'A)	-2490	2552	1750	32
H(8'A)	-2578	2655	2706	39
H(9'A)	-2238	4577	3212	47
H(10C)	-2841	2612	3731	56
H(10D)	-3326	3680	4031	56
H(11C)	241	4004	4098	53
H(11D)	-499	3150	4534	53
H(12B)	875	1871	4011	47
H(14B)	3062	1205	3284	41
H(15B)	3719	1415	2332	37
H(17C)	1735	4246	3330	36
H(17D)	3925	3864	3294	36
H(22D)	580	6361	125	48
H(22E)	2153	5530	-45	48
H(22F)	1613	5652	617	48
H(23D)	-4425	6214	480	55
H(23E)	-3688	6096	-162	55
H(23F)	-2383	6690	326	55
H(24D)	-4872	2738	787	47
H(24E)	-3044	1984	788	47
H(24F)	-3449	2774	264	47
H(25D)	-2309	5283	1726	55
H(25E)	-1165	5264	2349	55
H(25F)	-3484	5304	2303	55
H(1A)	5509	7796	5000	33
H(1B)	3446	8284	4817	33
H(2A)	5972	9291	5395	34
H(4A)	9236	9494	4092	33
H(6A)	7523	7560	3146	34

Table 2.12 Hydrogen coordinates (x 10^4) and isotropic displacement parameters ($Å^2$ x 10^3) for burk08, continued.

	x	y	z	U(eq)
H(8A)	7520	7976	2208	42
H(9A)	7036	10030	1918	47
H(10A)	7689	8307	1184	55
H(10B)	8053	9473	1006	55
H(11A)	4484	9707	997	48
H(11B)	5233	9030	475	48
H(12A)	4006	7567	866	51
H(14A)	1921	6607	1533	51
H(15A)	1349	6492	2497	47
H(17A)	3056	9645	1783	37
H(17B)	897	9204	1790	37
H(22A)	4520	10857	5088	52
H(22B)	2931	9993	5190	52
H(22C)	3464	10283	4545	52
H(23A)	9495	10813	4713	52
H(23B)	8725	10560	5338	52
H(23C)	7436	11240	4886	52
H(24A)	9919	7442	4112	51
H(24B)	8081	6697	4043	51
H(24C)	8507	7321	4634	51
H(25A)	7318	10215	3451	53
H(25B)	6128	10402	2845	53
H(25C)	8448	10439	2878	53

δ-lactone acid 148

Crystals of the ester-lactone **149** (176 mg, 1.04 mmol) were weighed into a scintillation vial, and a solution of NaOH (3.48 mL of a 0.3N aqueous solution, 1.04 mmol) was added via syringe, with stirring. The crystals immediately dissolved, and the solution was stirred for 10 min room temperature. After this period of time, a solution of NaOH (348 μL of a 3N aqueous solution, 1.04 mmol) was added dropwise over 10 min. and the orange solution stirred for an additional 20 min with the second equivalent. After this period of time, the solution was acidified with 2N HCl solution (until acidic by pH paper), which caused the precipitation of the δ-lactone acid **148** (63 mg, 39%) from the solution. The solid was collected by vacuum filtration, and it was washed with 3 mL of deionized H_2O. Diffraction quality crystals were obtained by perfusion of hexanes into an ethyl acetate solution of **148**. ^{1}H NMR (DMSO-*d*6, 300 MHz) δ 7.33 (d, *J* = 9.7 Hz, 1H), 6.18 (d, *J* = 9.7 Hz, 1H), 6.15 (s, 1H), 5.58 (d, *J* = 2.2 Hz, 1H); ^{13}C NMR (DMSO-*d*6, 75 MHz) δ 173.0, 166.7, 161.8, 143.4, 142.3, 122.4, 68.3.

Structure report for compound 148 (burk04)

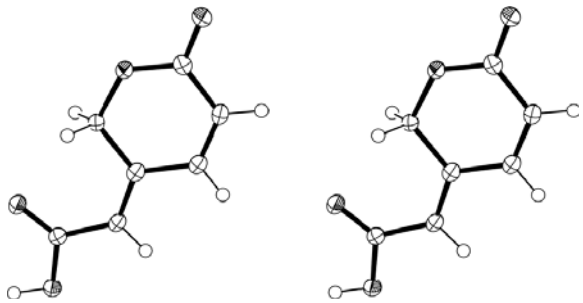

Figure 2.8 ORTEP stereopair drawing of the X-ray crystal structure of compound **148** with ellipsoids drawn at the 50% probability level

A colorless plate 0.10 x 0.10 x 0.02 mm in size was mounted on a Cryoloop with Paratone oil. Data were collected in a nitrogen gas stream at 100(2) K using phi and omega scans. Crystal-to-detector distance was 60 mm and exposure time was 10 seconds per frame using a scan width of 0.5°. Data collection was 97.8% complete to 67.00° in θ. A total of 2132 reflections were collected covering the indices, -12<=*h*<=11, -7<=*k*<=7, -11<=*l*<=11. 620 reflections were found to be symmetry independent, with an R_{int} of 0.0134. Indexing and unit cell refinement indicated a primitive, orthorhombic lattice. The space group was found to be Pnma (No. 62). The data were integrated using the Bruker SAINT software program and scaled using the SADABS software program. Solution by direct methods (SHELXS-97) produced a complete heavy-atom phasing model consistent with the proposed structure. All non-hydrogen atoms were refined anisotropically by full-matrix least-squares (SHELXL-97). All hydrogen atoms were placed using a riding model. Their positions were constrained relative to their parent atom using the appropriate HFIX command in SHELXL-97.

Table 2.13 Crystal data and structure refinement for burk04.

X-ray ID	burk04
Sample/notebook ID	BDJ4-46-1
Empirical formula	C7 H6 O4
Formula weight	154.12
Temperature	100(2) K
Wavelength	1.54178 Å
Crystal system	Orthorhombic
Space group	Pnma

Table 2.13 Crystal data and structure refinement for burk04, continued.

Unit cell dimensions	a = 10.5795(6) Å	α= 90°.
	b = 6.3810(4) Å	β= 90°.
	c = 9.6077(5) Å	γ = 90°.
Volume	648.59(6) $Å^3$	
Z	4	
Density (calculated)	1.578 Mg/m^3	
Absorption coefficient	1.140 mm^{-1}	
F(000)	320	
Crystal size	0.10 x 0.10 x 0.02 mm^3	
Crystal color/habit	colorless plate	
Theta range for data collection	6.22 to 68.46°.	
Index ranges	-12<=h<=11, -7<=k<=7, -11<=l<=11	
Reflections collected	2132	
Independent reflections	620 [R(int) = 0.0134]	
Completeness to theta = 67.00°	97.8 %	
Absorption correction	Semi-empirical from equivalents	
Max. and min. transmission	0.9776 and 0.8945	
Refinement method	Full-matrix least-squares on F^2	
Data / restraints / parameters	620 / 0 / 70	
Goodness-of-fit on F^2	1.075	
Final R indices [I>2sigma(I)]	R1 = 0.0307, wR2 = 0.0842	
R indices (all data)	R1 = 0.0340, wR2 = 0.0868	
Extinction coefficient	0.0012(4)	
Largest diff. peak and hole	0.289 and -0.209 $e.Å^{-3}$	

Table 2.14 Atomic coordinates (x 10^4) and equivalent isotropic displacement parameters ($Å^2$x 10^3) for burk04. U(eq) is defined as one third of the trace of the orthogonalized U^{ij} tensor.

	x	y	z	U(eq)
C(1)	2885(2)	2500	2898(2)	18(1)
C(2)	4224(2)	2500	3271(2)	20(1)
C(3)	4595(2)	2500	4597(2)	19(1)
C(4)	3694(2)	2500	5735(2)	18(1)
C(5)	2311(2)	2500	5375(2)	18(1)
C(6)	4144(2)	2500	7047(2)	18(1)
C(7)	3347(2)	2500	8298(2)	18(1)
O(1)	2014(1)	2500	3895(1)	20(1)
O(2)	2511(1)	2500	1696(1)	22(1)
O(3)	2202(1)	2500	8293(1)	24(1)
O(4)	4035(1)	2500	9460(1)	22(1)

Table 2.15 Bond lengths [Å] and angles [°] for burk04.

C(1)-O(2)	1.221(2)	C(3)-C(2)-H(2)	119.3
C(1)-O(1)	1.329(2)	C(1)-C(2)-H(2)	119.3
C(1)-C(2)	1.461(3)	C(2)-C(3)-C(4)	121.76(17)
C(2)-C(3)	1.333(3)	C(2)-C(3)-H(3)	119.1
C(2)-H(2)	0.9500	C(4)-C(3)-H(3)	119.1
C(3)-C(4)	1.450(3)	C(6)-C(4)-C(3)	118.23(17)
C(3)-H(3)	0.9500	C(6)-C(4)-C(5)	123.96(17)
C(4)-C(6)	1.348(3)	C(3)-C(4)-C(5)	117.82(16)
C(4)-C(5)	1.504(2)	O(1)-C(5)-C(4)	115.73(15)
C(5)-O(1)	1.456(2)	O(1)-C(5)-H(5A)	108.3
C(5)-H(5A)	0.9900	C(4)-C(5)-H(5A)	108.3
C(5)-H(5B)	0.9900	O(1)-C(5)-H(5B)	108.3
C(6)-C(7)	1.468(3)	C(4)-C(5)-H(5B)	108.3
C(6)-H(6)	0.9500	H(5A)-C(5)-H(5B)	107.4
C(7)-O(3)	1.212(2)	C(4)-C(6)-C(7)	124.27(17)
C(7)-O(4)	1.332(2)	C(4)-C(6)-H(6)	117.9
O(4)-H(4)	0.94(3)	C(7)-C(6)-H(6)	117.9

Table 2.15 Bond lengths [Å] and angles [°] for burk04, continued.

		O(3)-C(7)-O(4)	123.32(16)
O(2)-C(1)-O(1)	117.27(17)	O(3)-C(7)-C(6)	124.83(16)
O(2)-C(1)-C(2)	123.06(18)	O(4)-C(7)-C(6)	111.85(16)
O(1)-C(1)-C(2)	119.67(17)	C(1)-O(1)-C(5)	123.67(14)
C(3)-C(2)-C(1)	121.34(17)	C(7)-O(4)-H(4)	107.1(16)

Symmetry transformations used to generate equivalent atoms:

Table 2.16 Anisotropic displacement parameters ($Å^2 x\ 10^3$)for burk04. The anisotropic displacement factor exponent takes the form: $-2\pi^2[\ h^2 a^{*2} U^{11} + ... + 2\ h\ k\ a^*\ b^*\ U^{12}\ ]$

	U^{11}	U^{22}	U^{33}	U^{23}	U^{13}	U^{12}
C(1)	22(1)	14(1)	19(1)	0	2(1)	0
C(2)	17(1)	20(1)	23(1)	0	4(1)	0
C(3)	16(1)	18(1)	23(1)	0	1(1)	0
C(4)	16(1)	14(1)	23(1)	0	1(1)	0
C(5)	15(1)	22(1)	15(1)	0	0(1)	0
C(6)	14(1)	19(1)	22(1)	0	0(1)	0
C(7)	17(1)	17(1)	19(1)	0	-1(1)	0
O(1)	15(1)	29(1)	17(1)	0	0(1)	0
O(2)	22(1)	28(1)	17(1)	0	-1(1)	0
O(3)	16(1)	34(1)	21(1)	0	1(1)	0
O(4)	18(1)	32(1)	17(1)	0	-1(1)	0

Table 2.17 Hydrogen coordinates (x 10^4) and isotropic displacement parameters ($Å^2$x 10^3) for burk04.

	x	y	z	U(eq)
H(2)	4842	2500	2555	24
H(3)	5474	2500	4803	23
H(5A)	1916	1249	5803	21
H(5B)	1916	3751	5803	21
H(6)	5035	2500	7170	22
H(4)	3470(20)	2500	10210(30)	33

γ-lactone acid 156

Crystals of the ester-lactone **149** (291 mg, 1.74 mmol) were added to a scintillation vial, and an aqueous solution of NaOH (5.79 mL of a 0.3 M solution, 1.74 mmol) was added slowly with stirring. The solution stirred for 20 min at room temperature, then was acidified by the dropwise addition of 2N HCl until the mixture was acidic to pH paper. A precipitate formed, and the γ-lactone acid **156** (190 mg, 71%) was collected by vacuum filtration. ^{1}H NMR (DMSO-*d*6, 500 MHz) δ 6.85 (d, *J* = 12.5 Hz, 1H), 6.48 (s, 1H), 6.21 (d, *J* = 12.5 Hz, 1H), 5.16 (d, *J* = 1.8 Hz, 1H); ^{13}C NMR (DMSO-*d*6, 100 MHz) δ 172.8, 166.4, 129.9, 127.5, 122.0, 72.6.

Weinreb amide 158

A mixture of δ-lactone acid **148** (21 mg, 0.134 mmol), *N,O*-dimethylhydroxylamine hydrochloride (26 mg, 0.268 mmol), and PyBOP (78 mg, 0.150 mmol) in a scintillation vial was cooled to -20 °C. DMF (2 mL) was added via syringe, followed by i-Pr_2NEt (80 μL, 0.470 mmol), and the solution was allowed to slowly warm to room temperature as it stirred for 12 h. The solution was partitioned between H_2O and EtOAc, and the layers were separated. The aqueous layer was extracted with additional EtOAc, and the combined organic layers were washed with brine, dried over Na_2SO_4, filtered and concentrated under reduced pressure. The residue was purified by column chromatography (1:1 hexanes / ethyl acetate) to provide compound **158** (11 mg, 42%), for which the structure was not conclusively determined by NMR. ^{1}H NMR ($CDCl_3$, 400 MHz) δ 7.40-7.31 (m, 2H), 6.31 (d, J = 10.5 Hz, 1H), 3.73 (s, 3H), 3.43 (s, 2H), 3.20 (s, 3H); ^{13}C NMR ($CDCl_3$, 100 MHz) δ 170.6, 161.6, 149.7, 145.9, 116.1, 113.4, 61.6, 32.4; ESI-MS *m/z* 198.13 $[M+H]^+$.

***t*-butyl ester 160**

To a solution of the γ-lactone acid **156** (157 mg, 1.0 mmol) in CH_2Cl_2 (3 mL) was added $MgSO_4$ (491 mg, 4.1 mmol), freshly distilled *t*-BuOH (481 μL, 5.1 mmol), and H_2SO_4 (54 μL, 1.0 mmol), and the reaction flask was tightly stoppered and allowed to stir for 12 h. After this period of time, a saturated $NaHCO_3$ solution was added to quench the catalyst, and the mixture was partitioned between EtOAc and H_2O. The aqueous layer was extracted with additional EtOAc, and the combined

organic layers were dried over Na_2SO_4, filtered and concentrated under reduced pressure. The residue was purified by column chromatography (1:1 to 2:1 ethyl acetate / hexanes) to provide the *t*-butyl ester **160** (89 mg, 41%) as a clear oil. TLC (100% EtOAc): R_f = 0.6; ^{1}H NMR ($CDCl_3$, 400 MHz) δ 6.64 (dd, *J* = 12.5, 0.8 Hz, 1H), 6.23 (s, 1H), 6.04 (d, *J* = 12.5 Hz, 1H), 5.21 (d, *J* = 2.0 Hz, 1H), 1.50 (s, 9H); ^{13}C NMR ($CDCl_3$, 100 MHz) δ 173.1, 164.3, 159.7, 129.8, 128.3, 123.5, 82.3, 73.4, 28.1.

Lactol 161

A solution of *t*-butyl ester **160** (131 mg, 0.62 mmol) in CH_2Cl_2 (10 mL) was cooled to -78 °C, and to this stirred solution was added DIBAL-H (600 μL of a 1.0 M solution in hexanes, 0.06 mmol) in three 200 μL portions over 1 h. A new, higher R_f DNP active spot was observed on TLC of the reaction mixture, which was quenched at this time by the addition of a few drops of MeOH followed by a saturated aqueous solution of Rochelle's salt, and allowed to warm to ambient temperature. When the layers had separated, the aqueous layer was extracted with additional portions of CH_2Cl_2, and the combined organic layers were dried over Na_2SO_4, filtered and concentrated under reduced pressure. The residue was purified by column chromatography (1:1 to 2:1 ethyl acetate / hexanes gradient) to provide the lactol **161** (55 mg, 42%), which decomposed slowly in $CDCl_3$ to an aromatic product, presumably the corresponding furan. ^{1}H NMR ($CDCl_3$, 300 MHz) δ 6.47 (d, *J* = 12.5 Hz, 1H), 6.11-6.02 (m, 2H), 5.80 (d, *J* = 12.5 Hz, 1H), 5.03 (d, *J* = 14.2 Hz, 1H), 4.81

(d, *J* = 14.2 Hz, 1H), 2.83 (d, *J* = 8.8 Hz, 1H), 1.48 (s, 9H); ^{13}C NMR ($CDCl_3$, 75 MHz) δ 165.2, 141.3, 132.7, 131.4, 123.9, 102.4, 81.4, 74.6, 28.2.

Sulfone 168

The primary alcohol (203 mg, 0.573 mmol) obtained by the reduction of acetal **171** was dissolved in THF (5 mL). To the solution was added iPr_2NEt (300 μL, 1.72 mmol), and the stirred solution was cooled to 0 °C. To this solution was added MsCl (53 μL, 0.687 mmol), and the solution was allowed to slowly warm to room temperature with stirring. When none of the starting material remained by TLC analysis, the reaction mixture was partitioned between H_2O and EtOAc, and the aqueous layer was extracted with additional EtOAc. The combined organic layers were washed with brine, dried over Na_2SO_4, filtered, and concentrated under reduced pressure.

The crude mesylate residue was further dried by toluene azeotrope, and then was dissolved in THF (3 mL). A separate flask was charged with NaH (34 mg of a 60% dispersion in oil, 0.86 mmol), THF (2 mL), and PTSH (112 mg, 0.63 mmol), and the solution was stirred for 30 min and cooled to 0 °C. The solution of the crude mesylate was added to the reaction flask via syringe, and the reaction was allowed to warm to room temperature with stirring over 12 h. After this period of time the reaction mixture was partitioned between EtOAc and H_2O, the layers were separated, and the aqueous layer was extracted with additional EtOAc. The combined organic layers were washed with brine, dried over Na_2SO_4, filtered and concentrated under

reduced pressure. The residue was purified by column chromatography to provide the pure sulfide (155 mg, 52% over 2 steps) and recovered mesylate (88 mg) which accounted for most of the material balance.

Sulfide ^{1}H NMR ($CDCl_3$, 500 MHz) δ 7.59-7.49 (m, 5H), 7.25 (d, *J* = 8.5 Hz, 2H), 6.84 (d, *J* = 8.5 Hz, 2H), 4.65 (d, *J* = 11.2 Hz, 1H), 4.48 (d, *J* = 11.2 Hz, 1H), 3.77 (s, 3H), 3.75-3.36 (m, 5H), 2.17-2.06 (m, 1H), 2.01-1.89 (m, 1H), 0.88 (s, 9H), 0.05 (s, 6H); ^{13}C NMR ($CDCl_3$, 100 MHz) δ 159.3, 154.5, 133.8, 130.7, 130.1, 129.8, 129.7, 123.9, 113.9, 72.0, 55.4, 31.3, 29.9, 26.0, 18.4, -5.3, -5.3.

The purified sulfide (100 mg, 0.202 mmol) was then dissolved in EtOH (1 mL) and cooled to 0 °C. To this solution was added a solution of $(NH_4)_6Mo_7O_{24}$*$4H_2O$ (50 mg, 0.0404 mmol) in 30% w/w H_2O_2 (210 μL, 2.02 mmol), and the solution was allowed to warm to room temperature over 12 h. The reaction mixture was then extracted into Et_2O and H_2O, and the aqueous layer was extracted with additional Et_2O. The combined organic layers were washed with brine, dried over Na_2SO_4, filtered and concentrated under reduced pressure. The residue was purified by column chromatography (hexanes / ethyl acetate gradient) to provide sulfone **168** as a clear oil. ^{1}H NMR ($CDCl_3$, 400 MHz) δ 7.71-7.52 (m, 5H), 7.25 (d, *J* = 8.7 Hz, 2H), 6.88 (d, *J* = 8.7 Hz, 2H), 4.61 (d, *J* = 11.3 Hz, 1H), 4.47 (d, *J* = 11.3 Hz, 1H), 3.89-3.54 (m, 5H), 3.81 (s, 3H), 2.33-2.19 (m, 1H), 2.17-2.04 (m, 1H), 0.89 (s, 9H), 0.06 (s, 6H); ^{13}C NMR ($CDCl_3$, 100 MHz) δ 159.5, 153.6, 133.2, 131.6, 130.2, 129.8, 129.7, 125.2, 114.1, 71.9, 64.7, 55.4, 52.8, 26.0, 24.5, 18.4, -5.3, -5.3; ESI-MS *m/z* 571.03 $[M+K]^+$, 555.12 $[M+Na]^+$.

Julia adduct 166

To a solution of the sulfone **168** (81 mg, 0.152 mmol) in THF (2 mL) was added a solution of the aldehyde **167** (35 mg, 0.213 mmol) and the stirred solution was cooled to -78 °C. To this solution was added KHMDS (273 μL of a 15% w/w solution in toluene, 0.182 mmol) dropwise via syringe and the reaction was stirred at -78 °C for 90 min, and then was allowed to warm to room temperature. The reaction stirred for 30 min at room temperature, and then was quenched by the addition of saturated aqueous NH_4Cl (3 mL), and the mixture was extracted with Et_2O (3 x 10 mL). The combined organic layers were washed with brine, dried over Na_2SO_4, filtered, and concentrated under reduced pressure. The residue was purified by column chromatography (10:1 to 5:1 hexanes / ethyl acetate) to provide the Julia adduct **166** (49 mg, 67%) as a clear oil, containing a small amount of the aldehyde **167** as observed by ^{1}H NMR. TLC (10:1 hexanes / ethyl acetate): R_f = 0.4; ^{1}H NMR ($CDCl_3$, 400 MHz) δ 7.27 (d, *J* = 8.7 Hz, 2H), 6.86 (d, *J* = 8.7 Hz, 2H), 6.14 (d, *J* = 15.6 Hz, 1H), 5.86 (s, 1H), 5.81 (s, 1H), 5.64 (dt, *J* = 15.6, 7.2 Hz, 1H), 5.45 (q, *J* = 6.9 Hz, 1H), 4.60 (d, *J* = 11.5 Hz, 1H), 4.54 (d, *J* = 11.5 Hz, 1H), 3.80 (s, 3H), 3.66 (dd, *J* = 10.5, 5.9 Hz, 1H), 3.60 (dd, *J* = 10.5, 5.1 Hz, 1H), 3.50 (dq, *J* = 11.2, 5.4 Hz, 1H), 2.46-2.23 (m, 2H), 1.93 (s, 3H), 1.90 (s, 3H), 1.78 (s, 3H), 1.72 (d, *J* = 6.9 Hz, 3H), 0.91 (s, 9H), 0.06 (s, 6H); ^{13}C NMR ($CDCl_3$, 100 MHz) δ 159.2, 138.1, 135.3, 134.7, 133.8, 133.4, 132.2, 131.2, 129.5, 125.1, 124.9, 113.8, 79.7, 71.8, 65.4, 55.4, 35.3, 26.1, 19.3, 18.5, 16.9, 14.4, 14.0, -5.2, -5.2; ESI-MS *m/z* 487.99 $[M+NH_4]^+$, 471.20 $[M+H]^+$; HR-EI-MS *m/z* calcd. for $C_{29}H_{46}O_3Si_1$ $[M]^+$: 470.3211, found 470.3217.

Alcohol 181

To a solution of the diol **180** (241 mg, 1.10 mmol) in CH_2Cl_2 (10 mL) was added a solution of veratraldehyde dimethyl acetal (280 mg, 1.30 mmol) in 2 mL of CH_2Cl_2. The solution was cooled to 0 °C, PPTS (28 mg, 0.11 mmol) was added, and the reaction stirred for 30 min. After this period of time, TLC analysis of the reaction indicated the disappearance of starting material, and the formation of a new, higher R_f UV active product. The reaction mixture was partitioned between saturated $NaHCO_3$ and EtOAc, and the aqueous layer was extracted with additional EtOAc. The combined organic layers were washed with brine, dried over Na_2SO_4, filtered and concentrated under reduced pressure. The residue was purified by column chromatography (10:1 to 5:1 hexanes ethyl acetate gradient) to provide the DMP acetal (416 mg, > 100%, contaminated with the reagent) as a ~1.2:1 epimeric mixture.

A solution of the DMP acetal (400 mg, 1.10 mmol) in CH_2Cl_2 (15 mL) was cooled to -78 °C, and DIBAL-H (4.4 mL of a 1.0 M solution in hexanes, 4.40 mmol) was added via syringe. The solution was allowed to warm to 0 °C, and stirred for 30 min, after which time the reaction mixture was quenched by the dropwise addition of MeOH, followed by saturated aqueous Rochelle's salt solution. Once the layers had completely separated, the aqueous layer was extracted with additional CH_2Cl_2, and the combined organic layers were washed with brine, dried over Na_2SO_4, filtered and concentrated under reduced pressure. The residue was purified by column chromatography (1:1 to 1:2 hexanes / ethyl acetate gradient) to provide the alcohol

181 (203 mg, 50% over 2 steps) as a clear oil. TLC (100% ethyl acetate): $R_f = 0.5$; ^{1}H NMR ($CDCl_3$, 400 MHz) δ 6.92-6.80 (m, 3H), 4.55 (d, *J* = 11.3 Hz, 1H), 4.50 (d, *J* = 11.3, 1H), 3.89 (s, 3H), 3.87 (s, 3H), 3.79-3.52 (m, 5H), 2.42 (t, *J* = 6.4 Hz, 1H), 1.92-1.67 (m, 2H), 0.89 (s, 9H), 0.06 (s, 6H).

Propargylic alcohol 182

To a suspension of powdered 4 Å molecular sieves (20 mg) in CH_2Cl_2 (2mL) was added NMO (39 mg, 0.335 mmol), and a solution of the alcohol **181** (82 mg, 0.223 mmol). To the stirring solution was added TPAP (4 mg, 0.012 mmol), and the green solution turned black over 10 minutes. TLC analysis of the reaction mixture indicated the formation of the aldehyde (active with DNP stain), and so the mixture was filtered through a silica gel plug with CH_2Cl_2, and concentrated under reduced pressure to provide the aldehyde (61 mg, 74%) which was used without further purification in the next step. ^{1}H NMR ($CDCl_3$, 400 MHz) δ 9.65 (d, *J* = 9.65 Hz, 1H), 6.97-6.77 (m, 3H), 4.61 (d, *J* = 11.4 Hz, 1H), 4.50 (d, *J* = 11.4 Hz, 1H), 3.99-3.94 (m, 1H), 3.89 (s, 3H), 3.87 (s, 3H), 3.81-3.68 (m, 2H), 2.01-1.80 (m, 2H), 0.87 (s, 9H), 0.04 (s, 6H); ^{13}C NMR ($CDCl_3$, 100 MHz) δ 203.6, 149.2, 149.0, 130.1, 120.8, 111.4, 111.0, 80.6, 72.7, 58.2, 56.0, 56.0, 33.9, 26.0, 18.4, -5.3, -5.3.

To a suspension of K_2CO_3 (57 mg, 0.414 mmol) and TsN_3 (33 mg, 0.166 mmol) in MeCN (2 mL) was added dimethyl-2-oxopropylphosphonate (23 μL, 0.166 mmol). The suspension was stirred at room temperature for 2 h, after which a solution of the above described aldehyde (51 mg, 0.138 mmol) in MeOH (500 μL) was added

via syringe. The solution was allowed to stir for 12 h, and then was partitioned between EtOAc and H_2O. The aqueous layer was extracted with additional EtOAc, and the combined organic layers were washed with brine, dried over Na_2SO_4, filtered and concentrated under reduced pressure. The residue was purified by column chromatography (5:1 hexanes / ethyl acetate) to provide the terminal alkyne (14 mg, 29%). TLC (5:1 hexanes / ethyl acetate): R_f = 0.3; ^{1}H NMR ($CDCl_3$, 300 MHz) δ 6.96-6.76 (m, 3H), 4.74 (d, *J* = 11.2 Hz, 1H), 4.43 (d, *J* = 11.2 Hz, 1H), 4.34-4.22 (m, 1H), 3.89 (s, 3H), 3.88 (s, 3H), 3.81-3.70 (m, 2H), 2.48 (d, *J* = 2.0 Hz, 1H), 0.86 (s, 9H), 0.03 (s, 6H); ^{13}C NMR ($CDCl_3$, 75 MHz) δ 149.0, 148.8, 130.4, 120.9, 111.5, 110.9, 83.1, 74.0, 70.9, 65.3, 59.1, 56.0, 55.9, 38.9, 26.0, 18.4, -5.2.

A solution of the above described alkyne (14 mg, 0.038 mmol) in THF (2 mL) was cooled to -78 °C, and to the stirred solution was added n-BuLi (27 μL of a 1.54 M solution in hexanes, 0.042 mmol), and the solution was stirred for 30 min to effect complete deprotonation, after which a suspension of paraformaldehyde (2 mg, 0.058 mmol) in THF (100 μL) was added via syringe. The solution was allowed to warm to room temperature, and after 1 h TLC analysis indicated that a new lower R_f product had formed, and that some starting material remained. The reaction mixture was allowed to stir for an additional 12 h at room temperature, after which it was partitioned between H_2O and EtOAc, and the aqueous layer was extracted with additional EtOAc. The combined organic layers were dried over Na_2SO_4, filtered and concentrated under reduced pressure. Column chromatography of the residue (5:1 hexanes / ethyl acetate to 100% ethyl acetate gradient) provided recovered alkyne (6

mg) and the propargylic alcohol **182** (5 mg, 63% BORSM). TLC (5:1 hexanes / ethyl acetate): R_f = 0; ^{1}H NMR ($CDCl_3$, 400 MHz) δ 6.94-6.45 (m, 3H), 4.72 (d, *J* = 11.2 Hz, 1H), 4.42 (d, *J* = 11.2 Hz, 1H), 4.37-4.30 (m, 3H), 3.89 (s, 3H), 3.87 (s, 3H), 3.80-3.68 (m, 2H), 2.08-1.82 (m, 2H), 0.86 (s, 9H), 0.03 (s, 3H), 0.02 (s, 3H); ^{13}C NMR ($CDCl_3$, 100 MHz) δ 149.0, 130.5, 120.8, 111.4, 110.9, 85.1, 84.2, 70.9, 65.6, 59.1, 56.0, 55.9, 51.4, 39.0, 26.0, 18.4, -5.2.

Stannane 183

To a reaction flask was charged $(PPh_3)_2PdCl_2$ (1 mg, 0.001 mmol), followed by a solution of the propargylic alcohol **182** (5 mg, 0.013 mmol) in THF (500 μL) via syringe. To the stirred solution was added n-Bu_3SnH (5 μL, 0.017 mmol) dropwise via syringe. The solution darkened, and was stirred for 20 min at room temperature. The solution was concentrated under reduced pressure, and the residue was purified by column chromatography (hexanes / ethyl acetate gradient) to provide the stannane **183** (9 mg, 93%). ^{1}H NMR ($CDCl_3$, 400 MHz) δ 6.90-6.77 (m, 3H), 5.50 (dt, *J* = 8.9, 1.8 Hz, 1H), 4.52 (d, *J* = 11.4 Hz, 1H), 4.42-4.22 (m, 4H), 3.88 (s, 3H), 3.87 (s, 3H), 3.76-3.56 (m, 2H), 1.95 (t, *J* = 5.6 Hz, 1H), 1.97-1.84 (m, 1H), 1.64-1.40 (m, 6H), 1.40-1.21 (m, 6H), 1.04-0.78 (m, 24H), 0.03 (s, 6H).

Aldehyde 191

To a -78 °C solution of oxalyl chloride (335 μL, 3.95 mmol) in CH_2Cl_2 (10 mL) was added DMSO (590 μL, 8.26 mmol) dropwise via syringe, and the solution

was stirred for 10 min. To this solution was added a solution of the alcohol (813 mg, 3.59 mmol) derived from the DIBAL-H reduction of acetal **190** in CH_2Cl_2 (5 mL), and the reaction was stirred for 20 min. After this period of time, Et_3N (2.40 mL, 17.2 mmol) was added via syringe, and the solution was allowed to warm to room temperature with stirring. The solution was then diluted with CH_2Cl_2 and washed successively with saturated aqueous $NaHCO_3$, deionized H_2O, and brine. The organic layers were dried over Na_2SO_4, filtered, and concentrated under reduced pressure to provide the aldehyde **191** (620 mg, 78%). ^{1}H NMR ($CDCl_3$, 400 MHz) δ 9.80 (t, *J* = 1.8 Hz, 1H), 6.90-6.81 (m, 3H), 4.47 (s, 2H), 3.89 (s, 3H), 3.88 (s, 3H), 3.80 (t, *J* = 6.1 Hz, 2H), 2.70 (td, *J* = 6.1, 1.8 Hz, 2H).

Propargylic alcohol 193

To a stirred -78 °C solution of *t*-butyldimethyl(2-propynyloxy)silane (1.07 g, 7.08 mmol) in THF (80 mL) was added n-BuLi (3.10 mL of a 2.31 M solution in hexanes, 7.08 mmol) via syringe, and the solution stirred for 30 min to ensure complete deprotonation. To this solution was added a solution of aldehyde **191** (930 mg, 4.15 mmol) in THF (5 mL) via cannula, and the reaction stirred for 1 h at -78 °C, after which time TLC analysis indicated the disappearance of **191**. The reaction was quenched by the addition of a saturated aqueous NH_4Cl solution, and warmed to room temperature. The mixture was diluted with EtOAc, and the layers were separated. The aqueous layer was extracted with additional EtOAc, and the combined organic layers were washed with deionized water and brine, dried over Na_2SO_4, filtered, and concentrated under reduced pressure. Column chromatography of the residue

(hexanes / ethyl acetate gradient) provided the propargylic alcohol **193** (1.14 g, 70%) together with mixed fractions (0.41 g) that had additional **193** with unidentified impurities. ^{1}H NMR ($CDCl_3$, 400 MHz) δ 6.90-6.80 (m, 3H), 4.68-4.60 (m, 1H), 4.48 (d, *J* = 11.5 Hz, 1H), 4.44 (d, *J* = 11.5 Hz, 1H), 4.34 (d, *J* = 1.7 Hz, 2H), 3.89 (s, 3H), 3.88 (s, 3H), 3.87-3.79 (m, 1H), 3.70-3.62 (m, 1H), 3.02 (d, *J* = 6.1 Hz, 1H), 2.13-2.02 (m, 1H), 2.00-1.89 (m, 1H), 0.90 (s, 9H), 0.11 (s, 6H); ^{13}C NMR ($CDCl_3$, 100 MHz) δ 149.2, 148.8, 130.5, 120.5, 111.1, 111.0, 85.2, 83.7, 73.4, 67.6, 61.7, 60.6, 56.1, 56.0, 51.9, 36.8, 26.0, 21.2, 18.4, 14.4, -5.0; ESI-MS *m/z* 412.01 $[M+NH_4]^+$; HR-ESI-MS *m/z* calcd. for $C_{21}H_{34}O_5Si_1Na_1$: $[M+Na]^+$: 417.2068, found 417.2072.

Alcohol 194

To a solution of the propargylic alcohol **193** (1.14 g, 2.89 mmol) in DMF (15 mL) was added imidazole (530 mg, 7.80 mmol) and TBSCl (565 mg, 3.75 mmol). The solution was stirred at room temperature for 12 h, and then was partitioned between saturated aqueous $NaHCO_3$ and a 1:1 mixture of hexanes / diethyl ether. The aqueous layer was extracted with an additional portion of this mixture, and the combined organic layers were washed successively with deionized H_2O and brine. The solution was dried over Na_2SO_4, filtered and concentrated under reduced pressure. The residue was purified by column chromatography (hexanes / ethyl acetate gradient) to provide the bis-TBS ether (1.34 g, 91%) as a clear oil. *Bis-TBS ether* ^{1}H NMR ($CDCl_3$, 400 MHz) δ 6.91-6.79 (m, 3H), 4.62-4.56 (m, 1H), 4.43 (d, *J* = 11.4 Hz, 1H), 4.40 (d, *J* = 11.4 Hz, 1H), 4.31 (d, *J* = 1.7 Hz, 2H), 3.89 (s, 3H), 3.87 (s, 3H), 3.63-3.52 (m, 2H), 1.96 (dd, *J* = 12.8, 6.3 Hz, 2H), 0.90 (s, 9H), 0.89 (s, 9H), 0.13 (s, 3H),

0.10 (s, 6H), 0.10 (s, 3H); ^{13}C NMR ($CDCl_3$, 100 MHz) δ 149.1, 148.6, 131.1, 120.4, 111.1, 111.0, 86.2, 82.8, 73.1, 66.3, 60.1, 56.1, 55.9, 51.9, 38.8, 31.7, 25.9, 22.8, 18.4, 18.3, 14.3, -4.3, -4.9, -5.0.

A stock solution of 70% w/w HF-pyridine (0.5 mL) in THF (3 mL) and pyridine (3 mL) was prepared in a plastic vial, which corresponded to 85 mg HF / mL of the solution. A solution of the above described bis-TBS ether (340 mg, 0.668 mmol) in 1:1 THF-pyridine (3 mL) was stirred, as portions of the HF-pyridine stock solution (2.3 mL, 0.668 mmol) were added as needed based on occasional monitoring by TLC. When the starting material had been consumed, the reaction was quenched by the addition of saturated aqueous $NaHCO_3$. The mixture was partitioned between H_2O and EtOAc, and the aqueous layer was extracted with additional EtOAc. The combined organic layers were washed with brine, dried over Na_2SO_4, filtered and concentrated under reduced pressure. The residue was purified by column chromatography (hexanes / ethyl acetate gradient) to provide the alcohol **194** (244 mg, 92%) as a clear oil. ^{1}H NMR ($CDCl_3$, 400 MHz) δ 6.91-6.80 (m, 3H), 4.64-4.58 (m, 1H), 4.45 (d, *J* = 11.5 Hz, 1H), 4.39 (d, *J* = 11.5 Hz, 1H), 4.26 (dd, *J* = 6.2, 1.7 Hz, 1H), 3.89 (s, 3H), 3.88 (s, 3H), 3.63-3.52 (m, 2H), 1.96 (q, *J* = 6.4 Hz, 2H), 1.49 (t, *J* = 6.2 Hz, 1H), 0.90 (s, 9H), 0.13 (s, 3H), 0.10 (s, 3H); ^{13}C NMR ($CDCl_3$, 100 MHz) δ 149.1, 148.7, 131.1, 120.4, 111.2, 110.9, 87.4, 82.4, 73.1, 66.1, 60.1, 56.0, 51.3, 38.8, 25.9, 18.4, -4.4, -4.9.

Stannane 195

To a reaction flask was charged $(PPh_3)_2PdCl_2$ (34 mg, 0.048 mmol), and a solution of the alcohol **194** (191 mg, 0.484 mmol) in THF (5 mL). The suspension was stirred at room temperature as n-Bu_3SnH (170 μL, 0.629 mmol) was added dropwise via syringe. The solution darkened and was stirred for 20 min, then concentrated under reduced pressure. Column chromatography of the residue (hexanes / ethyl acetate gradient) provided the pure stannane **195** (207 mg, 62%). ^{1}H NMR ($CDCl_3$, 400 MHz) δ 6.90-6.80 (m, 3H), 5.53 (dt, *J* = 8.1, 1.9 Hz, 1H), 4.61 (td, *J* = 7.8, 5.7 Hz, 1H), 4.45-4.35 (m, 3H), 4.27 (ddd, *J* = 13.6, 5.4, 1.9 Hz, 1H), 3.89 (s, 3H), 3.88 (s, 3H), 3.57-3.41 (m, 2H), 1.92-1.78 (m, 1H), 1.81 (t, *J* = 5.4 Hz, 1H), 1.70-1.57 (m, 1H), 1.55-1.42 (m, 6H), 1.37-1.23 (m, 6H), 0.94-0.83 (m, 24H), 0.04 (s, 3H), 0.03 (s, 3H); ^{13}C NMR ($CDCl_3$, 100 MHz) δ 149.1, 148.7, 145.4, 143.1, 131.1, 120.3, 111.2, 111.0, 73.0, 67.1, 66.8, 63.8, 56.1, 55.9, 38.2, 29.4, 27.5, 26.0, 18.4, 13.9, 10.2, -4.2, -4.7.

Iodide 196

To a reaction flask was charged $(Ph_3P)_2PdCl_2$ (302 mg, 0.430 mmol) and a solution of the alcohol **194** (1.70 g, 4.30 mmol) in THF (50 mL). The solution stirred at room temperature as n-Bu_3SnH (1.51 mL, 5.60 mmol) was added slowly via syringe, and the darkened solution stirred for an additional 20 min. The solution was then concentrated under reduced pressure and redissolved in CH_2Cl_2 (50 mL), and cooled to 0 °C. A solution of I_2 (1.15 g, 4.50 mmol) was added via cannula, and the ice bath was allowed to melt. After the mixture had stirred for 30 min at room

temperature, solid KF on celite was added to adsorb the tin byproducts, and the suspension stirred for 2 h at room temperature. The reaction mixture was filtered and then concentrated under reduced pressure. Column chromatography of the residue (hexanes / ethyl acetate gradient) provided the iodide **196** (1.63 g, 72%) and 660 mg of impure material from mixed fractions. ^{1}H NMR ($CDCl_3$, 500 MHz) δ 6.90-6.98 (m, 3H), 6.25 (d, *J* = 9.2 Hz, 1H), 4.72 (dt, *J* = 9.2, 6.9 Hz, 1H), 4.43 (d, *J* = 11.5 Hz, 1H), 4.39 (d, *J* = 11.5 Hz, 1H), 4.26 (dd, *J* = 13.7, 6.9 Hz, 1H), 4.18 (dd, *J* = 13.7, 6.9 Hz, 1H), 3.89 (s, 3H), 3.88 (s, 3H), 3.56-3.46 (m, 2H), 2.81 (t, *J* = 6.9 Hz, 1H), 1.85-1.87 (m, 1H), 1.70-1.61 (m, 1H), 0.90 (s, 9H), 0.05 (s, 3H), 0.05 (s, 3H); ^{13}C NMR ($CDCl_3$, 125 MHz) δ 149.1, 145.8, 130.4, 120.5, 111.2, 111.2, 110.9, 103.5, 73.0, 68.1, 67.0, 66.1, 56.0, 55.9, 37.7, 25.9, 18.3, -4.3, -4.8.

Enyne 197

To a solution of the iodide **196** (849 mg, 1.62 mmol) and propargyl benzoate (359 mg, 2.24 mmol) in Et_3N (10 mL) was added $(PPh_3)_2PdCl_2$ (114 mg, 0.162 mmol) and CuI (93 mg, 0.486 mmol), and the reaction was stirred at room temperature. When TLC analysis indicated the consumption of iodide **196**, the reaction mixture was diluted with EtOAc and filtered through a celite plug. The solution was concentrated under reduced pressure, and the residue was purified by column chromatography (hexanes / ethyl acetate gradient) to provide the enyne **197** (719 mg, 80%). ^{1}H NMR ($CDCl_3$, 500 MHz) δ 8.08 (d, *J* = 8.0, 2H), 7.58 (t, *J* = 8.0 Hz, 1H), 7.45 (t, *J* = 8.0 Hz, 2H), 6.90-6.80 (m, 3H), 5.95 (d, *J* = 8.6 Hz, 1H), 5.06 (s, 2H), 4.72 (dt, *J* = 8.6, 7.0 Hz, 1H), 4.42 (d, *J* = 11.5 Hz, 1H), 4.40 (d, *J* = 11.5 Hz, 1H), 4.22-4.12 (m, 2H), 3.89

(s, 3H), 3.87 (s, 3H), 3.56-3.43 (m, 2H), 2.56 (t, J = 6.9 Hz, 1H), 1.99-1.87 (m, 1H), 1.72-1.63 (m, 1H), 0.87 (s, 9H), 0.05 (s, 3H), 0.03 (s, 3H); ^{13}C NMR ($CDCl_3$, 125 MHz) δ 166.1, 149.1, 148.7, 143.2, 133.5, 130.6, 130.0, 129.6, 128.6, 122.2, 120.5, 111.2, 110.9, 86.2, 83.1, 73.0, 66.2, 66.1, 60.8, 56.0, 55.9, 53.4, 38.0, 25.9, 18.3, -4.3, -4.8.

Bis-TBS ether 198

To a solution of the enyne **197** (719 mg, 1.30 mmol) in DMF (10 mL) was added imidazole (265 mg, 3.90 mmol) and TBSCl (294 mg, 1.95 mmol), and the reaction mixture was stirred at room temperature until no more starting material was visible by TLC. The reaction mixture was partitioned between saturated aqueous $NaHCO_3$ and a 1:1 mixture of hexanes / diethyl ether, and the layers were separated. The aqueous layer was extracted with an additional portion of the solvent mixture, and the combined organic layers were washed successively with deionized H_2O and brine. The organic layer was dried over Na_2SO_4, filtered and concentrated under reduced pressure. Column chromatography (hexanes / ethyl acetate gradient) provided the bis TBS ether **198** (644 mg, 74%). ^{1}H NMR ($CDCl_3$, 500 MHz) δ 8.08 (d, J = 8.0 Hz, 2H), 7.58 (t, J = 8.0 Hz, 1H), 7.45 (t, J = 8.0 Hz, 2H), 6.89-6.80 (m, 3H), 5.91 (d, J = 8.6 Hz, 1H), 5.05 (s, 2H), 4.70 (dt, J = 8.4, 5.2 Hz, 1H), 4.42 (d, J = 11.5 Hz, 1H), 4.39 (d, J = 11.5 Hz, 1H), 4.25 (d, J = 12.1 Hz, 1H), 4.12 (d, J = 12.1 Hz, 1H), 3.88 (s, 3H), 3.87 (s, 3H), 3.58-3.42 (m, 2H), 1.86-1.66 (m, 2H), 0.88 (s, 9H), 0.87 (s, 9H), 0.06 (s, 6H), 0.05 (s, 3H), 0.03 (s, 3H); ^{13}C NMR ($CDCl_3$, 125 MHz) δ 166.1, 149.0,

148.6, 143.4, 133.3, 131.2, 130.0, 129.8, 128.5, 121.6, 120.3, 111.0, 110.9, 87.2, 82.0, 73.0, 66.4, 66.0, 60.9, 56.0, 55.9, 53.5, 38.1, 26.0, 25.9, 18.5, 18.3, -4.2, -4.8, -5.1.

Diene 199

To a stirred solution of bis-TBS ether **198** (256 mg, 0.383 mmol) in CH_2Cl_2:H_2O (9:1 ratio, 10 mL) was added DDQ (95 mg, 0.421 mmol), and the initially green suspension faded to colorless with precipitation over the course of about 10 min. The suspension was filtered through a silica gel plug with CH_2Cl_2 / EtOAc (1:1), and the filtrate was concentrated under reduced pressure. The residue was purified by column chromatography (hexane / ethyl acetate gradient) to provide the primary alcohol (166 mg, 83%). ^{1}H NMR ($CDCl_3$, 400 MHz) δ 8.08 (d, *J* = 8.0 Hz, 2H), 7.58 (t, *J* = 8.0 Hz, 1H), 7.45 (t, *J* = 8.0 Hz, 2H), 5.99 (d, *J* = 8.9 Hz, 1H), 5.05 (s, 2H), 4.85 (dt, *J* = 8.9, 6.4 Hz, 1H), 4.24 (d, *J* = 12.1 Hz, 1H), 4.18 (d, *J* = 12.1 Hz, 1H), 3.79-3.62 (m, 2H), 2.72 (t, *J* = 5.8 Hz, 1H), 1.92-1.78 (m, 1H), 1.75-1.64 (m, 1H), 0.89 (s, 9H), 0.88 (s, 9H), 0.11 (s, 3H), 0.10 (s, 3H), 0.08 (s, 3H), 0.05 (s, 3H); ^{13}C NMR ($CDCl_3$, 100 MHz) δ 166.0, 143.7, 133.4, 130.0, 129.7, 128.5, 121.3, 87.1, 82.3, 68.2, 61.6, 59.9, 53.4, 40.0, 26.0, 25.9, 18.5, 18.2, -4.1, -4.8, -5.0, -5.2; ESI-MS *m/z* 541.33 $[M+Na]^+$, 536.12 $[M+NH_4]^+$; HR-ESI-MS *m/z* calcd. for $C_{28}H_{46}O_5Si_2Na_1$ $[M+Na]^+$: 541.2776, found 541.2766.

To a solution of the above described alcohol (63 mg, 0.12 mmol) in MeOH (5 mL) was added Pd-$BaSO_4$ (20 mg) and quinoline (40 μL) and the suspension stirred at room temperature. One balloon filled with H_2 was bubbled through the solution using

a 6" needle and a vent needle through the septum, and then the reaction mixture was filtered through celite with EtOAc. The resulting solution was stirred over $CuSO_4*xH_2O$ and filtered again through celite with EtOAc, and the solution was concentrated under reduced pressure. The residue was purified by column chromatography (hexane / ethyl acetate gradient) to provide the diene **199** (58 mg, 92%). ^{1}H NMR ($CDCl_3$, 400 MHz) δ 8.05 (d, *J* = 8.0 Hz, 2H), 7.56 (t, *J* = 8.0 Hz, 1H), 7.44 (t, *J* = 7.44 Hz, 2H), 6.18 (d, *J* = 11.6 Hz, 1H), 5.80 (dt, *J* = 11.6, 6.7 Hz, 1H), 5.51 (d, *J* = 8.7 Hz, 1H), 5.00 (d, *J* = 6.7 Hz, 2H), 4.84 (dt, *J* = 8.7, 5.6 Hz, 1H), 4.23 (d, *J* = 12.1 Hz, 1H), 4.19 (d, *J* = 12.1 Hz, 1H), 3.86-3.66 (m, 2H), 2.64 (t, *J* = 5.6 Hz, 1H), 1.96-1.69 (m, 2H), 0.89 (s, 9H), 0.88 (s, 9H), 0.10 (s, 3H), 0.09 (s, 3H), 0.08 (s, 3H), 0.06 (s, 3H); ^{13}C NMR ($CDCl_3$, 100 MHz) δ 166.5, 136.5, 134.1, 134.0, 133.1, 130.4, 129.8, 128.5, 126.0, 68.6, 62.0, 61.1, 60.2, 40.5, 26.0, 25.9, 18.4, 18.2, -4.1, -4.7, -5.2, -5.2; ESI-MS *m/z* 543.28 $[M+Na]^+$; HR-ESI-MS *m/z* calcd. for $C_{28}H_{48}O_5Si_2Na_1$ $[M+Na]^+$: 543.2932, found 543.2920.

Sulfone 200

To a reaction flask was charged PPh_3 (46 mg, 0.179 mmol) and PTSH (42 mg, 0.238 mmol). A solution of the diene **199** (62 mg, 0.119 mmol) in THF (5 mL) was added via syringe to the reaction flask, and the stirred solution was cooled to 0 °C. To the cooled solution was added DIAD (42 μL, 0.214 mmol) dropwise via syringe, and the solution was allowed to warm to room temperature as it stirred for 12 h. The reaction mixture was then partitioned between aqueous saturated $NaHCO_3$ and EtOAc, and the aqueous layer was extracted with additional EtOAc. The combined organic

layers were washed with deionized H_2O and brine, and then dried over Na_2SO_4. The organic layer was filtered and concentrated under reduced pressure, and the residue was purified by column chromatography (hexanes / ethyl acetate gradient) to provide the sulfide intermediate (79 mg, 97%). ^{1}H NMR ($CDCl_3$, 400 MHz) δ 8.04 (d, *J* = 8.0 Hz, 2H), 7.62-7.48 (m, 6H), 7.42 (t, *J* = 8.0 Hz, 2H), 6.18 (d, *J* = 11.7 Hz, 1H), 5.78 (dt, *J* = 11.7, 6.7 Hz, 1H), 5.44 (d, *J* = 8.4 Hz, 1H), 4.98 (d, *J* = 6.7 Hz, 2H), 4.72 (td, *J* = 8.4, 4.6 Hz, 1H), 4.24 (d, *J* = 12.0 Hz, 1H), 4.14 (d, *J* = 12.0 Hz, 1H), 3.48 (t, *J* = 7.1 Hz, 2H), 2.18-1.87 (m, 2H), 0.87 (s, 9H), 0.86 (s, 9H), 0.06 (s, 3H), 0.05 (s, 9H); ^{13}C NMR ($CDCl_3$, 100 MHz) δ 166.4, 154.5, 135.6, 134.9, 133.8, 133.7, 133.0, 130.4, 130.2, 129.9, 129.7, 128.5, 125.9, 123.9, 67.8, 62.0, 60.8, 37.8, 29.6, 26.1, 26.0, 25.9, 18.4, 18.2, -4.1, -4.7, -5.2; ESI-MS *m/z* 703.27 $[M+Na]^+$; HR-ESI-MS *m/z* calcd. for $C_{35}H_{52}O_4N_4Si_2S_1Na_1$ $[M+Na]^+$: 703.3140, found 703.3126.

A solution of the above described sulfide intermediate (124 mg, 0.182 mmol) in EtOH (5 mL) was cooled to 0 °C as it stirred. A separate solution of $(NH_4)_6Mo_7O_{24}$*$4H_2O$ (45 mg, 0.036 mmol) in H_2O_2 (278 μL of a 30% w/w aqueous solution, 2.73 mmol) was prepared, and then added to the cooled reaction flask. The ice bath was allowed to melt and the reaction warmed to room temperature as it stirred for 12 h. After this period of time the reaction mixture was partitioned between deionized H_2O and Et_2O, and the layers were separated. The aqueous layer was extracted with additional Et_2O, and the combined organic layers were washed with brine, dried over Na_2SO_4, filtered and concentrated under reduced pressure. The residue was purified by column chromatography (hexanes / ethyl acetate gradient) to

provide the sulfone **200** (91 mg, 70%). ^{1}H NMR ($CDCl_3$, 400 MHz) δ 8.03 (d, *J* = 7.6 Hz, 2H), 7.72-7.51 (m, 6H), 7.43 (t, *J* = 7.6 Hz, 2H), 6.17 (d, *J* = 12.6 Hz, 1H), 5.80 (dt, *J* = 12.6, 6.8 Hz), 5.41 (d, *J* = 8.3 Hz, 1H), 5.03-4.91 (m, 2H), 4.84 (dt, *J* = 8.3, 6.0 Hz, 1H), 4.25 (d, *J* = 12.3 Hz, 1H), 4.18 (d, *J* = 12.3 Hz, 1H), 3.91-3.80 (m, 2H), 2.21-2.13 (m, 2H), 0.88 (s, 9H), 0.88 (s, 9H), 0.09 (s, 3H), 0.07 (s, 6H), 0.06 (s, 3H).

Julia adduct 201

To a solution of the sulfone **200** (87 mg, 0.122 mmol) in THF (2 mL) was added a solution of the aldehyde **167** (2 mL of a 13.3 mg/mL stock solution, 0.162 mmol) in THF, and the solution was stirred and cooled to -78 °C. To the cooled reaction mixture was added KHMDS (222 μL of a 15% w/w solution in toluene, 0.146 mmol), and the yellow solution stirred for 1 h at -78 °C before being allowed to warm to room temperature, and was stirred for 30 min at room temperature. The reaction mixture was quenched by the addition of a saturated aqueous NH_4Cl solution, and then was diluted with Et_2O and deionized H_2O. The layers were separated and the aqueous layer was extracted with additional Et_2O. The combined organic layers were washed with brine, dried over Na_2SO_4, filtered and concentrated under reduced pressure. The residue was purified by column chromatography (hexane / diethyl ether gradient) to provide the Julia adduct **201** (52 mg, 66%). ^{1}H NMR ($CDCl_3$, 400 MHz) δ 8.05 (d, *J* = 8.0 Hz, 2H), 7.55 (t, *J* = 8.0 Hz, 1H), 7.43 (t, *J* = 8.0 Hz, 2H), 6.21 (d, *J* = 11.6 Hz, 1H), 6.14 (d, *J* = 15.5 Hz, 1H), 5.85 (s, 1H), 5.81-5.72 (m, 1H), 5.77 (s, 1H), 5.63 (dt, *J* = 15.5, 7.5 Hz, 1H), 5.47-5.38 (m, 1H), 5.43 (d, *J* = 8.7 Hz, 1H), 5.06-4.94 (m, 2H), 4.59-4.49 (m, 1H), 4.27 (d, *J* = 12.1 Hz, 1H), 4.14 (d, *J* = 12.1 Hz, 1H), 2.46-2.24 (m,

2H), 1.89 (s, 6H), 1.74 (s, 3H), 1.70 (d, *J* = 6.7 Hz, 3H), 0.89 (s, 9H), 0.88 (s, 9H), 0.07 (s, 6H), 0.06 (s, 3H), 0.05 (s, 3H); ESI-MS *m/z* 689.40 $[M+K]^+$, 673.39 $[M+Na]^+$, 668.17 $[M+NH_4]^+$; HR-ESI-MS *m/z* calcd. for $C_{39}H_{62}O_4Na_1Si_2$ $[M+Na]^+$: 673.4079, found 673.4091.

Alcohol 202

To the Julia adduct **201** (7 mg, 0.0106 mmol) was added NaOH (4 mL of a 1% w/v solution in MeOH), and the solution stirred at room temperature for 30 min, at which time TLC analysis indicated the disappearance of starting material. The reaction mixture was then partitioned between EtOAc and deionized H_2O, and the aqueous layer was extracted with additional EtOAc. The combined organic layers were washed with brine, dried over Na_2SO_4, filtered and concentrated under reduced pressure. The residue was purified by column chromatography to provide the alcohol **202** (4 mg, 71%). ^{1}H NMR ($CDCl_3$, 400 MHz) δ 6.11 (d, *J* = 16.0 Hz, 1H), 6.03 (d, *J* = 11.7 Hz, 1H), 5.87 (s, 1H), 5.80 (s, 1H), 5.74 (dt, *J* = 11.7, 6.6 Hz, 1H), 5.61 (dt, *J* = 16.0, 7.6 Hz, 1H), 5.45 (q, *J* = 6.9 Hz, 1H), 5.28 (d, *J* = 8.5 Hz, 1H), 4.54-4.45 (m, 1H), 4.28 (t, *J* = 6.2 Hz, 2H), 4.22 (d, *J* = 12.0 Hz, 1H), 4.11 (d, *J* = 12.0 Hz, 1H), 2.44-2.17 (m, 2H), 1.92 (s, 3H), 1.90 (s, 3H), 1.77 (s, 3H), 1.71 (d, *J* = 6.7 Hz, 3H), 1.64 (t, *J* = 6.2 Hz, 1H), 0.89 (s, 9H), 0.88 (s, 9H), 0.07 (s, 3H), 0.07 (s, 3H), 0.05 (s, 3H), 0.03 (s, 3H).

Pyran 204

To the alcohol **202** (4 mg, 0.007 mmol) was added NMO (1 mg, 0.011 mmol), and a small portion of powdered 4 Å molecular sieves, and the residue was dissolved in CH_2Cl_2 (200 μL). To this stirred suspension was added a catalytic amount of TPAP and the green solution turned black over a few min of stirring at room temperature. The suspension was filtered through a short silica gel plug, and the solution was concentrated under reduced pressure to yield a few mg of what is tentatively thought to be pyran **204**, possibly as an undetermined ratio of diastereomers. ^{1}H NMR spectral scans: Spectrum 2.73 - Spectrum 2.75, the lack of any aldehyde signal was noted. ESI-MS *m/z* 567.33 $[M+Na]^+$; HR-ESI-MS *m/z* calcd. for $C_{32}H_{56}O_3Na_1Si_2$ $[M+Na]^+$: 567.3660, found 567.3663.

Alkyne 205

A stirred solution of freshly distilled diisopropylamine (811 μL, 5.80 mmol) in THF (10 mL) was cooled to 0 °C, and n-BuLi (2.63 mL of a 2.2 M solution in hexanes, 5.85 mmol) was added via syringe. The LDA solution stirred at 0 °C for 30 min. A separate reaction flask was charged with tetronate **144** (696 mg, 5.52 mmol), which was dissolved in THF (5 mL) and cooled to -78 °C. The LDA solution was added to the cooled reaction flask via cannula, and the reaction mixture was stirred for 30 min at -78 °C. A solution of *tert*-butyldimethylsilylpropynal (929 mg, 5.52 mmol) in THF (3 mL) was added to the reaction flask via syringe. The reaction mixture stirred at -78 °C for 1 h, and then was quenched by the addition of saturated aqueous NH_4Cl. The mixture was warmed to room temperature and partitioned between

EtOAc and deionized H_2O. The aqueous layer was extracted with additional EtOAc, and the combined organic layers were washed with brine, dried over Na_2SO_4, filtered and concentrated under reduced pressure. The residue was purified by column chromatography to provide the propargylic alcohol precursor (773 mg, 48%). ^{1}H NMR ($CDCl_3$, 500 MHz) δ 5.57 (d, *J* = 6.3 Hz, 1H), 5.14 (d, *J* = 2.9 Hz, 1H), 5.12 (d, *J* = 2.9 Hz, 1H), 4.38 (s, 3H), 3.16 (d, *J* = 6.3 Hz, 1H), 0.92 (s, 9H), 0.10 (s, 6H); ^{13}C NMR ($CDCl_3$, 100 MHz) δ 168.9, 162.9, 149.4, 104.8, 103.9, 94.2, 90.5, 61.5, 55.5, 26.1, 16.6, -4.7.

To a solution of the above described propargylic alcohol precursor (773 mg, 2.63 mmol) in CH_2Cl_2 (25 mL) was added DMAP (16 mg, 0.132 mmol) and Et_3N (732 μL, 5.26 mmol), and the solution was stirred at room temperature. To the stirred solution was added benzoyl chloride (336 μL, 2.89 mmol) dropwise via syringe, and the reaction mixture stirred until TLC analysis indicated the disappearance of starting material. The reaction mixture was then partitioned between CH_2Cl_2 and saturated aqueous $NaHCO_3$. The aqueous layer was extracted with additional CH_2Cl_2, and the combined organic layers were washed successively with deionized H_2O and brine, and then dried over Na_2SO_4. The organic layer was filtered and concentrated under reduced pressure, and the residue was purified by column chromatography to provide the benzoate intermediate (539 mg, 54%). ^{1}H NMR ($CDCl_3$, 500 MHz) δ 8.04 (d, *J* = 8.0 Hz, 2H), 7.59 (t, *J* = 8.0 Hz, 1H), 7.46 (t, *J* = 8.0 Hz, 2H), 6.72 (s, 1H), 5.15 (d, *J* = 2.3 Hz, 1H), 5.13 (d, *J* = 2.3 Hz, 1H), 4.53 (s, 3H), 0.92 (s, 9H), 0.12 (s, 6H).

A solution of the above described benzoate intermediate (23 mg, 0.057 mmol) in THF (2 mL) was stirred and cooled to 0 °C. To the solution was added TBAF (60 μL of a 1.0 M solution in THF), and the darkened reaction mixture stirred for about 10 min, at which time TLC analysis indicated the disappearance of starting material. The reaction was quenched by the dropwise addition of AcOH, and the mixture was partitioned between deionized H_2O and EtOAc. The aqueous layer was extracted with additional EtOAc, and the combined organic layers were washed with brine, dried over Na_2SO_4, filtered and concentrated under reduced pressure. The residue was purified by column chromatography to provide the alkyne **205** (5 mg, 33%) which had an unidentified contaminant observed in the ^{1}H spectrum. ^{1}H NMR ($CDCl_3$, 500 MHz) δ 8.05 (d, *J* = 8.0 Hz, 2H), 7.60 (t, *J* = 8.0 Hz, 1H), 7.46 (t, *J* = 8.0 Hz, 2H), 6.75 (d, *J* = 2.3 Hz, 1H), 5.18 (d, *J* = 2.3 Hz, 1H), 5.15 (d, *J* = 2.3 Hz, 1H), 4.51 (s, 3H), 2.73 (d, *J* = 2.3 Hz, 1H); ^{13}C NMR ($CDCl_3$, 125 MHz) δ 167.4, 164.8, 164.5, 149.4, 133.8, 130.3, 130.0, 128.8, 100.8, 94.6, 79.7, 76.4, 61.6, 56.2.

Ene-yn-al 207

To a stirred solution of the bis-TBS ether **211** (290 mg, 0.455 mmol) and propargyl alcohol (34 μL, 0.592 mmol) in Et_3N (5 mL) at room temperature were added CuI (26 mg, 0.137 mmol) and $(PPh_3)_2PdCl_2$ (32 mg, 0.0455 mmol). The reaction stirred until the complete disappearance of the starting material **211** was observed by TLC, and then was filtered through a silica gel plug with EtOAc. The filtrate was concentrated under reduced pressure, and the residue was purified by column chromatography to provide the enyne intermediate (250 mg, 97%). ^{1}H NMR

($CDCl_3$, 400 MHz) δ 6.92-6.77 (m, 3H), 5.86 (d, *J* = 8.7 Hz, 1H), 4.70 (td, *J* = 8.7, 5.1 Hz, 1H), 4.41-4.36 (m, 4H), 4.23 (d, *J* = 12.1 Hz, 1H), 4.10 (d, *J* = 12.1 Hz, 1H), 3.88 (s, 3H), 3.87 (s, 3H), 3.58-3.42 (m, 2H), 1.87-1.64 (m, 2H), 0.89 (s, 9H), 0.86 (s, 9H), 0.07 (s, 6H), 0.04 (s, 3H), 0.03 (s, 3H); ^{13}C NMR ($CDCl_3$, 100 MHz) δ 149.1, 148.6, 142.9, 131.2, 121.7, 120.3, 111.2, 111.0, 86.3, 73.0, 66.1, 61.1, 55.9, 51.8, 38.1, 26.0, 26.0, 18.5, 18.3, -4.2, -4.8, -5.1.

To a reaction flask was charged the enyne intermediate described above (239 mg, 0.422 mmol), NMO (74 mg, 0.634 mmol), and powdered 4 Å molecular sieves (~50 mg). The mixture was suspended in CH_2Cl_2 (10 mL) and TPAP (7 mg, 0.021 mmol) was added with stirring at room temperature. The suspension turned from green to black, and when TLC analysis indicated the disappearance of starting material, the mixture was filtered through a short plug of silica gel with 1:1 CH_2Cl_2 : EtOAc. The filtrate was concentrated under reduced pressure to provide the ene-yn-al **207** (186 mg, 78%). ^1H NMR ($CDCl_3$, 500 MHz) δ 9.30 (s, 1H), 6.89-6.79 (m, 3H), 6.23 (d, *J* = 8.6 Hz, 1H), 4.74 (dt, *J* = 8.6, 5.2 Hz, 1H), 4.42 (d, *J* = 11.5 Hz, 1H), 4.38 (d, *J* = 11.5 Hz, 1H), 4.30 (d, *J* = 12.0 Hz, 1H), 4.16 (d, *J* = 12.0 Hz, 1H), 3.88 (s, 3H), 3.87 (s, 3H), 3.58-3.44 (m, 2H), 1.88-1.66 (m, 2H), 0.89 (s, 9H), 0.87 (s, 9H), 0.08 (s, 3H), 0.07 (s, 3H), 0.05 (s, 3H), 0.03 (s, 3H); ^{13}C NMR ($CDCl_3$, 125 MHz) δ 176.9, 150.0, 149.0, 148.6, 131.0, 120.4, 111.1, 111.0, 96.3, 87.7, 73.1, 66.2, 66.0, 60.3, 55.9, 37.8, 25.9, 25.8, 18.4, 18.2, -4.3, -4.8, -5.2.

Stannane 210

A solution of *i*-Pr_2NH (1.02 mL, 7.32 mmol) in THF (50 mL) was cooled to 0 °C with stirring, and then n-BuLi (3.58 mL of a 2.0 M solution in hexanes, 7.32 mmol) was added slowly via syringe, and the solution stirred for 30 min at 0 °C. A separate reaction flask was charged with tetronate **144** (885 mg, 7.03 mmol), and THF (50 mL), and the stirred solution was cooled to -78 °C. The LDA solution was added to the reaction flask via cannula, and the reaction stirred at -78 °C for 10 min as the solution darkened. A solution of aldehyde **209** (2.02 g, 5.9 mmol) in THF (20 mL) was then added via cannula, and the reaction stirred at -78 °C for 2 h, at which point TLC analysis indicated that the reaction mixture consisted mostly of a new product with different R_f than both of the starting materials. The reaction mixture was quenched by the addition of a saturated aqueous NH_4Cl solution, and then warmed to room temperature. The mixture was partitioned between deionized H_2O and EtOAc, and the aqueous layer was extracted with additional EtOAc. The combined organic layers were washed with brine, dried over Na_2SO_4, filtered and concentrated under reduced pressure. The residue was purified by column chromatography (5:1 to 2:1 hexane / ethyl acetate gradient) to provide the stannane **210** (1.86 g, 68%) as a colorless oil. TLC (2:1 hexanes / ethyl acetate): $R_f = 0.6$; ^1H NMR ($CDCl_3$, 500 MHz) δ 6.76 (dd, *J* = 12.6, 5.2 Hz, 1H), 6.21 (dd, *J* = 12.6, 1.7 Hz, 1H), 5.24-5.20 (m, 1H), 5.10-5.08 (m, 2H), 4.18 (s, 3H), 2.88 (d, *J* = 6.9 Hz, 1H), 1.57-1.42 (m, 6H), 1.36-1.25 (m, 6H), 1.01-0.83 (m, 15H); ^{13}C NMR ($CDCl_3$, 100 MHz) δ 169.4, 162.3, 149.5, 146.6, 133.7, 106.7, 93.8, 67.6, 61.2, 29.3, 27.5, 13.9, 11.1; HR-ESI-MS *m/z* calcd. for $C_{21}H_{37}O_4Sn_1$ $[M+H]^+$: 473.1708, found 473.1712.

Bis-TBS ether 211

To a solution of the iodide **196** (335 mg, 0.641 mmol) in DMF (6 mL) were added imidazole (131 mg, 1.92 mmol) and TBSCl (144 mg, 0.961 mmol). The solution stirred at room temperature until no more of the starting material was visible by TLC, and then the reaction mixture was partitioned between saturated aqueous $NaHCO_3$ and a 1:1 hexanes / diethyl ether solvent mixture. The aqueous layer was extracted with an additional portion of this mixture, and the combined organic layers were washed with deionized H_2O and brine, and then dried over Na_2SO_4 and filtered. The solution was concentrated under reduced pressure, and the residue was purified by column chromatography to provide the bis-TBS ether **211** (349 mg, 86%) as a clear oil. ^{1}H NMR ($CDCl_3$, 500 MHz) δ 6.89-6.79 (m, 3H), 6.23 (d, *J* = 8.6 Hz, 1H), 4.68 (dt, *J* = 8.6, 5.7 Hz, 1H), 4.42 (d, *J* = 11.5 Hz, 1H), 4.38 (d, *J* = 11.5 Hz, 1H), 4.30 (d, *J* = 12.9 Hz, 1H), 4.08 (d, *J* = 12.9 Hz, 1H), 3.89 (s, 3H), 3.88 (s, 3H), 3.58-3.41 (m, 2H), 1.86-1.64 (m, 2H), 0.90 (s, 9H), 0.87 (s, 9H), 0.08 (s, 3H), 0.07 (s, 3H), 0.04 (s, 6H); ^{13}C ($CDCl_3$, 125 MHz) δ 149.1, 148.7, 145.7, 131.1, 120.3, 111.0, 111.0, 103.5, 73.1, 68.0, 66.2, 65.7, 56.1, 56.0, 38.0, 26.0, 25.9, 18.5, 18.3, -4.3, -4.8, -5.0; HR-ESI-MS *m/z* calcd. for $C_{27}H_{49}I_1O_5Si_2Na_1$ $[M+Na]^+$: 659.2055, found 659.2072.

Stille adduct 212

To a reaction flask was charged LiCl (69 mg, 1.64 mmol), which was dried under high vacuum (0.1 mm Hg) with a heat gun for ~ 30 min, $AsPh_3$ (335 mg, 1.10 mmol), and Pd_2dba_3 (125 mg, 0.137 mmol). A solution of the bis-TBS ether **211** (349

mg, 0.547 mmol) and the stannane **210** (258 mg, 0.548 mmol) in freshly distilled NMP (5.5 mL) was prepared, and this solution was added to the reaction flask containing the solid reagents. The reaction mixture was stirred for 12 h at room temperature, during which time the solution changed from green to black. The reaction mixture was partitioned between Et_2O and deionized H_2O, and the aqueous layer was extracted twice with additional Et_2O. The combined organic layers were washed with brine, dried over Na_2SO_4, filtered and concentrated under reduced pressure. The residue was purified by column chromatography (4:1 to 2:1 hexanes / ethyl acetate) to provide the stille adduct **212a** (55 mg, 15%, "diastereomer A"), **212a/b** (202 mg, 53%, mix of diastereomers), and **212b** (91 mg, 24%, "diastereomer B") for a combined yield of 92%. *Diastereomer A* **212a**: ^{1}H NMR ($CDCl_3$, 400 MHz) δ 6.91-6.78 (m, 3H), 6.06 (d, *J* = 11.3 Hz, 1H), 5.92 (dd, *J* = 11.3, 9.2 Hz, 1H), 5.76 (d, *J* = 8.5 Hz, 1H), 5.68 (t, *J* = 8.5 Hz, 1H), 5.05 (d, *J* = 2.6 Hz, 1H), 5.04 (d, *J* = 2.6 Hz, 1H), 4.69 (td, *J* = 8.5, 4.7 Hz, 1H), 4.44 (d, *J* = 11.5 Hz, 1H), 4.40 (d, *J* = 11.5 Hz, 1H), 4.22 (d, *J* = 12.4 Hz, 1H), 4.18 (d, *J* = 12.4 Hz, 1H), 4.06 (s, 3H), 3.88 (s, 3H), 3.87 (s, 3H), 3.62-3.47 (m, 2H), 1.89-1.66 (m, 2H), 0.86 (s, 9H), 0.85 (s, 9H), 0.04 (s, 3H), 0.03 (s, 6H), 0.01 (s, 3H); ^{13}C NMR ($CDCl_3$, 100 MHz) δ 169.4, 161.5, 149.6, 149.1, 148.7, 136.7, 133.1, 131.1, 131.1, 120.5, 111.3, 111.0, 106.2, 93.3, 73.1, 66.3, 61.8, 61.1, 60.7, 56.0, 55.9, 38.9, 26.0, 25.9, 18.5, 18.2, -4.1, -4.7, -5.3, -5.3; ESI-MS *m/z* 713.39 $[M+Na]^+$, 708.11 $[M+NH_4]^+$. *Diastereomer B* **212b**: ^{1}H NMR ($CDCl_3$, 500 MHz) – see Spectrum 2.91, impure and difficult to analyze, ^{13}C NMR ($CDCl_3$, 100 MHz) δ 169.4, 161.9, 149.6, 149.0, 148.6, 136.8, 133.0, 131.2, 131.0, 130.9,

120.3, 111.2, 111.0, 106.6, 93.4, 73.1, 73.0, 66.5, 66.3, 61.8, 60.9, 59.5, 56.1, 55.9, 38.7, 26.0, 25.9, 18.5, 18.4, 18.2, -4.2, -4.7, -5.3.

Benzoate 213

A stirred solution of the stille adduct **212a** *Diastereomer A* (55 mg, 0.080 mmol) in CH_2Cl_2 (3 mL) was cooled to 0 °C, and DMAP (1 mg, 0.008 mmol) was added. To the solution was added Et_3N (45 μL, 0.32 mmol) followed by benzoyl chloride (18 μL, 0.16 mmol) via syringe. The solution was stirred until no more starting material was visible by TLC, and then was diluted with CH_2Cl_2 and saturated aqueous $NaHCO_3$, and the aqueous layer was extracted with an additional portion of CH_2Cl_2. The combined organic layers were washed with deionized H_2O and brine, then dried over Na_2SO_4, filtered and concentrated under reduced pressure. The residue was purified by column chromatography (4:1 to 2:1 hexanes / ethyl acetate gradient) to provide the benzoate **213** (24 mg, 38%). ^{1}H NMR ($CDCl_3$, 400 MHz) δ 8.05 (d, *J* = 8.0 Hz, 2H), 7.58-7.37 (m, 3H), 7.03 (d, *J* = 9.9 Hz, 1H), 6.92-6.80 (m, 3H), 6.35 (dd, *J* = 11.3, 9.9 Hz, 1H), 6.22 (d, *J* = 11.3 Hz, 1H), 5.43 (d, *J* = 8.6 Hz, 1H), 5.04 (d, *J* = 2.6 Hz, 1H), 5.02 (d, *J* = 2.6 Hz, 1H), 4.67 (td, *J* = 8.6, 4.4 Hz, 1H), 4.42 (s, 2H), 4.37 (s, 3H), 4.25 (d, *J* = 11.7 Hz, 1H), 4.14 (d, *J* = 11.7 Hz, 1H), 3.89 (s, 3H), 3.88 (s, 3H), 3.62-3.46 (m, 2H), 1.85-1.60 (m, 2H), 0.83 (s, 9H), 0.76 (s, 9H), 0.02 (s, 3H), 0.01 (s, 3H), -0.01 (s, 3H), -0.08 (s, 3H); ^{13}C NMR ($CDCl_3$, 100 MHz) δ 167.4, 165.9, 162.4, 149.6, 149.1, 148.7, 136.4, 135.7, 134.1, 133.3, 130.1, 128.5, 120.4, 111.3, 111.1, 103.1, 93.3, 73.0, 66.4, 66.0, 64.5, 61.1, 60.3, 56.1, 56.0, 38.6,

25.9, 25.9, 18.5, 18.2, -4.2, -4.7, -5.3, -5.3; HR-ESI-MS *m/z* calcd. for $C_{43}H_{62}O_{10}Si_2Na_1$ $[M+Na]^+$: 817.3774, found 817.3794.

Alcohol 214

The benzoate **213** (128 mg, 0.160 mmol) was dissolved in CH_2Cl_2 (1.5 mL) and H_2O (166 μL), and DDQ (40 mg, 0.176 mmol) was added at room temperature. The suspension turned from green to colorless, and TLC analysis indicated the formation of a new product and veratraldehyde. The reaction mixture was filtered through silica gel with 1:1 CH_2Cl_2 : EtOAc, and the filtrate was concentrated under reduced pressure. The residue was purified by column chromatography to provide the alcohol **214** (45 mg, 43%). ^{1}H NMR ($CDCl_3$, 400 MHz) δ 8.07 (d, *J* = 7.5 Hz, 2H), 7.56 (t, *J* = 7.5 Hz, 1H), 7.43 (t, *J* = 7.5 Hz, 2H), 7.01 (d, *J* = 9.9 Hz, 1H), 6.35 (dd, *J* = 11.3, 9.9 Hz, 1H), 6.20 (d, *J* = 11.3 Hz, 1H), 5.50 (d, *J* = 8.8 Hz, 1H), 5.05 (d, *J* = 2.6 Hz, 1H), 5.04 (d, *J* = 2.6 Hz, 1H), 4.74 (td, *J* = 8.8 Hz, 5.4 Hz, 1H), 4.36 (s, 3H), 4.30 (d, *J* = 11.7 Hz, 1H), 4.11 (d, *J* = 11.7 Hz, 1H), 3.80-3.69 (m, 2H), 1.89-1.58 (m, 2H), 0.86 (s, 9H), 0.78 (s, 9H), 0.06 (s, 3H), 0.04 (s, 3H), 0.03 (s, 3H), -0.06 (s, 3H); ^{13}C NMR ($CDCl_3$, 75 MHz) δ 167.4, 165.9, 162.5, 149.5, 136.2, 135.6, 134.1, 133.4, 128.6, 126.1, 103.1, 93.5, 68.2, 64.3, 61.3, 60.3, 60.1, 40.5, 25.9, 25.8, 18.5, 18.1, -4.1, -4.8, -5.3.

Sulfide 215

To a reaction flask was charged PTSH (21 mg, 0.121 mmol) and PPh_3 (24 mg, 0.091 mmol), and a solution of the alcohol **214** (39 mg, 0.060 mmol) in THF (2 mL)

was added, and the mixture was stirred at room temperature. The solution was cooled to 0 °C, and DIAD (21 μL, 0.108 mmol) was added via syringe. The reaction mixture was allowed to warm to room temperature as it stirred for 12 h, after which it was partitioned between saturated aqueous $NaHCO_3$ and EtOAc. The aqueous layer was extracted with additional EtOAc, and the combined organic layers were washed with deionized H_2O and brine, dried over Na_2SO_4, filtered and concentrated under reduced pressure. The residue was purified by column chromatography (hexanes / ethyl acetate gradient) to provide the sulfide **215** (25 mg, 52%). ^{1}H NMR ($CDCl_3$, 300 MHz) δ 8.04 (d, *J* = 7.5 Hz, 2H), 7.64-7.50 (m, 6H), 7.41 (t, *J* = 7.5 Hz, 2H), 7.02 (d, *J* = 9.7 Hz, 1H), 6.37 (dd, *J* = 11.1, 9.7 Hz, 1H), 6.20 (d, *J* = 11.1 Hz, 1H), 5.43 (d, *J* = 8.5 Hz, 1H), 5.05 (d, *J* = 2.6 Hz, 1H), 5.02 (d, *J* = 2.6 Hz, 1H), 4.66 (td, *J* = 8.5, 4.6 Hz, 1H), 4.35 (s, 3H), 4.25 (d, *J* = 11.6 Hz, 1H), 4.11 (d, *J* = 11.6 Hz, 1H), 3.53-3.35 (m, 2H), 2.11-1.95 (m, 2H), 0.82 (s, 9H), 0.77 (s, 9H), 0.00 (s, 9H), -0.08 (s, 3H); ^{13}C NMR ($CDCl_3$, 75 MHz) δ 167.5, 165.8, 162.5, 154.4, 149.5, 135.4, 135.3, 134.9, 133.9, 133.4, 130.0, 130.0, 128.6, 126.3, 124.0, 102.8, 93.5, 67.5, 64.2, 61.1, 60.4, 37.6, 29.9, 29.7, 25.9, 25.8, 18.5, 18.1, -4.1, -4.6, -5.3.

Sulfone 216

A stirred solution of the sulfide **215** (25 mg, 0.031 mmol) in EtOH (1 mL) was cooled to 0 °C, and then a solution of $(NH_4)_6Mo_7O_{24}$*$4H_2O$ (8 mg, 0.006 mmol) in H_2O_2 (48 μL of a 30% w/w aqueous solution, 0.471 mmol) was added slowly. The reaction mixture was allowed to warm to room temperature as it stirred for 12 h, and then it was partitioned between deionized H_2O and Et_2O. The aqueous layer was

extracted twice with additional portions of Et_2O, and the combined organic layers were washed with brine, dried over Na_2SO_4, filtered and concentrated under reduced pressure. Column chromatography (hexanes / ethyl acetate gradient) provided the sulfone **216** (17 mg, 65%). ^{1}H NMR ($CDCl_3$, 400 MHz) δ 8.03 (d, *J* = 8.0 Hz, 2H), 7.76-7.51 (m, 6H), 7.42 (t, *J* = 8.0 Hz, 2H), 7.02 (d, *J* = 10.1 Hz, 1H), 6.38 (dd, *J* = 11.2, 10.1 Hz, 1H), 6.17 (d, *J* = 11.2 Hz, 1H), 5.40 (d, *J* = 8.5 Hz, 1H), 5.06 (d, *J* = 2.6 Hz, 1H), 5.04 (d, *J* = 2.6 Hz, 1H), 4.79 (dt, *J* = 8.5, 5.8 Hz, 1H), 4.31 (s, 3H), 4.29 (d, *J* = 11.9 Hz, 1H), 4.11 (d, *J* = 11.9 Hz, 1H), 4.00-3.77 (m, 2H), 2.21-2.08 (m, 2H), 0.84 (s, 9H), 0.78 (s, 9H), 0.04 (s, 3H), 0.03 (s, 3H), 0.03 (s, 3H), -0.07 (s, 3H).

Julia adduct 217

A reaction flask was charged with the sulfone **216** (30 mg, 0.036 mmol), and then a solution of the aldehyde **167** (1.8 mL of a 20 mg / 5.5 mL solution in THF, ~6 mg, 0.039 mmol). The stirred solution was cooled to -78 °C, and then KHMDS (65 μL of a 15% w/w solution in toluene, 0.043 mmol) was added slowly via syringe causing the solution to turn yellow. The solution was stirred at -78 °C, then was allowed to warm to room temperature, and stirred at room temperature for 0.5 h. The reaction mixture was quenched at 0 °C by the addition of saturated aqueous NH_4Cl, then partitioned between deionized H_2O and Et_2O. The aqueous layer was extracted twice with additional Et_2O, and the combined organic layers were washed with brine, dried over Na_2SO_4, filtered and concentrated under reduced pressure. The residue was purified by column chromatography (100% toluene) to provide the Julia adduct **217** (10 mg, 37%) which eluted before mixed fractions with unreacted aldehyde **167**. ^{1}H

NMR ($CDCl_3$, 400 MHz) δ 8.07 (d, *J* = 8.0 Hz, 2H), 7.55 (t, *J* = 8.0 Hz, 1H), 7.42 (t, *J* = 8.0 Hz, 2H), 7.04 (d, *J* = 9.7 Hz, 1H), 6.36 (dd, *J* = 11.3, 9.7 Hz, 1H), 6.21 (d, *J* = 11.3 Hz, 1H), 6.12 (d, *J* = 15.6 Hz, 1H), 5.87 (s, 1H), 5.80 (s, 1H), 5.64 (dt, *J* = 15.6, 7.5 Hz, 1H), 5.48 (d, *J* = 8.4 Hz, 1H), 5.50-5.40 (m, 1H), 5.04 (d, *J* = 2.6 Hz, 1H), 5.02 (d, *J* = 2.6 Hz, 1H), 4.47 (td, *J* = 8.4, 4.6 Hz, 1H), 4.39 (s, 3H), 4.29 (d, *J* = 11.7 Hz, 1H), 4.12 (d, *J* = 11.7 Hz, 1H), 2.45-2.12 (m, 2H), 1.92 (s, 3H), 1.89 (s, 3H), 1.77 (s, 3H), 1.72 (d, *J* = 6.0 Hz, 3H), 0.86 (s, 9H), 0.78 (s, 9H), 0.05 (s, 3H), 0.03 (s, 3H), 0.01 (s, 3H), -0.07 (s, 3H).

Pyran 219

A reaction flask was charged with powdered 4 Å molecular sieves (10 mg), NMO (13 mg, 0.111 mmol), and a solution of stille adduct **212b** *"Diastereomer B"* (51 mg, 0.074 mmol) in CH_2Cl_2 (3 mL). To the stirred suspension was added TPAP (1 mg, 0.004 mmol) at room temperature, and the solution turned from green to black. The reaction mixture was filtered through a plug of silica with CH_2Cl_2, and the filtrate was concentrated under reduced pressure to provide the pyran **219** (10 mg, 20%) as a yellow oil, it fluoresced a bright yellow under long wave (365 nm) irradiation. ^{1}H NMR ($CDCl_3$, 500 MHz) δ 6.90-6.79 (m, 3H), 5.99 (d, *J* = 5.2 Hz, 1H), 5.94 (d, *J* = 5.7 Hz, 1H), 5.08 (d, *J* = 2.6 Hz, 1H), 5.06 (d, *J* = 2.6 Hz, 1H), 4.82 (d, *J* = 4.6 Hz, 1H), 4.42 (d, *J* = 11.5 Hz, 1H), 4.38 (d, *J* = 11.5 Hz, 1H), 4.30-4.24 (m, 1H), 4.15 (br, 2H), 4.13 (s, 3H), 3.87 (s, 3H), 3.87 (s, 3H), 3.64-3.50 (m, 2H), 2.03-1.90 (m, 2H), 0.89 (s, 9H), 0.87 (s, 9H), 0.04 (br, 9H), 0.02 (s, 3H); ^{13}C NMR ($CDCl_3$, 125 MHz) δ 167.2, 162.2, 149.7, 149.0, 148.6, 142.2, 131.2, 130.1, 120.1, 120.3, 118.3, 111.1,

110.9, 105.4, 102.1, 93.4, 79.8, 72.9, 69.4, 66.3, 64.5, 62.3, 56.0, 55.9, 32.7, 26.0, 18.5, 18.2, -4.2, -4.7, -5.1, -5.2.

Lactol 235

To a stirred -78 °C solution of the dienol **234** (1.06 g, 8.4 mmol) and α-acetoxy acrolein **226** (1.15 g, 10 mmol) in CH_2Cl_2 (75 mL) was added $MeAlCl_2$ (10 mL of a 1.0 M solution in hexanes, 10 mmol) dropwise via syringe. The solution stirred for 0.5 h at this temperature after which time no **234** was visible by TLC. The reaction was quenched by the addition of a saturated aqueous $NaHCO_3$ solution and allowed to warm to room temperature. The mixture was partitioned between deionized water and CH_2Cl_2, and the aqueous layer was extracted with an additional portion of CH_2Cl_2. The combined organic layers were washed with brine, dried over Na_2SO_4, filtered and concentrated under reduced pressure. Column chromatography of the residue provided the lactol **235** (1.4 g, 69%) as a mixture of epimers. *Major epimer* ^{1}H NMR ($CDCl_3$, 500 MHz) δ 5.79 (s, 1H), 5.08 (br, 1H), 3.92 (d, *J* = 8.6 Hz, 1H), 3.76 (d, *J* = 8.6 Hz, 1H), 2.48-2.37 (m, 1H), 2.14 (s, 3H), 1.90 (dd, *J* = 13.7, 4.6 Hz, 1H), 1.70 (s, 3H), 1.49 (t, *J* = 13.7 Hz, 1H), 1.22 (s, 3H), 1.05 (d, *J* = 6.9 Hz, 3H); ^{13}C NMR ($CDCl_3$, 100 MHz) δ 170.2, 137.4, 125.9, 101.3, 81.3, 77.8, 43.3, 39.9, 29.2, 21.9, 21.6, 21.0, 19.1.

Lactone 236

A reaction flask was charged with powdered 4 Å molecular sieves (100 mg), NMO (301 mg, 2.60 mmol), and then a solution of the lactol **235** (412 mg, 1.71 mmol)

in freshly distilled MeCN (4 mL). To the stirred suspension was added TPAP (30 mg, 0.086 mmol) at room temperature, and the color slowly changed from green to black over 3-4 hours, and stirring continued until **235** was no longer visible by TLC. The suspension was concentrated to about 1 mL of liquid volume, and then was filtered through a short plug of silica with CH_2Cl_2 : EtOAc (4:1) to provide the lactone **236** (329 mg, 81%) as an oil which solidified at 4 °C. Diffraction quality crystals were obtained by perfusion of hexanes into an ethyl acetate solution of **236**. ^{1}H NMR ($CDCl_3$, 400 MHz) δ 5.08 (s, 1H), 4.24 (d, *J* = 8.2 Hz, 1H), 4.02 (d, *J* = 8.2 Hz, 1H), 2.31-2.20 (m, 1H), 2.07 (br, 1H), 2.06 (d, *J* = 0.9 Hz, 1H), 1.72 (s, 3H), 1.06 (s, 3H), 1.04 (d, *J* = 7.5 Hz, 3H); ^{13}C NMR ($CDCl_3$, 100 MHz) δ 175.8, 170.0, 139.0, 126.2, 79.6, 78.7, 43.1, 35.2, 31.8, 21.7, 20.9, 20.7, 19.3.

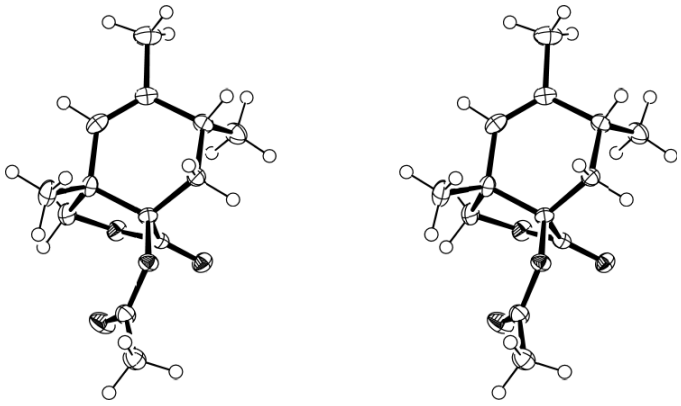

Figure 2.9 ORTEP stereopair drawing of the X-ray crystal structure of lactone **236** with ellipsoids drawn at the 50% probability level

Structure report for lactone 236 (Burk10):

Table 2.18 Crystal data and structure refinement for burk10.

Identification code	burk10	
Empirical formula	C13 H18 O4	
Formula weight	238.27	
Temperature	123(2) K	
Wavelength	0.71073 Å	
Crystal system	Monoclinic	
Space group	P2(1)	
Unit cell dimensions	a = 6.507(5) Å	α= 90°
	b = 12.432(9) Å	β= 100.905(10)°
	c = 7.892(6) Å	γ = 90°
Volume	626.9(8) $Å^3$	
Z	2	
Density (calculated)	1.262 g/cm^3	
Absorption coefficient	0.093 mm^{-1}	
F(000)	256	
Crystal size	0.24 x 0.14 x 0.12 mm^3	
Crystal color, habit	Colorless block	
Theta range for data collection	2.63 to 25.36°	
Index ranges	-7<=h<=7, -14<=k<=9, -8<=l<=9	
Reflections collected	5126	
Independent reflections	1806 [R(int) = 0.0306]	
Completeness to theta = 25.00°	96.9 %	
Absorption correction	Multi-scan	
Refinement method	Full-matrix least-squares on F^2	
Data / restraints / parameters	1806 / 1 / 158	
Goodness-of-fit on F^2	1.041	
Final R indices [I>2sigma(I)]	R1 = 0.0314, wR2 = 0.0811	
R indices (all data)	R1 = 0.0329, wR2 = 0.0828	
Absolute structure parameter	0.4(10)	
Largest diff. peak and hole	0.204 and -0.180 e $Å^{-3}$	

Table 2.19 Atomic coordinates (x 10^4) and equivalent isotropic displacement parameters ($Å^2$x 10^3)for burk10. U(eq) is defined as one third of the trace of the orthogonalized U^{ij} tensor.

	x	y	z	U(eq)
O(1)	-1066(2)	8723(1)	6855(2)	19(1)
O(2)	2377(2)	8292(1)	7381(2)	31(1)
O(3)	1191(2)	7238(1)	4105(2)	23(1)
O(4)	782(2)	9007(1)	3625(2)	24(1)
C(1)	-5914(3)	6124(2)	1560(3)	32(1)
C(2)	-4470(3)	6775(2)	2893(2)	22(1)
C(3)	-4492(3)	7986(2)	2645(2)	21(1)
C(4)	-3567(3)	8555(2)	4335(2)	19(1)
C(5)	-1512(3)	8072(2)	5287(2)	18(1)
C(6)	931(3)	8792(2)	7755(2)	23(1)
C(7)	1073(3)	9564(2)	9219(2)	27(1)
C(8)	-3225(3)	6306(2)	4227(2)	23(1)
C(9)	-1605(3)	6846(2)	5596(2)	21(1)
C(10)	578(3)	6460(2)	5296(3)	25(1)
C(11)	289(3)	8192(2)	4271(2)	18(1)
C(12)	-2001(4)	6544(2)	7394(2)	29(1)
C(13)	-3496(3)	8310(2)	1097(2)	27(1)

Table 2.20 Bond lengths [Å] and angles [°] for burk10.

O(1)-C(6)	1.361(2)	C(3)-C(4)	1.529(3)
O(1)-C(5)	1.461(2)	C(3)-C(13)	1.541(2)
O(2)-C(6)	1.210(2)	C(4)-C(5)	1.527(3)
O(3)-C(11)	1.341(3)	C(5)-C(11)	1.547(2)
O(3)-C(10)	1.455(3)	C(5)-C(9)	1.547(3)
O(4)-C(11)	1.205(3)	C(6)-C(7)	1.492(3)
C(1)-C(2)	1.507(3)	C(8)-C(9)	1.516(3)
C(2)-C(8)	1.335(3)	C(9)-C(12)	1.536(3)

Table 2.20 Bond lengths [Å] and angles [°] for burk10, continued.

C(2)-C(3)	1.518(3)	C(9)-C(10)	1.559(3)
C(6)-O(1)-C(5)	119.60(13)	O(2)-C(6)-O(1)	123.39(18)
C(11)-O(3)-C(10)	110.25(14)	O(2)-C(6)-C(7)	125.64(19)
C(8)-C(2)-C(1)	121.4(2)	O(1)-C(6)-C(7)	110.96(16)
C(8)-C(2)-C(3)	121.65(19)	C(2)-C(8)-C(9)	127.2(2)
C(1)-C(2)-C(3)	116.91(19)	C(8)-C(9)-C(12)	109.54(17)
C(2)-C(3)-C(4)	110.71(16)	C(8)-C(9)-C(5)	111.52(17)
C(2)-C(3)-C(13)	111.49(16)	C(12)-C(9)-C(5)	113.89(16)
C(4)-C(3)-C(13)	114.54(16)	C(8)-C(9)-C(10)	106.63(16)
C(5)-C(4)-C(3)	114.27(16)	C(12)-C(9)-C(10)	112.46(17)
O(1)-C(5)-C(4)	102.36(14)	C(5)-C(9)-C(10)	102.42(15)
O(1)-C(5)-C(11)	109.69(15)	O(3)-C(10)-C(9)	105.24(16)
C(4)-C(5)-C(11)	112.71(15)	O(4)-C(11)-O(3)	123.13(15)
O(1)-C(5)-C(9)	114.82(15)	O(4)-C(11)-C(5)	126.06(18)
C(4)-C(5)-C(9)	114.07(16)	O(3)-C(11)-C(5)	110.71(15)
C(11)-C(5)-C(9)	103.46(14)		

Table 2.21 Anisotropic displacement parameters ($Å^2 x\ 10^3$) for burk10. The anisotropic displacement factor exponent takes the form: $-2\pi^2[\ h^2\ a^{*2}U^{11} + ... + 2\ h\ k\ a^*\ b^*\ U^{12}]$

	U^{11}	U^{22}	U^{33}	U^{23}	U^{13}	U^{12}
O(1)	20(1)	20(1)	18(1)	-5(1)	2(1)	1(1)
O(2)	24(1)	37(1)	30(1)	-9(1)	-1(1)	7(1)
O(3)	21(1)	21(1)	28(1)	-2(1)	8(1)	4(1)
O(4)	23(1)	22(1)	28(1)	0(1)	8(1)	-3(1)
C(1)	24(1)	34(2)	37(1)	-14(1)	5(1)	-3(1)
C(2)	20(1)	25(1)	22(1)	-5(1)	7(1)	-2(1)
C(3)	18(1)	24(1)	22(1)	-1(1)	3(1)	1(1)
C(4)	17(1)	19(1)	22(1)	0(1)	4(1)	1(1)
C(5)	18(1)	18(1)	18(1)	-3(1)	4(1)	-1(1)
C(6)	23(1)	25(1)	20(1)	1(1)	3(1)	0(1)
C(7)	27(1)	29(1)	23(1)	-3(1)	2(1)	2(1)

Table 2.21 Anisotropic displacement parameters ($Å^2 x\ 10^3$) for burk10. The anisotropic displacement factor exponent takes the form: $-2\pi^2[h^2 a^{*2} U^{11} + ... + 2 h k a^* b^* U^{12}]$, continued.

	U^{11}	U^{22}	U^{33}	U^{23}	U^{13}	U^{12}
C(8)	26(1)	18(1)	28(1)	-5(1)	12(1)	-4(1)
C(9)	26(1)	15(1)	23(1)	1(1)	6(1)	3(1)
C(10)	26(1)	21(1)	27(1)	2(1)	5(1)	6(1)
C(11)	17(1)	21(1)	17(1)	-3(1)	1(1)	0(1)
C(12)	46(1)	20(1)	23(1)	4(1)	10(1)	1(1)
C(13)	26(1)	36(1)	20(1)	4(1)	4(1)	-1(1)

Table 2.22 Hydrogen coordinates ($x\ 10^4$) and isotropic displacement parameters ($Å^2 x\ 10^3$) for burk10.

	x	y	z	U(eq)
H(1A)	-5783	5360	1868	48
H(1B)	-5537	6232	427	48
H(1C)	-7361	6358	1518	48
H(3)	-5997	8204	2350	25
H(4A)	-3329	9320	4084	23
H(4B)	-4603	8530	5106	23
H(7A)	2405	9461	10021	40
H(7B)	-87	9437	9825	40
H(7C)	995	10302	8774	40
H(8)	-3371	5549	4330	28
H(10A)	1604	6449	6396	30
H(10B)	481	5729	4790	30
H(12A)	-3318	6868	7569	44

Table 2.22 Hydrogen coordinates (x 10^4) and isotropic displacement parameters ($Å^2$ x 10^3) for burk10, continued.

	x	y	z	U(eq)
H(12B)	-847	6811	8276	44
H(12C)	-2090	5760	7485	44
H(13A)	-2110	7978	1213	41
H(13B)	-3357	9094	1068	41
H(13C)	-4388	8063	25	41

Spirotetronate 237

To a stirred -30 °C solution of the lactone **236** (200 mg, 0.839 mmol) in THF (7 mL) was added a solution of TBSCl (328 mg, 2.18 mmol) in THF (7 mL). To this stirred solution was added KHMDS (3.31 mL of a 15% w/w solution in toluene, 2.18 mmol) slowly via syringe, and the solution was allowed to slowly warm to room temperature. The solution stirred at room temperature for 3 h, and then was quenched by the addition of a saturated aqueous NH_4Cl solution, and then the mixture was diluted with EtOAc and deionized H_2O. The aqueous layer was extracted with additional EtOAc, and the combined organic layers were washed with brine, dried over Na_2SO_4, filtered and concentrated under reduced pressure to provide the intermediate spirotetronic acid. *Crude Dieckmann product intermediate*: ^1H NMR ($CDCl_3$, 400 MHz) see Spectrum 2.107

The crude intermediate described above was dissolved in toluene (10 mL) and MeOH (4 mL), and to the stirred solution was added $TMSCHN_2$ (840 μL of a 2.0 M solution in hexanes, 1.67 mmol) via syringe. The solution stopped bubbling and retained the yellow color part of the way through the addition. The solution stirred for 30 min at room temperature, and then the excess $TMSCHN_2$ was quenched by the dropwise addition of AcOH. When the yellow color had faded, the reaction mixture was concentrated under reduced pressure and the residue was purified by column chromatography to provide the spirotetronate **237** (86 mg, 28% over 2 steps) and an unidentified lower R_f product. ^{1}H NMR ($CDCl_3$, 500 MHz) δ 5.05 (s, 1H), 4.99 (s, 1H), 3.83 (s, 3H), 3.52 (d, *J* = 10.0 Hz, 1H), 3.38 (d, *J* = 3.38 Hz, 1H), 2.51-2.35 (m, 1H), 1.73-1.66 (m, 2H), 1.69 (s, 3H), 1.02 (d, *J* = 6.9 Hz, 3H), 0.88 (s, 9H), 0.01 (s, 6H).

Tricyclic acetal 238

To a cooled (0 °C) and stirred solution of the spirotetronate **237** (86 mg, 0.235 mmol) in THF (2 mL) was added TBAF (469 μL of a 1.0 M solution in THF, 0.469 mmol) slowly via syringe. When no more starting material remained by TLC, the reaction was partitioned between EtOAc and deionized water, and the aqueous layer was extracted with additional EtOAc. The combined organic layers were washed with brine, dried over Na_2SO_4, filtered and concentrated under reduced pressure. The residue was purified by column chromatography (hexanes / ethyl acetate gradient) to provide the tricyclic acetal **238**. ^{1}H NMR ($CDCl_3$, 400 MHz) δ 5.10 (s, 1H), 3.60 (s, 2H), 3.32 (s, 3H), 2.86 (s, 2H), 2.48-2.35 (m, 1H), 1.80-1.75 (m, 2H), 1.71 (s, 3H),

1.06 (s, 3H), 1.05 (d, 3H); ^{13}C NMR ($CDCl_3$, 100 MHz) δ 173.2, 139.7, 124.0, 110.7, 94.9, 51.1, 47.8, 39.6, 36.5, 29.3, 25.8, 22.3, 20.9, 18.7.

Aldol adduct 241

To a stirred -78 °C solution of freshly distilled ethyl propionate **239** (356 μL, 3.10 mmol) in CH_2Cl_2 (11 mL) was added Bu_2BOTf (1.23 g, 4.50 mmol) slowly via syringe. The solution stirred for 30 min, and then i-Pr_2NEt (1.08 mL, 6.20 mmol) was added dropwise via syringe. The solution stirred at -78 °C for 4 h, and then a solution of the aldehyde **240** (500 mg, 4.0 mmol) in CH_2Cl_2 (2 mL) slowly via syringe, and the solution continued to stir at this temperature for 2 h, and then was allowed to warm to 0 °C over 3 h. The reaction was quenched by the addition of a pH 7 buffered solution, and MeOH. The quenched reaction mixture was cooled to 0 °C, then a solution of 30 mL of a 2:1 MeOH / 30% aqueous H_2O_2 mixture was slowly added. The solution was then diluted with deionized H_2O and CH_2Cl_2, and the layers were separated. The aqueous layer was extracted with additional CH_2Cl_2 and the combined organic layers were washed with a saturated aqueous $NaHCO_3$ solution, brine, and then dried over Na_2SO_4. The organic layer was then filtered and concentrated under reduced pressure, and column chromatography of the residue provided the aldol adduct **241** (368 mg, 53%). ^{1}H NMR ($CDCl_3$, 500 MHz) δ 5.93 (s, 1H), 5.37 (q, *J* = 6.9 Hz, 1H), 4.28 (m, 1H), 4.13 (q, *J* = 7.5 Hz, 2H), 2.71-2.68 (m, 1H), 2.40 (d, *J* = 3.4 Hz, 1H), 1.73 (s, 3H), 1.73 (s, 3H), 1.67 (d, *J* = 6.9 Hz, 2H), 1.25 (t, *J* = 7.5 Hz, 3H), 1.15 (d, *J* = 7.4 Hz, 3H).

Diels-Alder adduct 243

To a stirred -78 °C solution of the aldol adduct **241** (366 mg, 1.62 mmol) and α-acetoxy acrolein **226** (221 mg, 1.94 mmol) in CH_2Cl_2 (15 mL) was added $MeAlCl_2$ (1.94 mL of a 1.0 M solution in hexanes, 1.94 mmol), and the solution stirred at -78 °C for 30 min. After this period of time, TLC analysis indicated that starting material was still present, so the reaction was warmed to -50 °C and monitored by TLC. The reaction was quenched by the addition of a saturated aqueous $NaHCO_3$ solution and warmed to room temperature. The mixture was partitioned between deionized water and CH_2Cl_2, and the aqueous layer was extracted with an additional portion of CH_2Cl_2. The combined organic layers were washed with brine, dried over Na_2SO_4, filtered and concentrated under reduced pressure. Column chromatography of the residue provided the Diels-Alder adduct **243** (202 mg, 37%) as a mixture of epimers and diastereomers and unreacted aldol adduct **241** (177 mg) so that the yield was 70.8% BORSM. ^{1}H NMR ($CDCl_3$, 400 MHz) – mixture of epimers and diastereomers, see Spectrum 2.119, and ^{13}C NMR ($CDCl_3$, 100 MHz) - Spectrum 2.120.

Lactone 244

A reaction flask was charged with powdered 4 Å molecular sieves (30 mg), NMO (28 mg, 0.242 mmol), and then a solution of the Diels-Alder adduct **243** (55 mg, 0.162 mmol) in freshly distilled MeCN (1 mL). The suspension was stirred at room temperature as TPAP (3 mg, 0.008 mmol) was added, and the suspension slowly turned from green to black. The reaction mixture was filtered through a short silica gel plug with CH_2Cl_2:EtOAc (4:1) and the filtrate was concentrated to provide the

lactone **244** (49 mg, 90%) as a 1.7:1 mixture of diastereomers. ^{1}H NMR – diastereomers, see Spectrum 2.121. ESI-MS *m/z* 361.12 $[M+Na]^+$, 355.99 $[M+NH_4]^+$, 338.87 $[M+H]^+$.

Diels-Alder adduct 245

To a stirred -78 °C solution of the silyl ether **242** (64 mg, 0.188 mmol) and α-acetoxy acrolein **226** (26 mg, 0.225 mmol) in CH_2Cl_2 (2 mL) was added $MeAlCl_2$ (225 μL of a 1.0 M solution in hexanes, 0.225 mmol) slowly via syringe. The reaction was allowed to warm to -50 °C for 30 min, and then was quenched by the addition of saturated aqueous $NaHCO_3$ and warmed to room temperature. The mixture was partitioned between deionized H_2O and CH_2Cl_2, and the aqueous layer was extracted with an additional portion of CH_2Cl_2. The combined organic layers were washed with brine, dried over Na_2SO_4, filtered and concentrated under reduced pressure. The residue was purified by column chromatography to provide the Diels-Alder adduct **245** (14 mg, 17%) as a mixture of epimers and diastereomers, and the silyl ether **242** (33 mg) such that the yield was 34% BORSM. ^{1}H NMR ($CDCl_3$, 500 MHz) – mixture of epimers and diastereomers, see Spectrum 2.122.

Lactone 246

The Diels-Alder adduct **245** (14 mg, 0.0315 mmol) was oxidized in the same fashion as the oxidation of **243** to **244** described above. The lactone **246** (12 mg, 90%) was obtained, and the ^{1}H NMR ($CDCl_3$, 400 MHz) – see Spectrum 2.123 indicated a 1.9:1 mixture of diastereomers.

Ester 251

A stirred solution of the dienol **234** (1.05 g, 8.36 mmol) in THF (15 mL) was cooled to -78 °C, and then n-BuLi (4.70 mL of a 1.96 M solution in hexanes, 9.2 mmol) was added slowly via syringe. The solution stirred at this temperature for 15 min before MsCl (712 μL, 9.2 mmol) was added, and reaction stirred for an additional 15 min. To the reaction mixture was then transferred a solution of LiBr (3.27 g, 37.6 mmol) in THF (7 mL) via cannula, and the mixture was allowed to warm to room temperature, and stirred for 1 h.

A separate reaction flask was charged with THF (25 mL) and freshly distilled ethyl propionate (885 μL, 7.69 mmol), and stirred as it was cooled to -78 °C. LiHMDS (7.89 mL of a 1.06 M solution in THF, 8.36 mmol) was added via syringe, and the reaction mixture stirred at this temperature for 30 min. After this period of time, the solution of the crude mesylate / bromide described above was transferred via cannula to the reaction flask, and the reaction stirred at -78 °C for 10 min, then was allowed to warm to room temperature. The mixture stirred at room temperature for 12 h, then was quenched by the addition of a saturated aqueous NH_4Cl solution. The mixture was partitioned between deionized H_2O and Et_2O, and the aqueous layer was extracted with additional Et_2O. The combined organic layers were washed with brine, dried over Na_2SO_4, filtered and concentrated under reduced pressure. Column chromatography of the residue (15:1 hexanes / Et_2O) provided the ester **251** (460 mg, 28%). ^{1}H NMR ($CDCl_3$, 400 MHz) δ 5.64 (s, 1H), 5.31 (q, J = 6.8 Hz, 1H), 4.11 (q, J

= 7.1 Hz, 2H), 2.67-2.58 (m, 1H), 2.39 (dd, *J* = 13.4, 7.3 Hz, 1H), 2.07 (dd, *J* = 13.4, 7.7 Hz, 1H), 1.73 (s, 3H), 1.69 (s, 3H), 1.66 (d, *J* = 6.8 Hz, 3H), 1.24 (t, *J* = 7.1 Hz, 3H), 1.11 (d, *J* = 6.9 Hz, 3H).

Silyl ether 252

To a stirred -78 °C solution of the ester **251** (460 mg, 2.20 mmol) in Et_2O (20 mL) was added DIBAL-H (5.1 mL of a 1.5 M solution in toluene, 7.66 mmol) slowly via syringe. The reaction stirred until no more **251** remained by TLC analysis (2:1 hexanes / Et_2O), and then was quenched by the dropwise addition of MeOH until gas evolution stopped, and then a saturated aqueous solution of Rochelle's salt. The mixture was allowed to warm to room temperature and stirred until the layers separated. The aqueous layer was extracted twice with additional Et_2O, and the combined organic layers were washed with brine, dried over Na_2SO_4, filtered and concentrated under reduced pressure. The residue was purified by column chromatography to provide the intermediate alcohol (310 mg, 84%). ^{1}H NMR ($CDCl_3$, 400 MHz) δ 5.66 (s, 1H), 5.32 (q, *J* = 6.8 Hz, 1H), 3.52 (dt, *J* = 10.9, 5.5 Hz, 1H), 3.44 (dt, *J* = 10.9, 5.5 Hz, 1H), 2.17-2.05 (m, 1H), 1.93-1.80 (m, 2H), 1.75 (s, 3H), 1.73 (s, 3H), 1.67 (d, *J* = 6.8 Hz, 3H), 1.39 (t, *J* = 5.5 Hz, 1H), 0.89 (d, *J* = 6.5 Hz, 3H); ^{13}C NMR ($CDCl_3$, 100 MHz) δ 133.9, 133.6, 130.7, 123.6, 68.7, 45.4, 34.0, 17.9, 16.9, 16.9, 13.8.

To a solution of the above described intermediate alcohol (310 mg, 1.84 mmol) in DMF (5 mL) was added imidazole (238 mg, 3.49 mmol) and TIPSCl (433 μL, 2.00

mmol). The solution stirred for 12 h at room temperature, and then it was partitioned between saturated aqueous $NaHCO_3$ and 1:1 hexanes / Et_2O. The organic layer was washed with deionized H_2O and then brine, and then was dried over Na_2SO_4, filtered and concentrated under reduced pressure. The residue was purified by column chromatography (100% hexanes to 30:1 hexanes / Et_2O gradient) to provide the silyl ether **252** (460 mg, 78%). ^{1}H NMR ($CDCl_3$, 400 MHz) δ 5.61 (s, 1H), 5.31 (q, *J* = 6.8 Hz, 1H), 3.53 (dd, *J* = 9.5, 5.7 Hz, 1H), 3.46 (dd, *J* = 9.5, 6.3 Hz, 1H), 2.21 (dd, *J* = 12.6, 5.5 Hz, 1H), 1.89-1.75 (m, 2H), 1.72 (s, 3H), 1.70 (s, 3H), 1.67 (d, *J* = 6.8 Hz, 3H), 1.10-0.99 (m, 21 H), 0.86 (d, *J* = 6.5 Hz, 3H).

Diels-Alder adduct 253

To a stirred -78 °C solution of the silyl ether **252** (460 mg, 1.42 mmol) and α-acetoxy acrolein **226** (290 mg, 2.51 mmol) in CH_2Cl_2 (12 mL) was added $MeAlCl_2$ (1.70 mL of a 1.0 M solution in hexanes, 1.70 mmol) slowly via syringe. The reaction was monitored by TLC, and after 0.5 h, no more starting material **252** was visible. The reaction was quenched by the addition of a saturated aqueous $NaHCO_3$ solution, and allowed to warm to room temperature. The mixture was partitioned between deionized H_2O and CH_2Cl_2, and the aqueous layer was extracted with an additional portion of CH_2Cl_2. The combined organic layers were washed with brine, dried over Na_2SO_4, filtered and concentrated under reduced pressure. The residue was purified by column chromatography to provide the Diels-Alder adduct **253** (330 mg, 53%) as a 1:1 mixture of diastereomers. ^{1}H NMR ($CDCl_3$, 400 MHz) – see Spectrum 2.128, mixture of diastereomers.

Ester 254

The Diels-Alder adduct **253** (400 mg, 0.912 mmol) was dissolved in *t*-BuOH (18.8 mL) and acetone (6.3 mL), and the stirred solution was cooled to 0 °C. To the solution was added KH_2PO_4 (4.74 mL of a 1.25 M aqueous solution, 5.93 mmol), followed by $KMnO_4$ (6.38 mL of a 0.5 M aqueous solution, 3.19 mmol), and the solution was stirred at 0 °C for 10 min, then allowed to warm to room temperature and stirred for 1 h. The reaction was quenched by the addition of a 10% aqueous $Na_2S_2O_3$ solution, and the mixture was partitioned between deionized H_2O and EtOAc. The aqueous layer was extracted with three portions of EtOAc, and the combined organic layers were dried over Na_2SO_4, filtered and concentrated under reduced pressure. The crude residue was taken up in toluene (10 mL) and MeOH (2 mL), and the stirred mixture was cooled to 0 °C. To the mixture was added $TMSCHN_2$ (5.8 mL of a 10% w/w solution in hexanes, 3.65 mmol) and the solution was allowed to warm to room temperature and stirred an additional 0.5 h. The reaction was re-cooled to 0 °C, quenched by the addition of saturated aqueous $NaHCO_3$, and partitioned between deionized H_2O and EtOAc. The aqueous layer was extracted twice with additional EtOAc, and the combined organic layers were washed with brine, dried over Na_2SO_4, filtered and concentrated under reduced pressure. The residue was purified by column chromatography to provide the ester **254** (157 mg, 37%) still as the mixture of diastereomers. ^1H NMR ($CDCl_3$, 400 MHz) – see Spectrum 2.129. Mixture of diastereomers.

Aldehyde 255

A solution of the ester **254** (180 mg, 0.384 mmol) in MeCN (2 mL) was stirred in a plastic vial. To the solution was added HF-py (0.1 mL of a 70% w/w solution, 3.84 mmol), and the solution was stirred until no more of the starting material **254** could be observed by TLC. The solution was quenched by the cautious addition of saturated aqueous $NaHCO_3$, and then was partitioned between deionized H_2O and EtOAc. The aqueous layer was extracted with two additional portions of EtOAc, and the combined organic layers were washed with brine, dried over Na_2SO_4, filtered and concentrated under reduced pressure. The residue was purified by column chromatography to provide the intermediate alcohol (101 mg, 84%), still as the mixture of diastereomers. ^1H NMR ($CDCl_3$, 500 MHz) – see Spectrum 2.130. Mixture of diastereomers. ESI-MS *m/z* 335.11 $[M+Na]^+$, 329.93 $[M+NH_4]^+$, 312.94 $[M+H]^+$.

A reaction flask was charged with powdered 4 Å molecular sieves (50 mg), NMO (18 mg, 0.149 mmol), and a solution of the above described intermediate alcohol (31 mg, 0.099 mmol) in CH_2Cl_2 (1 mL). The suspension was stirred at room temperature as TPAP (single crystal, catalytic amount) was added. The suspension turned from green to black and a new higher R_f, DNP active spot was observed by TLC concurrently with the disappearance of the intermediate alcohol. The suspension was filtered through a short silica gel plug with 4:1 CH_2Cl_2:EtOAc, and the filtrate was concentrated under reduced pressure to provide the aldehyde **255** (32 mg,

quantitative) still as the mixture of diastereomers. ^{1}H NMR ($CDCl_3$, 400 MHz) – see Spectrum 2.131. Mix of diastereomers.

Aldehyde 256

A reaction flask was charged with 4 Å molecular sieves, aldehyde **255** (30 mg, 0.097 mmol as a solution in 2 mL toluene), and freshly distilled piperidine (12 μL, 0.121 mmol). The stirred mixture was heated to 80 °C for 3 h, then cooled to room temperature and filtered through a celite plug, which was washed with a few mL of THF. The filtrate was concentrated under reduced pressure, and the crude enamine residue was taken up in THF (2 mL), and the solution was stirred and cooled to -95 °C with a liquid N_2 / hexanes bath. To the cooled solution was added PhSeCl (23 mg, 121 mmol, solution in 300 μL THF) slowly over 5 min. The solution was warmed to -78 °C where it was stirred for 20 min, then was quenched by the addition of H_2O (500 μL) and Et_2O (5 mL). The mixture was warmed to room temperature and stirred for 3 h, then diluted with Et_2O and deionized H_2O. The aqueous layer was extracted with three portions of additional Et_2O and the combined organic layers were washed successively with aqueous saturated $NaHCO_3$ and brine. The solution was dried over Na_2SO_4, filtered and concentrated under reduced pressure. The residue was then suspended in MeOH:THF:H_2O (2 mL: 1 mL : 1 mL) and stirred at 0 °C while $NaIO_4$ (41 mg, 0.193 mmol) was added, and the solution was allowed to warm to room temperature and stirred for 1 h. Two more additions of $NaIO_4$ (41 mg, 0.193 mmol) each at 0 °C, then stirring at room temperature for 1 h were needed to consume the starting α-selenoaldehydes by TLC analysis. When the starting material had been

consumed, the reaction was cooled to 0 °C and diluted with Et_2O, and quenched by the addition of saturated aqueous $Na_2S_2O_3$ (3 mL). The mixture was partitioned between deionized H_2O and Et_2O, and the aqueous layer was extracted with two additional portions of Et_2O. The combined organic layers were washed with brine, dried over Na_2SO_4, filtered and concentrated under reduced pressure. Column chromatography (hexane / Et_2O gradient) of the residue provided the aldehyde **256**, as a single diastereomer. ^{1}H NMR ($CDCl_3$, 300 MHz) δ 9.49 (s, 1H), 6.25 (s, 1H), 6.13 (s, 1H), 4.66 (s, 1H), 3.76 (s, 3H), 2.66 (dd, *J* = 14.6, 5.3 Hz, 1H), 2.48 (d, *J* = 12.4 Hz, 1H), 2.14-1.96 (m, 3H), 2.06 (s, 3H), 1.62 (s, 3H), 1.06 (s, 3H), 1.06 (d, *J* = 6.8 Hz, 3H).

Benzoate 260

To a stirred -78 °C solution of the triene-ester **259** (839 mg, 4.03 mmol) in Et_2O (40 mL) was added DIBAL-H (5.9 mL of a 1.5 M solution in toluene, 8.86 mmol) slowly via syringe, and the reaction was stirred for 1.5 h at this temperature. The reaction was quenched by the dropwise addition of MeOH, and then a saturated aqueous Rochelle's salt solution, and then allowed to warm to room temperature with stirring. When the layers had separated, the aqueous layer was extracted twice with additional Et_2O, and the combined organic layers were washed with brine, dried over Na_2SO_4, filtered and concentrated under reduced pressure. The residue (670 mg) was dissolved in CH_2Cl_2, and to the solution was added DMAP (49 mg, 0.403 mmol) and Et_3N (841 μL, 6.04 mmol) and the solution was stirred and cooled to 0 °C. To the cooled solution was added BzCl (557 μL, 4.83 mmol) via syringe, and the solution stirred until no more of the alcohol intermediate (R_f < 0.1 in 5:1 hexanes / Et_2O) was

visible, and the product **260** (R_f = 0.5 in 5:1 hexanes / Et_2O) was the predominant component of the mixture. The mixture was then partitioned between CH_2Cl_2 and saturated $NaHCO_3$, and the aqueous layer was washed with additional CH_2Cl_2. The combined organic layers were washed with deionized H_2O, brine, and then dried over Na_2SO_4. The organic layer was then filtered and concentrated under reduced pressure, and the residue was purified by column chromatography (8:1 to 6:1 hexanes / Et_2O) to provide the benzoate **260** (700 mg, 64% over 2 steps). TLC (5:1 hexanes / Et_2O): R_f = 0.5; ^{1}H NMR ($CDCl_3$, 400 MHz) δ 8.07 (d, *J* = 7.5 Hz, 2H), 7.56 (t, *J* = 7.5 Hz, 1H), 7.45 (t, *J* = 7.5 Hz, 2H), 6.05 (s, 1H), 5.84 (s, 1H), 5.45 (q, *J* = 6.8 Hz, 1H), 4.76 (s, 2H), 1.92 (s, 6H), 1.77 (s, 3H), 1.71 (d, *J* = 6.8 Hz, 3H); ^{13}C NMR ($CDCl_3$, 100 MHz) δ 166.6, 135.0, 133.9, 133.5, 133.0, 131.2, 130.5, 129.9, 129.8, 128.5, 125.2, 71.5, 18.8, 16.9, 16.0, 14.0; FTIR (film) νmax 2969, 2917, 2855, 1719, 1449, 1265, 1178, 1108, 1020, 715 cm^{-1}; ESI-MS *m/z* 292.79 $[M+Na]^+$; HR-ESI-MS *m/z* calcd. for $C_{18}H_{22}O_2Na_1$ $[M+Na]^+$: 293.1512, found 293.1513.

Diels-Alder adduct 261

To a stirred -78 °C solution of the benzoate **260** (913 mg, 3.38 mmol) and α-acetoxy acrolein **226** (770 mg, 6.75 mmol) in CH_2Cl_2 (40 mL) was added $MeAlCl_2$ (3.56 mL of a 1.0 M solution in hexanes, 3.55 mmol) slowly via syringe, and the solution stirred at this temperature for 0.5 h. The reaction was then quenched by the addition of a saturated aqueous $NaHCO_3$ solution and allowed to warm to room temperature. The mixture was then partitioned between deionized H_2O and CH_2Cl_2, and the aqueous layer was extracted with additional CH_2Cl_2. The combined organic

layers were washed with brine, dried over Na_2SO_4, filtered and concentrated under reduced pressure. The residue was purified by column chromatography (4:1 to 3:1 hexanes / Et_2O) to provide the Diels-Alder adduct **261** (747 mg, 58%) as a single diastereomer. TLC (3:1 hexanes / Et_2O): $R_f = 0.2$; ^1H NMR ($CDCl_3$, 400 MHz) δ 9.66 (s, 1H), 8.06 (d, *J* = 7.5 Hz, 2H), 7.57 (t, *J* = 7.5 Hz, 1H), 7.45 (t, *J* = 7.5 Hz, 2H), 5.33 (s, 1H), 5.20 (s, 1H), 4.62 (d, *J* = 12.5 Hz, 1H), 4.58 (d, *J* = 12.5 Hz, 1H), 2.52 (dd, *J* = 14.0, 5.3 Hz, 1H), 2.11 (s, 3H), 2.05-1.95 (m, 1H), 1.89 (dd, *J* = 14.0, 11.3 Hz, 1H), 1.83 (s, 3H), 1.73 (s, 3H), 1.29 (s, 3H), 1.05 (d, *J* = 6.9 Hz, 3H); ^{13}C NMR ($CDCl_3$, 100 MHz) δ 199.4, 170.7, 166.4, 135.9, 133.1, 132.8, 130.9, 130.3, 129.8, 128.5, 127.7, 86.3, 71.6, 44.9, 31.9, 30.5, 23.1, 21.0, 18.1, 15.3; FTIR (film) νmax 2966, 2932, 2878, 1663, 1602, 1448, 1374, 1112, 1025, 716 cm^{-1}; ESI-MS *m/z* 407.15 $[M+Na]^+$, 384.92 $[M+H]^+$, 408.17 $[M+NH_4]^+$; HR-ESI-MS *m/z* calcd. for $C_{23}H_{28}O_5Na_1$ $[M+Na]^+$: 407.1829, found 407.1833.

Ester 262

To a stirred 0 °C solution of the Diels-Alder adduct **261** (1.69 g, 4.40 mmol) in MeOH (50 mL) were added successively KOH (44 mL of a 0.78 M solution in MeOH, 34.3 mmol) and I_2 (22 mL of a 0.78 M solution in MeOH, 17.2 mmol), and the darkened solution stirred at this temperature for 45 min. At this time, additional portions of KOH (8.8 mL of the 0.78 M solution in MeOH, 6.86 mmol) and I_2 (4.4 mL of the 0.78 M solution in MeOH, 3.43 mmol) were added, and stirring continued for 30 min at 0 °C. After this period of time, H_2SO_4 (41 mL of a 2N aqueous solution, 82 mmol) was added, and the mixture was allowed to warm to room temperature. The

mixture was diluted with deionized H_2O and Et_2O, and the aqueous layer was extracted with two additional portions of Et_2O. The combined organic layers were washed with saturated aqueous $Na_2S_2O_3$, then brine, then were dried over Na_2SO_4, filtered and concentrated under reduced pressure. The residue was purified by column chromatography (5:2 hexanes / Et_2O to 100% Et_2O gradient) to provide the ester **262** (546 mg, 33%) and then the diol **263** (193 mg, 16%). *Ester **262***: TLC (1:1 hexanes / Et_2O): R_f = 0.4; ^{1}H NMR ($CDCl_3$, 400 MHz) δ 8.05 (d, *J* = 8.0 Hz, 2H), 7.57 (t, *J* = 8.0 Hz, 1H), 7.45 (t, *J* = 8.0 Hz, 2H), 5.31 (s, 1H), 5.19 (s, 1H), 4.64 (d, *J* = 12.8 Hz, 1H), 4.60 (d, *J* = 12.8 Hz, 1H), 3.68 (s, 3H), 3.12 (s, 1H), 2.41-2.28 (m, 1H), 1.94-1.87 (m, 2H), 1.84 (s, 3H), 1.75 (s, 3H), 1.19 (s, 3H), 1.05 (d, *J* = 7.1 Hz, 3H); ^{13}C NMR ($CDCl_3$, 100 MHz) δ 176.0, 166.4, 136.0, 133.1, 133.0, 130.8, 130.5, 129.7, 128.5, 127.6, 78.1, 72.1, 52.5, 45.7, 37.3, 30.3, 22.8, 21.1, 18.3, 15.0; FTIR (film) νmax 3429 br, 2959, 2872, 1716, 1643, 1448, 1367, 1273, 1112, 1031, 716 cm^{-1}; ESI-MS *m/z* 395.05 $[M+Na]^+$, 389.90 $[M+NH_4]^+$, HR-ESI-MS *m/z* calcd. for $C_{22}H_{28}O_5Na_1$ $[M+Na]^+$: 395.1829, found 395.1825.

Diol 263

To a stirred 0 °C solution of ester **262** (511 mg, 1.37 mmol) in MeOH (29 mL) was added KOH (13.7 mL of a 1.0 M solution in MeOH, 13.7 mmol), and the solution was stirred at 0 °C for 2 h, then at room temperature for 2 h. The reaction was then diluted with deionized H_2O and EtOAc, and the aqueous layer was washed with three additional portions of EtOAc. The combined organic layers were washed with brine, dried over Na_2SO_4, filtered and concentrated under reduced pressure. Column

chromatography (1:1 hexanes / EtOAc) provided the diol **263** (310 mg, 84%) and starting ester **262** (79 mg), such that the yield was 99% BORSM. TLC (1:1 hexanes / EtOAc): R_f = 0.3; ^{1}H NMR ($CDCl_3$, 500 MHz) δ 5.17 (s, 2H), 3.89 (d, *J* = 5.8 Hz, 2H), 3.75 (s, 3H), 3.04 (s, 1H), 2.39-2.28 (m, 1H), 1.90-1.87 (m, 2H), 1.76 (s, 3H), 1.74 (s, 3H), 1.18 (s, 3H), 1.05 (d, *J* = 6.9 Hz, 3H); ^{13}C NMR ($CDCl_3$, 125 MHz) δ 175.8, 135.6, 135.5, 130.1, 127.9, 78.3, 70.8, 52.4, 45.5, 37.3, 30.2, 22.9, 21.1, 18.3, 14.8; FTIR (film) νmax 3456 br, 2959, 2872, 1723, 1441, 1381, 1260, 1152, 1125, 1025, 863, 756; ESI-MS *m/z* 307.09 $[M+K]^+$, 291.07 $[M+Na]^+$, 285.90 $[M+NH_4]^+$, 268.90 $[M+H]^+$; HR-ESI-MS *m/z* calcd. for $C_{15}H_{24}O_4Na_1$ $[M+Na]^+$: 291.1567, found 291.1570.

***p*-bromobenzoate 264**

To a reaction flask were charged *p*-bromobenzoic acid (32 mg, 0.160 mmol), CSA (18 mg, 0.080 mmol), DMAP (21 mg, 0.168 mmol), and a solution of the diol **263** (43 mg, 0.160 mmol) in CH_2Cl_2 (5 mL). The solution was stirred as DCC (53 mg, 0.256 mmol) was added in one portion. The reaction was allowed to stir for 3 h at room temperature, and then was diluted with CH_2Cl_2 and 10% aqueous citric acid. The layers were separated, and the organic layer was washed successively with saturated aqueous $NaHCO_3$, deionized H_2O, and then brine. The organic layer was dried over Na_2SO_4, filtered, and concentrated under reduced pressure. The residue was purified by column chromatography (5:3 hexanes / Et_2O) to provide the *p*-bromobenzoate **264** (57 mg, 80%). Diffraction quality crystals were obtained by perfusion of hexanes into an EtOAc solution of **264**, and a neat sample of **264**

solidified in the freezer (mp of the amorphous solid = 49-51 °C (uncorrected). TLC (5:3 hexanes / Et_2O): R_f = 0.2; ^{1}H NMR ($CDCl_3$, 500 MHz) δ 7.91 (d, *J* = 8.6 Hz, 2H), 7.59 (d, *J* = 8.6 Hz, 2H), 5.30 (s, 1H), 5.18 (s, 1H), 4.63 (d, *J* = 11.5 Hz, 1H), 4.58 (d, *J* = 11.5 Hz, 1H), 3.69 (s, 3H), 3.11 (s, 1H), 2.40-2.29 (m, 1H), 1.91-1.87 (m, 2H), 1.83 (s, 3H), 1.75 (s, 3H), 1.19 (s, 3H), 1.05 (d, *J* = 6.9 Hz, 3H); ^{13}C NMR ($CDCl_3$, 100 MHz) δ 175.8, 165.7, 136.1, 133.4, 131.9, 131.2, 130.6, 129.4, 128.2, 127.5, 78.1, 72.5, 52.5, 45.7, 37.4, 30.3, 22.8, 21.1, 18.3, 15.1; ESI-MS *m/z* 474.95 $[M+Na]^+$, 467.76 $[M+H]^+$; HR-ESI-MS *m/z* calcd. for $C_{22}H_{27}Br_1O_5Na_1$ $[M+Na]^+$: 473.0934, found 473.0929.

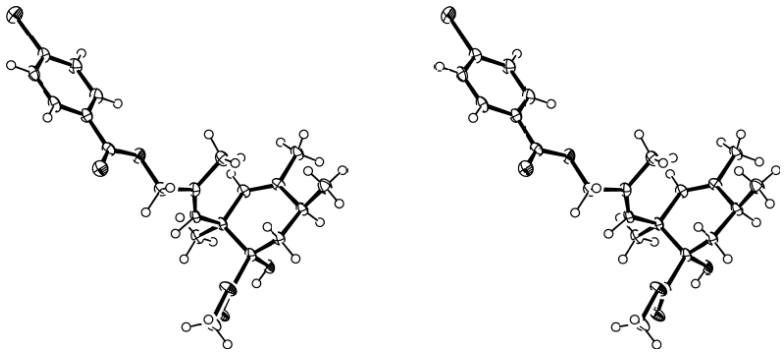

Figure 2.10 ORTEP stereopair drawing of the X-ray crystal structure of compound **264** with ellipsoids drawn at the 50% probability level

Structure report for compound 264 (burk12):

Sample bdj7-134-1

Data collected on June 16-17, 2009

A colorless crystal of sample bdj7-134-1was mounted on a Cryoloop with Paratone-N oil. Data were collected on a Bruker APEX II CCD systems using Mo K alpha radiation in a nitrogen gas stream at 100(2) K using phi and omega scans. Crystal-to-detector distance was 60 mm and exposure time was 10 seconds per frame using a scan width of 0.5°. Indexing and unit cell refinement indicated a primitive, triclinic, P-1. The data were integrated using the Bruker SHELXTL software program and scaled using the SADABS software program. Solution by direct methods (SHELXS) and all non-hydrogen atoms were refined anisotropically by full-matrix least-squares (SHELXL-97).

All hydrogen atoms were placed using a riding model except hydrogen atom on O5 which was allowed to refine. Intramolecular hydrogen bonding noted between O5-H5A and O4. Two residual electron density peaks of 1.47 e/A^3 found at 0.91 and 0.93 Angstroms from atom Br1.

Table 2.23 Crystal data and structure refinement for BURK12.

Identification code	burk12	
Empirical formula	C22 H27 Br O5	
Formula weight	451.35	
Temperature	100(2) K	
Wavelength	0.71073 Å	
Crystal system	Triclinic	
Space group	P-1	
Unit cell dimensions	a = 9.745(3) Å	α= 69.894(5)°.
	b = 10.404(3) Å	β= 67.400(6)°.
	c = 11.659(4) Å	γ = 87.178(5)°.
Volume	1020.2(6) $Å^3$	
Z	2	

Table 2.23 Crystal data and structure refinement for BURK12, continued.

Density (calculated)	1.469 Mg/m^3
Absorption coefficient	2.045 mm^{-1}
F(000)	468
Crystal size	0.10 x 0.10 x 0.10 mm^3
Crystal color and habit	Colorless/.block
Theta range for data collection	2.02 to 27.43°.
Index ranges	-12<=h<=12, -13<=k<=13, -14<=l<=11
Reflections collected	7424
Independent reflections	4169 [R(int) = 0.0458]
Completeness to theta = 25.00°	96.9 %
Absorption correction	multi-scan/sadabs
Max. and min. transmission	0.8216 and 0.8216
Refinement method	Full-matrix least-squares on F^2
Data / restraints / parameters	4169 / 0 / 261
Goodness-of-fit on F^2	1.052
Final R indices [I>2sigma(I)]	R1 = 0.0594, wR2 = 0.1469
R indices (all data)	R1 = 0.0717, wR2 = 0.1568
Largest diff. peak and hole	1.474 and -1.580 $e.Å^{-3}$

Table 2.24 Atomic coordinates (x 10^4) and equivalent isotropic displacement parameters ($Å^2$x 10^3) for BURK12. U(eq) is defined as one third of the trace of the orthogonalized U^{ij} tensor.

	x	y	z	U(eq)
Br(1)	6266(1)	5115(1)	-3092(1)	30(1)
O(1)	-375(3)	6063(3)	1416(3)	28(1)
O(2)	124(3)	4046(3)	2615(3)	24(1)
O(3)	-5403(3)	2105(3)	7061(3)	28(1)
O(4)	-6312(3)	64(3)	7272(3)	29(1)
O(5)	-4526(3)	-1220(3)	8450(3)	21(1)

Table 2.24 Atomic coordinates (x 10^4) and equivalent isotropic displacement parameters ($Å^2$x 10^3) for BURK12. U(eq) is defined as one third of the trace of the orthogonalized U^{ij} tensor, continued.

	x	y	z	U(eq)
C(1)	2717(4)	4004(4)	556(4)	23(1)
C(2)	4025(4)	3998(4)	-488(4)	24(1)
C(3)	4470(4)	5112(4)	-1660(4)	22(1)
C(4)	3647(4)	6242(4)	-1816(4)	22(1)
C(5)	2338(4)	6229(4)	-766(4)	22(1)
C(6)	1866(4)	5119(4)	417(4)	20(1)
C(7)	431(4)	5154(4)	1508(4)	21(1)
C(8)	-1287(4)	3978(4)	3705(4)	22(1)
C(9)	-1354(4)	2721(4)	4860(4)	19(1)
C(10)	-2339(4)	1662(4)	5243(4)	18(1)
C(11)	-2673(4)	227(4)	6294(4)	18(1)
C(12)	-1405(4)	-319(3)	6719(4)	18(1)
C(13)	-1283(4)	-408(4)	7832(4)	19(1)
C(14)	-2416(4)	124(4)	8839(4)	20(1)
C(15)	-3547(4)	904(4)	8321(4)	19(1)
C(16)	-4041(4)	176(3)	7590(4)	18(1)
C(17)	-5375(4)	766(4)	7285(4)	20(1)
C(18)	-6693(5)	2703(5)	6824(5)	40(1)
C(19)	-254(4)	2873(4)	5434(4)	24(1)
C(20)	-3025(4)	-744(4)	5683(4)	21(1)
C(21)	-29(4)	-1070(4)	8178(4)	24(1)
C(22)	-1677(5)	1031(4)	9267(4)	29(1)

Table 2.25 Bond lengths [Å] and angles [°] for BURK12.

Br(1)-C(3)	1.898(4)	C(11)-C(16)	1.570(5)
O(1)-C(7)	1.202(4)	C(12)-C(13)	1.320(5)

Table 2.25 Bond lengths [Å] and angles [°] for BURK12, continued.

O(2)-C(7)	1.341(4)	C(12)-H(12A)	0.9500
O(2)-C(8)	1.455(4)	C(13)-C(21)	1.495(5)
O(3)-C(17)	1.328(4)	C(13)-C(14)	1.515(5)
O(3)-C(18)	1.454(5)	C(14)-C(15)	1.524(5)
O(4)-C(17)	1.204(5)	C(14)-C(22)	1.525(5)
O(5)-C(16)	1.429(4)	C(14)-H(14A)	1.0000
O(5)-H(5A)	0.82(5)	C(15)-C(16)	1.527(5)
C(1)-C(2)	1.385(5)	C(15)-H(15A)	0.9900
C(1)-C(6)	1.393(5)	C(15)-H(15B)	0.9900
C(1)-H(1A)	0.9500	C(16)-C(17)	1.523(5)
C(2)-C(3)	1.380(5)	C(18)-H(18A)	0.9800
C(2)-H(2A)	0.9500	C(18)-H(18B)	0.9800
C(3)-C(4)	1.390(5)	C(18)-H(18C)	0.9800
C(4)-C(5)	1.384(5)	C(19)-H(19A)	0.9800
C(4)-H(4A)	0.9500	C(19)-H(19B)	0.9800
C(5)-C(6)	1.385(5)	C(19)-H(19C)	0.9800
C(5)-H(5B)	0.9500	C(20)-H(20A)	0.9800
C(6)-C(7)	1.494(5)	C(20)-H(20B)	0.9800
C(8)-C(9)	1.503(5)	C(20)-H(20C)	0.9800
C(8)-H(8A)	0.9900	C(21)-H(21A)	0.9800
C(8)-H(8B)	0.9900	C(21)-H(21B)	0.9800
C(9)-C(10)	1.331(5)	C(21)-H(21C)	0.9800
C(9)-C(19)	1.504(5)	C(22)-H(22A)	0.9800
C(10)-C(11)	1.523(5)	C(22)-H(22B)	0.9800
C(10)-H(10A)	0.9500	C(22)-H(22C)	0.9800
C(11)-C(12)	1.518(5)		
C(11)-C(20)	1.536(5)		

C(7)-O(2)-C(8)	115.8(3)	C(2)-C(1)-H(1A)	119.9
C(17)-O(3)-C(18)	115.4(3)	C(6)-C(1)-H(1A)	119.9
C(16)-O(5)-H(5A)	104(3)	C(3)-C(2)-C(1)	119.0(3)
C(2)-C(1)-C(6)	120.2(4)	C(3)-C(2)-H(2A)	120.5
C(1)-C(2)-H(2A)	120.5	C(11)-C(12)-H(12A)	116.5
C(2)-C(3)-C(4)	121.7(4)	C(12)-C(13)-C(21)	121.5(3)
C(2)-C(3)-Br(1)	119.3(3)	C(12)-C(13)-C(14)	122.1(3)
C(4)-C(3)-Br(1)	119.0(3)	C(21)-C(13)-C(14)	116.4(3)
C(5)-C(4)-C(3)	118.5(4)	C(13)-C(14)-C(15)	111.8(3)
C(5)-C(4)-H(4A)	120.7	C(13)-C(14)-C(22)	112.2(3)
C(3)-C(4)-H(4A)	120.7	C(15)-C(14)-C(22)	109.8(3)
C(4)-C(5)-C(6)	120.7(3)	C(13)-C(14)-H(14A)	107.6
C(4)-C(5)-H(5B)	119.6	C(15)-C(14)-H(14A)	107.6
C(6)-C(5)-H(5B)	119.6	C(22)-C(14)-H(14A)	107.6
C(5)-C(6)-C(1)	119.7(3)	C(14)-C(15)-C(16)	111.3(3)
C(5)-C(6)-C(7)	118.3(3)	C(14)-C(15)-H(15A)	109.4

Table 2.25 Bond lengths [Å] and angles [°] for BURK12, continued.

C(1)-C(6)-C(7)	121.9(3)	C(16)-C(15)-H(15A)	109.4
O(1)-C(7)-O(2)	123.0(4)	C(14)-C(15)-H(15B)	109.4
O(1)-C(7)-C(6)	124.4(4)	C(16)-C(15)-H(15B)	109.4
O(2)-C(7)-C(6)	112.6(3)	H(15A)-C(15)-H(15B)	108
O(2)-C(8)-C(9)	106.9(3)	O(5)-C(16)-C(17)	106.1(3)
O(2)-C(8)-H(8A)	110.3	O(5)-C(16)-C(15)	107.6(3)
C(9)-C(8)-H(8A)	110.3	C(17)-C(16)-C(15)	112.8(3)
O(2)-C(8)-H(8B)	110.3	O(5)-C(16)-C(11)	109.8(3)
C(9)-C(8)-H(8B)	110.3	C(17)-C(16)-C(11)	111.6(3)
H(8A)-C(8)-H(8B)	108.6	C(15)-C(16)-C(11)	108.9(3)
C(10)-C(9)-C(8)	118.4(3)	O(4)-C(17)-O(3)	124.2(3)
C(10)-C(9)-C(19)	129.1(3)	O(4)-C(17)-C(16)	122.4(3)
C(8)-C(9)-C(19)	112.5(3)	O(3)-C(17)-C(16)	113.4(3)
C(9)-C(10)-C(11)	133.4(3)	O(3)-C(18)-H(18A)	109.5
C(9)-C(10)-H(10A)	113.3	O(3)-C(18)-H(18B)	109.5
C(11)-C(10)-H(10A)	113.3	H(18A)-C(18)-H(18B)	109.5
C(12)-C(11)-C(10)	115.5(3)	O(3)-C(18)-H(18C)	109.5
C(12)-C(11)-C(20)	107.2(3)	H(18A)-C(18)-H(18C)	109.5
C(10)-C(11)-C(20)	106.3(3)	H(18B)-C(18)-H(18C)	109.5
C(12)-C(11)-C(16)	106.4(3)	C(9)-C(19)-H(19A)	109.5
C(10)-C(11)-C(16)	110.8(3)	C(9)-C(19)-H(19B)	109.5
C(20)-C(11)-C(16)	110.5(3)	H(19A)-C(19)-H(19B)	109.5
C(13)-C(12)-C(11)	126.9(3)	C(9)-C(19)-H(19C)	109.5
C(13)-C(12)-H(12A)	116.5	H(19A)-C(19)-H(19C)	109.5
H(19B)-C(19)-H(19C)	109.5	H(21A)-C(21)-H(21C)	109.5
C(11)-C(20)-H(20A)	109.5	H(21B)-C(21)-H(21C)	109.5
C(11)-C(20)-H(20B)	109.5	C(14)-C(22)-H(22A)	109.5
H(20A)-C(20)-H(20B)	109.5	C(14)-C(22)-H(22B)	109.5
C(11)-C(20)-H(20C)	109.5	H(22A)-C(22)-H(22B)	109.5
H(20A)-C(20)-H(20C)	109.5	C(14)-C(22)-H(22C)	109.5
H(20B)-C(20)-H(20C)	109.5	H(22A)-C(22)-H(22C)	109.5
C(13)-C(21)-H(21A)	109.5	H(22B)-C(22)-H(22C)	109.5
C(13)-C(21)-H(21B)	109.5		
H(21A)-C(21)-H(21B)	109.5		
C(13)-C(21)-H(21C)	109.5		

Symmetry transformations used to generate equivalent atoms:

Table 2.26 Anisotropic displacement parameters ($Å^2 x\ 10^3$)for BURK12. The anisotropic displacement factor exponent takes the form: $-2\pi^2[\ h^2 a^{*2} U^{11} + ... + 2\ h\ k\ a^*\ b^*\ U^{12}\ ]$

	U^{11}	U^{22}	U^{33}	U^{23}	U^{13}	U^{12}
Br(1)	34(1)	21(1)	29(1)	-7(1)	-8(1)	7(1)
O(1)	31(2)	17(1)	31(2)	-2(1)	-14(1)	10(1)
O(2)	28(1)	17(1)	20(1)	-1(1)	-10(1)	11(1)
O(3)	28(1)	21(1)	43(2)	-11(1)	-24(1)	17(1)
O(4)	28(1)	27(2)	40(2)	-9(1)	-24(1)	9(1)
O(5)	26(1)	13(1)	25(1)	-2(1)	-15(1)	4(1)
C(1)	30(2)	13(2)	24(2)	-3(1)	-14(2)	10(1)
C(2)	29(2)	16(2)	29(2)	-6(2)	-15(2)	11(2)
C(3)	28(2)	17(2)	23(2)	-8(2)	-13(2)	6(1)
C(4)	31(2)	16(2)	23(2)	-4(2)	-17(2)	4(1)
C(5)	32(2)	15(2)	26(2)	-6(2)	-19(2)	10(2)
C(6)	25(2)	16(2)	22(2)	-6(2)	-13(2)	6(1)
C(7)	23(2)	15(2)	25(2)	-4(2)	-14(2)	7(1)
C(8)	23(2)	17(2)	26(2)	-6(2)	-12(2)	11(1)
C(9)	24(2)	15(2)	19(2)	-7(1)	-12(2)	12(1)
C(10)	23(2)	18(2)	18(2)	-8(1)	-14(1)	11(1)
C(11)	23(2)	14(2)	20(2)	-6(1)	-14(1)	9(1)
C(12)	23(2)	12(2)	23(2)	-6(1)	-12(2)	8(1)
C(13)	21(2)	12(2)	28(2)	-8(1)	-14(2)	8(1)
C(14)	22(2)	19(2)	22(2)	-7(2)	-14(2)	8(1)
C(15)	23(2)	17(2)	22(2)	-8(1)	-13(2)	10(1)
C(16)	23(2)	12(2)	19(2)	-3(1)	-13(1)	9(1)
C(17)	26(2)	17(2)	20(2)	-5(1)	-14(2)	9(1)
C(18)	41(3)	34(2)	60(3)	-17(2)	-38(2)	27(2)
C(19)	30(2)	17(2)	27(2)	-4(2)	-17(2)	5(2)
C(20)	27(2)	17(2)	26(2)	-10(2)	-16(2)	9(1)
C(21)	26(2)	24(2)	27(2)	-9(2)	-17(2)	12(2)
C(22)	31(2)	35(2)	32(2)	-21(2)	-18(2)	12(2)

Table 2.27 Hydrogen coordinates (x 10^4) and isotropic displacement parameters ($Å^2$x 10^3) for BURK12.

	x	y	z	U(eq)
H(1A)	2399	3245	1369	27
H(2A)	4607	3238	-398	29
H(4A)	3975	7006	-2625	26
H(5B)	1758	6990	-858	27
H(8A)	-2133	3909	3451	26
H(8B)	-1340	4813	3939	26
H(10A)	-2963	1838	4760	22
H(12A)	-615	-630	6120	22
H(14A)	-2975	-689	9644	23
H(15A)	-3095	1845	7712	23
H(15B)	-4429	983	9075	23
H(18A)	-6594	3696	6629	60
H(18B)	-7603	2283	7615	60
H(18C)	-6751	2532	6067	60
H(19A)	-233	1988	6091	36
H(19B)	-555	3561	5862	36
H(19C)	742	3169	4722	36
H(20A)	-2161	-701	4877	31
H(20B)	-3892	-462	5459	31
H(20C)	-3246	-1687	6324	31
H(21A)	530	-1516	7544	36
H(21B)	-433	-1758	9076	36
H(21C)	639	-368	8140	36
H(22A)	-1064	485	9719	43
H(22B)	-2448	1398	9874	43
H(22C)	-1045	1793	8484	43
H(5A)	-5150(50)	-1450(50)	8230(40)	22(12)

Table 2.28 Hydrogen bonds for BURK12 [Å and °].

D-H...A	d(D-H)	d(H...A)	d(D...A)	<(DHA)
O(5)-H(5A)...O(4)	0.82(5)	2.14(5)	2.655(4)	120(4)

Symmetry transformations used to generate equivalent atoms:

Bis-acetate 265

To a stirred 0 °C solution of the diol **263** (310 mg, 1.16 mmol) in Ac_2O (9.8 mL, 104 mmol) was added $Sc(OTf)_3$ (284 mg dissolved in 1.8 mL MeCN, 0.577 mmol) via cannula, and the solution stirred for 30 seconds at this temperature. The reaction was quenched by the addition of a saturated aqueous $NaHCO_3$ solution, and was transferred to a beaker so that the gas evolution could be more easily controlled. Solid $NaHCO_3$ (5 g) was also added, and the mixture stirred until gas evolution ceased. The mixture was then diluted with Et_2O and deionized H_2O, and the aqueous layer was extracted twice with additional portions of Et_2O. The combined organic layers were washed with brine, dried over Na_2SO_4, filtered and concentrated under reduced pressure. The residue was purified by column chromatography (3:2 hexanes / EtOAc, isocratic) to provide the bis-acetate **265** (393 mg, 97%). TLC (1:1 hexanes / EtOAc): $R_f = 0.5$; ^1H NMR ($CDCl_3$, 400 MHz) δ 5.15 (s, 1H), 5.10 (s, 1H), 4.36 (d, *J* = 12.4 Hz, 1H), 4.30 (d, *J* = 12.4 Hz, 1H), 3.69 (s, 3H), 2.60 (dd, *J* = 14.0, 4.9 Hz, 1H), 2.06 (s, 3H), 2.05 (s, 3H), 1.98-1.87 (m, 1H), 1.82 (dd, *J* = 14.0, 11.6 Hz, 1H),

1.74 (s, 3H), 1.70 (s, 3H), 1.28 (s, 3H), 1.01 (d, J = 6.9 Hz, 3H); ^{13}C NMR ($CDCl_3$, 100 MHz) δ 171.0, 170.9, 170.3, 135.4, 132.2, 131.1, 127.7, 83.4, 71.5, 52.0, 45.1, 34.0, 30.6, 23.2, 21.1, 20.8, 18.0, 14.9; FTIR (film) νmax 2948, 1736, 1440, 1370, 1230, 1111, 1021, 913, 733 cm^{-1}; ESI-MS *m/z* 375.05 $[M+Na]^+$, 369.91 $[M+NH_4]^+$; HR-ESI-MS *m/z* calcd. for $C_{19}H_{28}O_6Na$ $[M+Na]^+$: 375.1778, found 375.1782.

Mono-acetate 266

To a stirred -78 °C solution of the bis-acetate **265** (98 mg, 0.276 mmol) in THF (5.5 mL) was added DIBAL-H (738 μL of a 1.5 M solution in toluene, 1.10 mmol) dropwise via syringe over 10 min, and the solution stirred for 2 h at this temperature. The reaction was quenched by the dropwise addition of MeOH followed by a saturated aqueous solution of Rochelle's salt, and then was allowed to warm to room temperature. When the layers had separated, the mixture was diluted with deionized H_2O and EtOAc, and the aqueous layer was extracted with additional portions of EtOAc. The combined organic layers were washed with brine, dried over Na_2SO_4, filtered and concentrated under reduced pressure. Column chromatography of the residue (3:1 to 1:1 hexanes / ethyl acetate gradient) provided the mono-acetate **266** (54 mg, 63%). TLC (1:1 hexanes / EtOAc): R_f = 0.3; ^{1}H NMR ($CDCl_3$, 400 MHz) δ 5.16 (s, 1H), 5.08 (s, 1H), 3.88 (d, J = 6.0 Hz, 2H), 3.71 (s, 3H), 2.59 (dd, J = 13.8, 4.7 Hz, 1H), 2.06 (s, 3H), 2.00-1.86 (m, 1H), 1.85 (dd, J = 13.8, 11.6 Hz, 1H), 1.75 (s, 3H), 1.71 (s, 3H), 1.43 (t, J = 6.0 Hz, 1H), 1.28 (s, 3H), 1.02 (d, J = 6.8 Hz, 3H); ^{13}C NMR ($CDCl_3$, 100 MHz) δ 171.3, 170.4, 137.1, 135.1, 128.2, 128.1, 83.6, 70.6, 52.0, 45.0,

34.0, 30.6, 23.4, 21.1, 20.8, 18.0, 14.7; FTIR (film) νmax 2949, 1734, 1438, 1370, 1268, 1016, 909, 732 cm^{-1}; ESI-MS *m/z* 348.97 $[M+K]^+$, 333.06 $[M+Na]^+$, 327.94 $[M+NH_4]^+$, 292.87 $[M+H-H_2O]^+$; HR-ESI-MS *m/z* calcd. for $C_{17}H_{26}O_5Na_1$ $[M+Na]^+$: 333.1672, found 333.1675.

Silyl ether 267

To a stirred solution of the mono-acetate **266** (205 mg, 0.660 mmol) in DMF (7 mL) were added imidazole (112 mg, 1.65 mmol) and TBSCl (200 mg, 1.32 mmol) at room temperature. The solution stirred until only the product was visible by TLC, and then was diluted with saturated aqueous $NaHCO_3$ and 1:1 hexanes / Et_2O. The aqueous layer was extracted with an additional portion of the solvent mixture, and the combined organic layers were washed with deionized H_2O, then brine, then were dried over Na_2SO_4, filtered and concentrated under reduced pressure. Column chromatography of the residue (5:1 to 3:1 hexanes / EtOAc gradient) provided the silyl ether **267** (229 mg, 82%). TLC (1:1 hexanes / EtOAc): R_f = 0.7; ^1H NMR ($CDCl_3$, 400 MHz) δ 5.18 (s, 1H), 5.12 (s, 1H), 3.88 (s, 2H), 3.69 (s, 3H), 2.59 (dd, *J* = 13.3, 4.2 Hz, 1H), 2.05 (s, 3H), 2.01-1.80 (m, 2H), 1.70 (s, 3H), 1.67 (s, 3H), 1.28 (s, 3H), 1.01 (d, *J* = 6.7 Hz, 3H), 0.89 (s, 9H), 0.04 (s, 6H); ^{13}C NMR ($CDCl_3$, 100 MHz) δ 171.1, 170.4, 136.3, 134.6, 128.6, 126.3, 83.7, 69.7, 52.0, 44.9, 34.0, 30.6, 26.1, 23.3, 20.8, 18.5, 18.1, 14.5, -5.1, -5.2; FTIR (film) νmax 2956, 2857, 1738, 1437, 1370, 1256, 1106, 908, 837, 777, 733 cm^{-1}; ESI-MS *m/z* 447.09 $[M+Na]^+$, 441.87 $[M+NH_4]^+$; HR-ESI-MS *m/z* calcd. for $C_{23}H_{40}O_5Si_1Na_1$ $[M+Na]^+$: 447.2537, found 447.2540.

Spirotetronate 268

To a stirred -78 °C solution of the silyl ether **267** (229 mg, 0.539 mmol) in THF (5.4 mL) and freshly distilled HMPA (2 mL) was added LiHMDS (1.17 mL of a 1.06 M solution in THF, 1.24 mmol) slowly via syringe, and the reaction was stirred at this temperature for 30 min, then allowed to warm to room temperature slowly over 1 h. The reaction was allowed to stir at room temperature for 15 min, and then $(MeO)_2SO_2$ (128 μL, 1.35 mmol) was added via syringe, and the reaction stirred for an additional 2 h at room temperature before being partitioned between deionized H_2O and Et_2O. The aqueous layer was extracted with two portions of additional Et_2O, and the combined organic layers were washed with brine, dried over Na_2SO_4, filtered and concentrated under reduced pressure. The residue was purified by column chromatography (4:1 to 1:1 hexanes / EtOAc) to provide the spirotetronate **268** (155 mg, 71%). TLC (1:1 hexanes / EtOAc): R_f = 0.6; ^{1}H NMR ($CDCl_3$, 400 MHz) δ 5.54 (s, 1H), 5.30 (s, 1H), 5.06 (s, 1H), 3.91 (s, 2H), 3.82 (s, 3H), 2.50-2.36 (m, 1H), 1.96 (dd, *J* = 13.7, 10.5 Hz, 1H), 1.78 (dd, *J* = 13.7, 6.4 Hz, 1H), 1.70 (s, 3H), 1.66 (s, 3H), 1.06 (s, 3H), 1.01 (d, *J* = 7.1 Hz, 3H), 0.90 (s, 9H), 0.06 (s, 6H); ^{13}C NMR ($CDCl_3$, 100 MHz) δ 184.7, 172.1, 135.1, 134.6, 128.4, 127.4, 89.6, 88.0, 69.7, 59.5, 44.3, 37.2, 31.6, 26.1, 22.3, 21.1, 18.5, 18.4, 14.8, -5.1, -5.1; FTIR (film) νmax 2957, 2858, 1747, 1625, 1440, 1361, 1253, 1207, 1173, 1093, 1019, 961, 909, 837, 808, 778, 732 cm^{-1}; ESI-MS *m/z* 429.08 $[M+Na]^+$, 406.82 $[M+H]^+$; HR-ESI-MS *m/z* calcd. for $C_{23}H_{38}O_4Si_1Na_1$ $[M+Na]^+$: 429.2432, found 429.2436.

Stannane 269

To a stirred -78 °C solution of the spirotetronate **268** (155 mg, 0.381 mmol) in THF (5 mL) was added *t*-BuLi (305 μL of a 1.5 M solution in pentane, 0.457 mmol) slowly via syringe, and the solution turned lemon yellow. The lithiation was allowed to proceed at this temperature for 30 min, and then the aldehyde **209** (967 μL of a 150 mg/mL solution in THF, 0.419 mmol) was added via syringe, and the reaction stirred at -78 °C for 20 min. The reaction was quenched by the addition of a saturated aqueous NH_4Cl solution and allowed to warm to room temperature. The mixture was partitioned between deionized H_2O and EtOAc, and the aqueous layer was extracted twice with additional EtOAc. The combined organic layers were washed with brine, dried over Na_2SO_4, filtered and concentrated under reduced pressure. The residue was purified by column chromatography (2:1 to 1:1 hexanes / EtOAc gradient) to provide the stannane **269** (274 mg, 96%) as a 1:1 mixture of diastereomers. ^{1}H NMR ($CDCl_3$, 400 MHz) - Spectrum 2.151. (diastereomeric mixture) and ^{13}C NMR ($CDCl_3$, 125 MHz) - Spectrum 2.152. ESI-MS *m/z* 775.19 $[M+Na]^+$, 752.95 $[M+H]^+$; HR-ESI-MS *m/z* calcd. for $C_{38}H_{68}O_5Si_1Sn_1Na_1$ $[M+Na]^+$: 775.3750, found 775.3763.

Sulfone 271

To a reaction flask was charged PPh_3 (846 mg, 3.23 mmol), PTSH (766 mg, 4.30 mmol), and the primary alcohol **270** (427 mg dissolved in 10 mL THF, 2.15 mmol), and the solution was stirred as it cooled to 0 °C. To the solution was added DIAD (762 μL, 3.87 mmol) slowly via syringe, and the reaction was allowed to warm to room temperature as it stirred for 12 h. The mixture was then partitioned between

saturated aqueous $NaHCO_3$ and EtOAc, and the aqueous layer was extracted with an additional portion of EtOAc. The combined organic layers were washed with deionized water, then brine, then dried over Na_2SO_4, filtered, and concentrated under reduced pressure. The residue was purified by column chromatography (3:1 to 2:1 hexanes / EtOAc) to provide the sulfide intermediate (540 mg, 70%). *Sulfide intermediate* TLC (1:1 hexanes / EtOAc): R_f = 0.5; ^{1}H NMR ($CDCl_3$, 500 MHz) δ 7.64-7.49 (m, 5H), 4.81-4.76 (m, 1H), 4.28 (d, *J* = 15.0 Hz, 1H), 4.19 (d, *J* = 15.0 Hz, 1H), 3.87-3.80 (m, 1H), 3.56-3.48 (m, 1H), 3.50 (t, *J* = 7.1 Hz, 2H), 2.46-2.38 (m, 2H), 2.07 (p, *J* = 7.1 Hz, 2H), 1.88-1.48 (m, 6H); ^{13}C NMR ($CDCl_3$, 125 MHz) δ 154.2, 133.8, 130.3, 129.9, 124.0, 96.9, 84.5, 62.2, 54.7, 32.3, 30.4, 27.9, 25.5, 19.2, 17.9; FTIR (film) νmax 2946, 2865, 1602, 1501, 1387, 1119, 1022, 765, 693 cm^{-1}; ESI-MS *m/z* 396.94 $[M+K]^+$, 380.99 $[M+Na]^+$, 358.78 $[M+Na]^+$; HR-ESI-MS *m/z* calcd. for $C_{18}H_{22}N_4O_2S_1Na_1$ $[M+Na]^+$: 381.1356, found 381.1357.

The above described sulfide intermediate (540 mg, 1.50 mmol) was dissolved in EtOH (15 mL) and the solution was stirred and cooled to 0 °C. To the cooled solution was added $(NH_4)_6Mo_7O_{24}$*$4H_2O$ (370 mg, 0.300 mmol dissolved in 2.3 mL / 22.5 mmol 30% w/w aqueous H_2O_2), and the solution warmed to room temperature as it stirred for 12 h. The mixture was partitioned between EtOAc and deionized H_2O, and the aqueous layer was extracted with an additional portion of EtOAc. The combined organic layers were washed with brine, dried over Na_2SO_4, filtered and concentrated under reduced pressure. The residue was purified by column chromatography (3:1 to 1:1 hexanes / EtOAc) to provide the sulfone **271** (540 mg,

92%). TLC (1:1 hexanes / EtOAc): R_f = 0.5; ^{1}H NMR ($CDCl_3$, 400 MHz) δ 7.72-7.57 (m, 5H), 4.81-4.75 (m, 1H), 4.30 (d, *J* = 15.4 Hz, 1H), 4.20 (d, *J* = 15.4 Hz, 1H), 3.92-3.79 (m, 2H), 3.57-3.48 (m, 1H), 2.50 (t, *J* = 6.8 Hz, 2H), 2.24-2.14 (m, 2H), 1.91-1.48 (m, 6H); ^{13}C NMR ($CDCl_3$, 125 MHz) δ 153.5, 133.1, 131.7, 129.9, 125.2, 97.1, 83.2, 78.7, 62.2, 55.1, 54.6, 30.4, 25.5, 21.5, 19.2, 17.8; FTIR (film) νmax 2952, 2872, 1500, 1343, 1155, 1022, 768, 693 cm^{-1}; ESI-MS *m/z* 412.93 $[M+Na]^+$, 407.86 $[M+NH_4]^+$, 390.43 $[M+H]^+$; HR-ESI-MS *m/z* calcd. for $C_{18}H_{22}N_4O_4S_1Na_1$ $[M+Na]^+$: 413.1254, found 413.1252.

Propargylic alcohol 272

To a stirred solution of the sulfone **271** (4.74 g, 12.1 mmol) in EtOH (100 mL) was added PPTS (305 mg, 1.21 mmol) and the reaction was heated to 60 °C. The deprotection was monitored by TLC, and when no more of the starting material **271** remained, the reaction was cooled to room temperature and evaporated under reduced pressure. Column chromatography of the residue (1:1 hexanes / EtOAc) provided the pure propargylic alcohol **272** (3.56 g, 95%). TLC (1:1 hexanes / EtOAc): R_f = 0.3; ^{1}H NMR ($CDCl_3$, 400 MHz) δ 7.73-7.56 (m, 5H), 4.26 (dt, *J* = 6.1, 2.1 Hz, 2H), 3.93-3.85 (m, 2H), 2.49 (tt, *J* = 6.8, 2.1 Hz, 2H), 2.23-2.13 (m, 2H), 1.72 (t, *J* = 6.1 Hz, 1H), ^{13}C NMR ($CDCl_3$, 125 MHz) δ 153.5, 133.1, 131.7, 129.9, 125.2, 83.1, 81.0, 55.1, 51.3, 21.5, 17.7; FTIR (film) νmax 3369 br, 2912, 1723, 1495, 1340, 1155, 1014, 765, 691; ESI-MS *m/z* 344.80 $[M+K]^+$, 328.90 $[M+Na]^+$, 306.91 $[M+H]^+$; HR-ESI-MS *m/z* calcd. for $C_{13}H_{15}N_4O_3S_1$ $[M+H]^+$: 307.0859, found 307.0861.

Vinyl iodide 273

To a reaction flask was charged $(PPh_3)_2PdCl_2$ (22 mg, 0.031 mmol) and a solution of the propargylic alcohol **272** (188 mg, 0.614 mmol) in THF (6.5 mL). The solution was stirred as n-Bu_3SnH (190 μL, 0.706 mmol) was added slowly via syringe, and the darkened solution was stirred for 20 min at room temperature. The reaction mixture was concentrated under reduced pressure, then dissolved in CH_2Cl_2, and cooled to 0 °C. The cooled solution stirred as I_2 (155 mg solution in 8 mL CH_2Cl_2, 0.614 mmol) was added via cannula, and the reaction mixture was allowed to warm to room temperature, and stirred at room temperature for 30 min. Solid KF on celite was added, and the suspension stirred an additional 2 h at room temperature. The suspension was filtered and concentrated under reduced pressure, and column chromatography of the residue (2:1 to 1:1 hexanes / ethyl acetate) provided the iodide **273** (68 mg, 26%) and undesired byproducts and regioisomers (132 mg). TLC (1:1 hexanes / EtOAc): R_f = 0.4; ^{1}H NMR ($CDCl_3$, 500 MHz) δ 7.70-7.60 (m, 5H), 6.29 (t, *J* = 8.0 Hz, 1H), 4.23 (d, *J* = 6.5 Hz, 2H), 3.78-3.74 (m, 2H), 2.40 (q, *J* = 7.5 Hz, 2H), 2.11 (p, *J* = 7.5 Hz, 2H), 1.94 (t, *J* = 6.5 Hz, 1H); ^{13}C NMR ($CDCl_3$, 125 MHz) δ 153.5, 140.2, 133.1, 131.7, 129.9, 125.2, 105.2, 65.3, 55.0, 29.2, 21.7; FTIR (film) νmax 3402 br, 2946, 1730, 1496, 1341, 1157, 1043, 769, 691; ESI-MS *m/z* 456.79 $[M+Na]^+$, 451.70 $[M+NH_4]^+$, 434.78 $[M+H]^+$, 416.71 $[M-H_2O+H]^+$; HR-ESI-MS *m/z* calcd. for $C_{13}H_{15}I_1N_4O_3S_1Na_1$ $[M+Na]^+$: 456.9802, found 456.9797.

SEM ether 274

To a stirred solution of the vinyl iodide **273** (690 mg, 1.59 mmol) was added i-Pr_2NEt (1.38 mL, 7.95 mmol), and then SEMCl (843 μL, 4.77 mmol) via syringe. The solution stirred at room temperature for 12 h, and then was partitioned between CH_2Cl_2 and saturated aqueous $NaHCO_3$. The aqueous layer was extracted with an additional portion of CH_2Cl_2, and the combined aqueous layers were washed with deionized H_2O, brine, dried over Na_2SO_4, filtered, and concentrated under reduced pressure. The residue was purified by column chromatography (hexanes / ethyl acetate gradient) to provide the SEM ether **275** (594 mg, 66%). ^{1}H NMR ($CDCl_3$, 500 MHz) δ 7.74-7.57 (m, 5H), 6.40 (t, *J* = 7.7 Hz, 1H), 4.68 (s, 2H), 4.24 (s, 2H), 3.88-3.72 (m, 2H), 3.70-3.65 (m, 2H), 2.40 (q, *J* = 7.7 Hz, 2H), 2.13-2.06 (m, 2H), 0.98-0.91 (m, 2H), 0.02 (s, 9H); ^{13}C NMR ($CDCl_3$, 125 MHz) δ 153.4, 142.4, 133.1, 131.7, 129.9, 125.1, 99.9, 93.3, 68.6, 65.9, 55.0, 29.4, 21.7, 18.2, -1.2; ESI-MS *m/z* 586.80 $[M+Na]^+$, 581.73 $[M+NH_4]^+$; HR-ESI-MS *m/z* calcd. for $C_{19}H_{29}I_1N_4O_4S_1Si_1Na_1$ $[M+Na]^+$: 587.0620, found 587.0616.

Stille adduct 275

A reaction flask was charged with LiCl (463 mg, 1.09 mmol) that was dried under high vacuum (0.1 mm Hg) with a heat gun for ~ 30 min. After the reaction flask had cooled to room temperature, $AsPh_3$ (222 mg, 0.728 mmol) and Pd_2dba_3 (83 mg, 0.091 mmol) were added, followed by a solution of the stannane **269** (274 mg, 0.364 mmol) and the SEM ether **274** (205 mg, 0.364 mmol) in freshly distilled NMP (5 mL) which was transferred to the reaction flask via syringe. The mixture stirred for

12 h at room temperature, after which it was partitioned between Et_2O and deionized H_2O, and the aqueous layer was extracted with two additional portions of Et_2O. The combined organic layers were washed with brine, dried over Na_2SO_4, filtered and concentrated under reduced pressure. Column chromatography of the residue provided the Stille adduct **275** (137 mg, 42%) and stannane **269** (44 mg) such that the BORSM yield was 49%. ^{1}H NMR ($CDCl_3$, 500 MHz) - Spectrum 2.163; ^{13}C NMR ($CDCl_3$, 125 MHz) – Spectrum 2.164 (mixture of diastereomers); ESI-MS *m/z* 921.18 $[M+Na]^+$; HR-ESI-MS *m/z* calcd. for $C_{45}H_{70}N_4O_9S_1Si_2Na_1$ $[M+Na]^+$: 921.4294, found 921.4306.

Bis TBS ether 276

To a stirred 0 °C solution of the Stille adduct **275** (85 mg, 0.095 mmol) in CH_2Cl_2 (1.5 mL) was added *i*-Pr_2NEt (74 μL, 0.425 mmol) and then TBSOTf (43 μL, 0.189 mmol) via syringe. The reaction stirred at this temperature for 2 h, and then was partitioned between CH_2Cl_2 and saturated aqueous $NaHCO_3$. The aqueous layer was extracted with additional CH_2Cl_2, and the combined organic layers were washed with brine and dried over Na_2SO_4. The solution was filtered and concentrated under reduced pressure, and the residue was purified by column chromatography to provide the bis-TBS ether **276** (59 mg, 62%). ^{1}H NMR ($CDCl_3$, 400 MHz) - Spectrum 2.165; ^{13}C NMR ($CDCl_3$, 125 MHz) – Spectrum 2.166 (mix of diastereomers); FTIR (film) νmax 2952, 2932, 2858, 1740, 1638, 1348, 1249, 1152, 1058, 841, 779 cm^{-1}; ESI-MS *m/z* 1051.43 $[M+K]^+$, 1035.47 $[M+Na]^+$; HR-ESI-MS *m/z* calcd. for $C_{51}H_{84}N_4O_9S_1Si_3Na_1$ $[M+Na]^+$: 1035.5159, found 1035.5174.

Primary alcohol 277

To a mixture of pyridine (1 mL) and THF (4 mL) in a plastic vial was added HF-py (450 μL of a 70% w/w solution) and the mixture was stirred, to make a 3.2 M solution of HF in THF-py. To a solution of the bis-TBS ether **276** (70 mg, 0.069 mmol) in THF (300 μL) and pyridine (100 μL) was added 5 equivalents of the HF-py stock solution (100 μL) and the mixture was stirred at room temperature for 2 h, after which time only starting material was visible by TLC. An additional 300 μL of the stock solution was then added, and the mixture stirred for 12 h, after which time it was partitioned between saturated aqueous $NaHCO_3$ and EtOAc, and the aqueous layer was extracted with two additional portions of EtOAc. The combined organic layers were washed with brine, dried over Na_2SO_4, filtered and concentrated under reduced pressure. The residue was purified by column chromatography to provide the primary alcohol **277** (53 mg, 86%). ^{1}H NMR ($CDCl_3$, 500 MHz) - Spectrum 2.167; ^{13}C NMR ($CDCl_3$, 125 MHz) – Spectrum 2.168 (mix of diastereomers); ESI-MS *m/z* 937.30 $[M+K]^+$, 921.36 $[M+Na]^+$; HR-ESI-MS *m/z* calcd. for $C_{45}H_{70}N_4O_9S_1Si_2Na_1$ $[M+Na]^+$: 921.4294, found 921.4297.

Aldehyde 278

To a reaction flask was charged powdered 4 Å molecular sieves (5 mg), NMO (10 mg, 0.088 mmol), and a solution of the primary alcohol **277** (53 mg, 0.059 mmol) in CH_2Cl_2 (2 mL). To this stirred suspension was added TPAP (1 mg, 0.003 mmol) and the color changed from green to black over a few minutes, and the consumption of

277 was observed by TLC. Filtration of the reaction mixture through a short silica gel plug with 4:1 CH_2Cl_2 and concentration of the filtrate under reduced pressure provided the aldehyde **278** (44 mg, 84%). ^{1}H NMR ($CDCl_3$, 500 MHz) - Spectrum 2.169; ^{13}C NMR ($CDCl_3$, 125 MHz) – Spectrum 2.170 (mix of diastereomers); ESI-MS *m/z* 935.26 $[M+K]^+$, 919.35 $[M+Na]^+$; HR-ESI-MS *m/z* calcd. for $C_{45}H_{68}N_4O_9S_1Si_2Na_1$ $[M+Na]^+$: 919.4138, found 919.4151.

Macrocycle 279

To a stirred -78 °C solution of the aldehyde **278** (43 mg, 0.048 mmol) in THF (10 mL) was slowly added KHMDS (105 μL of a 0.5 M solution in toluene, 0.053 mmol) via syringe. The solution stirred for 1 h at -78 °C and then was allowed to warm to room temperature. The reaction stirred at room temperature for 1 h, and then was quenched by the addition of a saturated aqueous NH_4Cl solution. The mixture was partitioned between EtOAc and deionized H_2O, and the aqueous layer was extracted with two additional portions of EtOAc. The combined organic layers were washed with brine, dried over Na_2SO_4, filtered and concentrated under reduced pressure. Column chromatography of the residue provided the crude macrocycle **279** (16 mg, 50%) which appeared to be a single diastereomer by ^{13}C NMR. ^{1}H NMR ($CDCl_3$, 500 MHz) *crude* δ 6.13 (dd, *J* = 12.5, 8.3 Hz, 1H), 5.91 (dd, *J* = 8.3, 1.3 Hz, 1H), 5.83 (d, *J* = 12.5 Hz, 1H), 5.61 (d, *J* = 15.6 Hz, 1H), 5.56 (s, 1H), 5.53 (d, *J* = 7.8 Hz, 1H), 5.40-5.31 (m, 1H), 5.09 (s, 1H), 4.53 (s, 2H), 4.16-4.09 (m, 2H), 4.07 (s, 3H), 3.68-3.57 (m, 2H), 2.63 (dd, *J* = 14.6, 9.3 Hz, 1H), 2.49-2.14 (m, 5H), 1.84 (s, 3H), 1.82-1.76 (m, 1H), 1.73 (s, 3H), 1.22 (s, 3H), 1.13 (d, *J* = 7.5 Hz, 3H), 0.96-0.90

(m, 2H), 0.85 (s, 9H), 0.06-0.00 (m, 15H); ^{13}C NMR ($CDCl_3$, 125 MHz) δ 177.9, 171.3, 140.5, 135.0, 134.5, 134.3, 133.2, 132.7, 131.9, 128.7, 127.9, 124.4, 105.7, 92.0, 85.7, 65.1, 62.7, 61.7, 60.5, 59.2, 43.9, 36.3, 32.8, 31.7, 29.9, 28.5, 27.4, 25.9, 22.1, 21.2, 20.5, 18.3, 18.2, 18.1, 14.4, 12.9, -1.2, -3.1, -4.4; ESI-MS *m/z* 693.52 $[M+Na]^+$; HR-ESI-MS *m/z* calcd. for $C_{38}H_{62}O_6Si_2Na_1$ $[M+Na]^+$: 693.3977, found 693.3984.

Alcohol 280

To a stirred solution of the macrocycle **279** (17 mg, 0.025 mmol) in THF (1 mL) in a plastic vial was added TBAF (50 μL of a 1.0 M solution in THF, 0.050 mmol) and the solution stirred at room temperature for 2 h, after which time TLC analysis indicated the consumption of starting material. The reaction mixture was partitioned between deionized H_2O and EtOAc, and the aqueous layer was extracted with additional EtOAc. The combined organic layers were washed with brine, dried over Na_2SO_4, filtered and concentrated under reduced pressure. The residue was purified by column chromatography to provide the crude alcohol **280** (8 mg, 57%). ^{1}H NMR ($CDCl_3$, 500 MHz) *crude* δ 6.06 (dd, *J* = 12.2, 8.5 Hz, 1H), 5.87 (d, *J* = 12.2 Hz, 1H), 5.61-5.54 (m, 1H), 5.57 (d, *J* = 15.5 Hz, 1H), 5.53 (s, 1H), 5.35 (ddd, *J* = 15.5, 10.3, 5.3 Hz, 1H), 5.29-5.20 (m, 1H), 5.08 (s, 1H), 4.53 (s, 2H), 4.26-4.08 (m, 2H), 4.14 (s, 3H), 3.67-3.45 (m, 2H), 2.63 (dd, *J* = 14.6, 9.3 Hz, 1H), 2.48-2.12 (m, 5H), 1.84 (s, 3H), 1.75-1.71 (m, 1H), 1.73 (s, 3H), 1.21 (s, 3H), 1.14 (d, *J* = 7.4 Hz, 3H), 0.95-0.88 (m, 2H), 0.02 (s, 9H); ^{13}C NMR ($CDCl_3$, 125 MHz) δ 178.7, 172.0, 140.4, 136.0, 134.4, 134.3, 133.6, 132.7, 130.1, 129.8, 127.9, 124.5, 104.5, 92.2, 86.7, 65.3,

62.1, 61.2, 59.9, 43.8, 35.9, 32.8, 31.7, 28.5, 27.5, 22.0, 20.5, 18.3, 13.0, -1.2; ESI-MS *m/z* 579.32 $[M+Na]^+$; HR-ESI-MS *m/z* calcd. for $C_{32}H_{48}O_6Si_1Na_1$ $[M+Na]^+$: 579.3112, found 579.3114.

2.8 Spectral overlays of compound 217 with IMDA reaction products

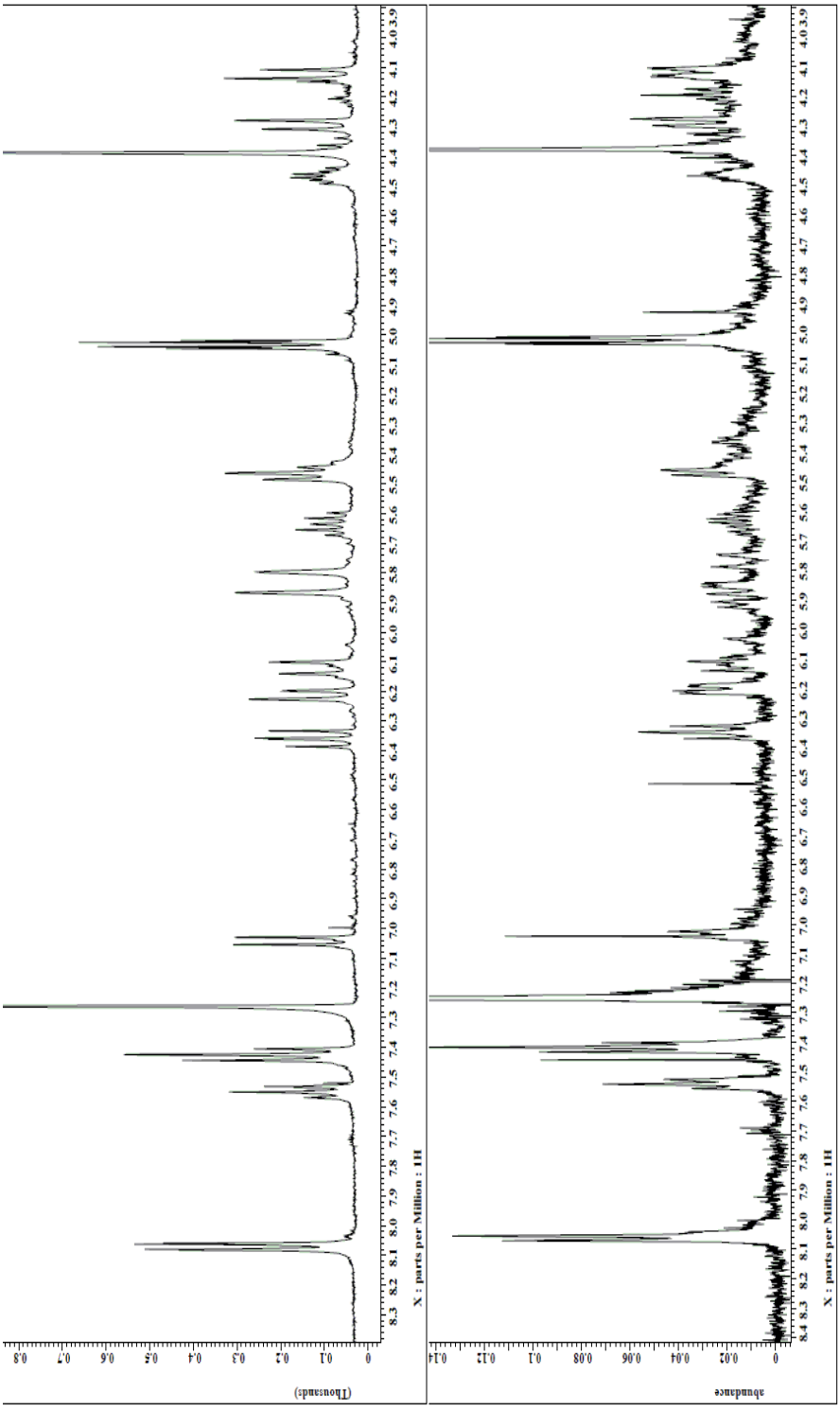

Figure 2.11 Compound **217** (left) and IMDA product 1 (right)

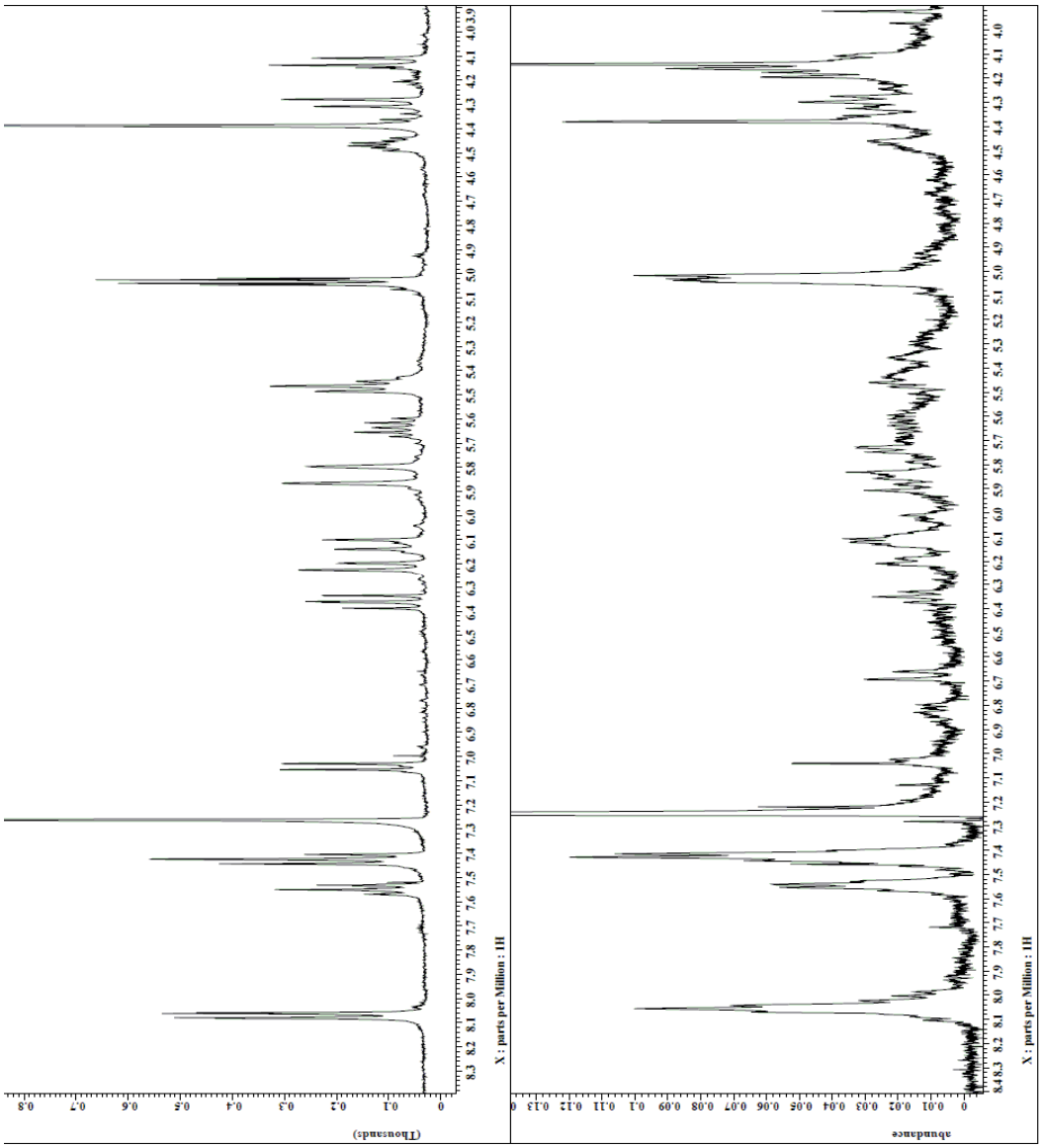

Figure 2.12 Compound **217** (left) and IMDA product 2 (right)

2.9 Spectral overlay of compound 280 with spirohexenolide B (129)

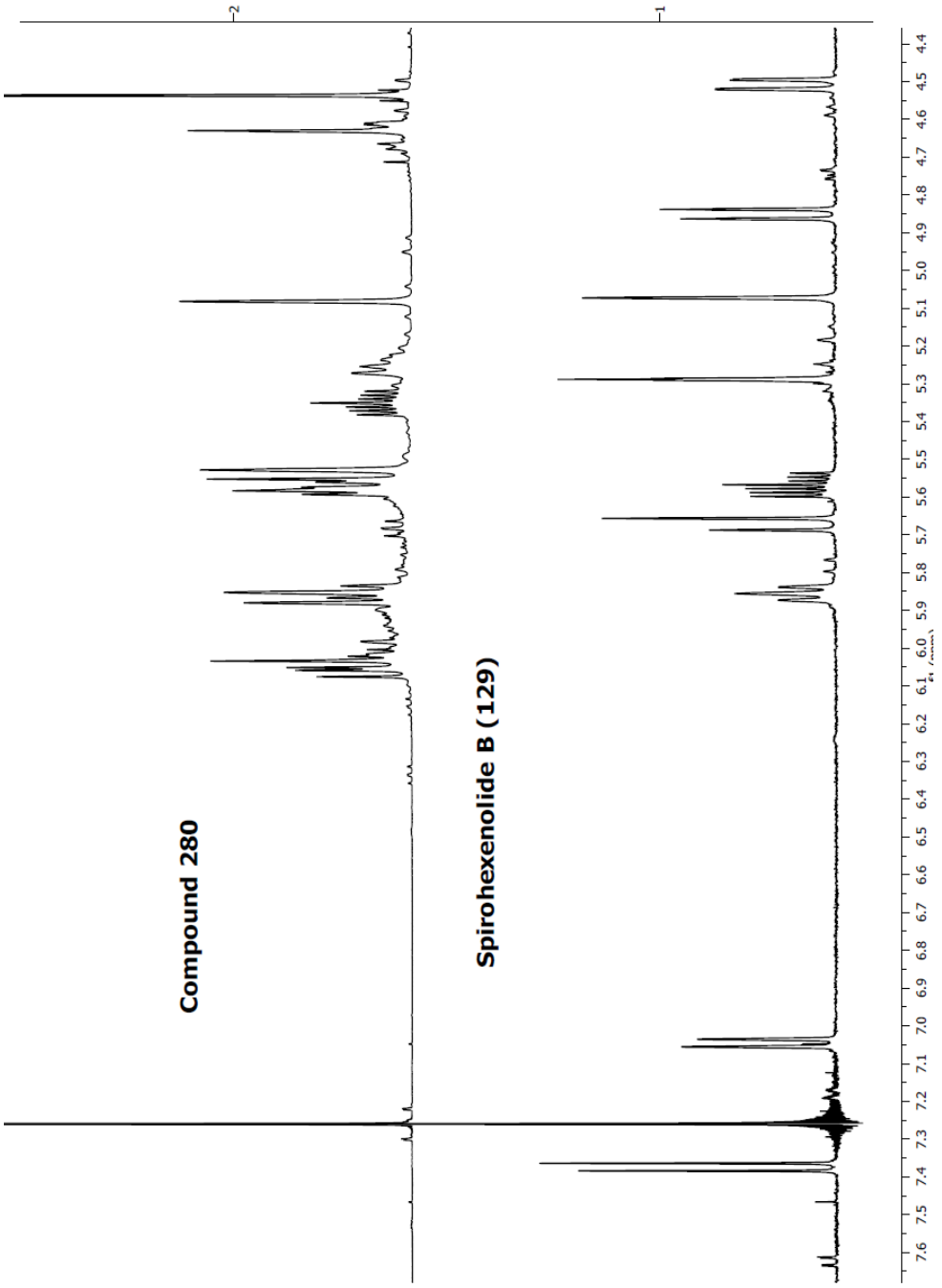

Figure 2.13 Spectral overlay of compound **280** with spirohexenolide B (**129**)

2.10 Selected NMR spectra

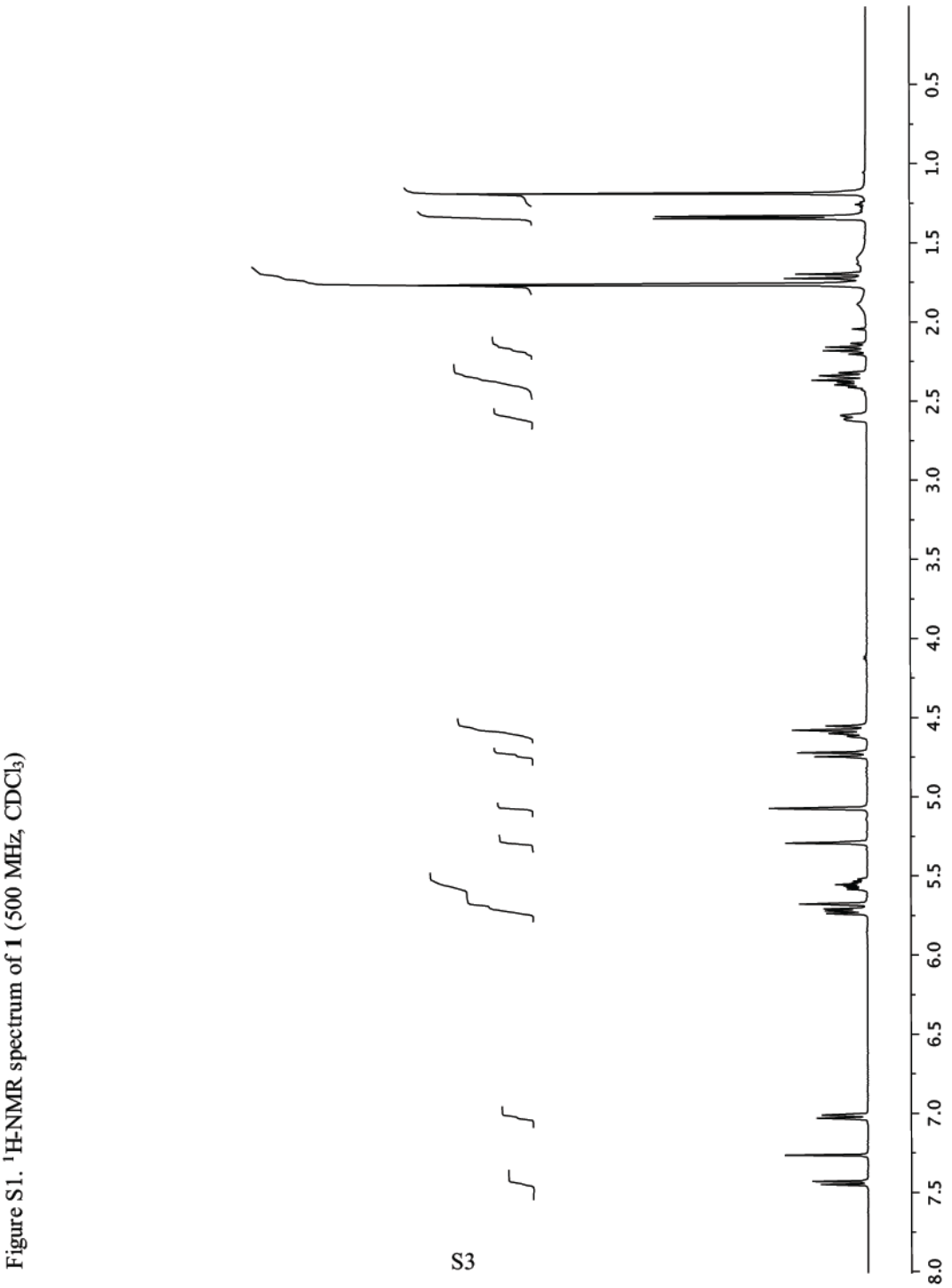

Spectrum 2.1 ^{1}H NMR ($CDCl_3$, 500 MHz) of spirohexenolide A **128**

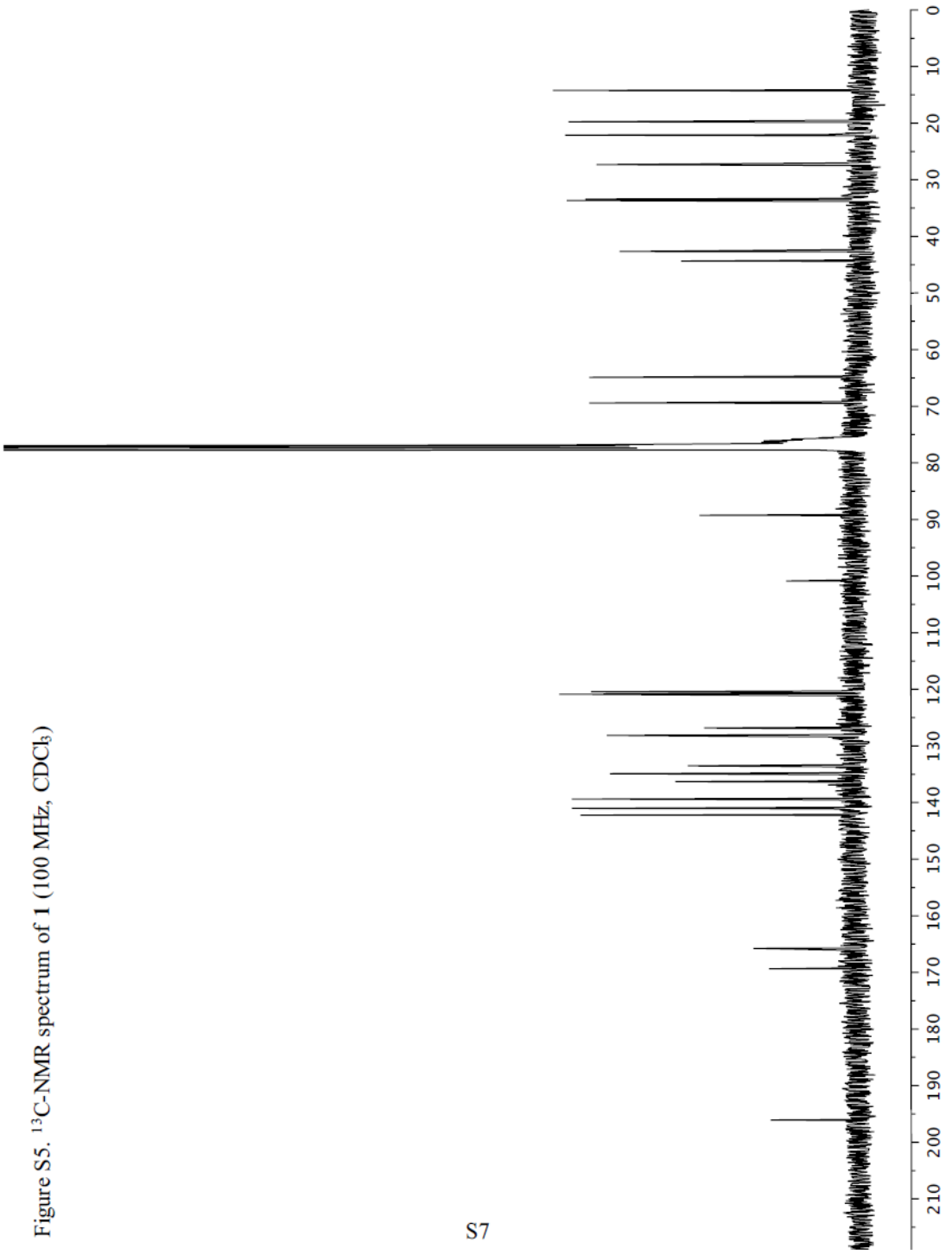

Figure S5. ^{13}C-NMR spectrum of **1** (100 MHz, $CDCl_3$)

S7

Spectrum 2.2 ^{13}C NMR ($CDCl_3$, 100 MHz) of spirohexenolide A **128**

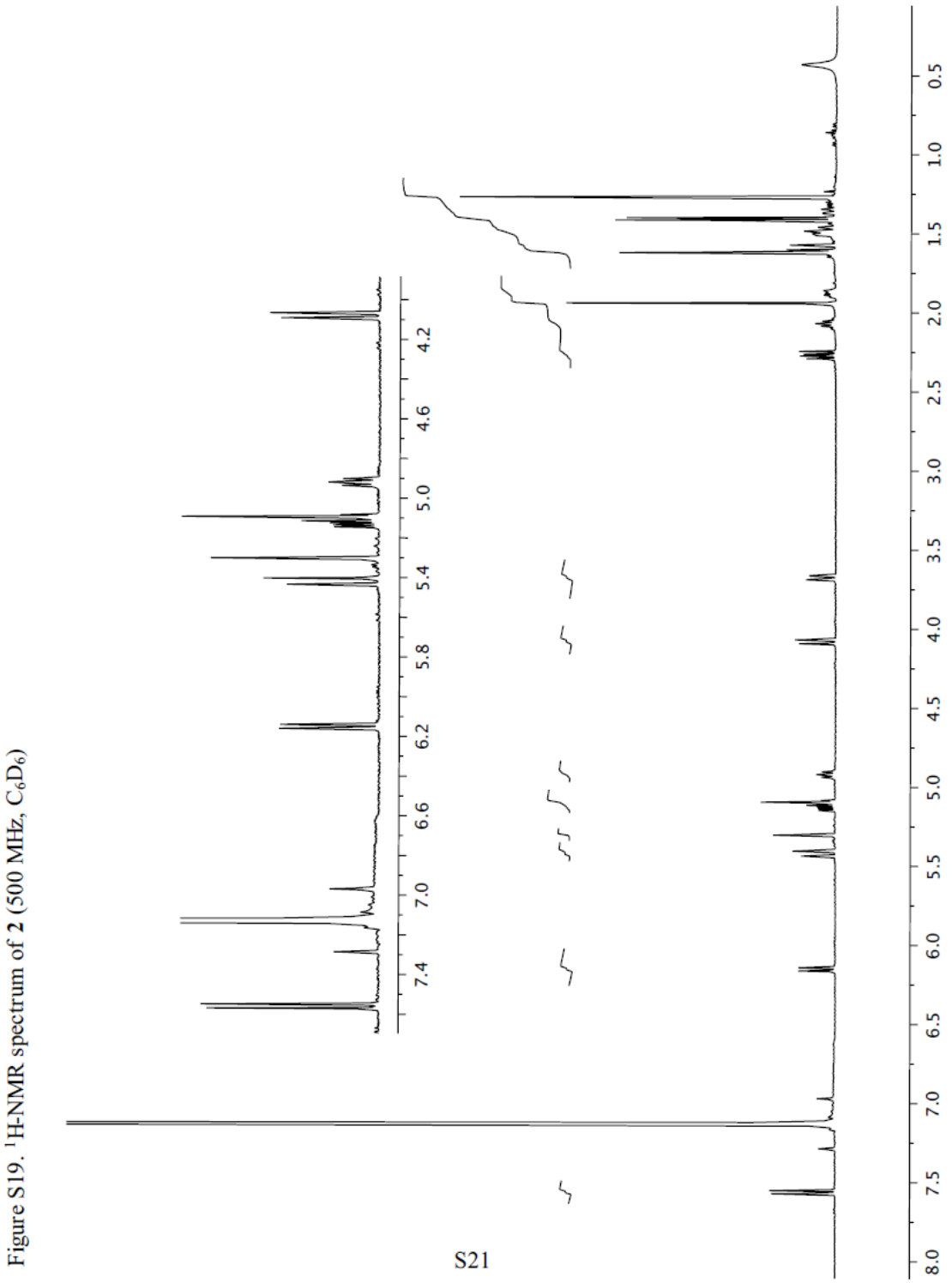

Spectrum 2.3 ^{1}H NMR (C_6D_6, 500 MHz) of spirohexenolide B **129**

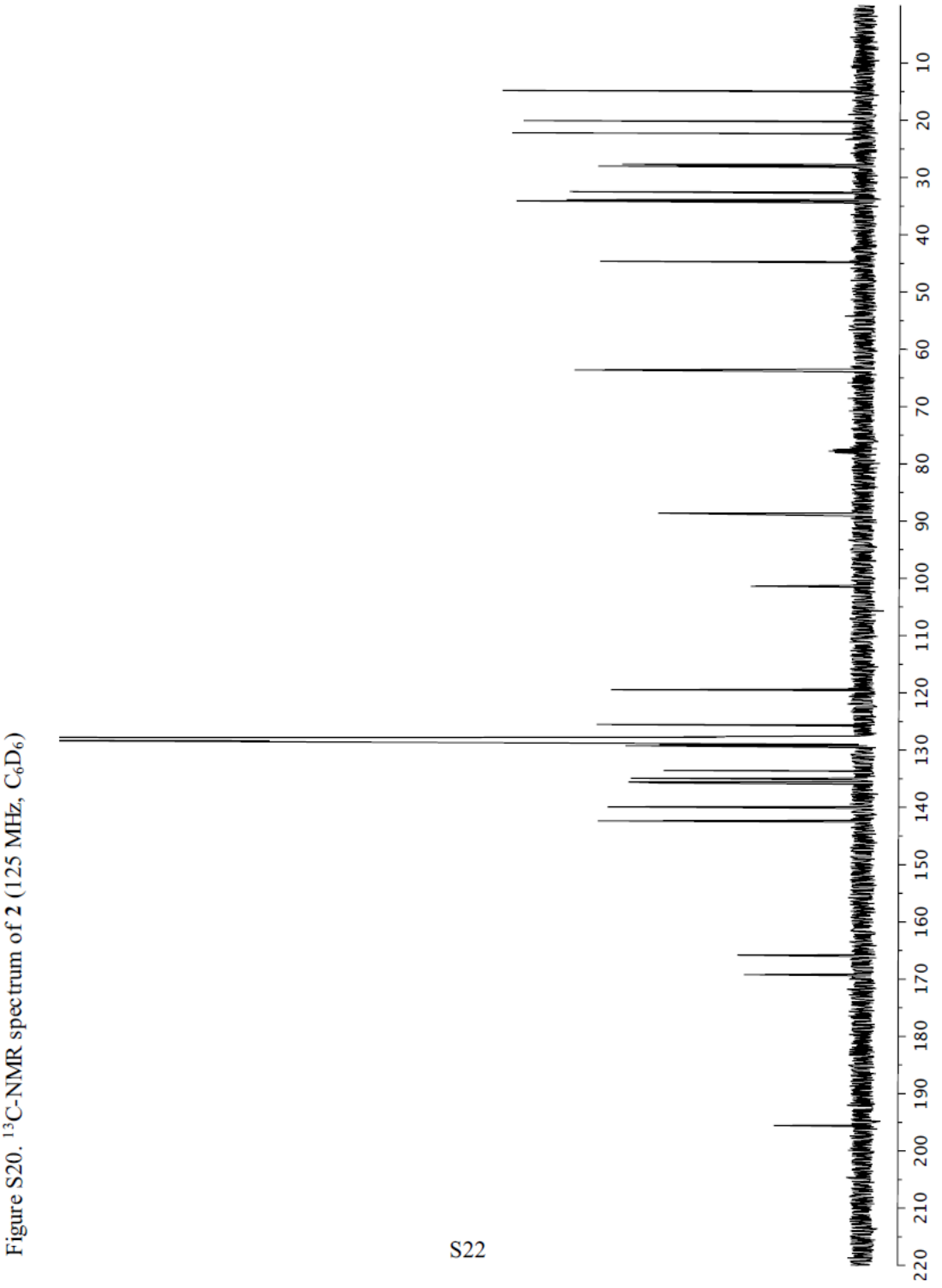

Spectrum 2.4 ^{13}C NMR (C_6D_6, 125 MHz) of spirohexenolide B **129**

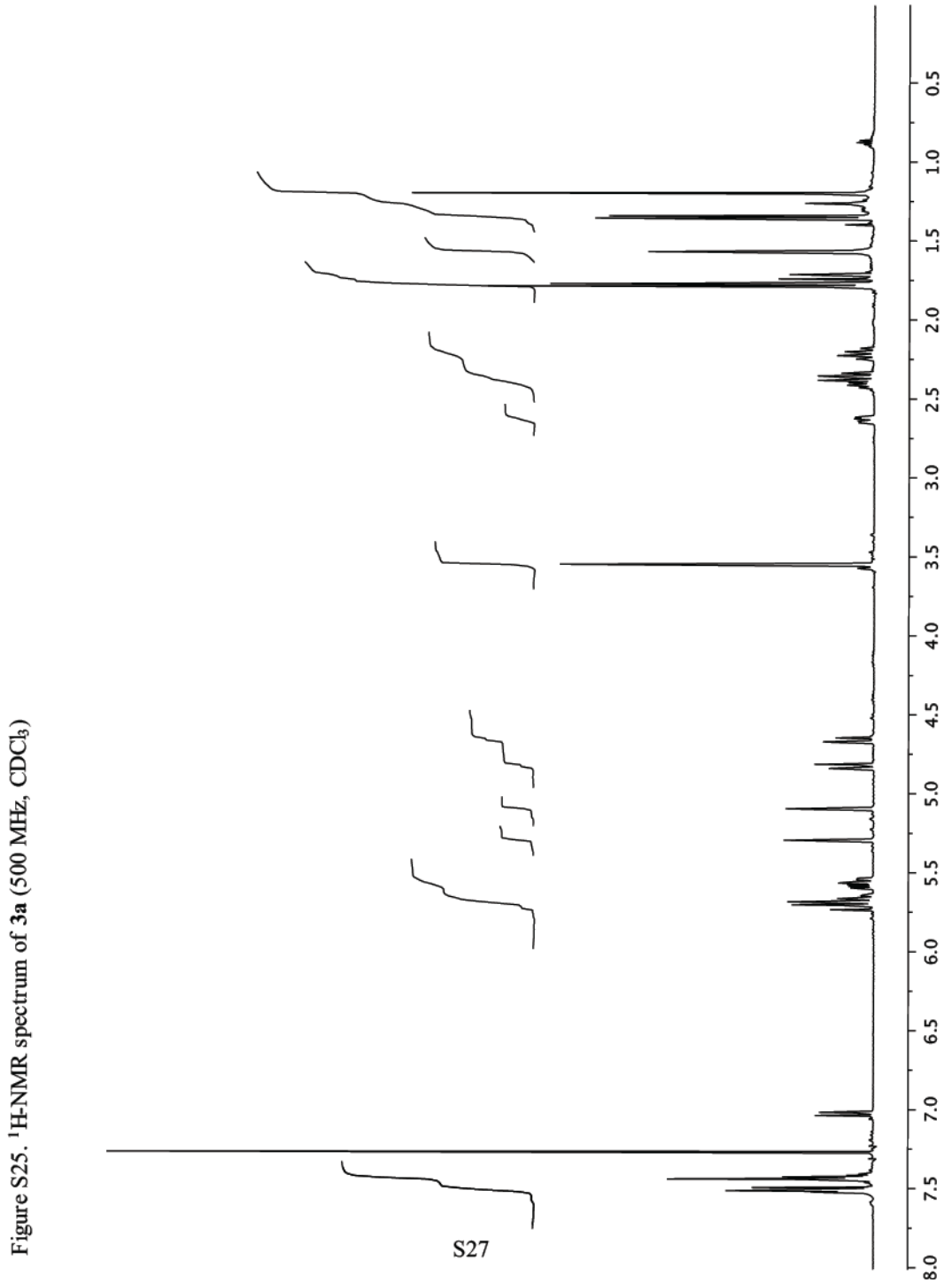

Spectrum 2.5 ^{1}H NMR ($CDCl_3$, 500 MHz) of compound **130a**

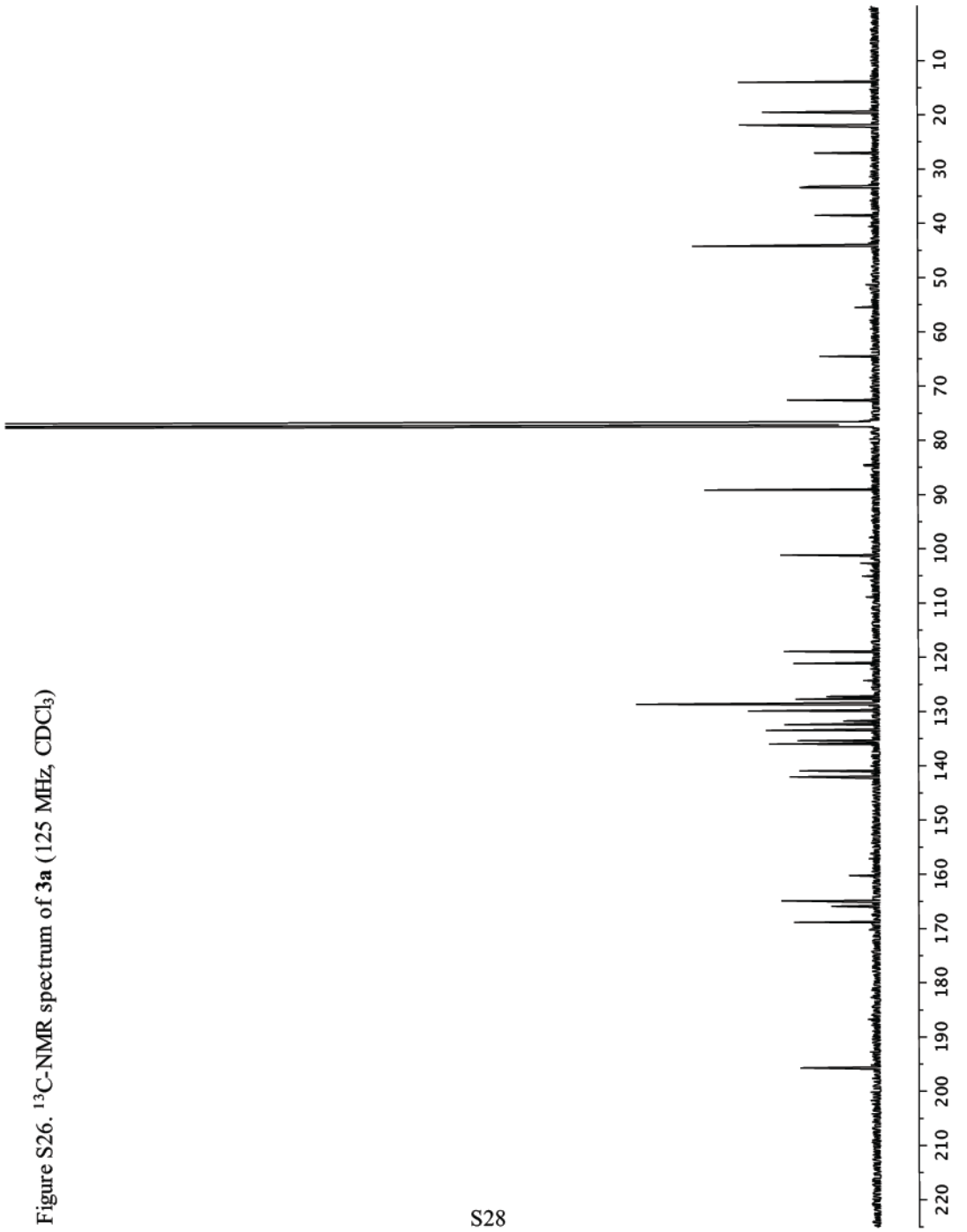

Figure S26. ^{13}C-NMR spectrum of **3a** (125 MHz, $CDCl_3$)

S28

Spectrum 2.6 ^{13}C NMR ($CDCl_3$, 125 MHz) of compound **130a**

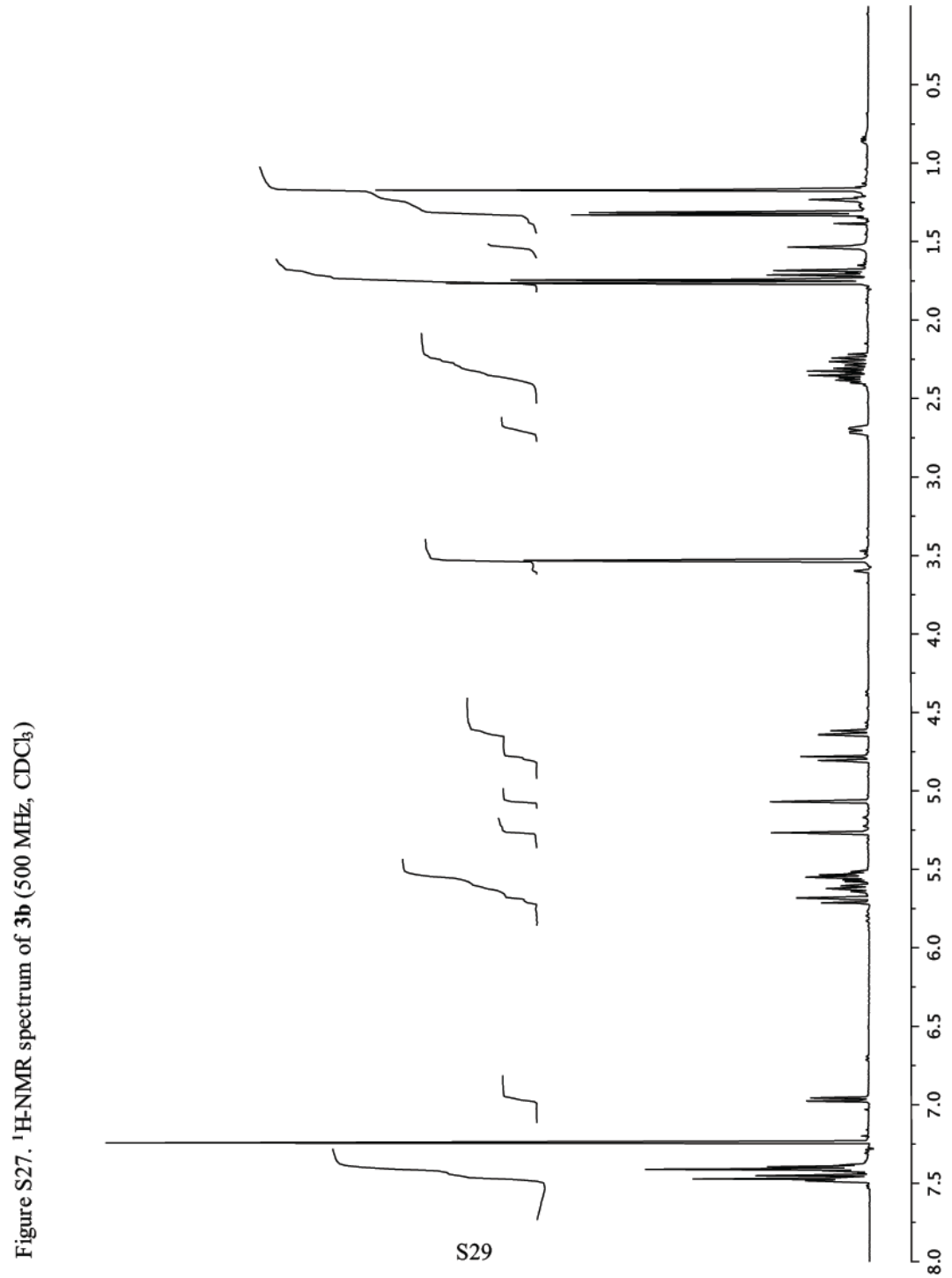

Spectrum 2.7 ^{1}H NMR ($CDCl_3$, 500 MHz) of compound **130b**

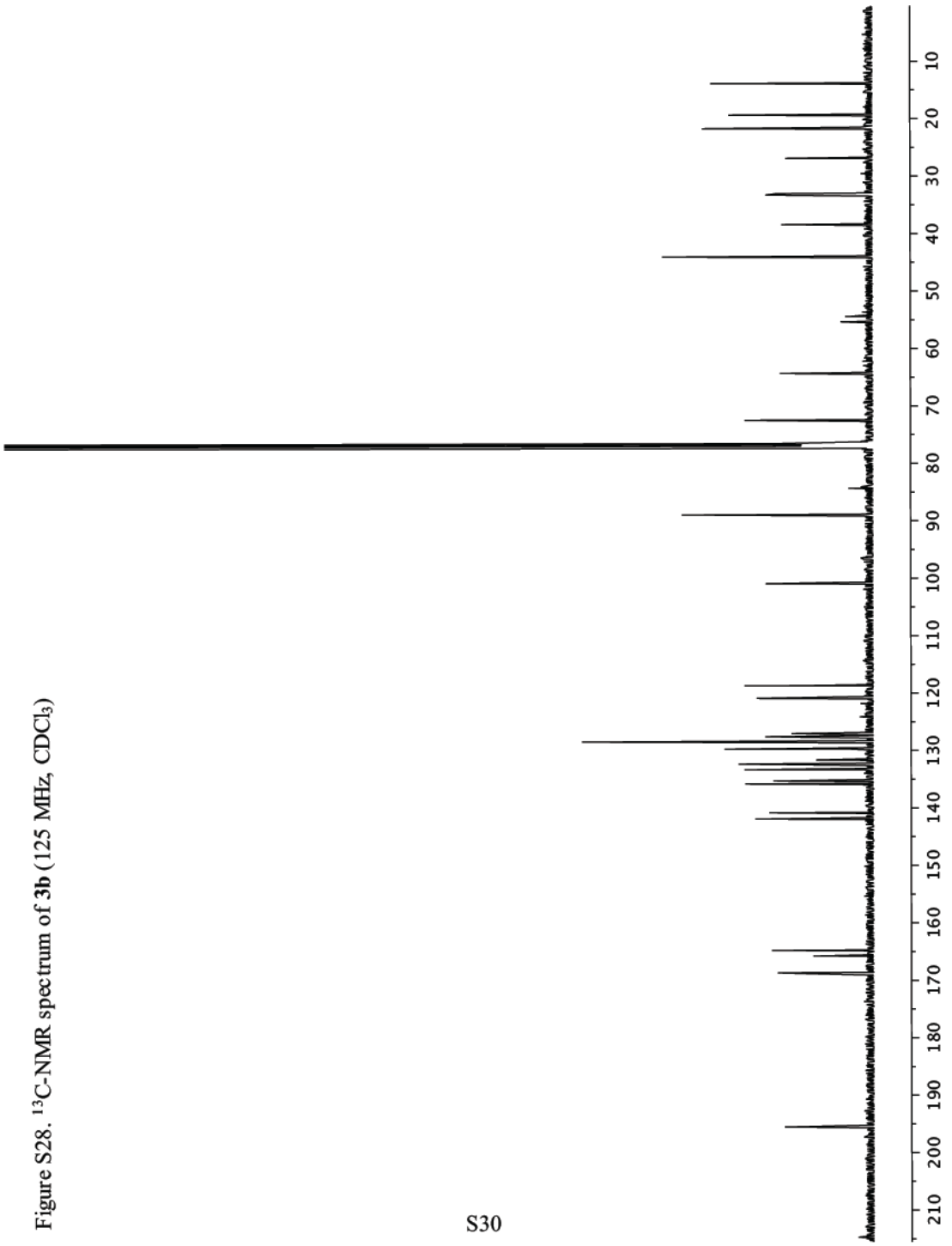

Spectrum 2.8 ^{13}C NMR ($CDCl_3$, 125 MHz) of compound **130b**

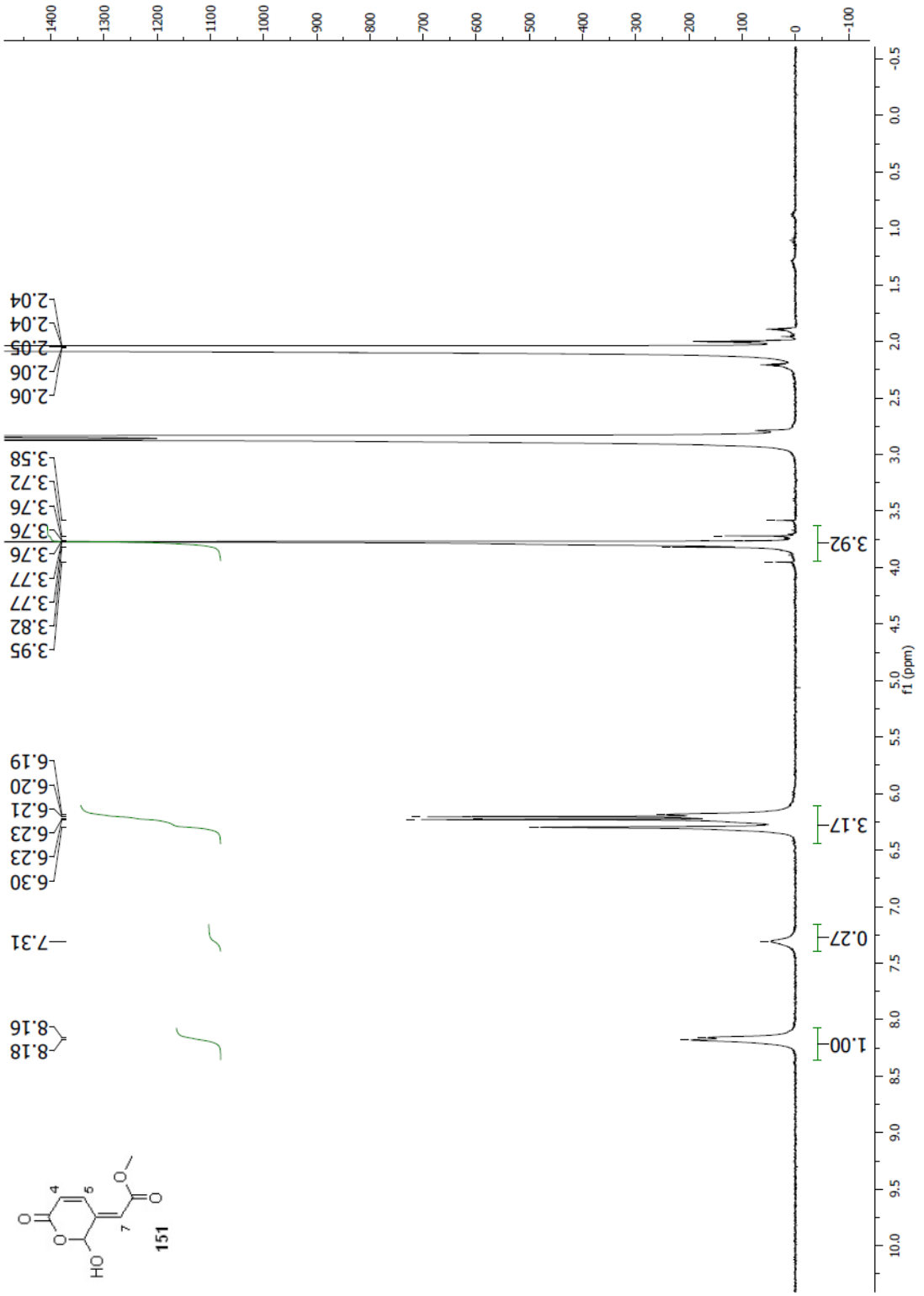

Spectrum 2.9 ^{1}H NMR ($(CD_3)_2CO$, 400 MHz) of compound **151**

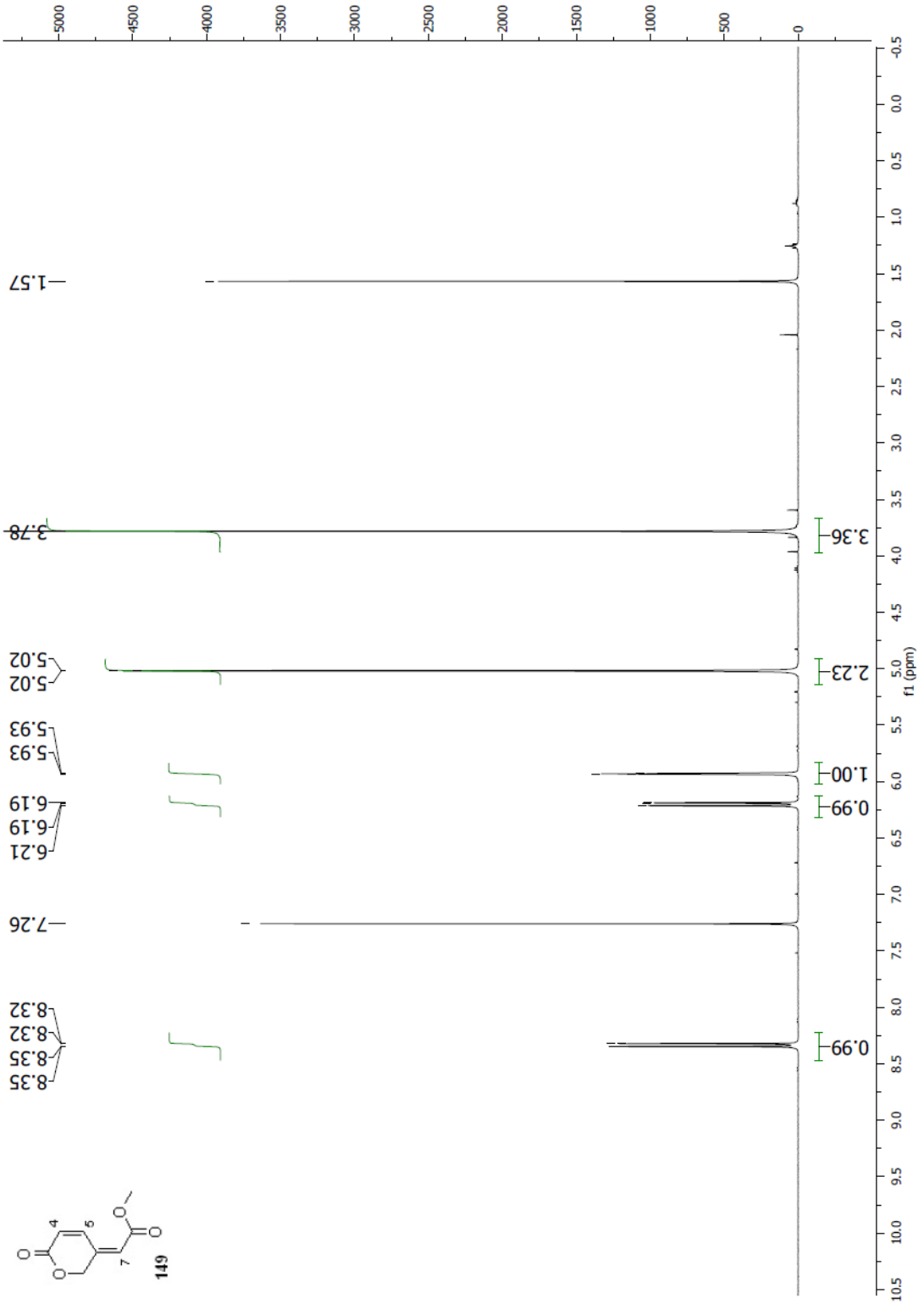

Spectrum 2.10 ^{1}H NMR ($CDCl_3$, 400 MHz) of compound **149**

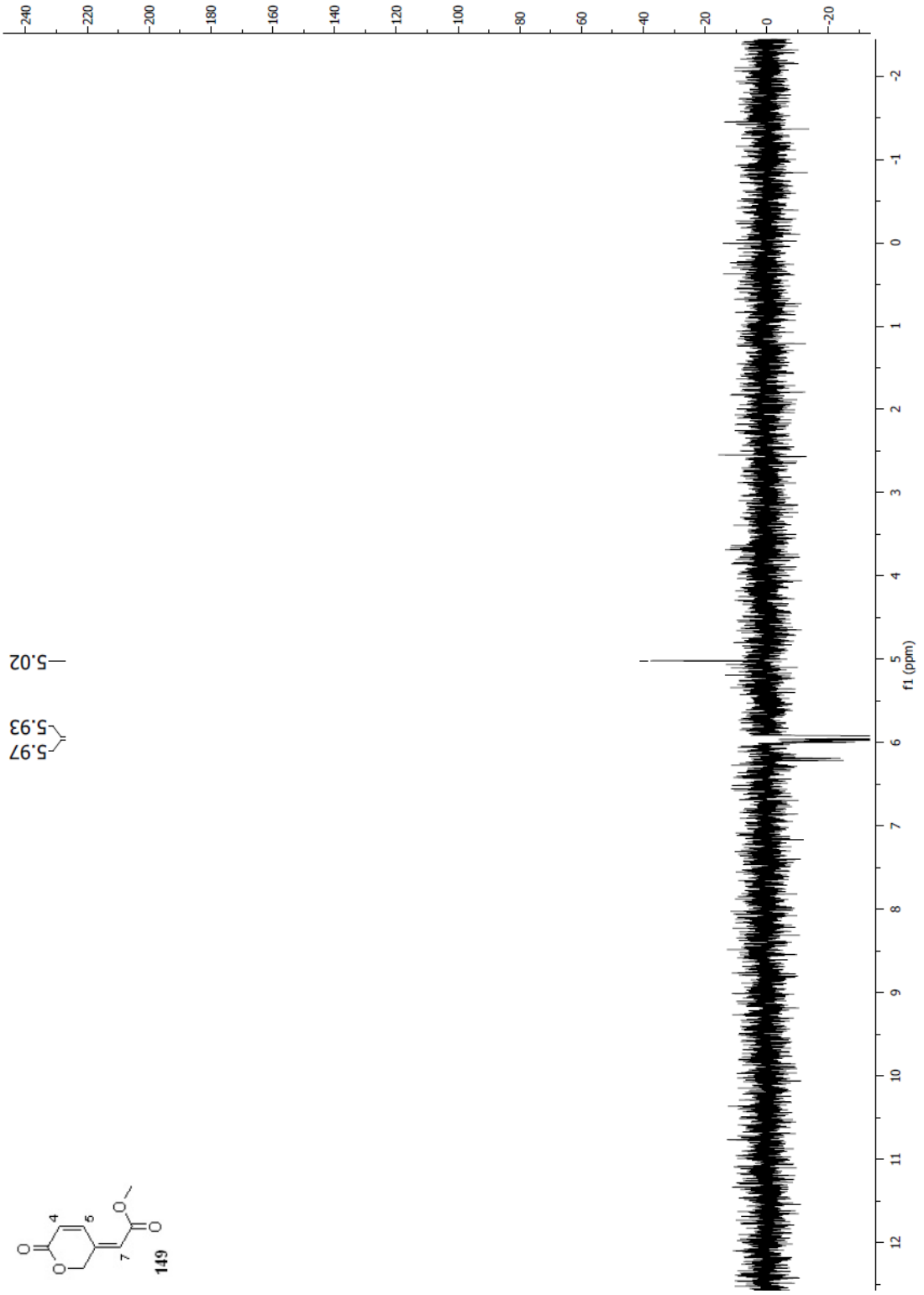

Spectrum 2.11 NOESY1D ($CDCl_3$, 400 MHz) of compound **149**, irradiation at H-7 methine δ 5.93 ppm

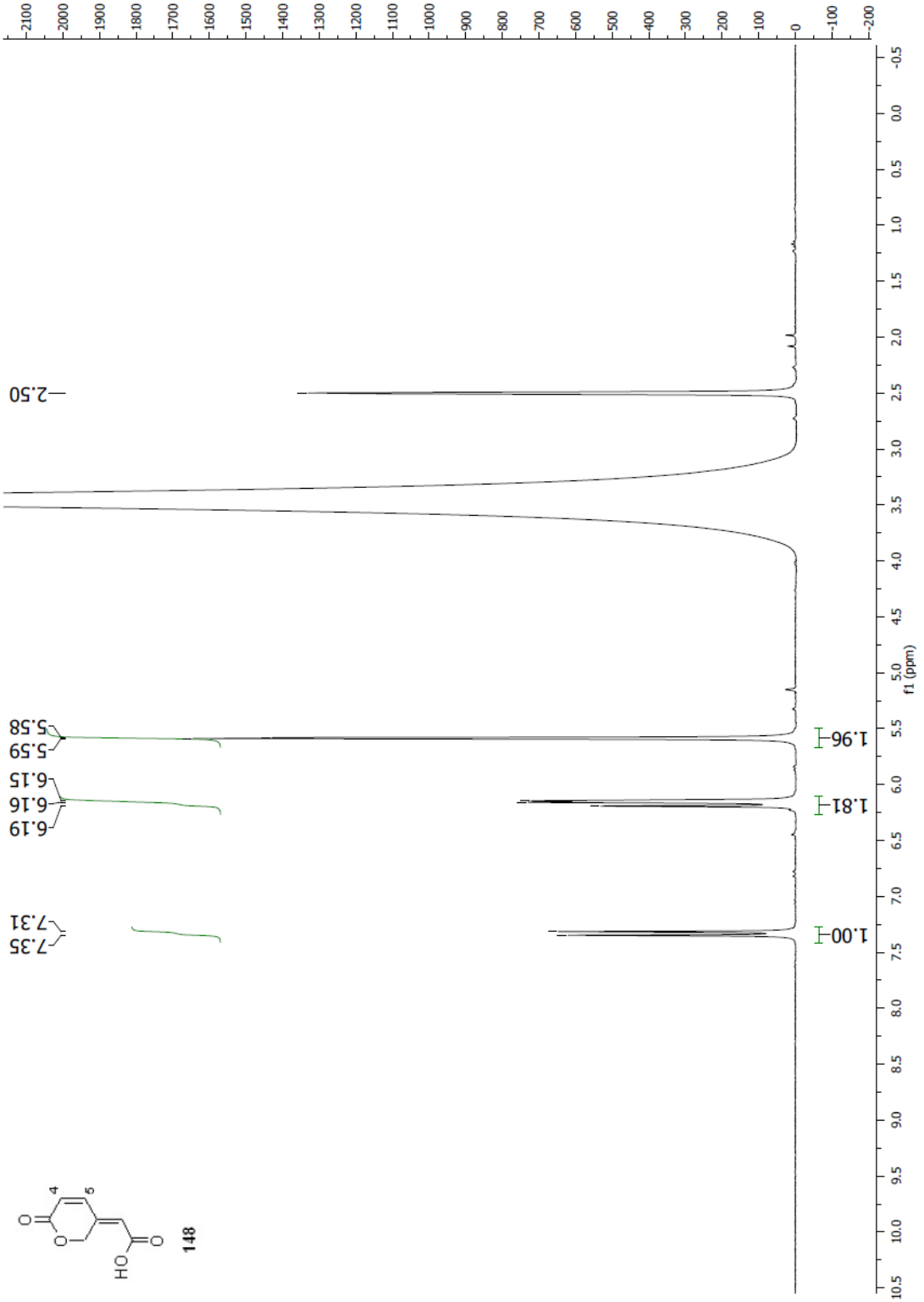

Spectrum 2.12 ^{1}H NMR (DMSO-*d*6, 300 MHz) of compound **148**

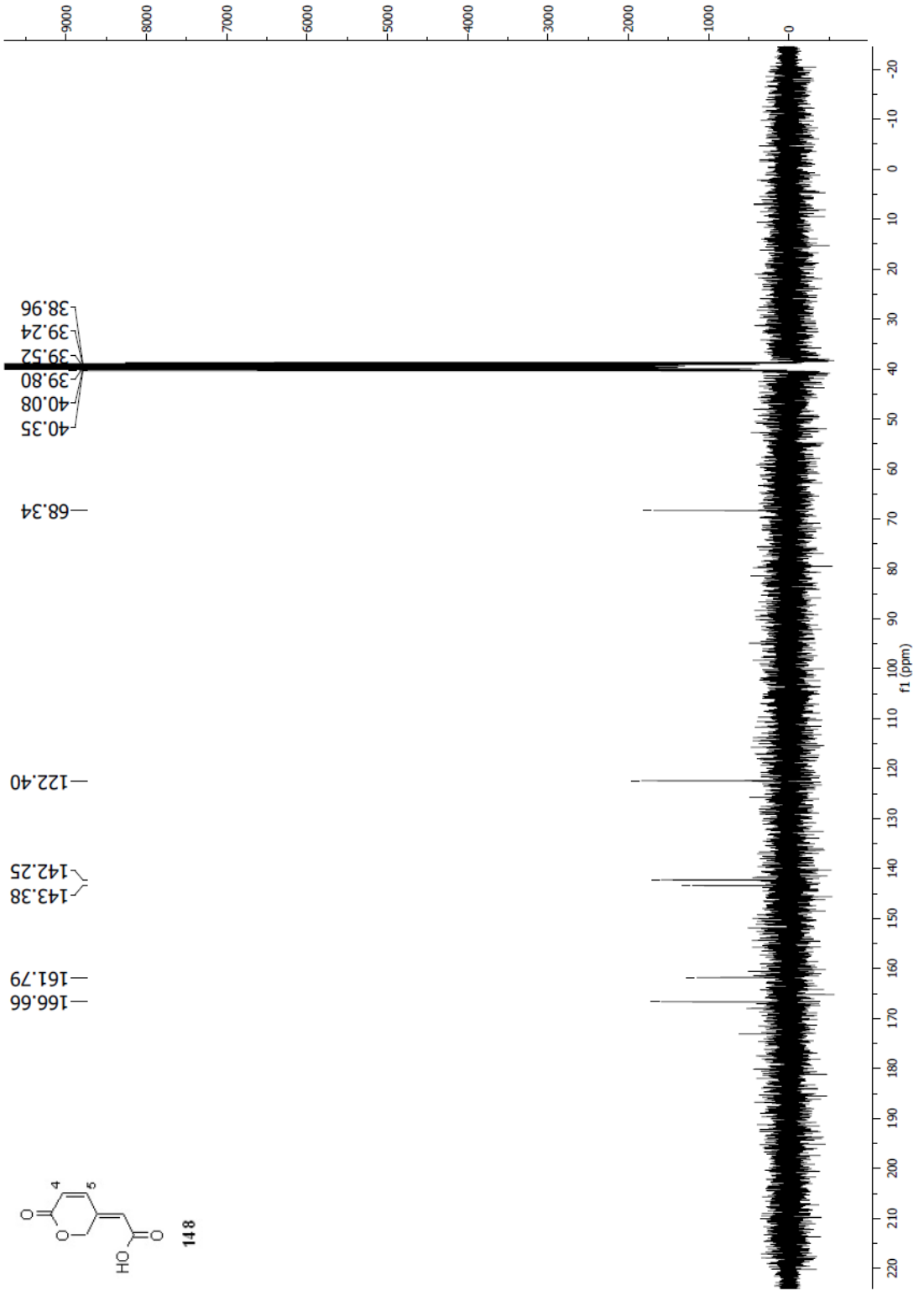

Spectrum 2.13 ^{13}C NMR (DMSO-*d*6, 75 MHz) of compound **148**

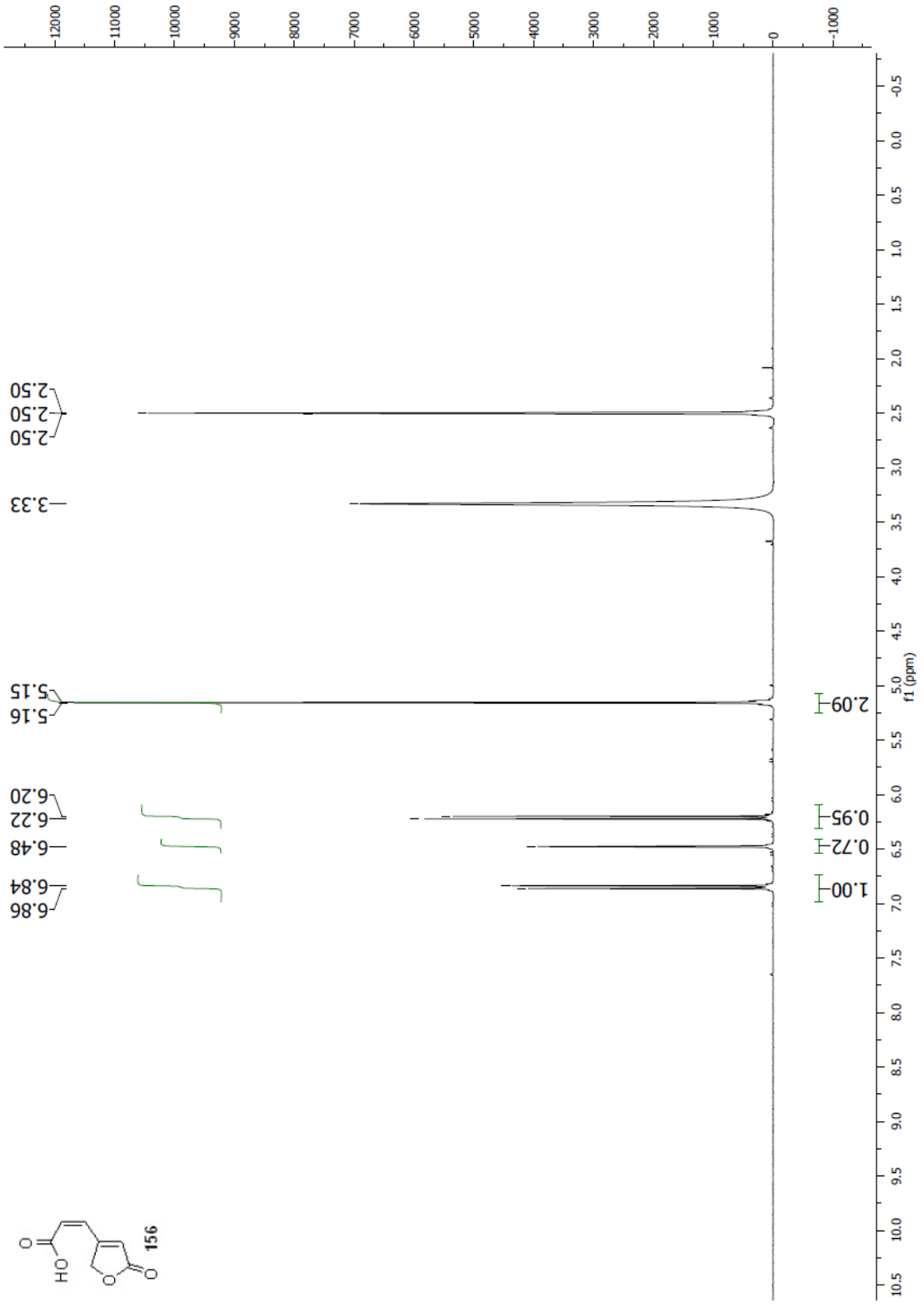

Spectrum 2.14 ^{1}H NMR (DMSO-*d*6, 500 MHz) of compound **156**

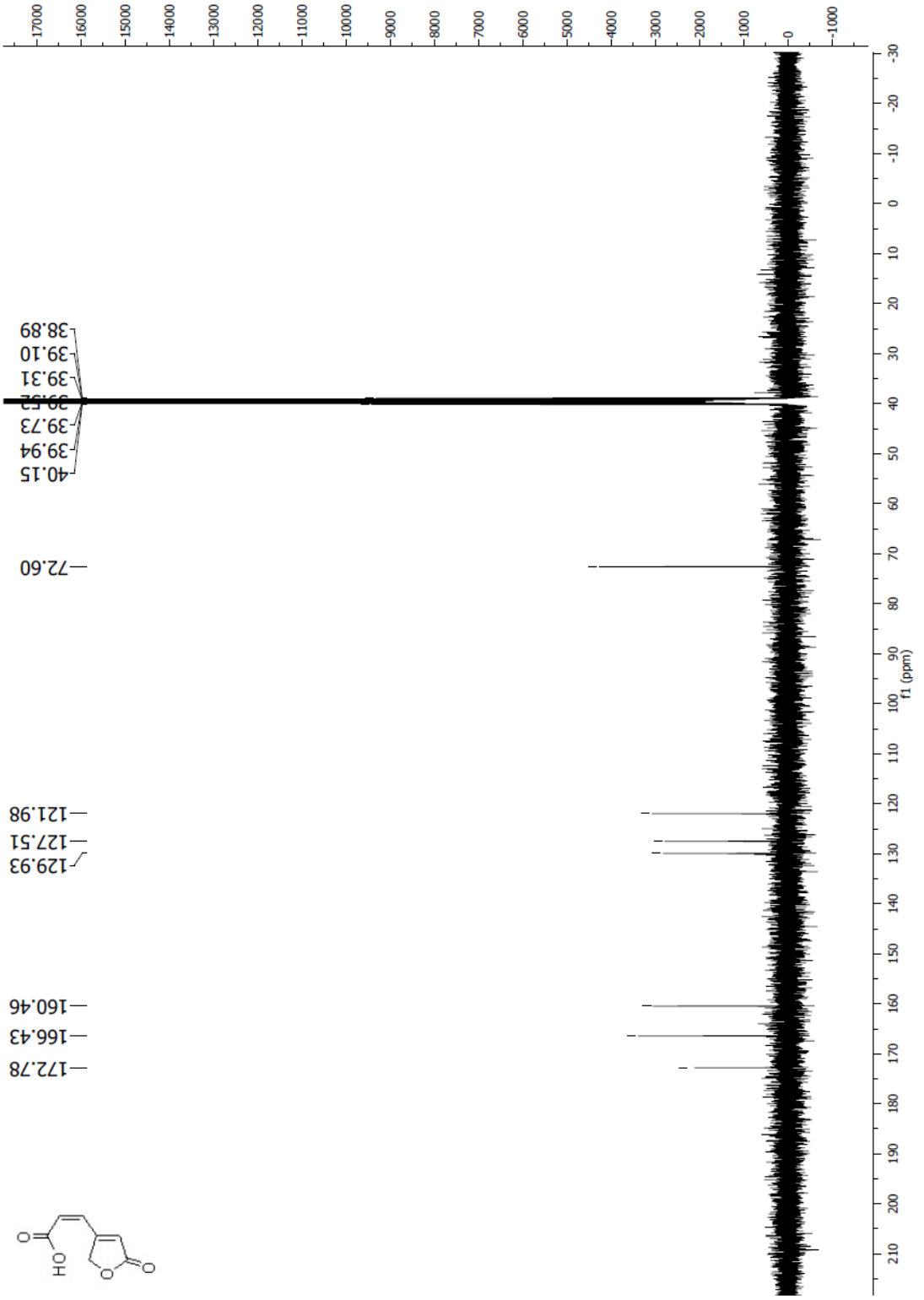

Spectrum 2.15 ^{13}C NMR (DMSO-*d*6, 100 MHz) of compound **156**

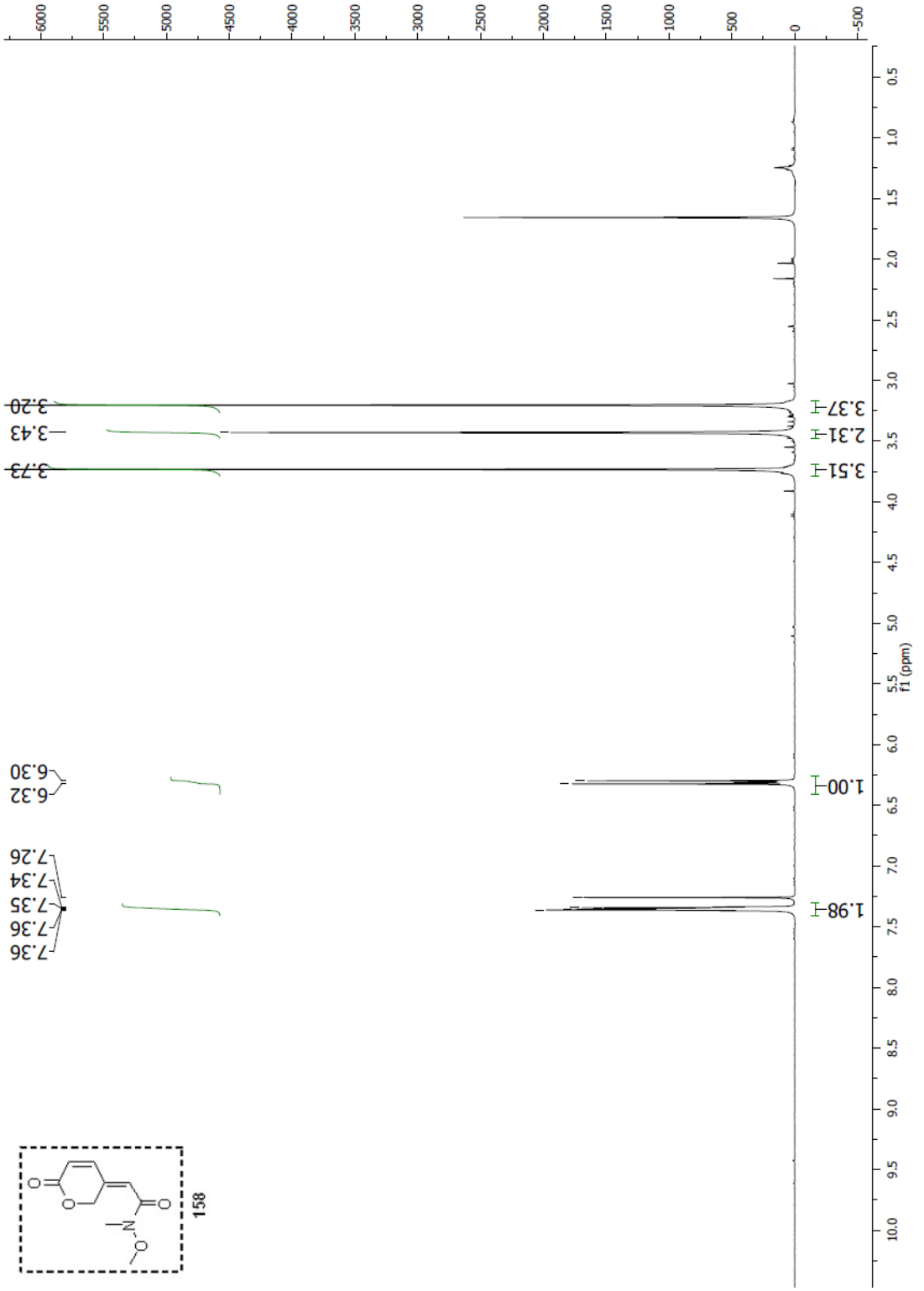

Spectrum 2.16 ^{1}H NMR ($CDCl_3$, 400 MHz) of compound **158**

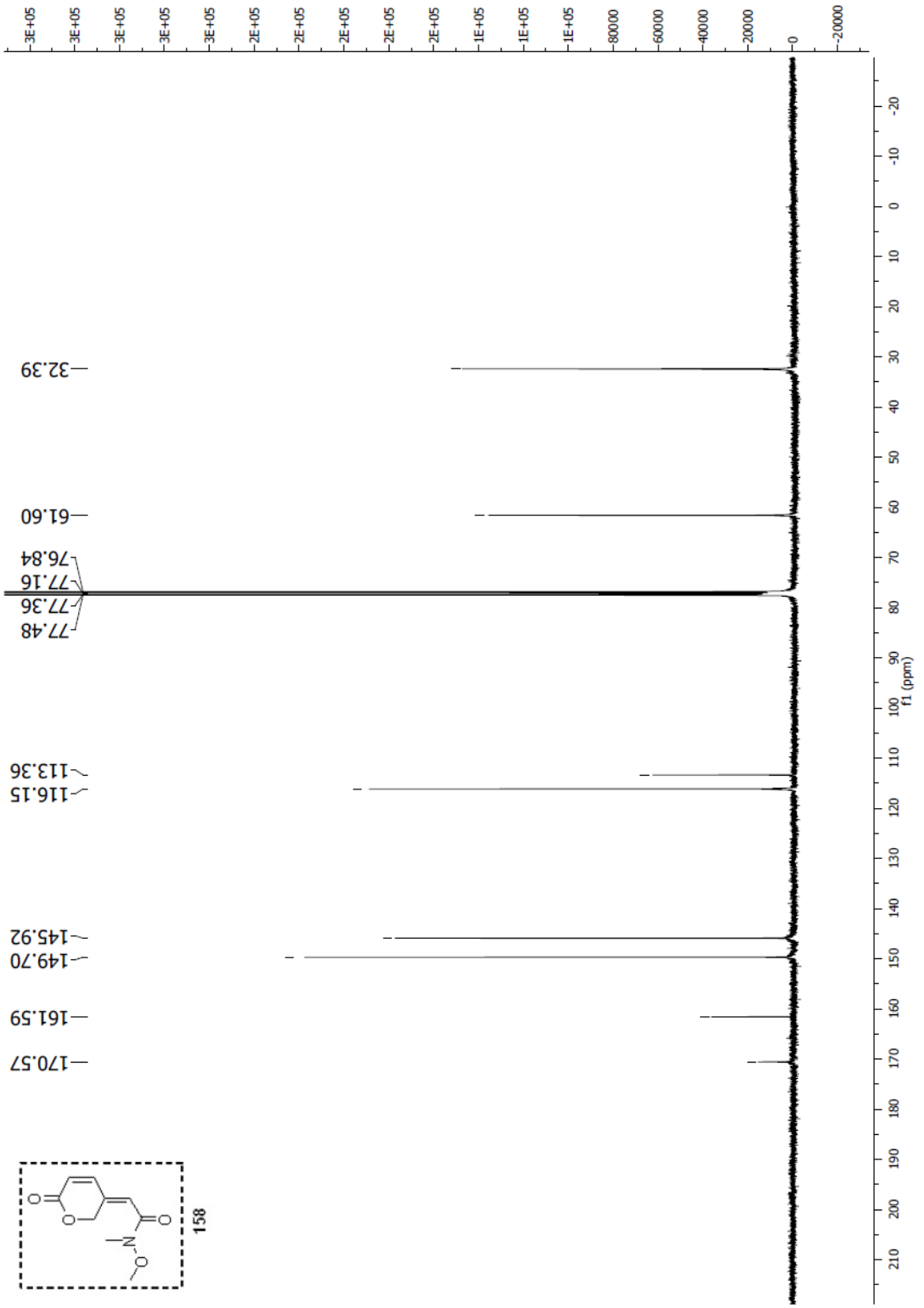

Spectrum 2.17 ^{13}C NMR ($CDCl_3$, 100 MHz) of compound **158**

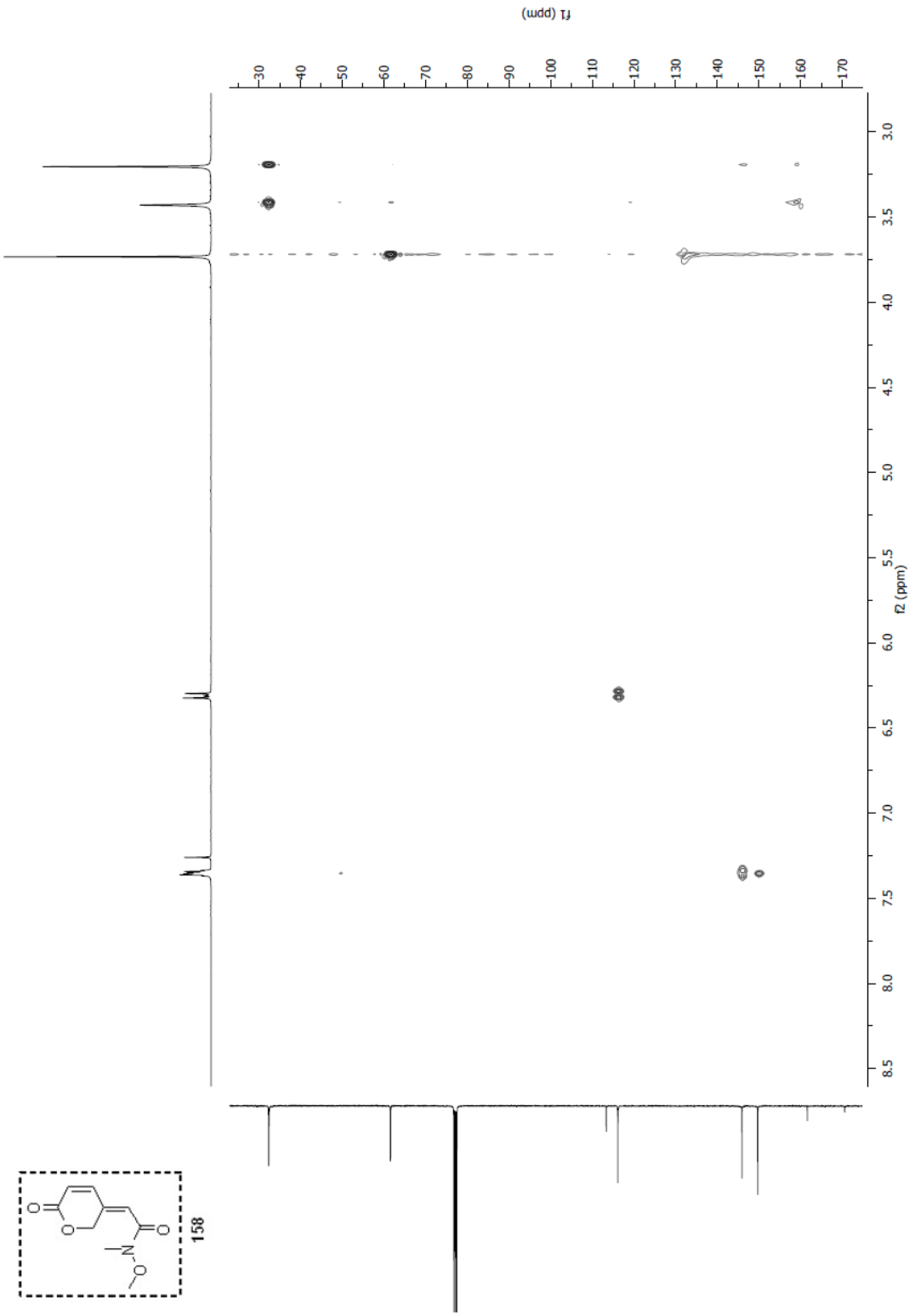

Spectrum 2.18 ^{1}H-^{13}C gHMQC NMR ($CDCl_3$, 400 MHz – 100 MHz) of compound **158**

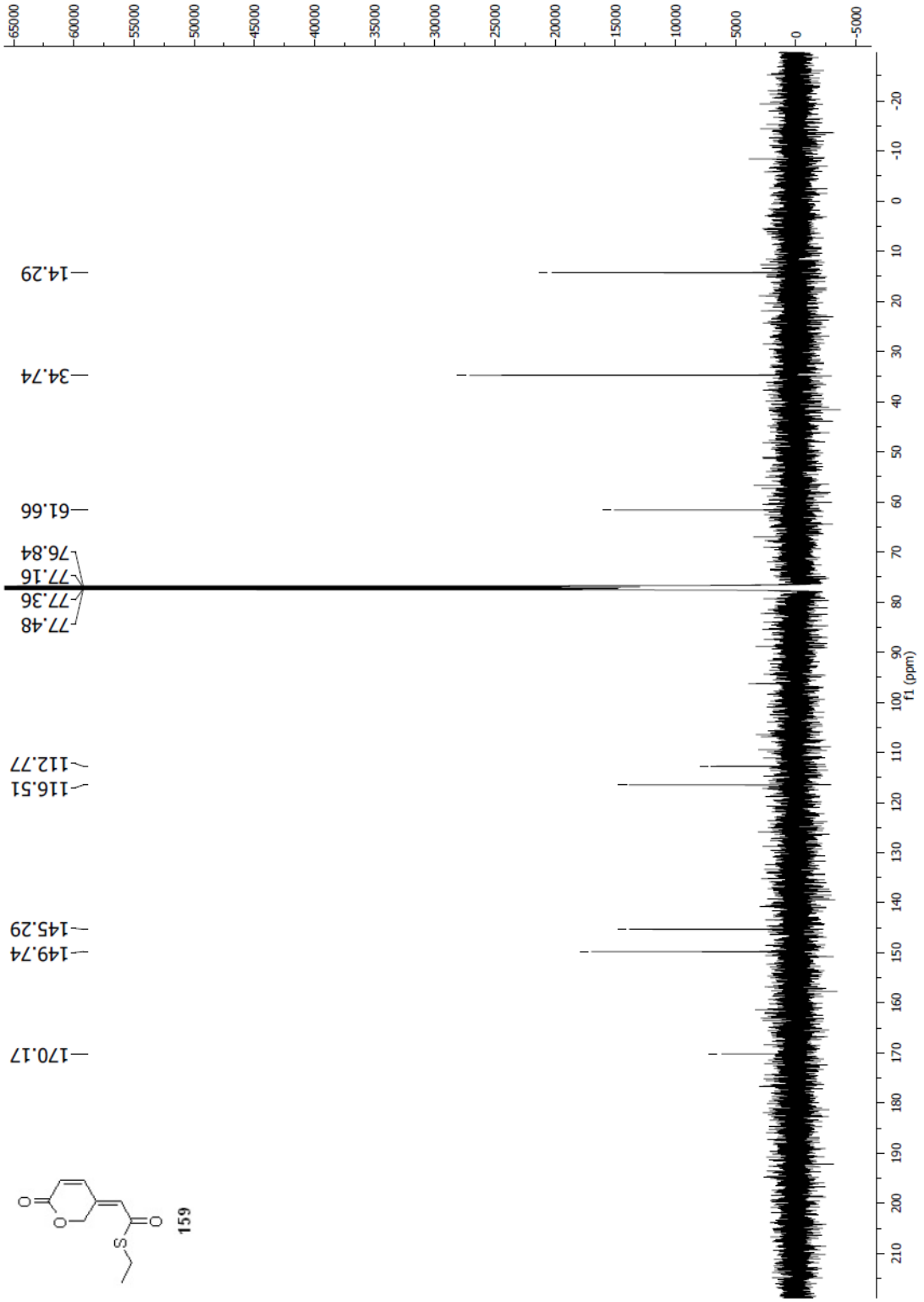

Spectrum 2.19 ^{1}H NMR ($CDCl_3$, 100 MHz) of compound **159**

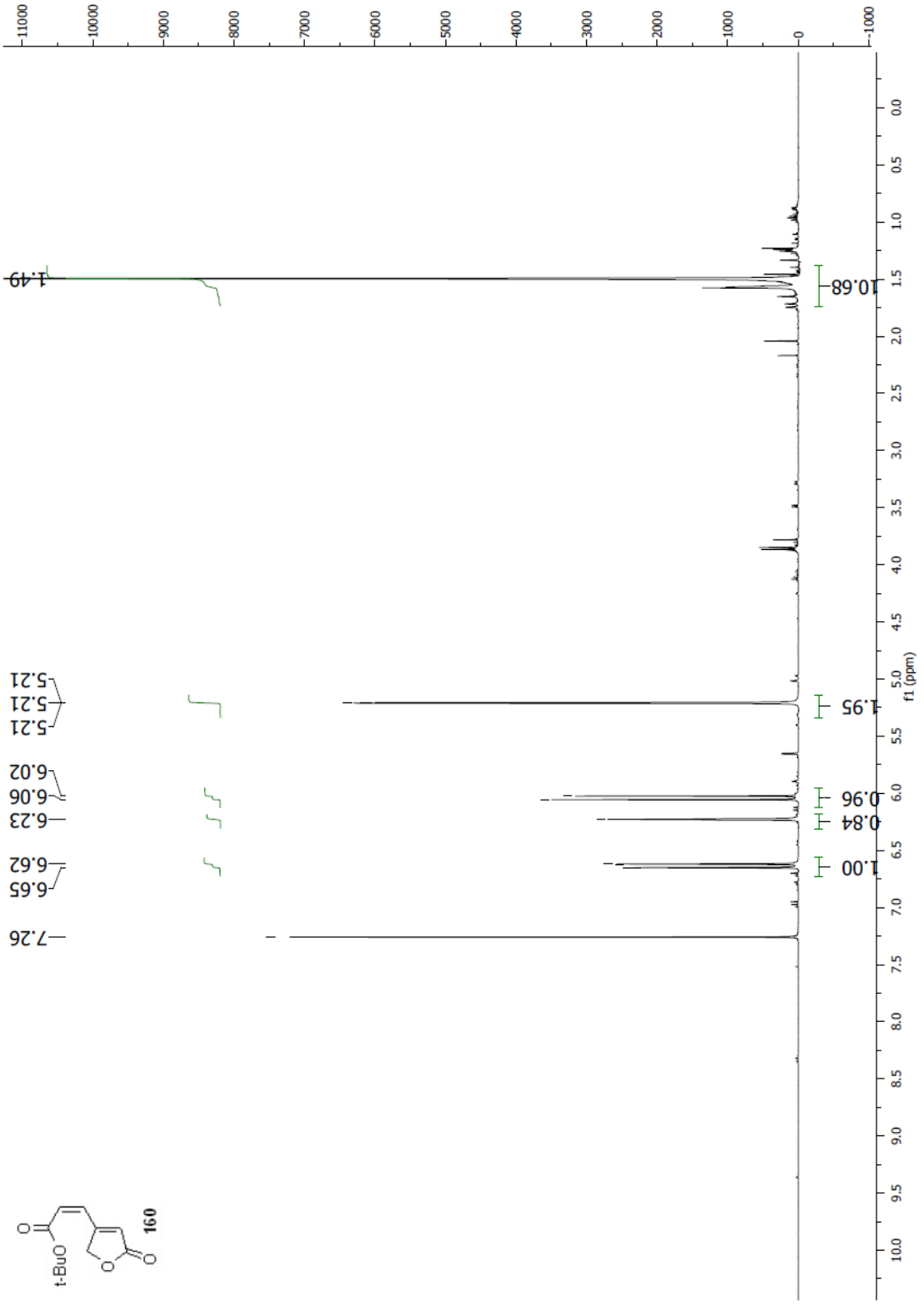

Spectrum 2.20 ^{1}H NMR ($CDCl_3$, 400 MHz) of compound **160**

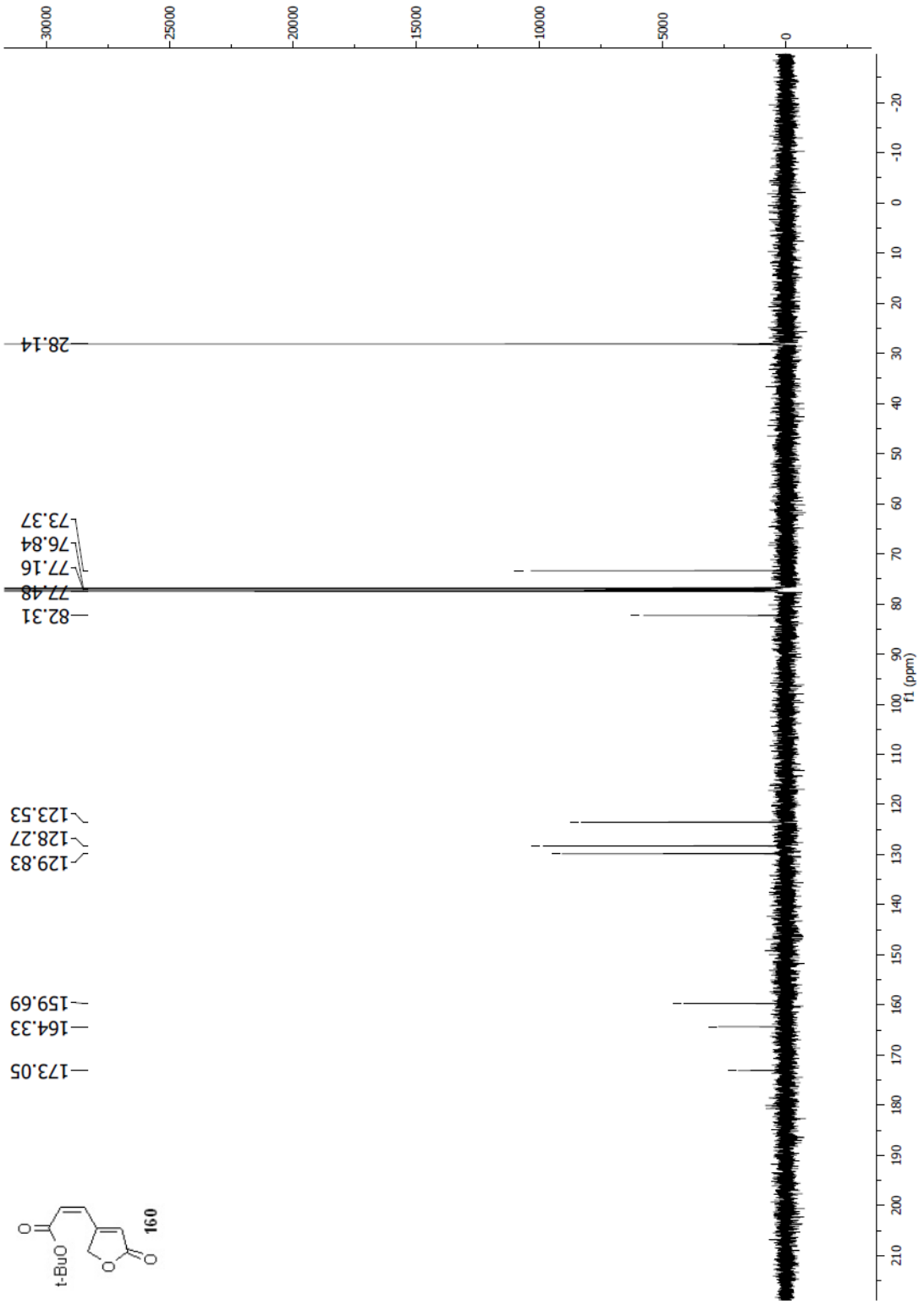

Spectrum 2.21 ^{13}C NMR ($CDCl_3$, 100 MHz) of compound **160**

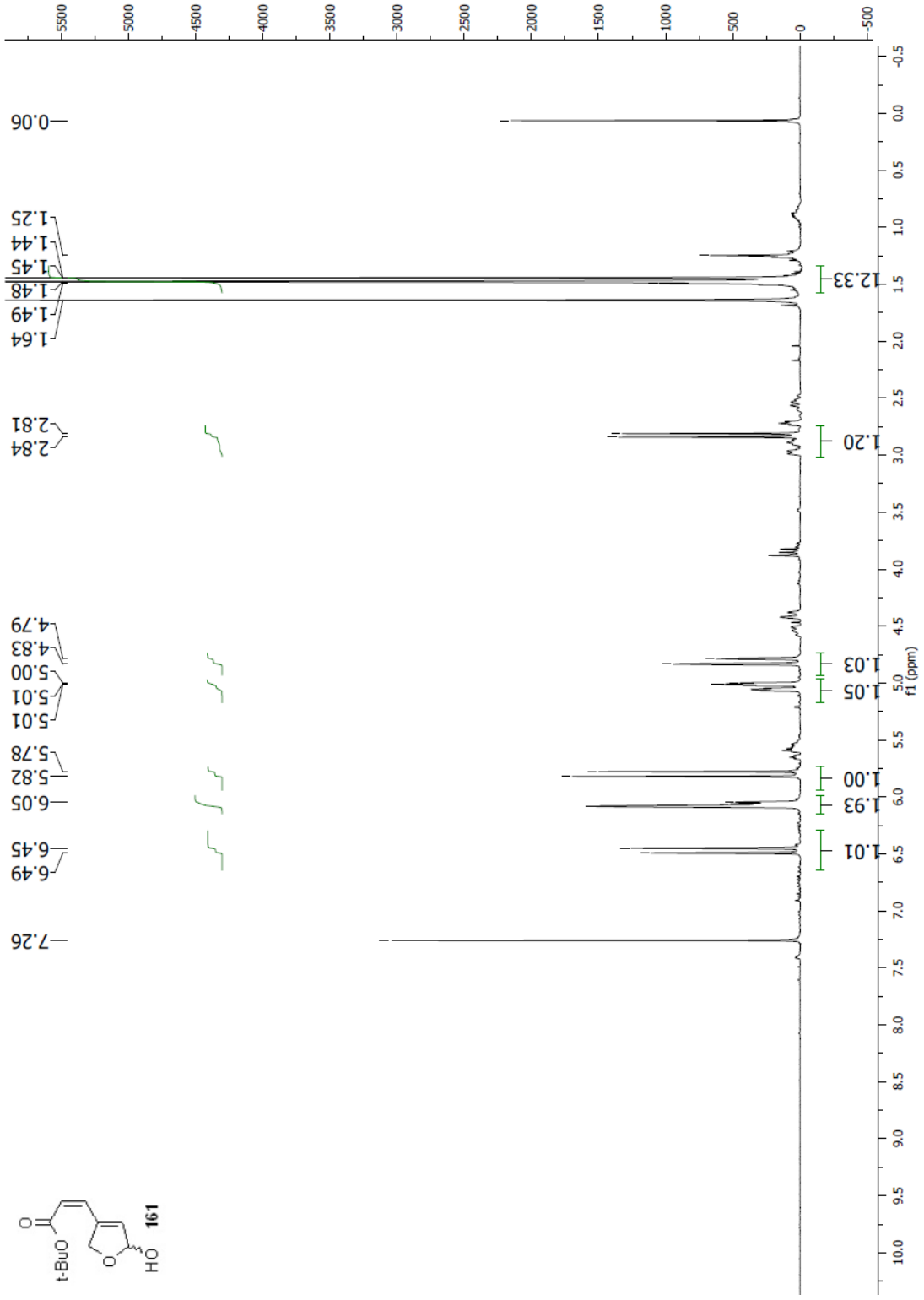

Spectrum 2.22 ^{1}H NMR ($CDCl_3$, 300 MHz) of compound **161**

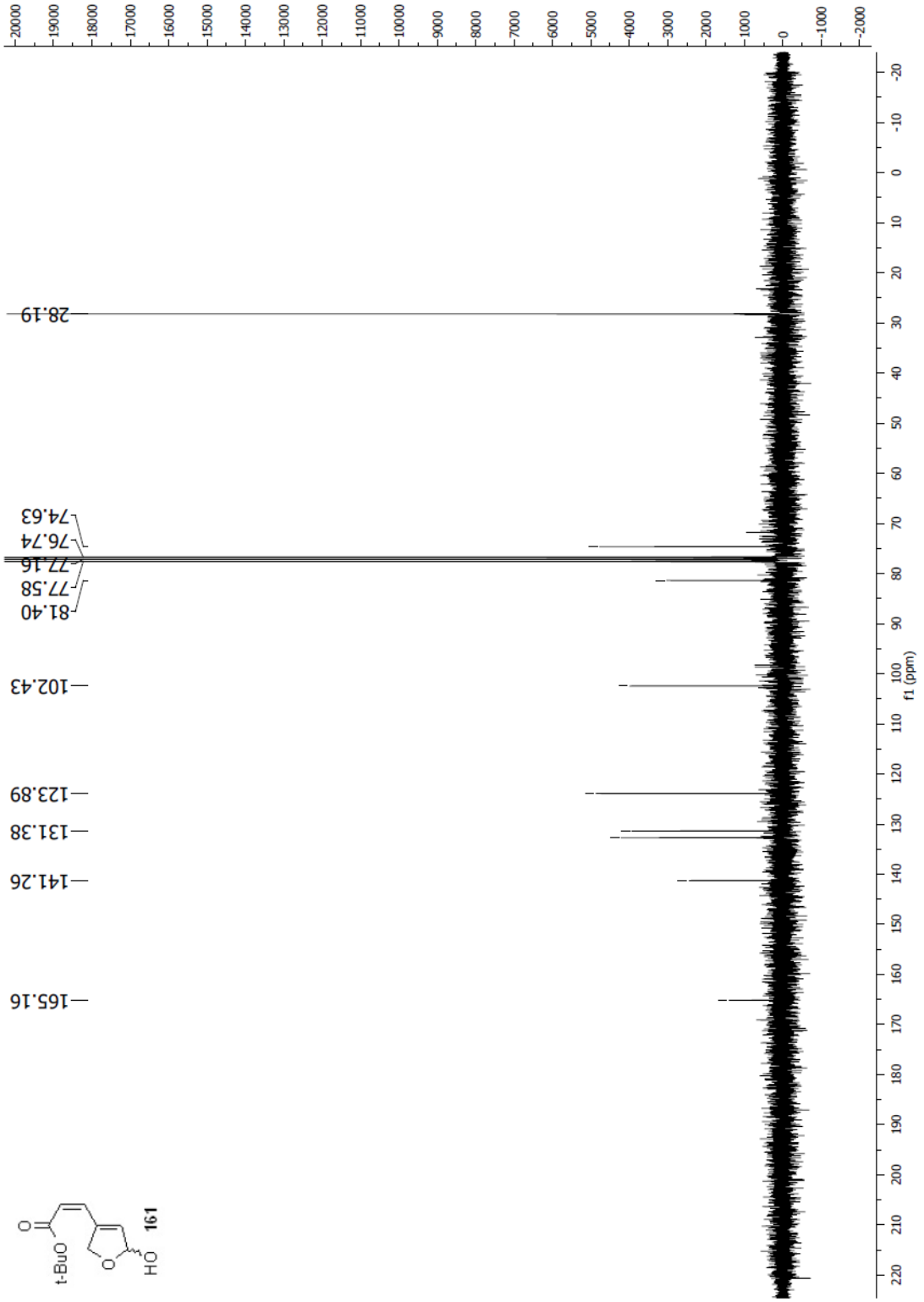

Spectrum 2.23 ^{13}C NMR ($CDCl_3$, 75 MHz) of compound **161**

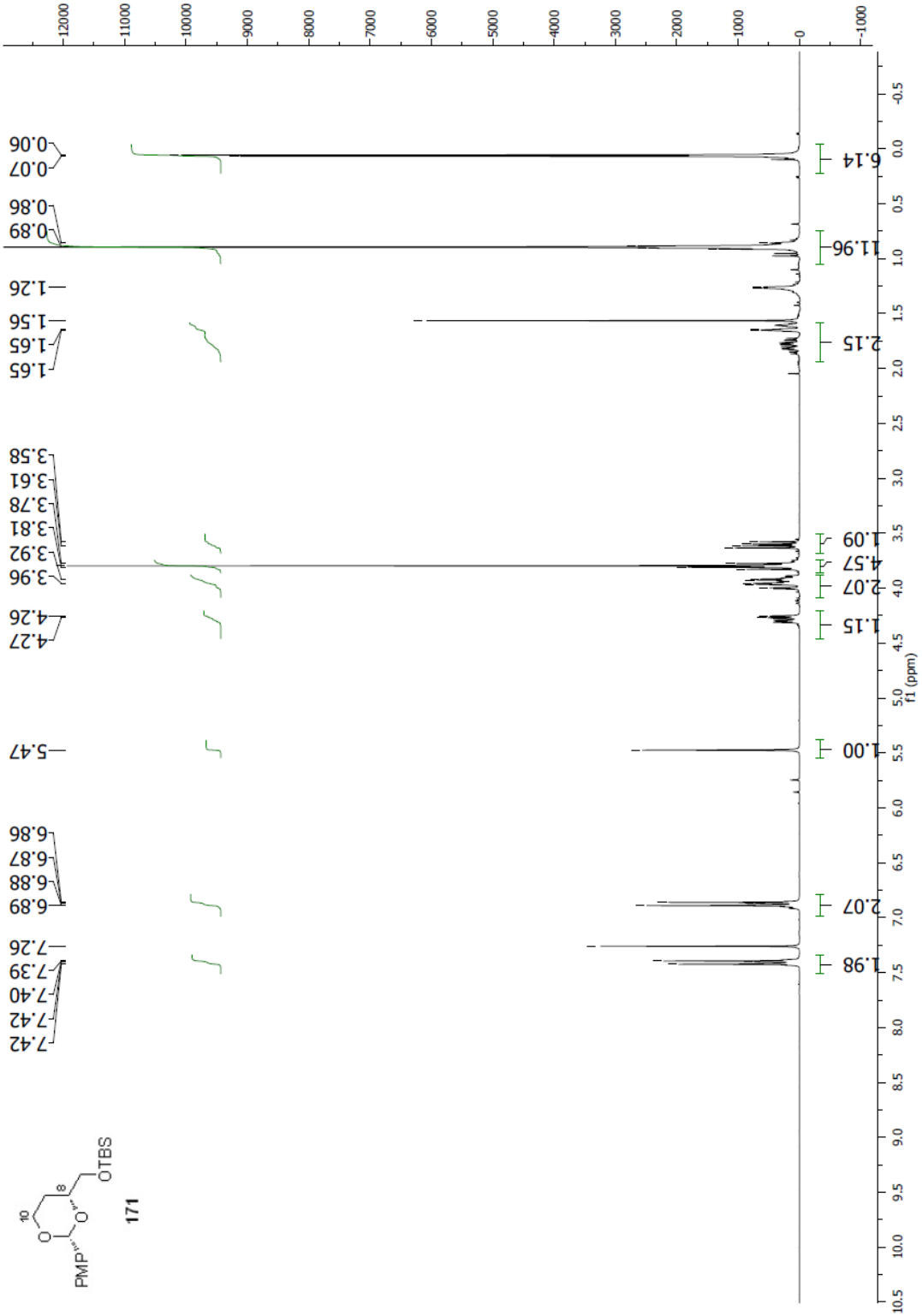

Spectrum 2.24 ^{1}H NMR ($CDCl_3$, 300 MHz) of compound **171**

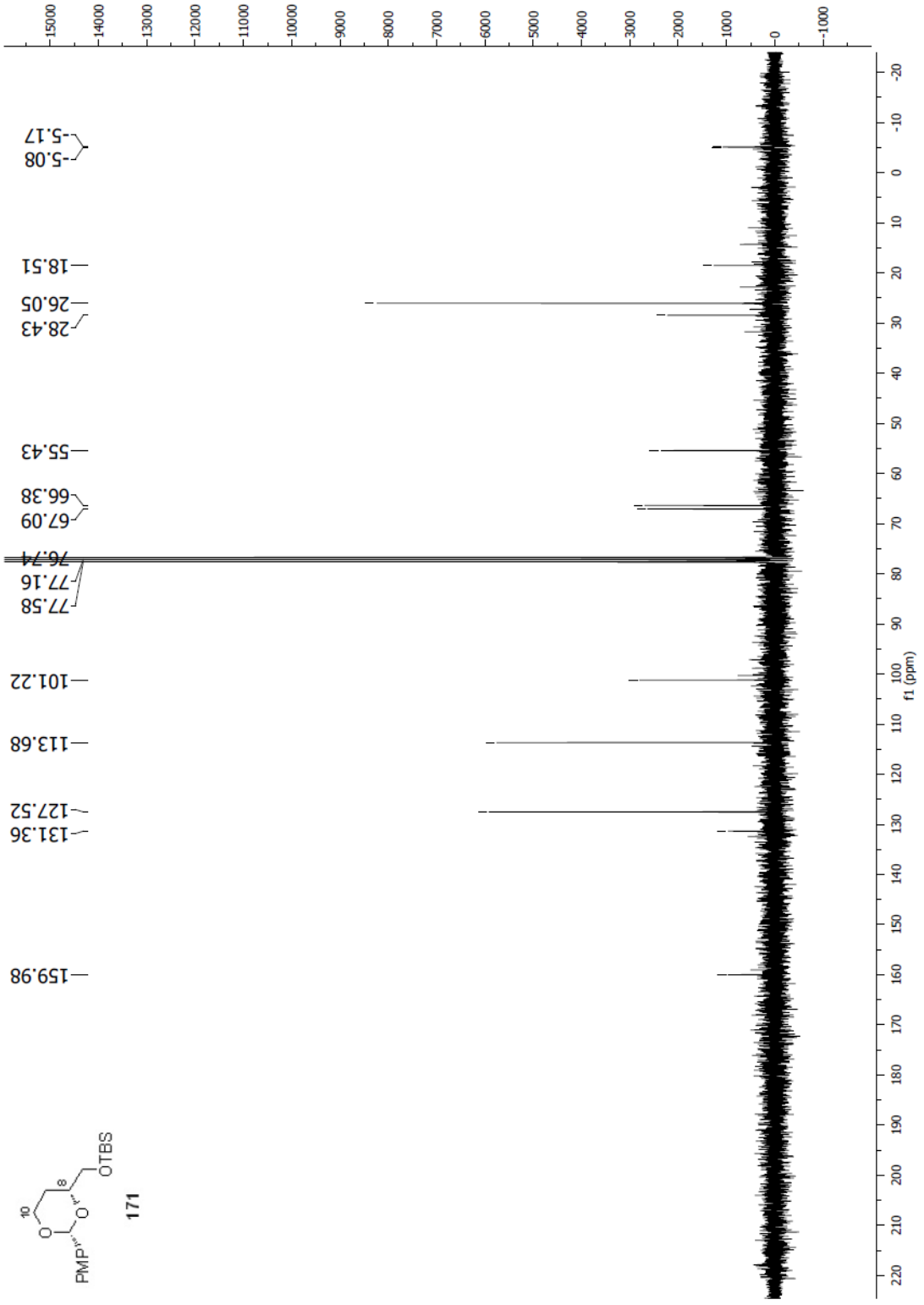

Spectrum 2.25 ^{13}C NMR ($CDCl_3$, 75 MHz) of compound **171**

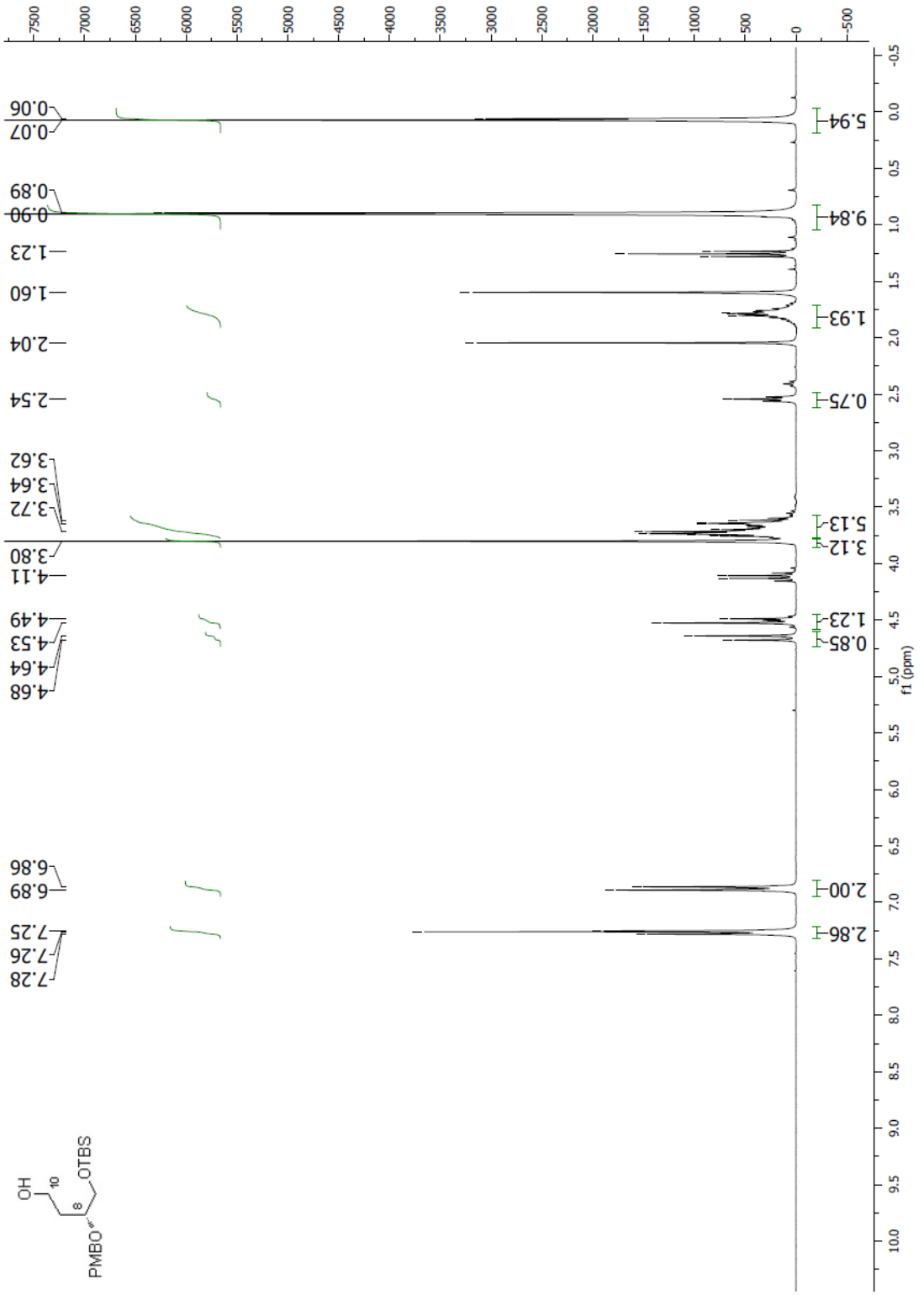

Spectrum 2.26 ^{1}H NMR ($CDCl_3$, 300 MHz) of reduction product of **171**

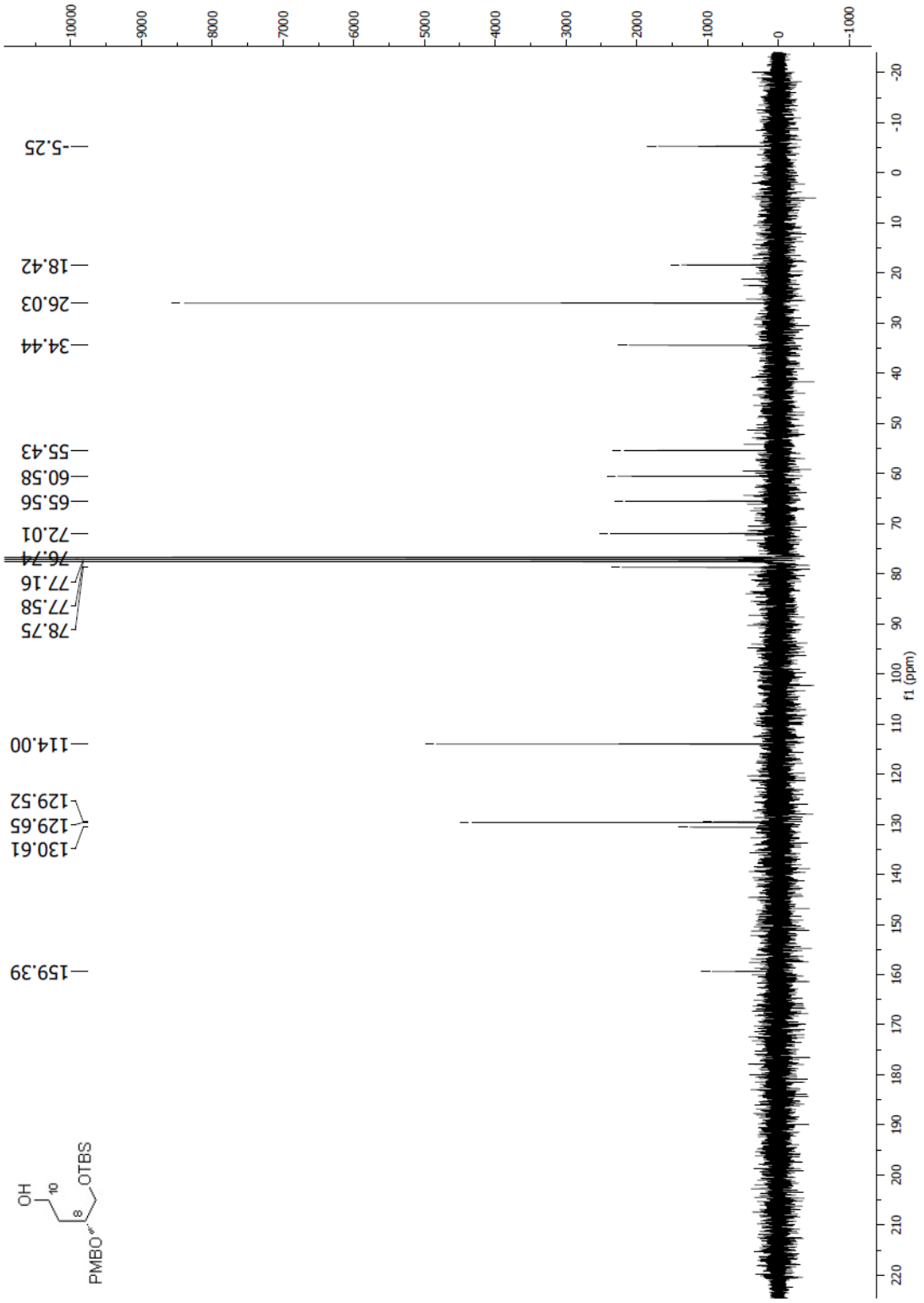

Spectrum 2.27 ^{13}C NMR ($CDCl_3$, 75 MHz) of reduction product of **171**

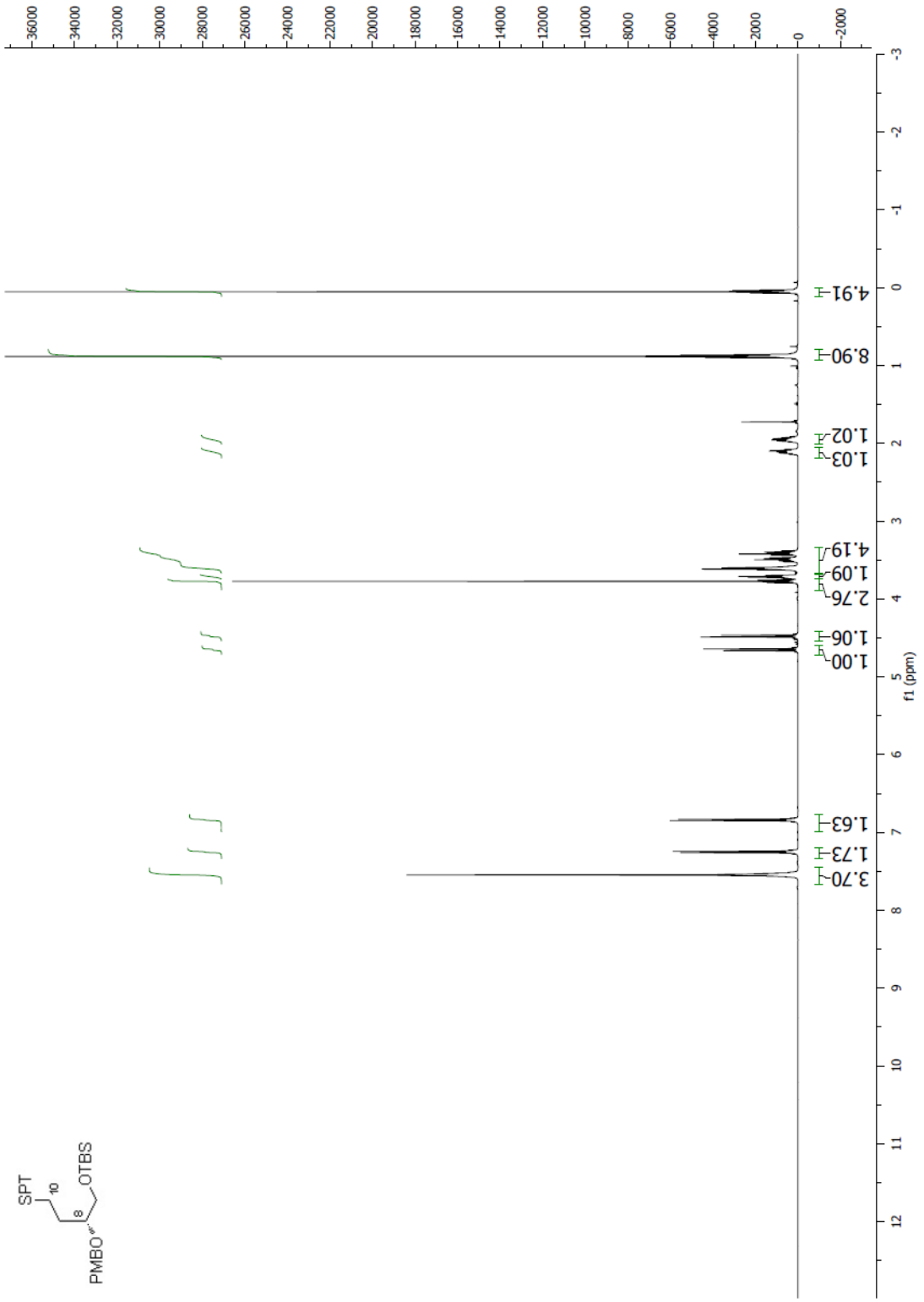

Spectrum 2.28 ^{1}H NMR ($CDCl_3$, 500 MHz) of sulfide precursor to **168**

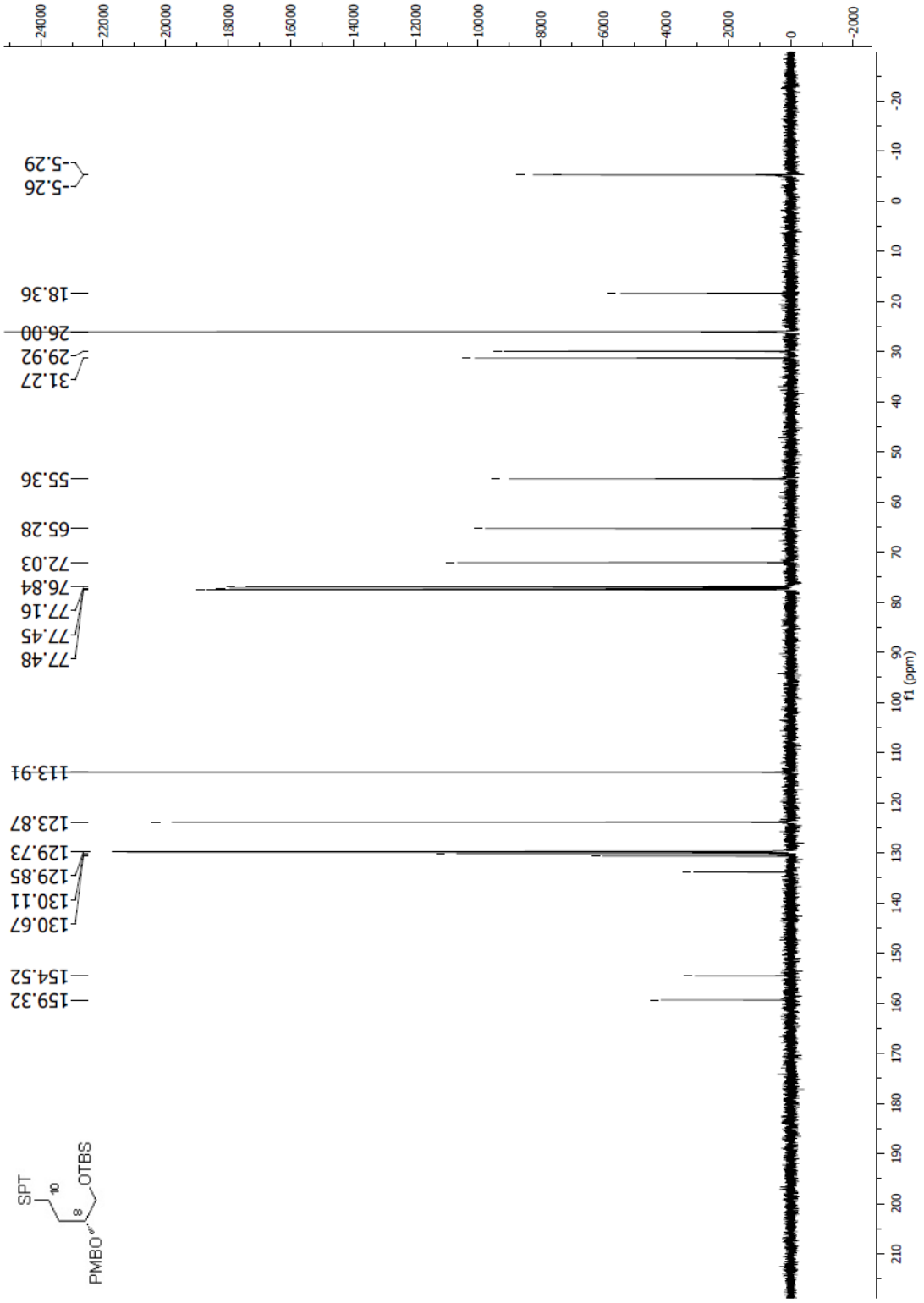

Spectrum 2.29 ^{13}C NMR ($CDCl_3$, 100 MHz) of sulfide precursor to **168**

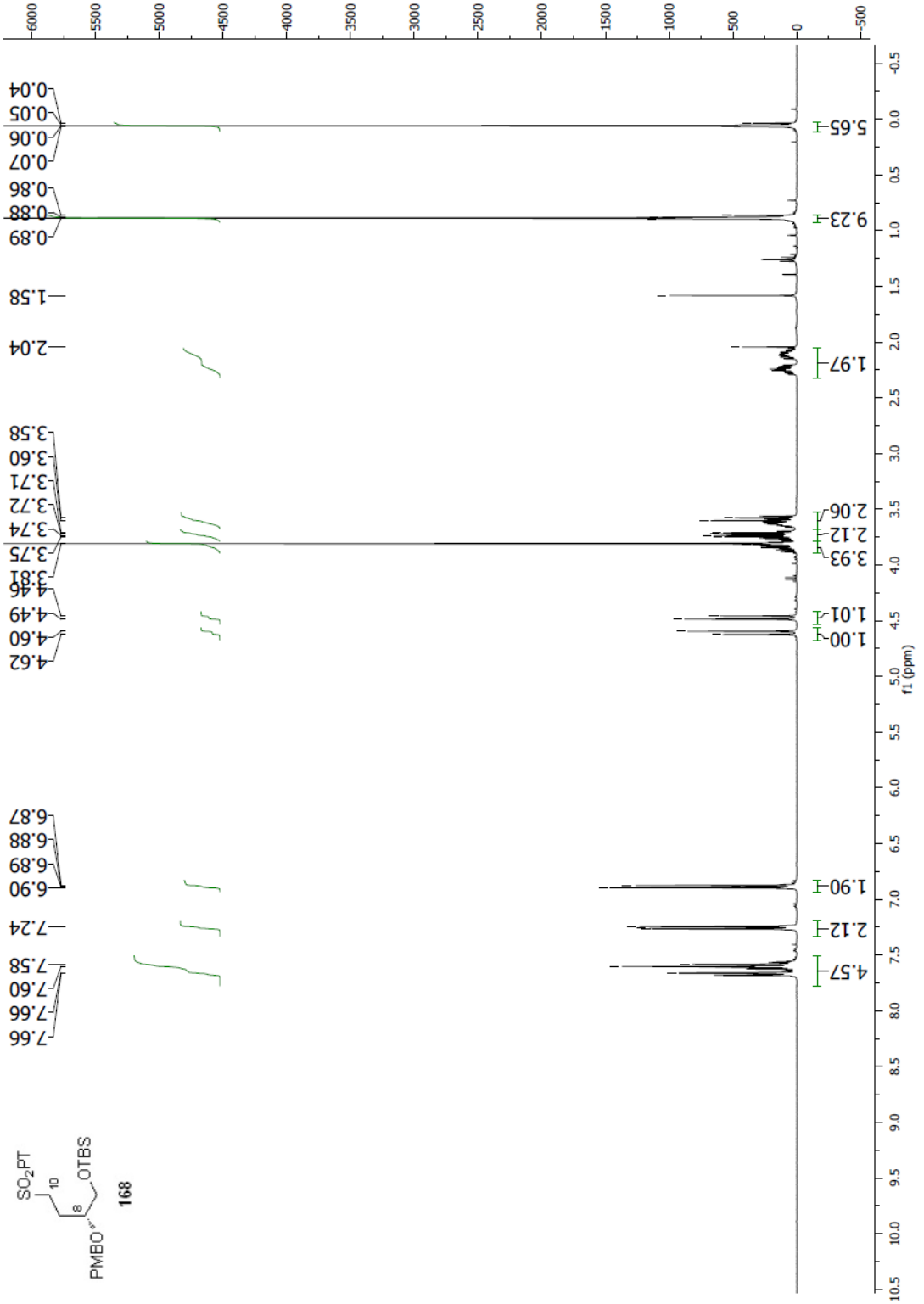

Spectrum 2.30 ^{1}H NMR ($CDCl_3$, 400 MHz) of compound **168**

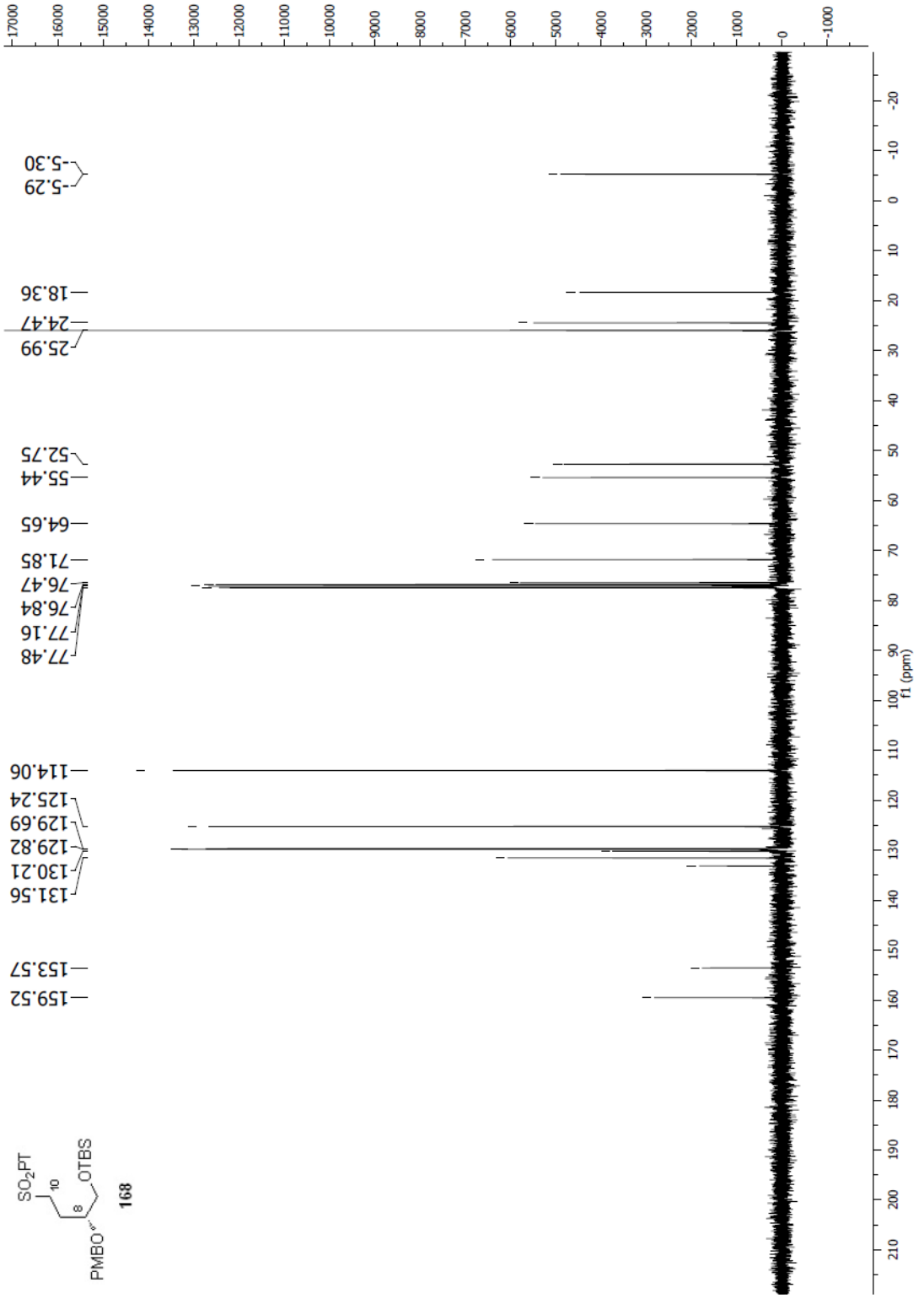

Spectrum 2.31 ^{13}C NMR ($CDCl_3$, 100 MHz) of compound **168**

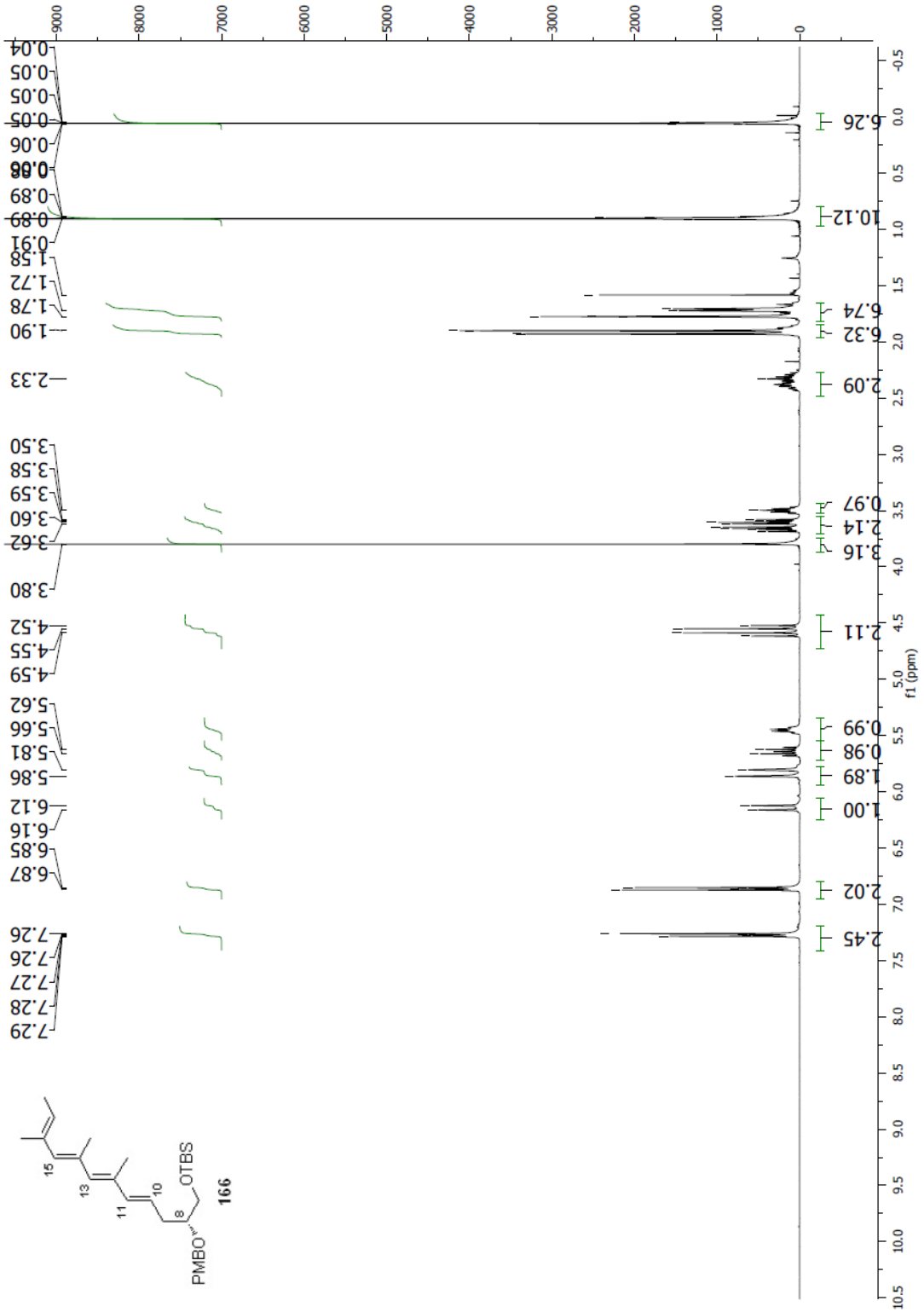

Spectrum 2.32 ^{1}H NMR ($CDCl_3$, 400 MHz) of compound **166**

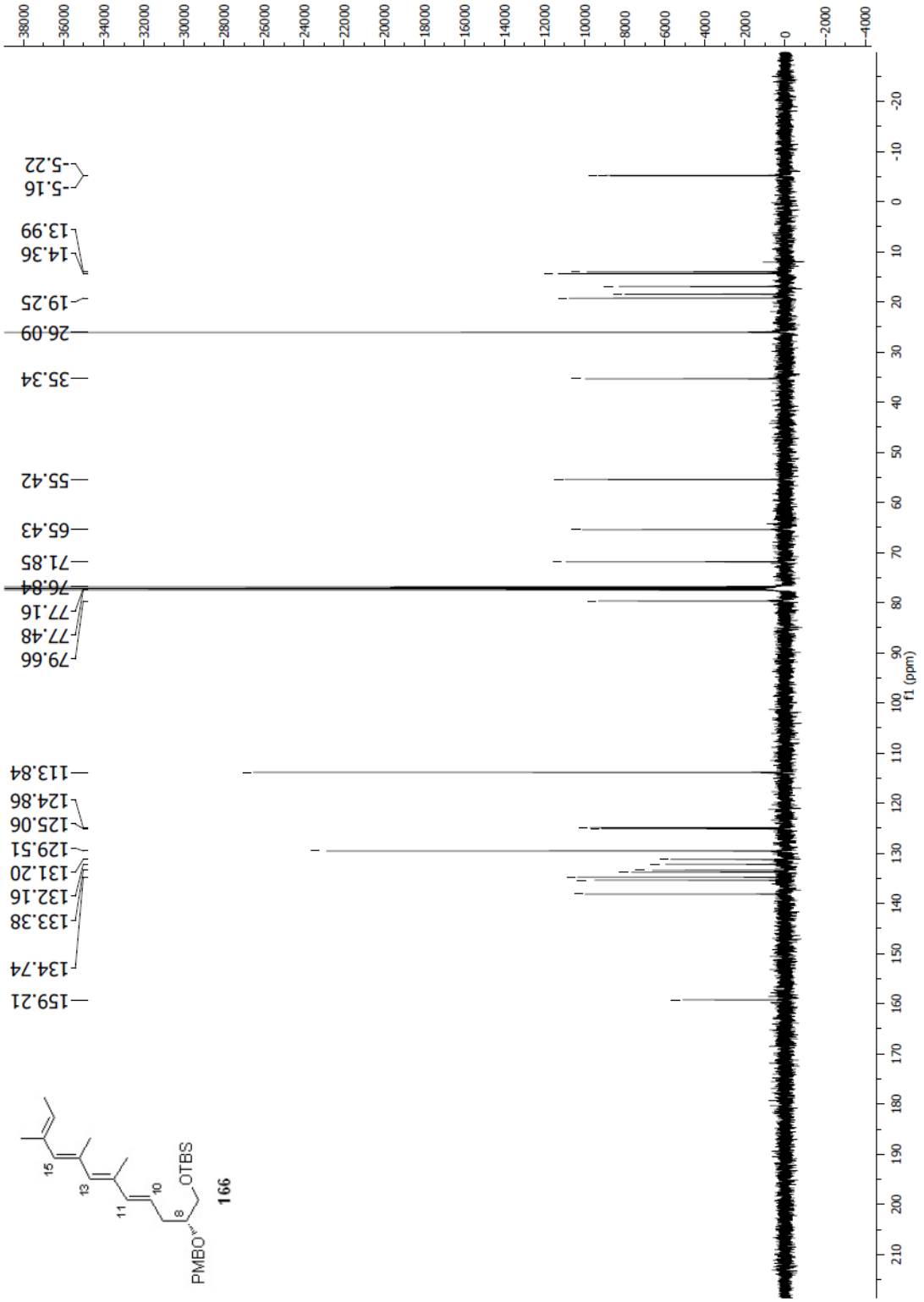

Spectrum 2.33 ^{13}C NMR ($CDCl_3$, 100 MHz) of compound **166**

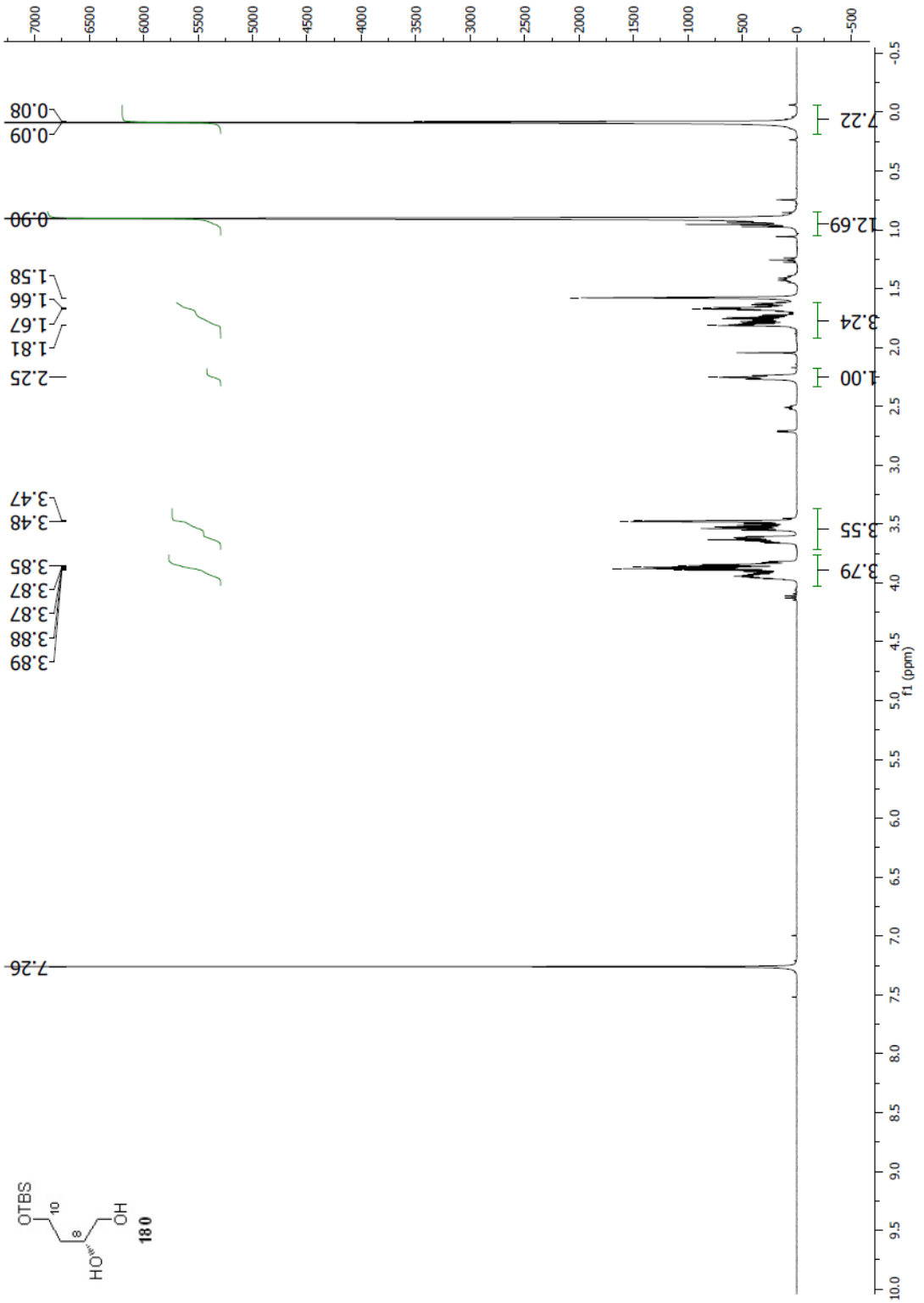

Spectrum 2.34 ^{1}H NMR ($CDCl_3$, 400 MHz) of compound **180**

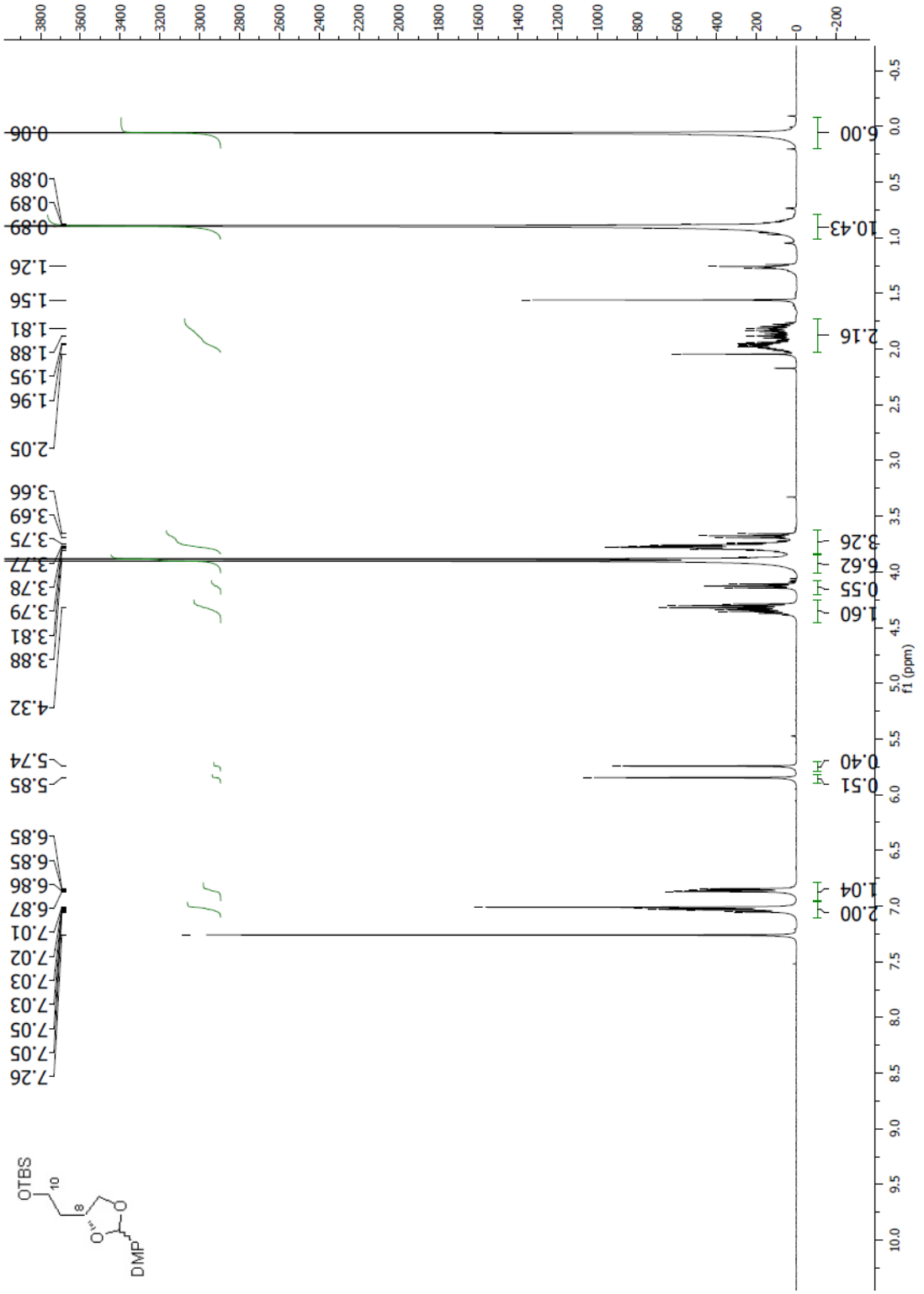

Spectrum 2.35 ^{1}H NMR ($CDCl_3$, 400 MHz) of the DMP acetal of **180**

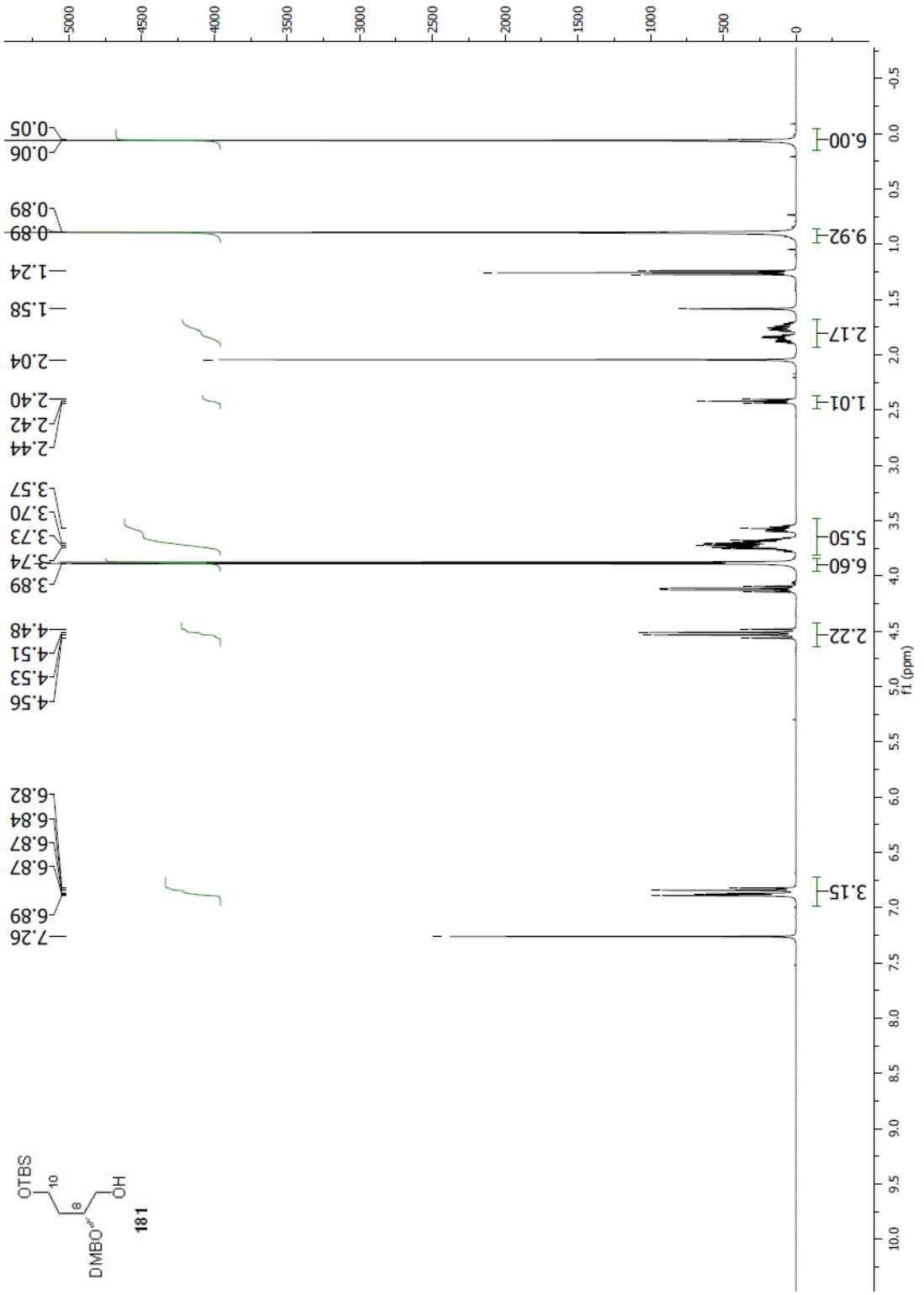

Spectrum 2.36 ^{1}H NMR ($CDCl_3$, 400 MHz) of compound **181**

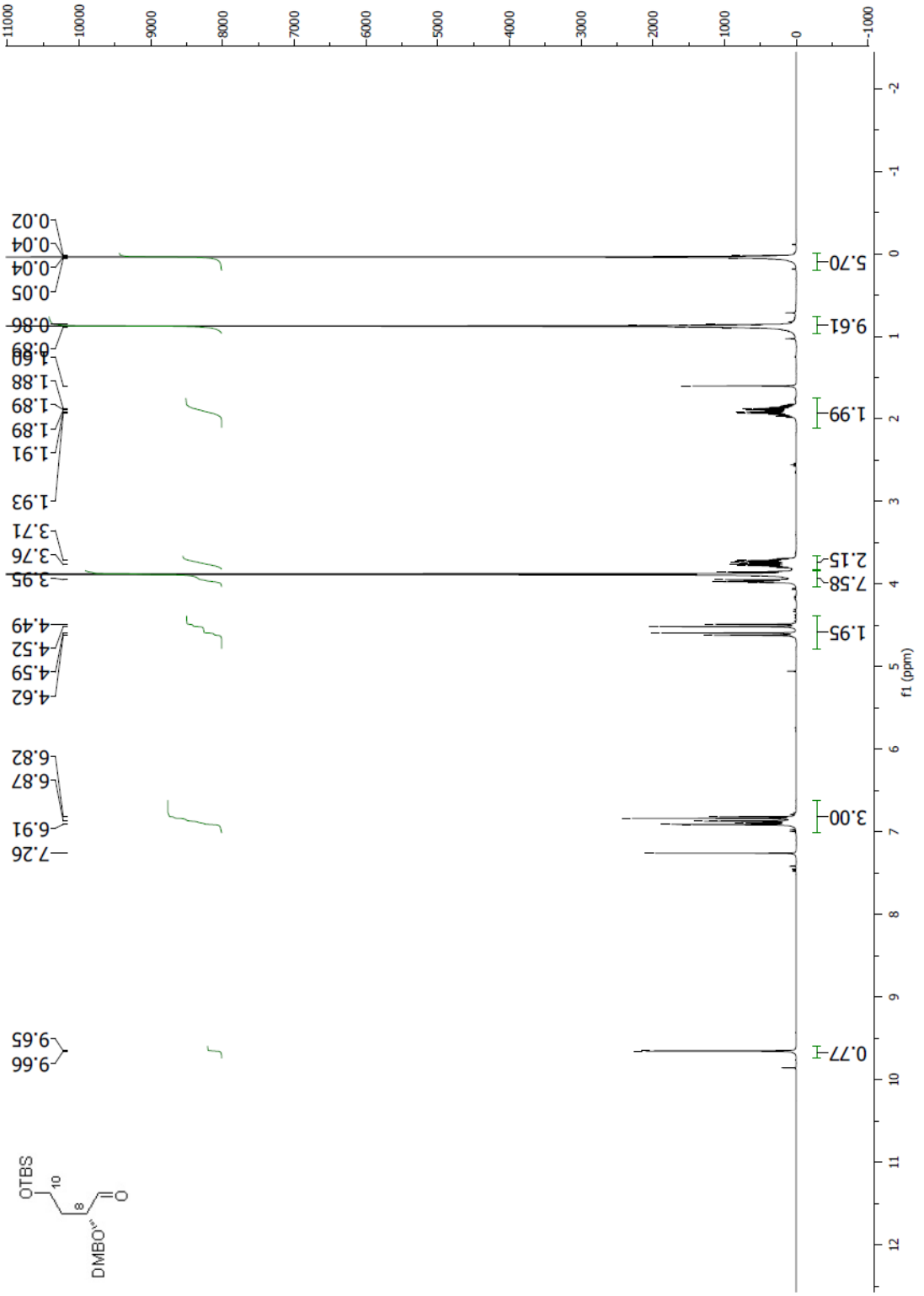

Spectrum 2.37 ^{1}H NMR ($CDCl_3$, 400 MHz) of oxidation product of **181**

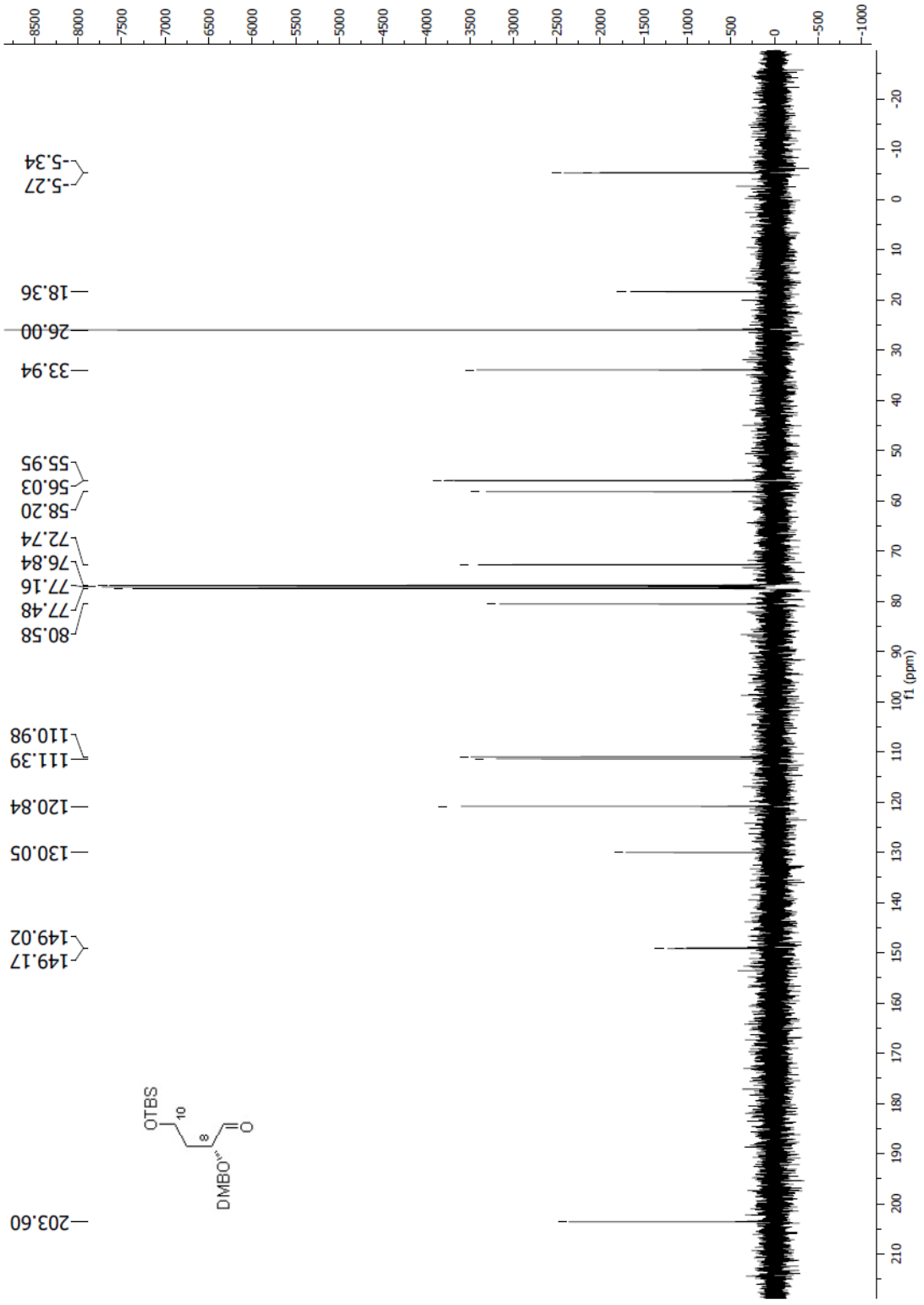

Spectrum 2.38 ^{13}C NMR ($CDCl_3$, 100 MHz) of the oxidation product of **181**

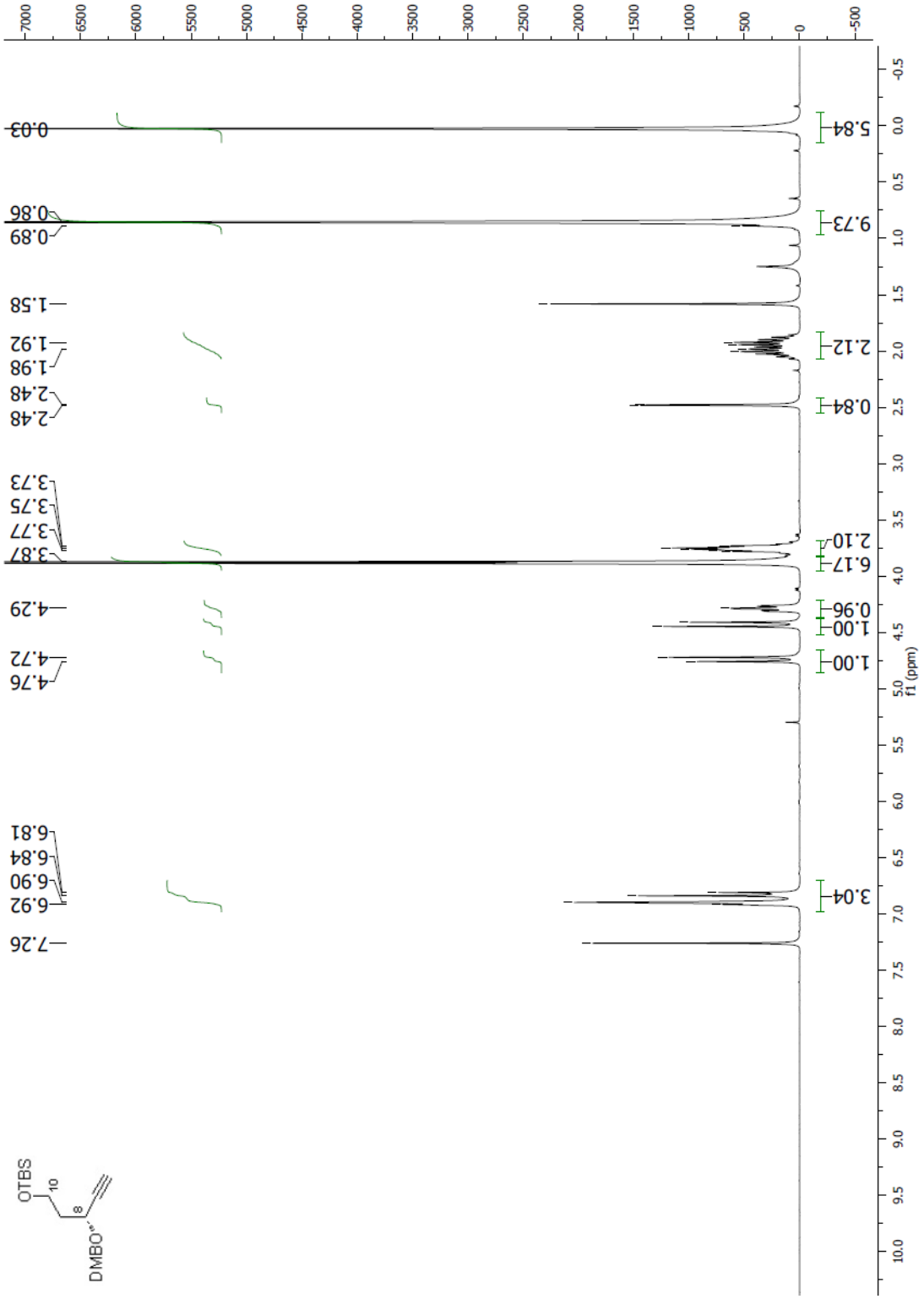

Spectrum 2.39 ^{1}H NMR ($CDCl_3$, 300 MHz) of the alkyne precursor to **182**

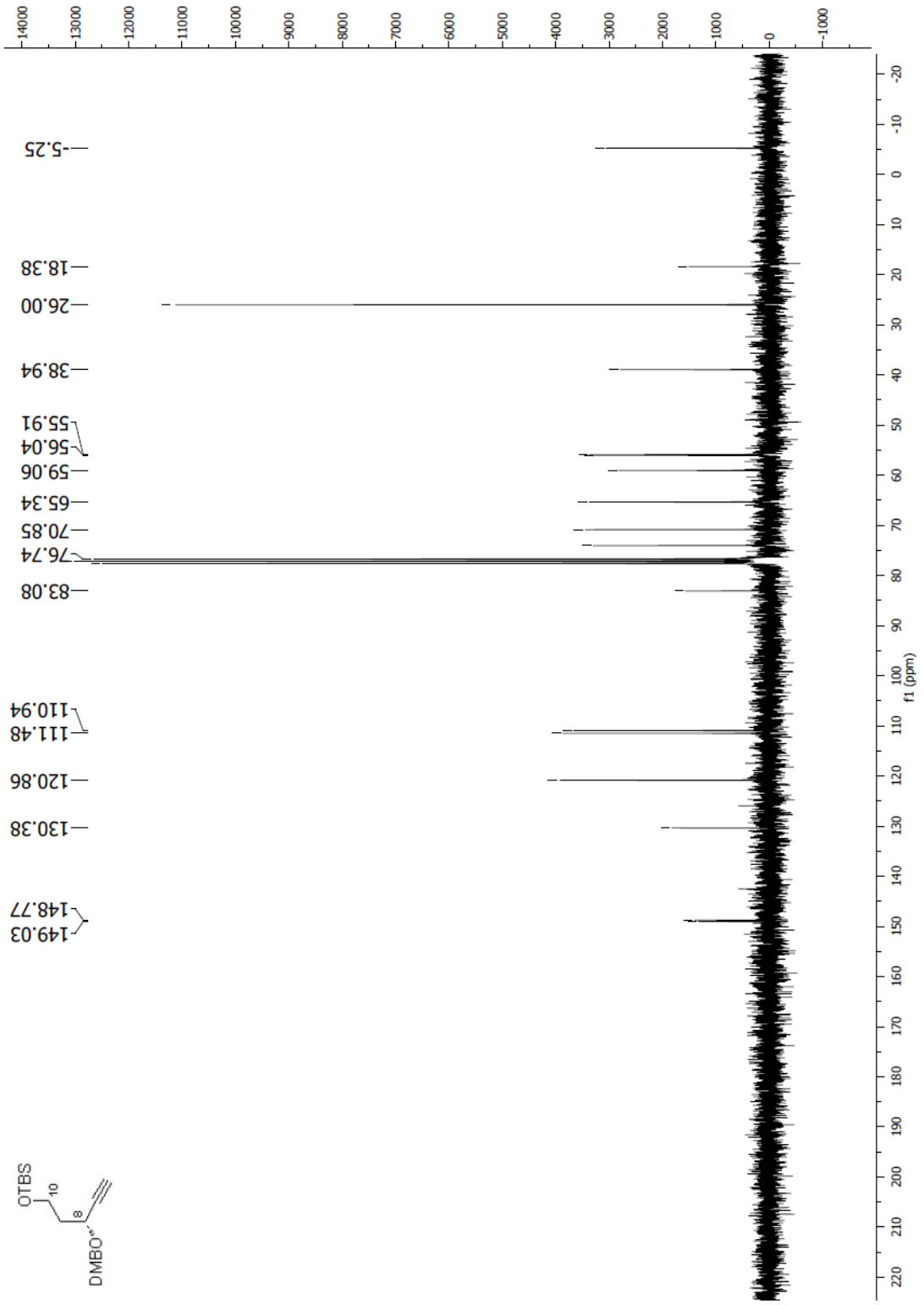

Spectrum 2.40 ^{13}C NMR ($CDCl_3$, 75 MHz) of the alkyne precursor to **182**

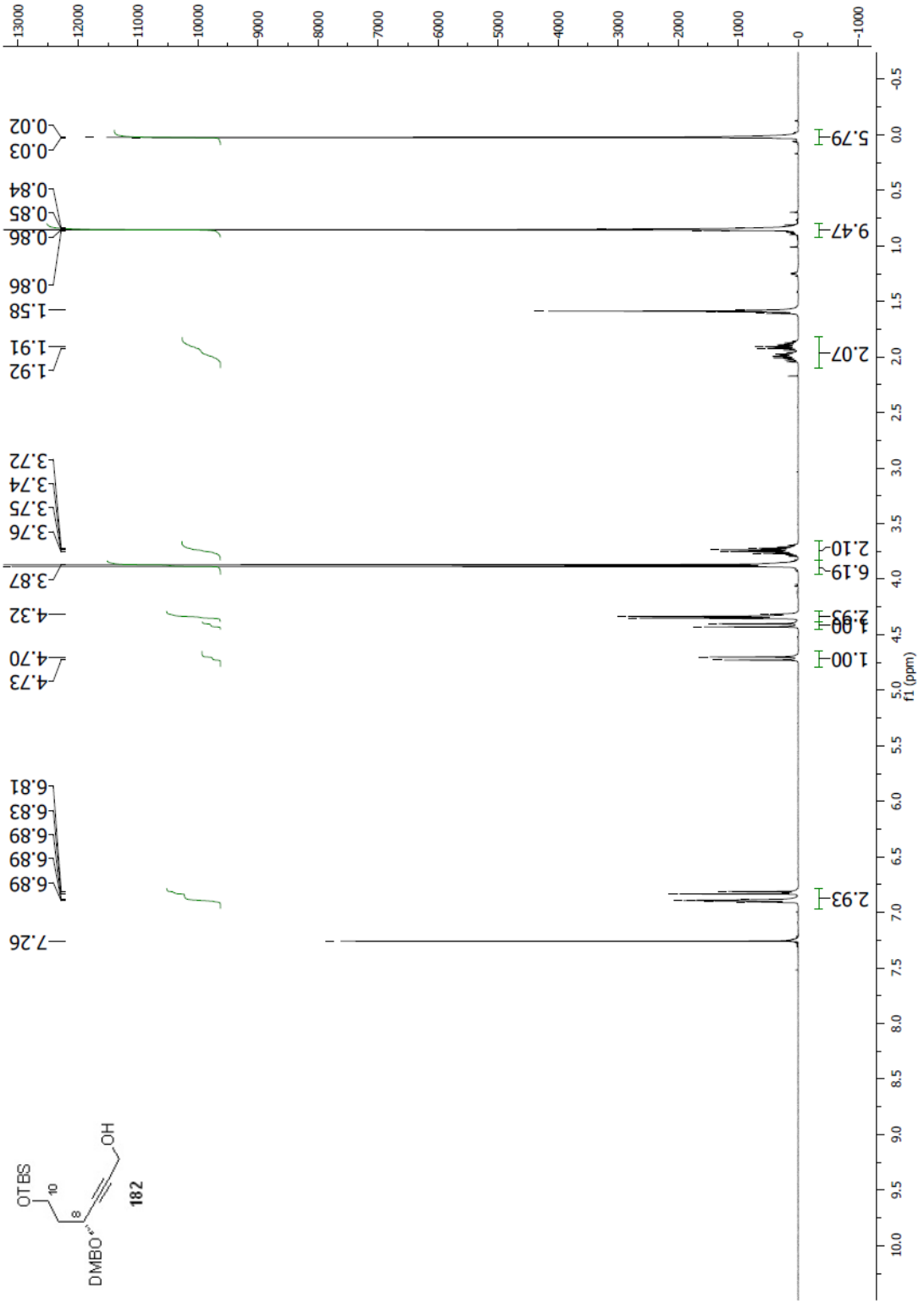

Spectrum 2.41 ^{1}H NMR ($CDCl_3$, 400 MHz) of compound **182**

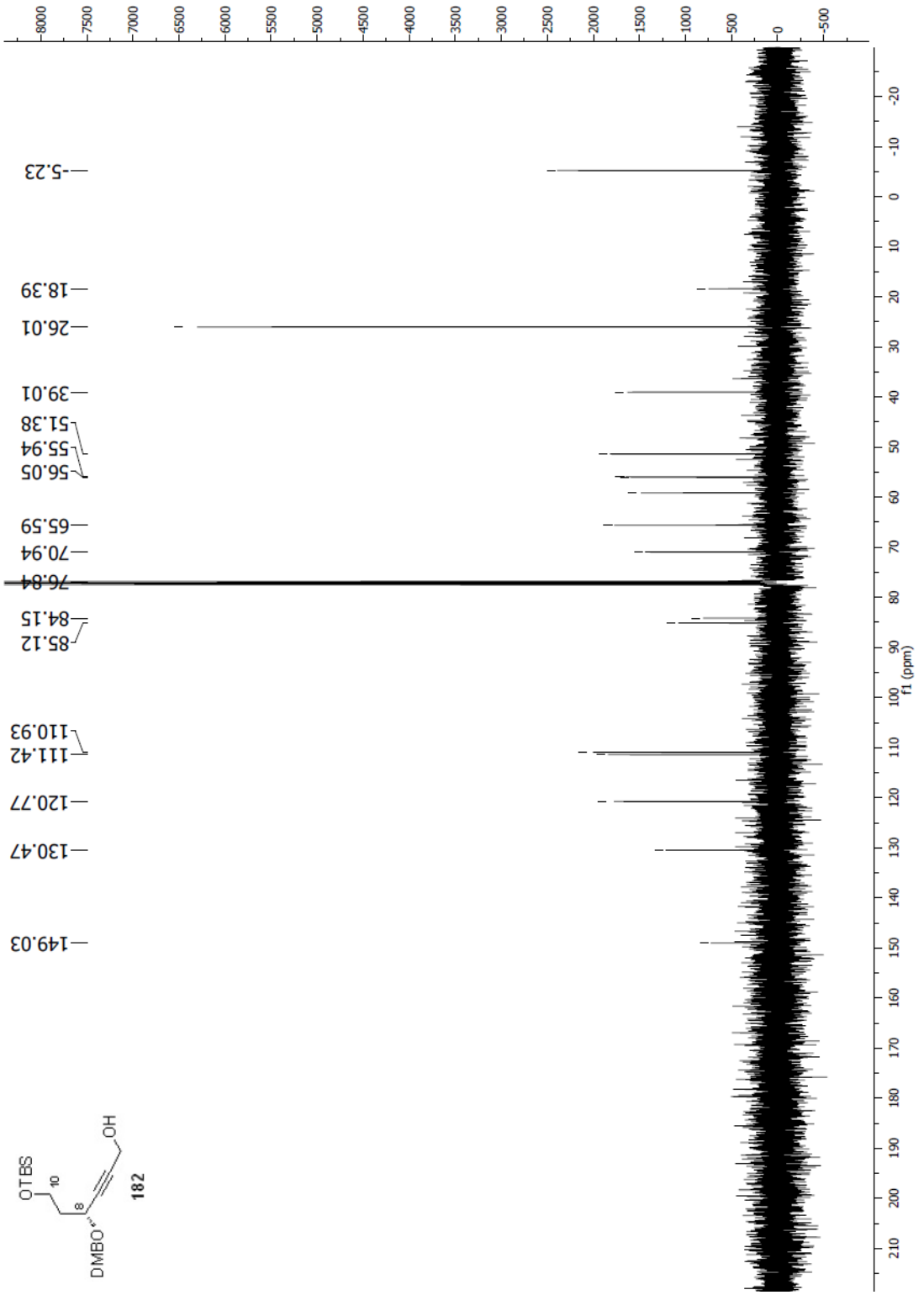

Spectrum 2.42 ^{13}C NMR ($CDCl_3$, 100 MHz) of compound **182**

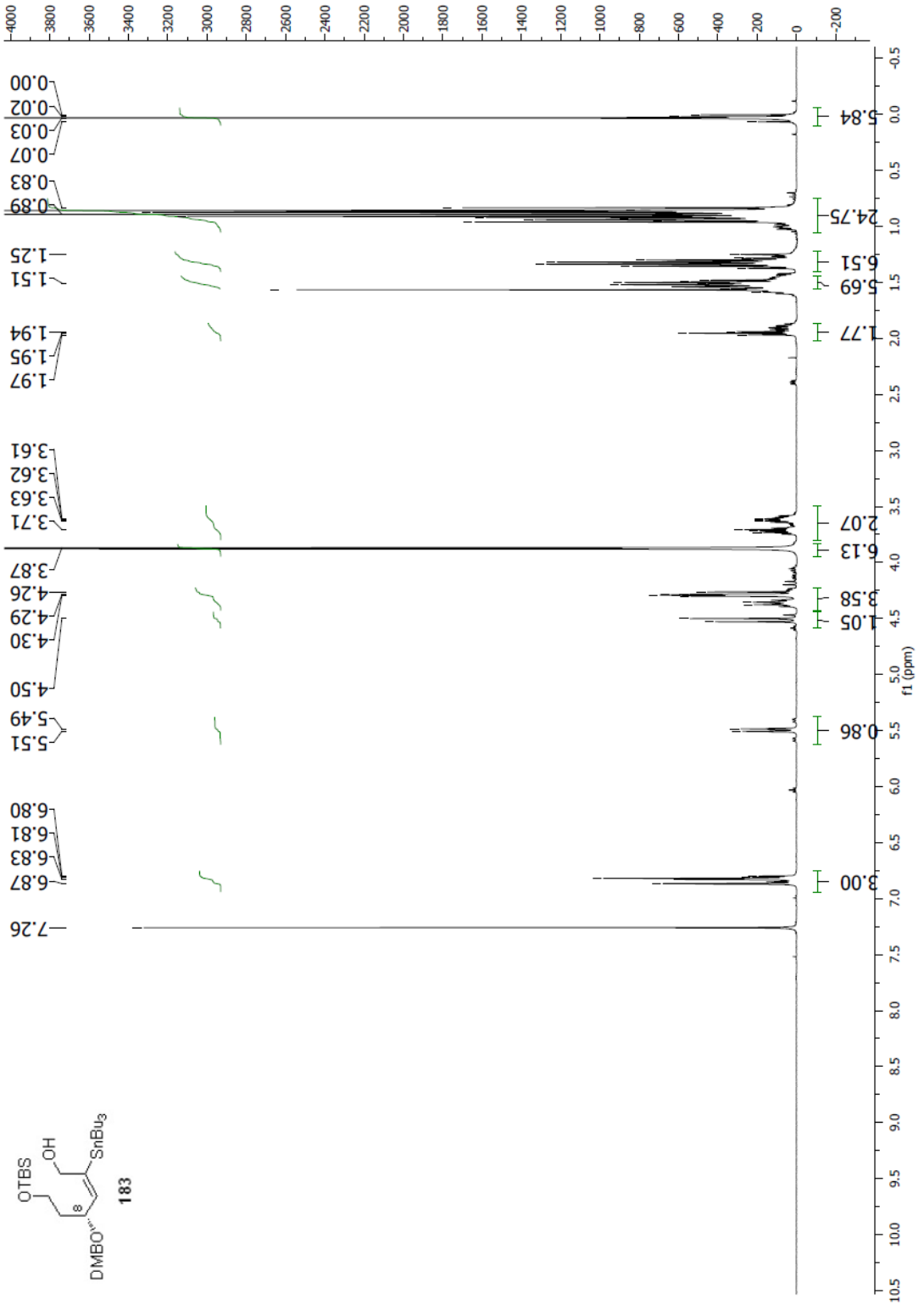

Spectrum 2.43 ^{1}H NMR ($CDCl_3$, 400 MHz) of compound **183**

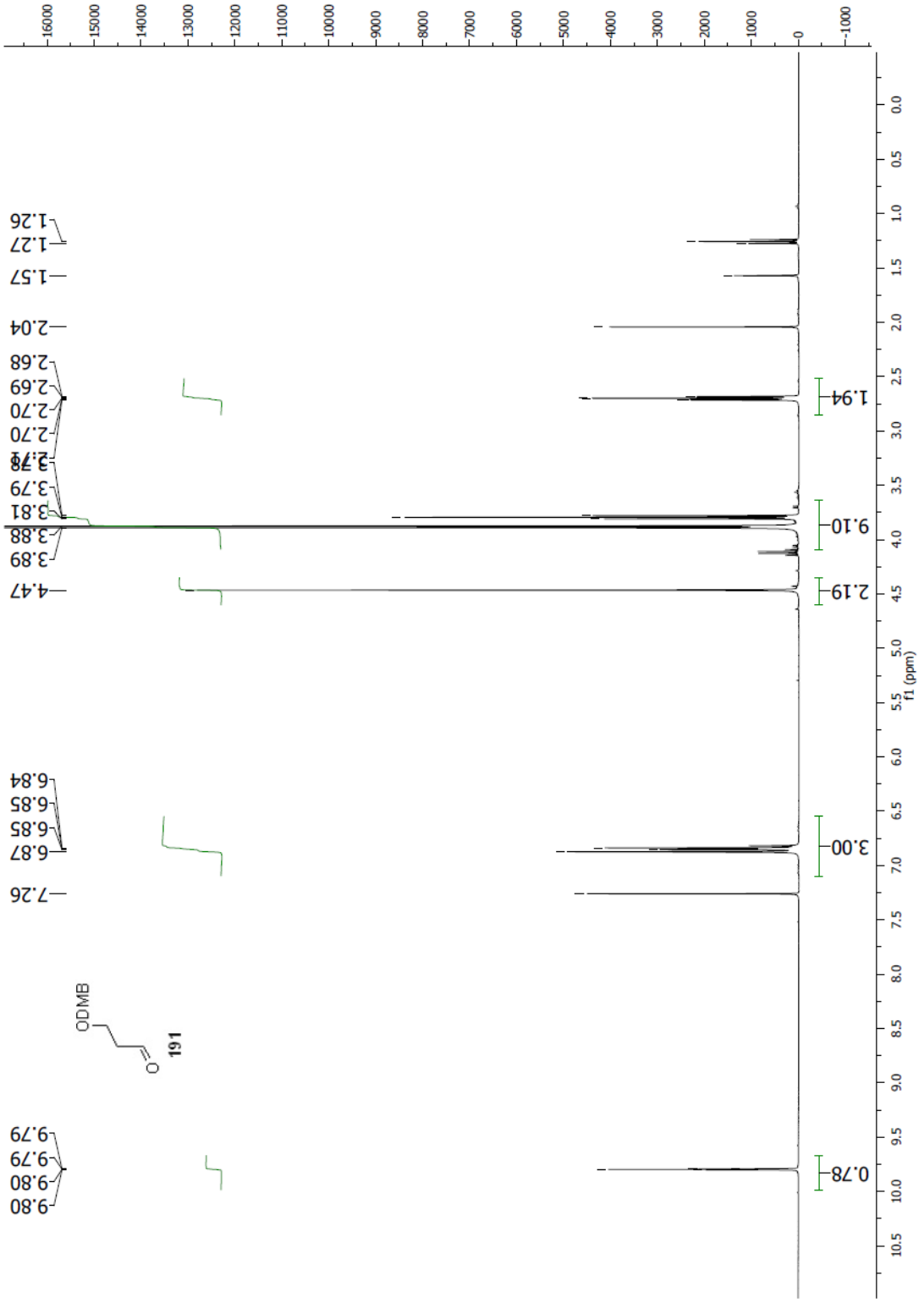

Spectrum 2.44 ^{1}H NMR ($CDCl_3$, 400 MHz) of compound **191**

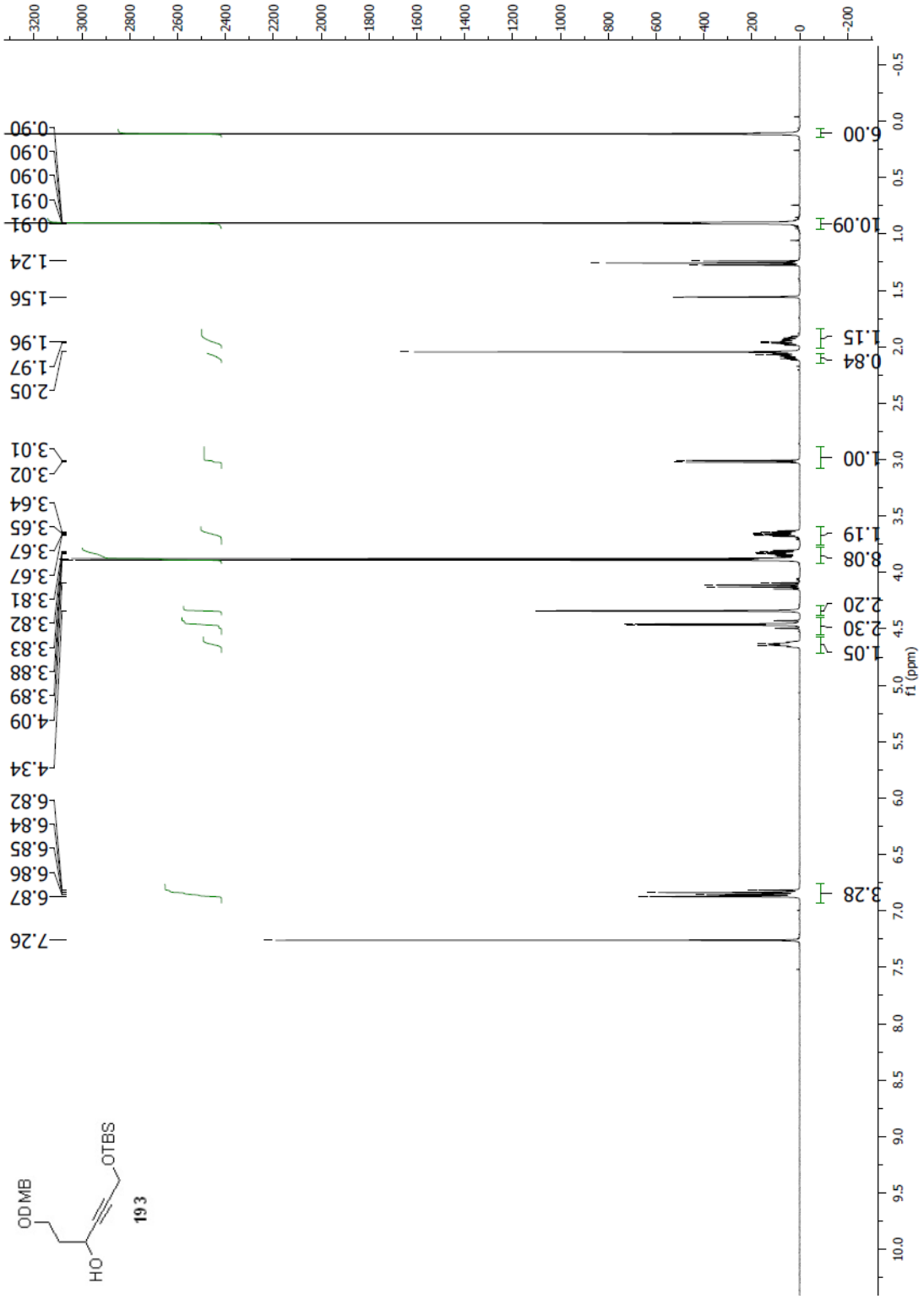

Spectrum 2.45 ^{1}H NMR ($CDCl_3$, 400 MHz) of compound **193**

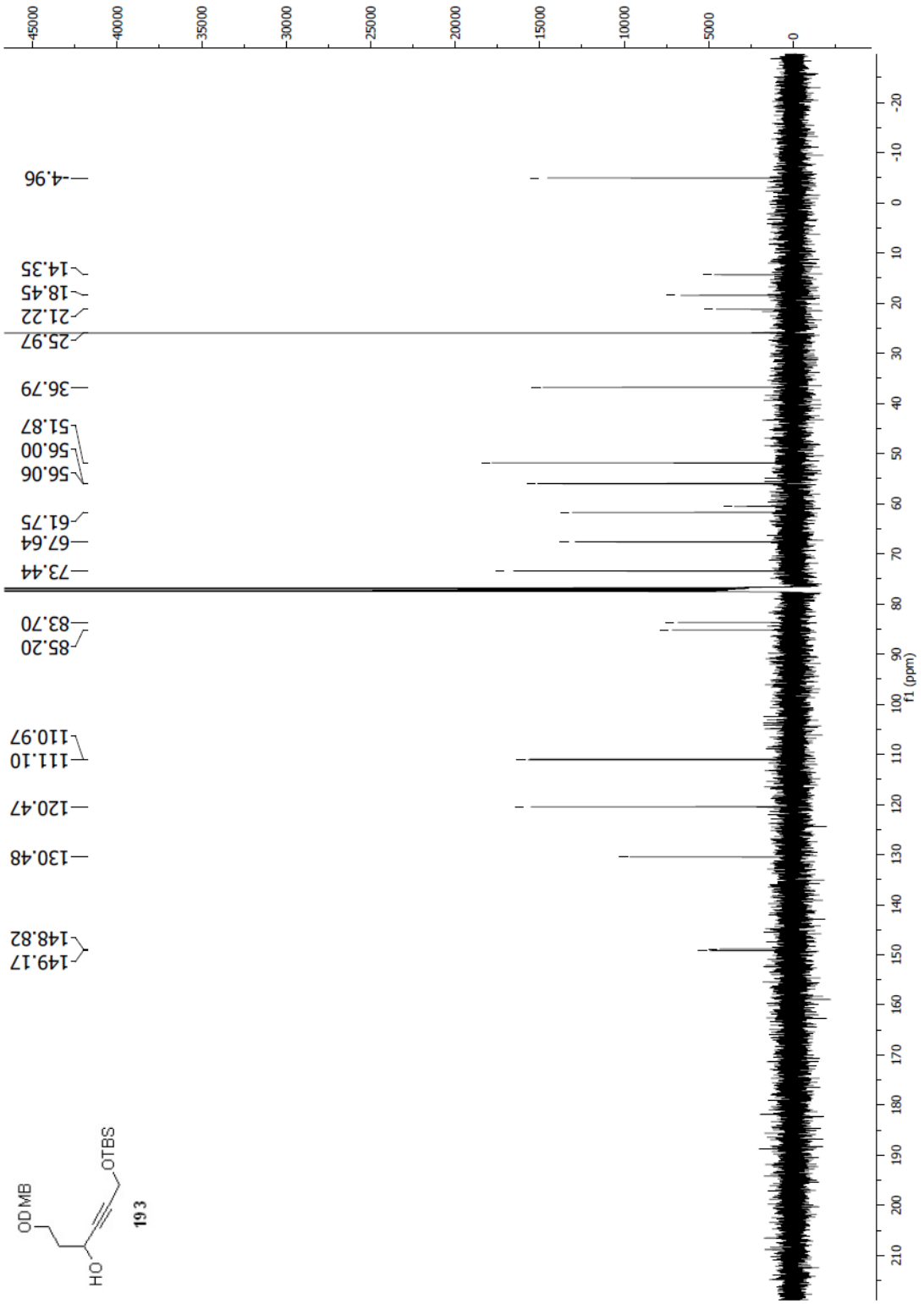

Spectrum 2.46 ^{13}C NMR ($CDCl_3$, 100 MHz) of compound **193**

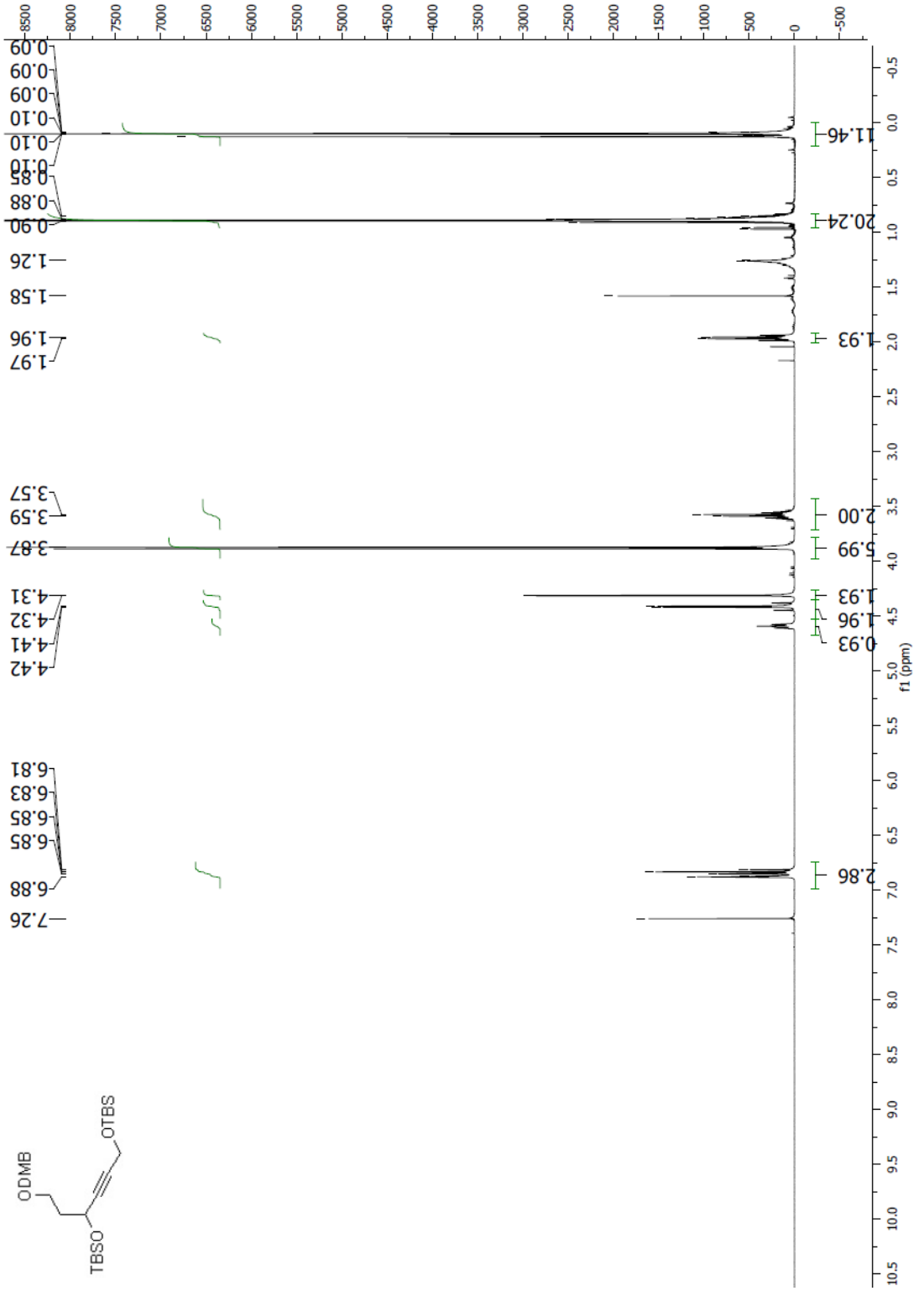

Spectrum 2.47 ^{1}H NMR ($CDCl_3$, 400 MHz) of the TBS ether of compound **193**

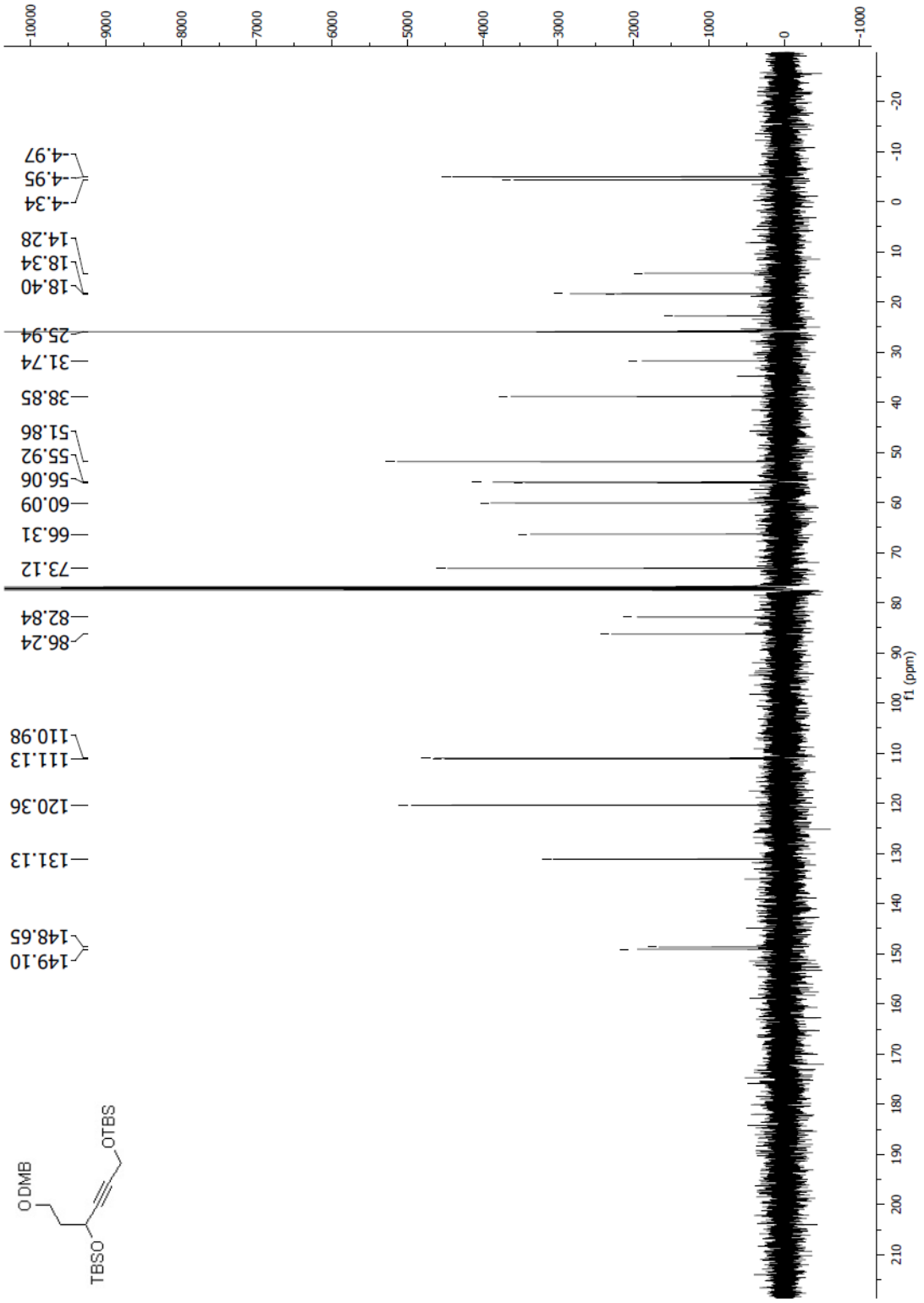

Spectrum 2.48 ^{13}C NMR ($CDCl_3$, 100 MHz) of the TBS ether of compound **193**

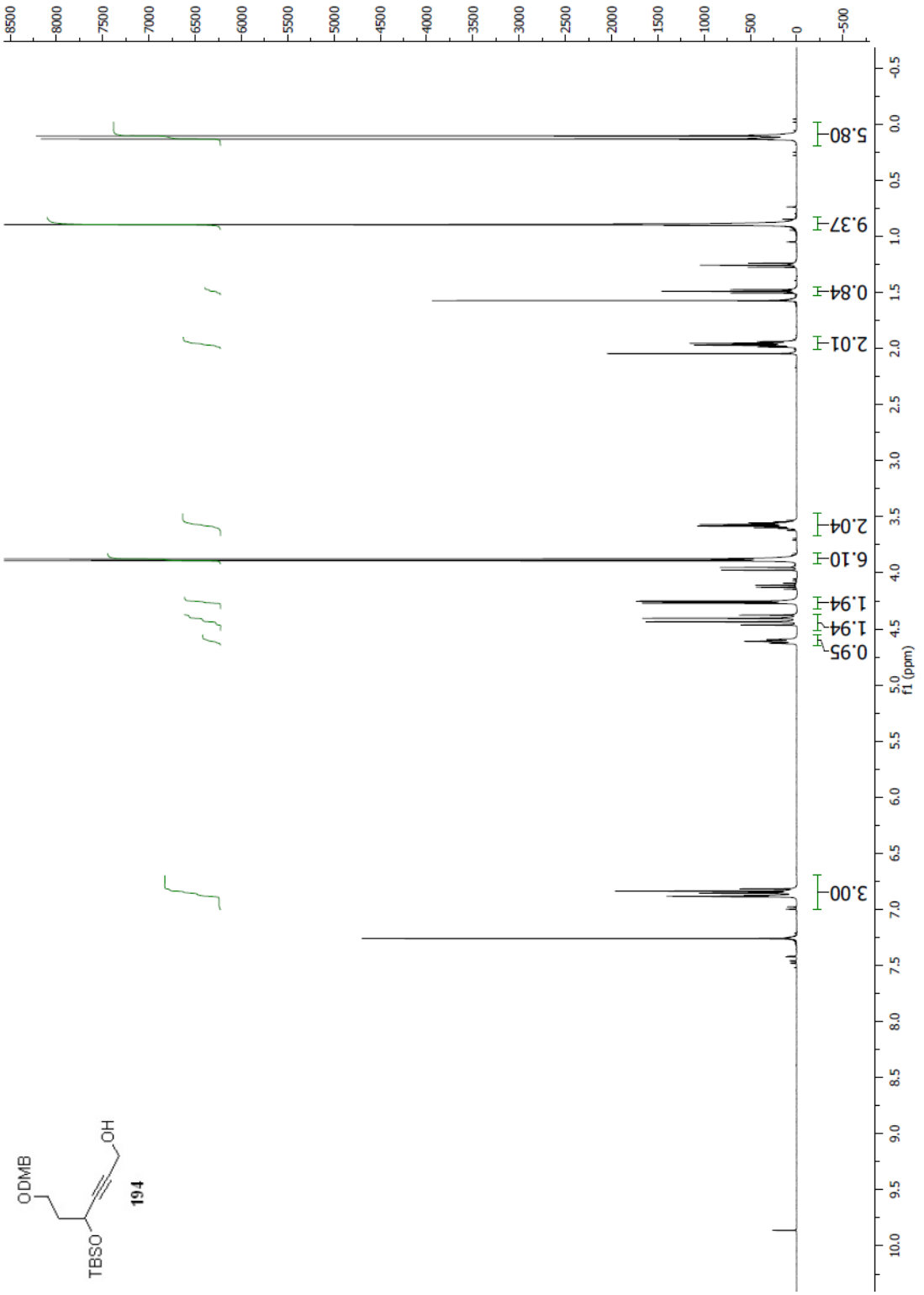

Spectrum 2.49 ^{1}H NMR ($CDCl_3$, 400 MHz) of compound **194**

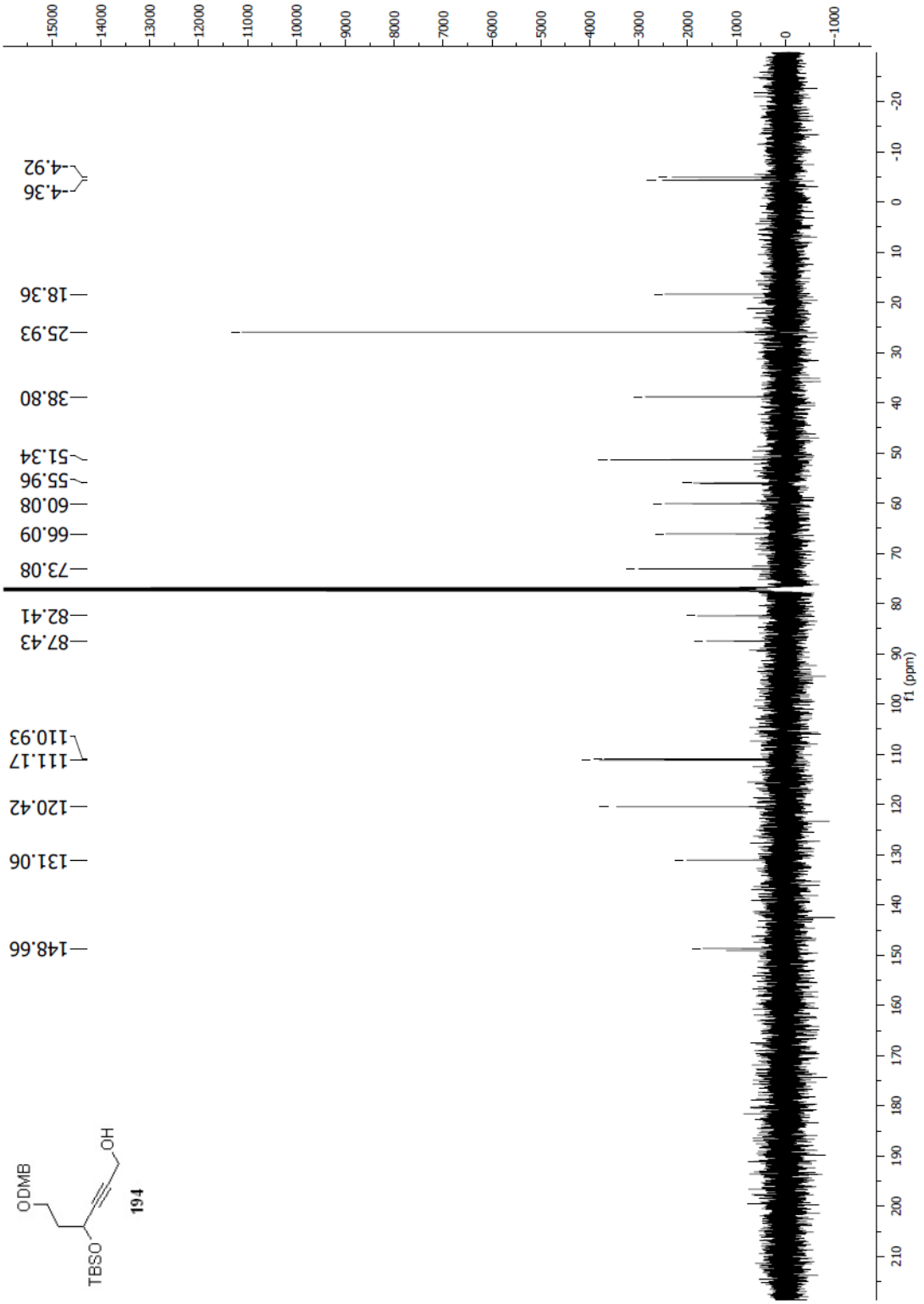

Spectrum 2.50 ^{13}C NMR ($CDCl_3$, 100 MHz) of compound **194**

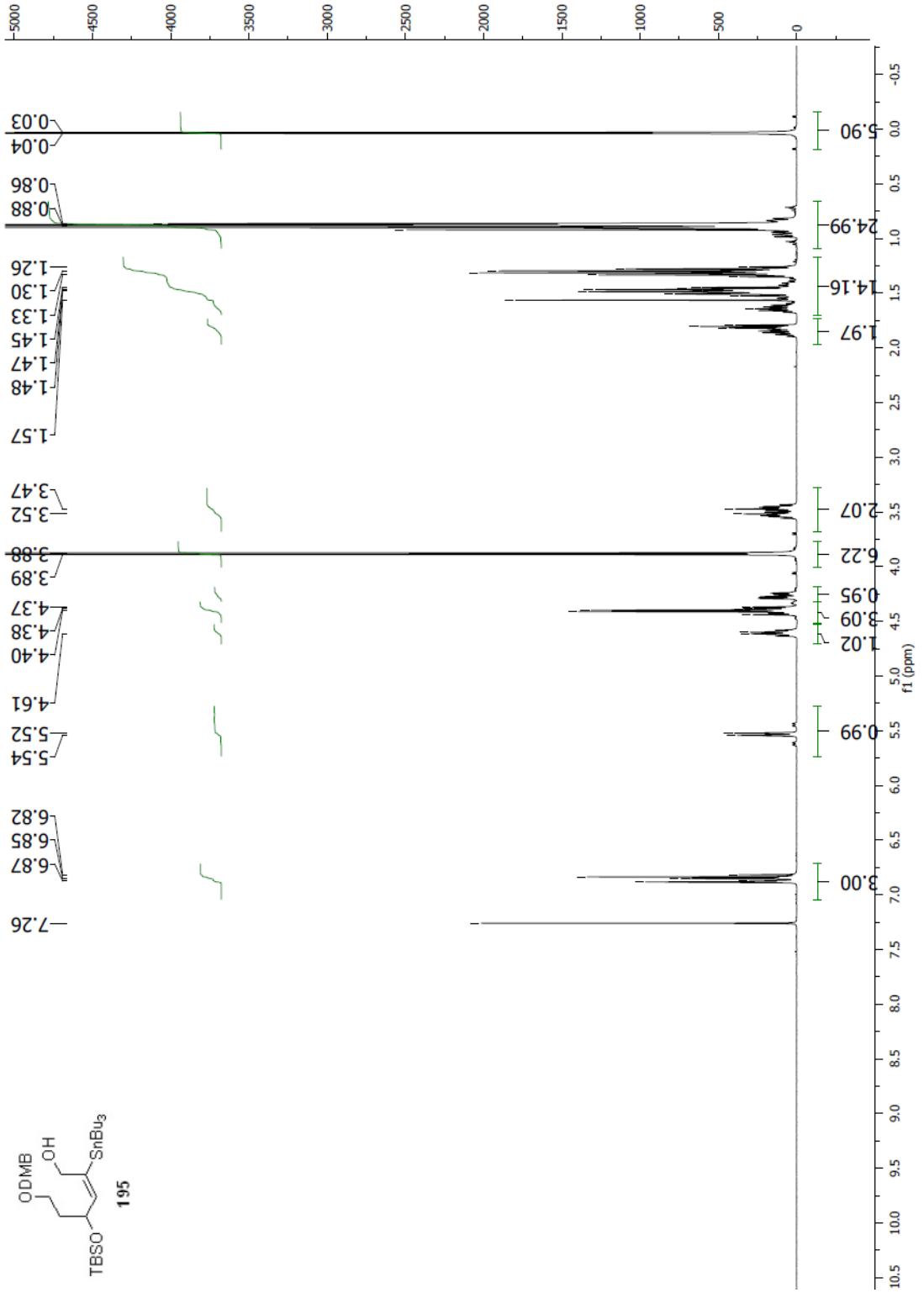

Spectrum 2.51 ^{1}H NMR ($CDCl_3$, 400 MHz) of compound **195**

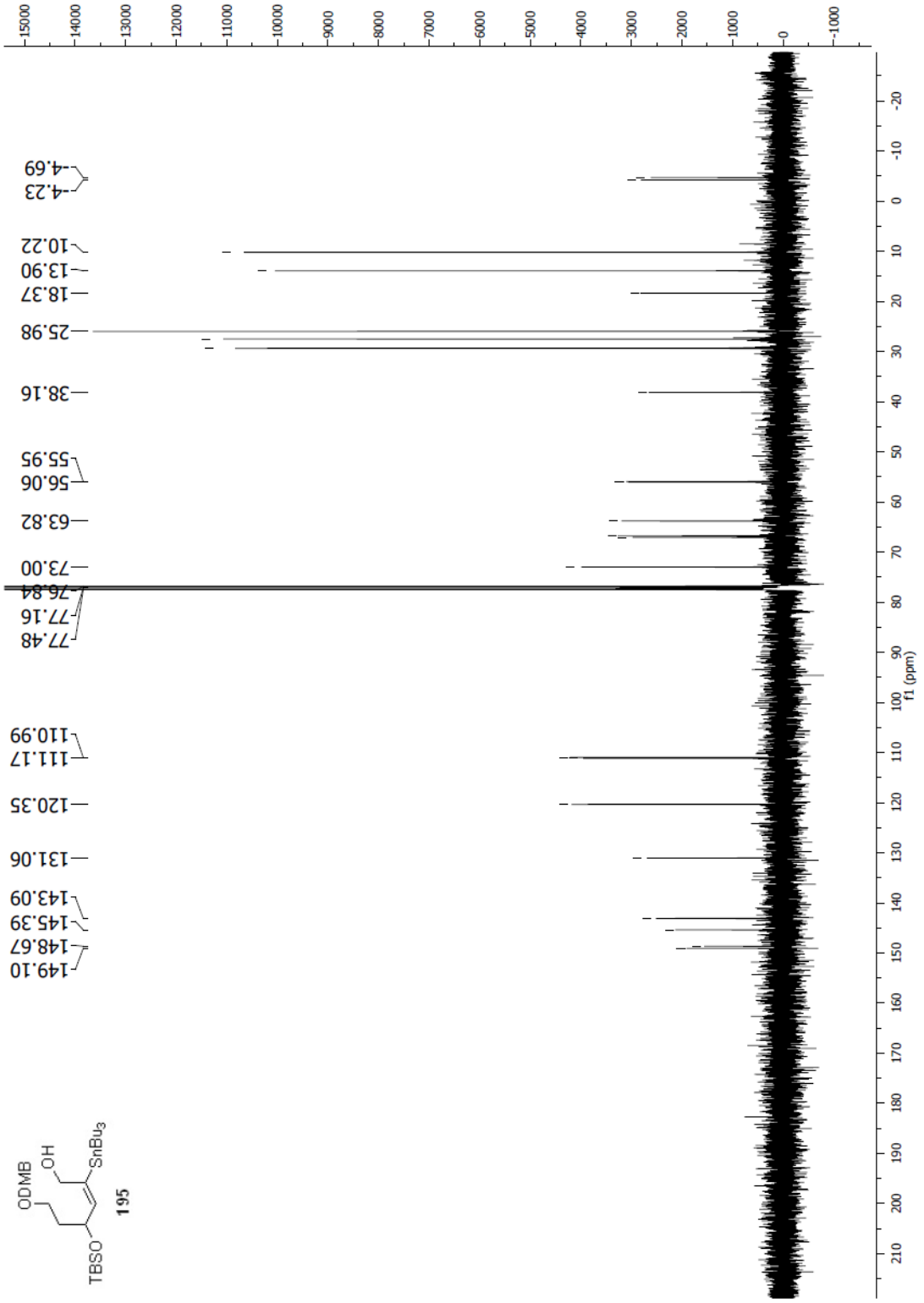

Spectrum 2.52 ^{13}C NMR ($CDCl_3$, 100 MHz) of compound **195**

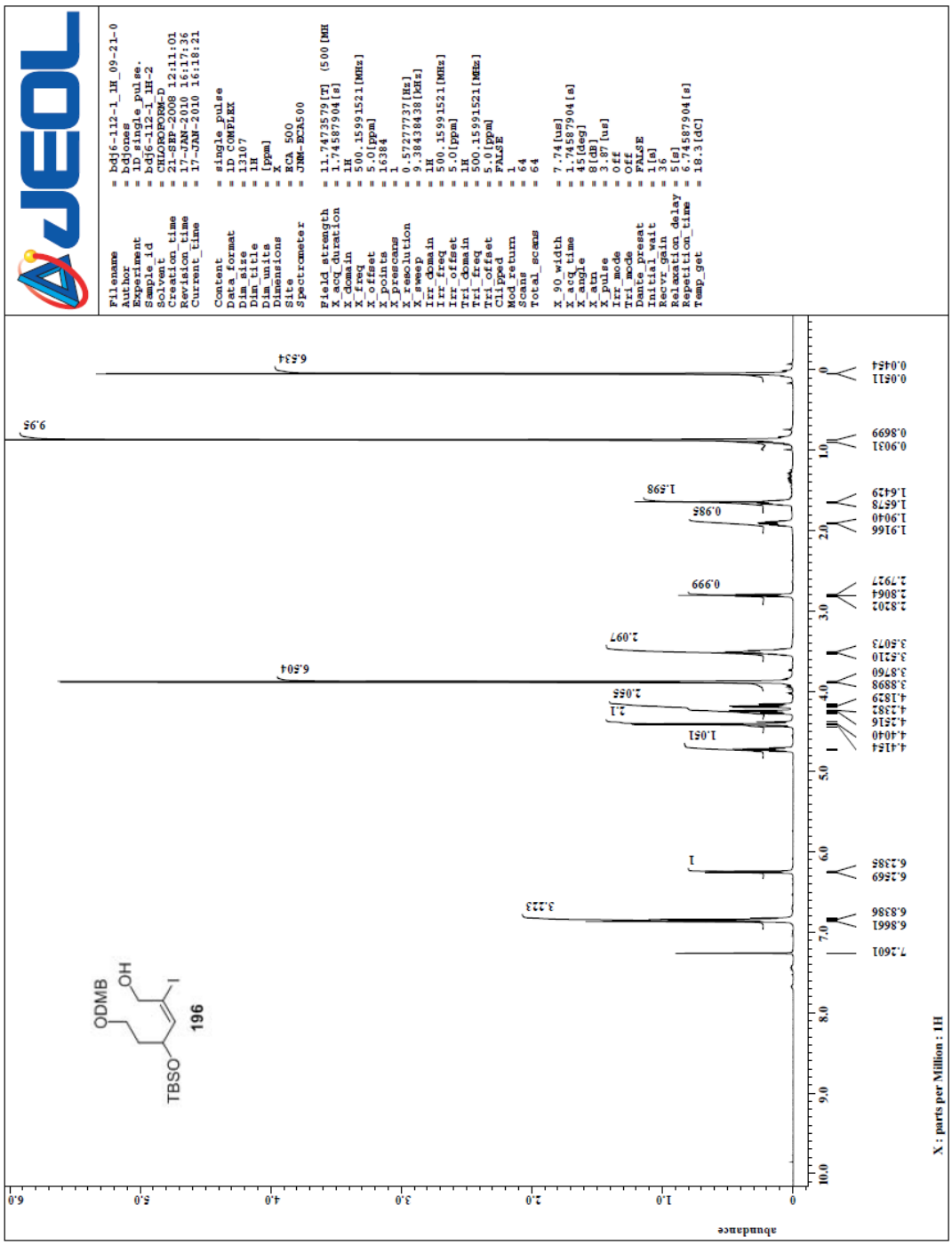

Spectrum 2.53 ^{1}H NMR ($CDCl_3$, 500 MHz) of compound **196**

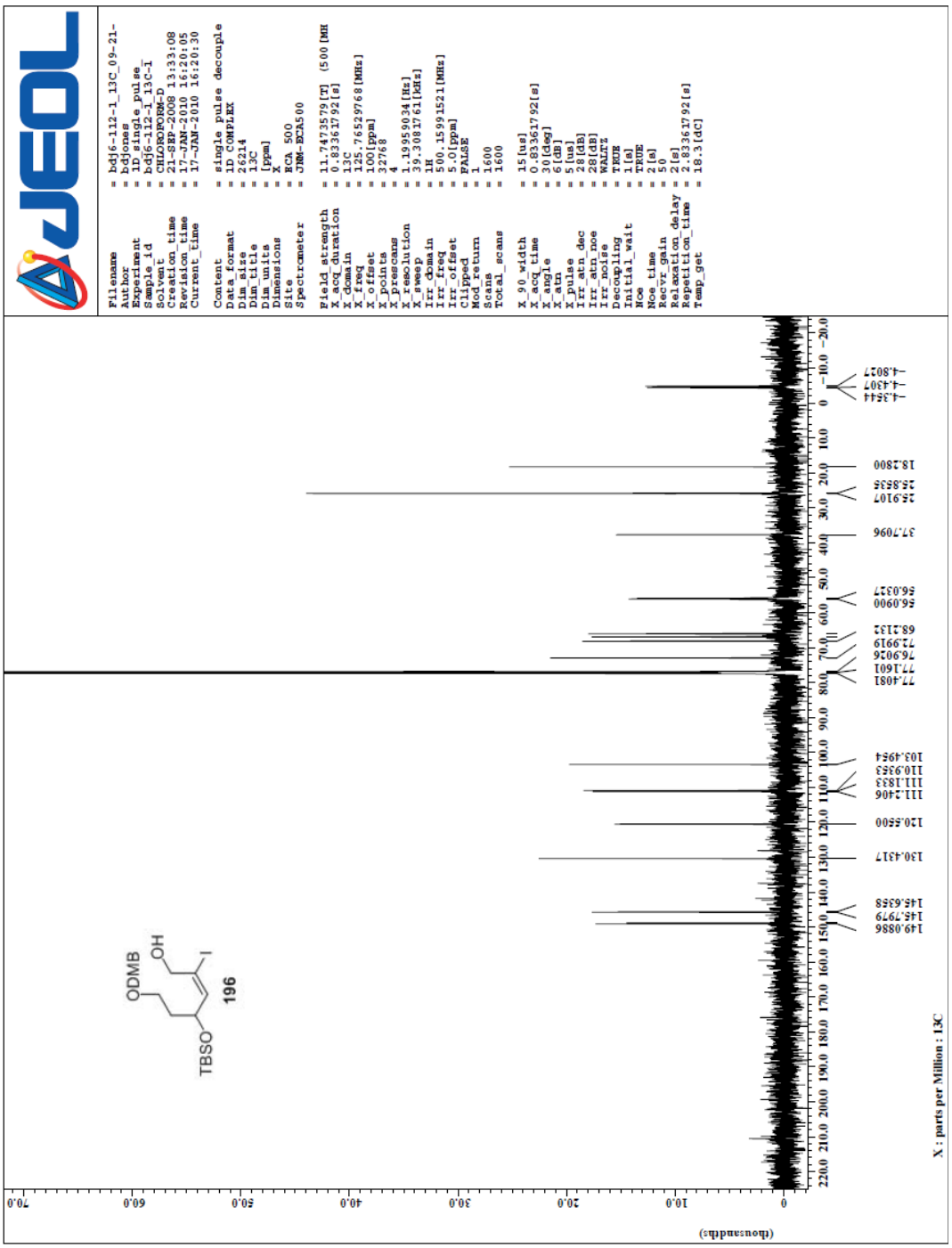

Spectrum 2.54 ^{13}C NMR ($CDCl_3$, 125 MHz) of compound **196**

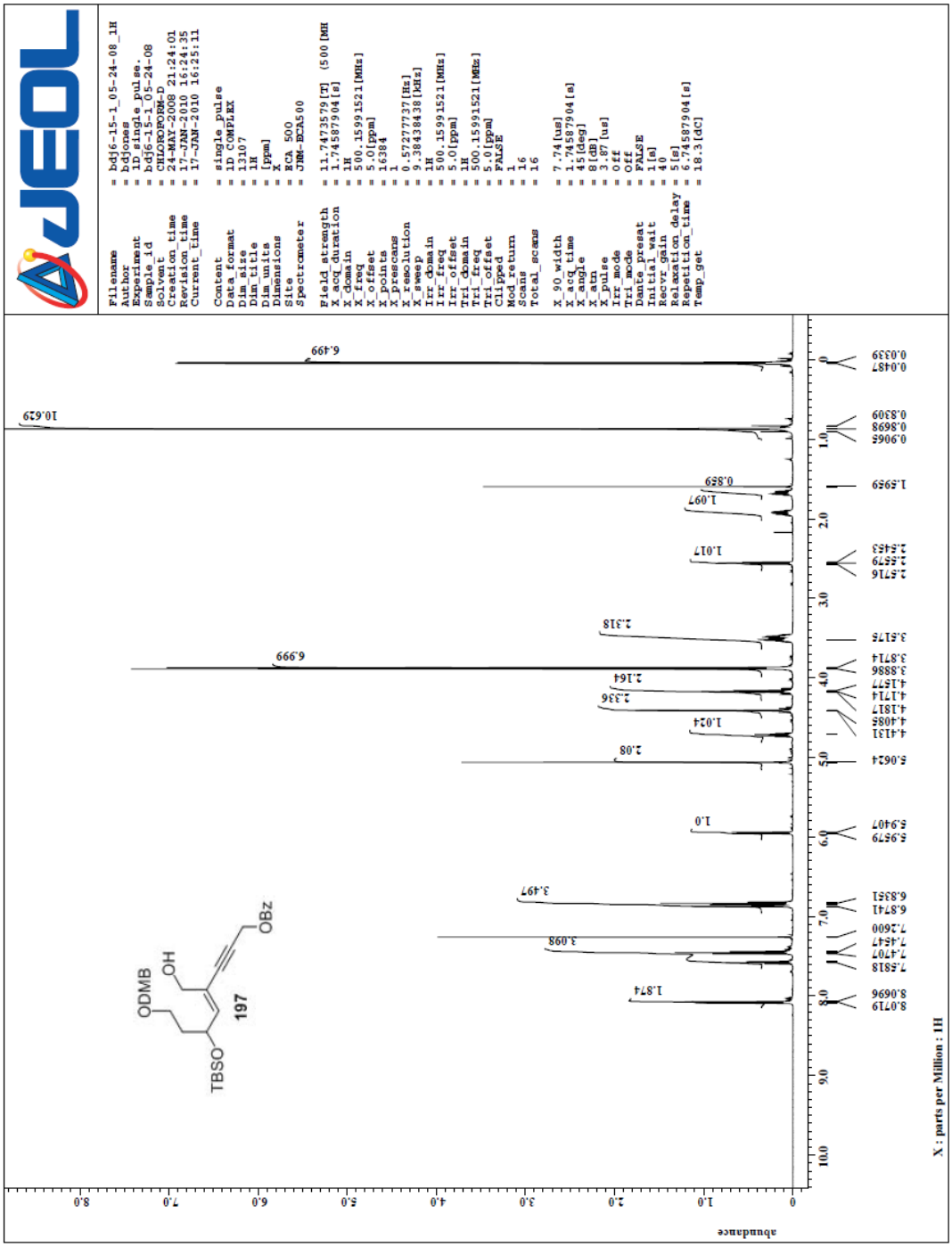

Spectrum 2.55 ^{1}H NMR ($CDCl_3$, 500 MHz) of compound **197**

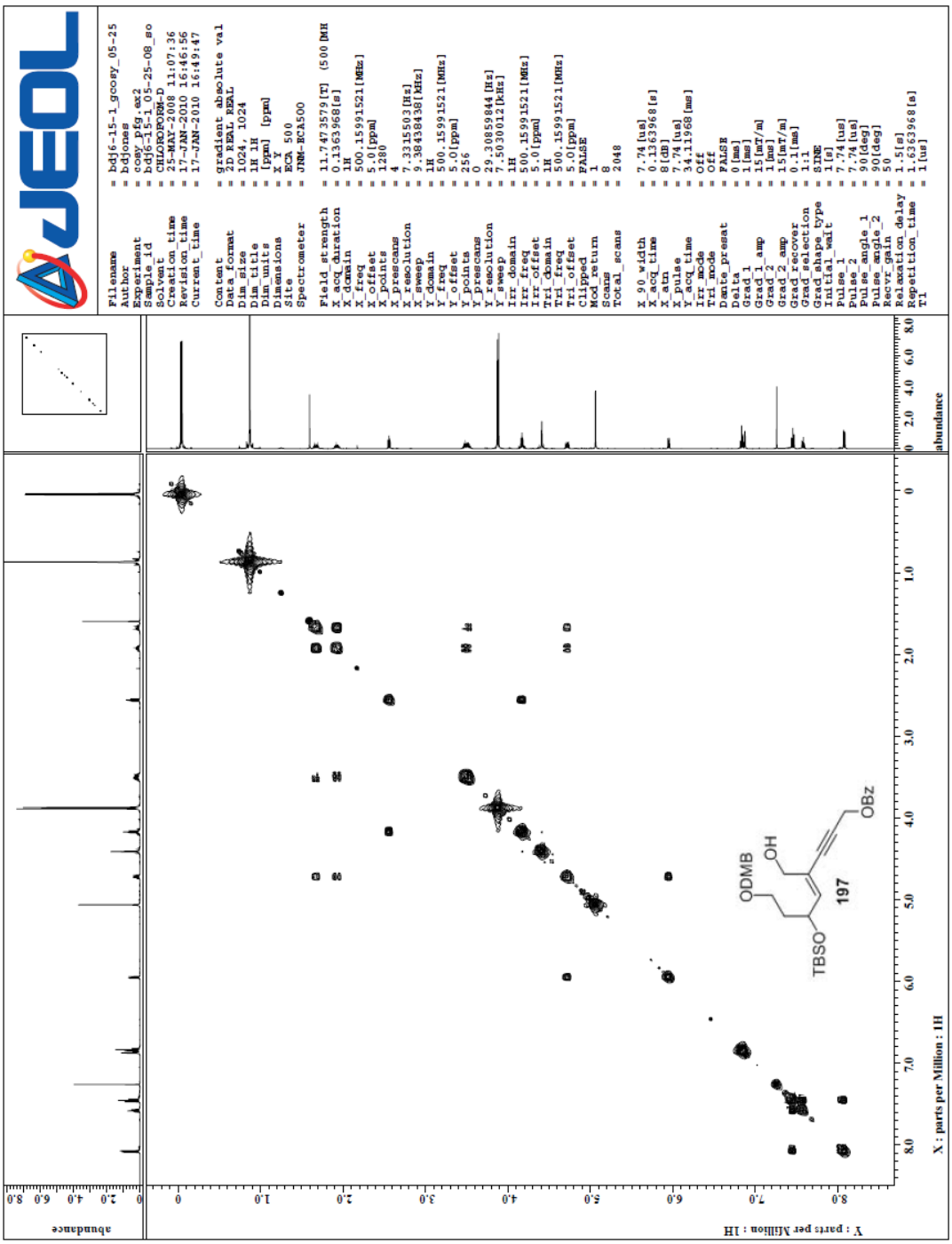

Spectrum 2.56 gCOSY NMR ($CDCl_3$, 500 MHz) of compound **197**

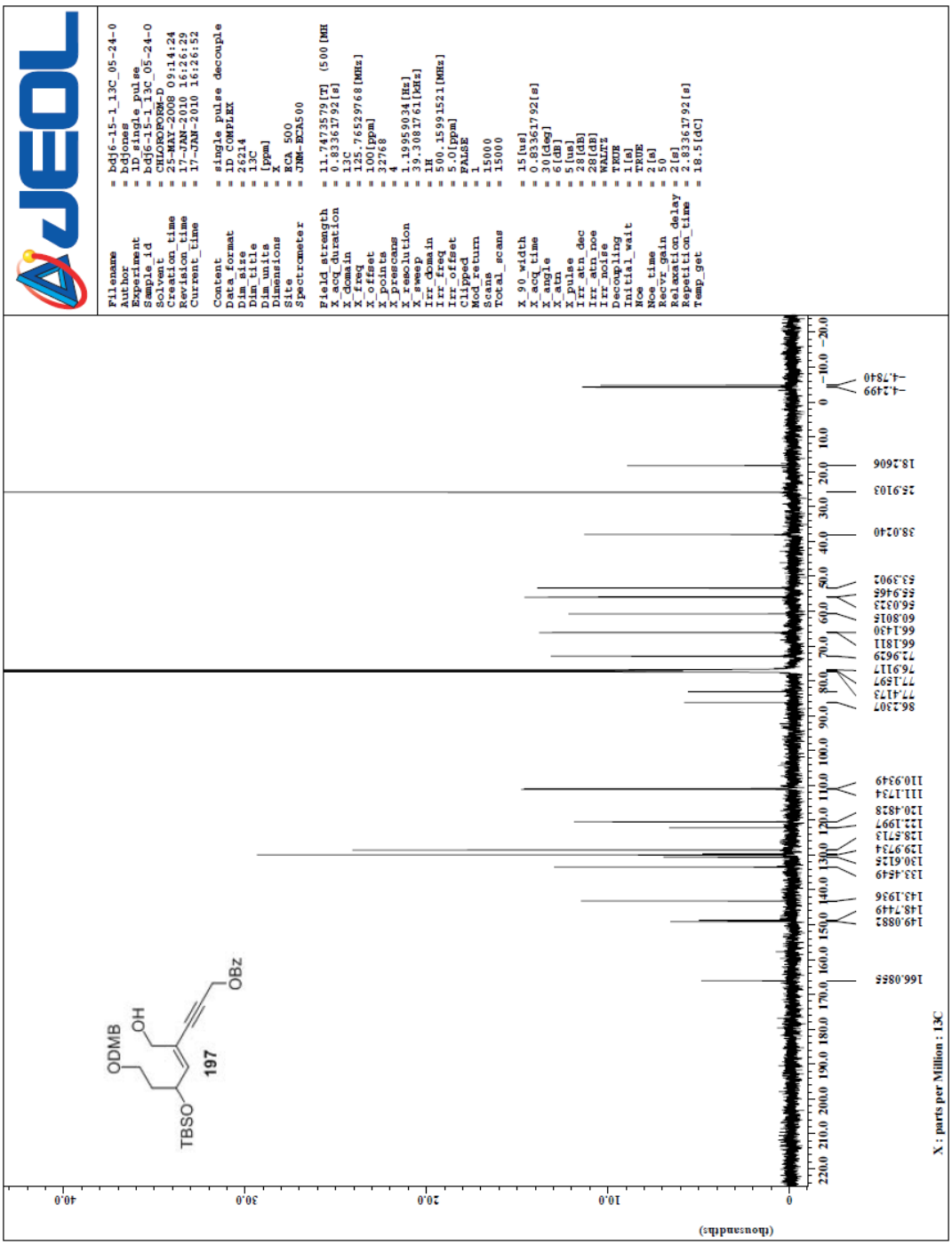

Spectrum 2.57 ^{13}C NMR ($CDCl_3$, 125 MHz) of compound **197**

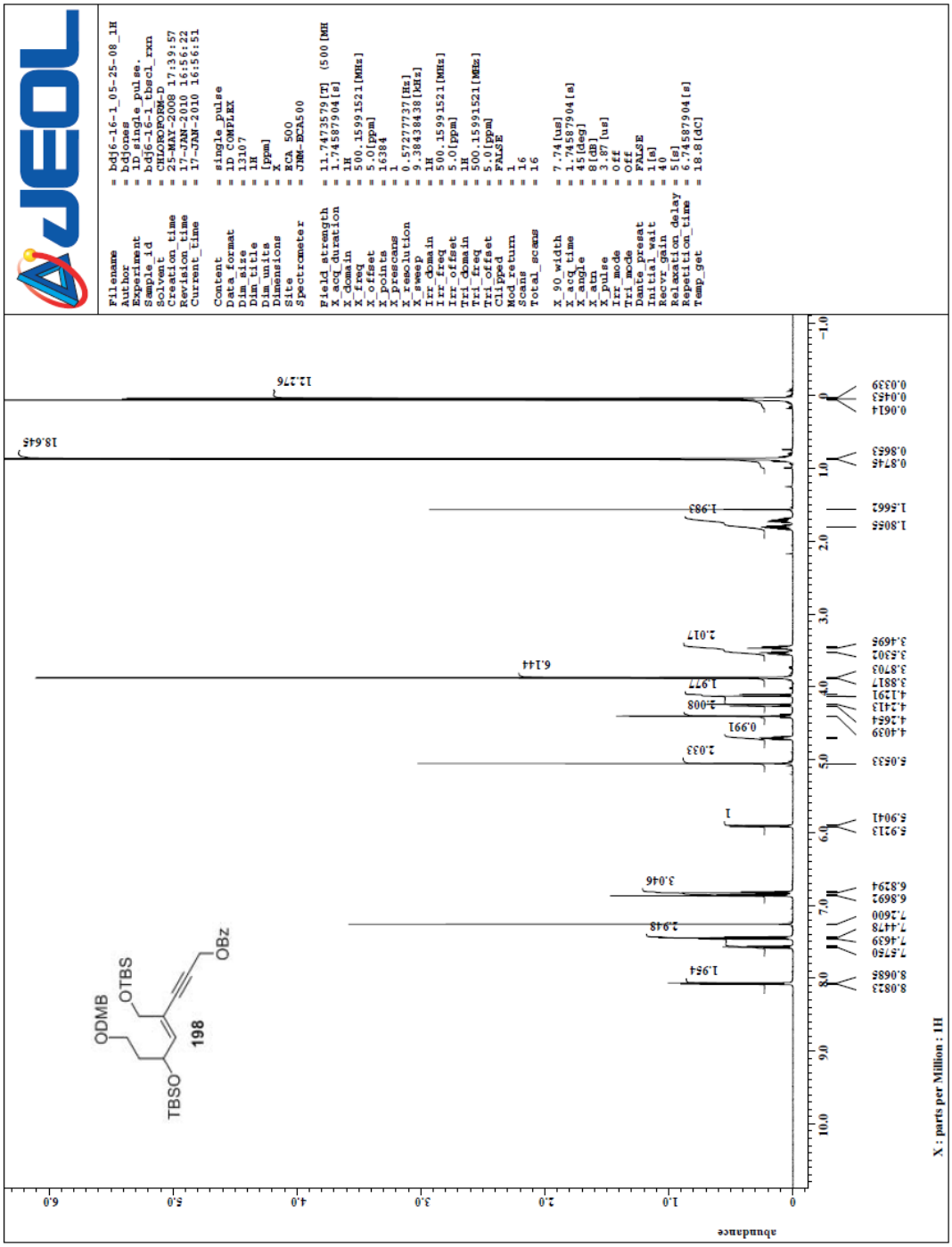

Spectrum 2.58 ^{1}H NMR ($CDCl_3$, 500 MHz) of compound **198**

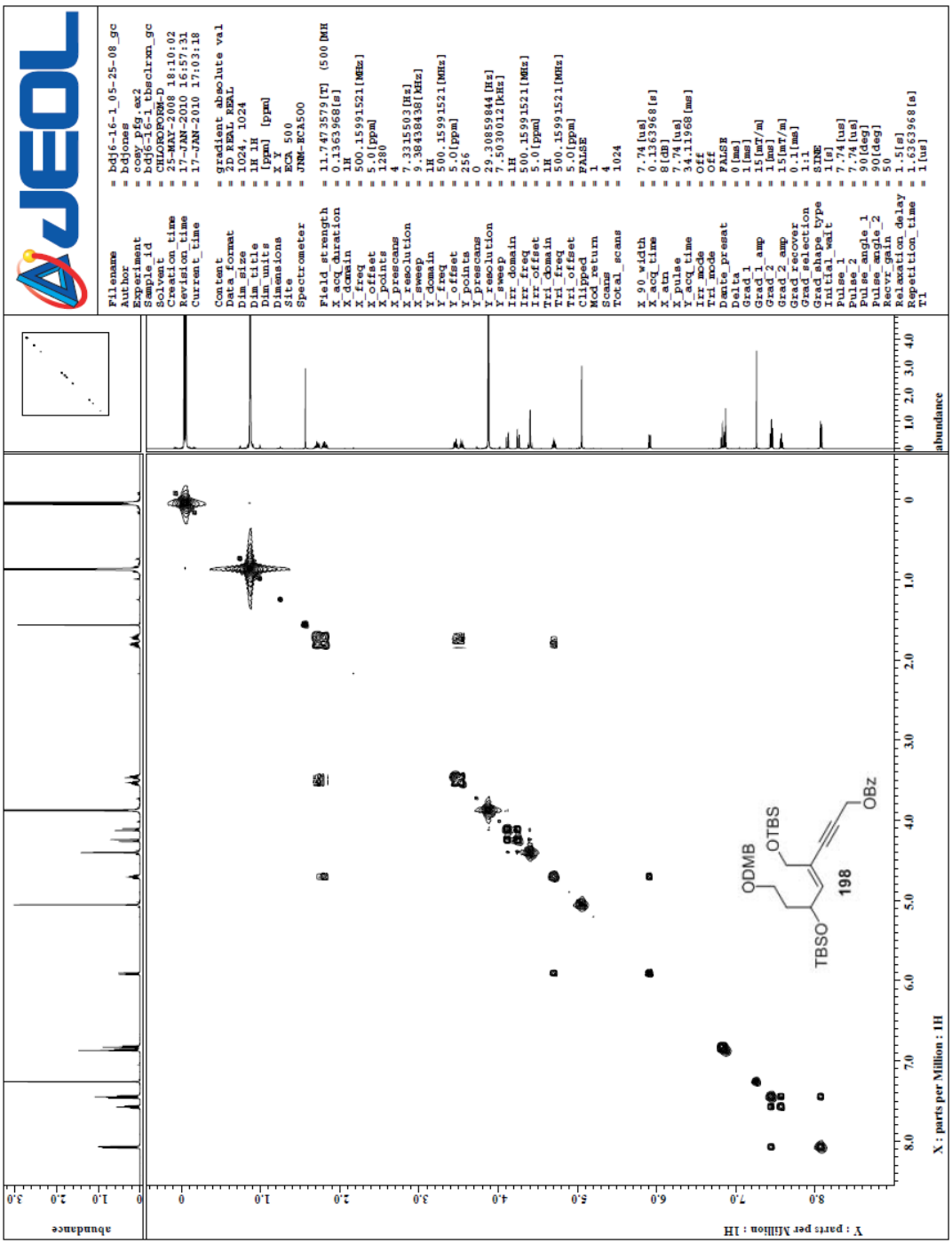

Spectrum 2.59 gCOSY NMR ($CDCl_3$, 500 MHz) of compound **198**

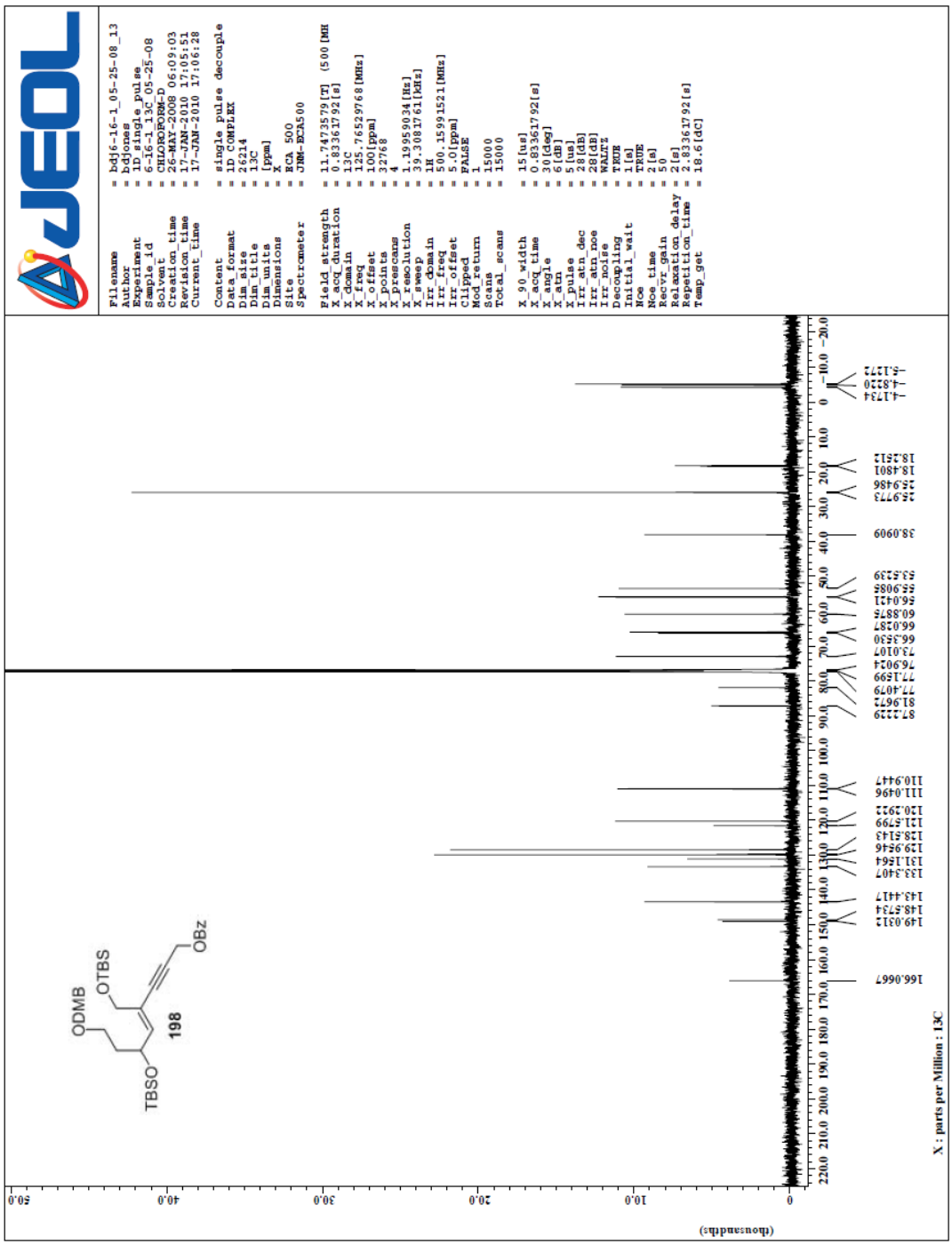

Spectrum 2.60 ^{13}C NMR ($CDCl_3$, 125 MHz) of compound **198**

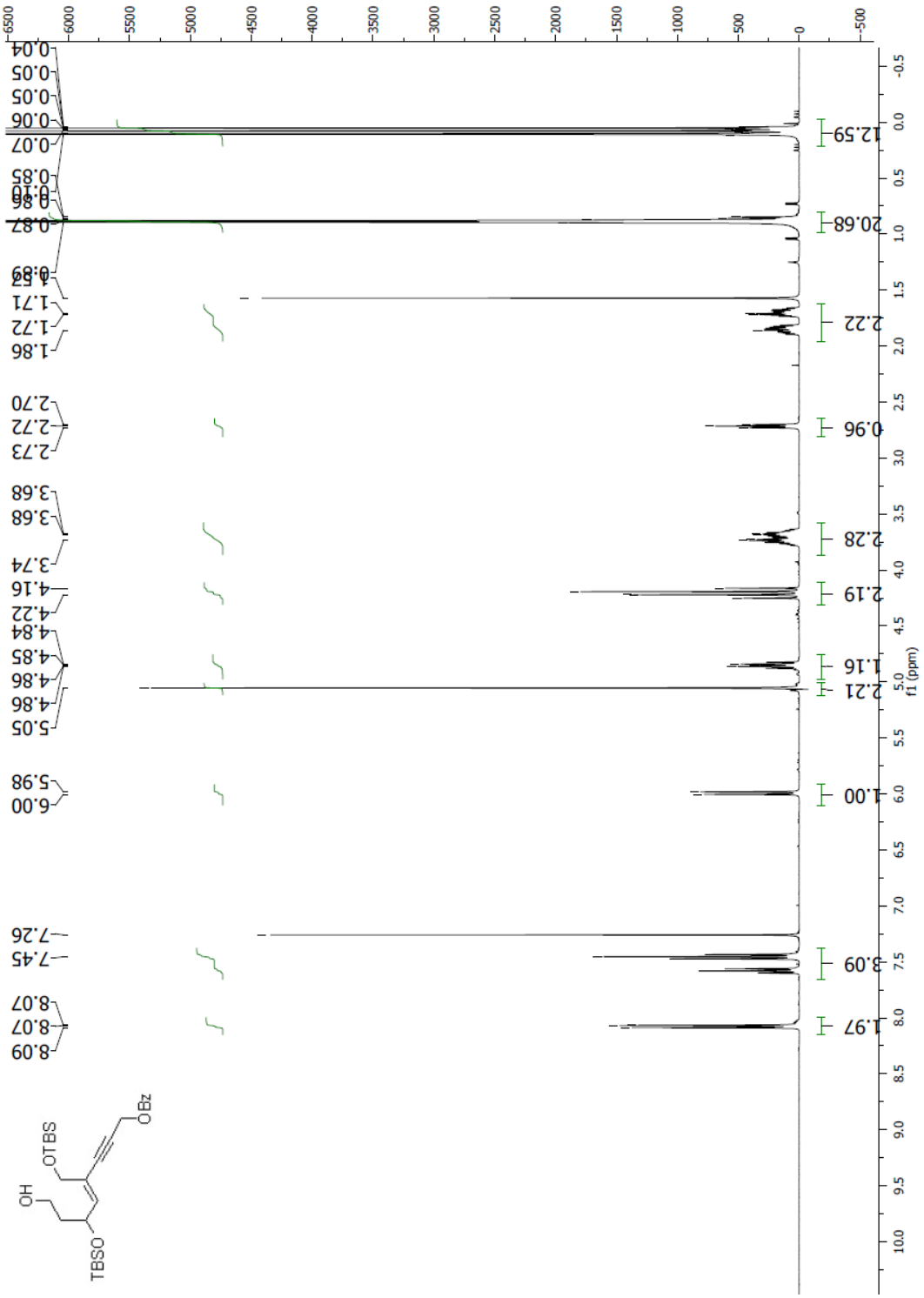

Spectrum 2.61 ^{1}H NMR ($CDCl_3$, 400 MHz) of the enyne precursor to **199**

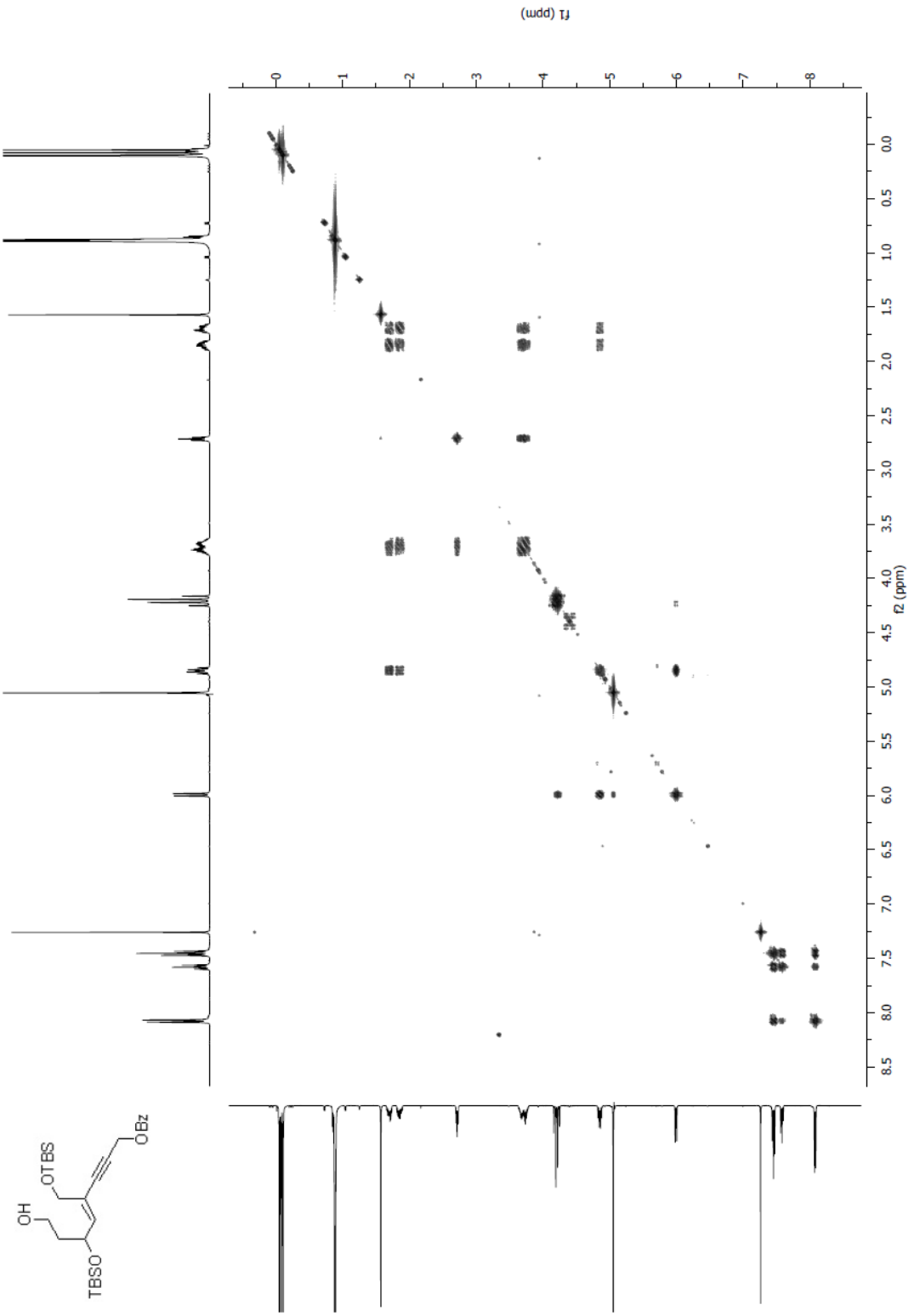

Spectrum 2.62 gCOSY NMR ($CDCl_3$, 400 MHz) of the enyne precursor to **199**

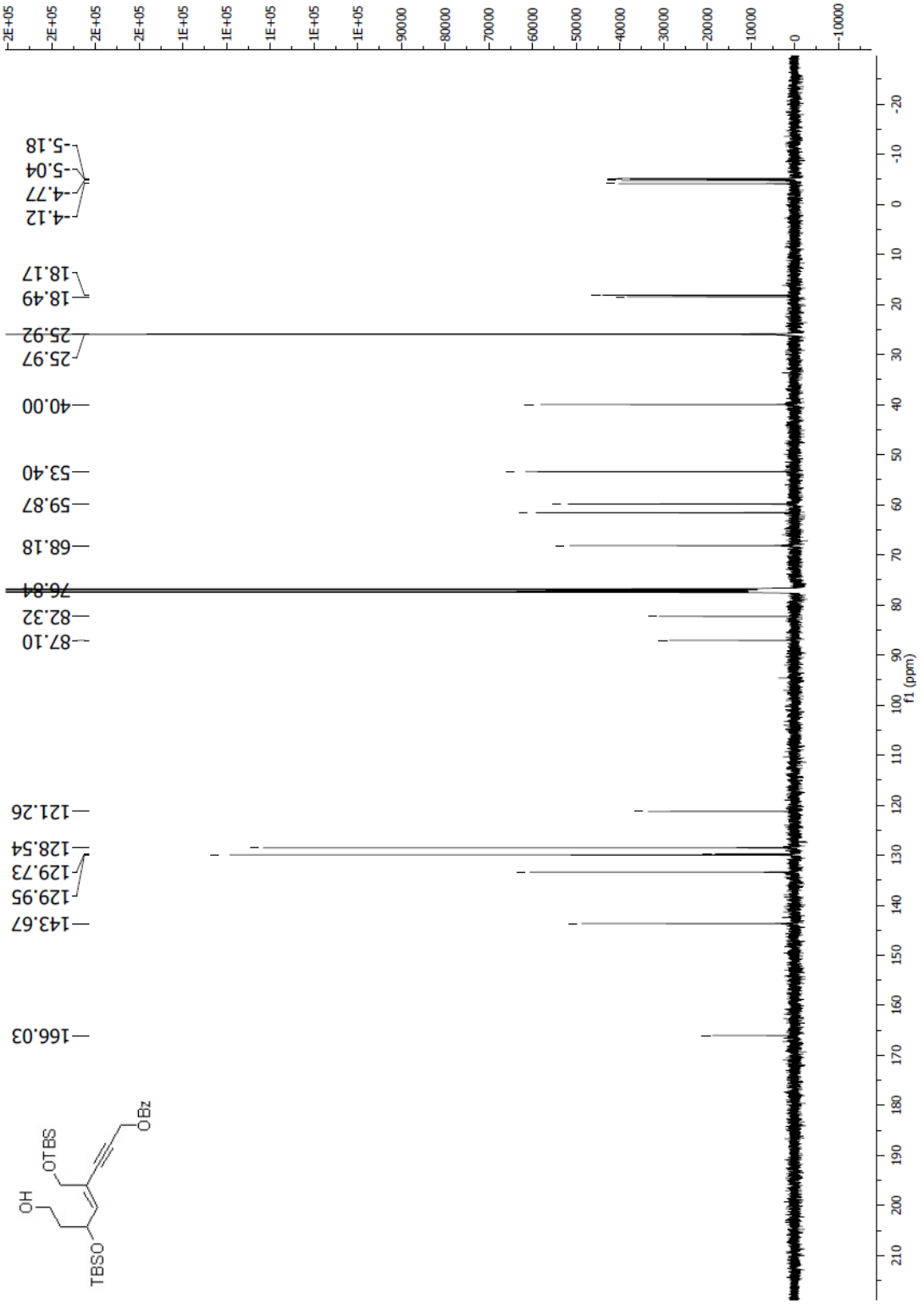

Spectrum 2.63 ^{13}C NMR ($CDCl_3$, 100 MHz) of the enyne precursor to **199**

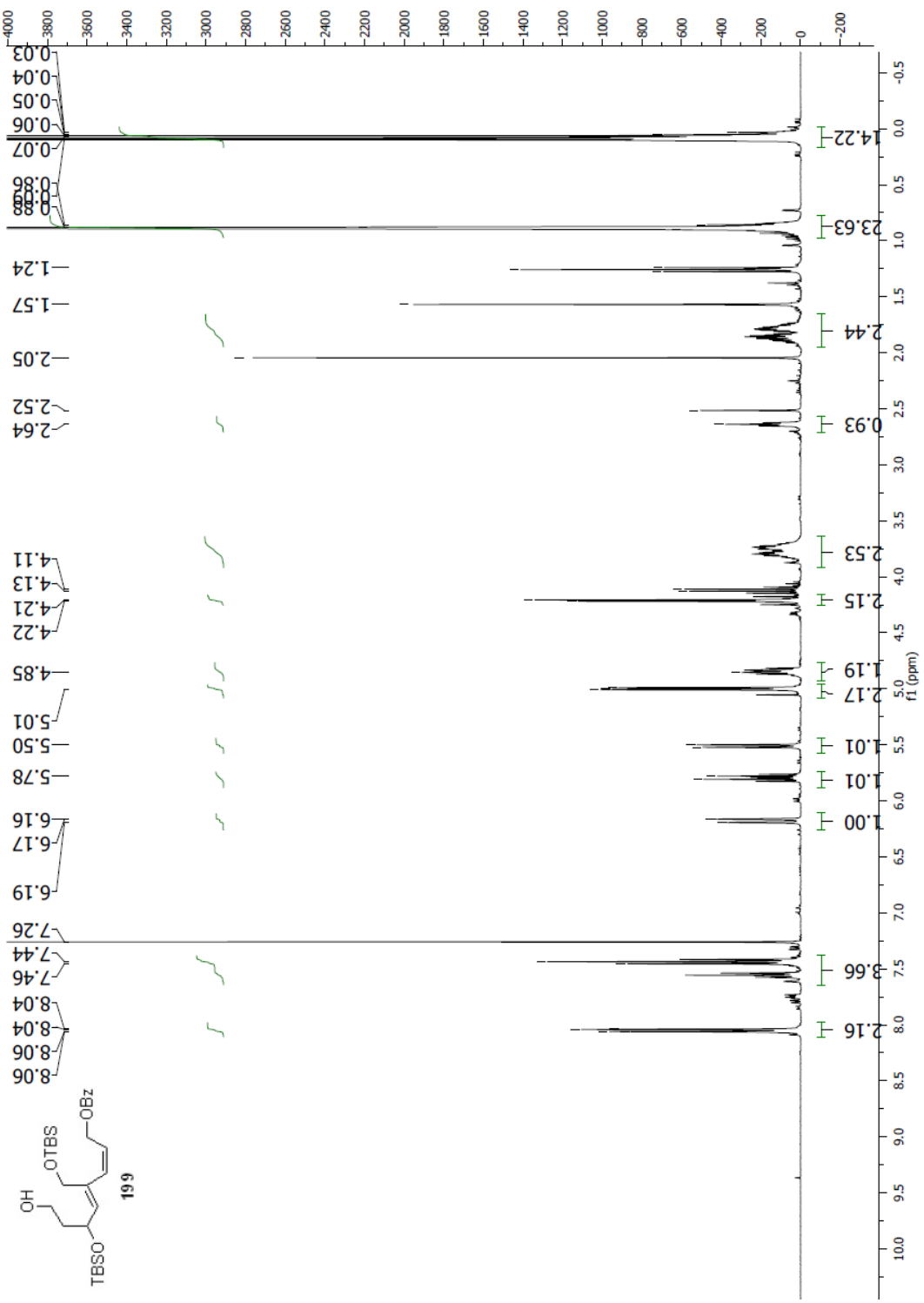

Spectrum 2.64 ^{1}H NMR ($CDCl_3$, 400 MHz) of compound **199**

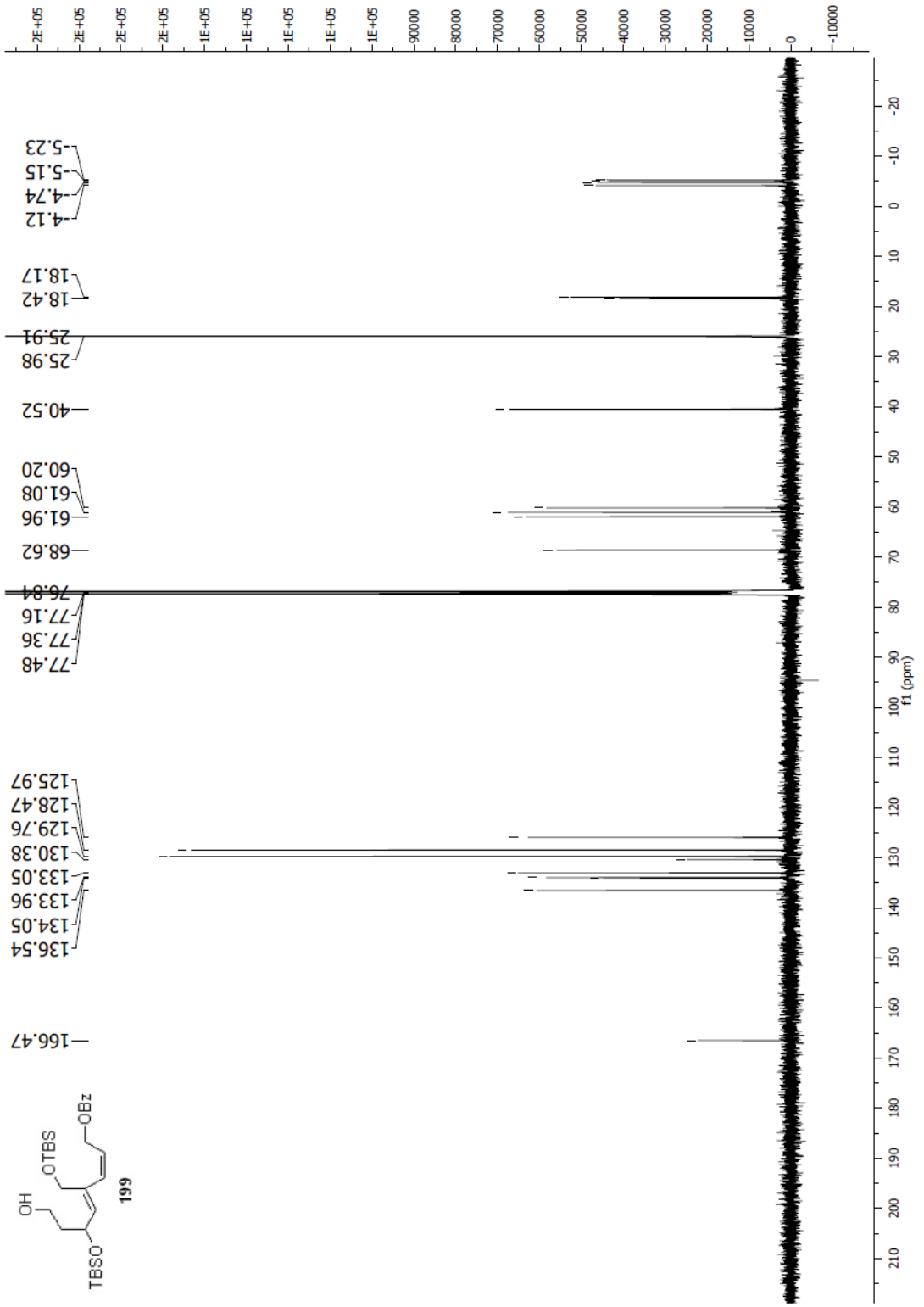

Spectrum 2.65 ^{13}C NMR ($CDCl_3$, 100 MHz) of compound **199**

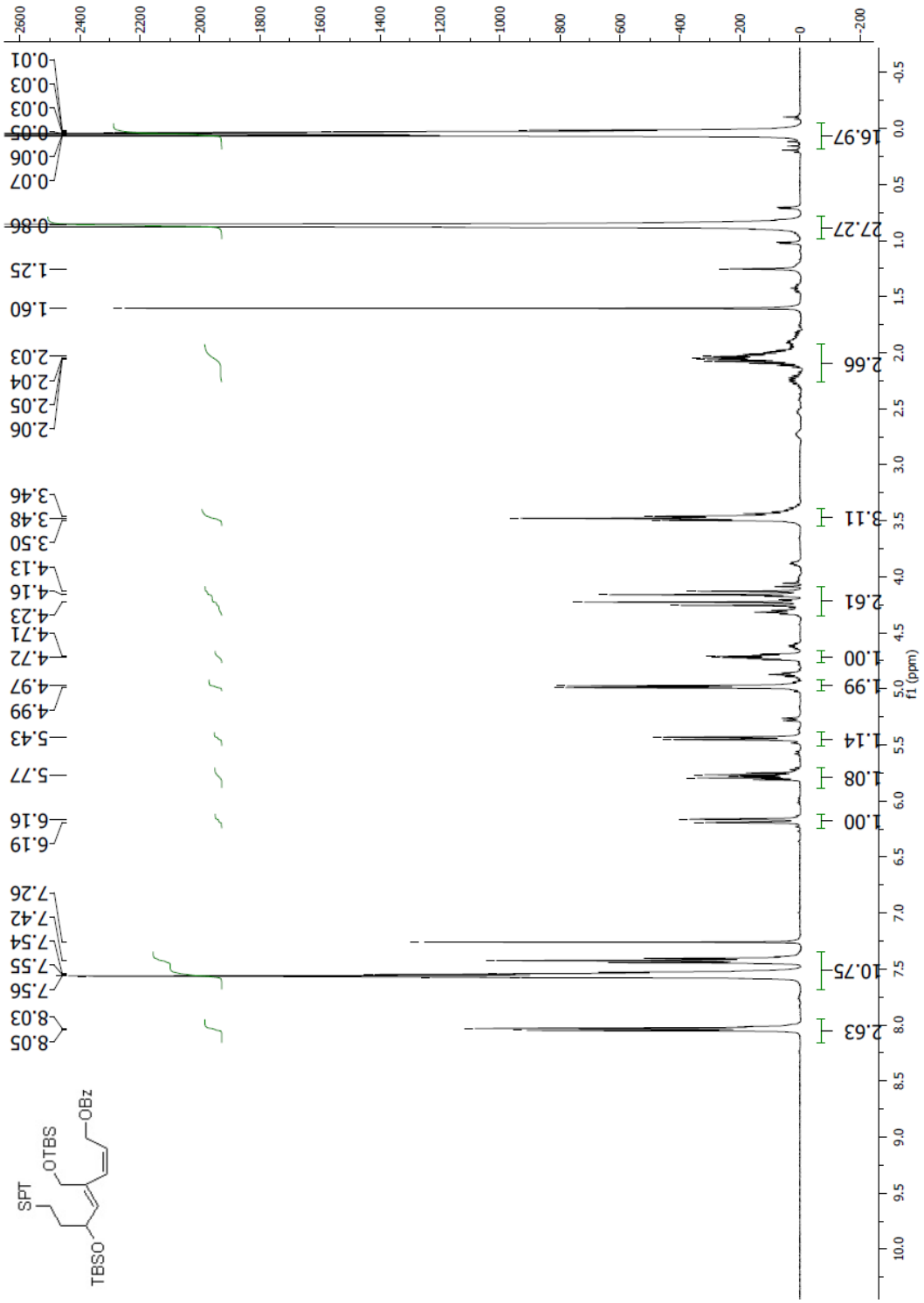

Spectrum 2.66 ^{1}H NMR ($CDCl_3$, 400 MHz) of the sulfide precursor to **200**

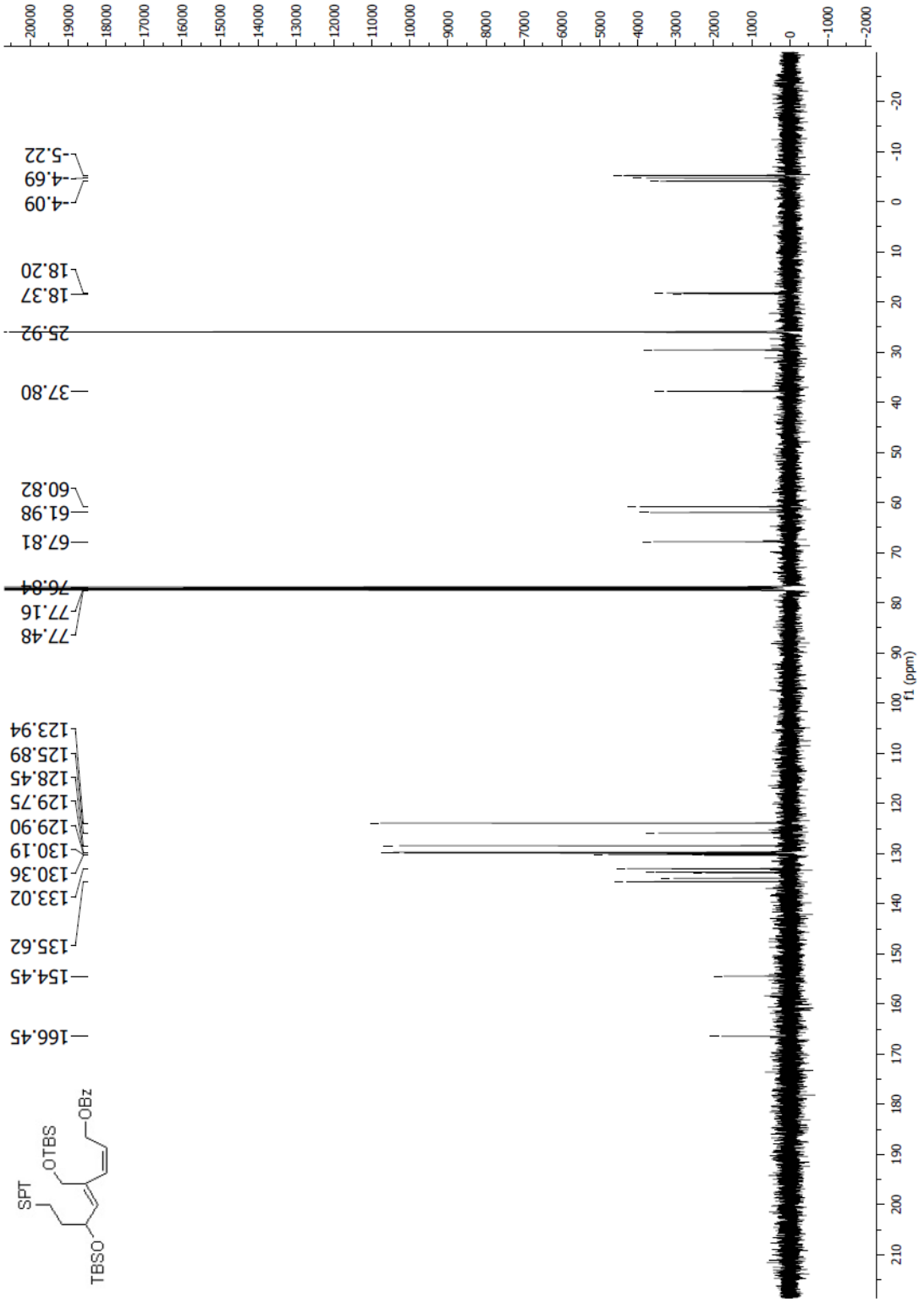

Spectrum 2.67 ^{13}C NMR ($CDCl_3$, 400 MHz) of the sulfide precursor to **200**

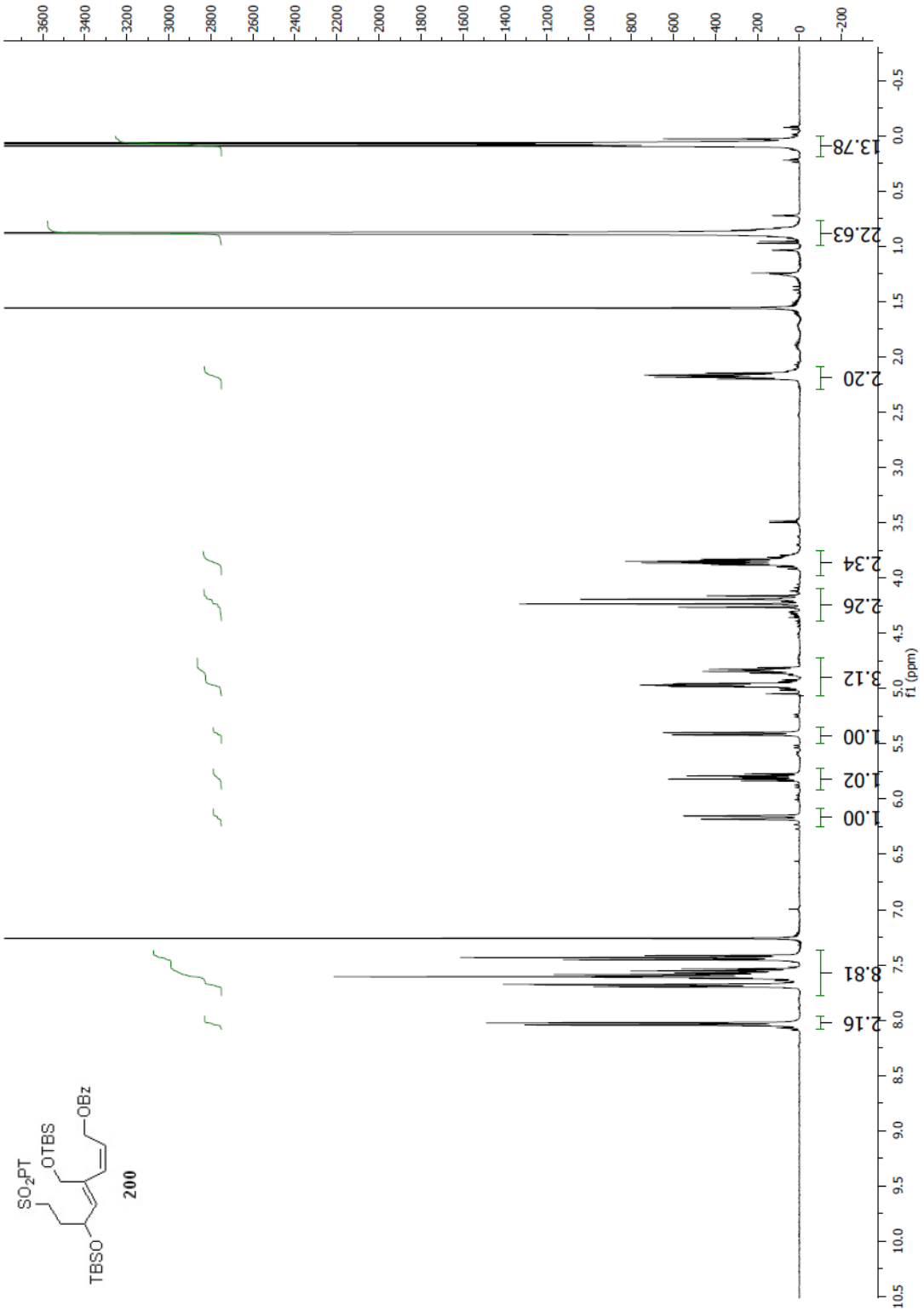

Spectrum 2.68 ^{1}H NMR ($CDCl_3$, 400 MHz) of compound **200**

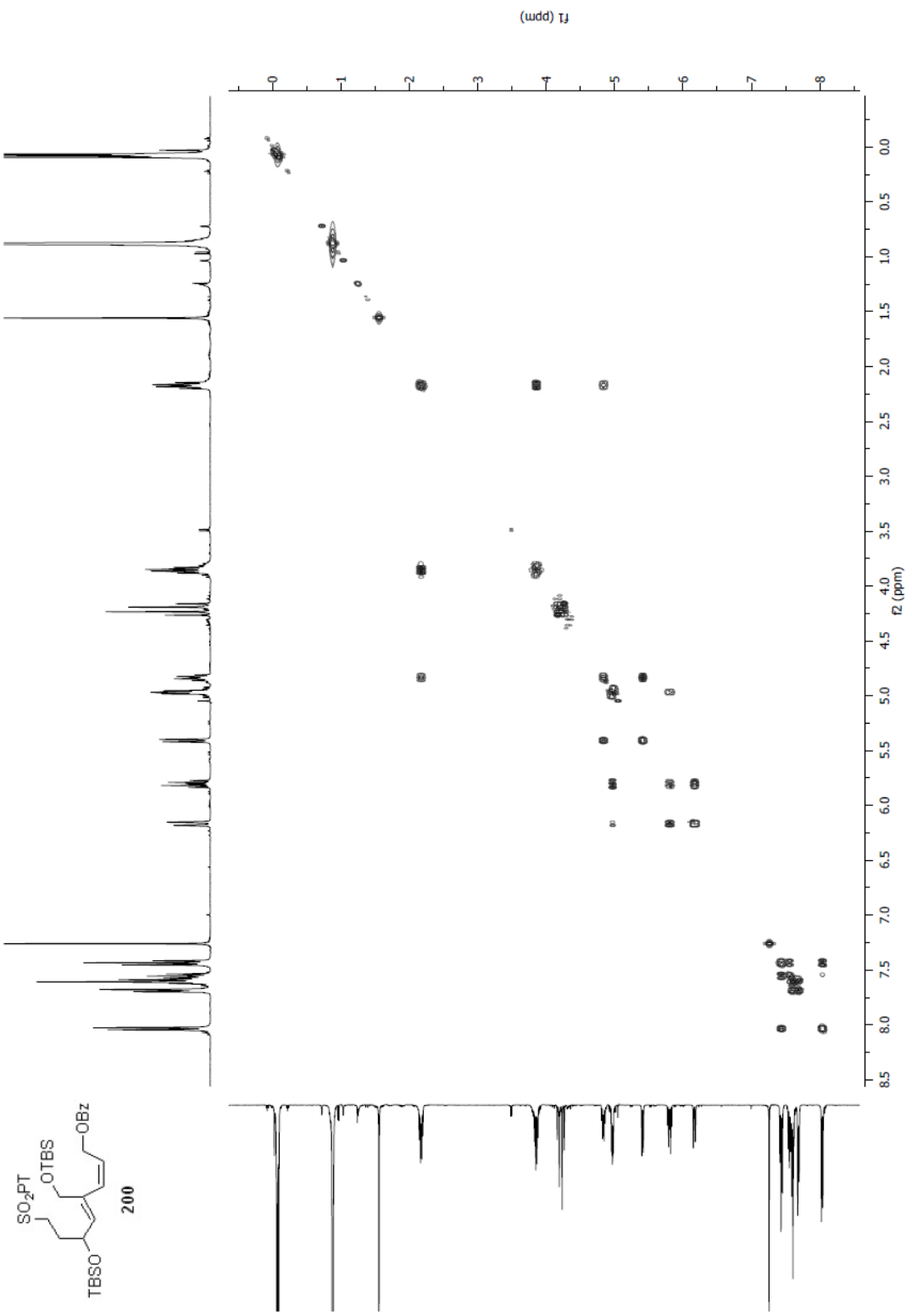

Spectrum 2.69 gCOSY NMR ($CDCl_3$, 400 MHz) of compound **200**

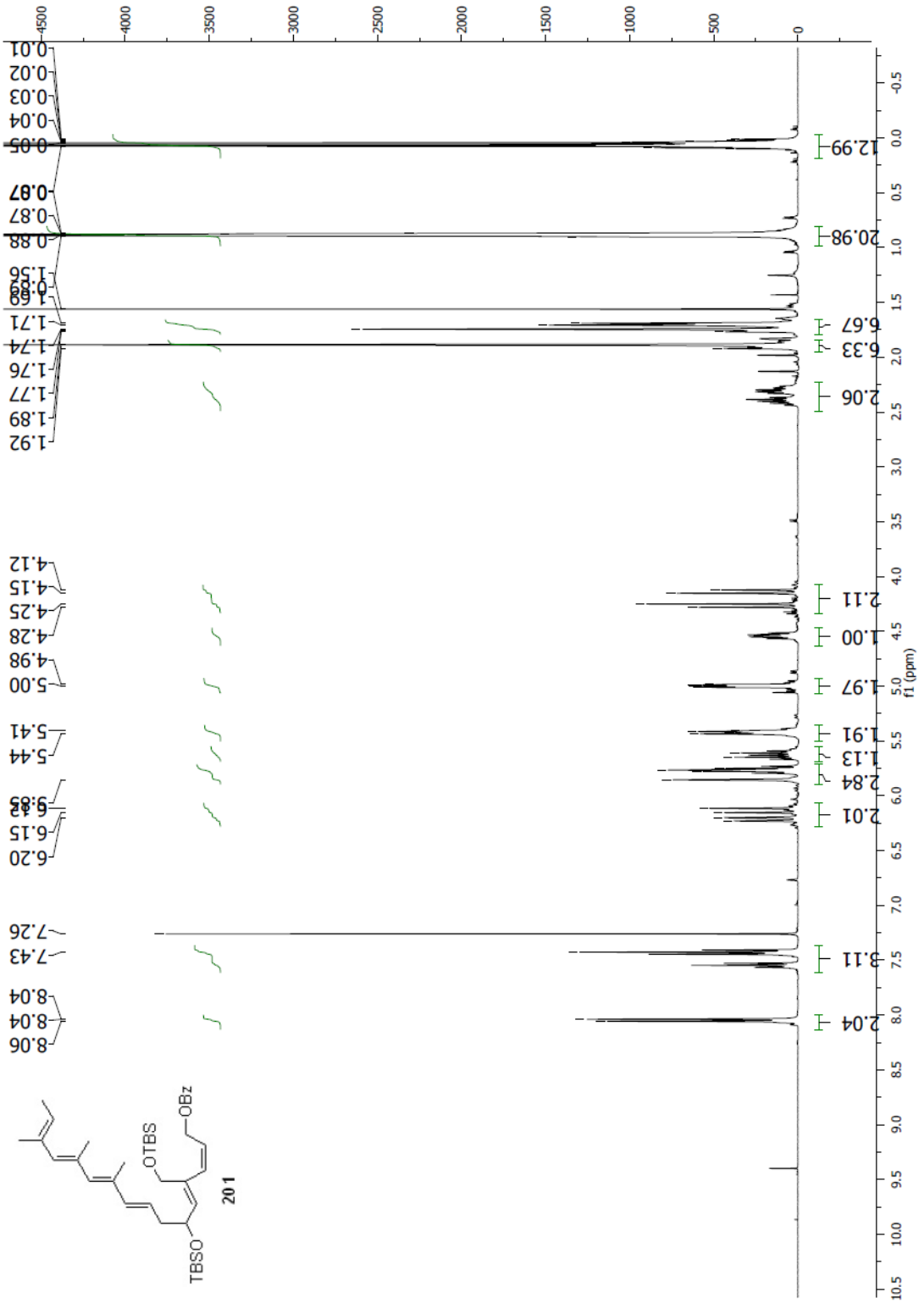

Spectrum 2.70 ^{1}H NMR ($CDCl_3$, 400 MHz) of compound **201**

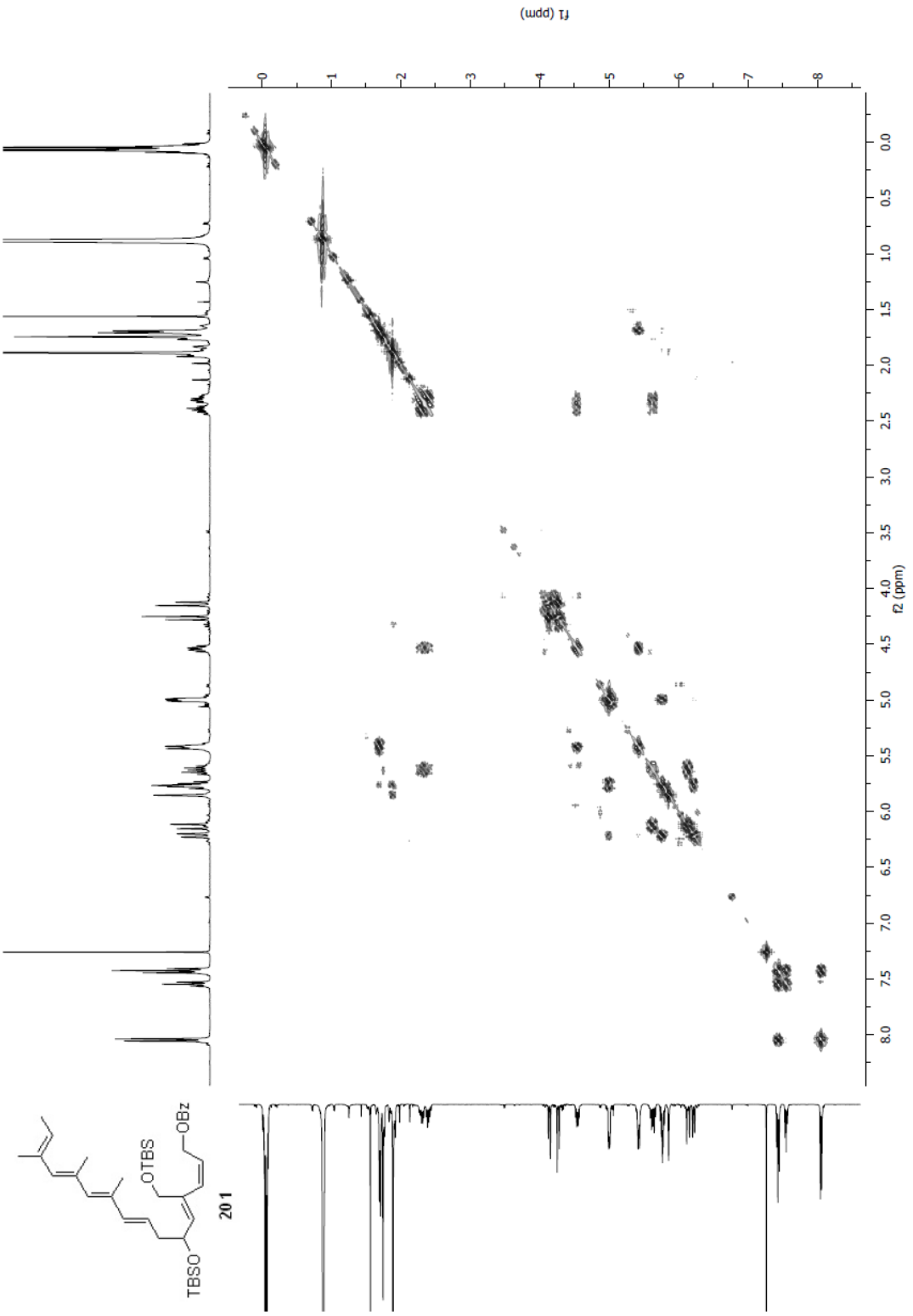

Spectrum 2.71 gCOSY NMR ($CDCl_3$, 400 MHz) of compound **201**

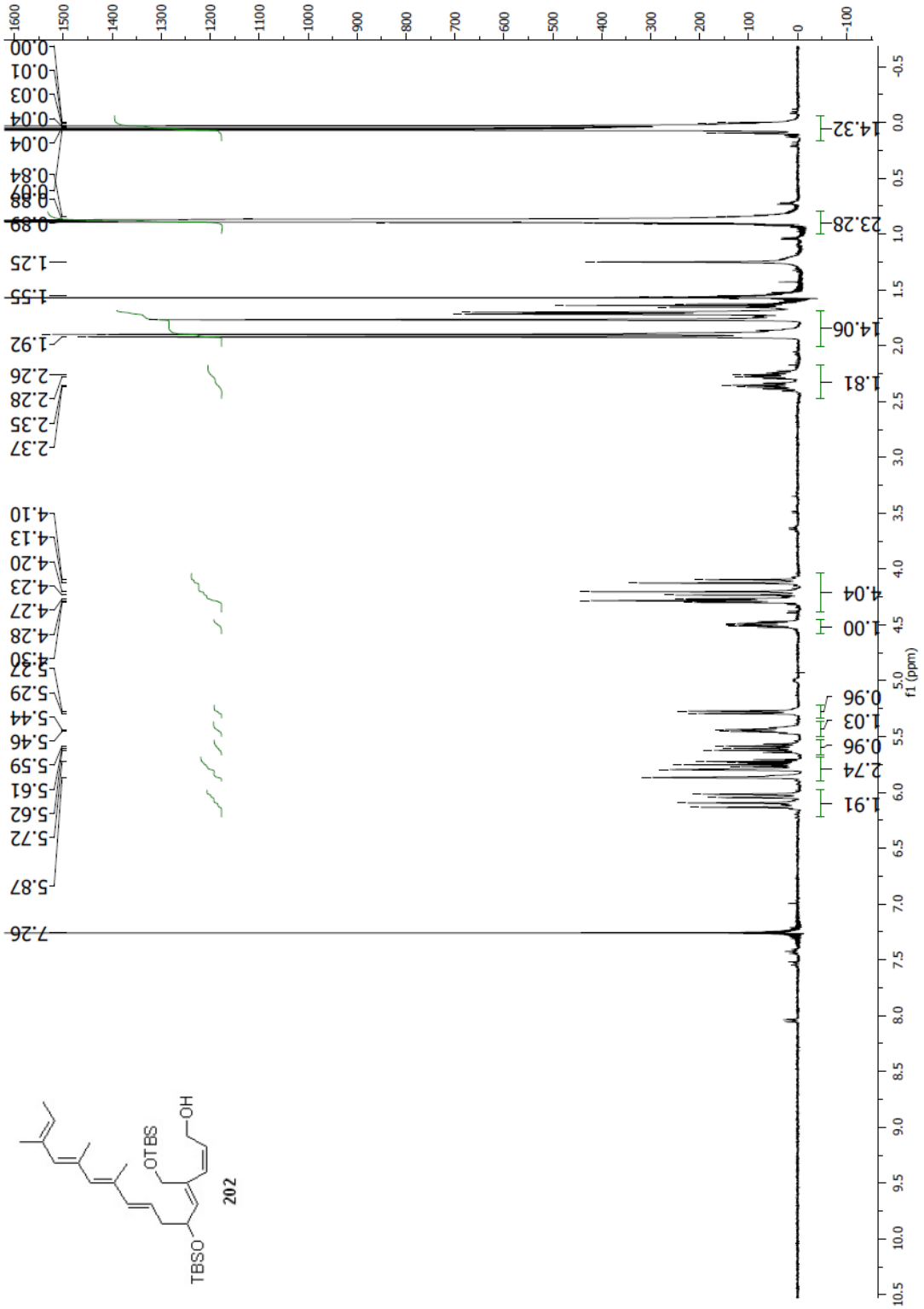

Spectrum 2.72 ^{1}H NMR ($CDCl_3$, 400 MHz) of compound **202**

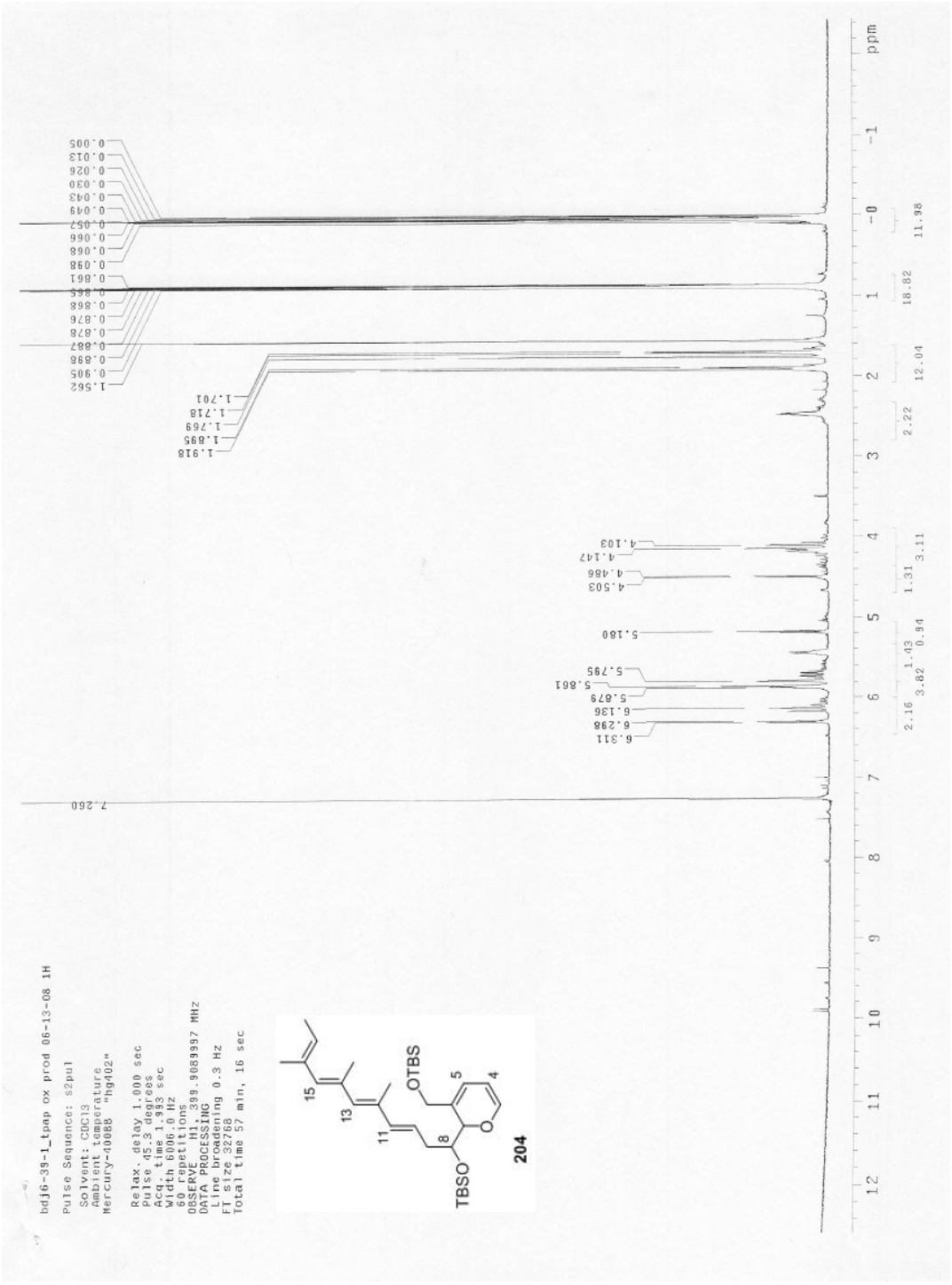

Spectrum 2.73 ^{1}H NMR ($CDCl_3$, 400 MHz) of oxidation product **204**

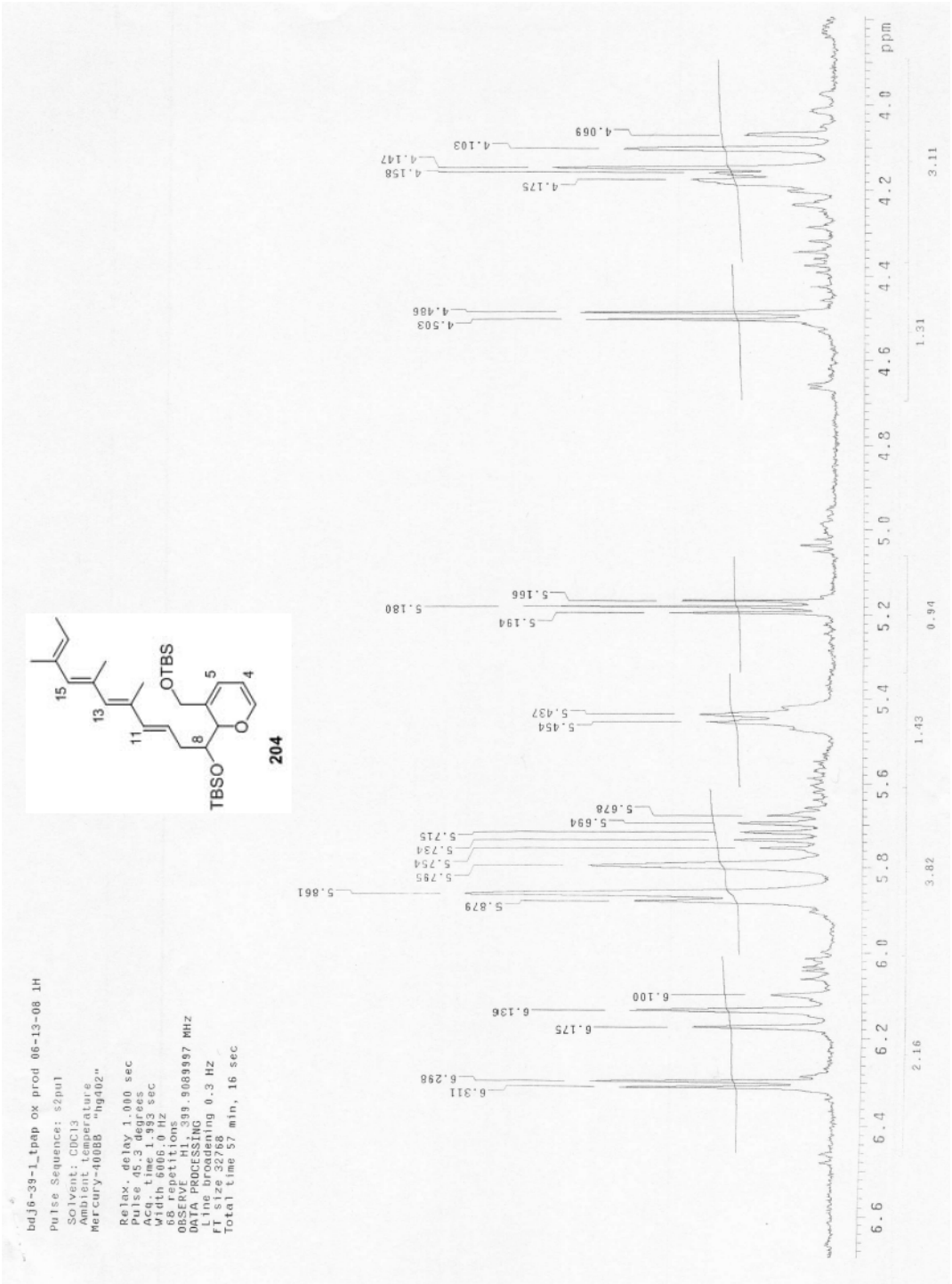

Spectrum 2.74 ^{1}H NMR ($CDCl_3$, 400 MHz) expansion of Spectrum 2.73

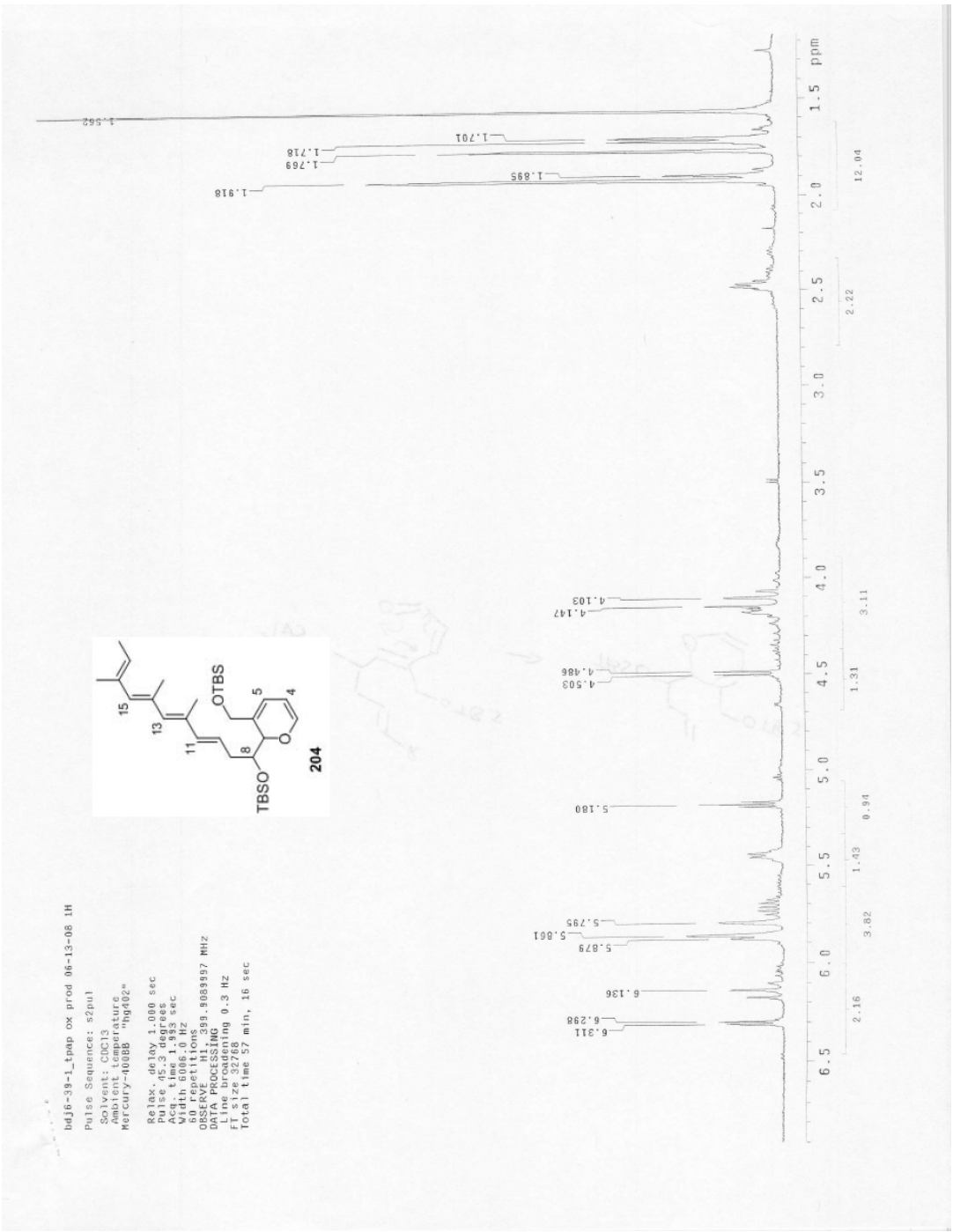

Spectrum 2.75 ^{1}H NMR ($CDCl_3$, 400 MHz) expansion of Spectrum 2.73

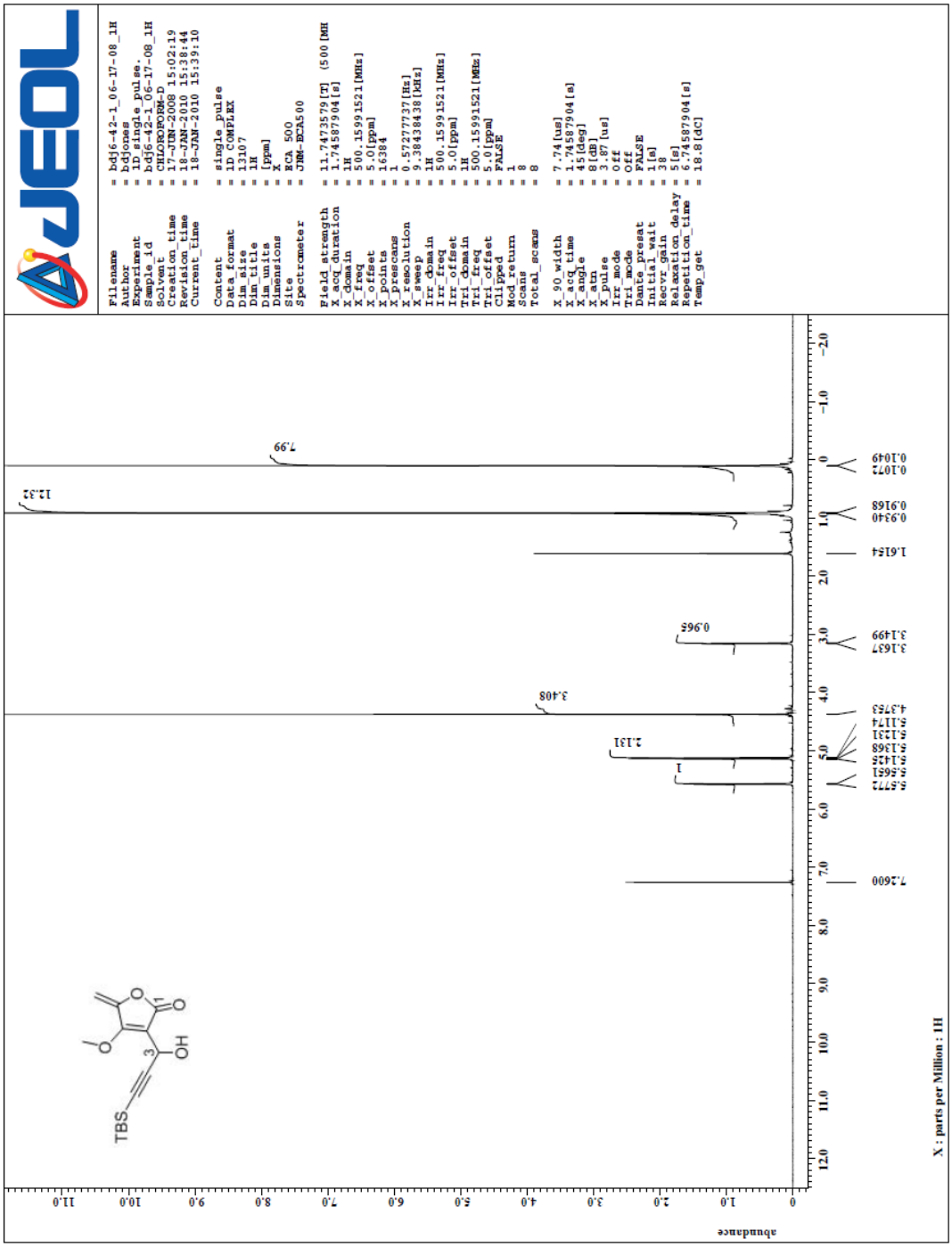

Spectrum 2.76 ^{1}H NMR ($CDCl_3$, 500 MHz) of the adduct precursor to **205**

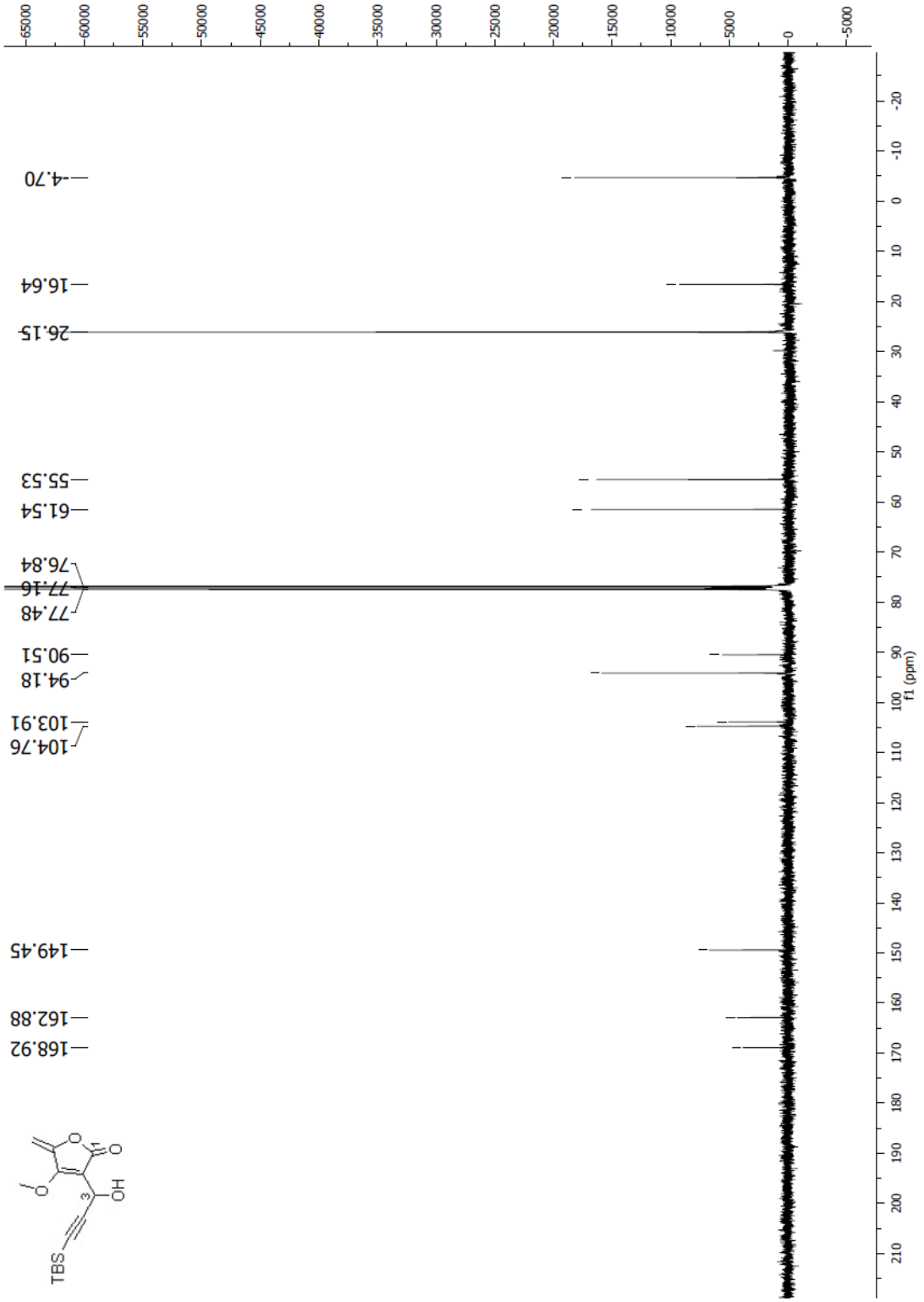

Spectrum 2.77 ^{13}C NMR ($CDCl_3$, 100 MHz) of the adduct precursor to **205**

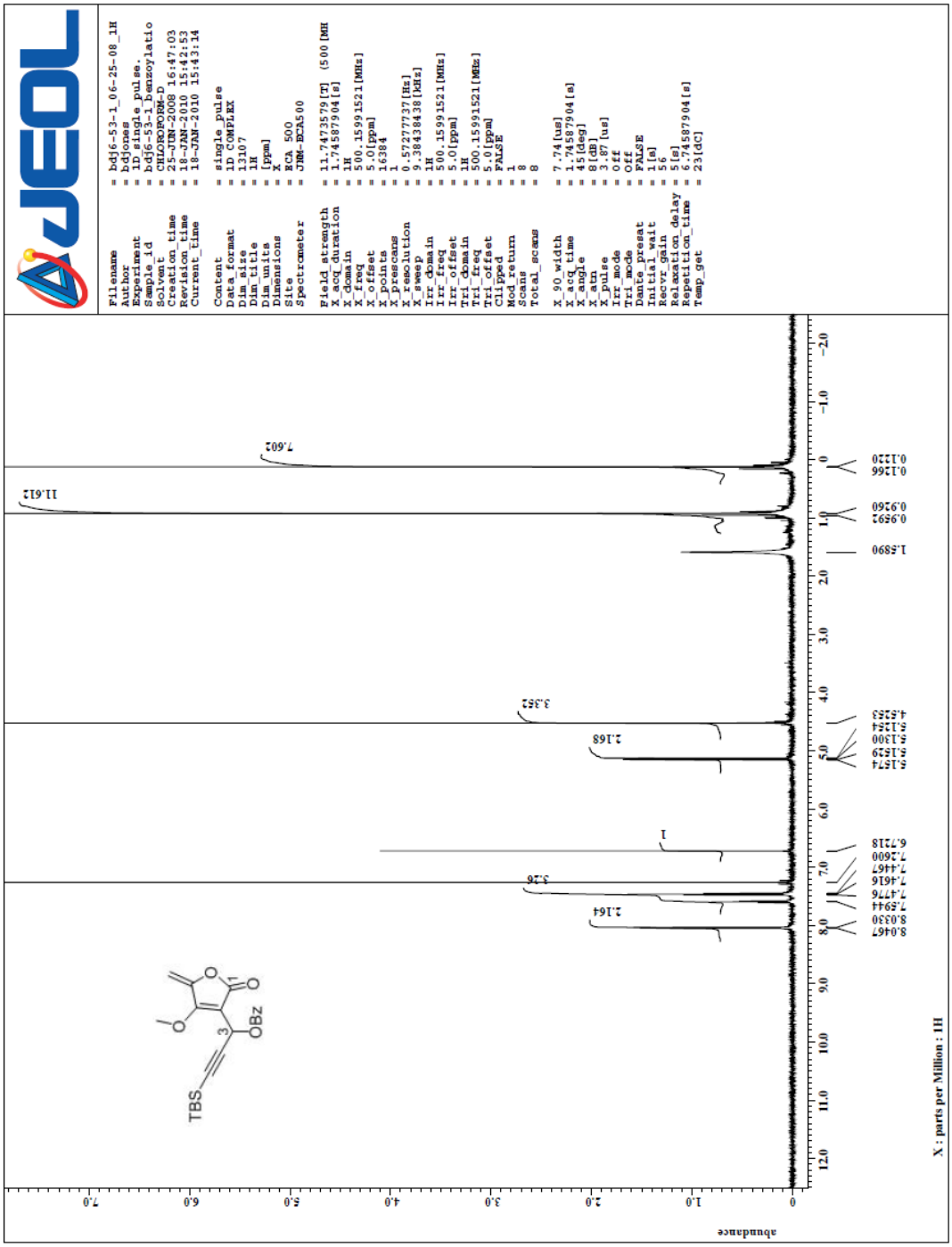

Spectrum 2.78 ^{1}H NMR ($CDCl_3$, 500 MHz) of the benzoate precursor to **205**

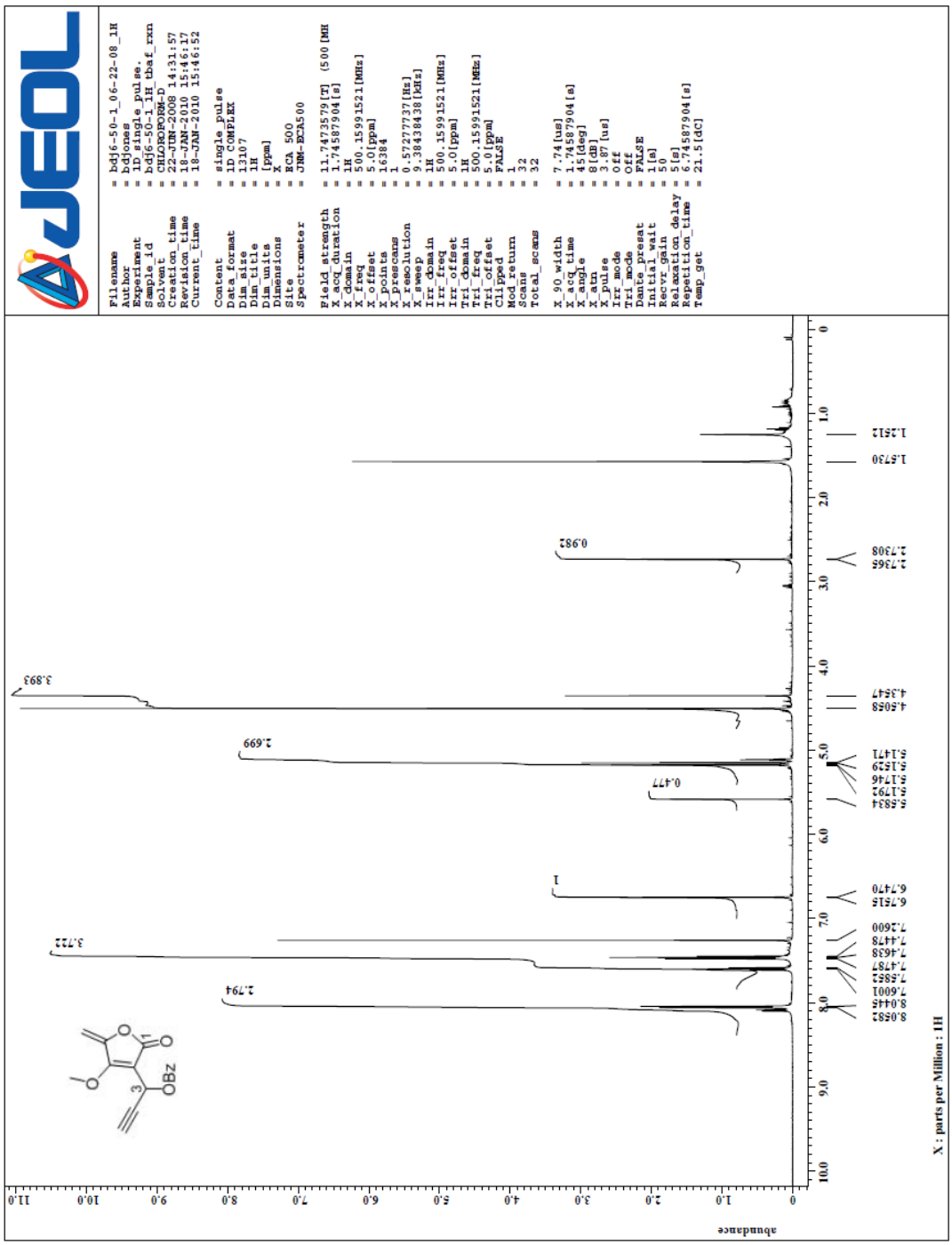

Spectrum 2.79 ^{1}H NMR ($CDCl_3$, 500 MHz) of compound **205**

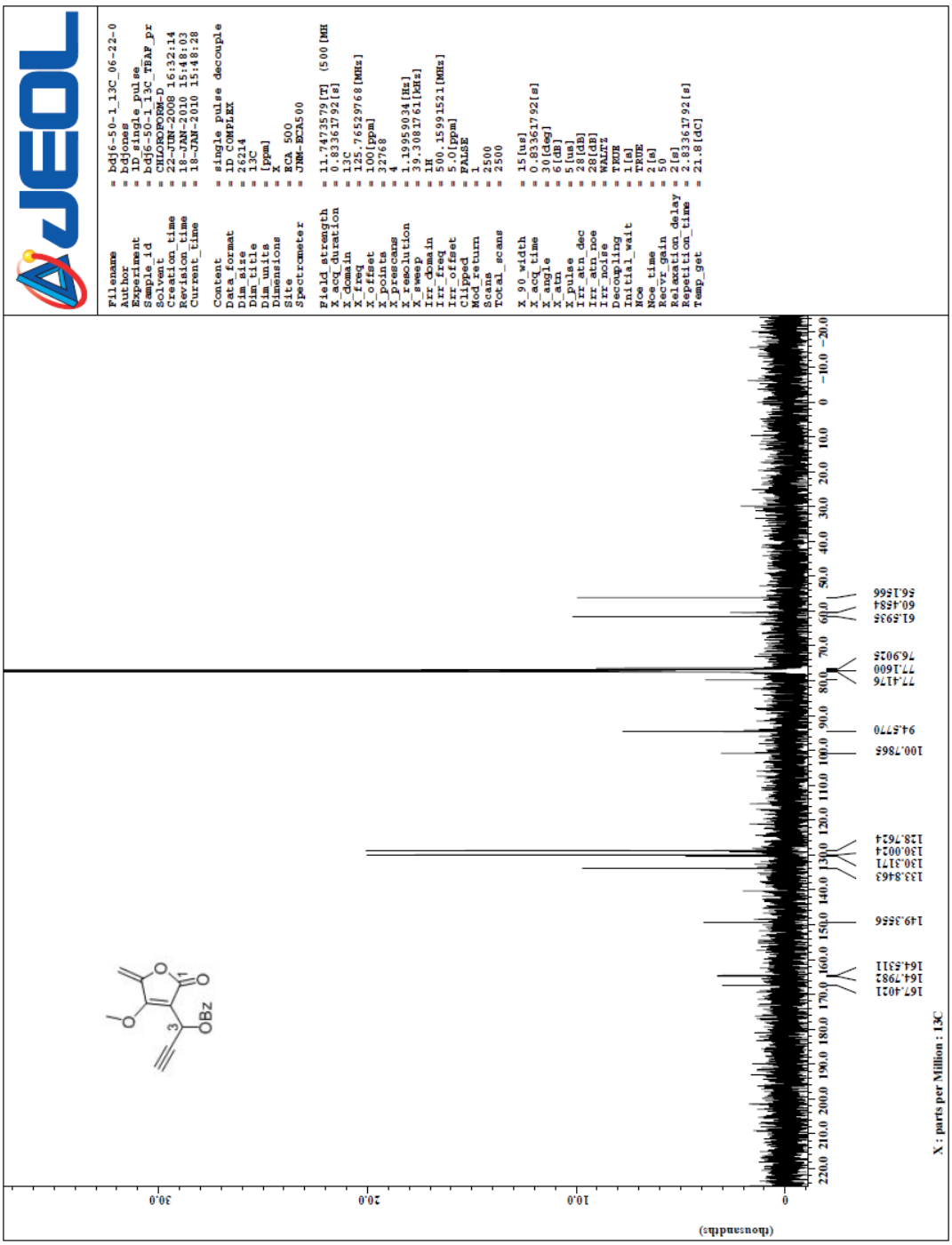

Spectrum 2.80 ^{13}C NMR ($CDCl_3$, 125 MHz) of compound **205**

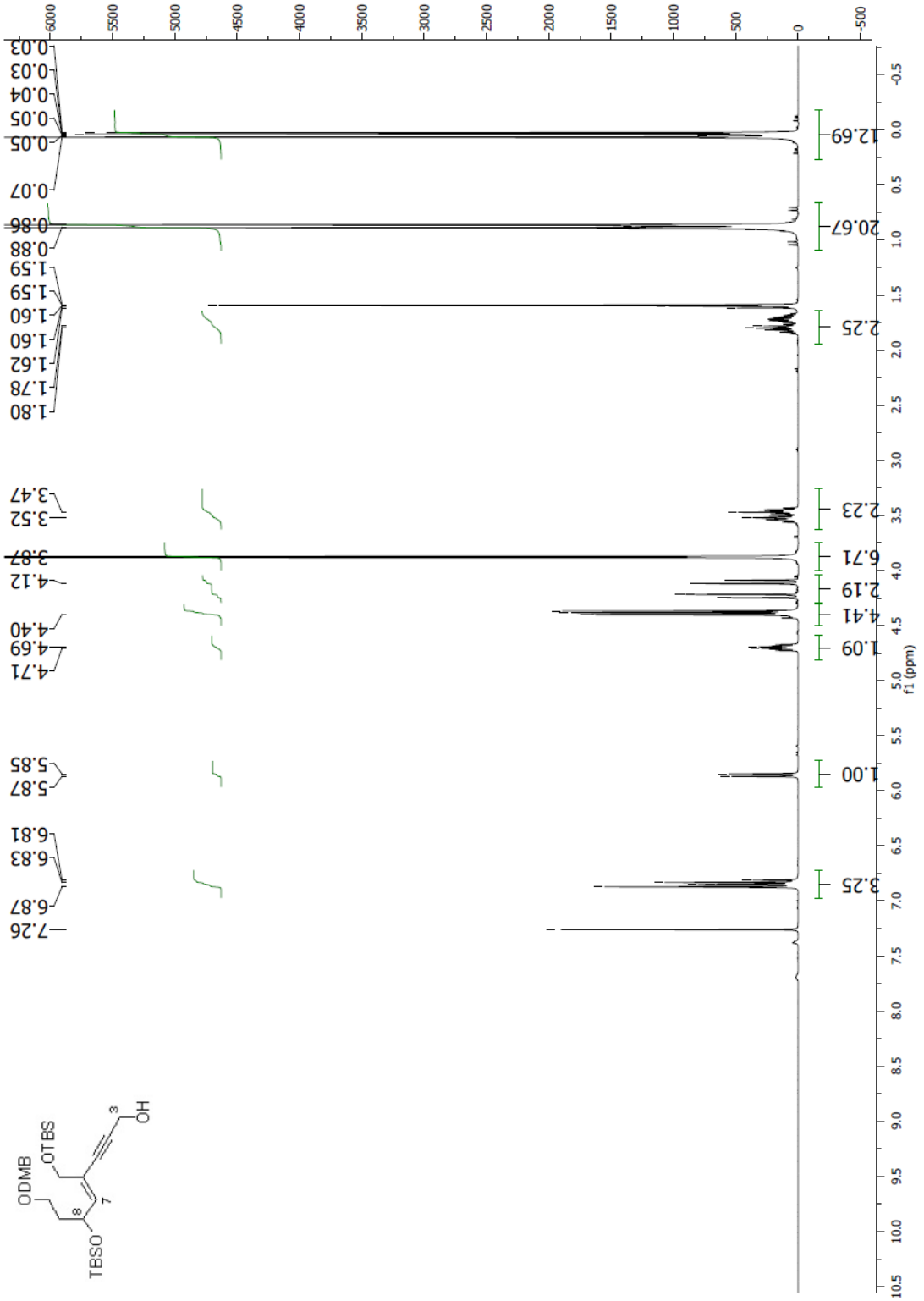

Spectrum 2.81 ^{1}H NMR ($CDCl_3$, 400 MHz) of Sonogashira adduct precursor to **207**

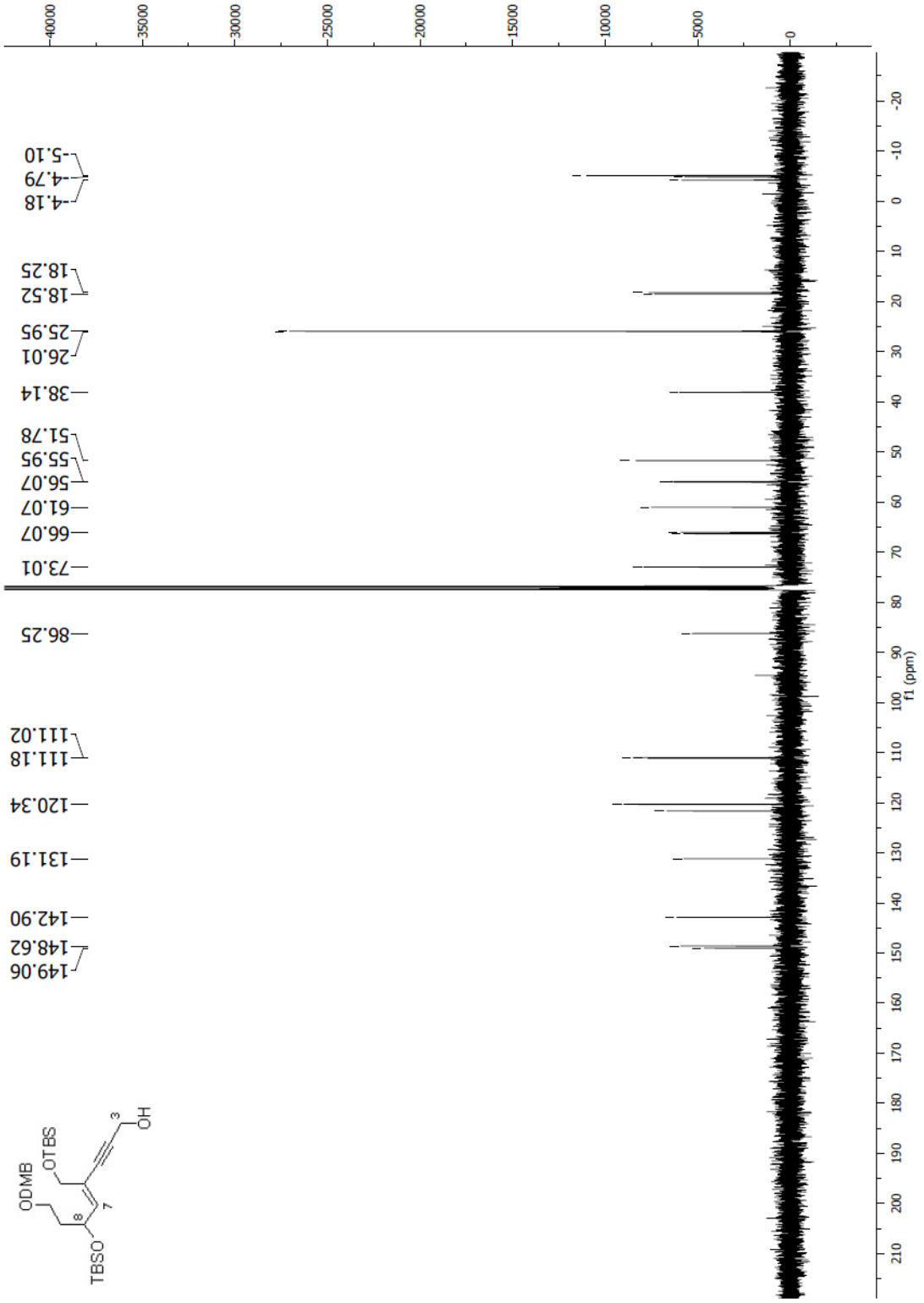

Spectrum 2.82 ^{13}C NMR ($CDCl_3$, 100 MHz) of Sonogashira adduct precursor to **207**

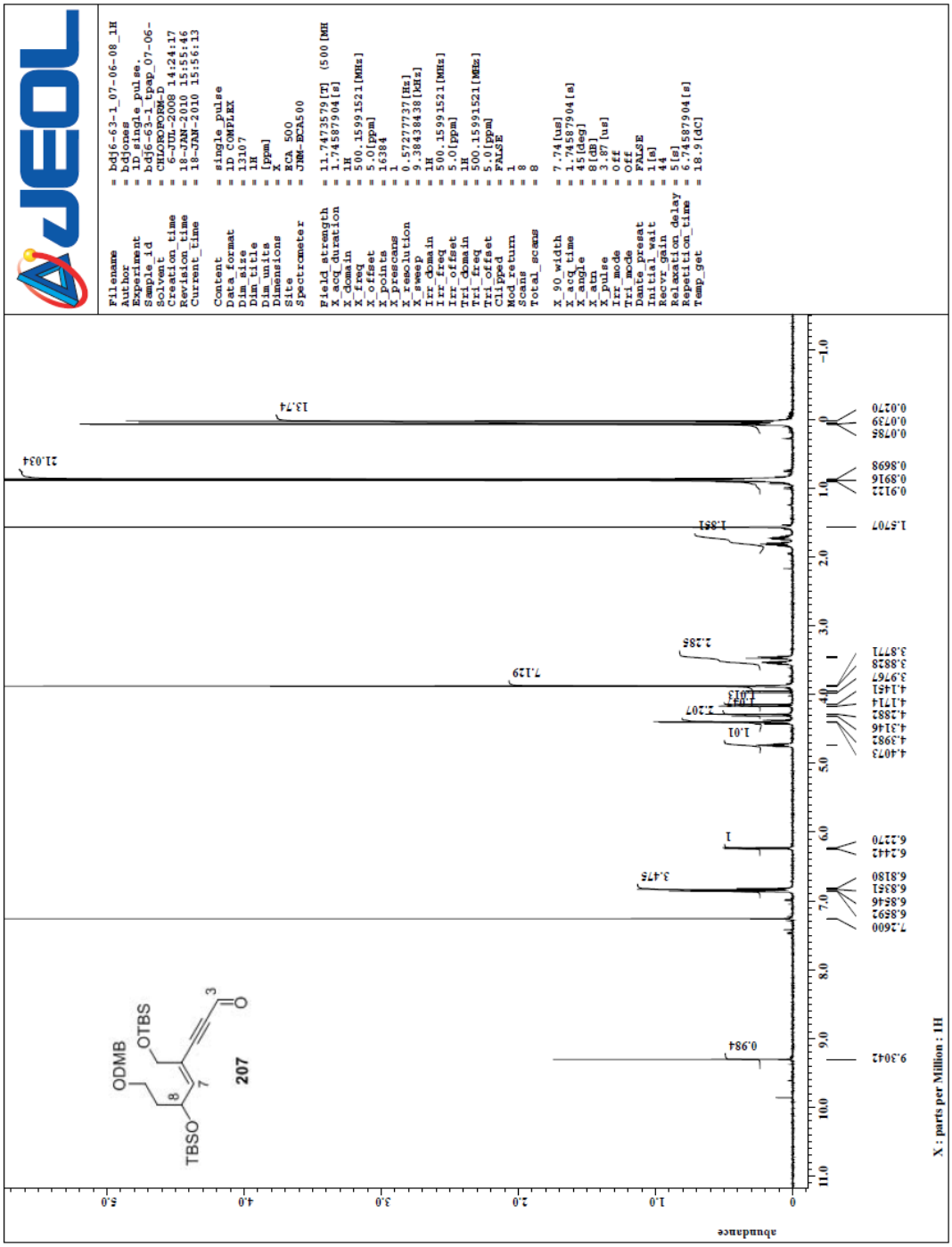

Spectrum 2.83 ^{1}H NMR ($CDCl_3$, 500 MHz) of compound **207**

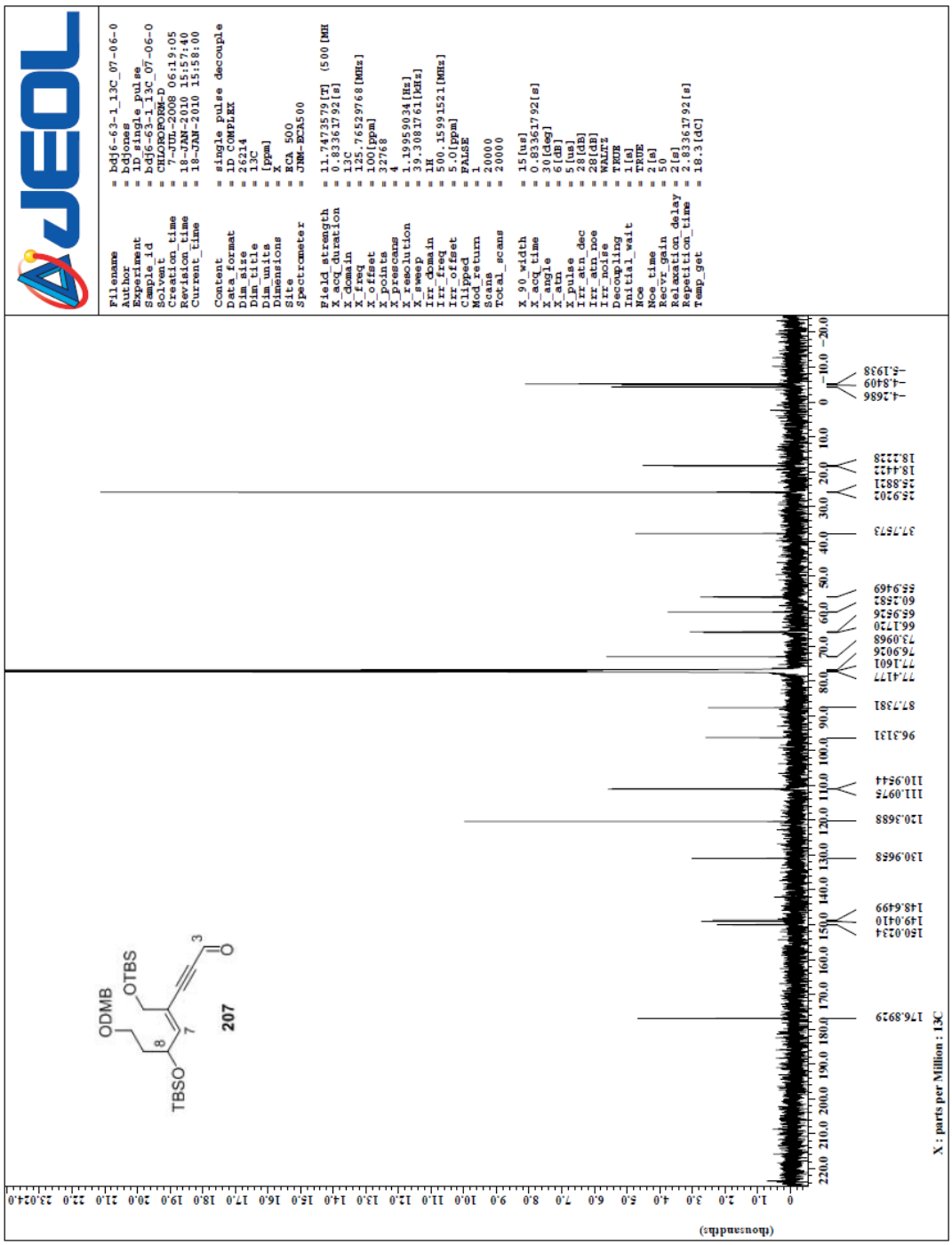

Spectrum 2.84 ^{13}C NMR ($CDCl_3$, 125 MHz) of compound **207**

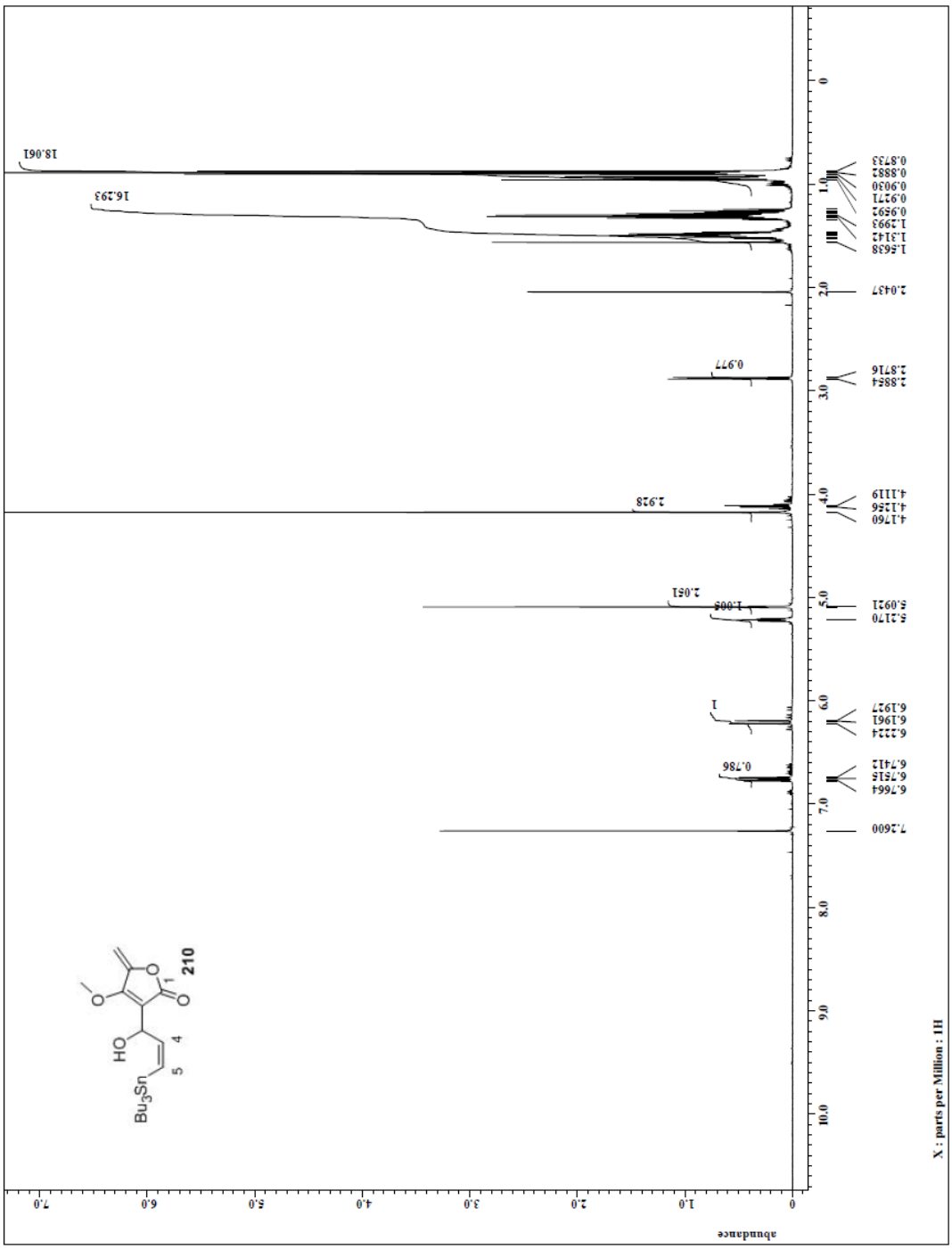

Spectrum 2.85 ^{1}H NMR ($CDCl_3$, 500 MHz) of compound **210**

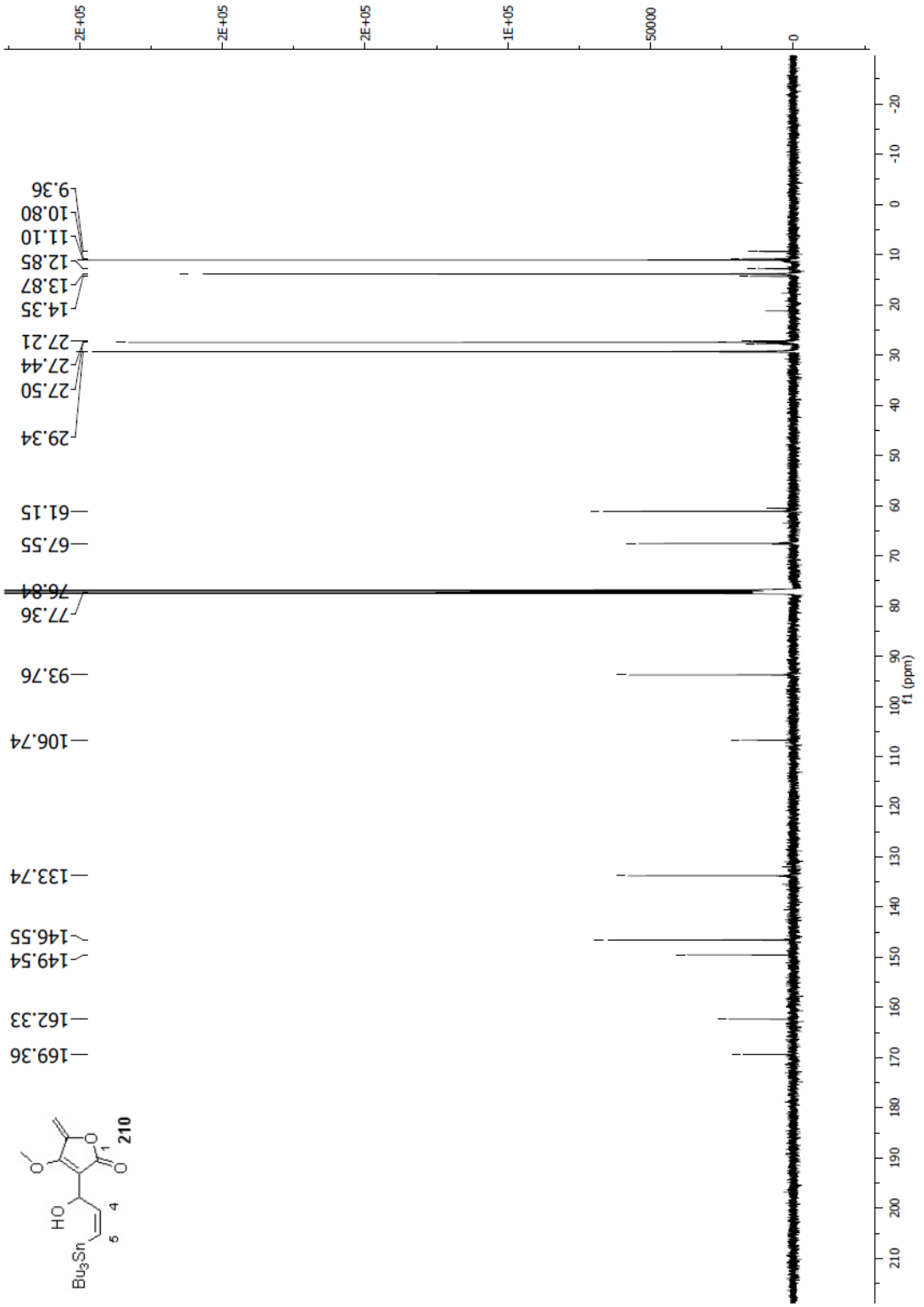

Spectrum 2.86 ^{13}C NMR ($CDCl_3$, 100 MHz) of compound **210**

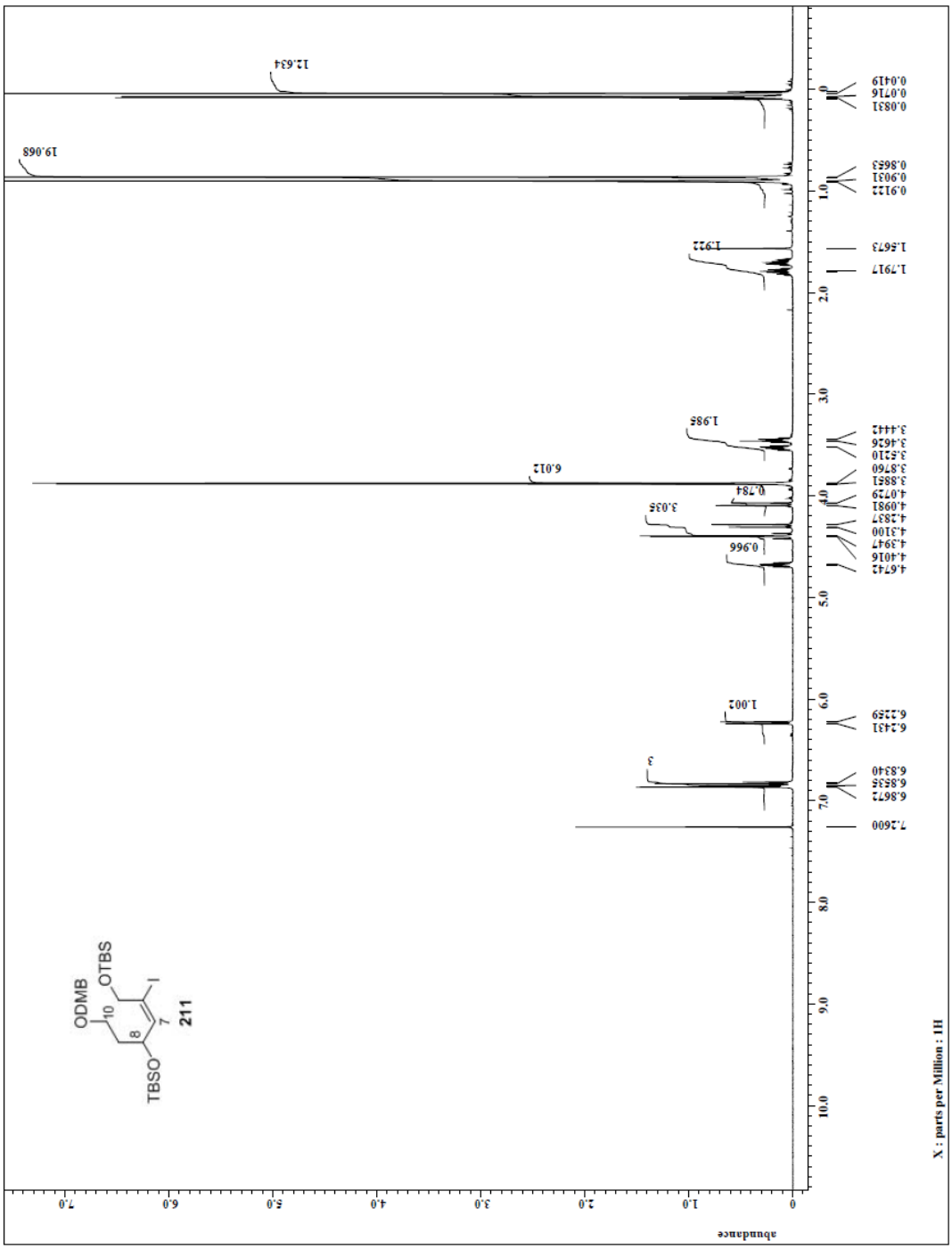

Spectrum 2.87 ^{1}H NMR ($CDCl_3$, 500 MHz) of compound **211**

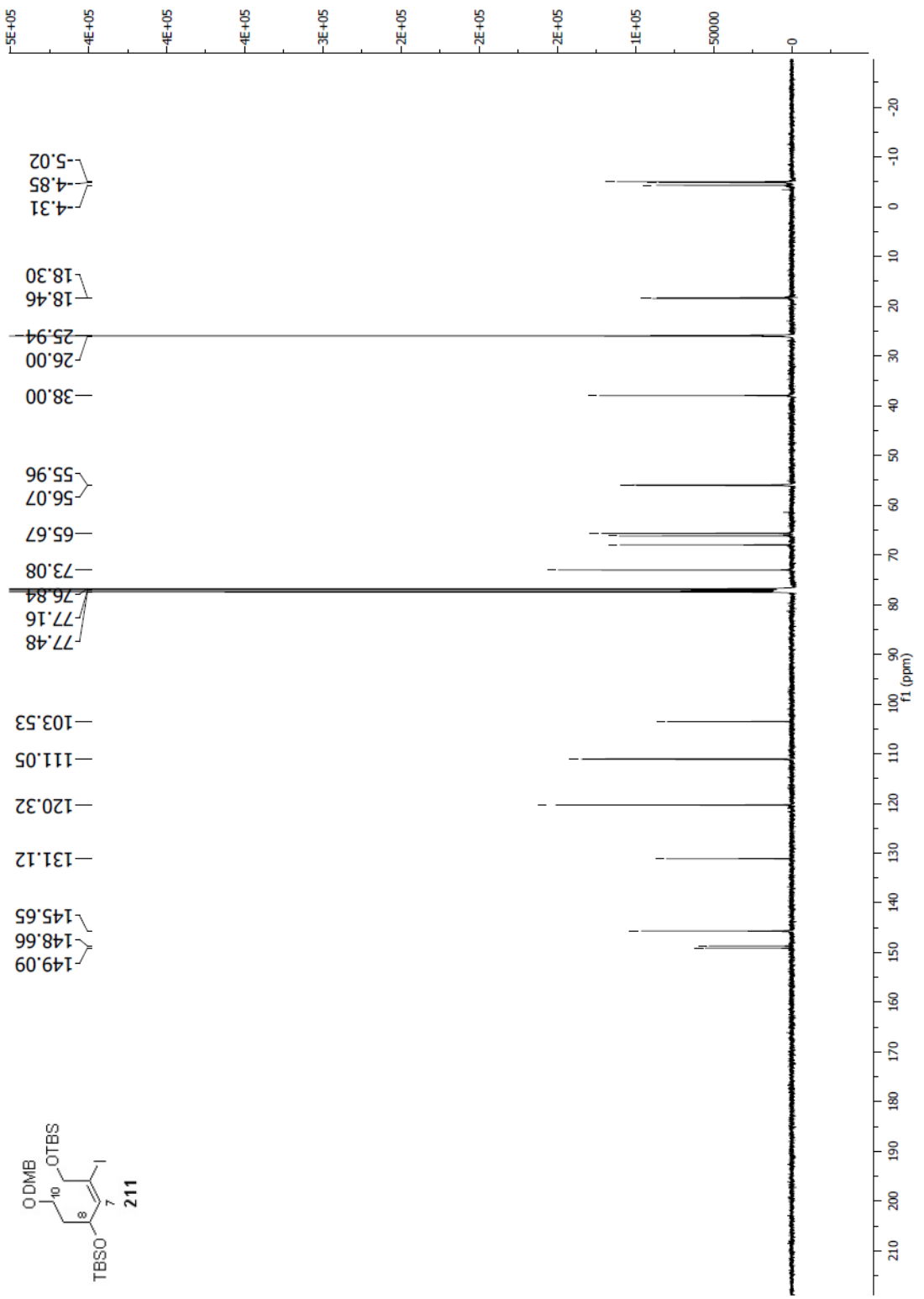

Spectrum 2.88 ^{13}C NMR ($CDCl_3$, 100 MHz) of compound **211**

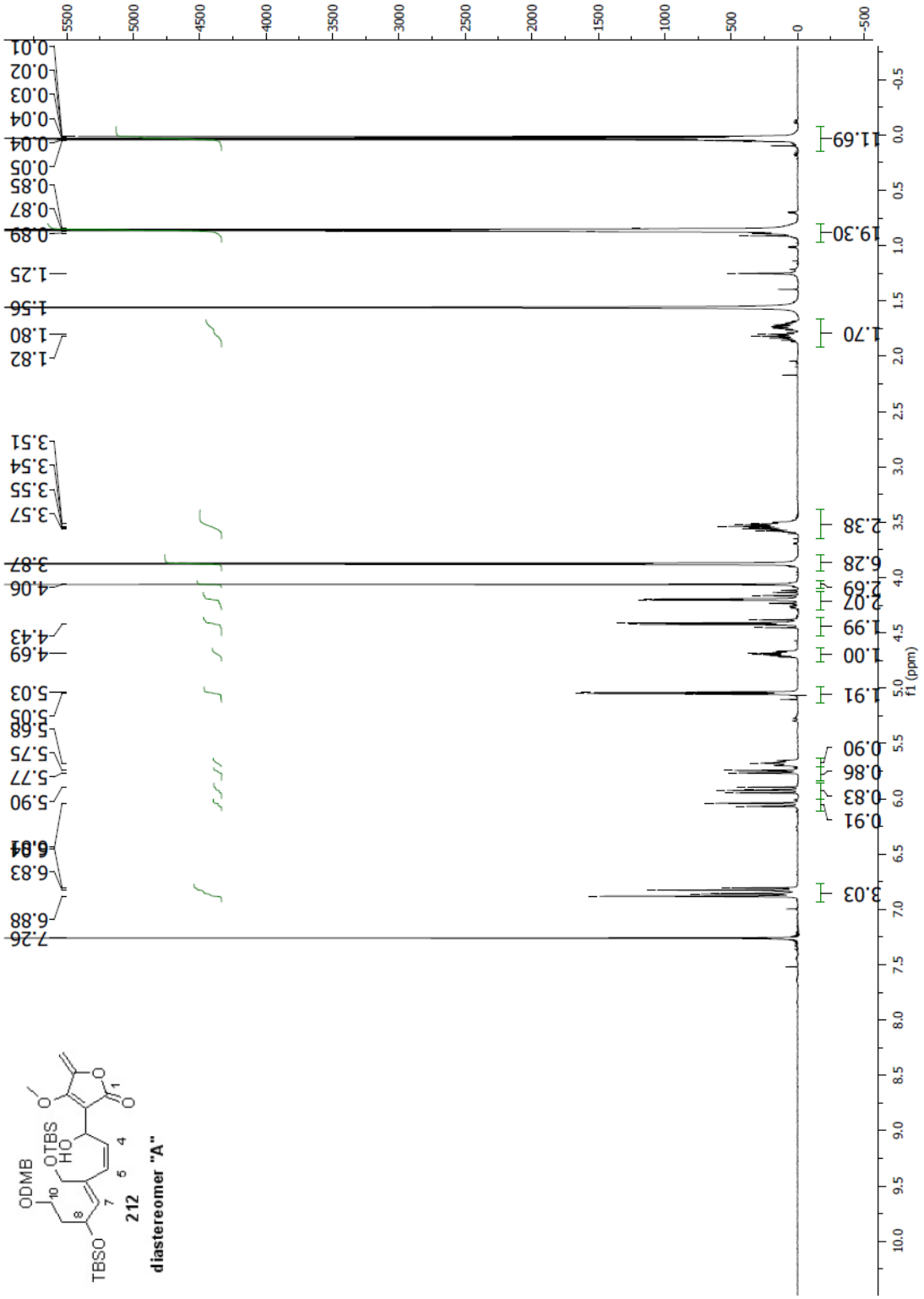

Spectrum 2.89 ^{1}H NMR ($CDCl_3$, 400 MHz) of compound **212a**

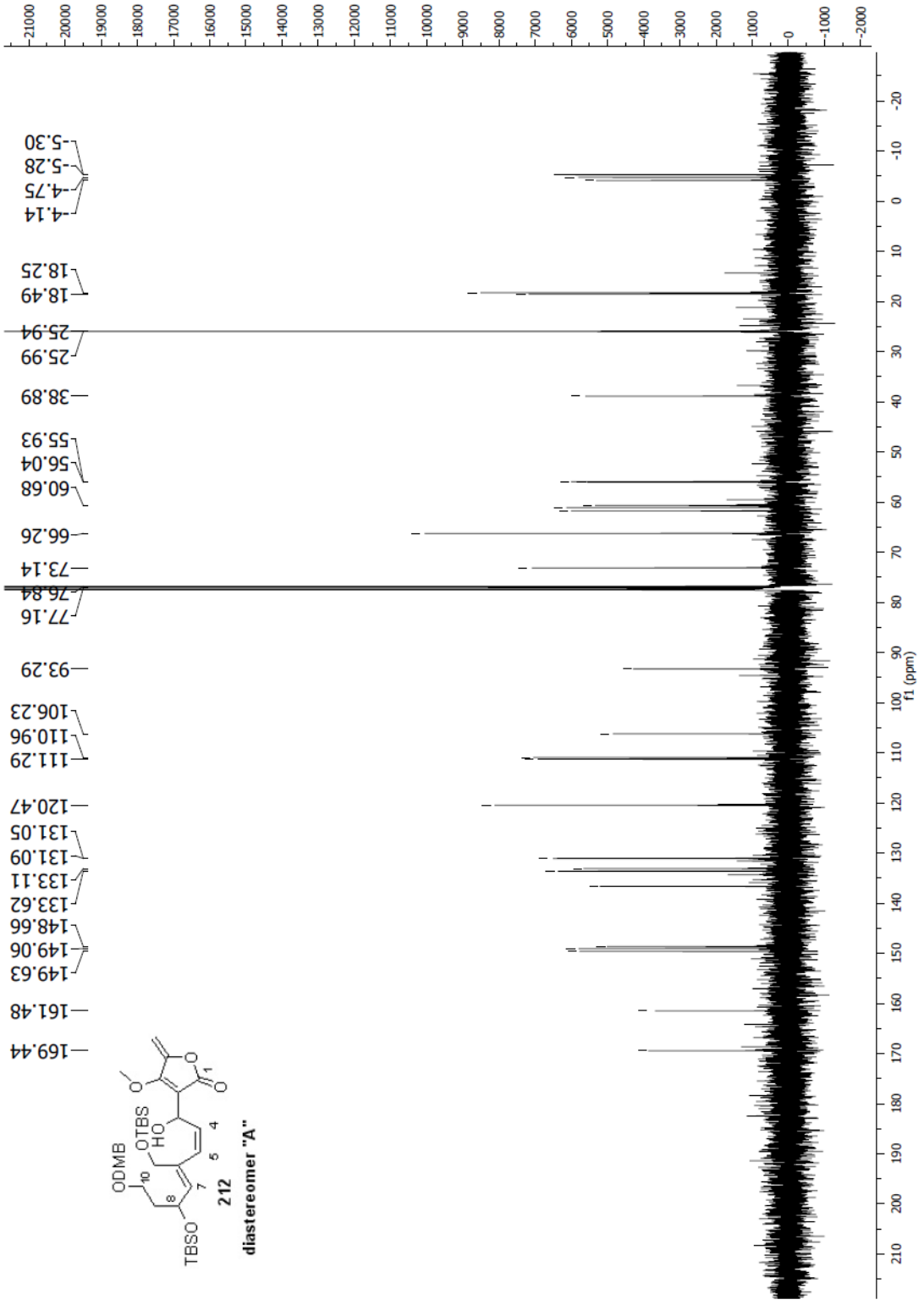

Spectrum 2.90 ^{13}C NMR ($CDCl_3$, 100 MHz) of compound **212a**

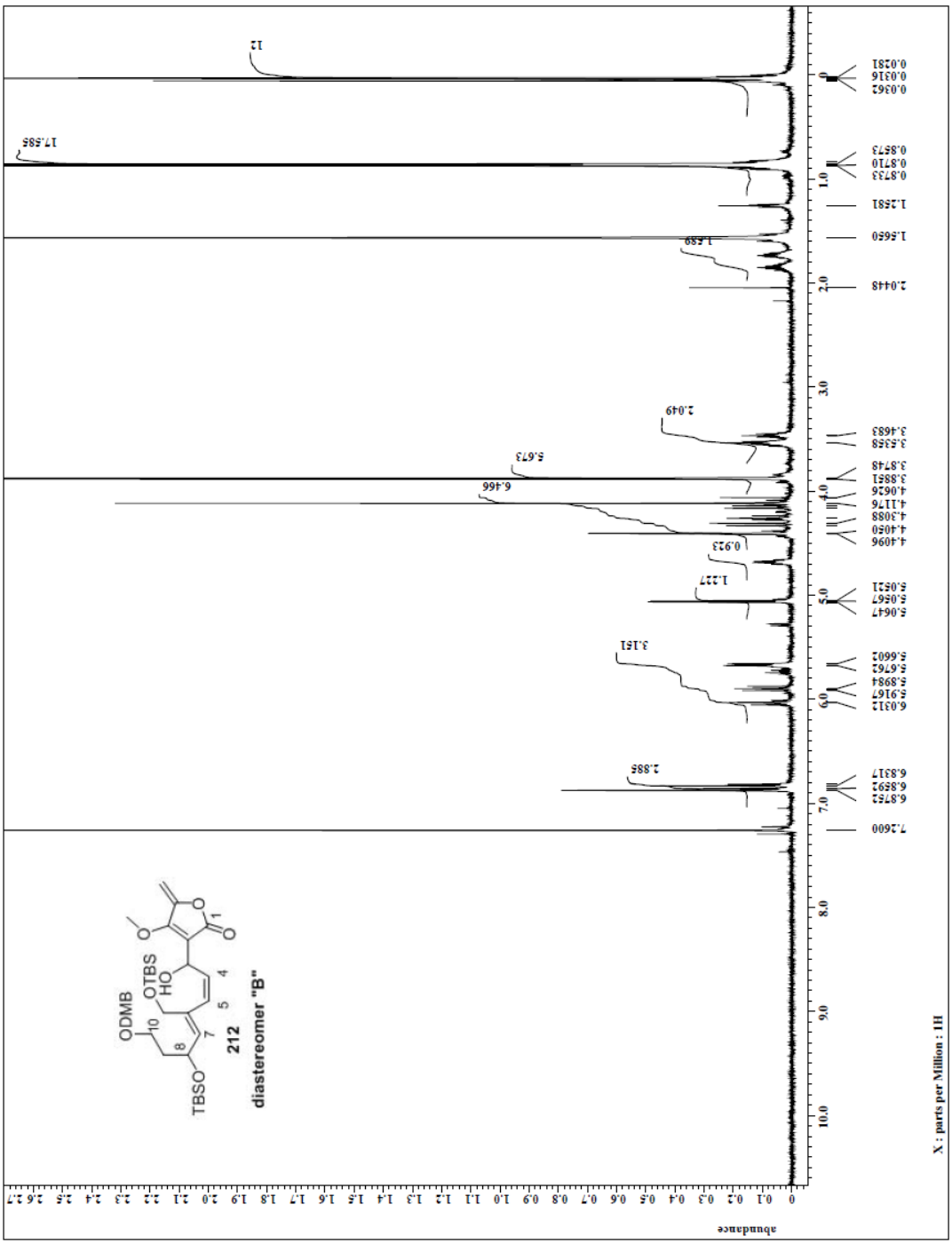

Spectrum 2.91 ^{1}H NMR ($CDCl_3$, 500 MHz) of compound **212b**

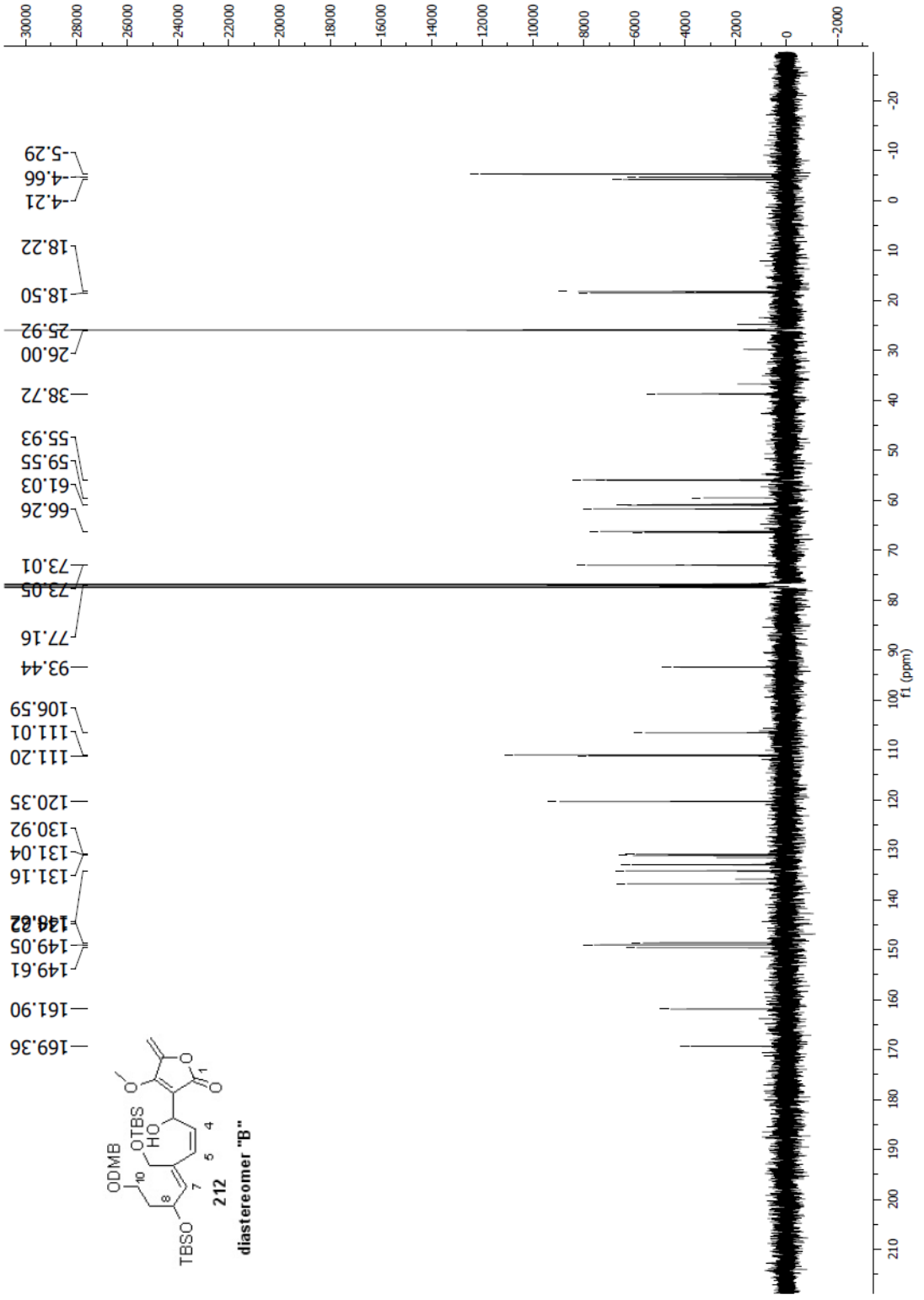

Spectrum 2.92 ^{13}C NMR ($CDCl_3$, 100 MHz) of compound **212b**

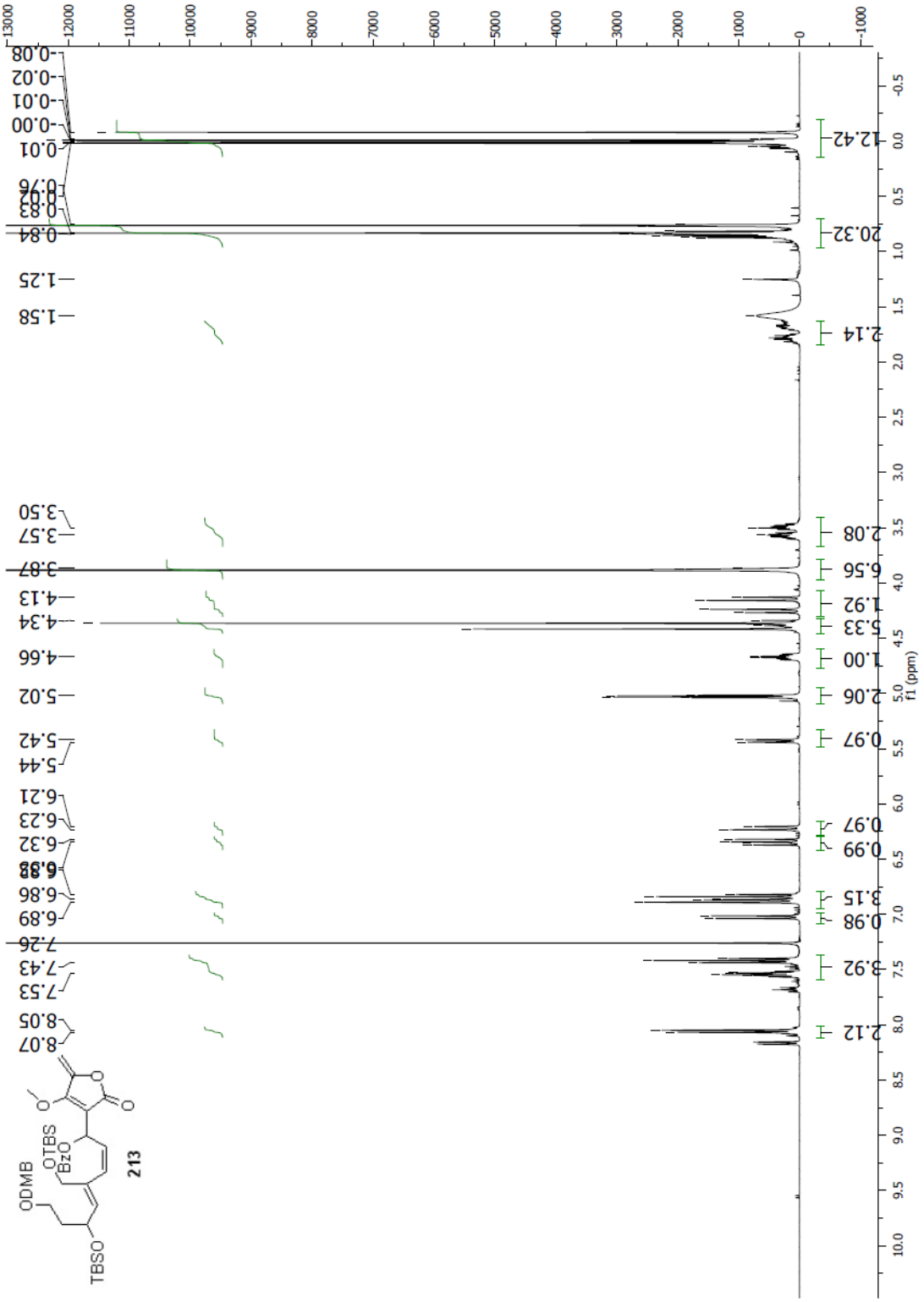

Spectrum 2.93 ^{1}H NMR ($CDCl_3$, 400 MHz) of compound **213**

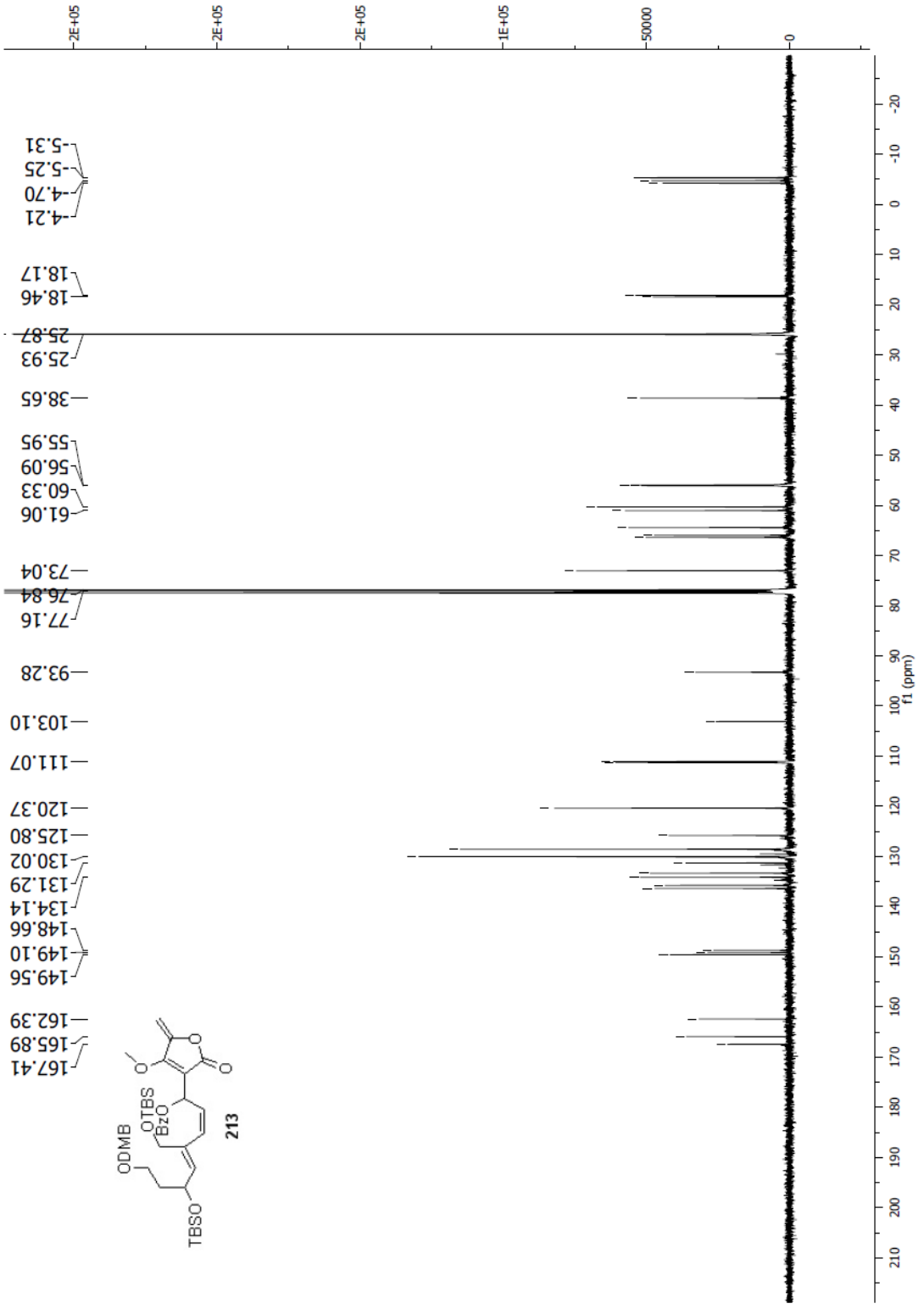

Spectrum 2.94 ^{13}C NMR ($CDCl_3$, 100 MHz) of compound **213**

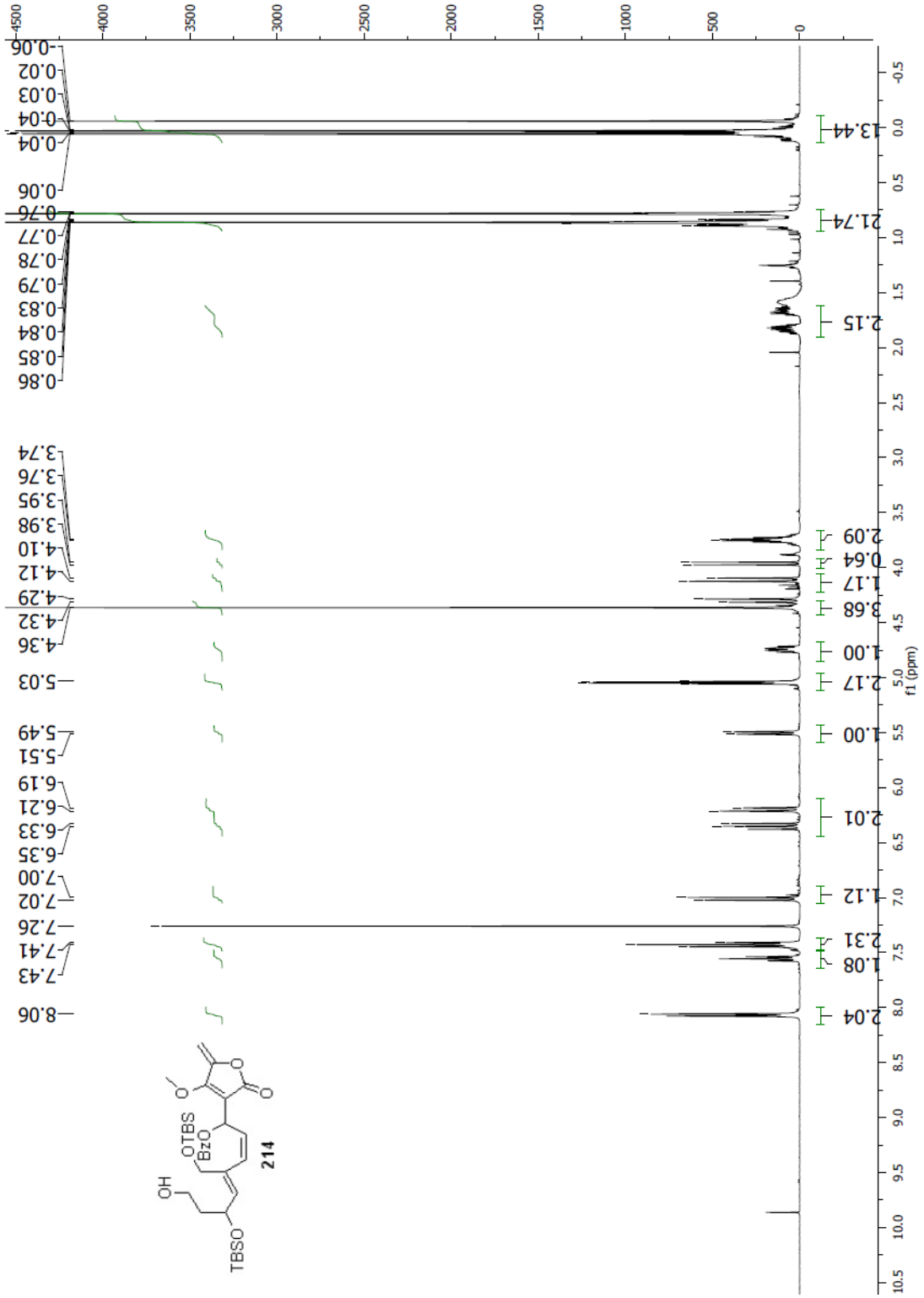

Spectrum 2.95 ^{1}H NMR ($CDCl_3$, 400 MHz) of compound **214**

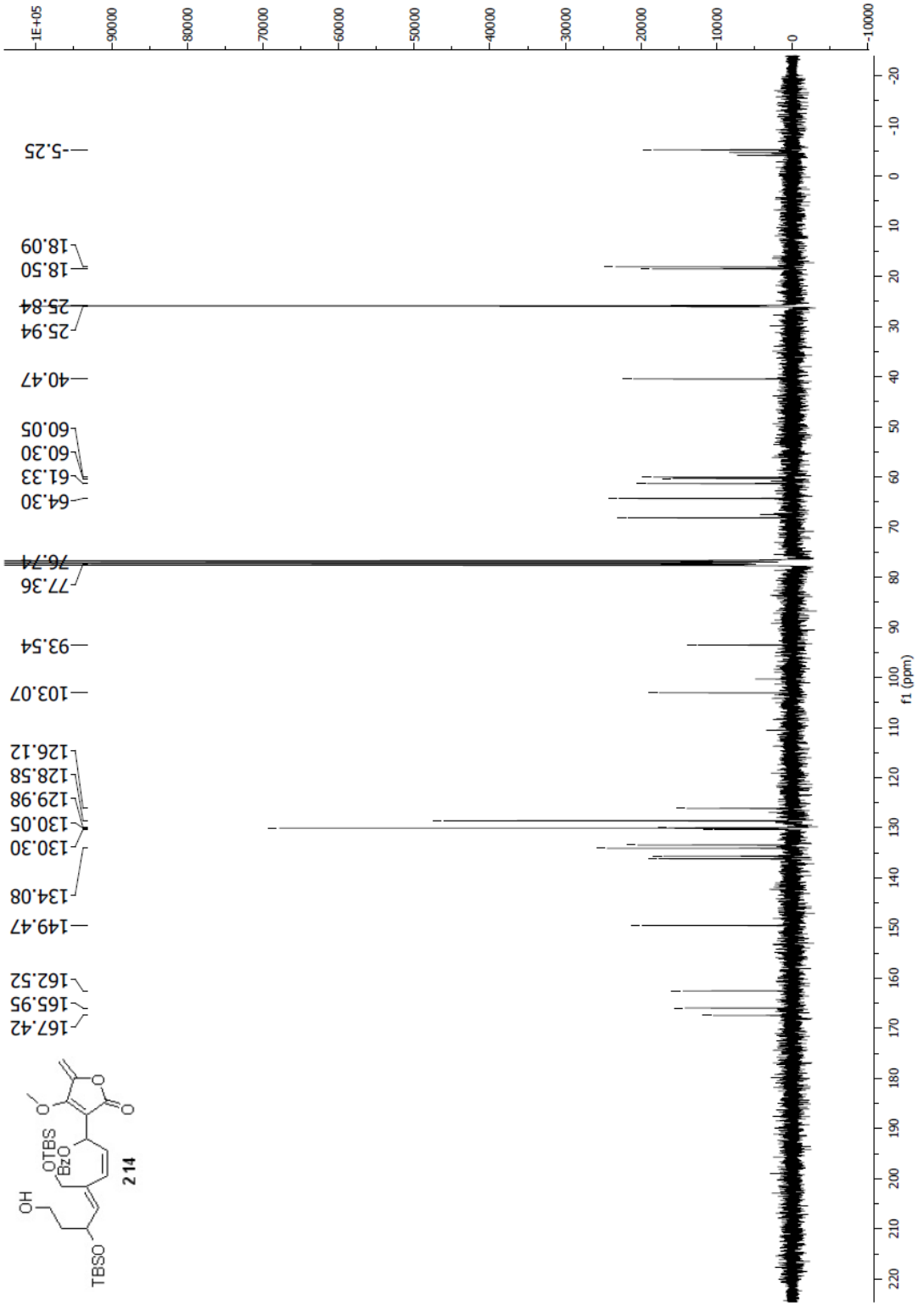

Spectrum 2.96 ^{13}C NMR ($CDCl_3$, 75 MHz) of compound **214**

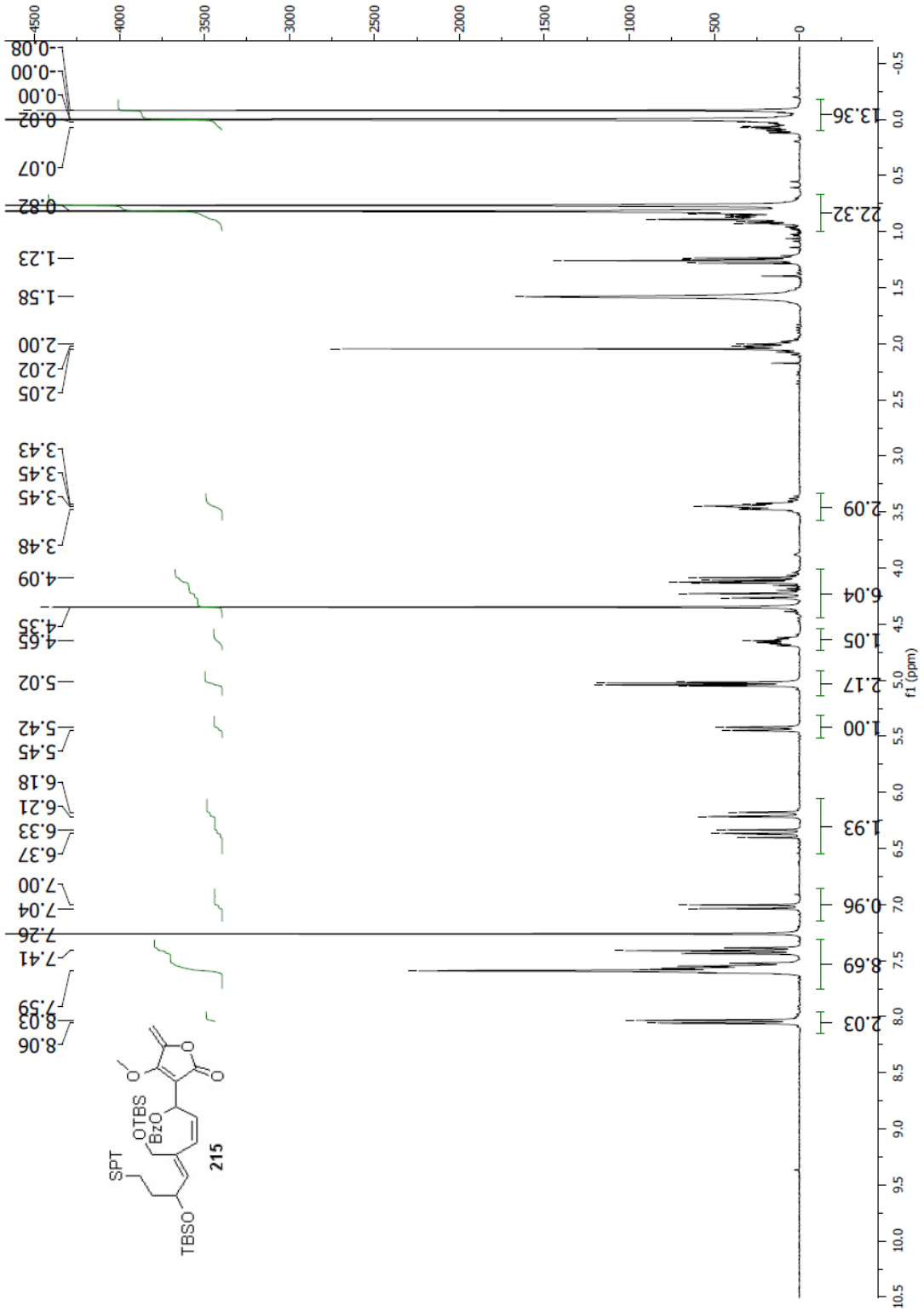

Spectrum 2.97 ^{1}H NMR ($CDCl_3$, 300 MHz) of compound **215**

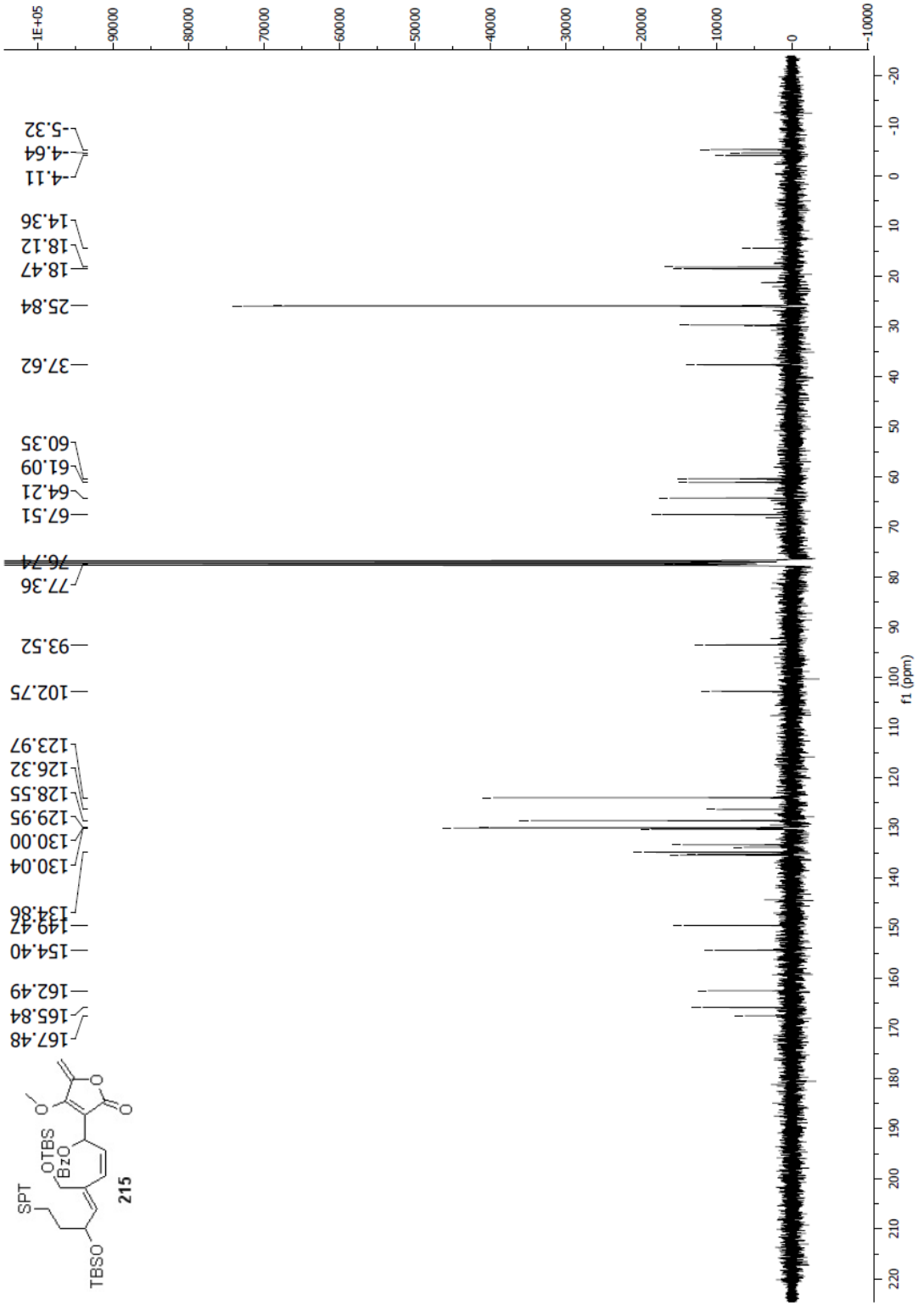

Spectrum 2.98 ^{13}C NMR ($CDCl_3$, 75 MHz) of compound **215**

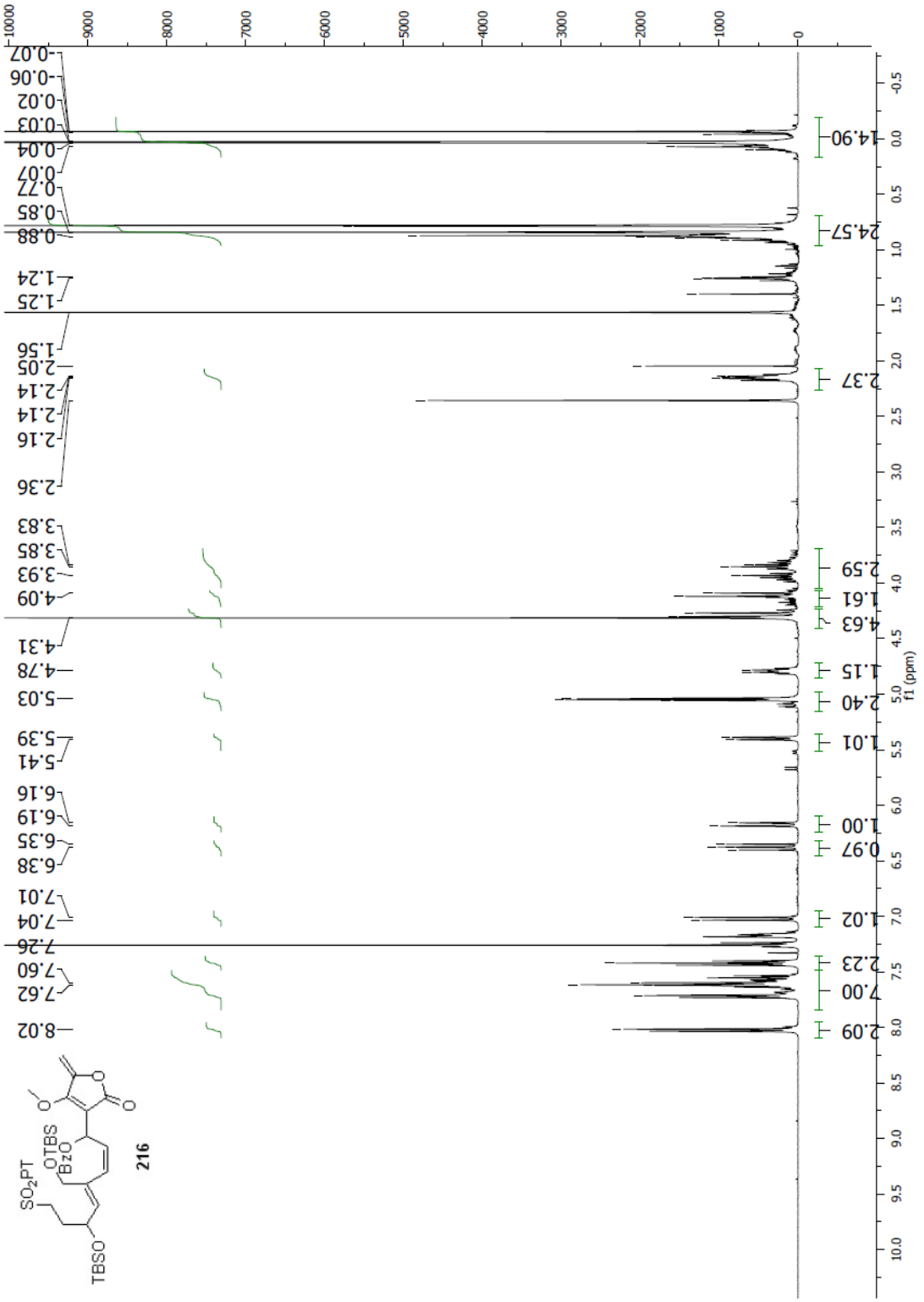

Spectrum 2.99 ^{1}H NMR ($CDCl_3$, 400 MHz) of compound **216**

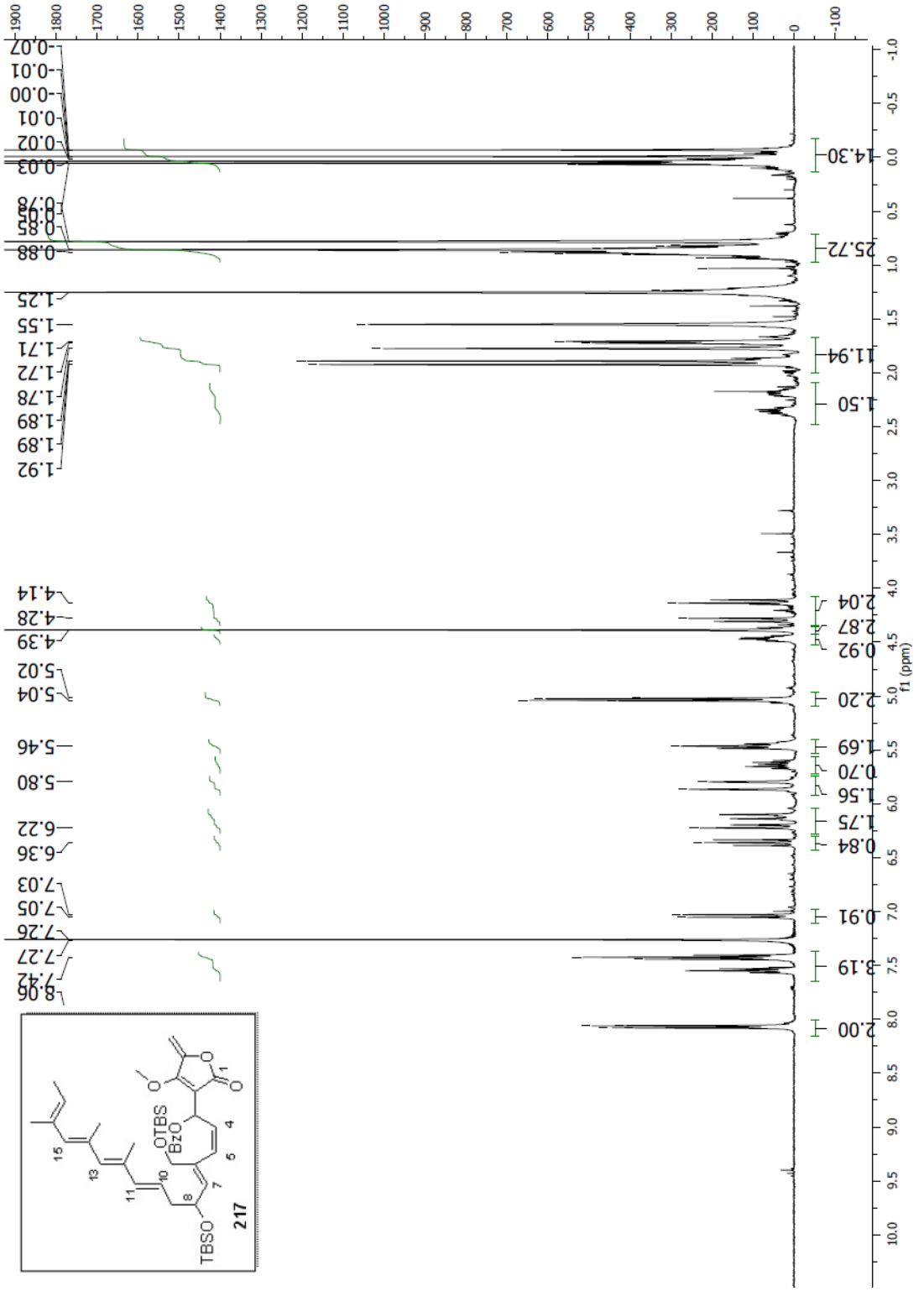

Spectrum 2.100 ^{1}H NMR ($CDCl_3$, 400 MHz) of compound **217**

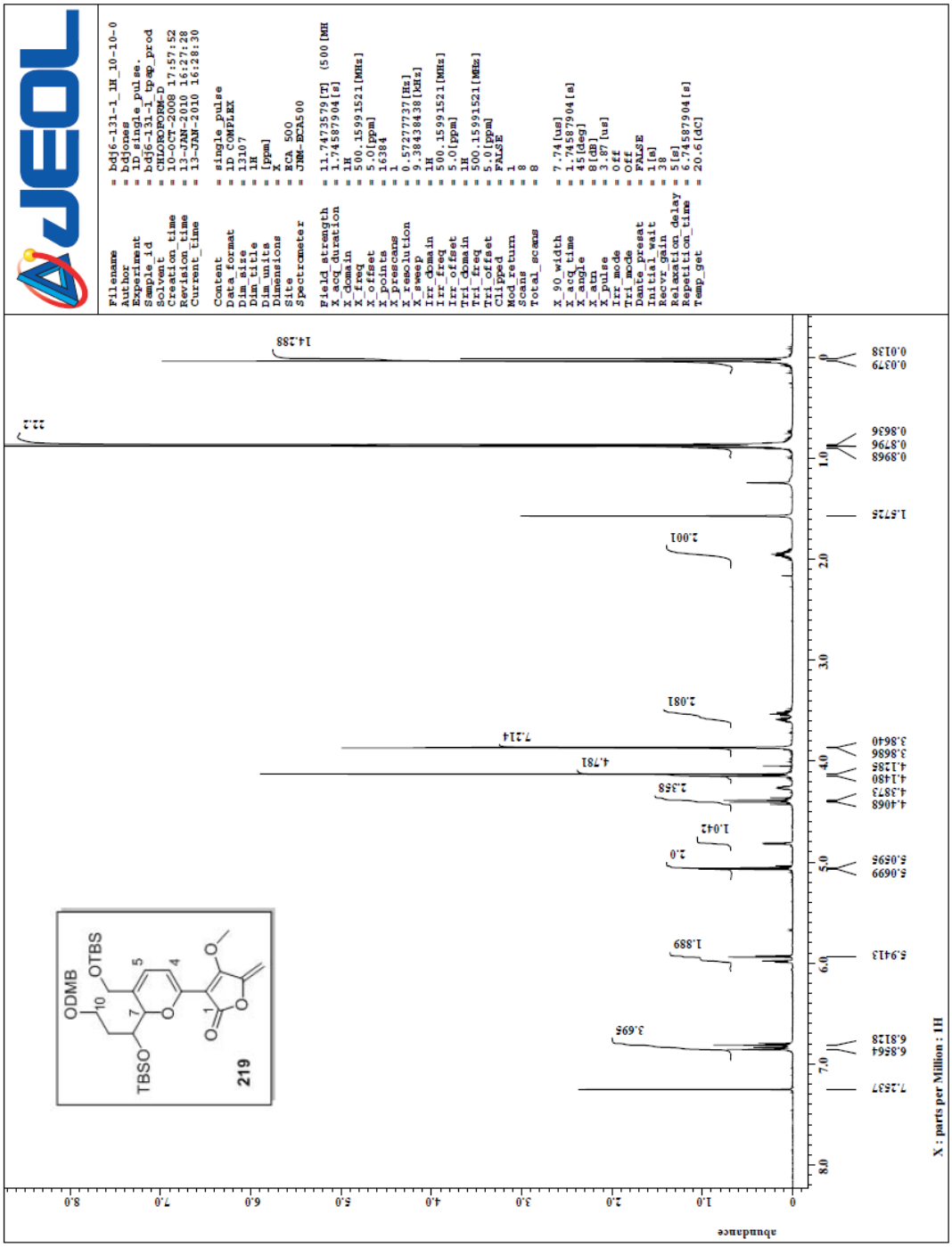

Spectrum 2.101 ^{1}H NMR ($CDCl_3$, 500 MHz) of compound **219**

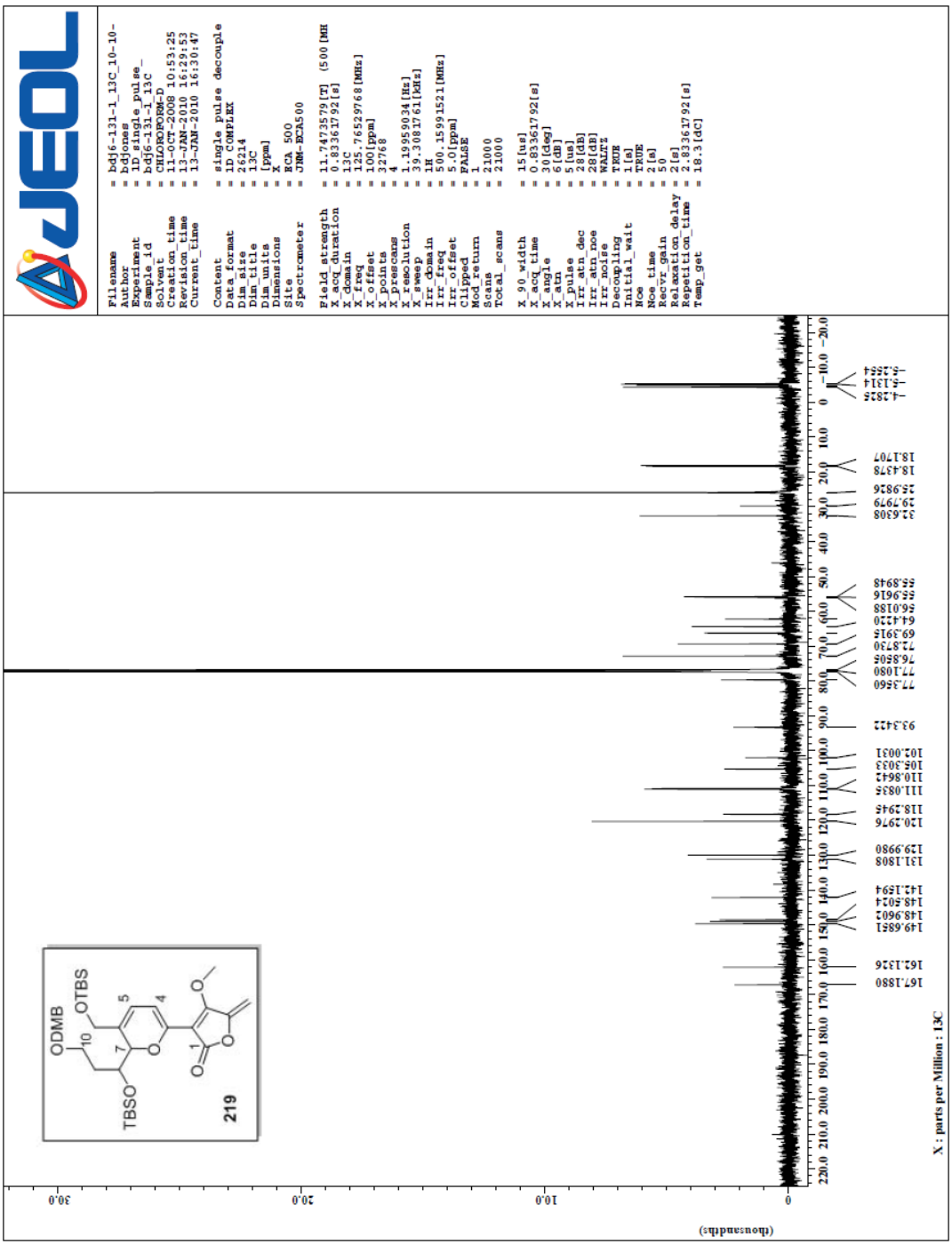

Spectrum 2.102 ^{13}C NMR ($CDCl_3$, 125 MHz) of compound **219**

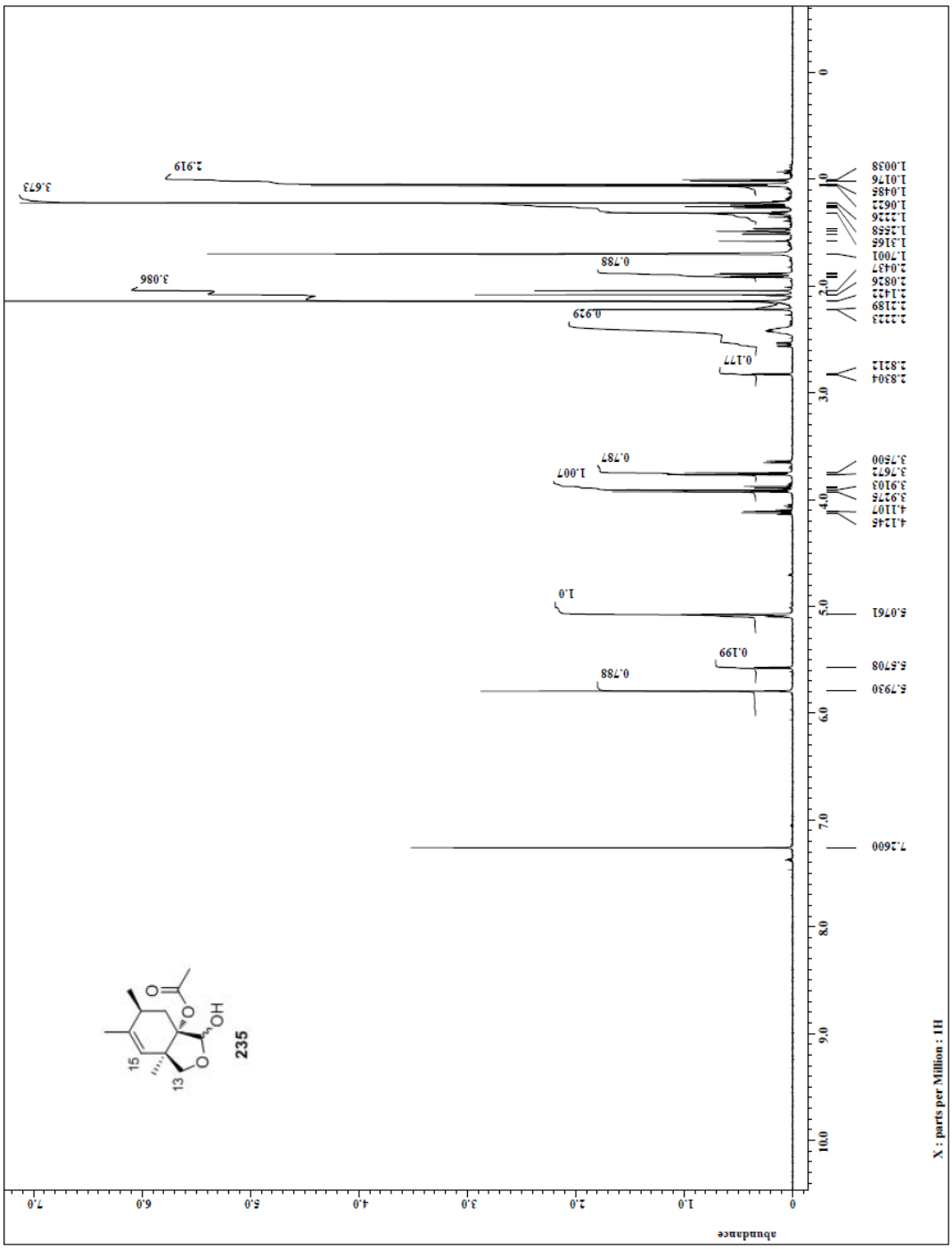

Spectrum 2.103 ^{1}H NMR ($CDCl_3$, 500 MHz) of compound **235**

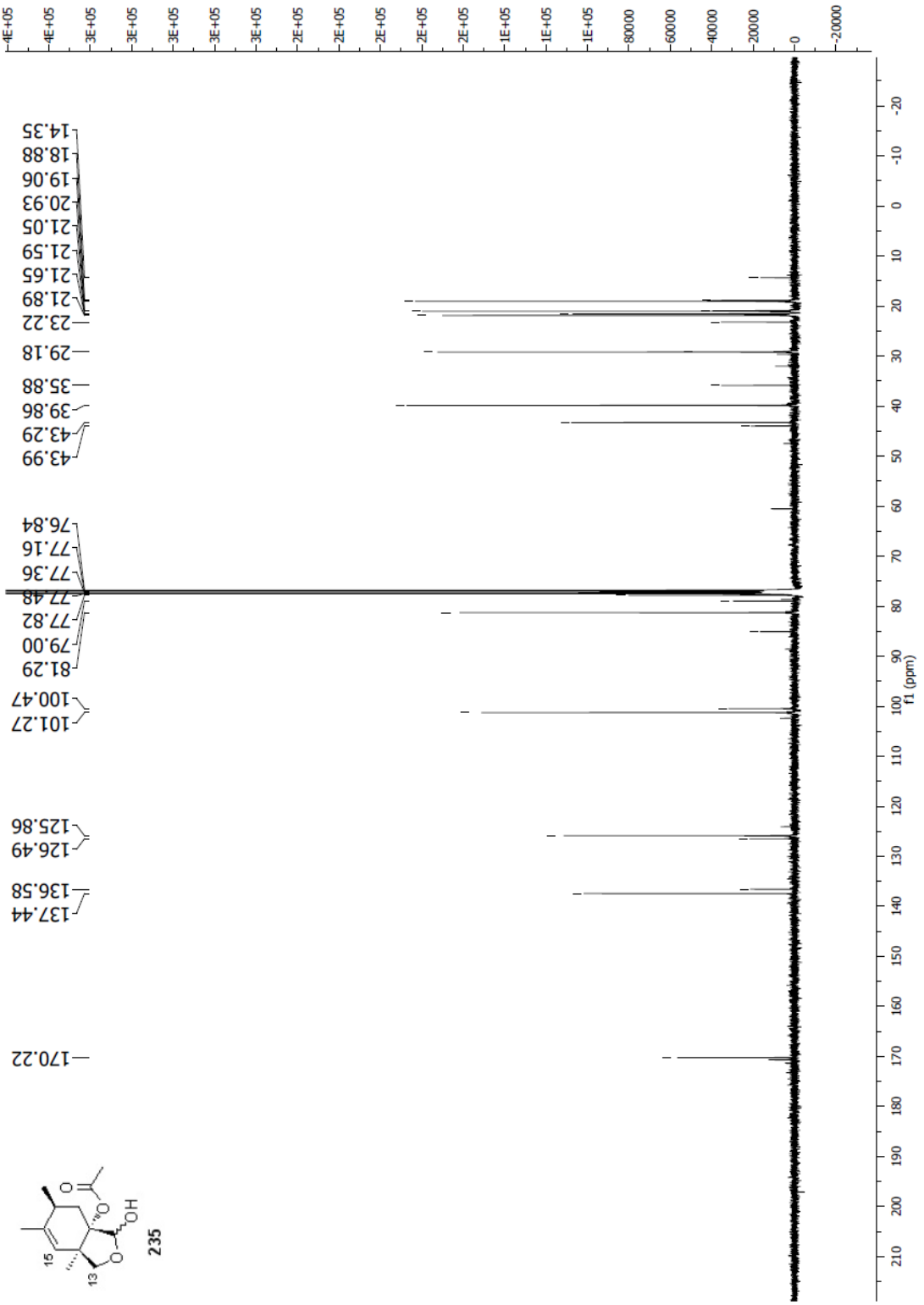

Spectrum 2.104 ^{13}C NMR ($CDCl_3$, 100 MHz) of compound **235**

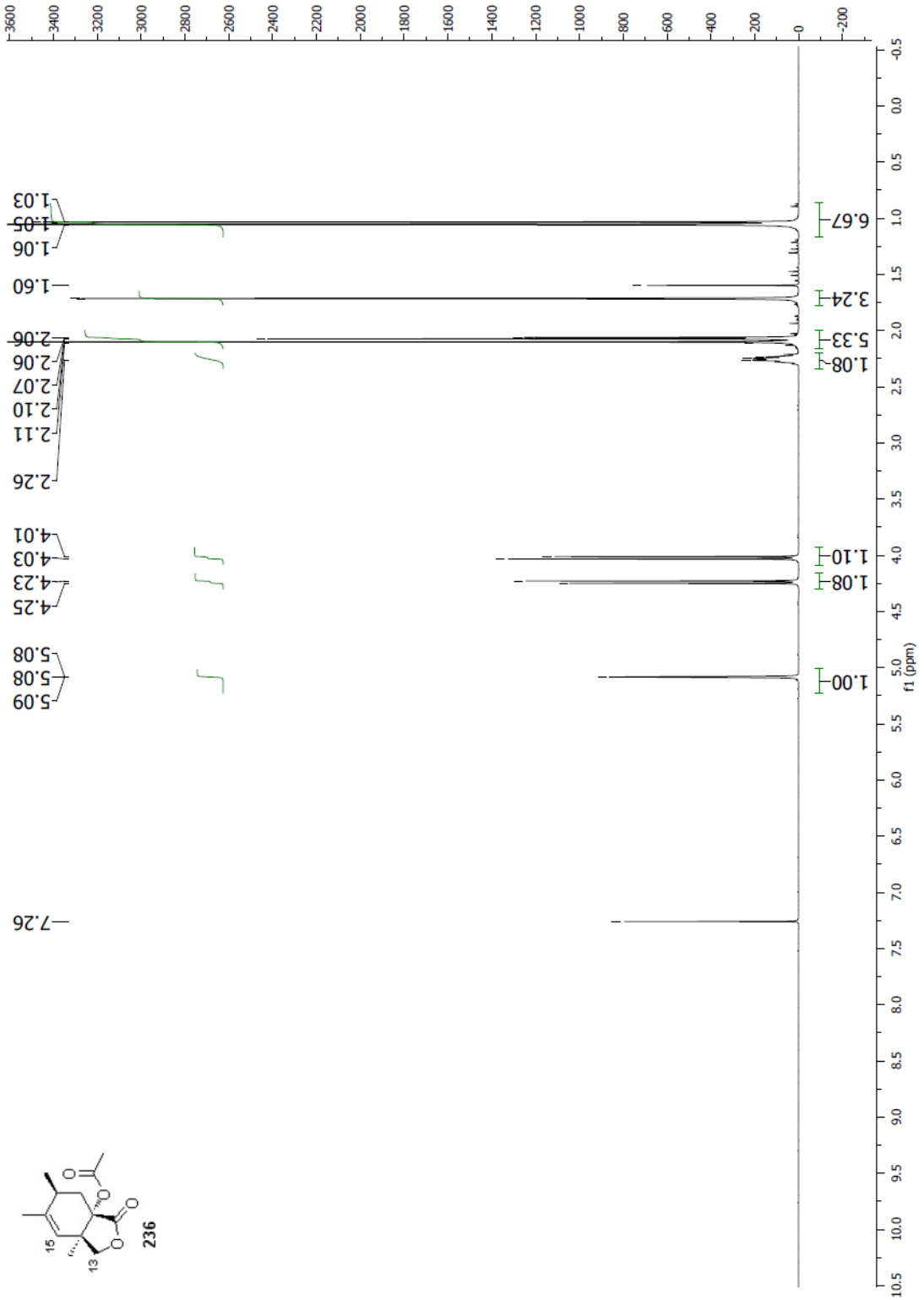

Spectrum 2.105 ^{1}H NMR ($CDCl_3$, 400 MHz) of compound **236**

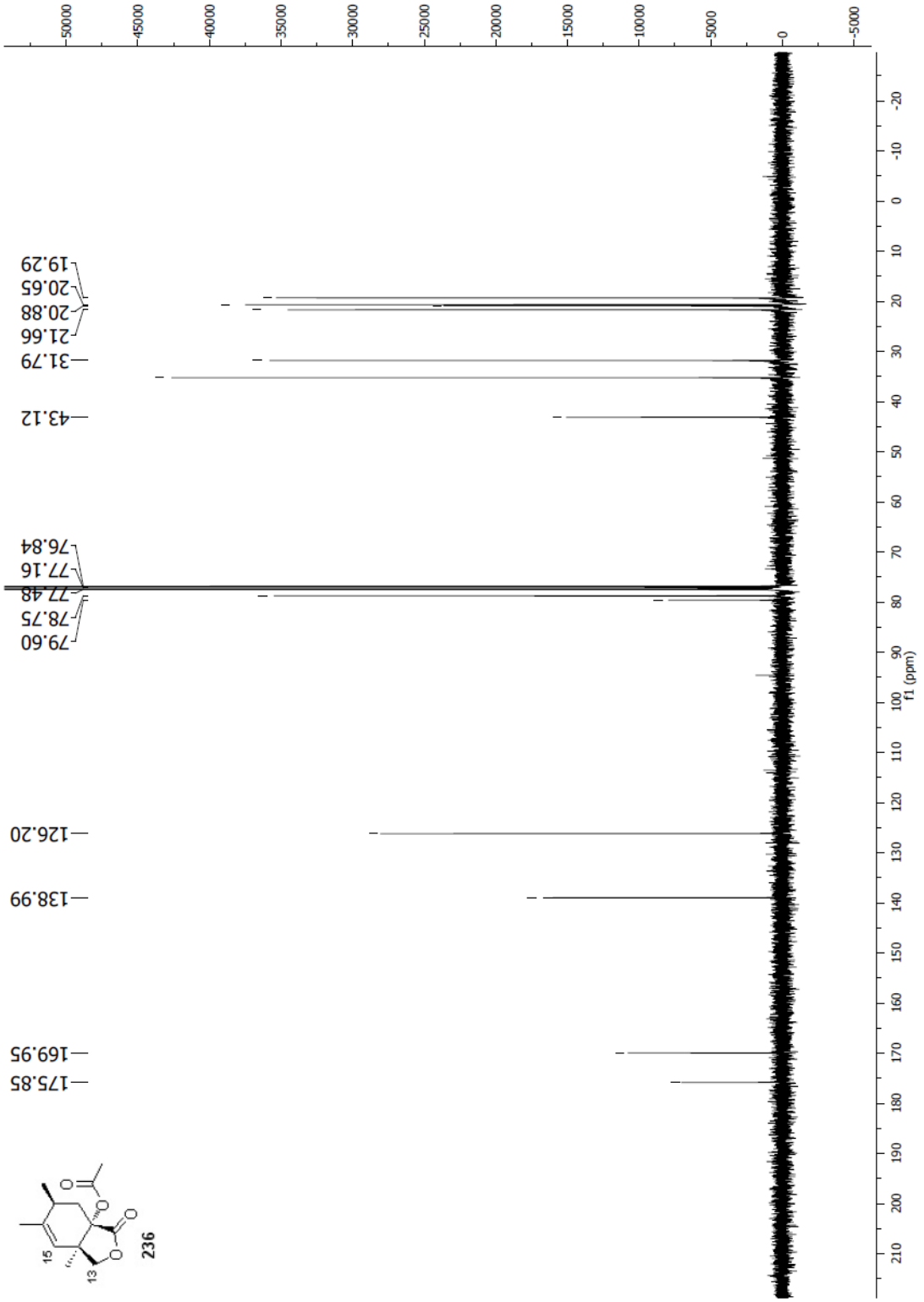

Spectrum 2.106 ^{13}C NMR ($CDCl_3$, 100 MHz) of compound **236**

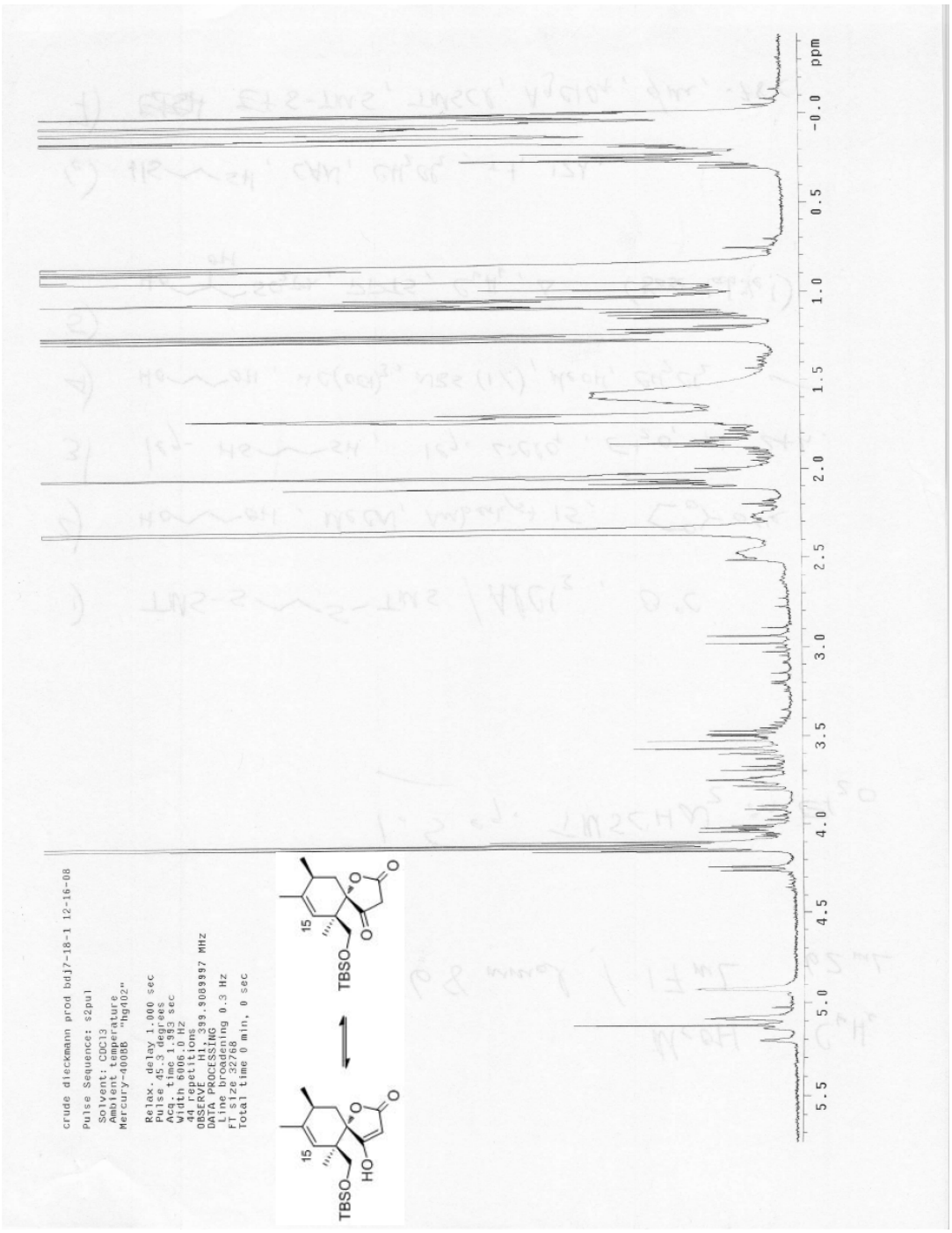

Spectrum 2.107 ^{1}H NMR ($CDCl_3$, 400 MHz) of the crude Dieckmann precursor to compound **237**

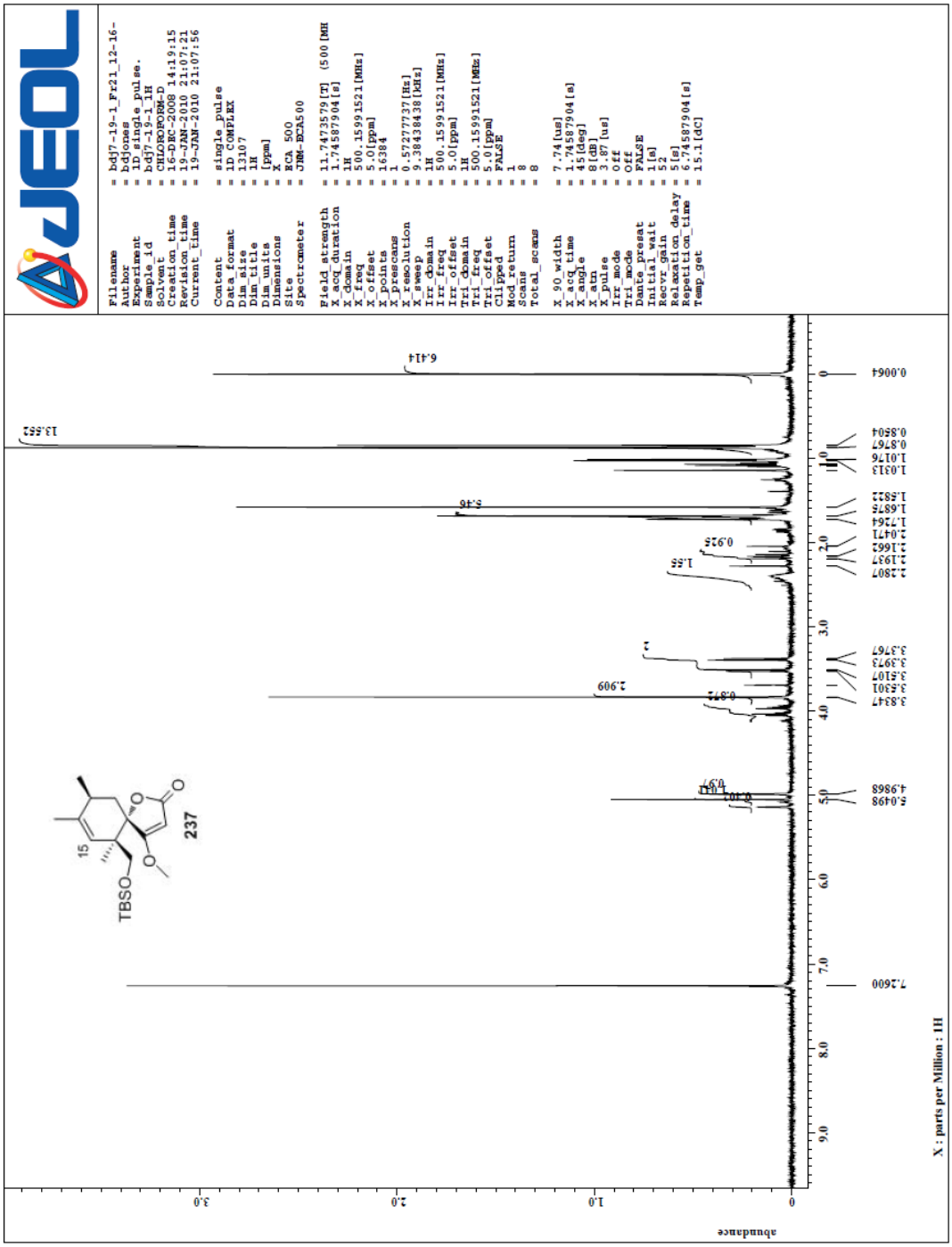

Spectrum 2.108 ^{1}H NMR ($CDCl_3$, 500 MHz) of compound **237**

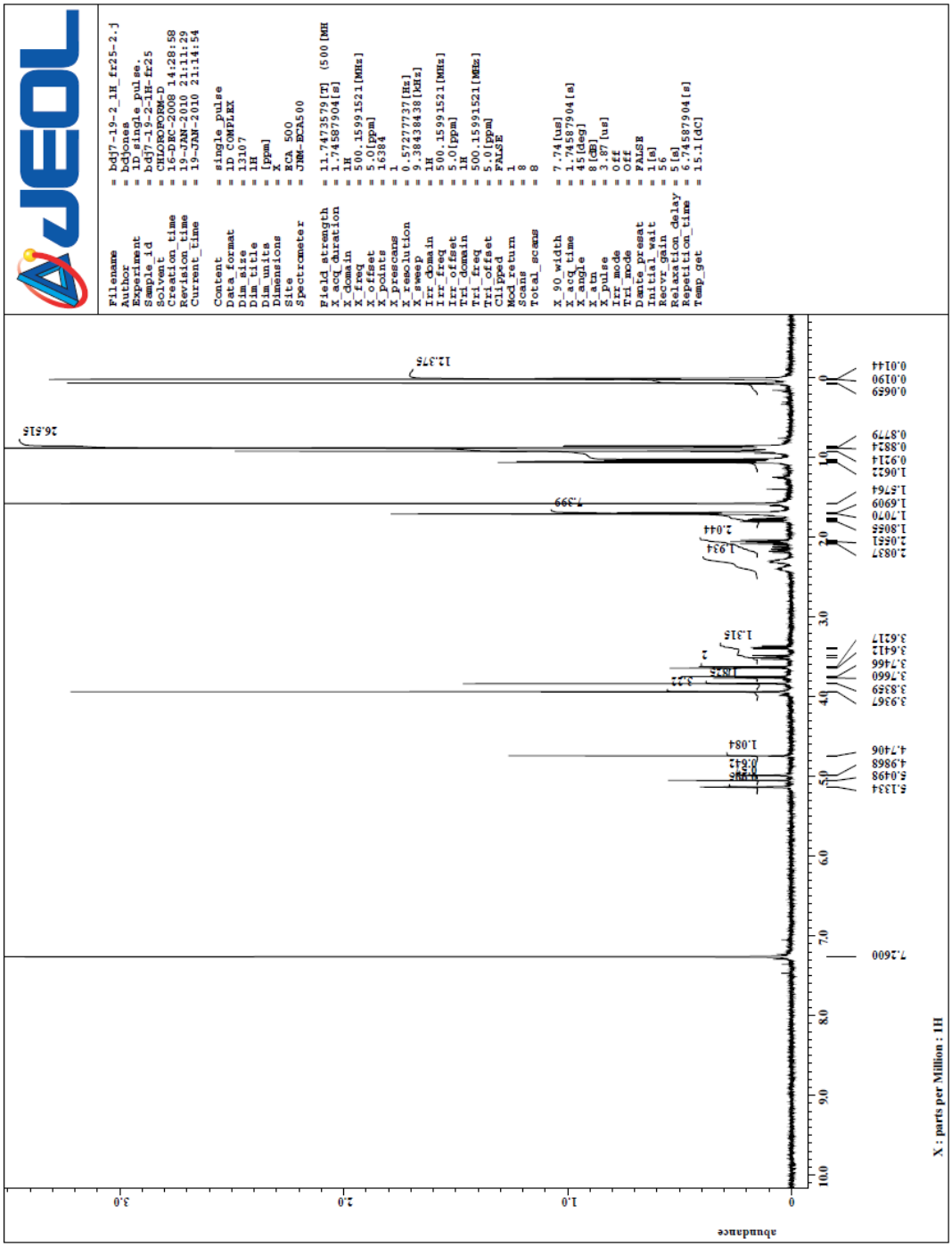

Spectrum 2.109 ^{1}H NMR ($CDCl_3$, 500 MHz) of side product obtained with **237**

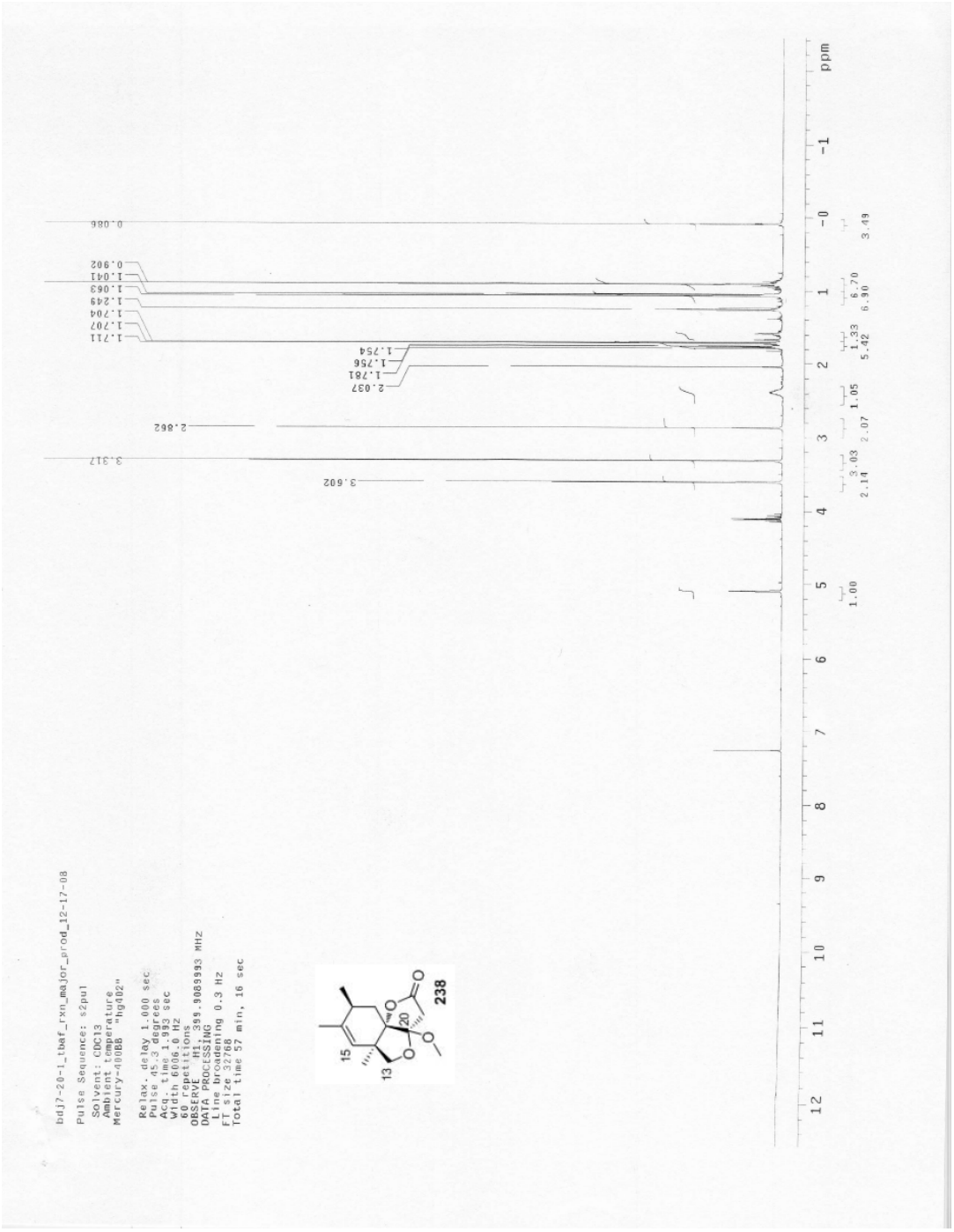

Spectrum 2.110 ^{1}H NMR ($CDCl_3$, 400 MHz) of compound **238**

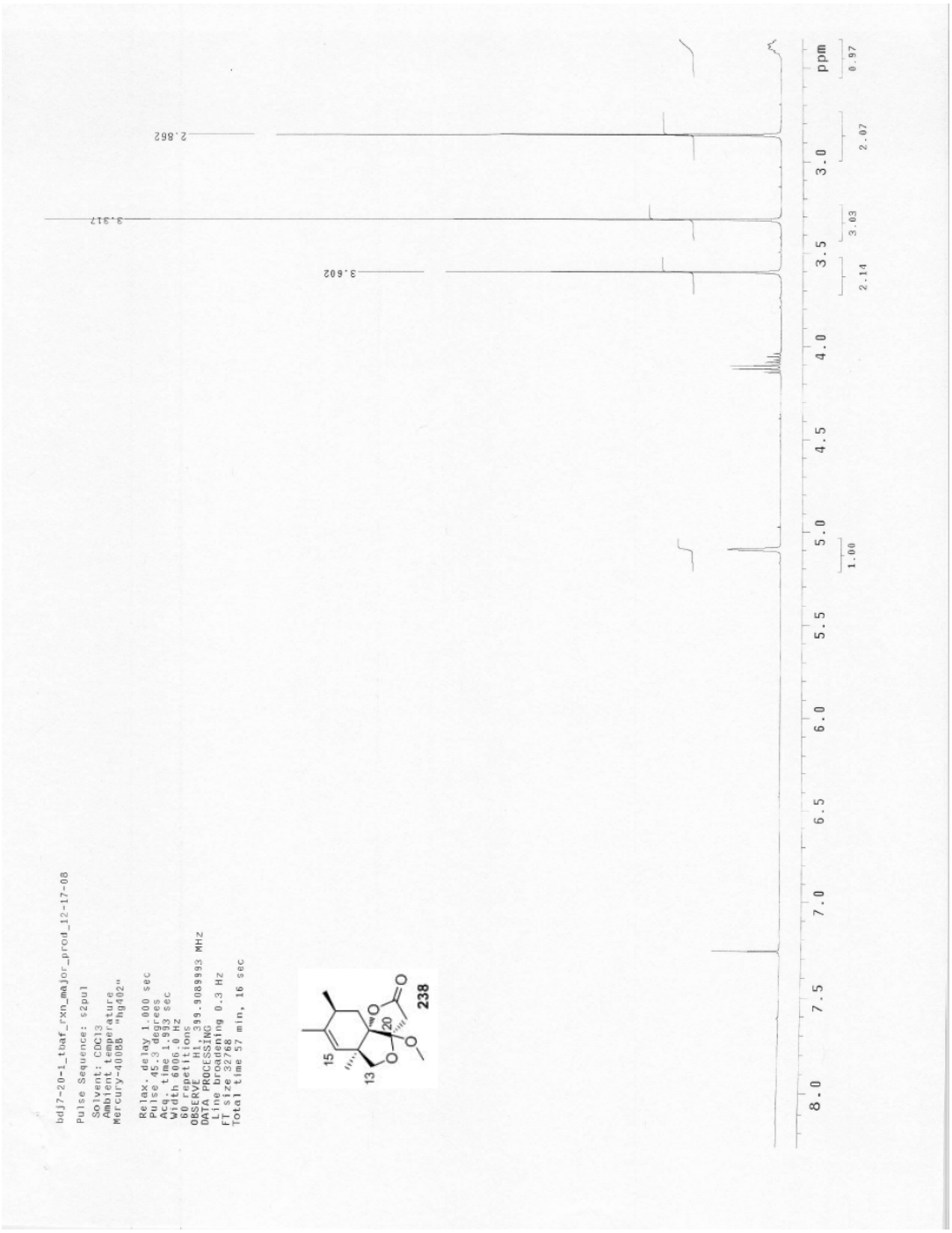

Spectrum 2.111 Expansion of Spectrum 2.110

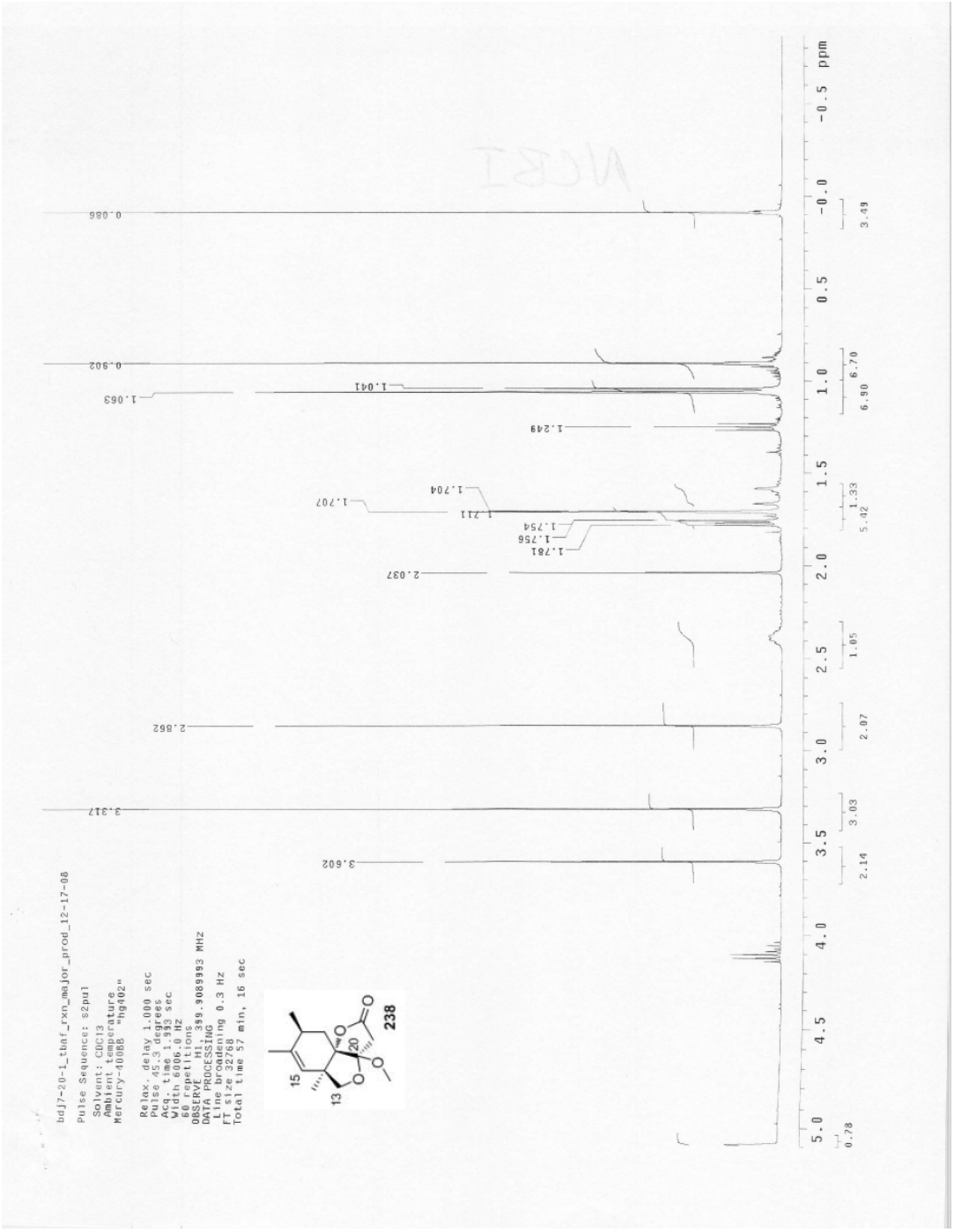

Spectrum 2.112 Expansion of Spectrum 2.110

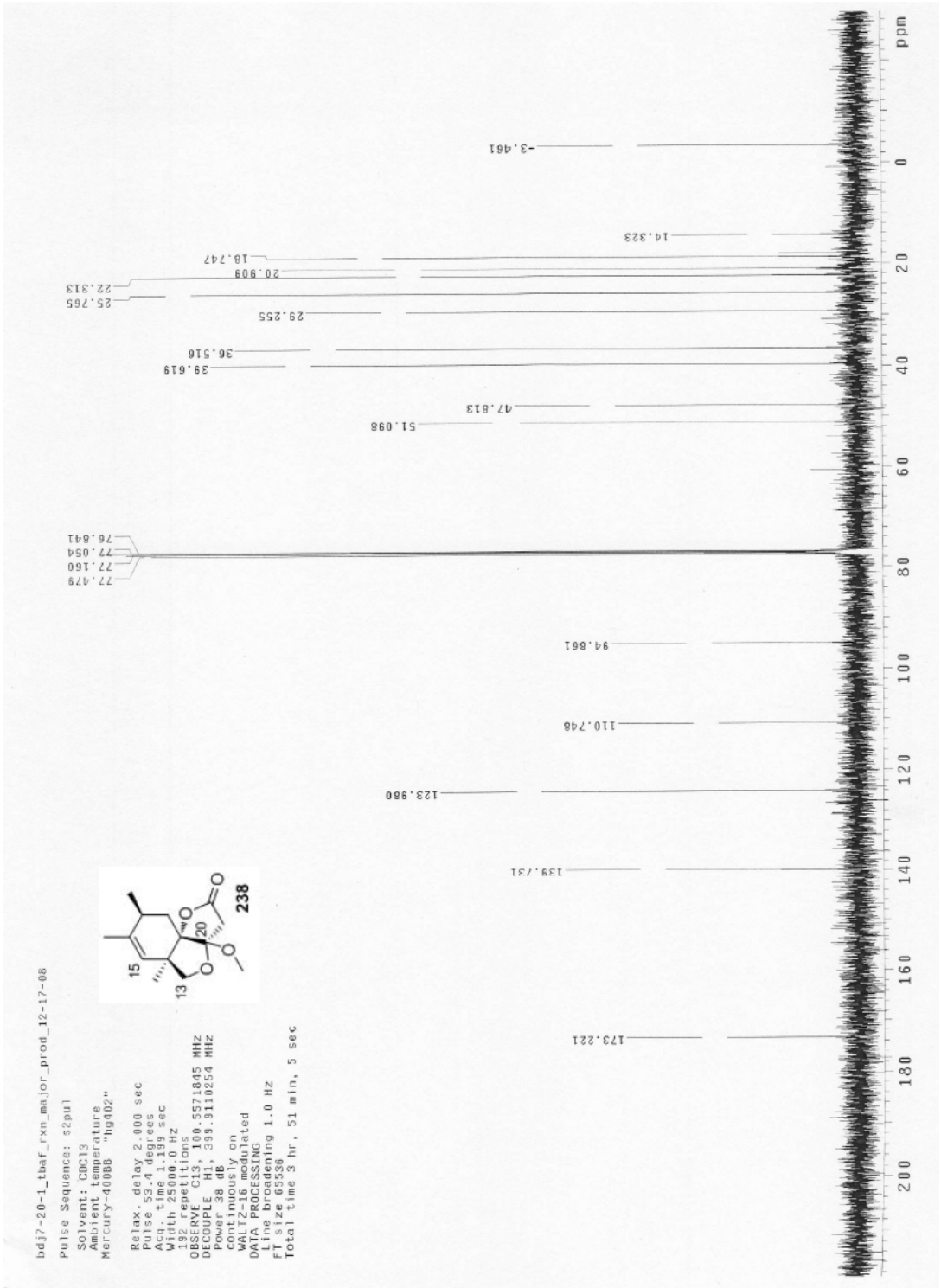

Spectrum 2.113 ^{13}C NMR ($CDCl_3$, 100 MHz) of compound **238**

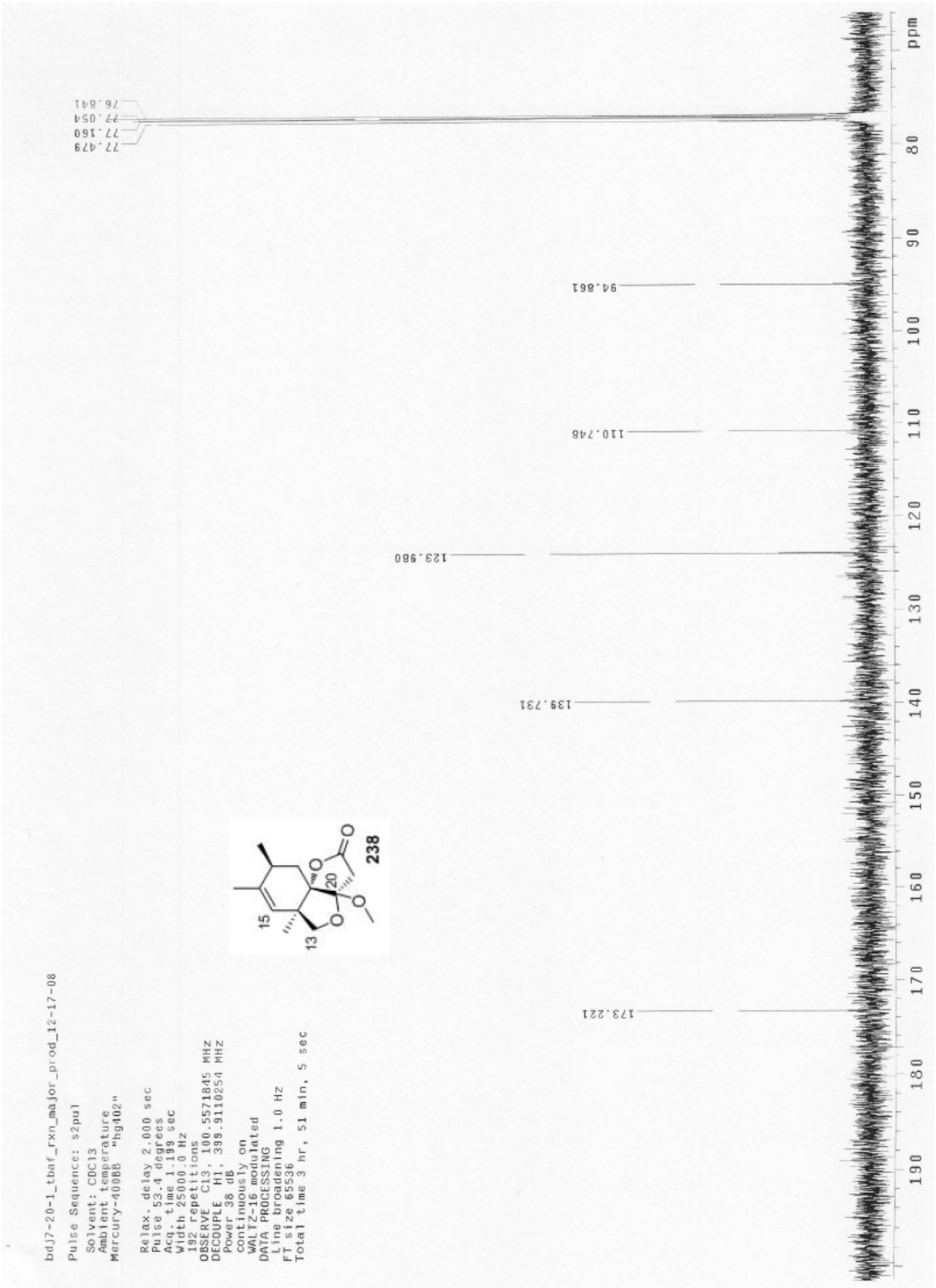

Spectrum 2.114 Expansion of Spectrum 2.113

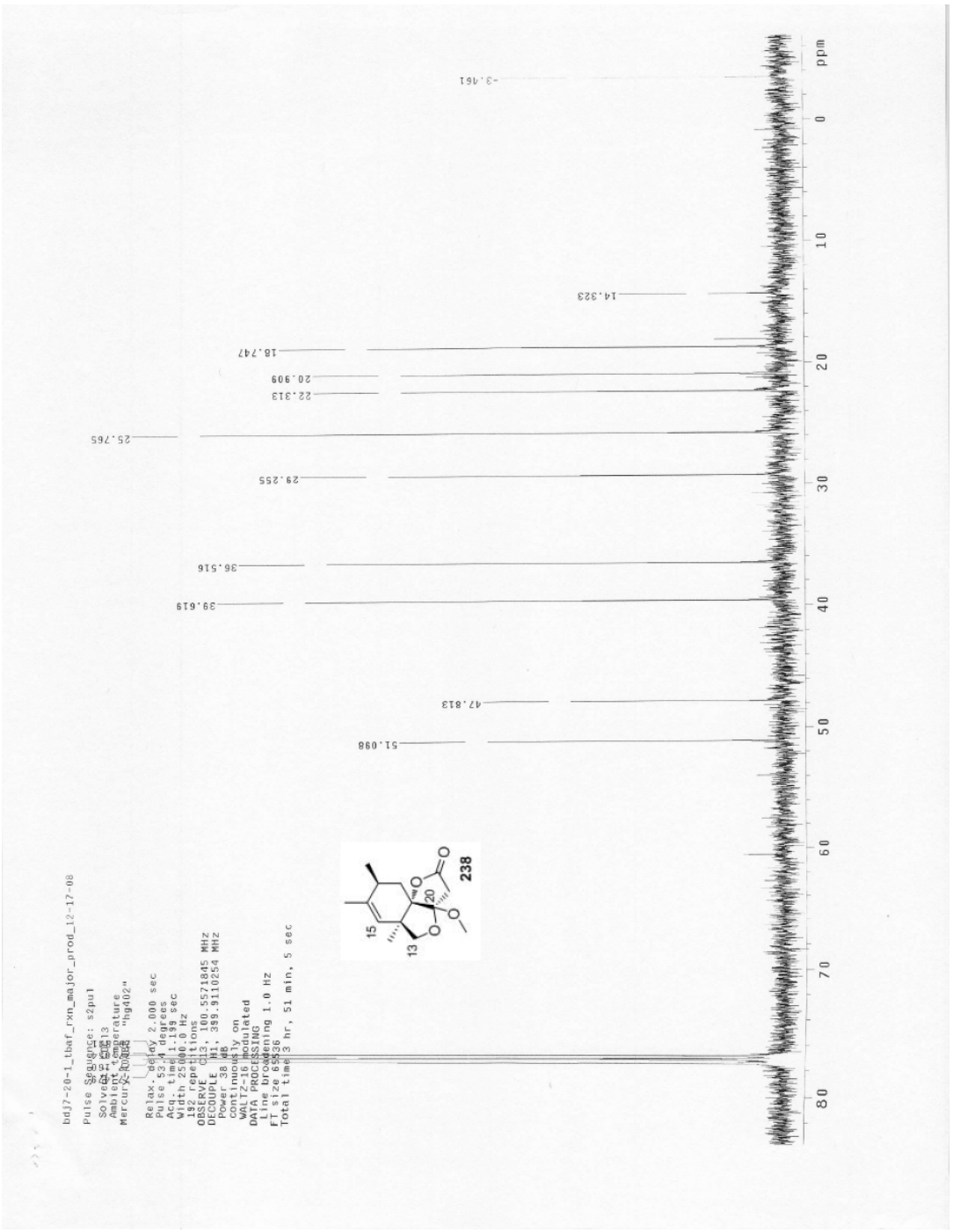

Spectrum 2.115 Expansion of Spectrum 2.113

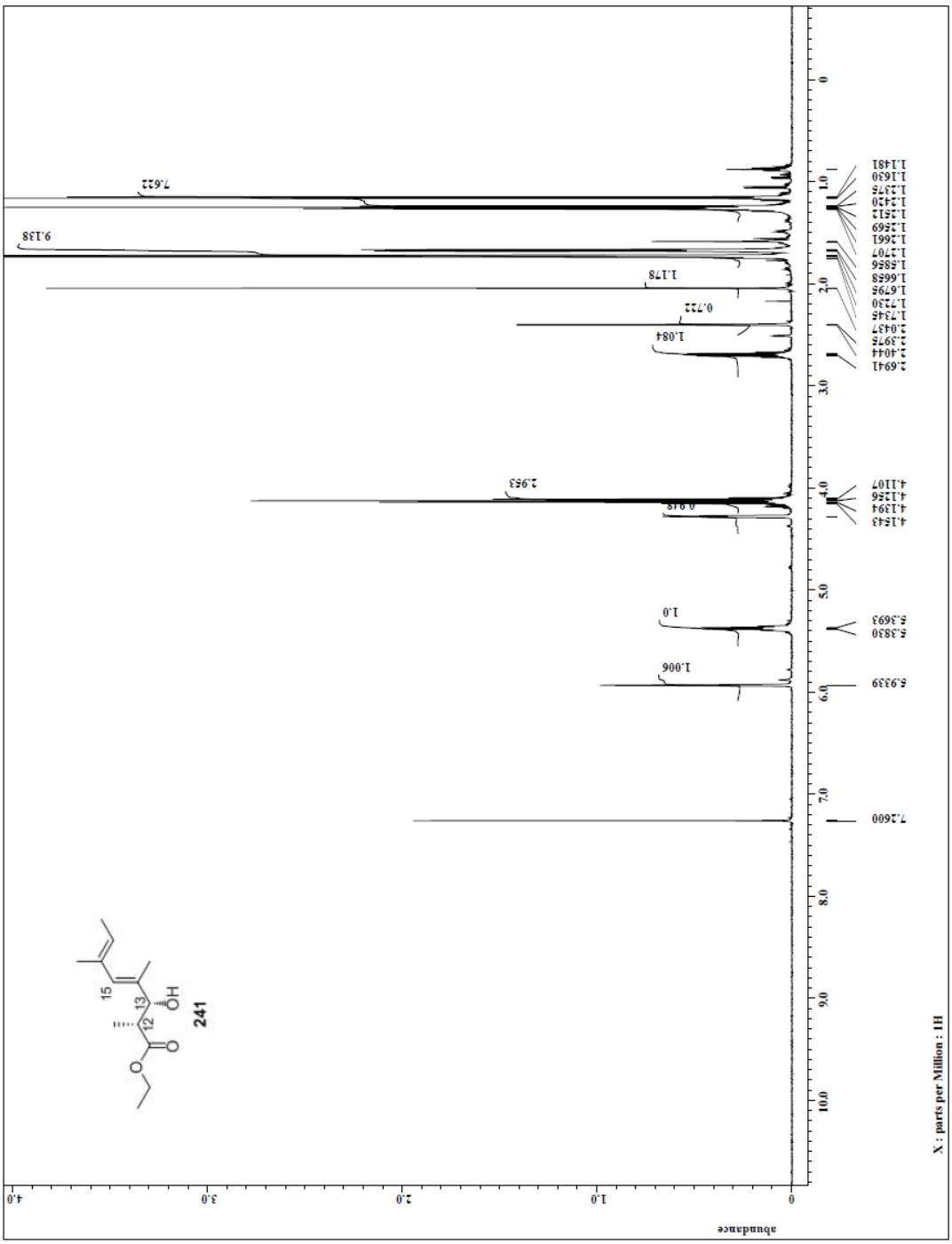

Spectrum 2.116 ^{1}H NMR ($CDCl_3$, 500 MHz) of compound **241**

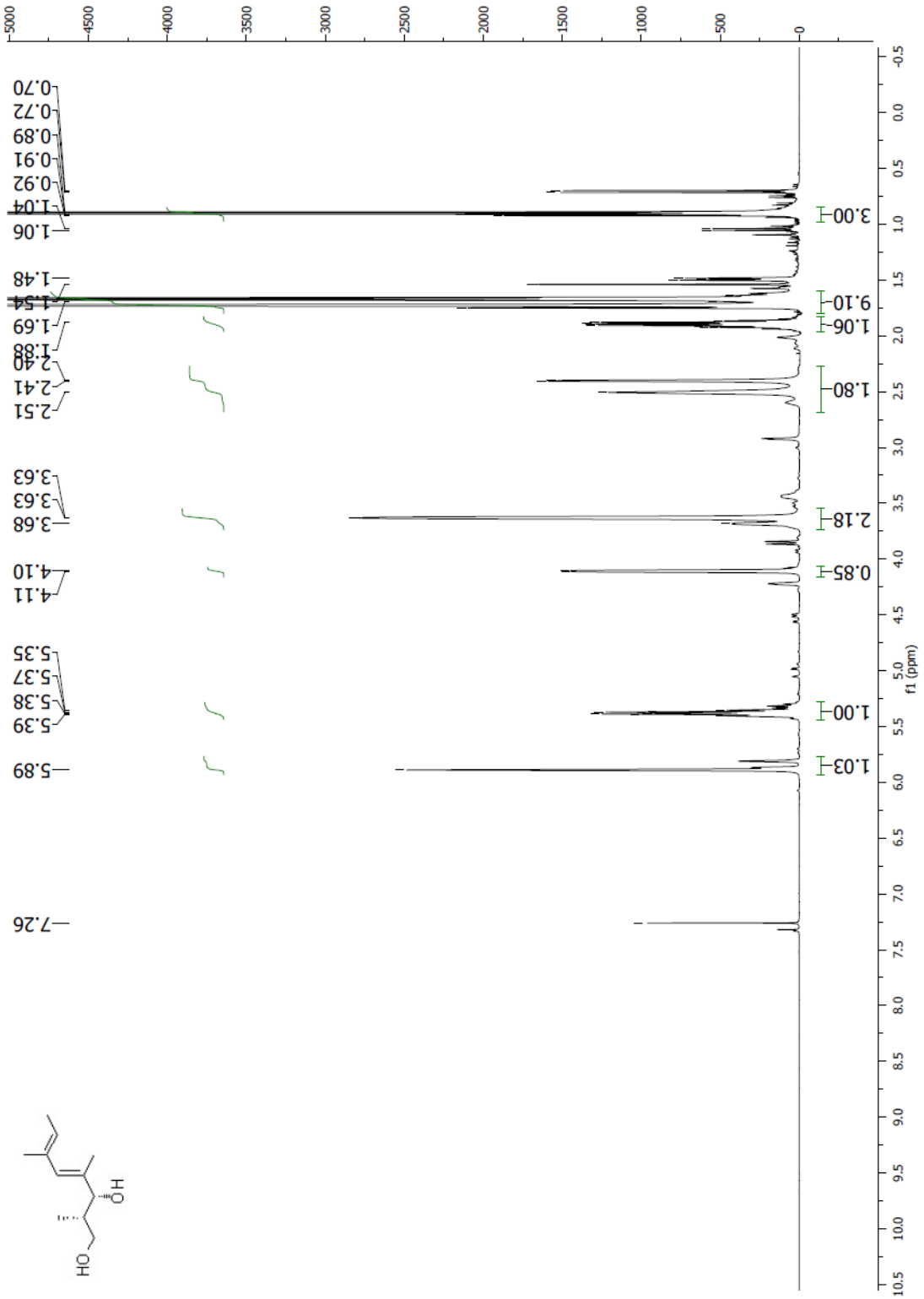

Spectrum 2.117 ^{1}H NMR ($CDCl_3$, 400 MHz) of diol precursor to **242**

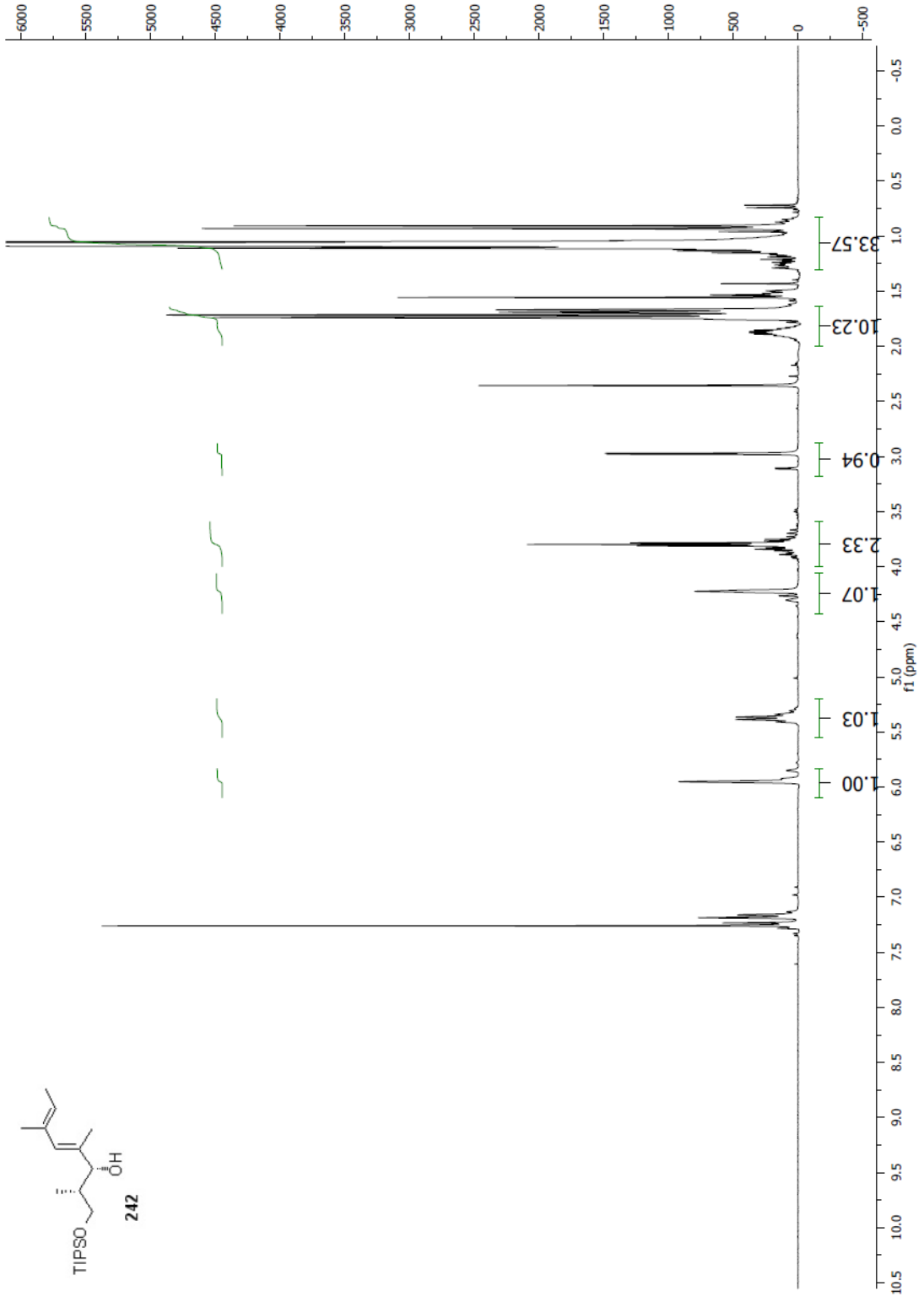

Spectrum 2.118 ^{1}H NMR ($CDCl_3$, 300 MHz) of compound **242**

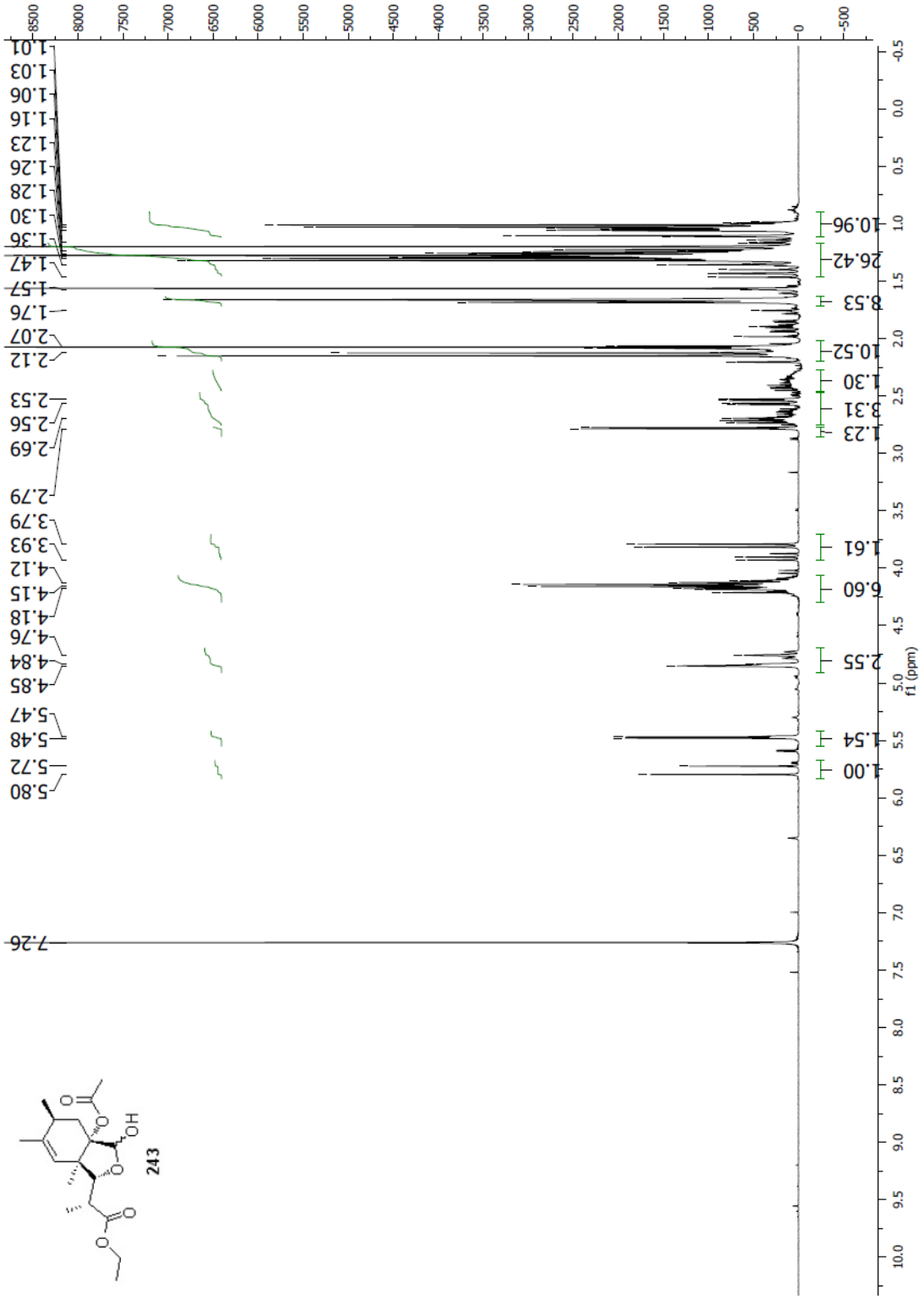

Spectrum 2.119 ^{1}H NMR ($CDCl_3$, 400 MHz) of compound **243**

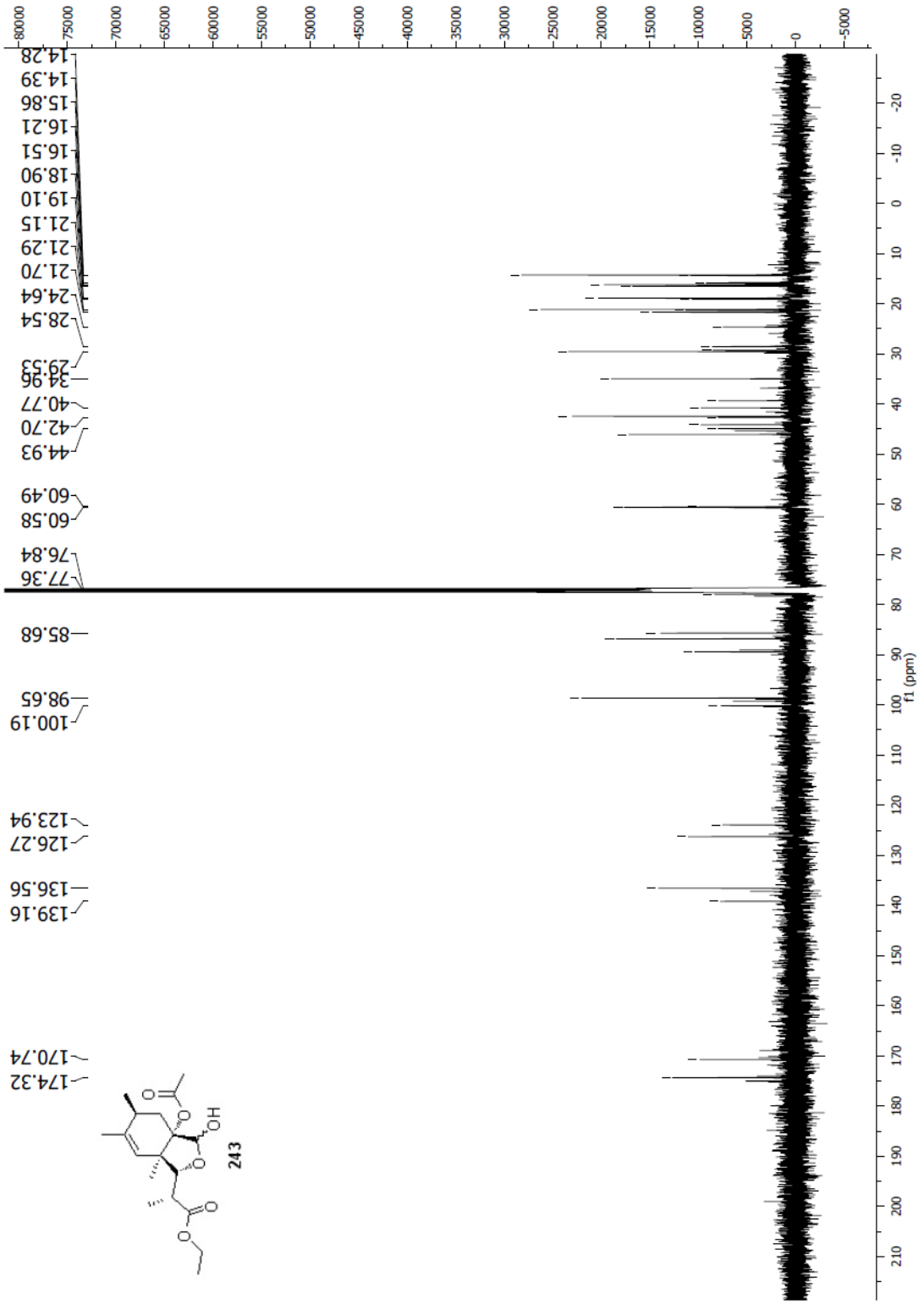

Spectrum 2.120 ^{13}C NMR ($CDCl_3$, 100 MHz) of compound **243**

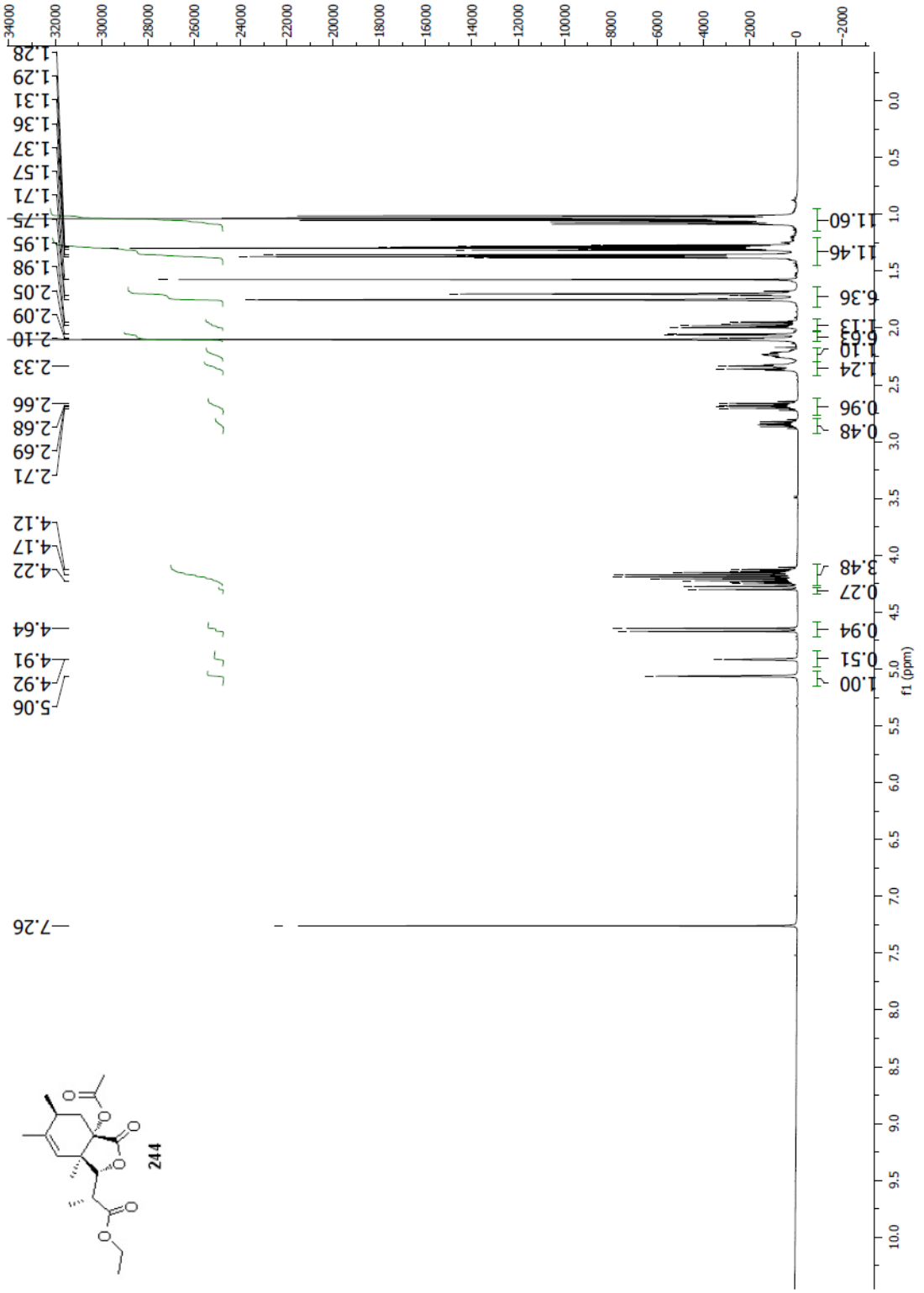

Spectrum 2.121 ^{1}H NMR ($CDCl_3$, 400 MHz) of compound **244**

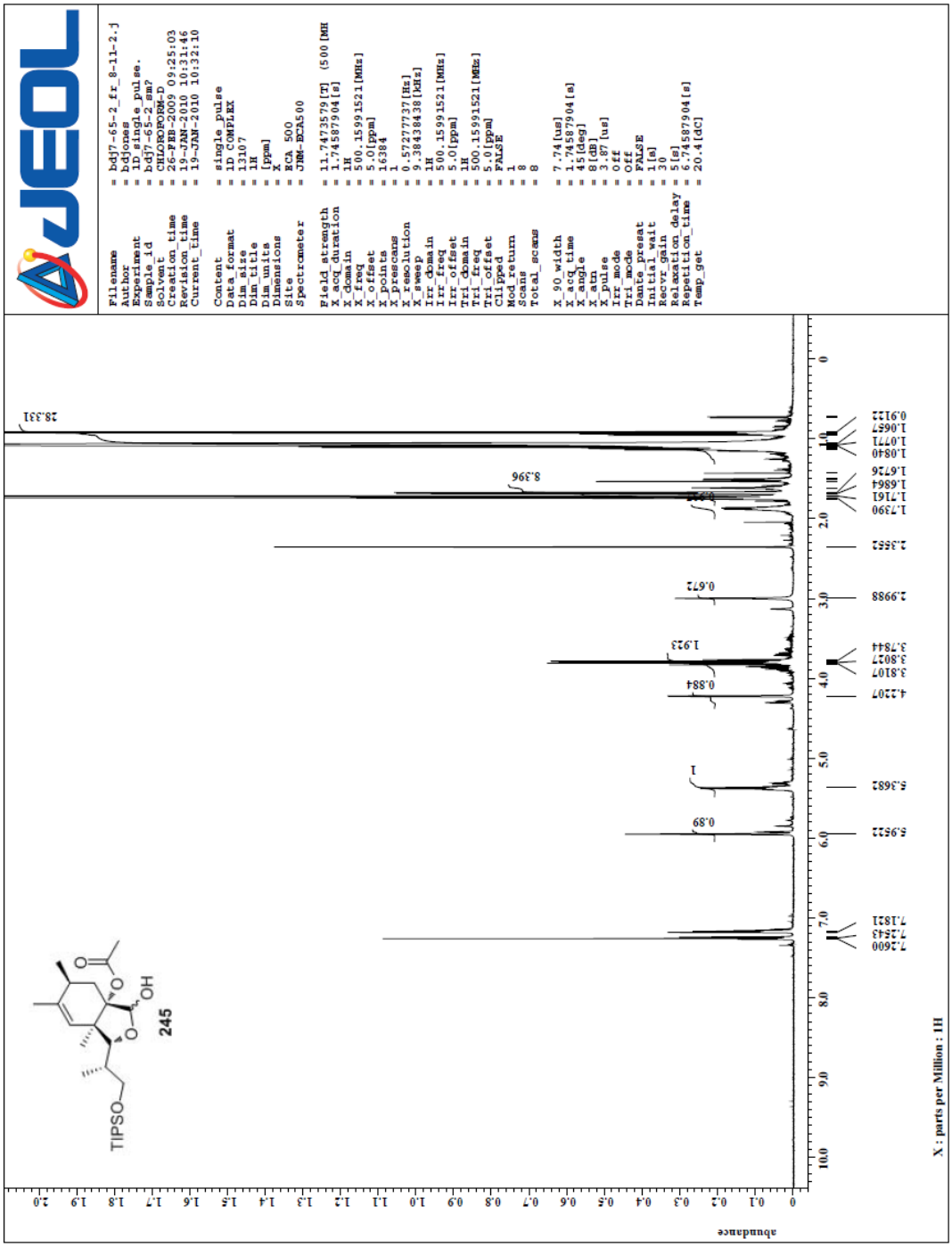

Spectrum 2.122 ^{1}H NMR ($CDCl_3$, 500 MHz) of compound **245**

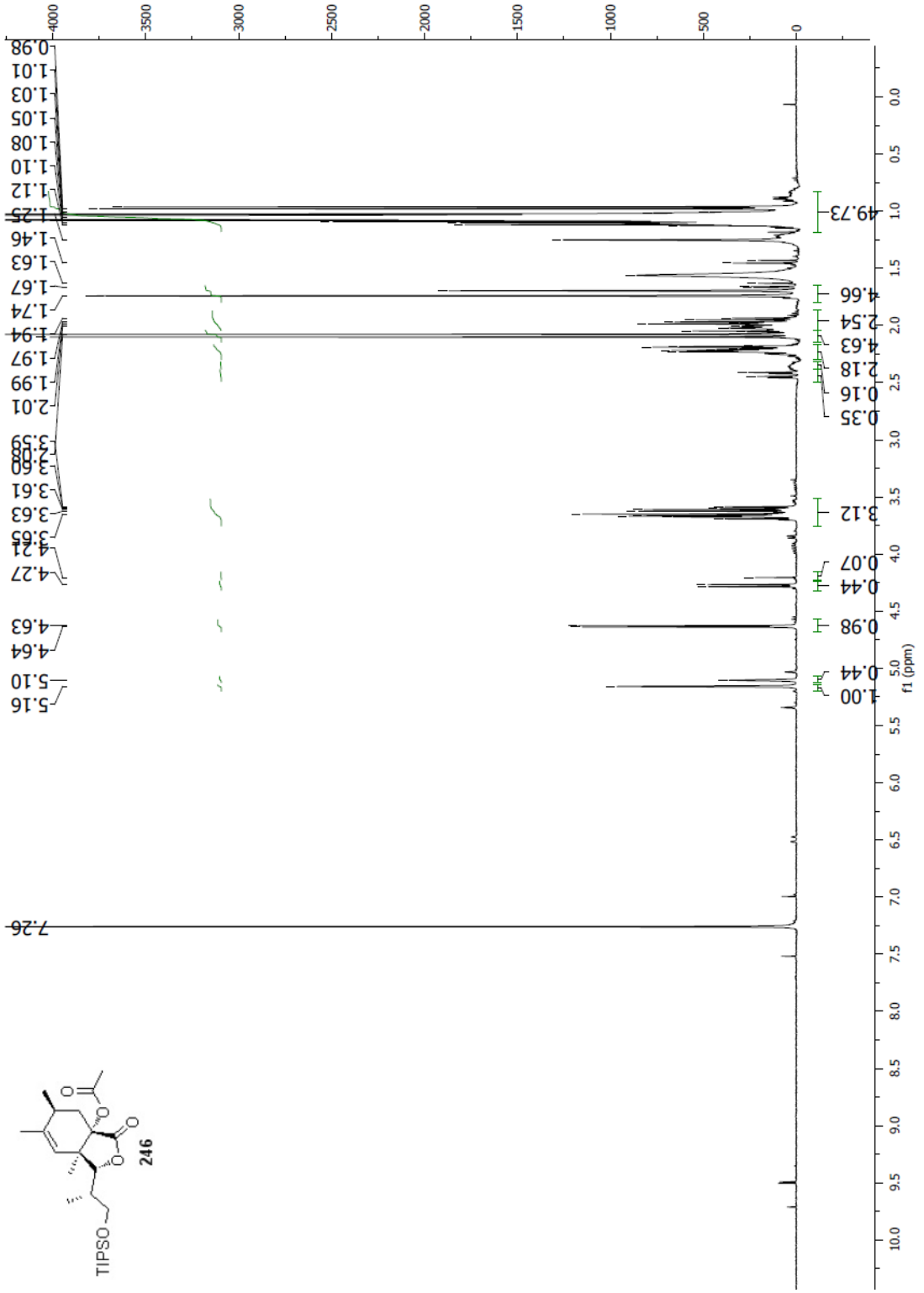

Spectrum 2.123 ^{1}H NMR ($CDCl_3$, 400 MHz) of compound **246**

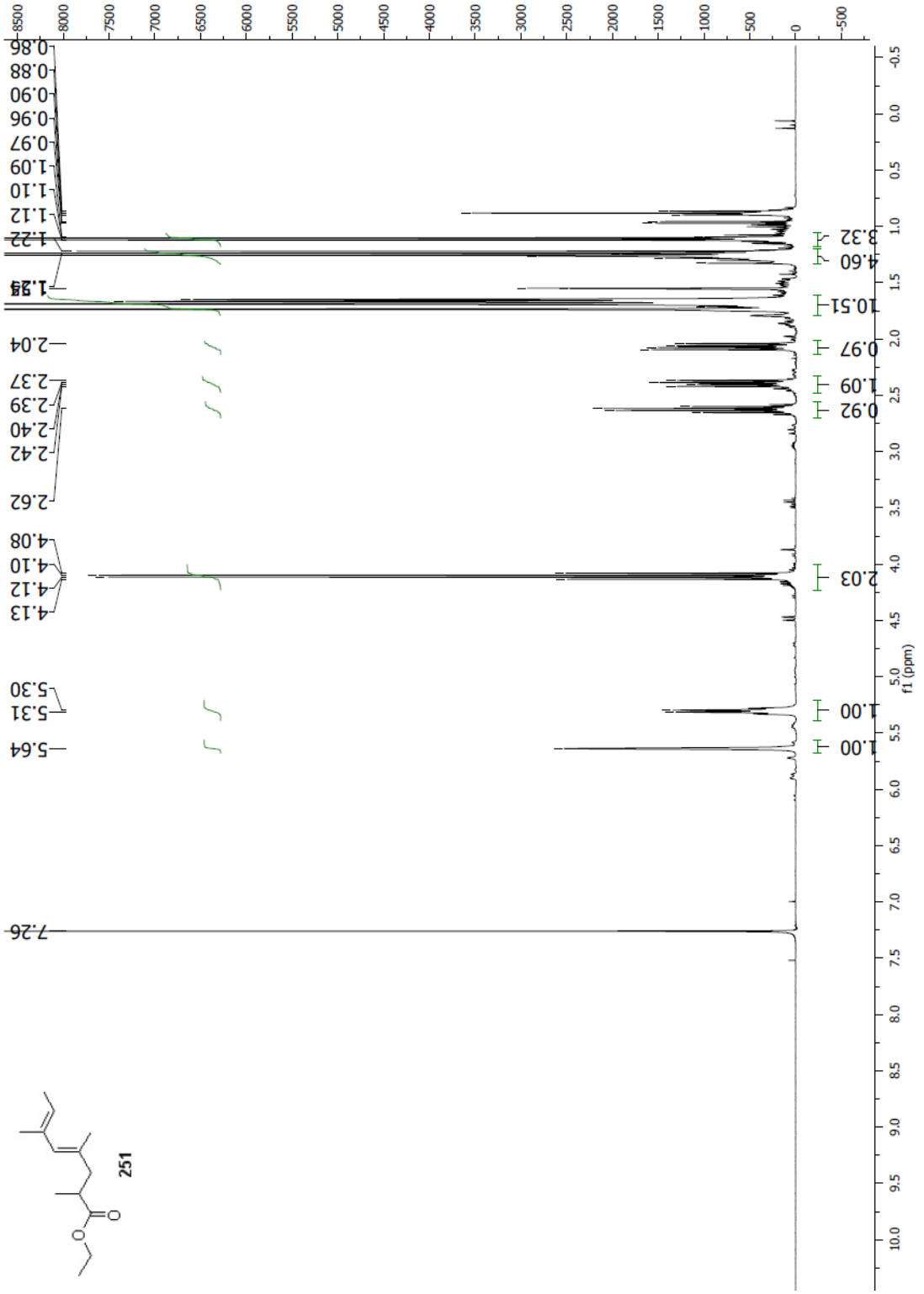

Spectrum 2.124 ^{1}H NMR ($CDCl_3$, 400 MHz) of compound **251**

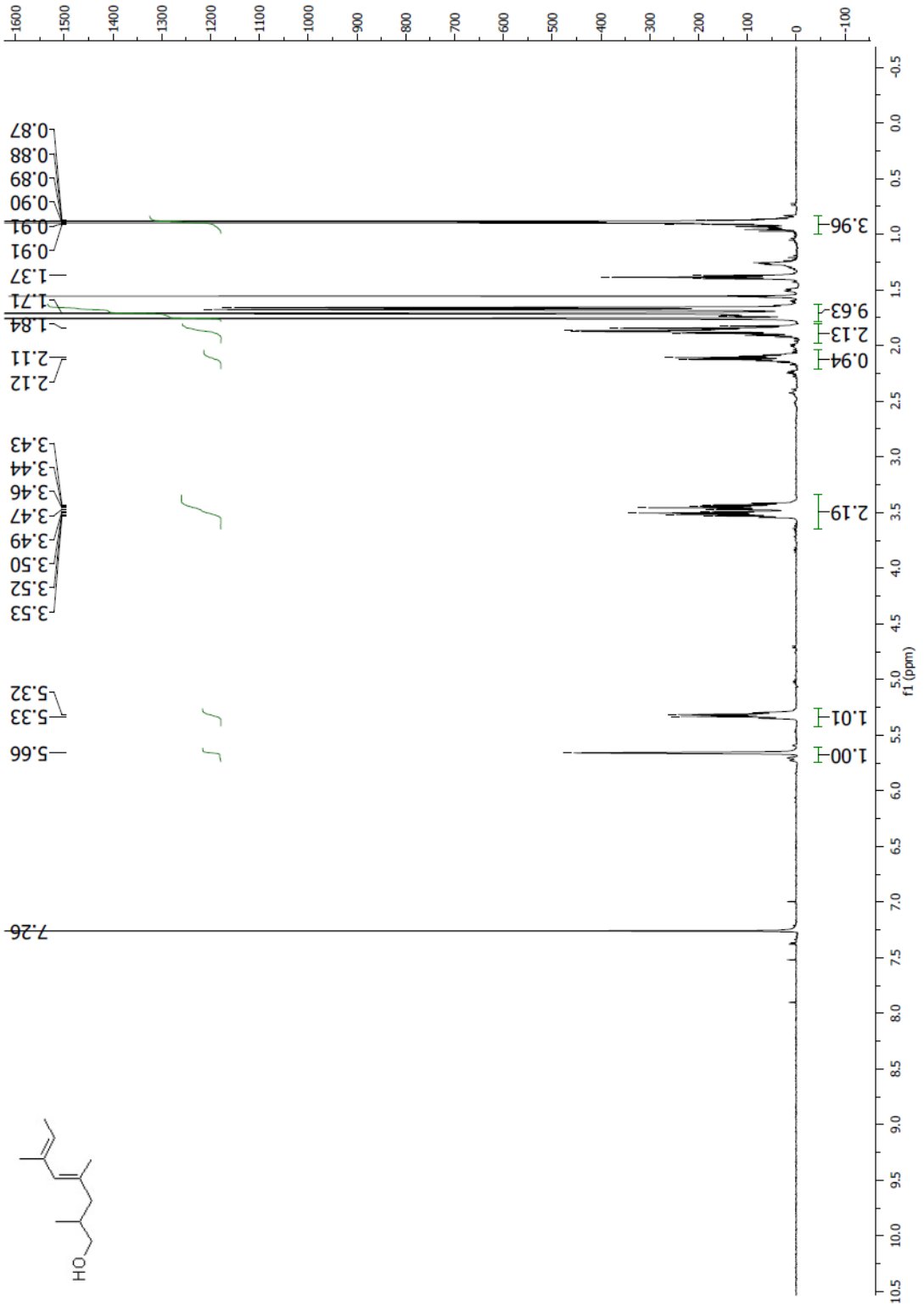

Spectrum 2.125 ^{1}H NMR ($CDCl_3$, 400 MHz) of alcohol precursor to **252**

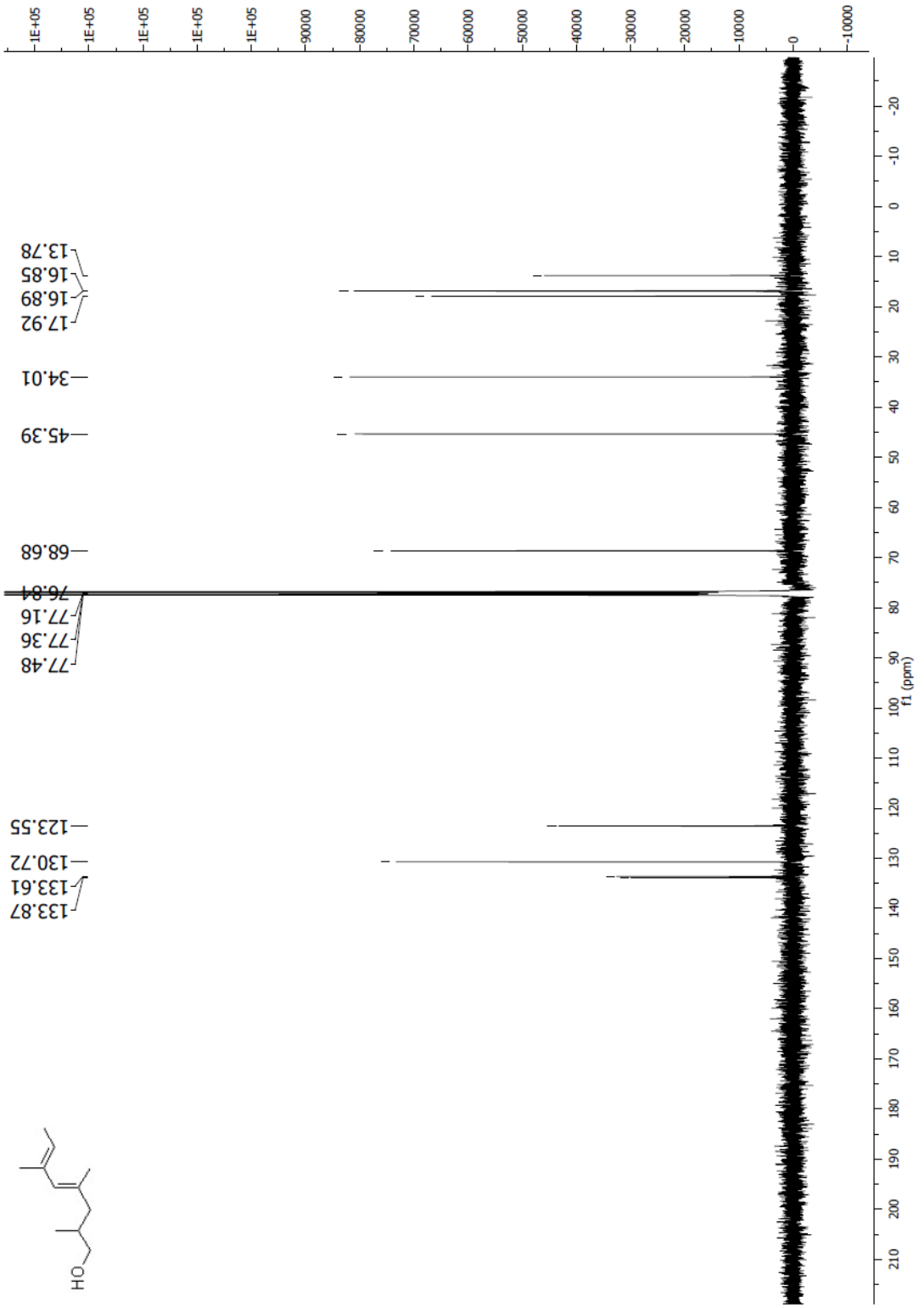

Spectrum 2.126 ^{13}C NMR ($CDCl_3$, 100 MHz) of alcohol precursor to **252**

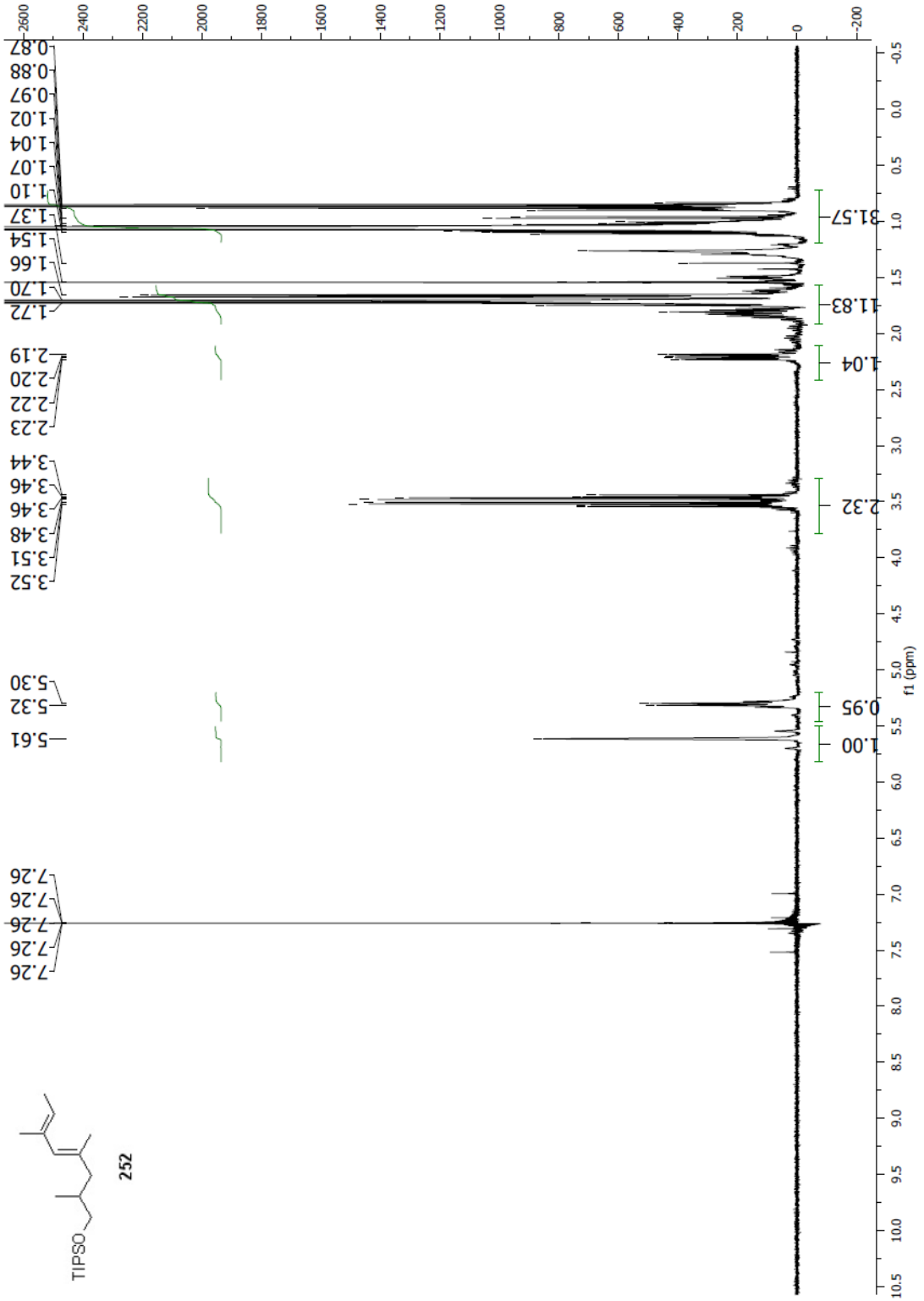

Spectrum 2.127 ^{1}H NMR ($CDCl_3$, 400 MHz) of compound **252**

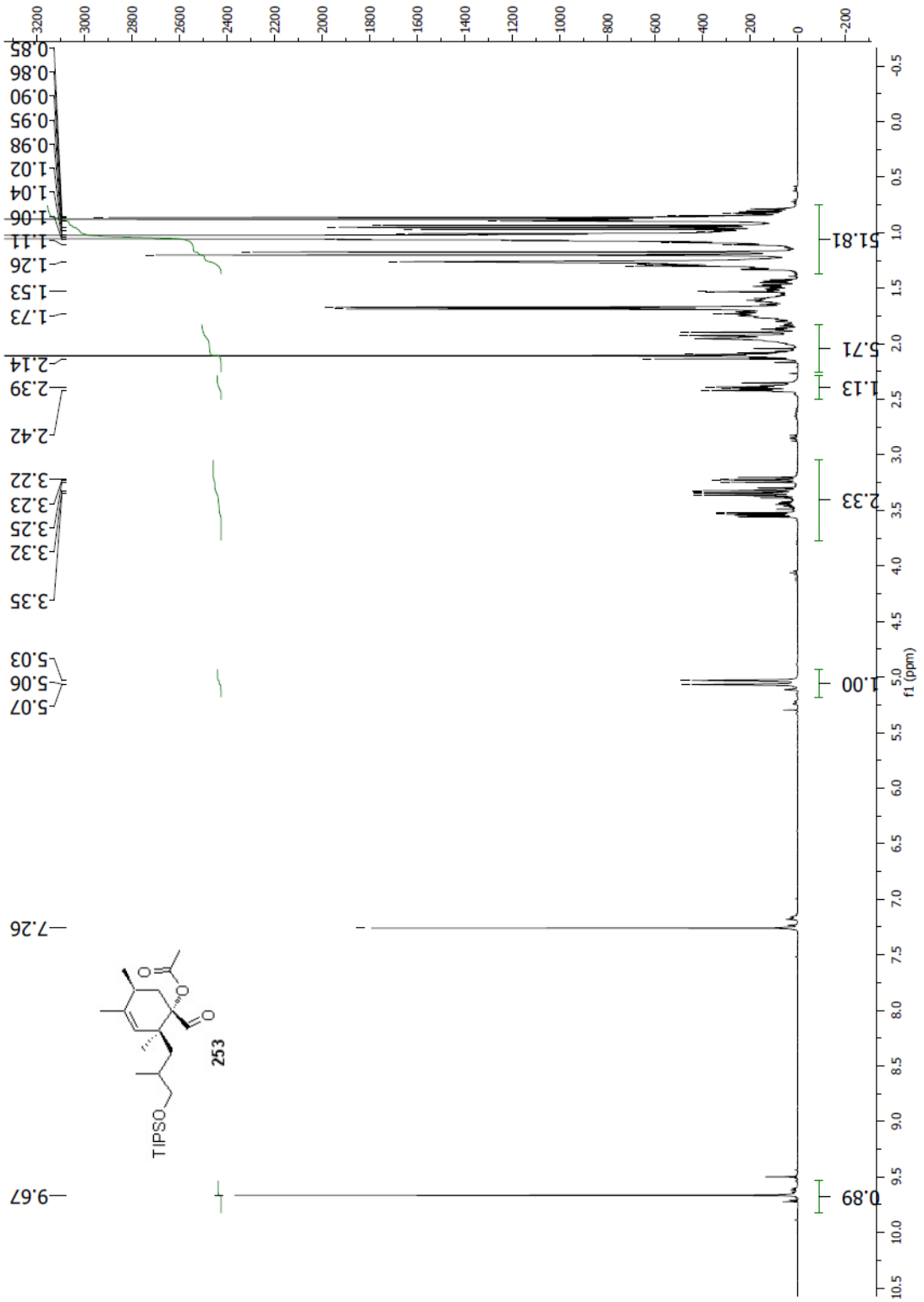

Spectrum 2.128 ^{1}H NMR ($CDCl_3$, 400 MHz) of compound **253**

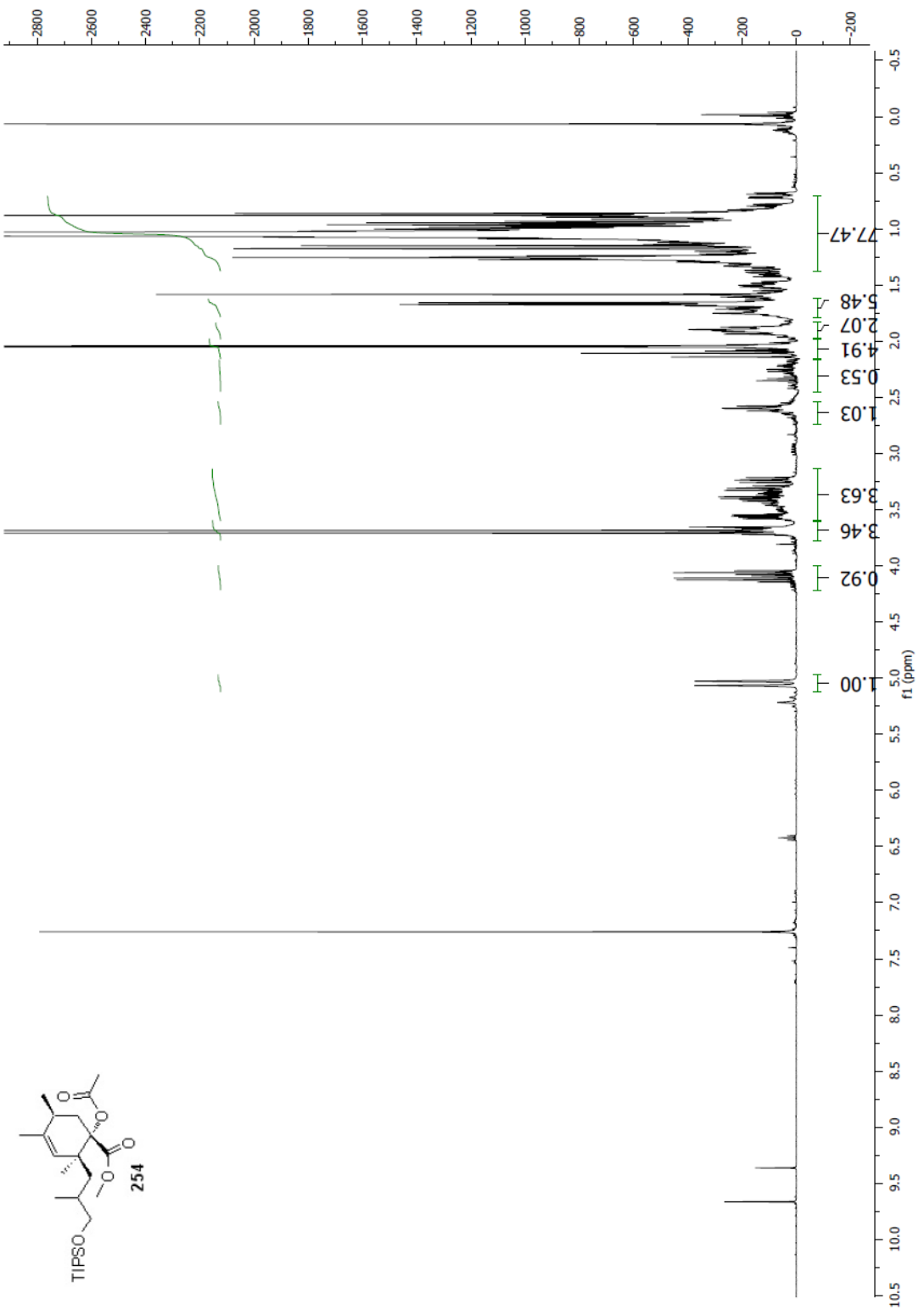

Spectrum 2.129 ^{1}H NMR ($CDCl_3$, 400 MHz) of compound **254**

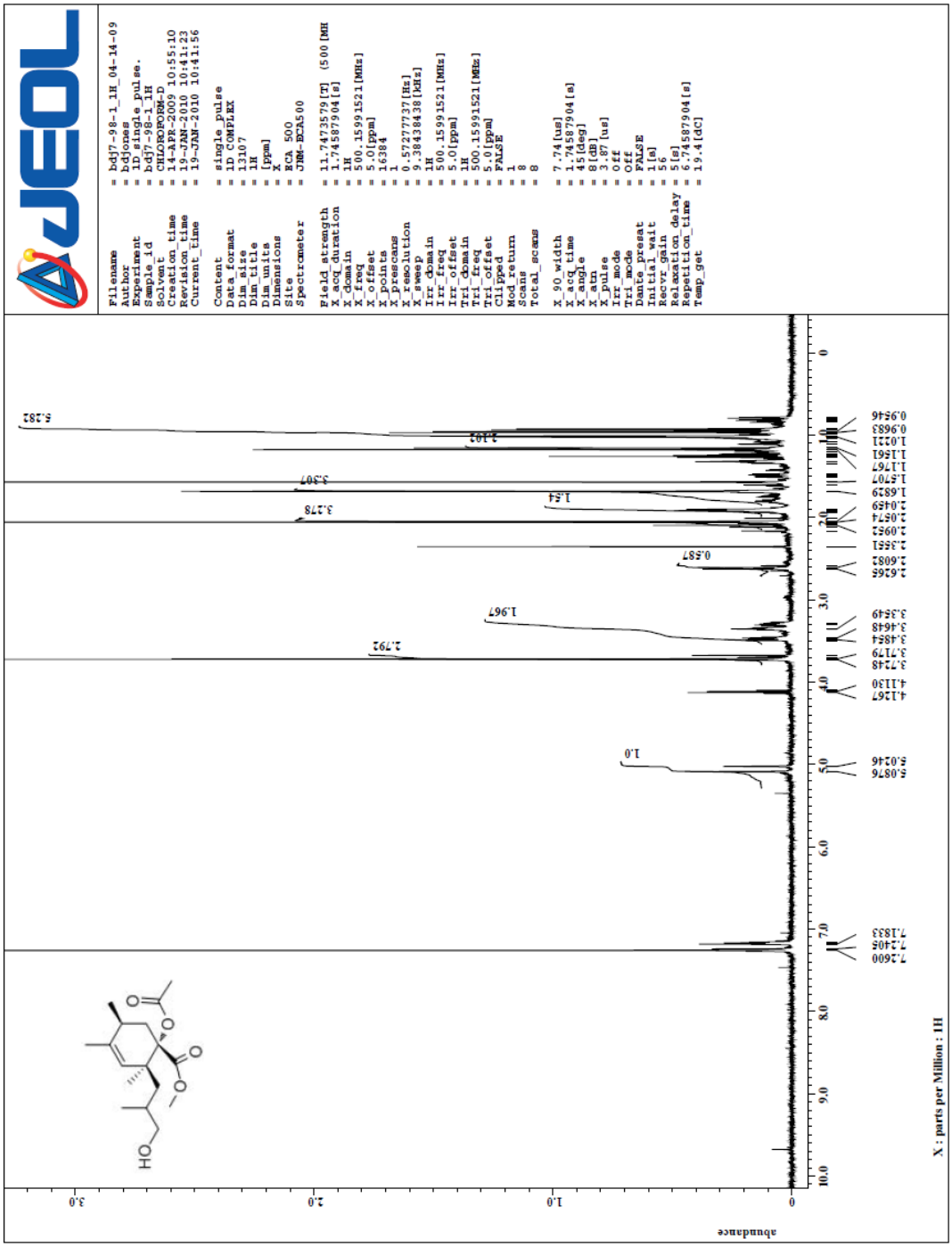

Spectrum 2.130 ^{1}H NMR ($CDCl_3$, 500 MHz) of the alcohol precursor to **255**

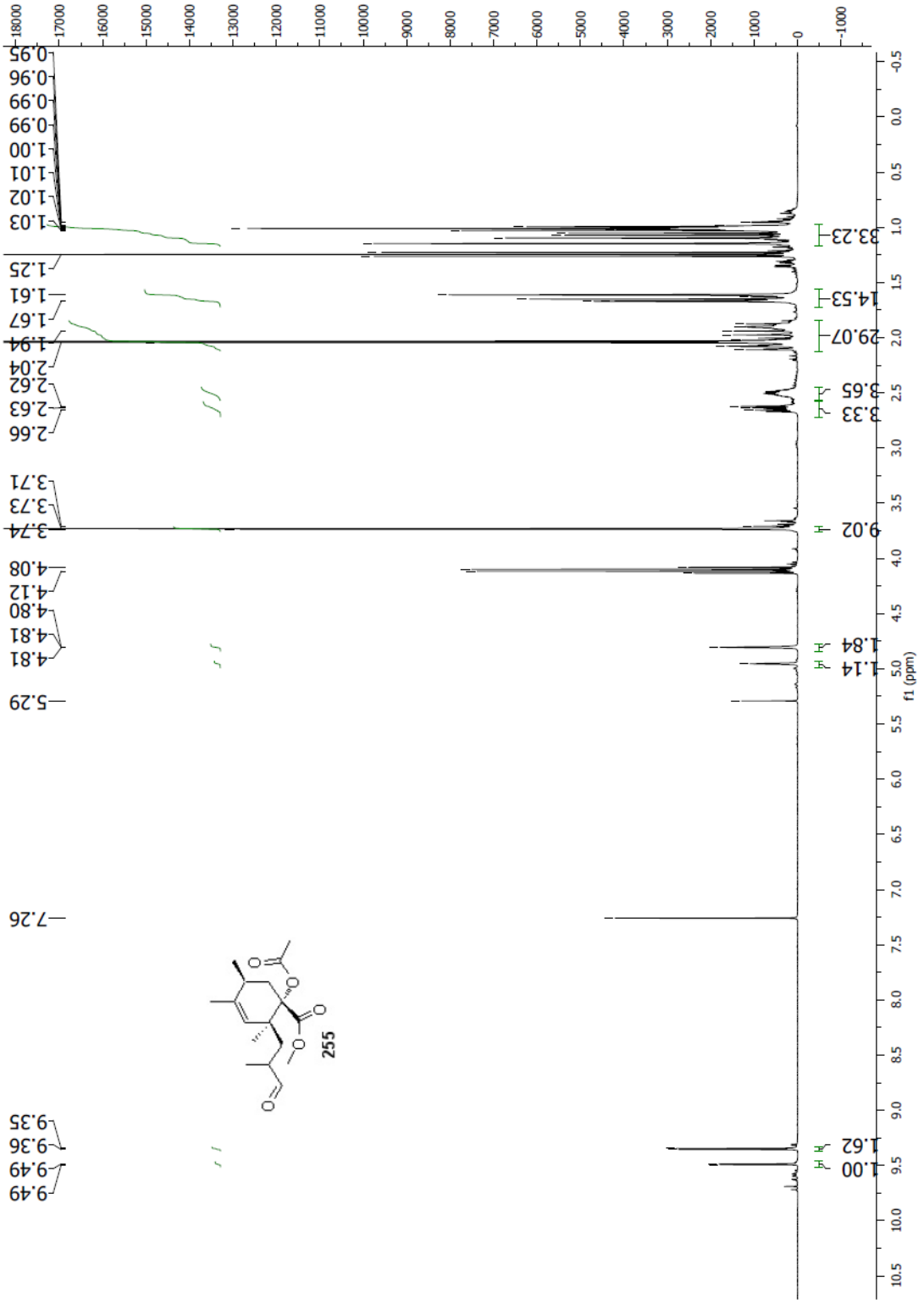

Spectrum 2.131 ^{1}H NMR ($CDCl_3$, 400 MHz) of compound **255**

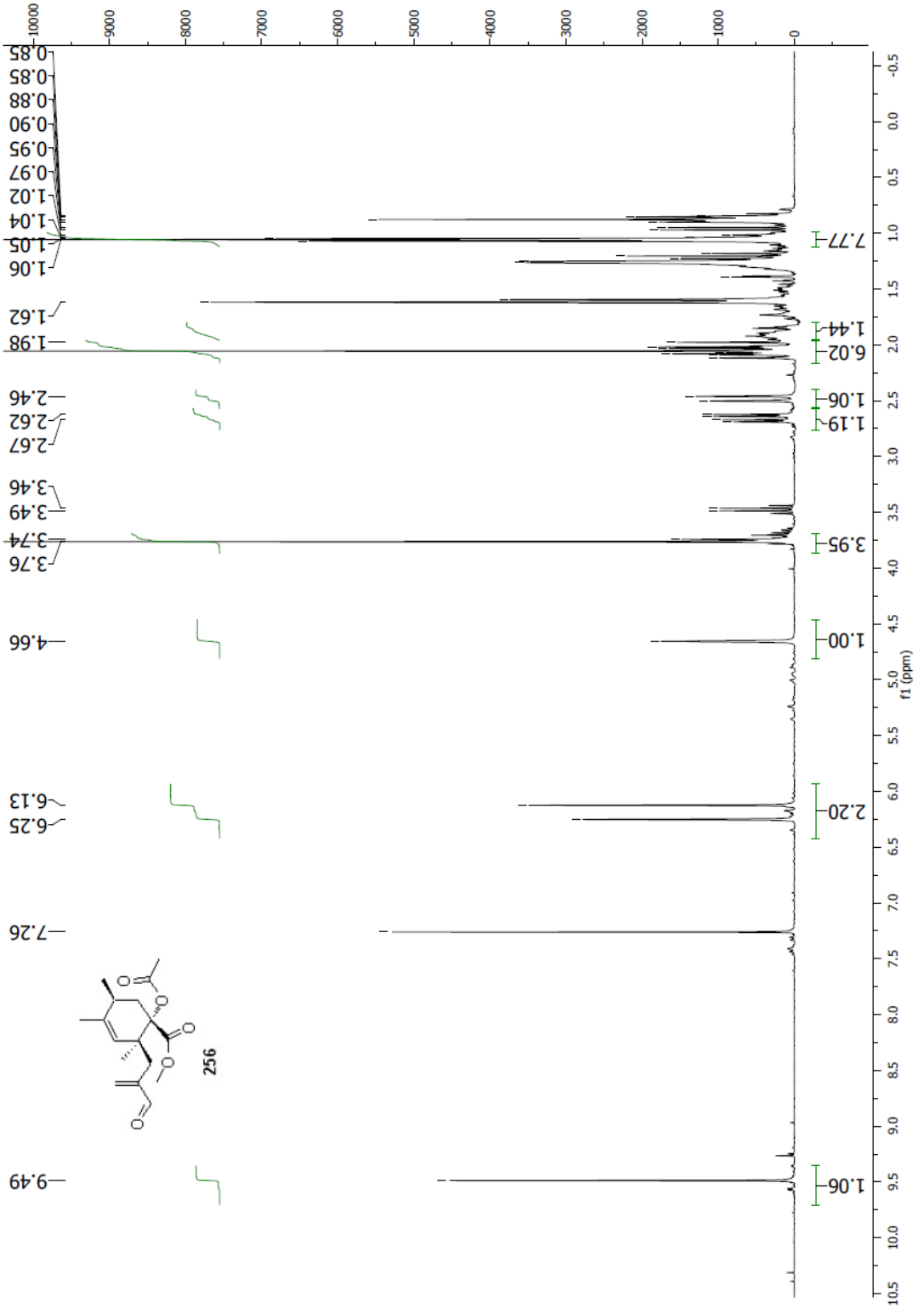

Spectrum 2.132 ^{1}H NMR ($CDCl_3$, 300 MHz) of compound **256**

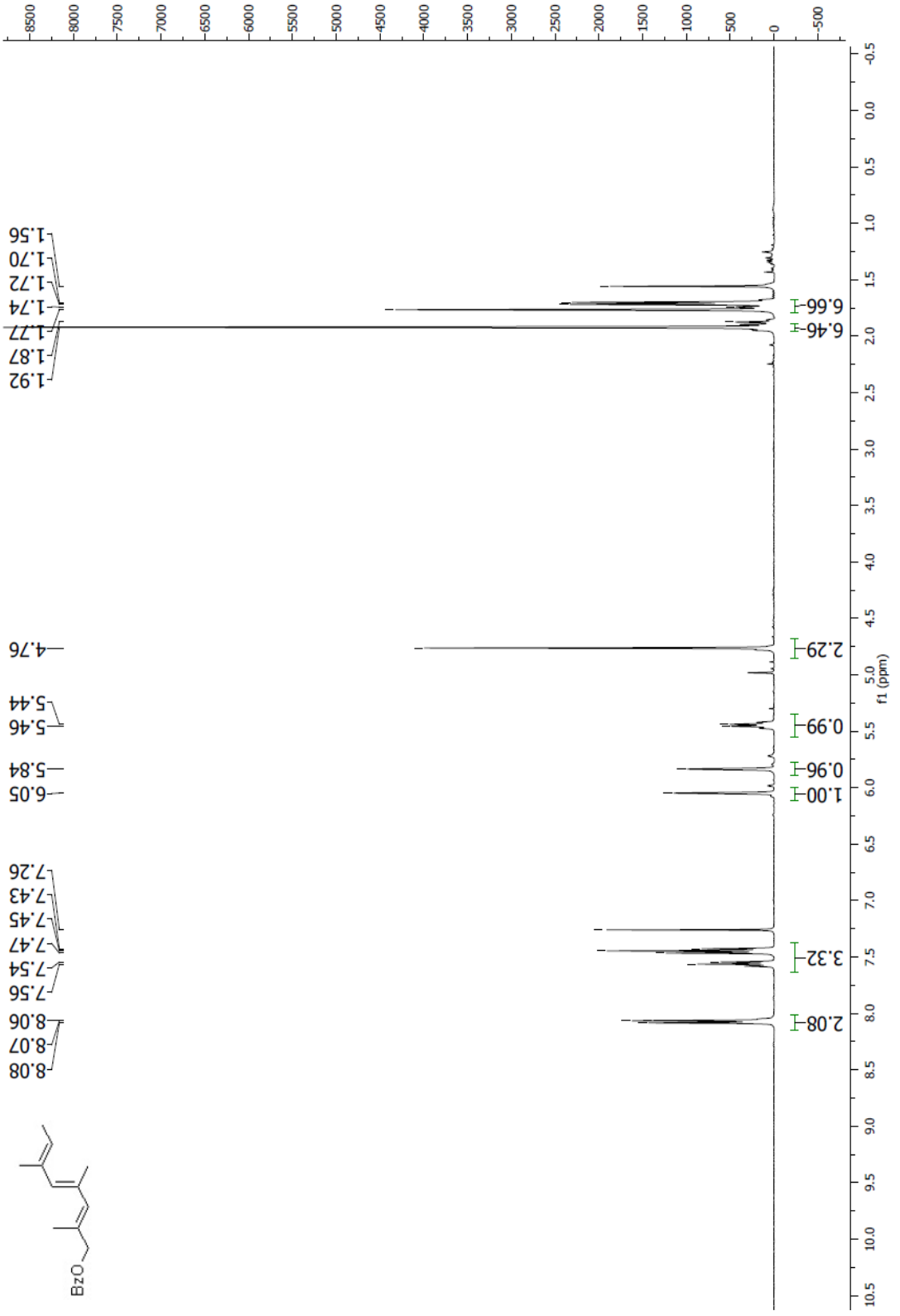

Spectrum 2.133 ^{1}H NMR ($CDCl_3$, 400 MHz) of compound **260**

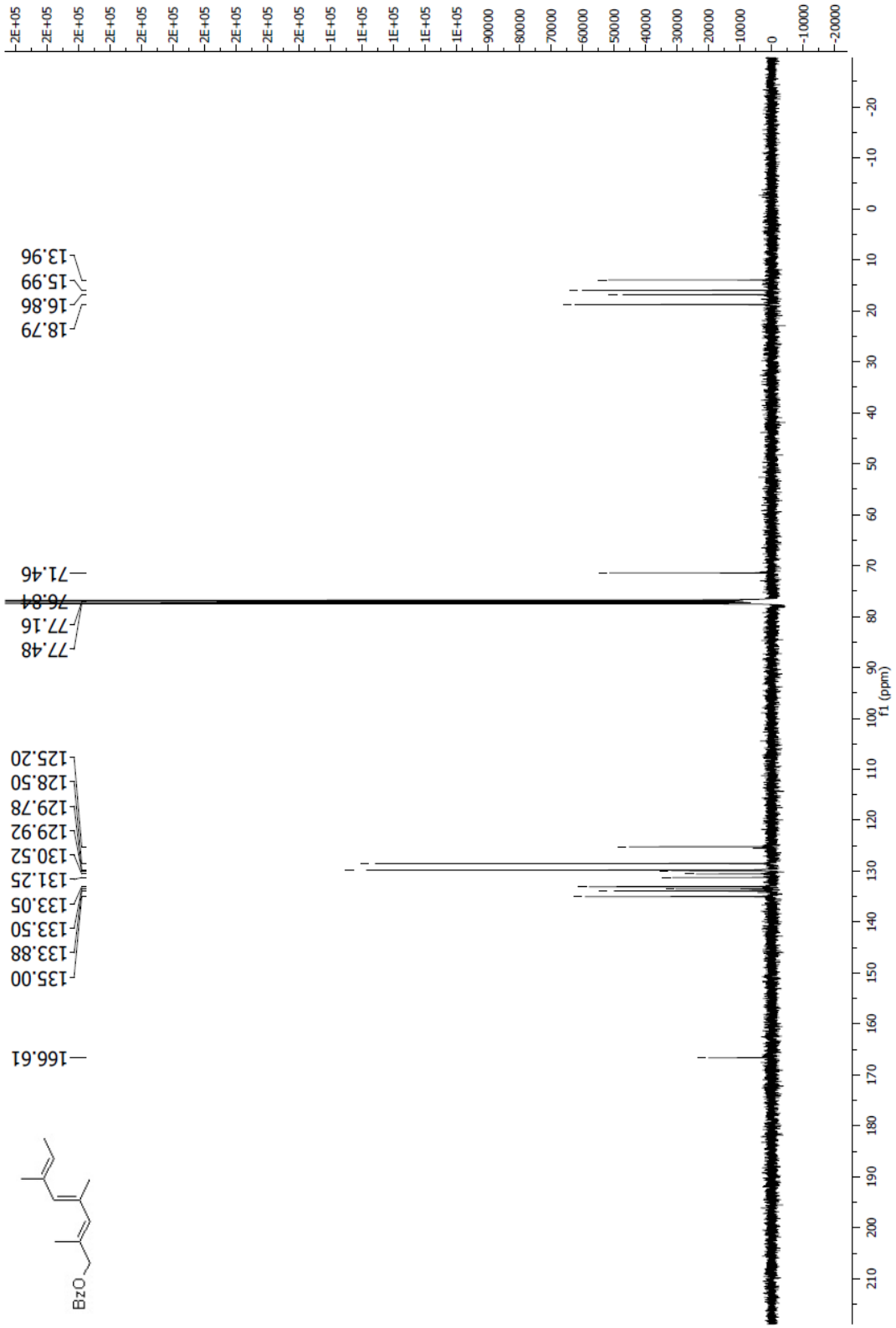

Spectrum 2.134 ^{1}H NMR ($CDCl_3$, 100 MHz) of compound **260**

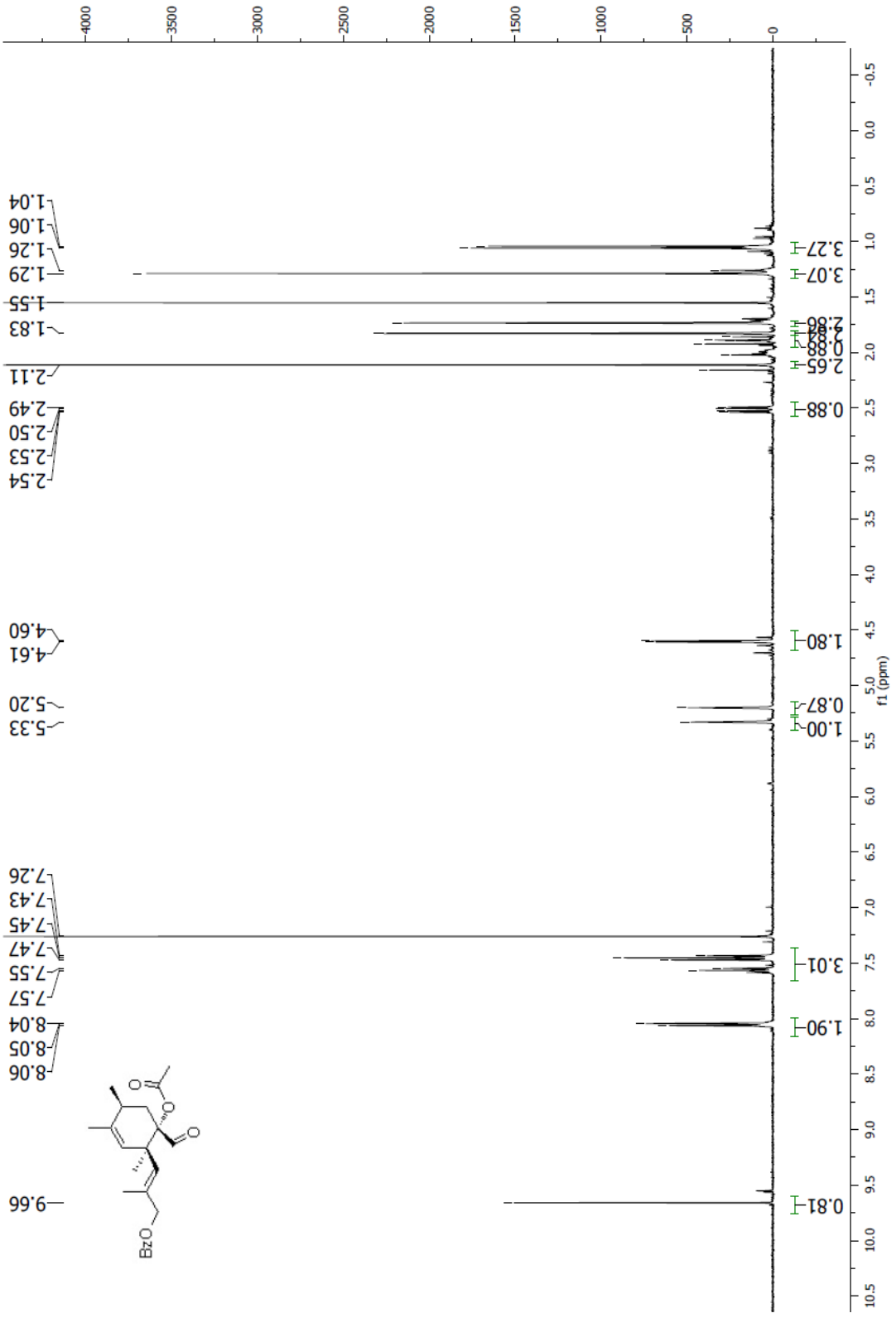

Spectrum 2.135 ^{1}H NMR ($CDCl_3$, 400 MHz) of compound **261**

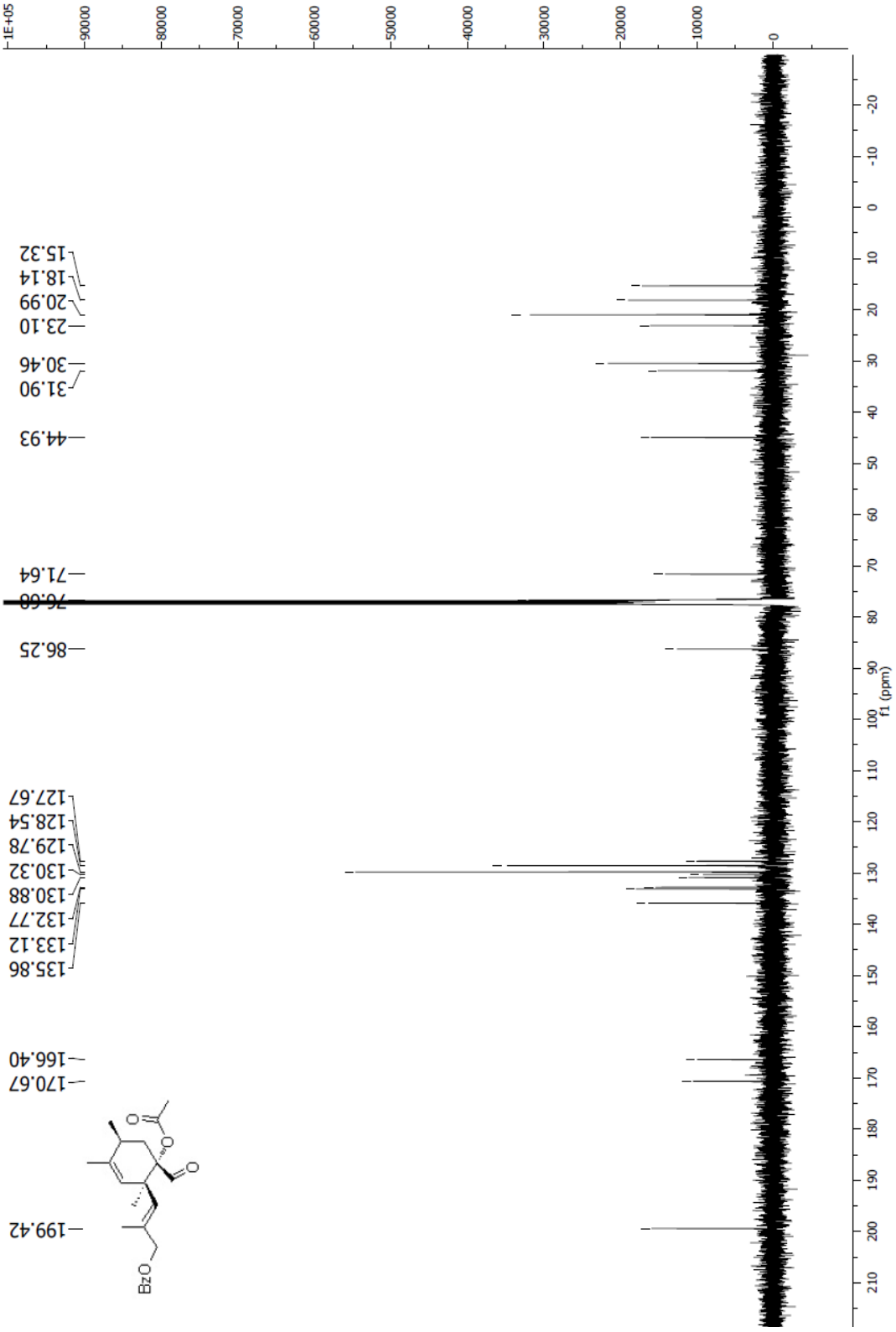

Spectrum 2.136 ^{13}C NMR ($CDCl_3$, 100 MHz) of compound **261**

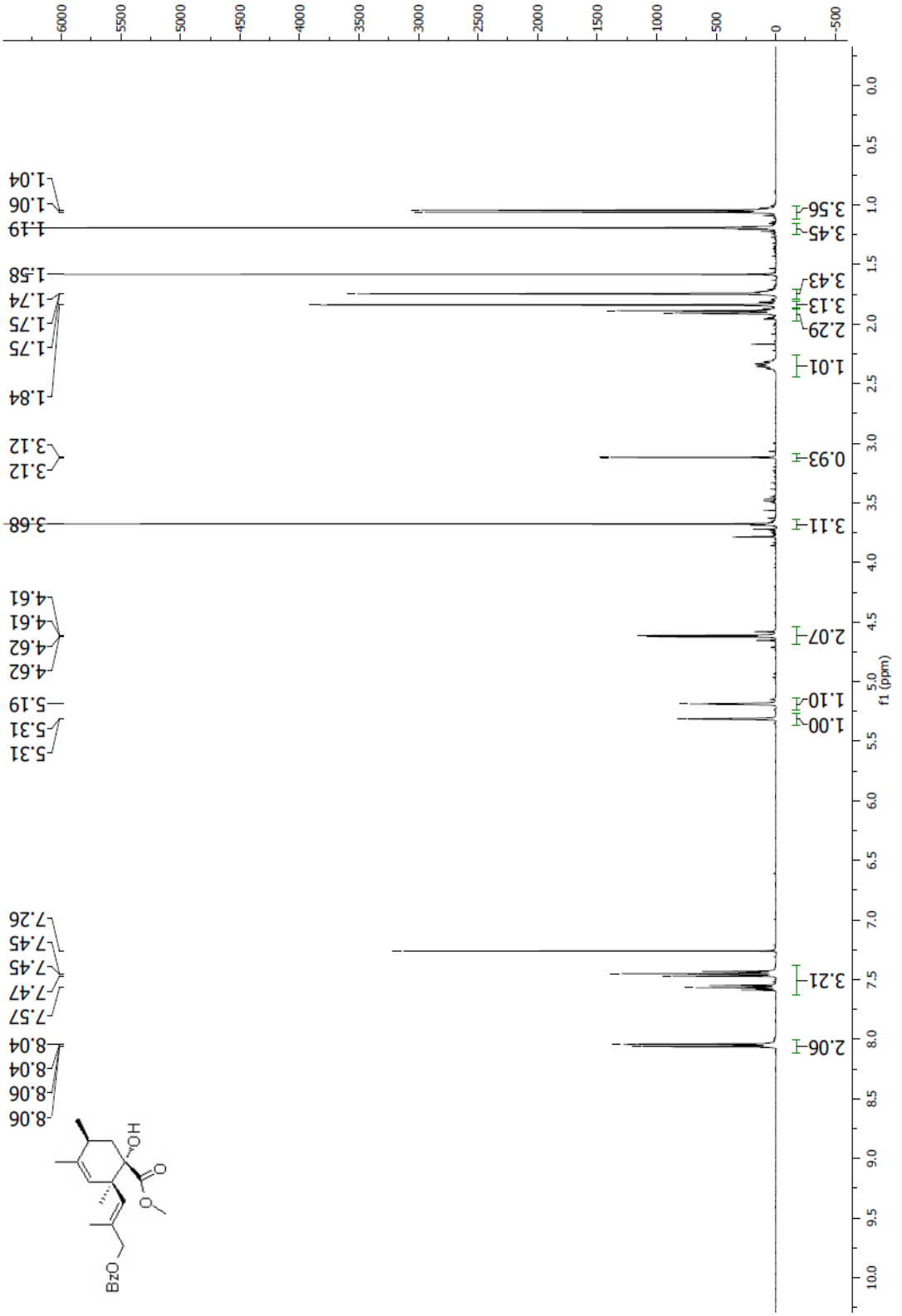

Spectrum 2.137 ^{1}H NMR ($CDCl_3$, 400 MHz) of compound **262**

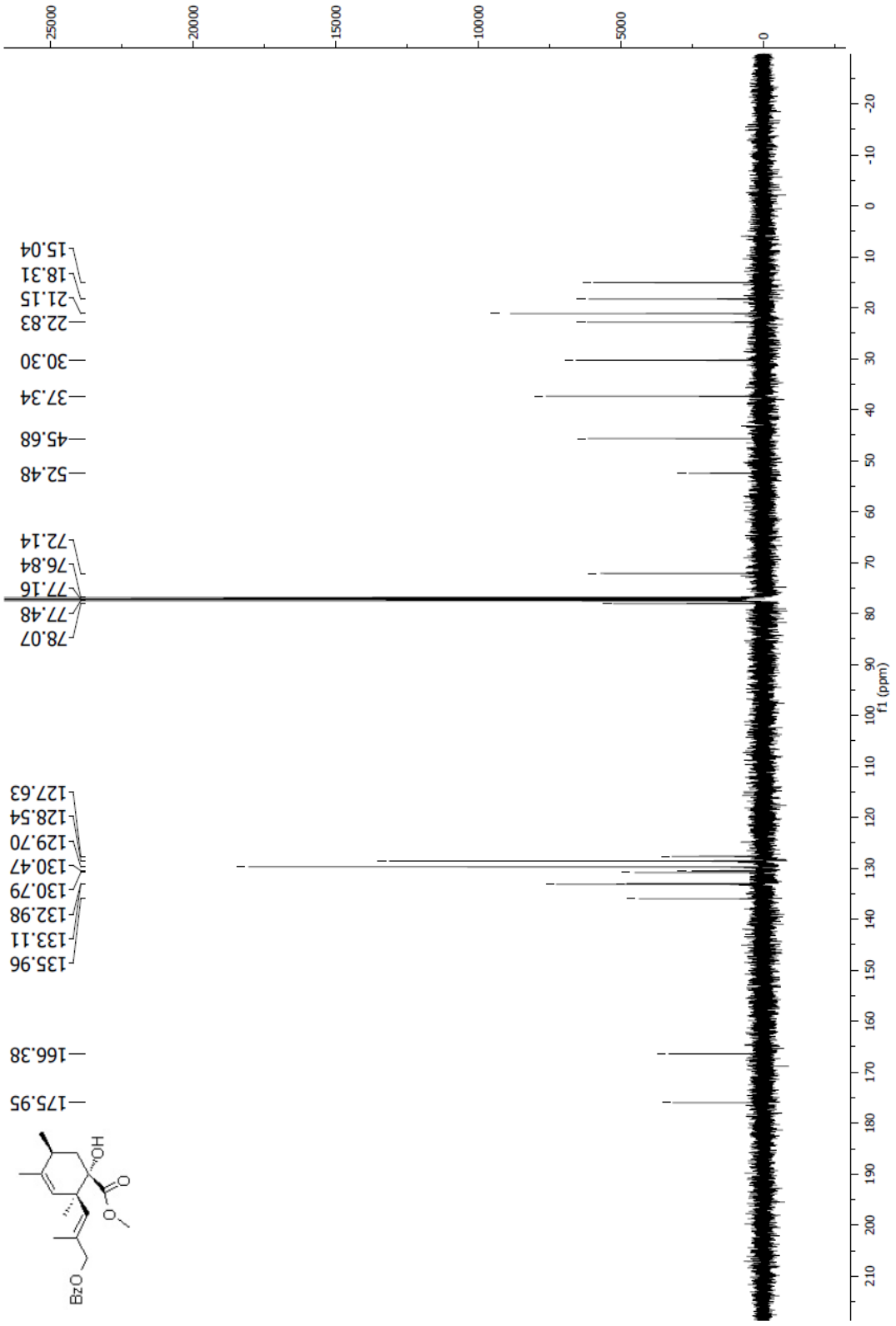

Spectrum 2.138 ^{13}C NMR ($CDCl_3$, 100 MHz) of compound **262**

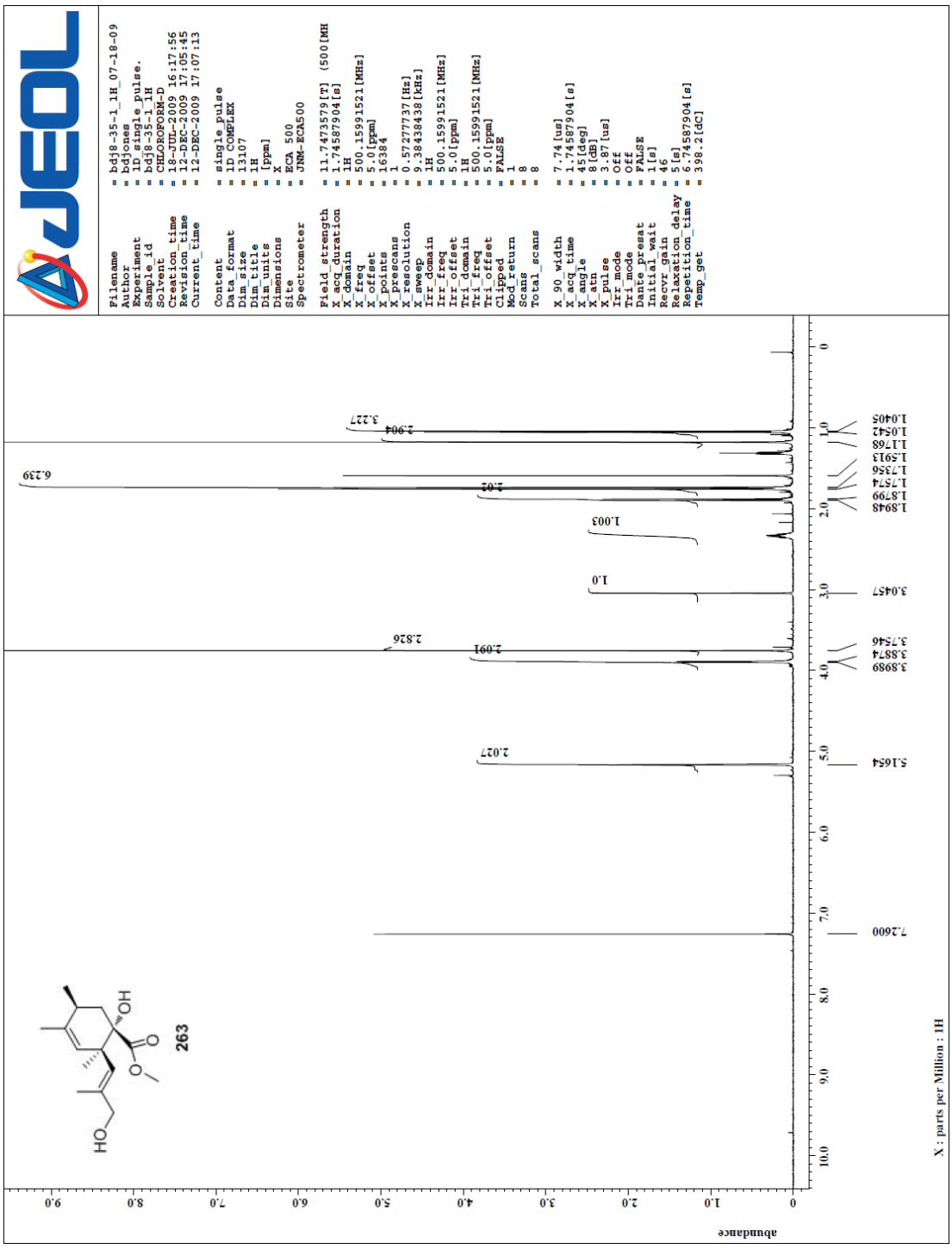

Spectrum 2.139 ^{1}H NMR ($CDCl_3$, 500 MHz) of compound **263**

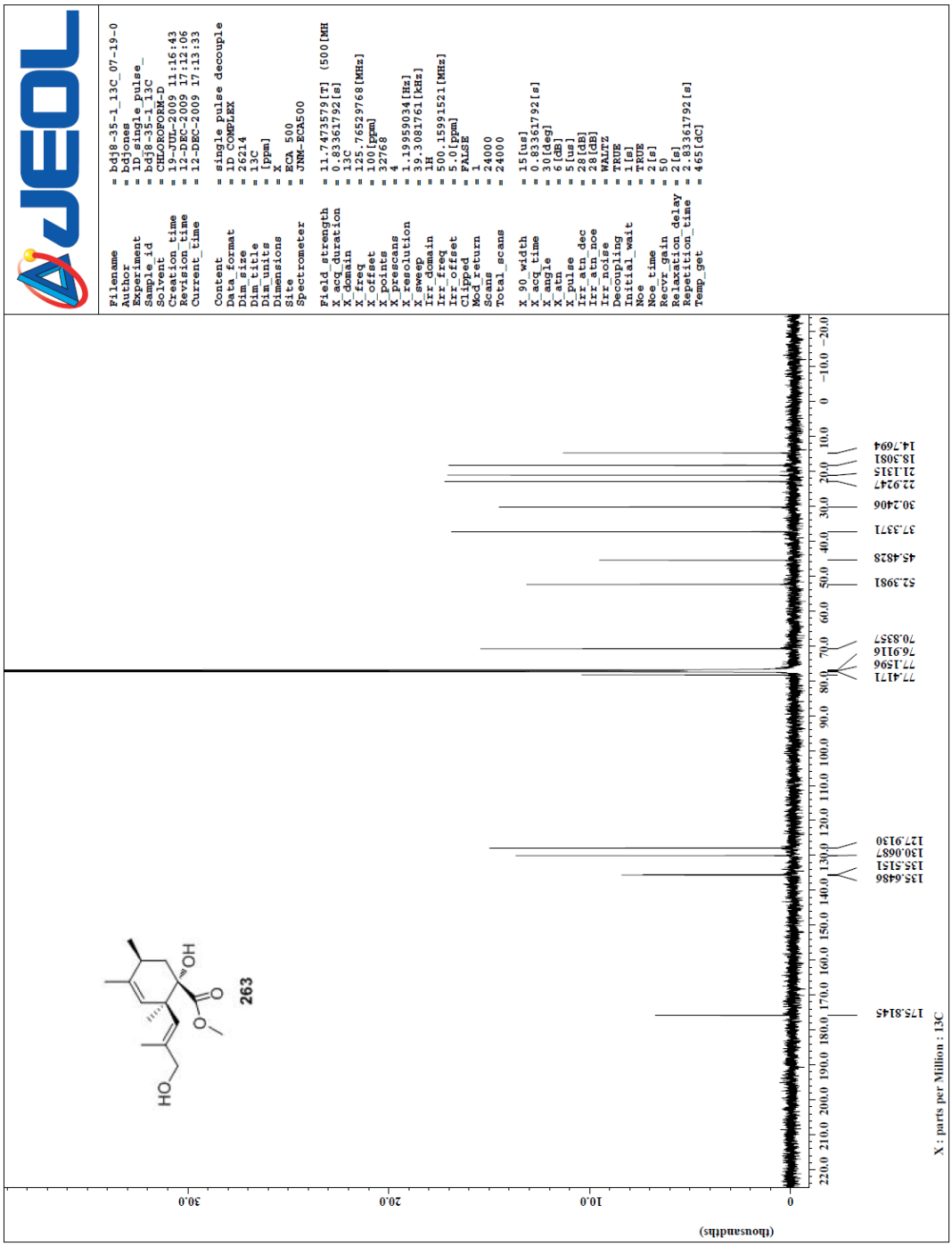

Spectrum 2.140 ^{13}C NMR ($CDCl_3$, 125 MHz) of compound **263**

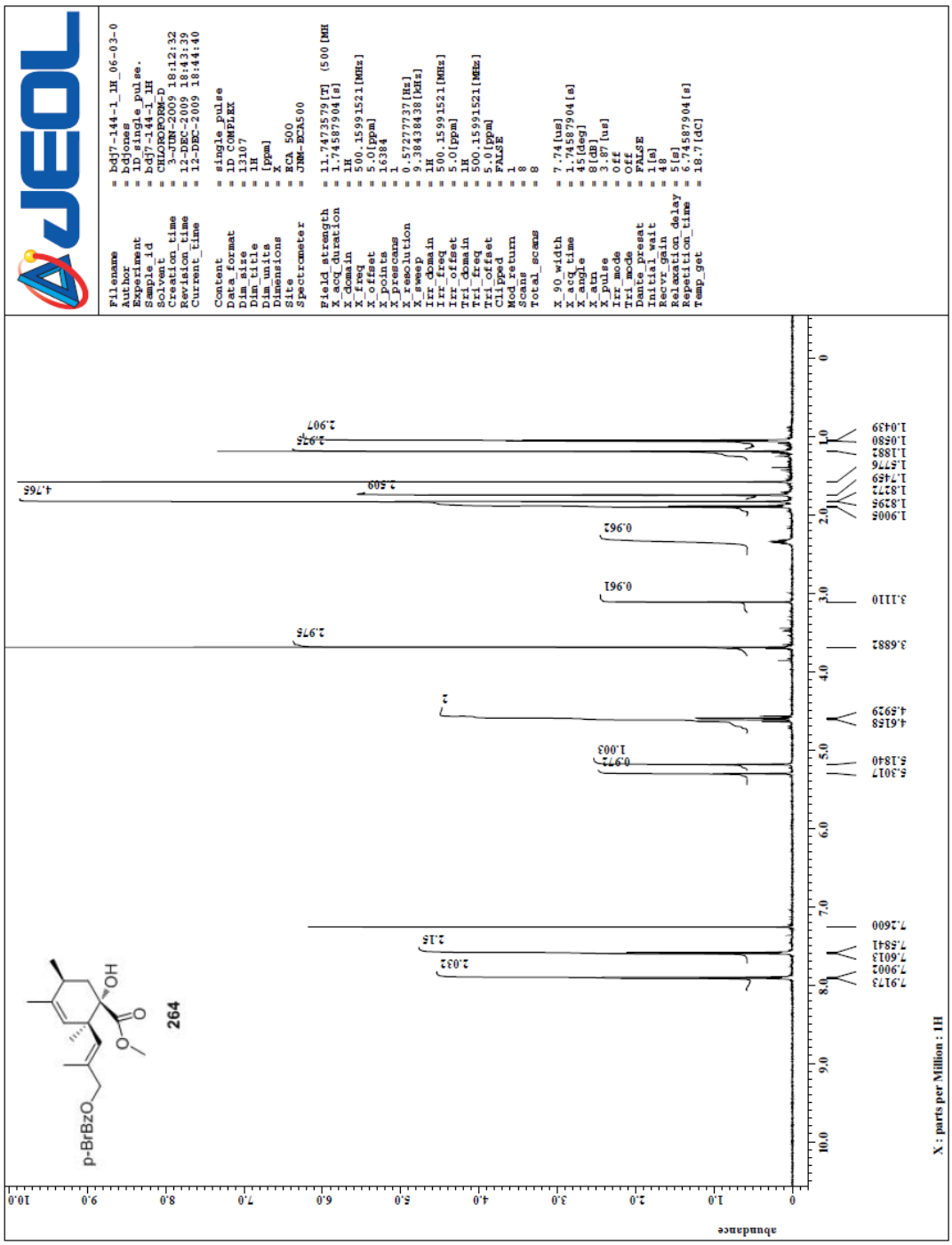

Spectrum 2.141 ^{1}H NMR ($CDCl_3$, 500 MHz) of compound **264**

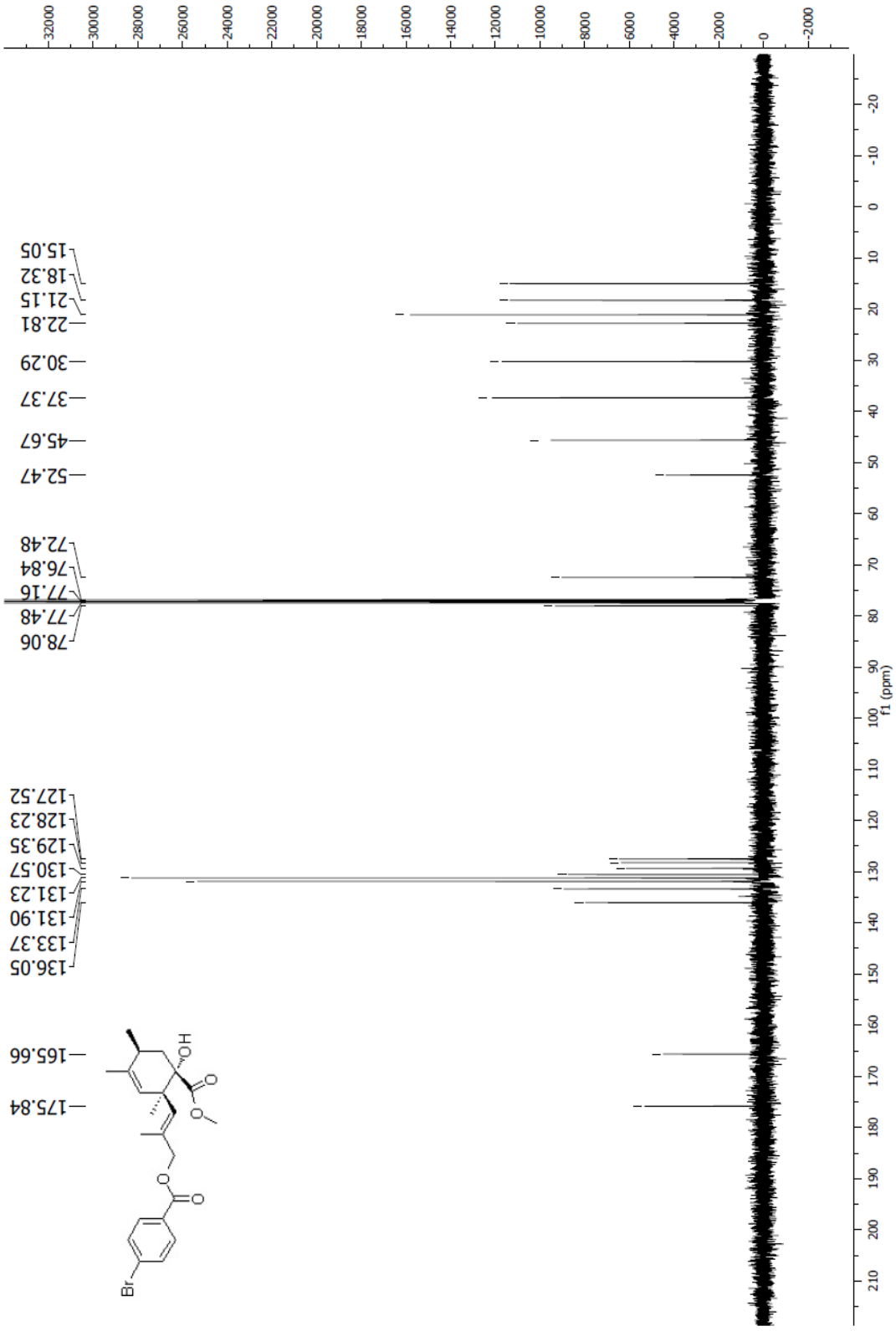

Spectrum 2.142 ^{13}C NMR ($CDCl_3$, 100 MHz) of compound **264**

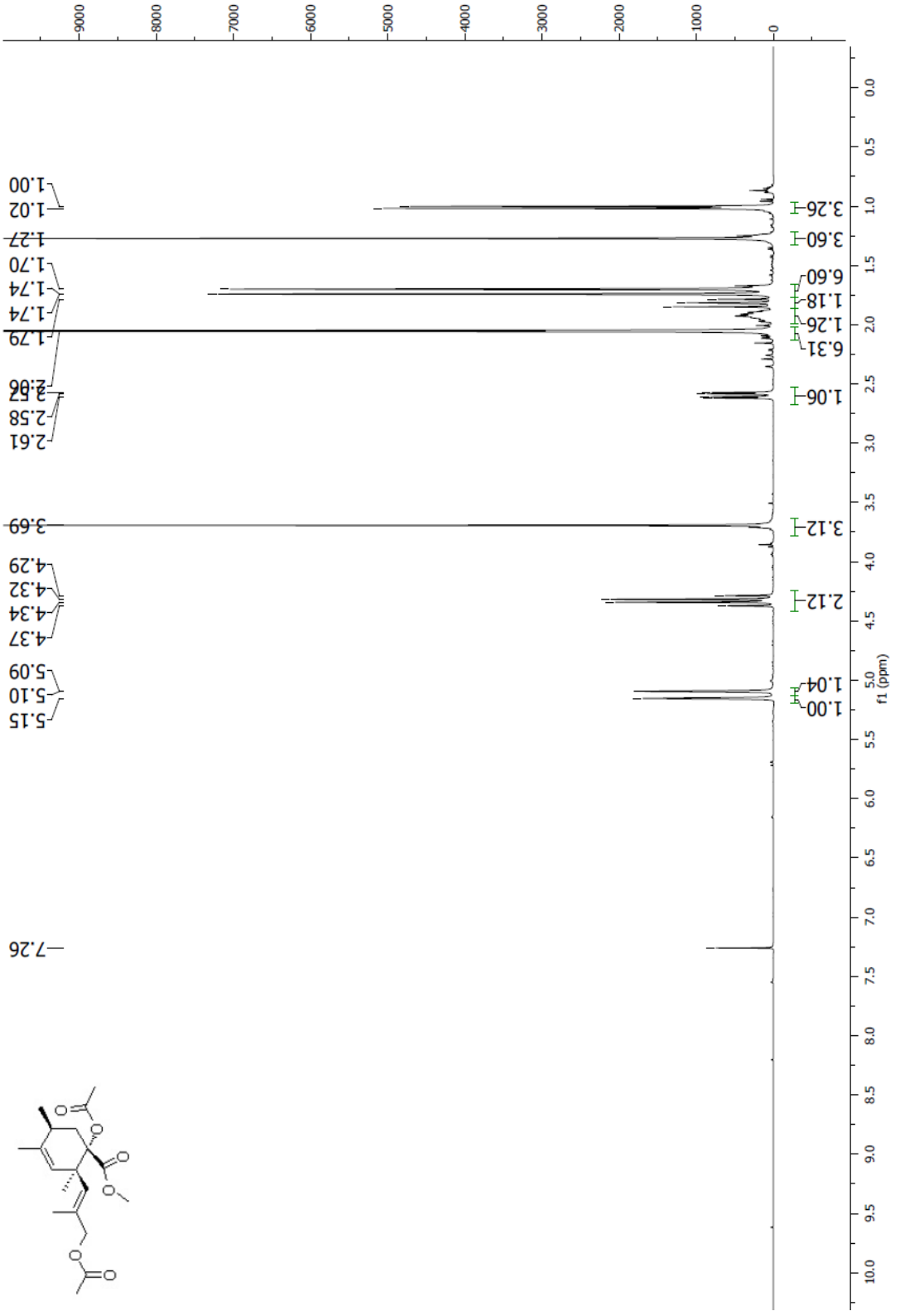

Spectrum 2.143 ^{1}H NMR ($CDCl_3$, 400 MHz) of compound **265**

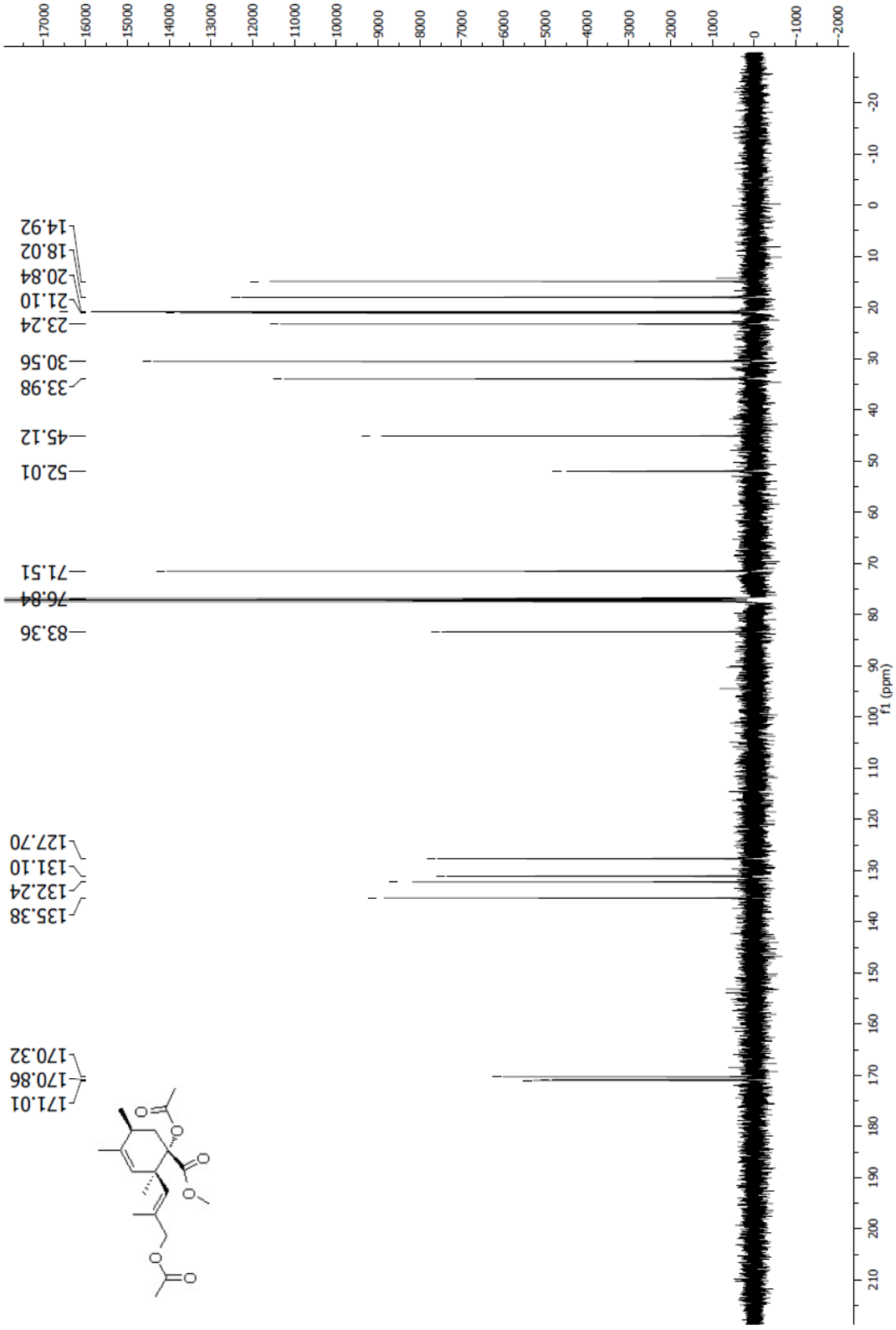

Spectrum 2.144 ^{13}C NMR ($CDCl_3$, 100 MHz) of compound **265**

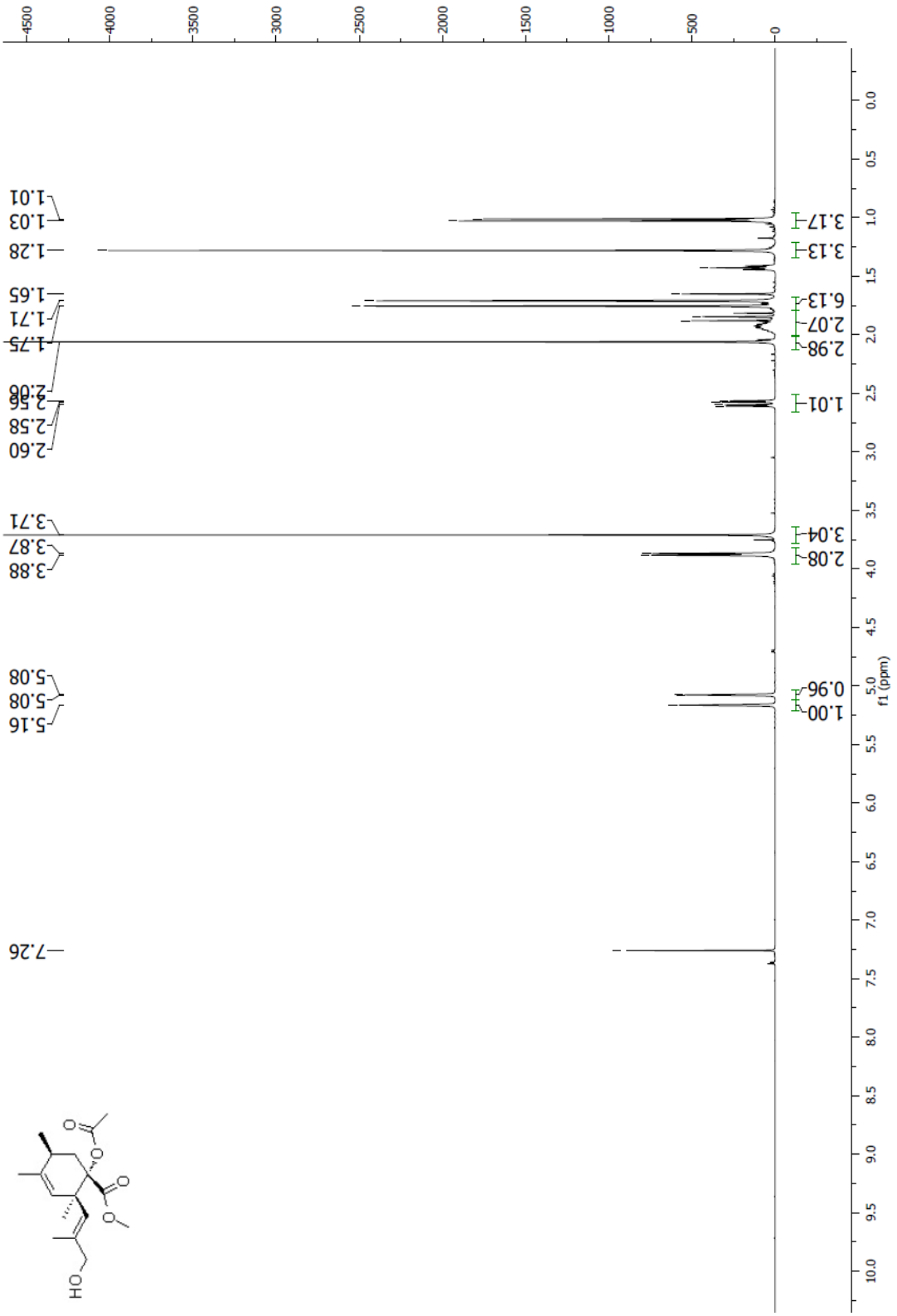

Spectrum 2.145 ^{1}H NMR ($CDCl_3$, 400 MHz) of compound **266**

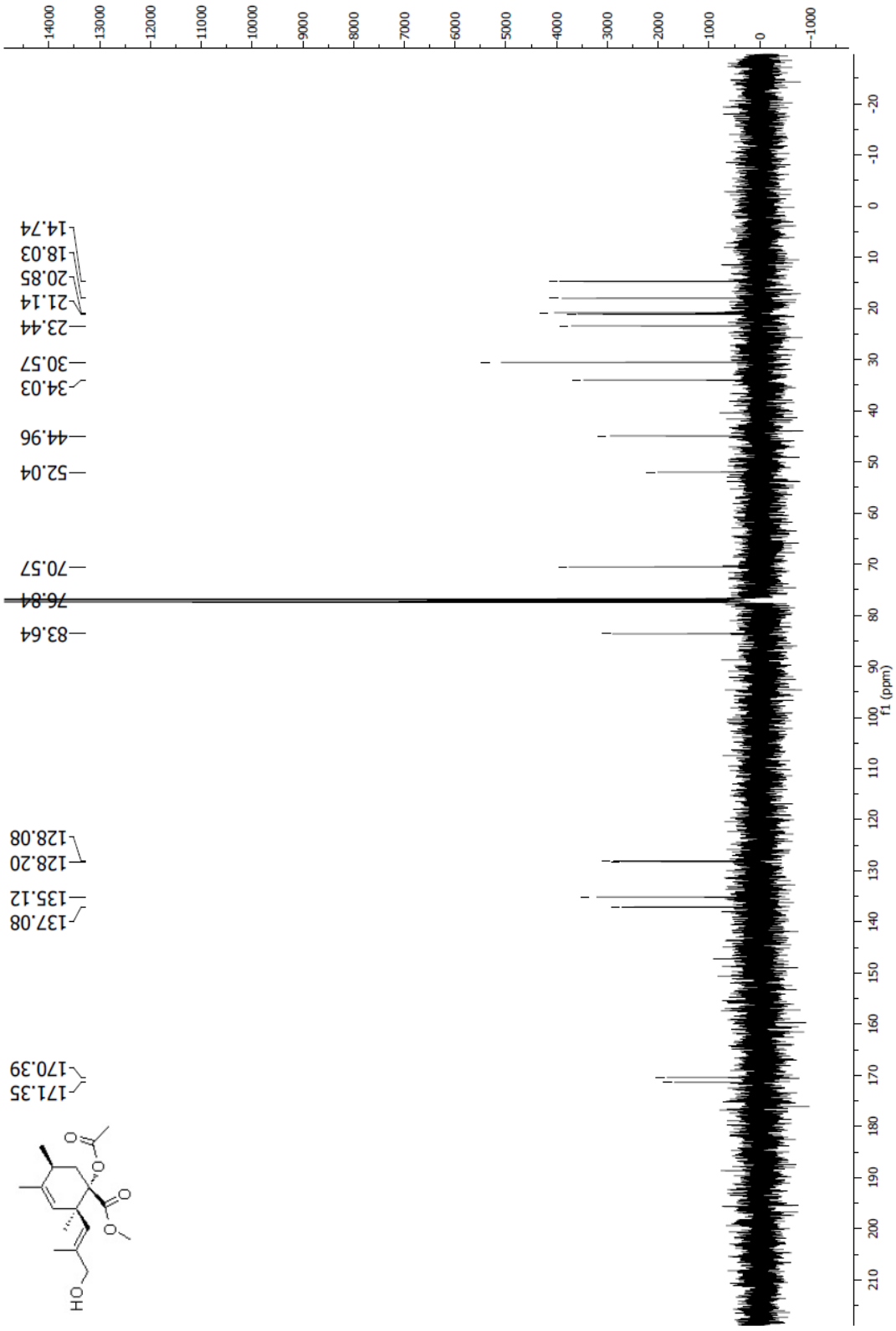

Spectrum 2.146 ^{13}C NMR ($CDCl_3$, 100 MHz) of compound **266**

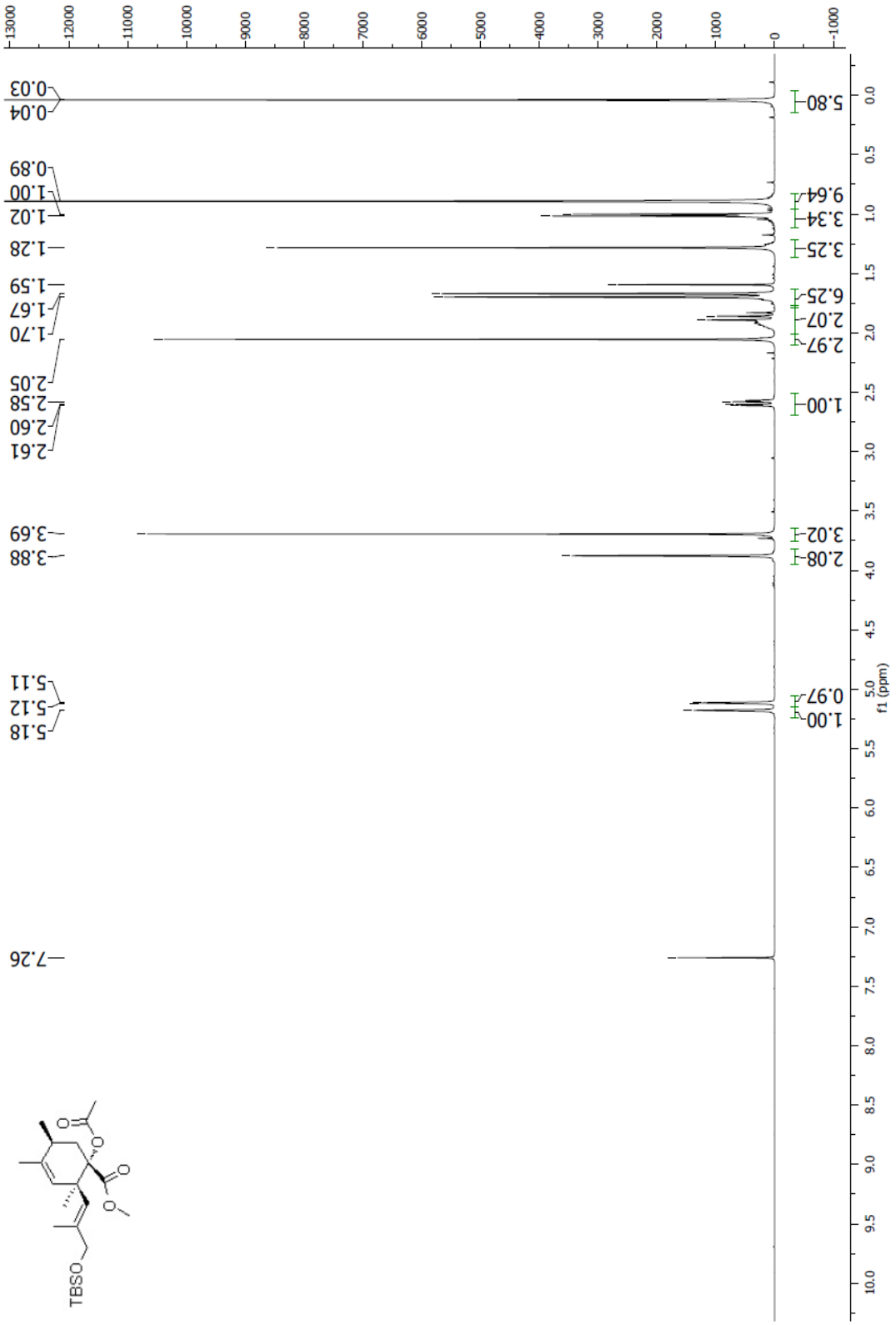

Spectrum 2.147 ^{1}H NMR ($CDCl_3$, 400 MHz) of compound **267**

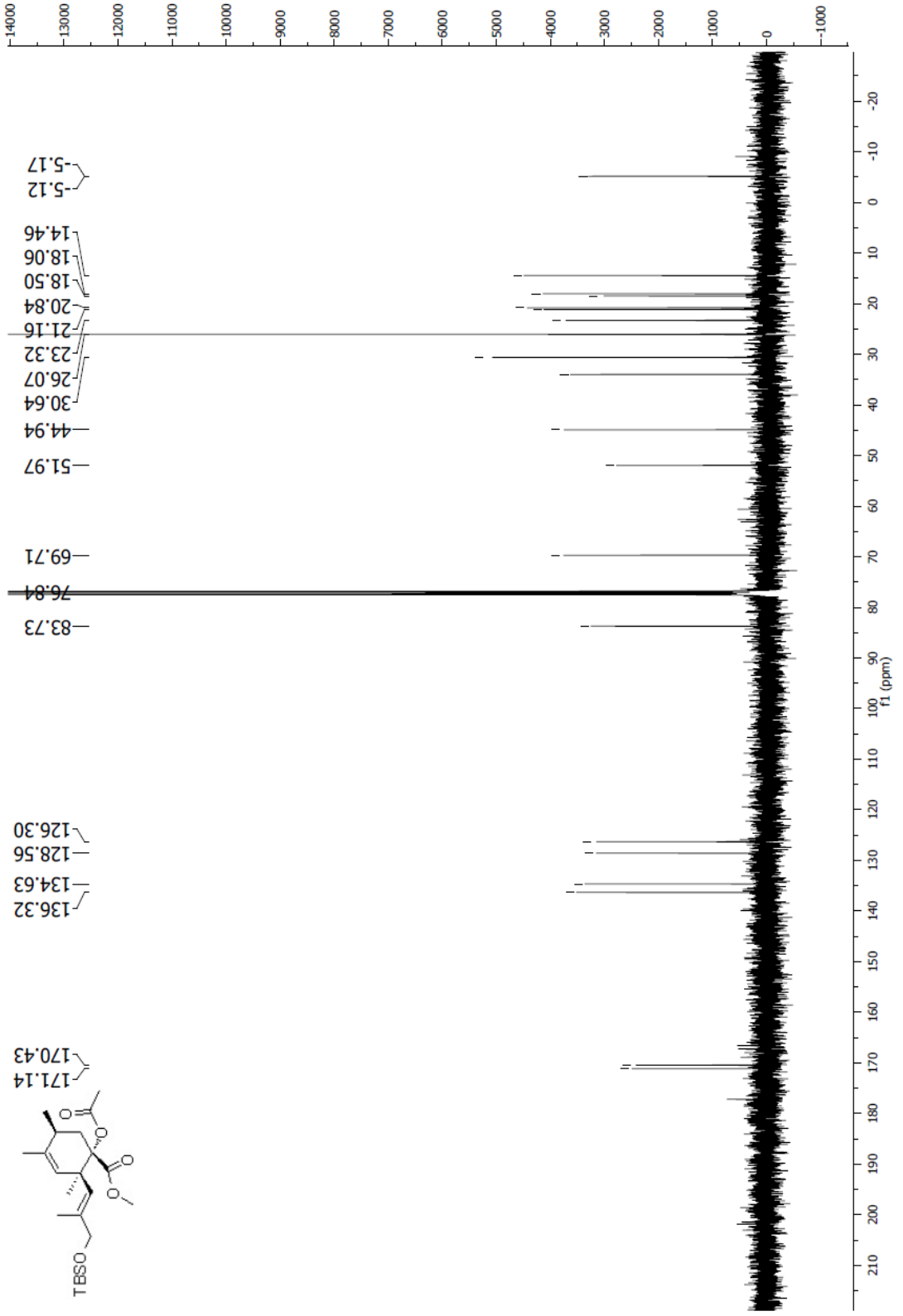

Spectrum 2.148 ^{13}C NMR ($CDCl_3$, 100 MHz) of compound **267**

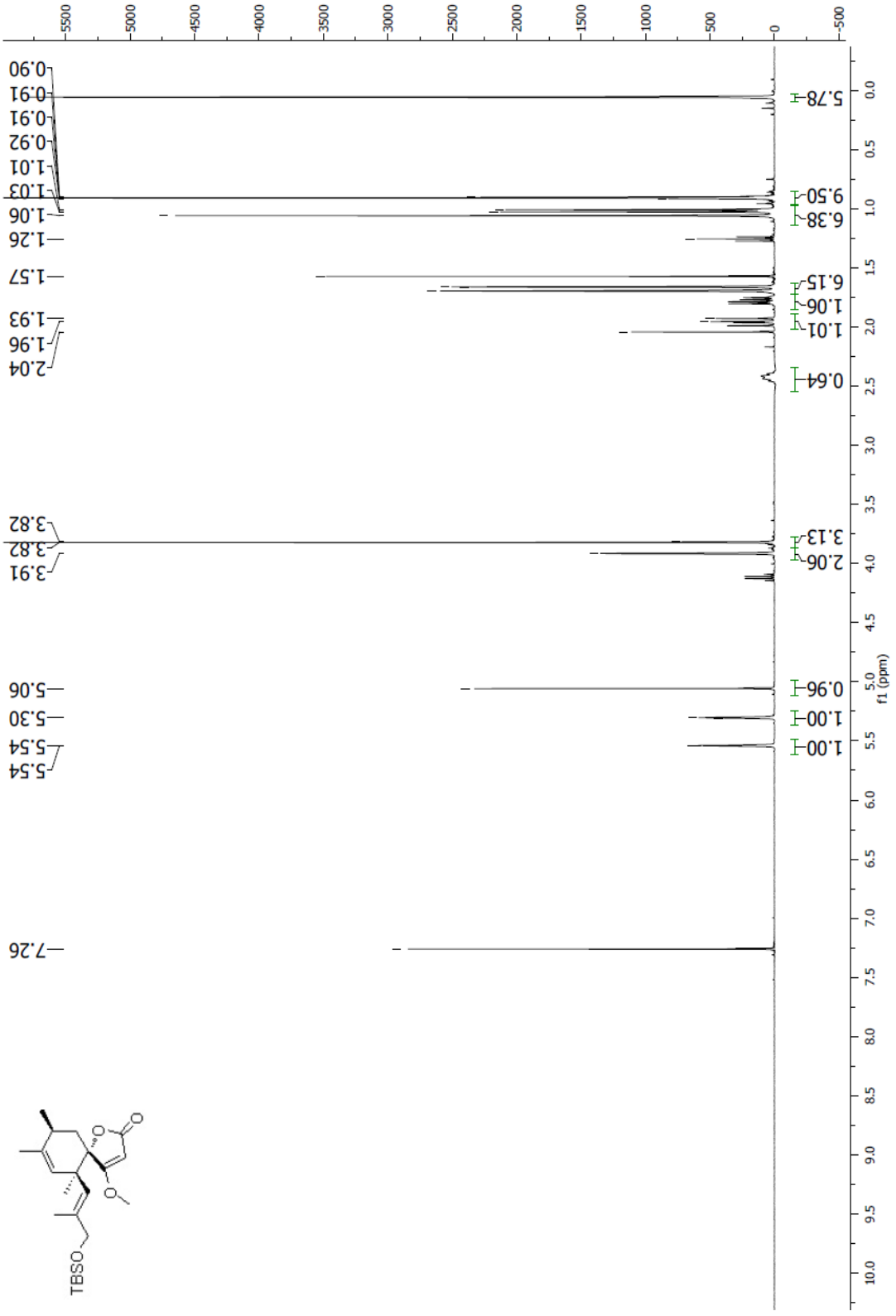

Spectrum 2.149 ^{1}H NMR ($CDCl_3$, 400 MHz) of compound **268**

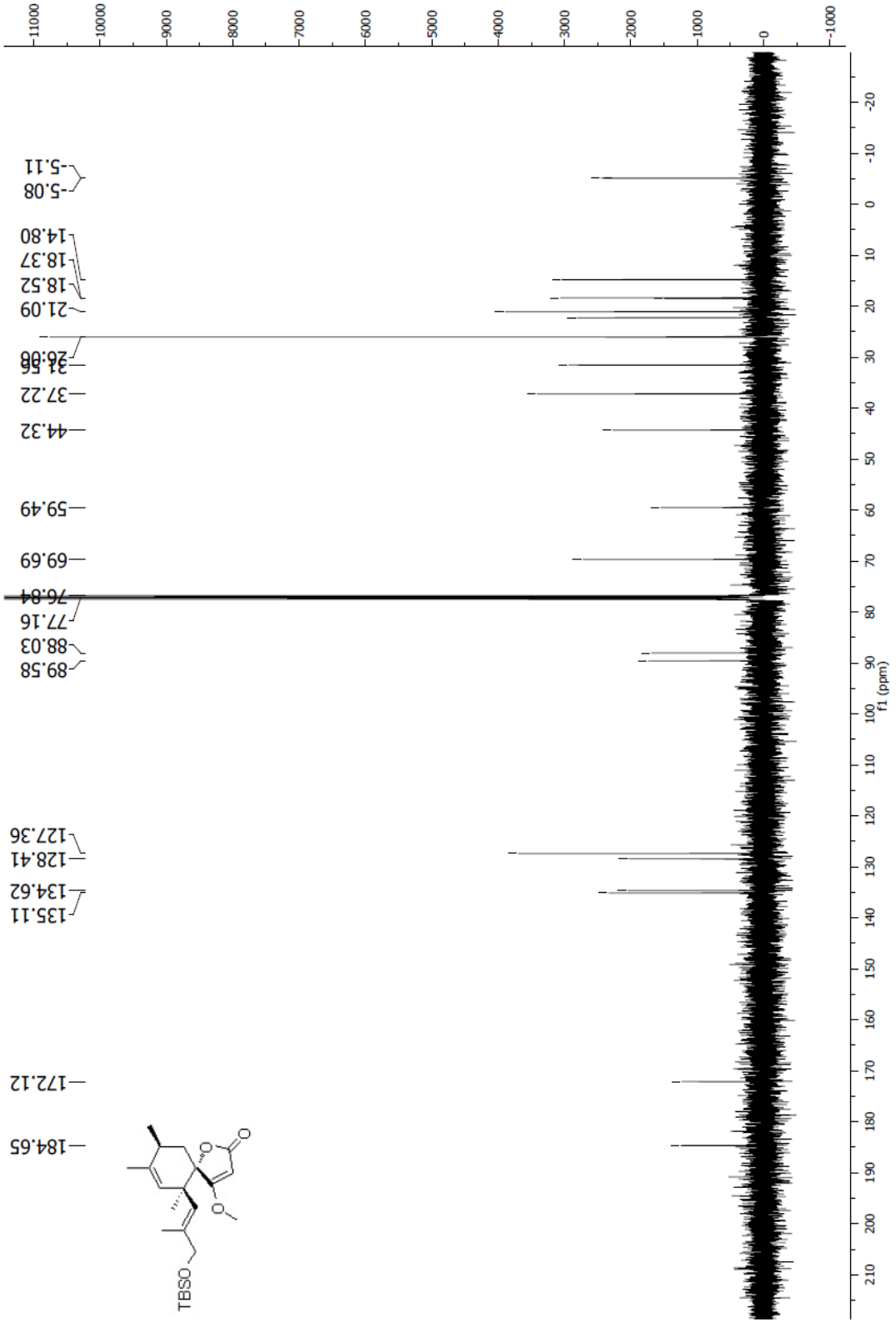

Spectrum 2.150 ^{13}C NMR ($CDCl_3$, 100 MHz) of compound **268**

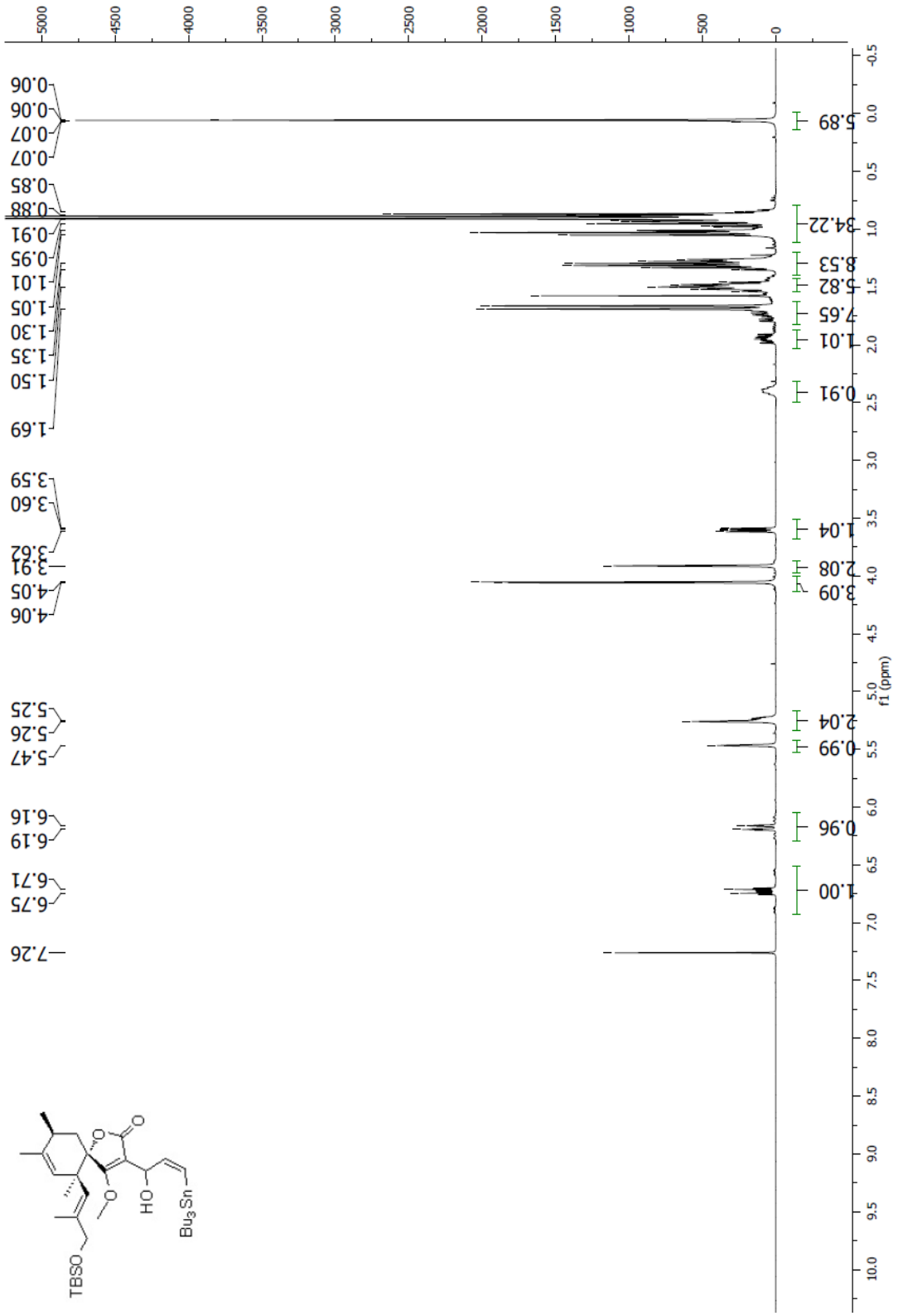

Spectrum 2.151 ^{1}H NMR ($CDCl_3$, 400 MHz) of compound **269**

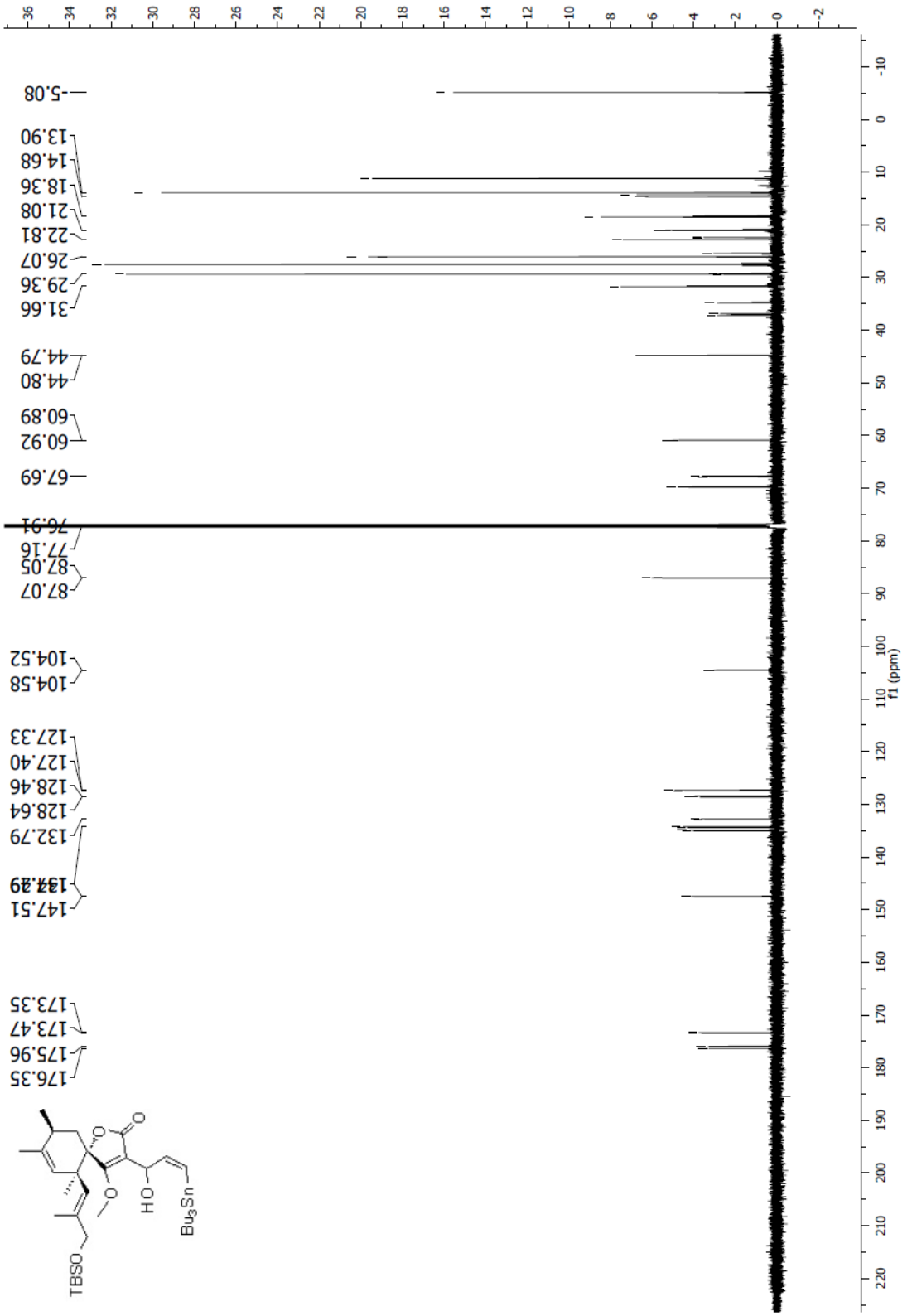

Spectrum 2.152 ^{13}C NMR ($CDCl_3$, 125 MHz) of compound **269**

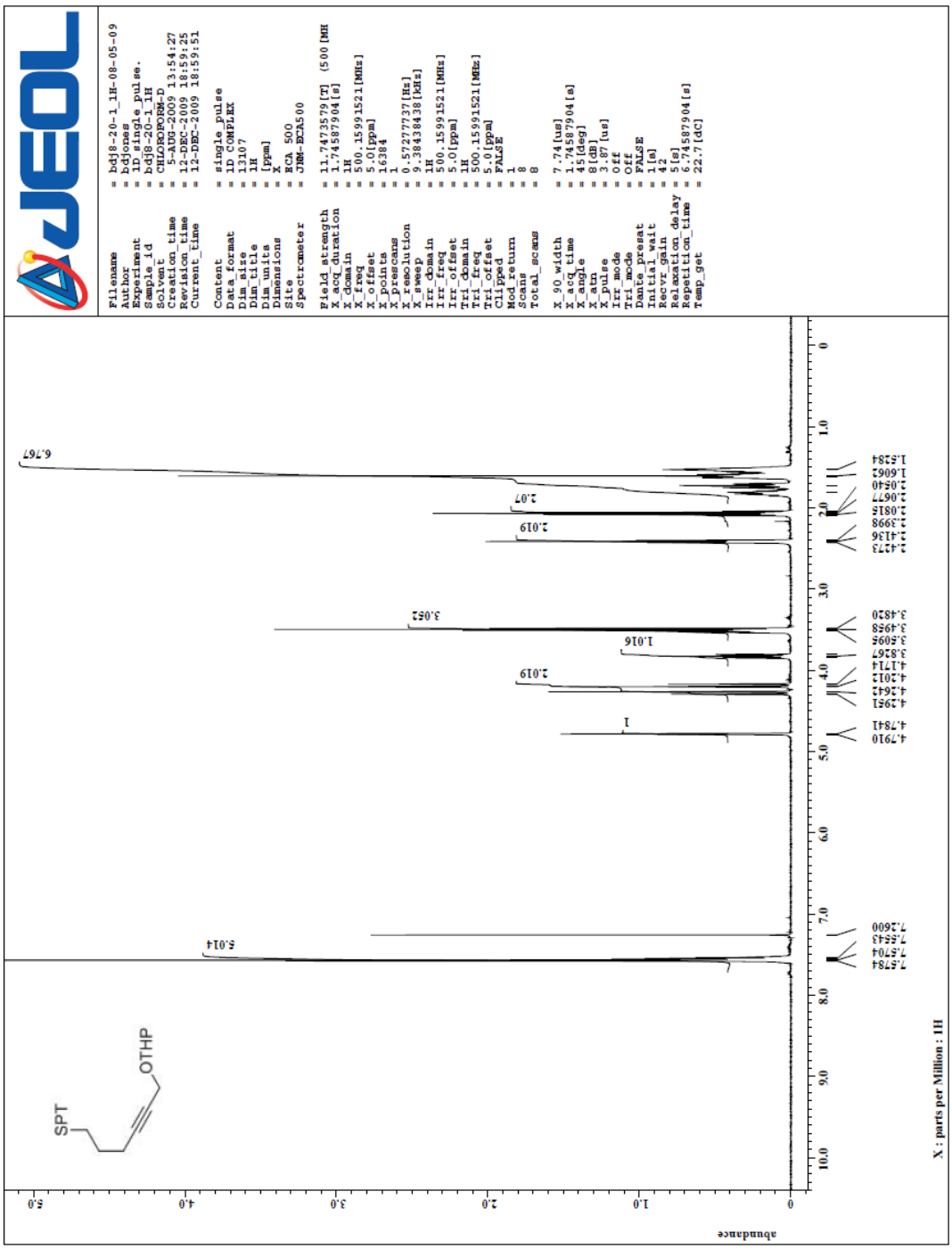

Spectrum 2.153 ^{1}H NMR ($CDCl_3$, 500 MHz) of sulfide precursor to **271**

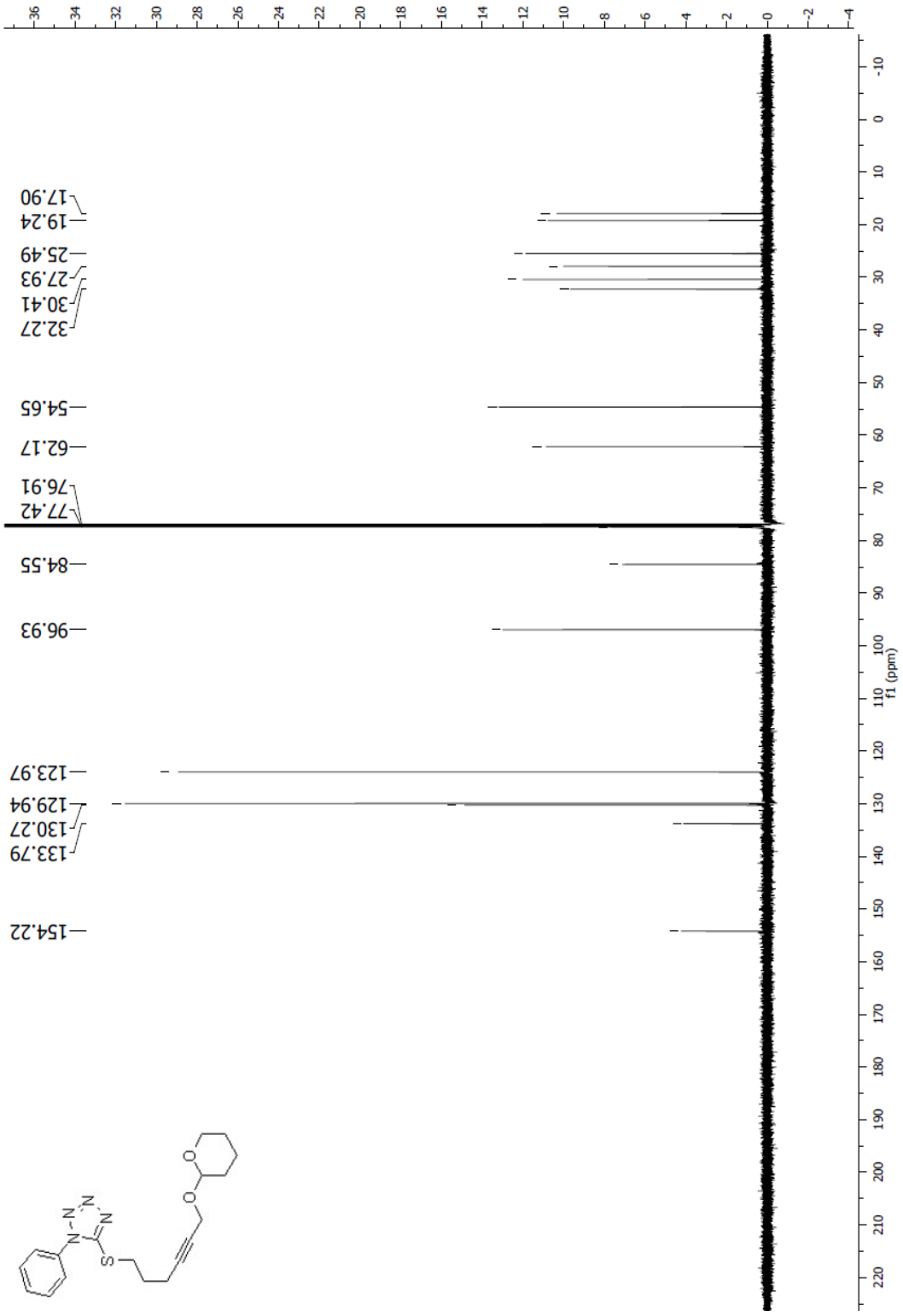

Spectrum 2.154 ^{13}C NMR ($CDCl_3$, 125 MHz) of sulfide precursor to **271**

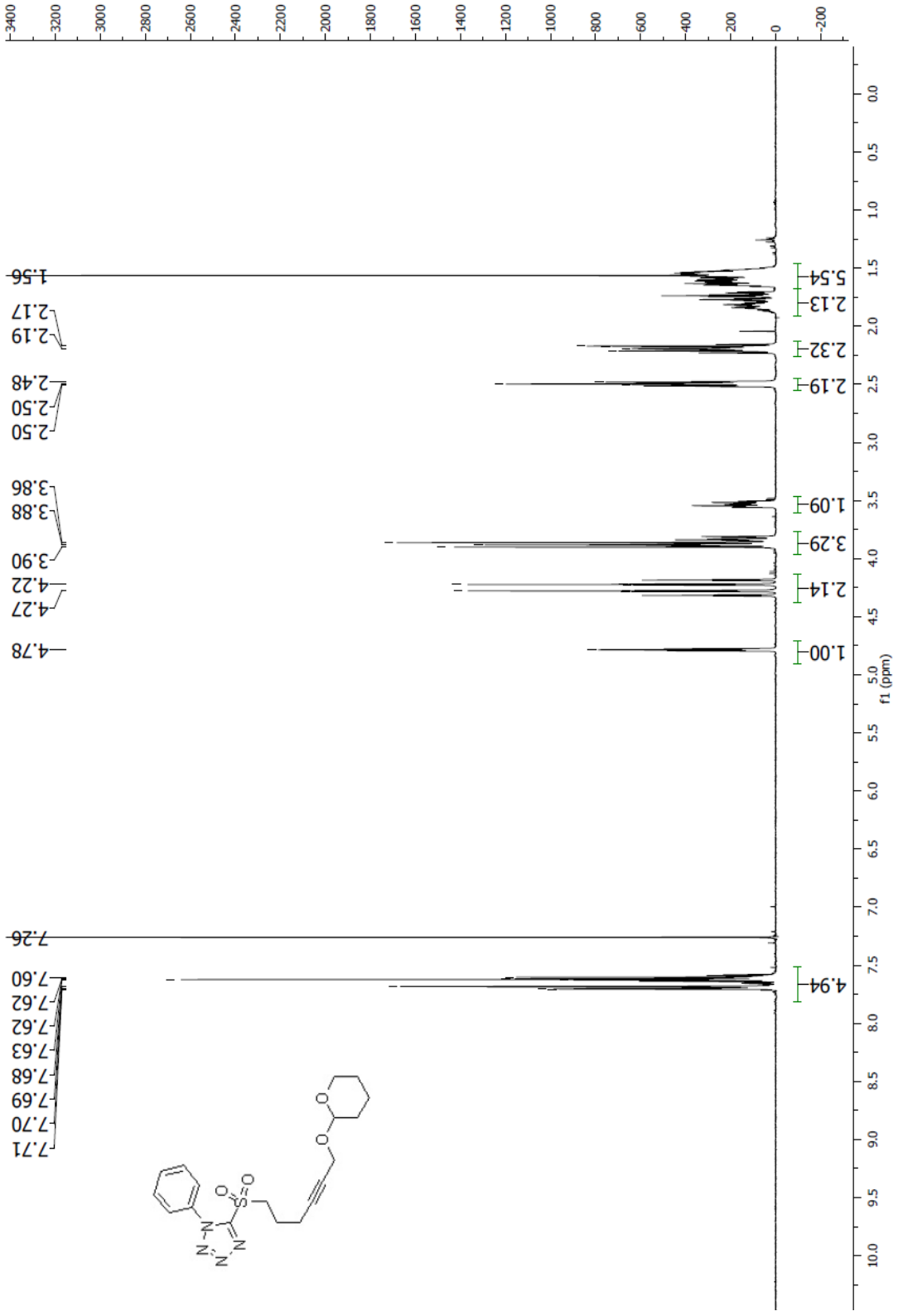

Spectrum 2.155 ^{1}H NMR ($CDCl_3$, 400 MHz) of compound **271**

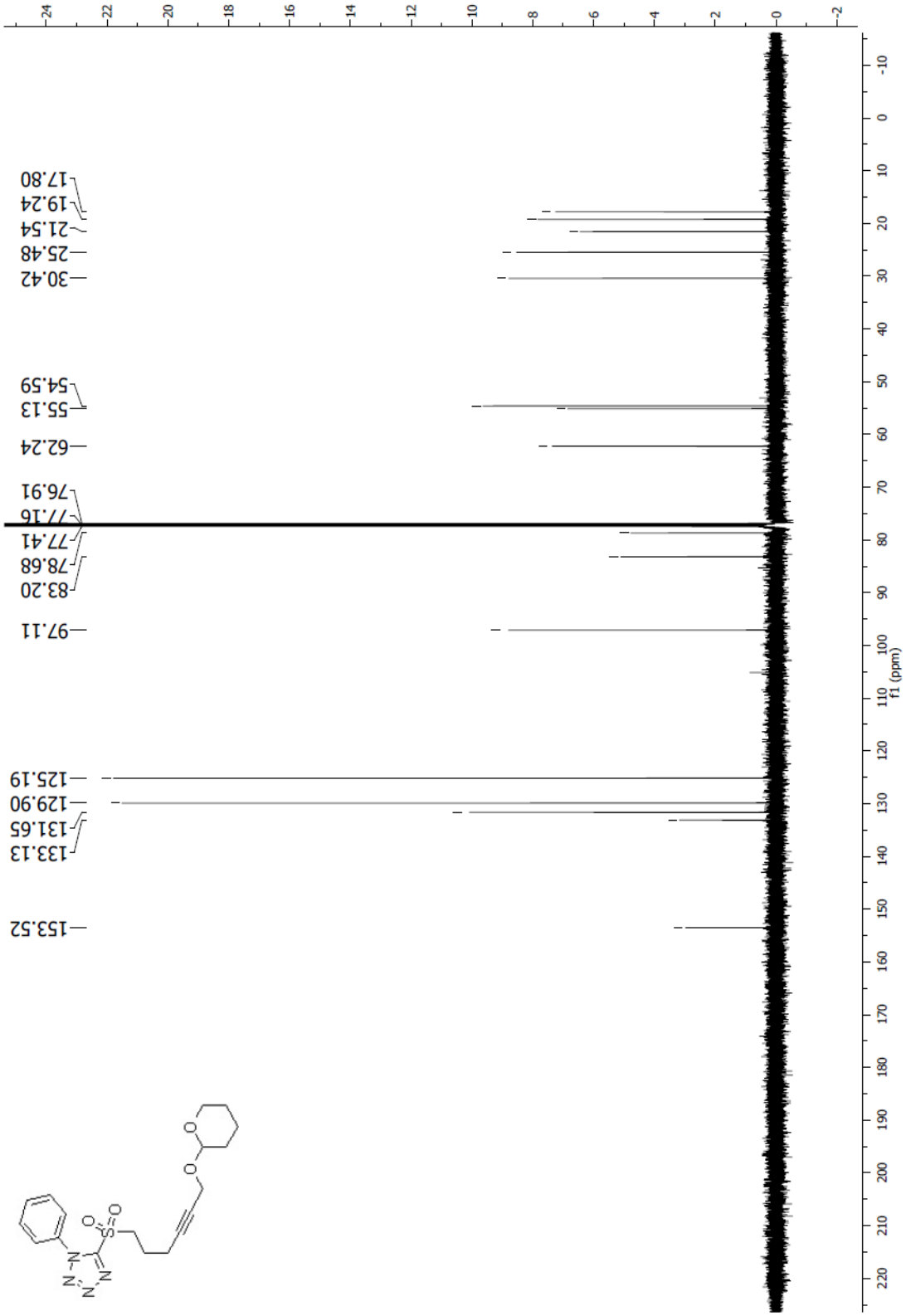

Spectrum 2.156 ^{13}C NMR ($CDCl_3$, 125 MHz) of compound **271**

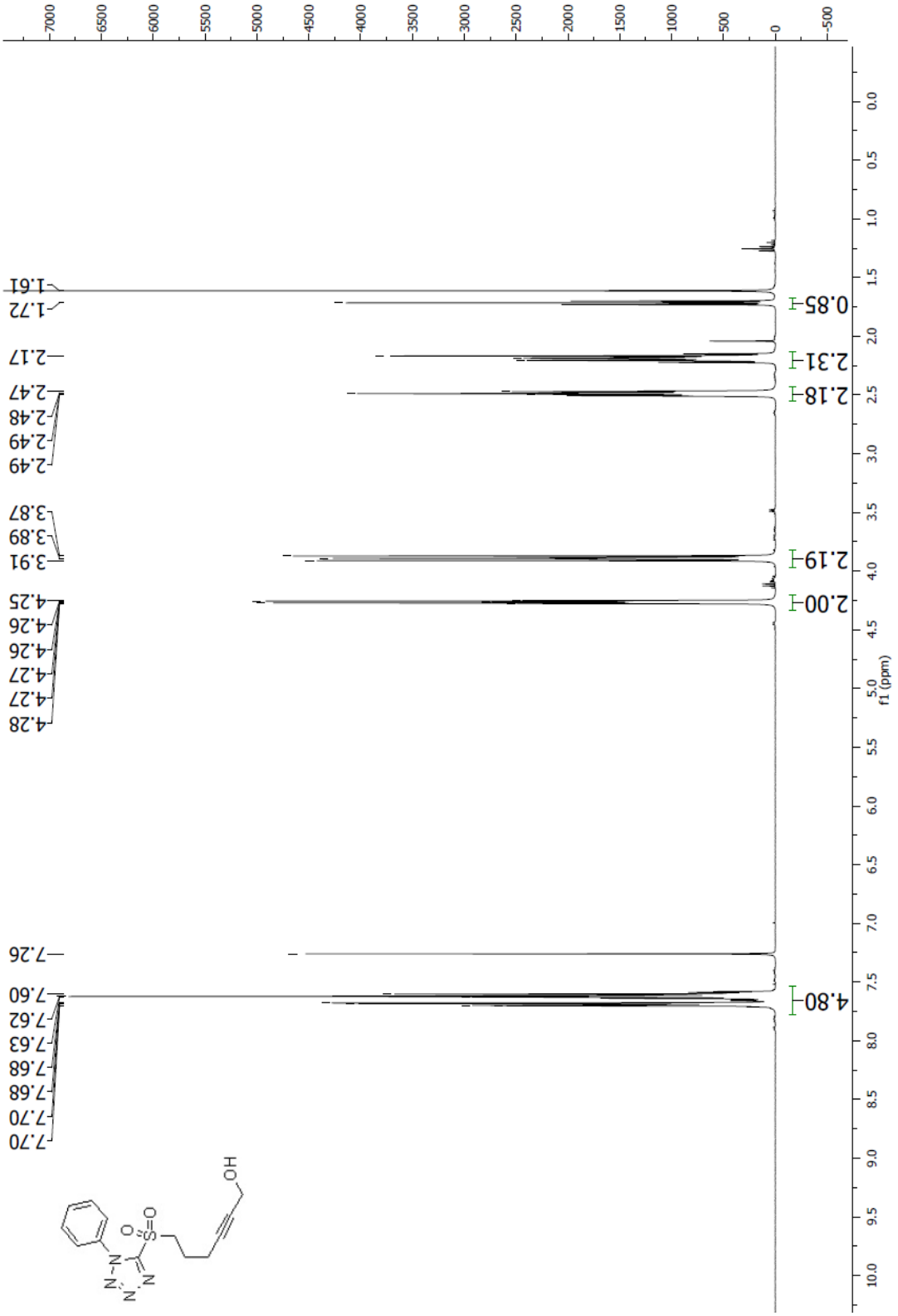

Spectrum 2.157 ^{1}H NMR ($CDCl_3$, 400 MHz) of compound **272**

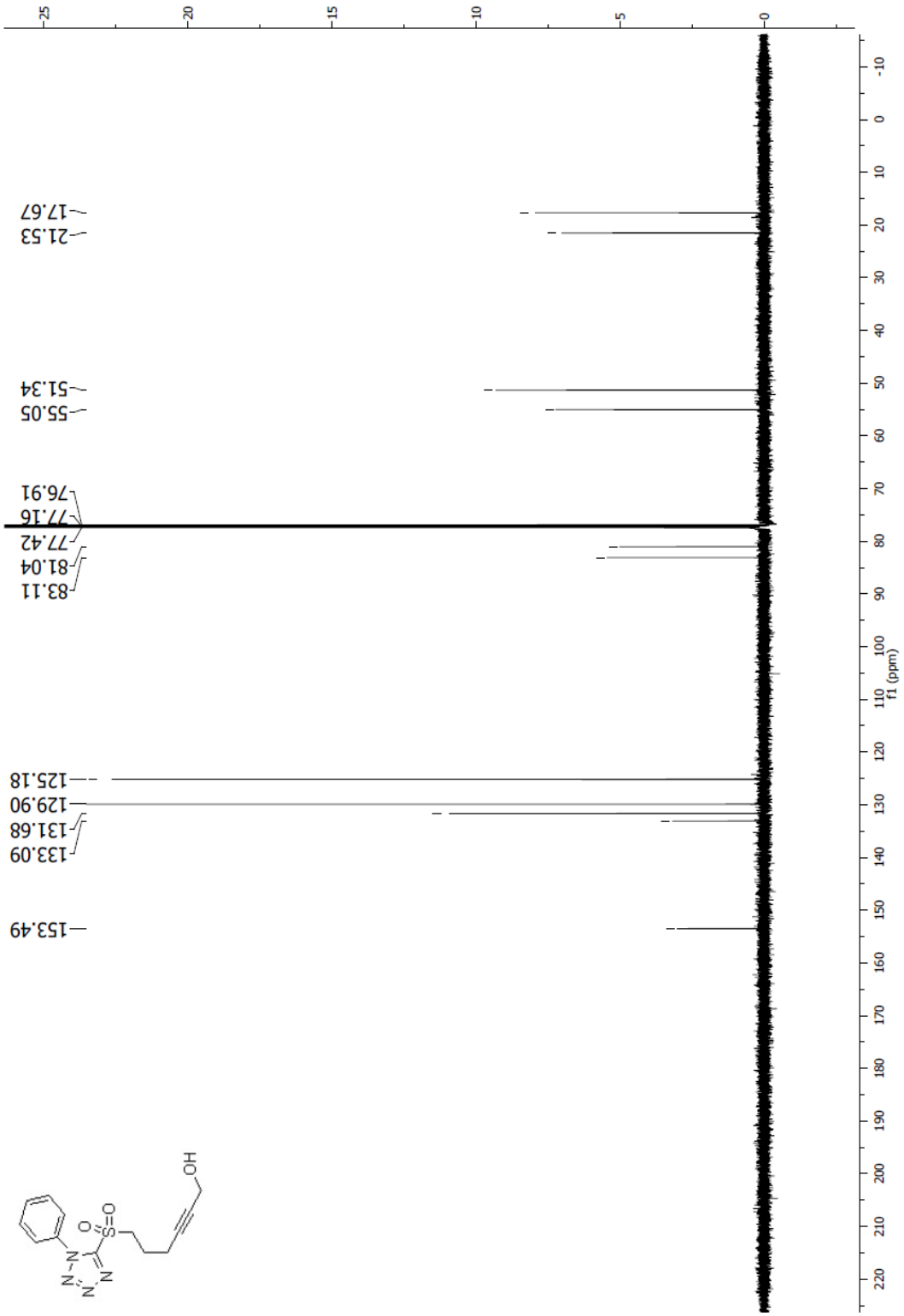

Spectrum 2.158 ^{13}C NMR ($CDCl_3$, 125 MHz) of compound **272**

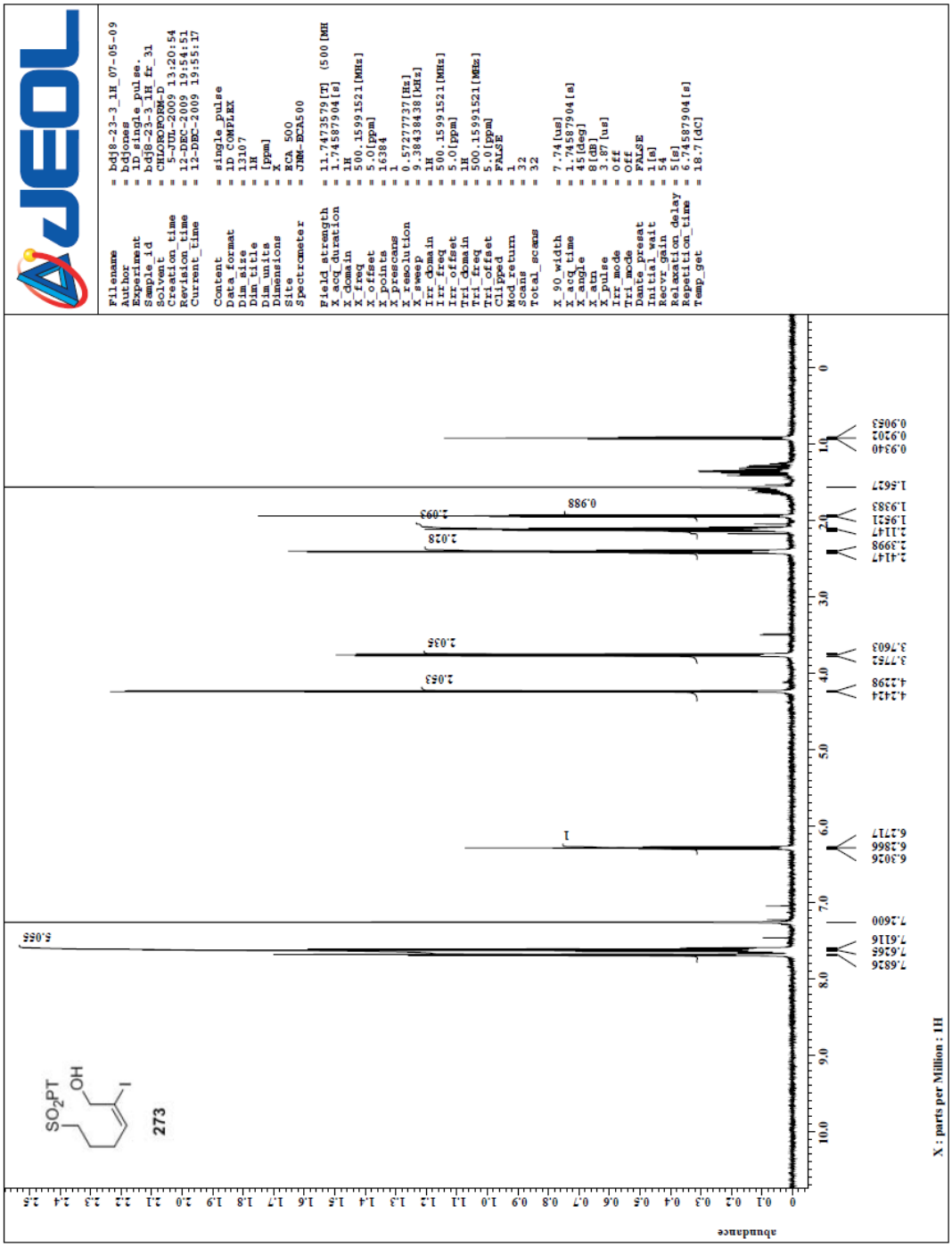

Spectrum 2.159 ^{1}H NMR ($CDCl_3$, 500 MHz) of compound **273**

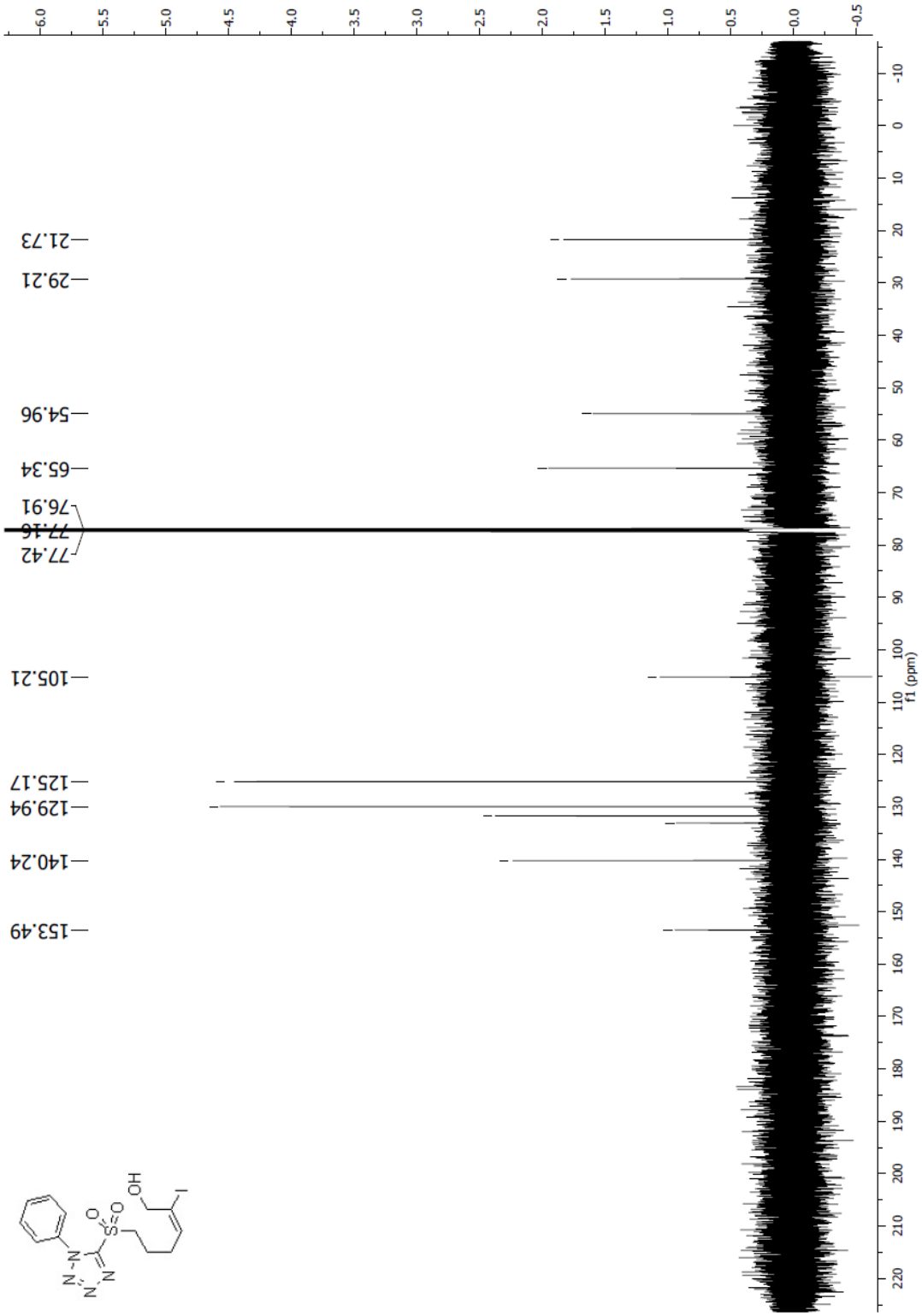

Spectrum 2.160 ^{13}C NMR ($CDCl_3$, 125 MHz) of compound **273**

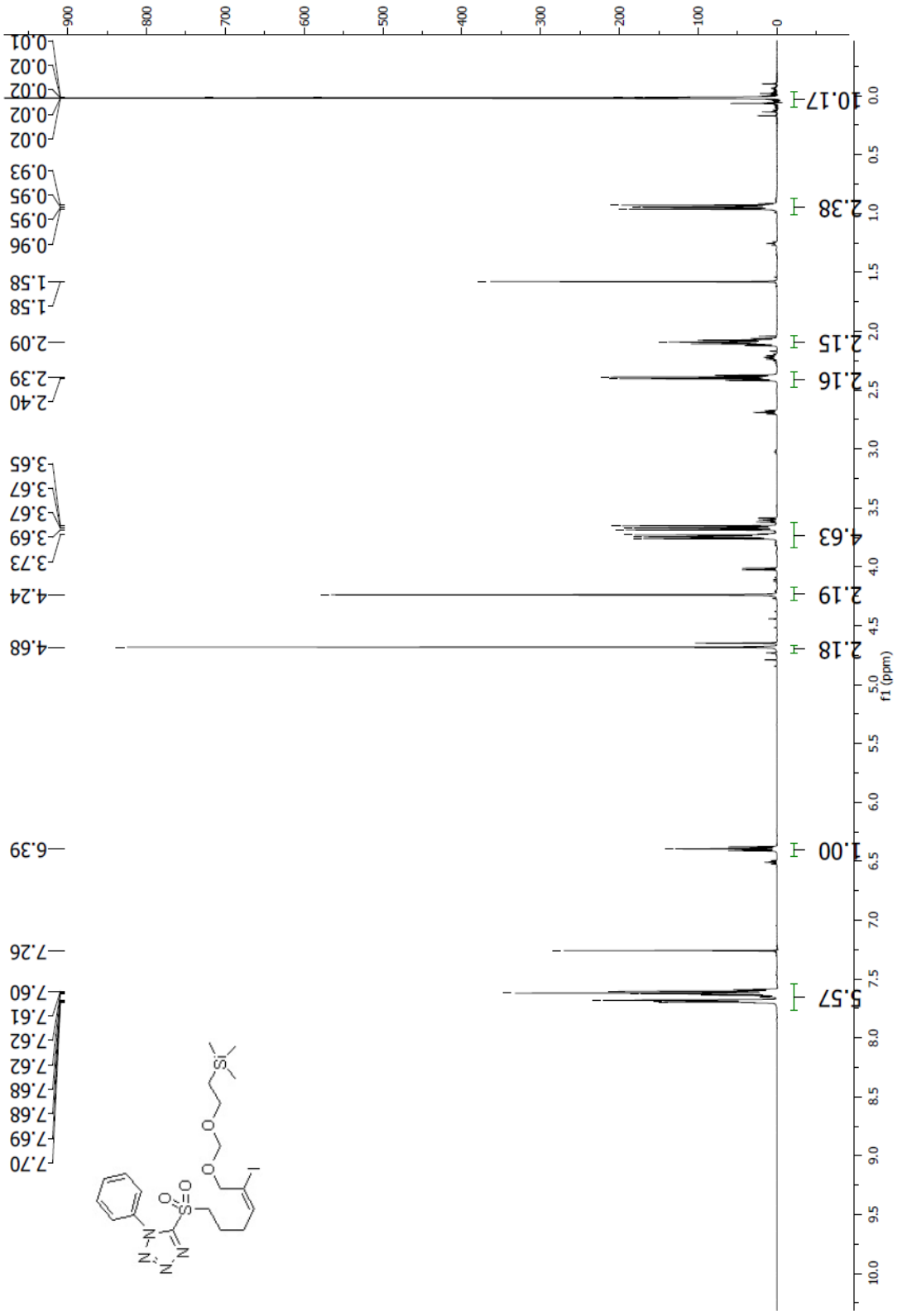

Spectrum 2.161 ^{1}H NMR ($CDCl_3$, 500 MHz) of compound **274**

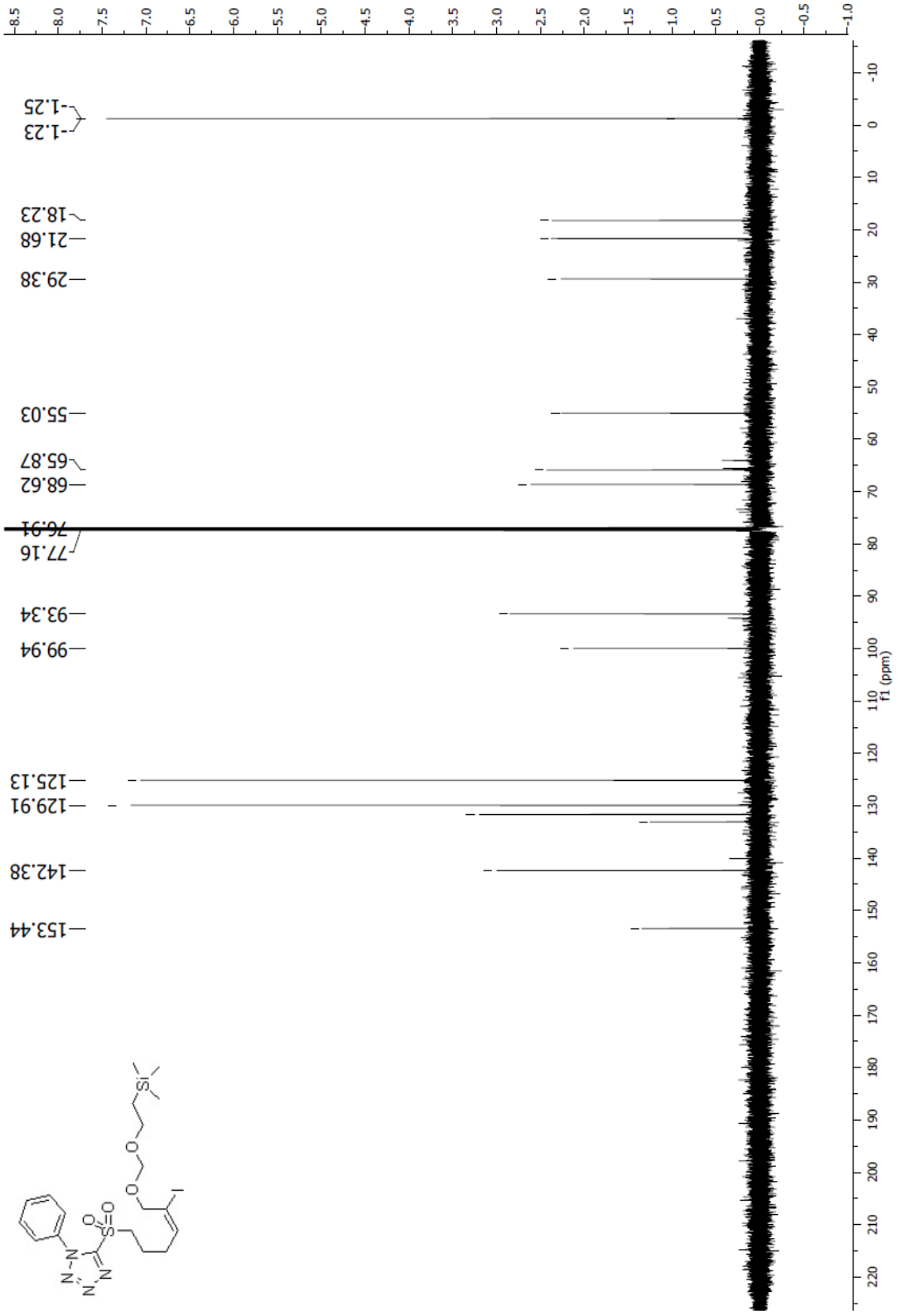

Spectrum 2.162 ^{13}C NMR ($CDCl_3$, 125 MHz) of compound **274**

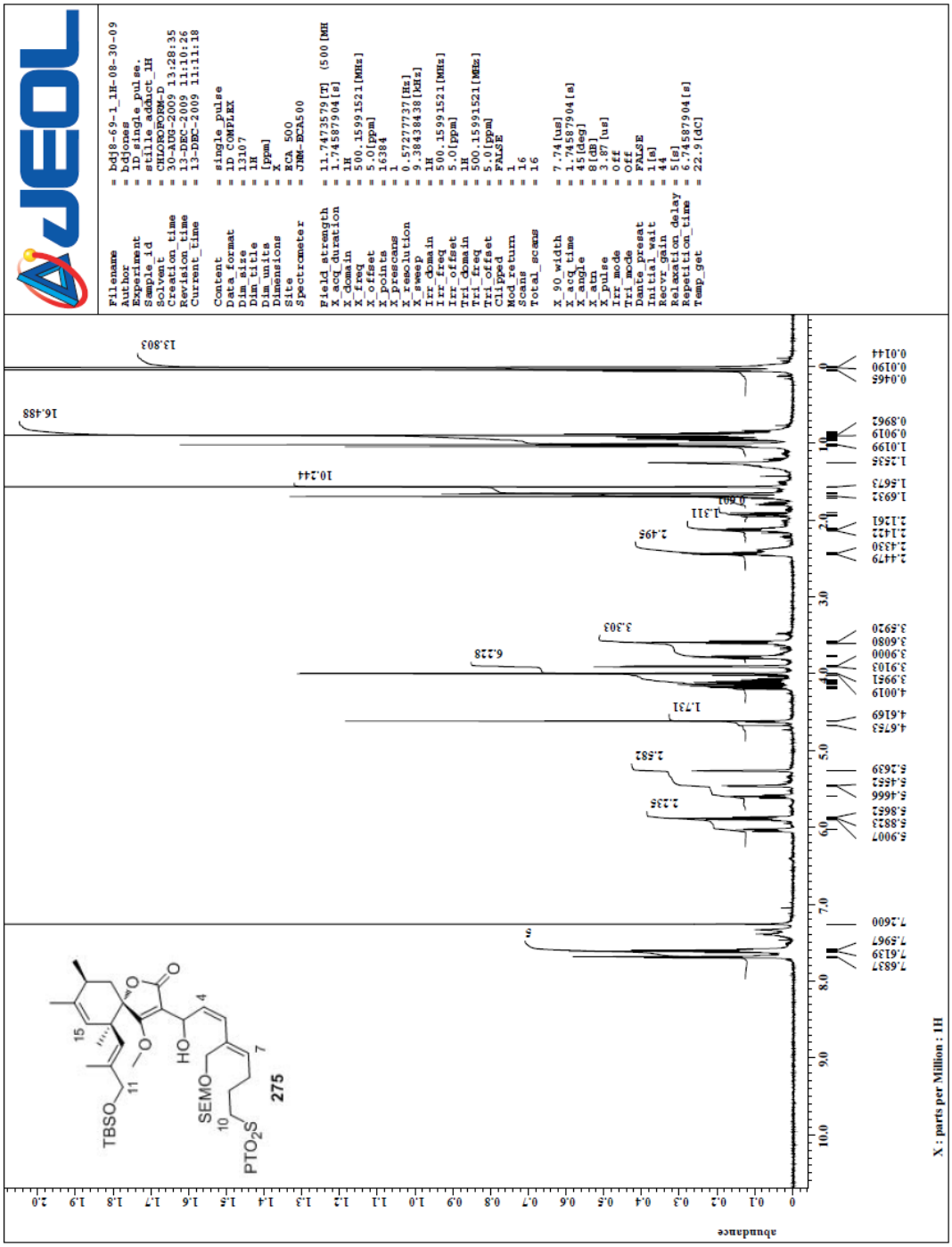

Spectrum 2.163 ^{1}H NMR ($CDCl_3$, 500 MHz) of compound **275**

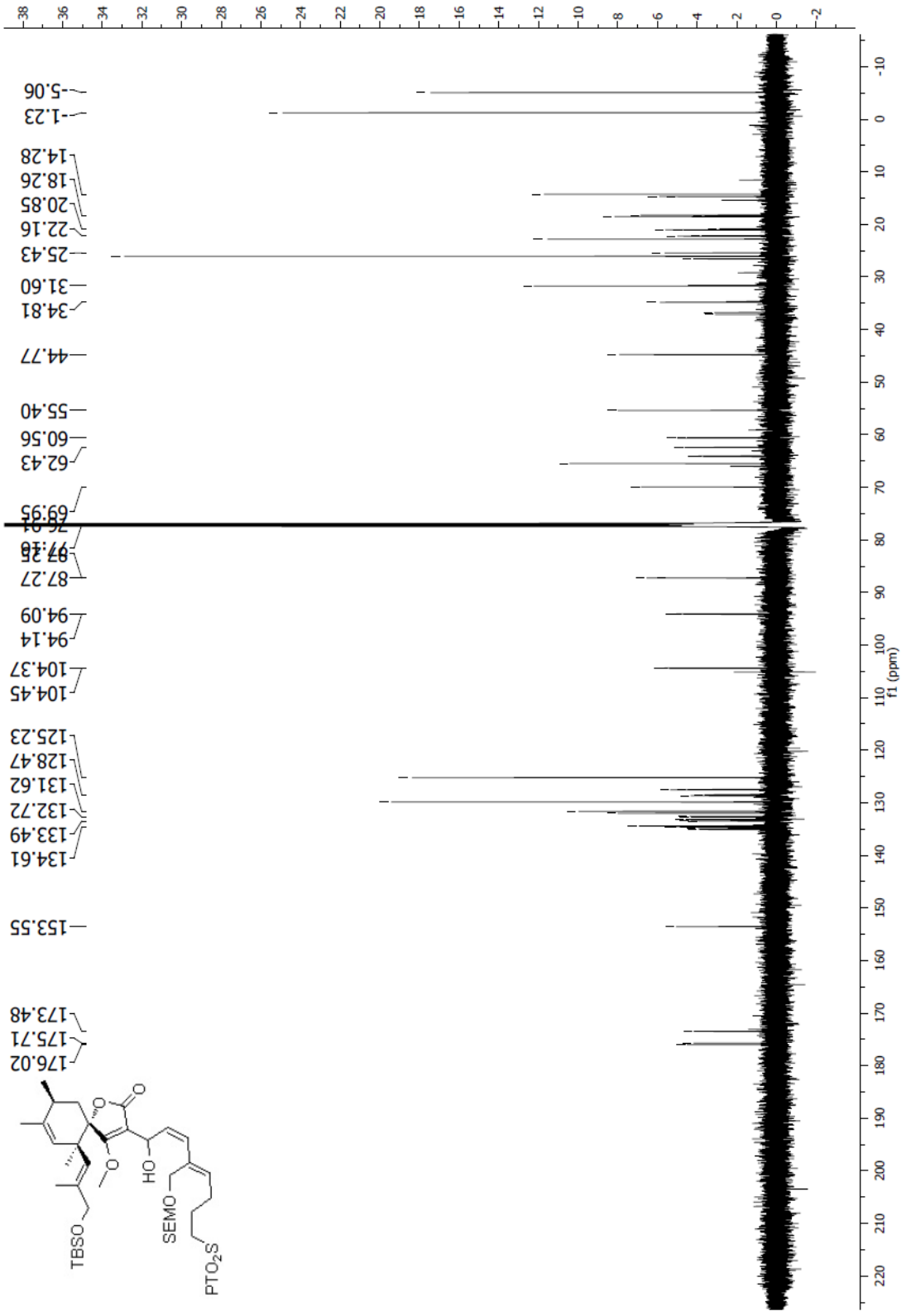

Spectrum 2.164 ^{13}C NMR ($CDCl_3$, 125 MHz) of compound **275**

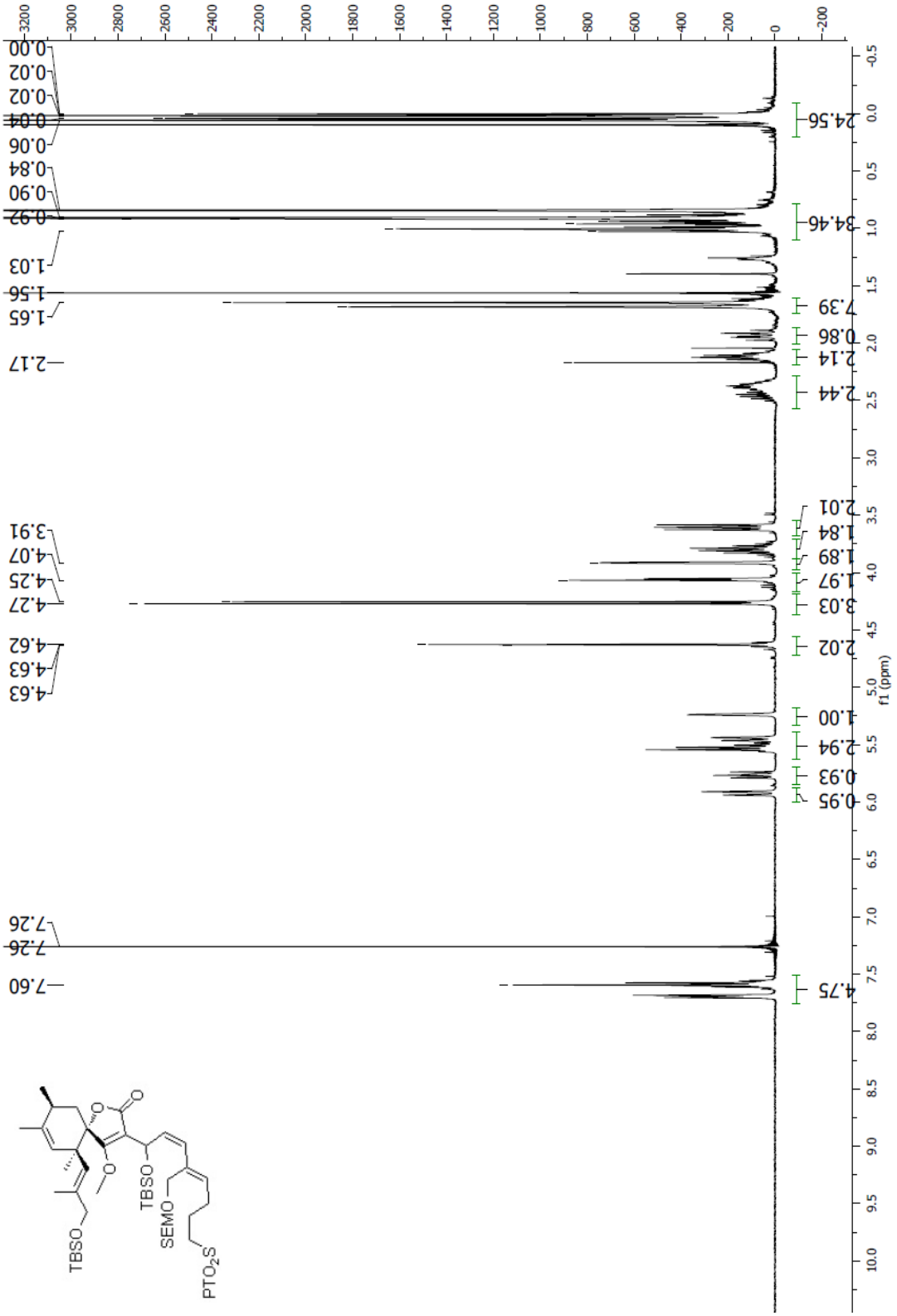

Spectrum 2.165 ^{1}H NMR ($CDCl_3$, 400 MHz) of compound **276**

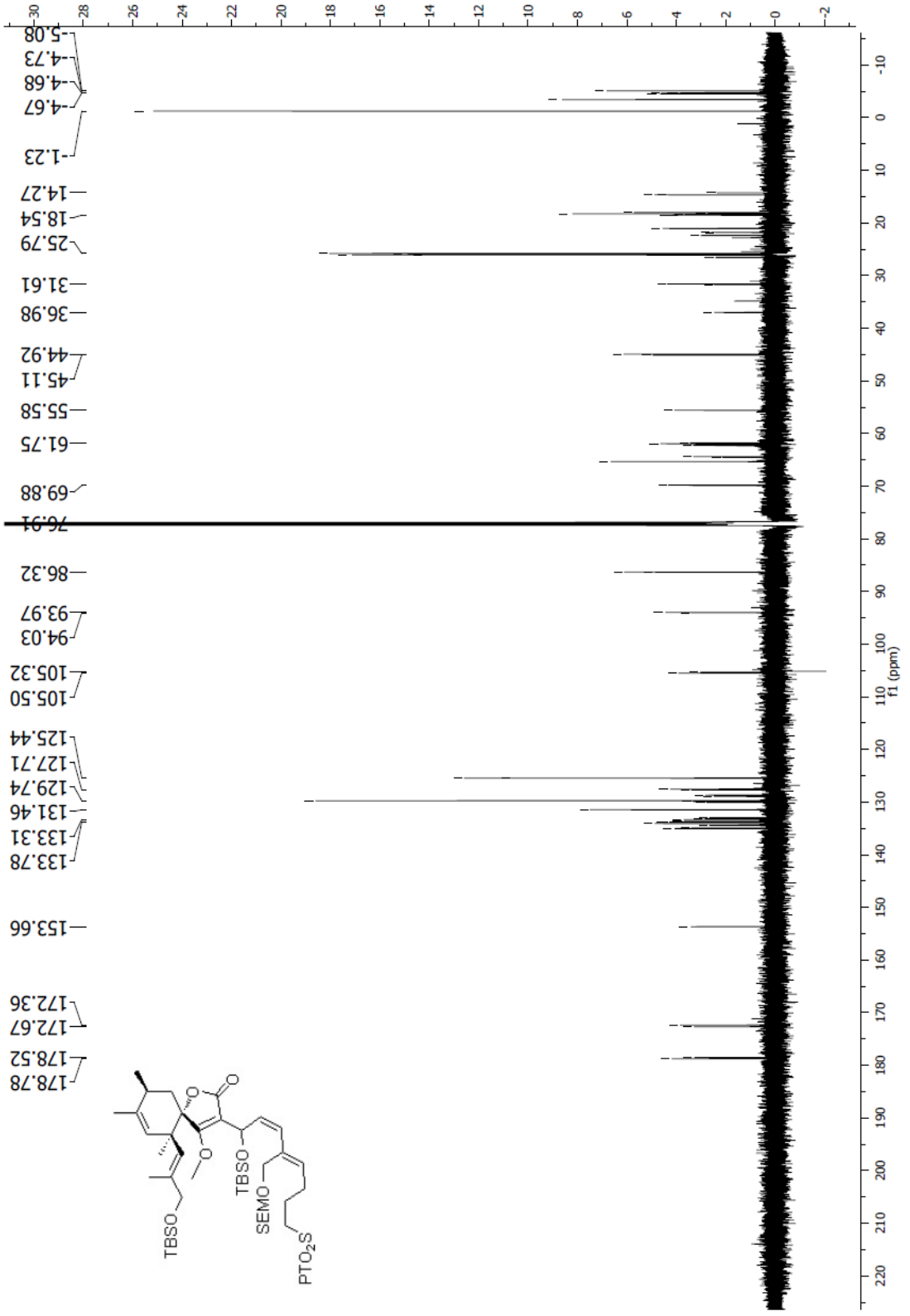

Spectrum 2.166 ^{13}C NMR ($CDCl_3$, 125 MHz) of compound **276**

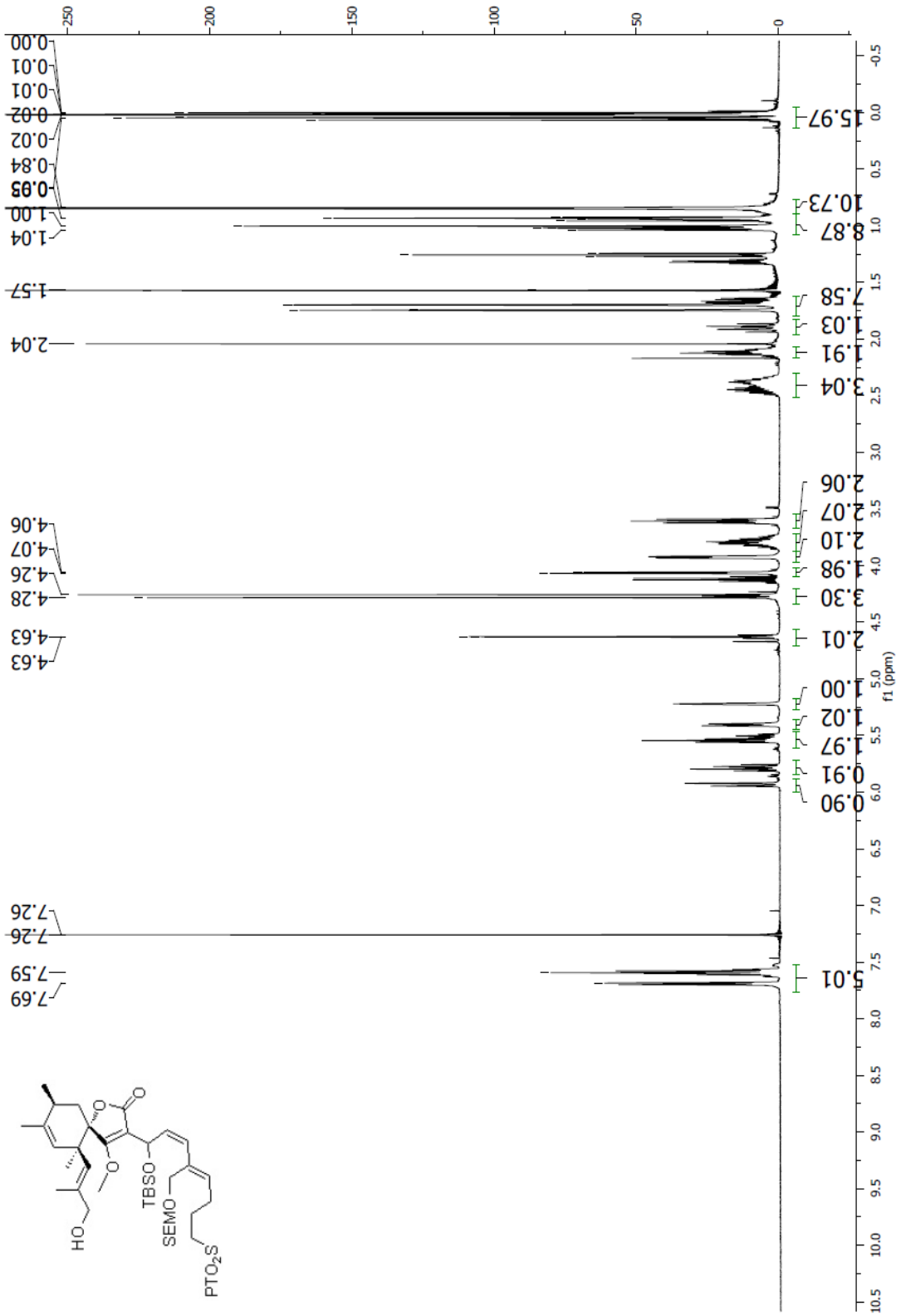

Spectrum 2.167 ^{1}H NMR ($CDCl_3$, 500 MHz) of compound **277**

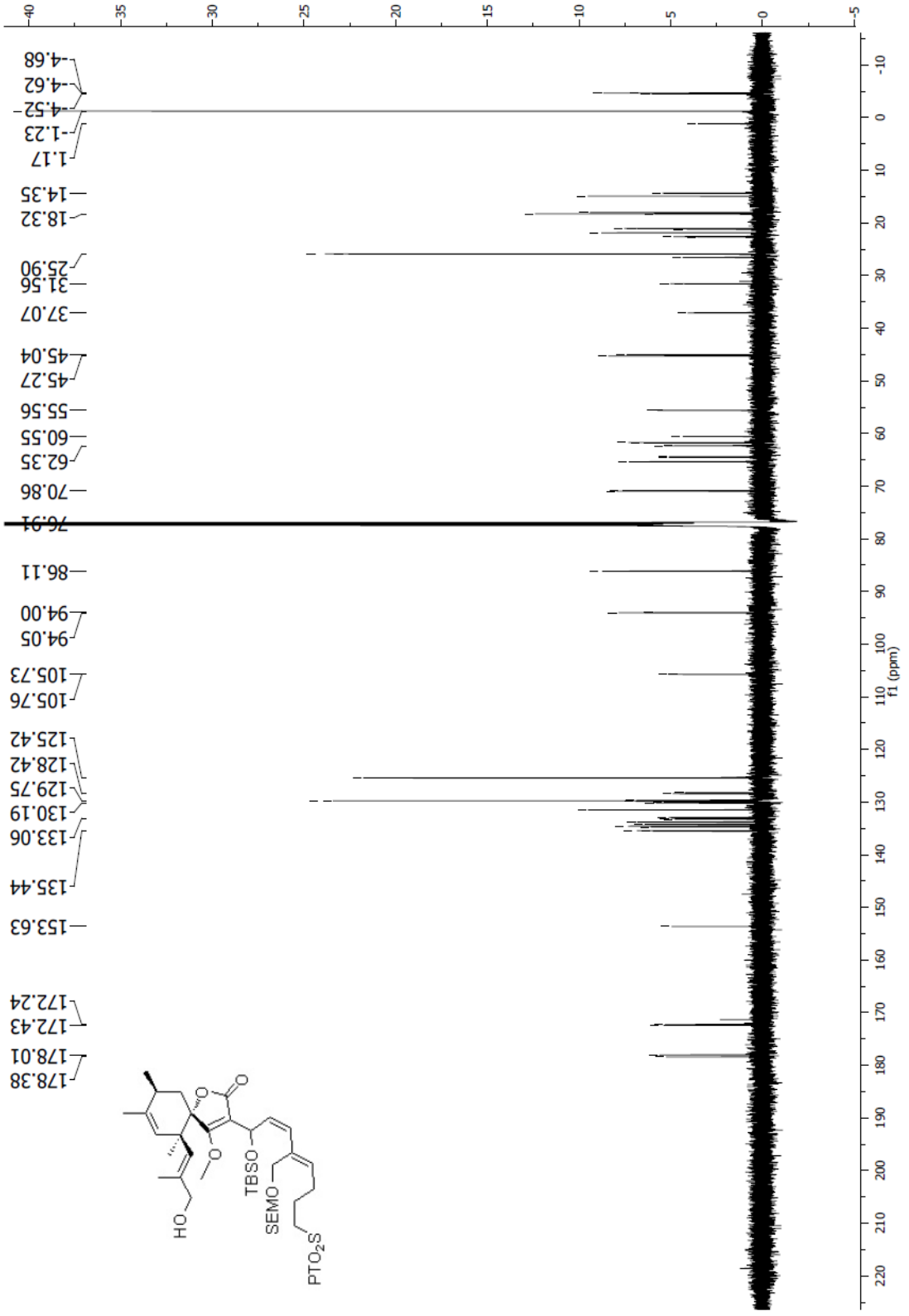

Spectrum 2.168 ^{13}C NMR ($CDCl_3$, 125 MHz) of compound **277**

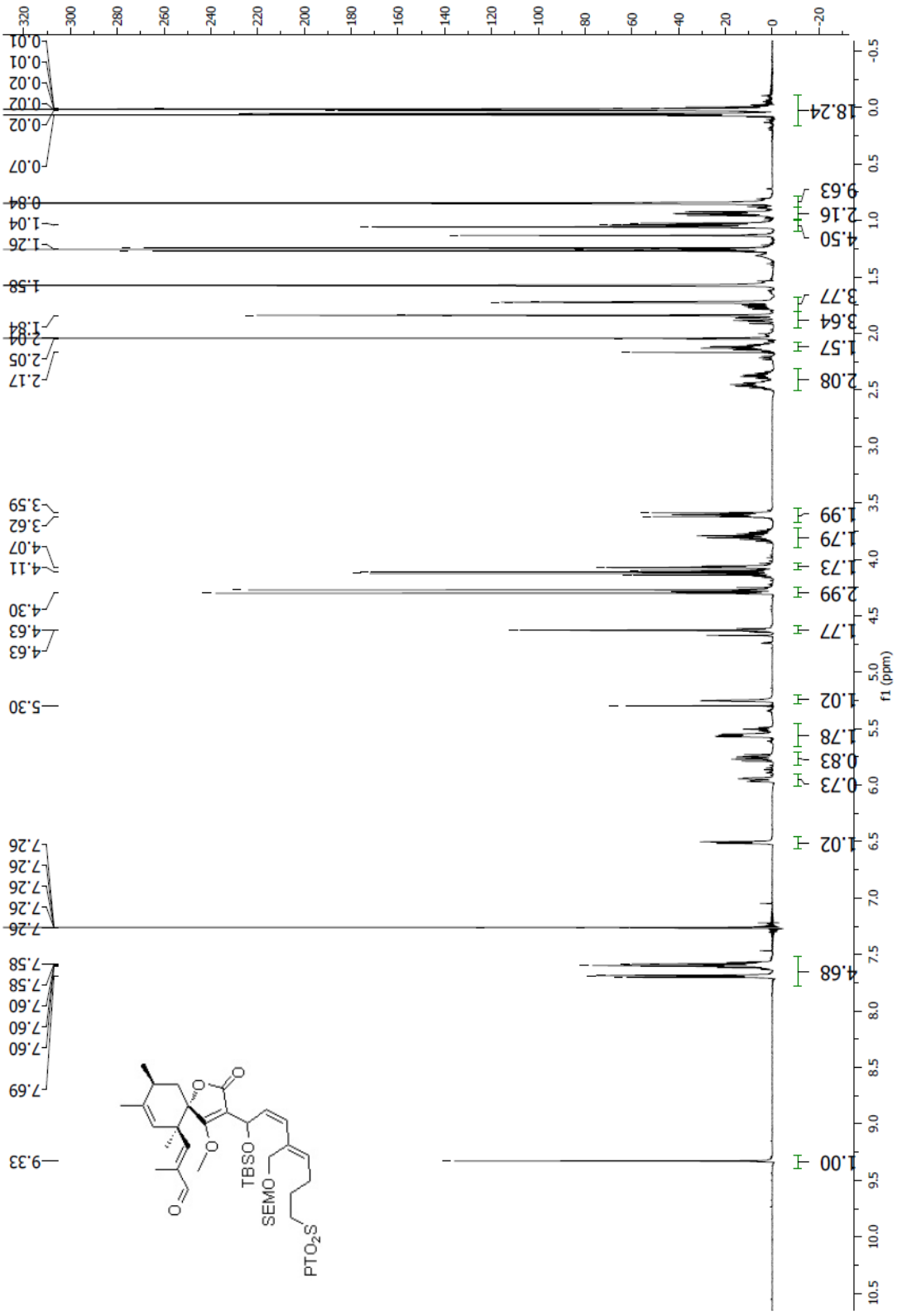

Spectrum 2.169 ^{1}H NMR ($CDCl_3$, 500 MHz) of compound **278**

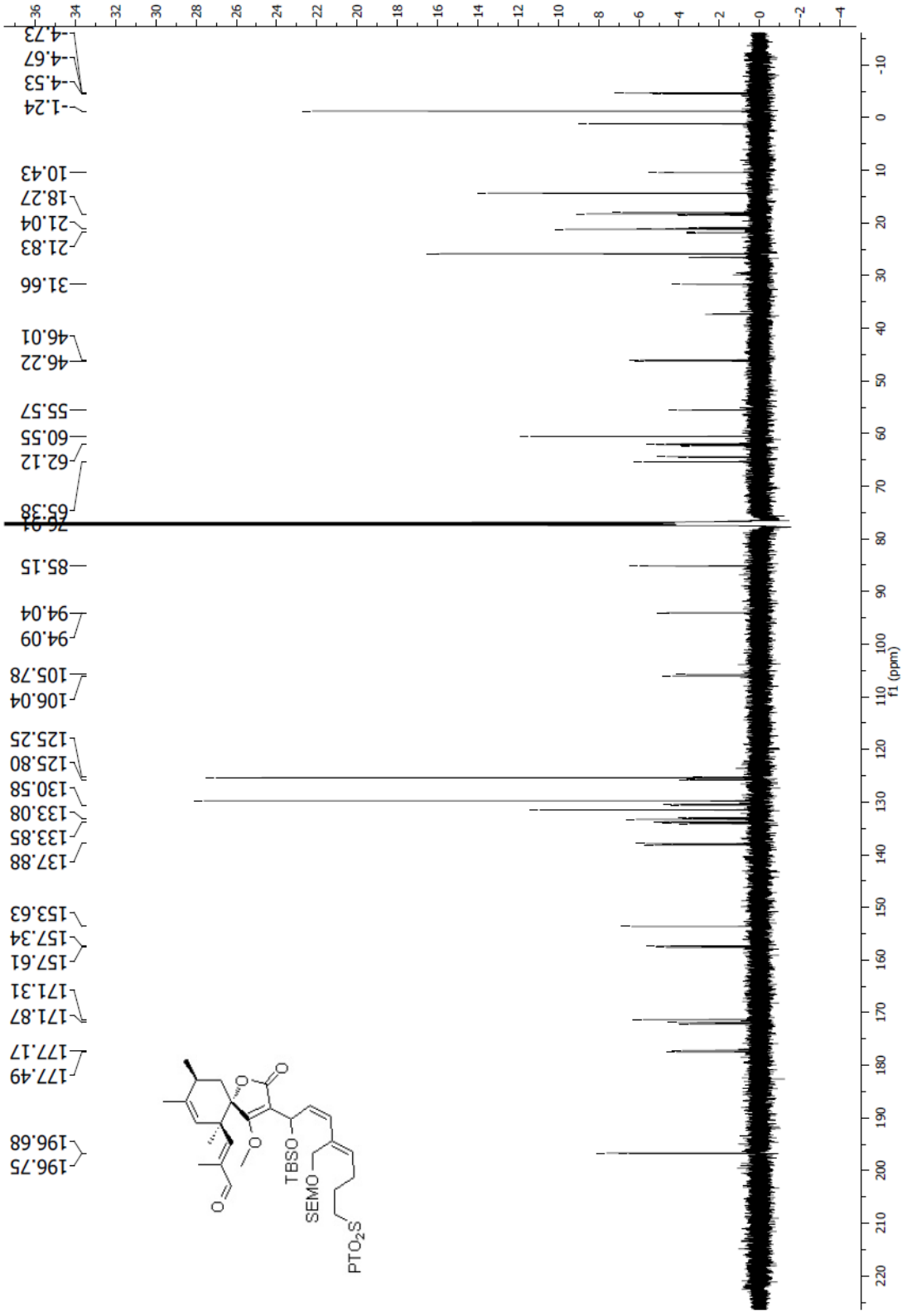

Spectrum 2.170 ^{13}C NMR ($CDCl_3$, 125 MHz) of compound **278**

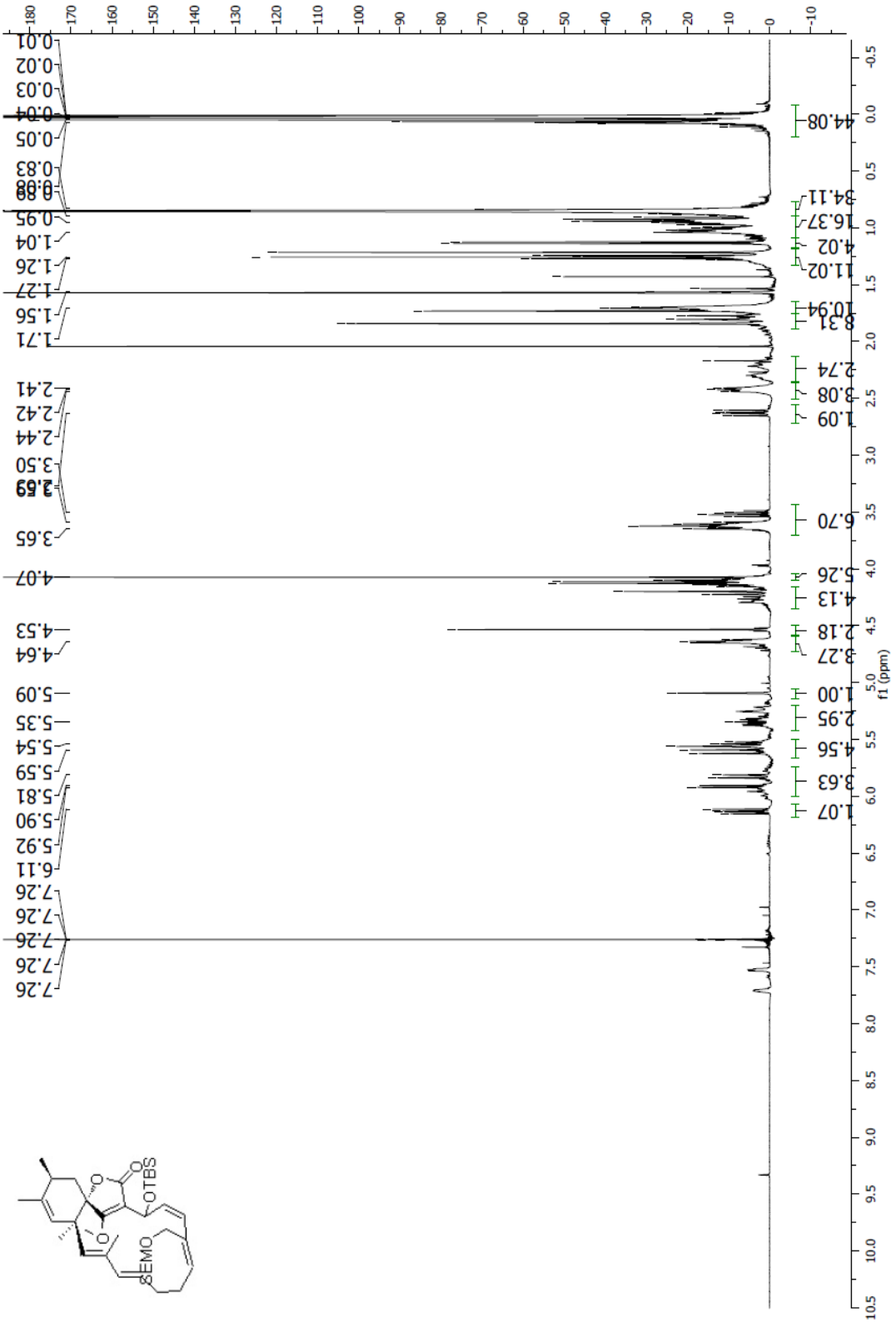

Spectrum 2.171 ^{1}H NMR ($CDCl_3$, 500 MHz) of compound **279**

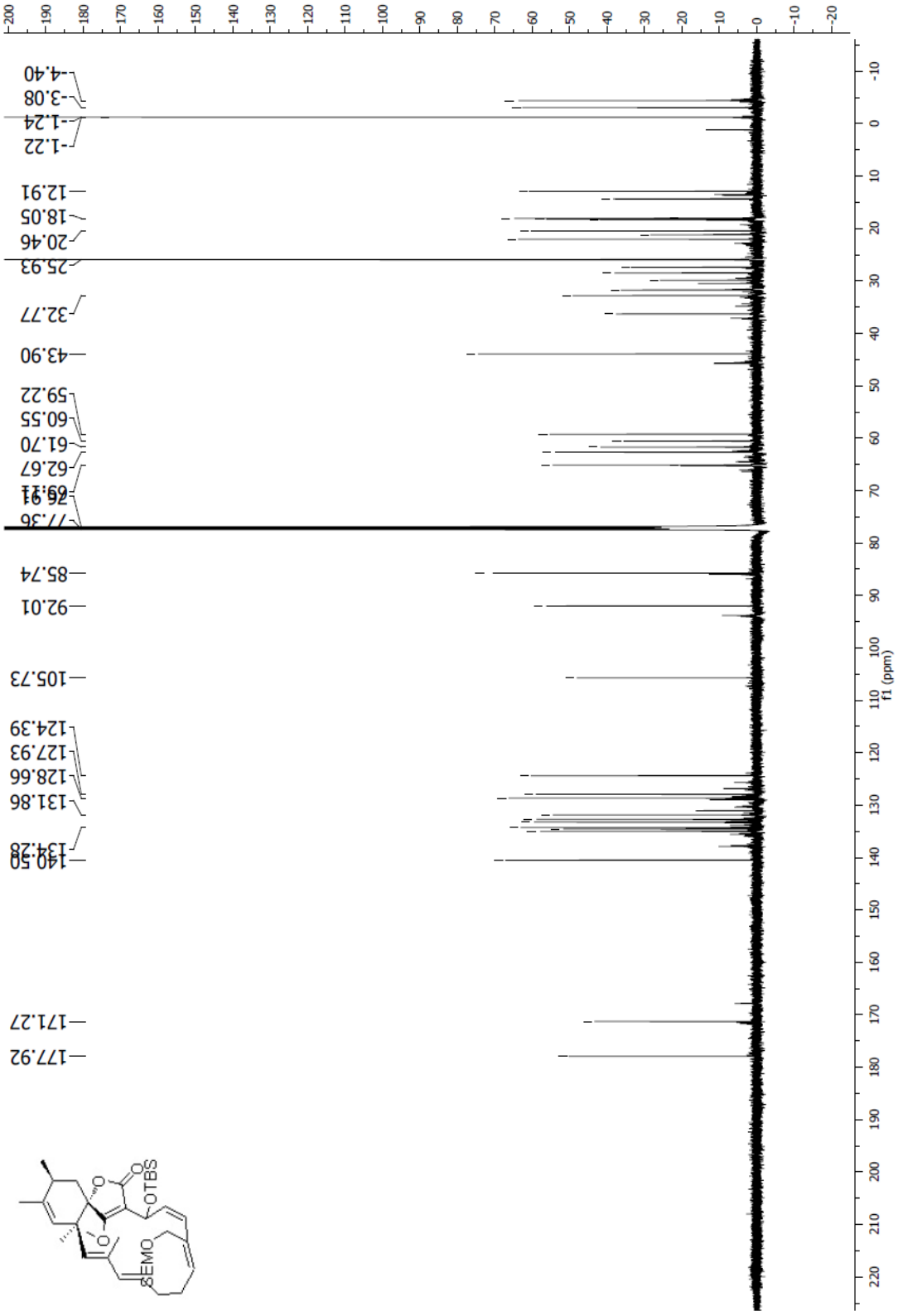

Spectrum 2.172 ^{13}C NMR ($CDCl_3$, 125 MHz) of compound **279**

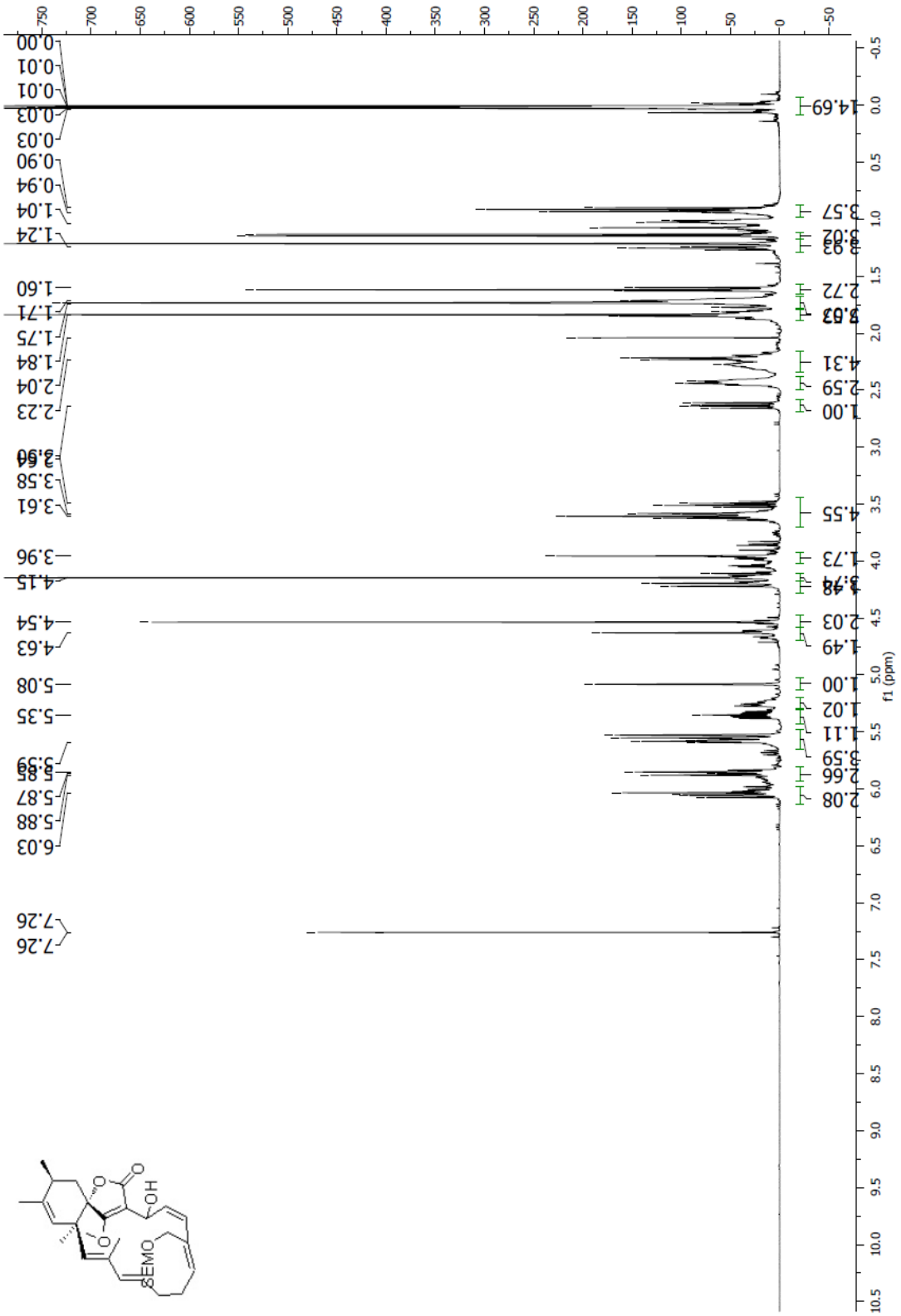

Spectrum 2.173 ^{1}H NMR ($CDCl_3$, 500 MHz) of compound **280**

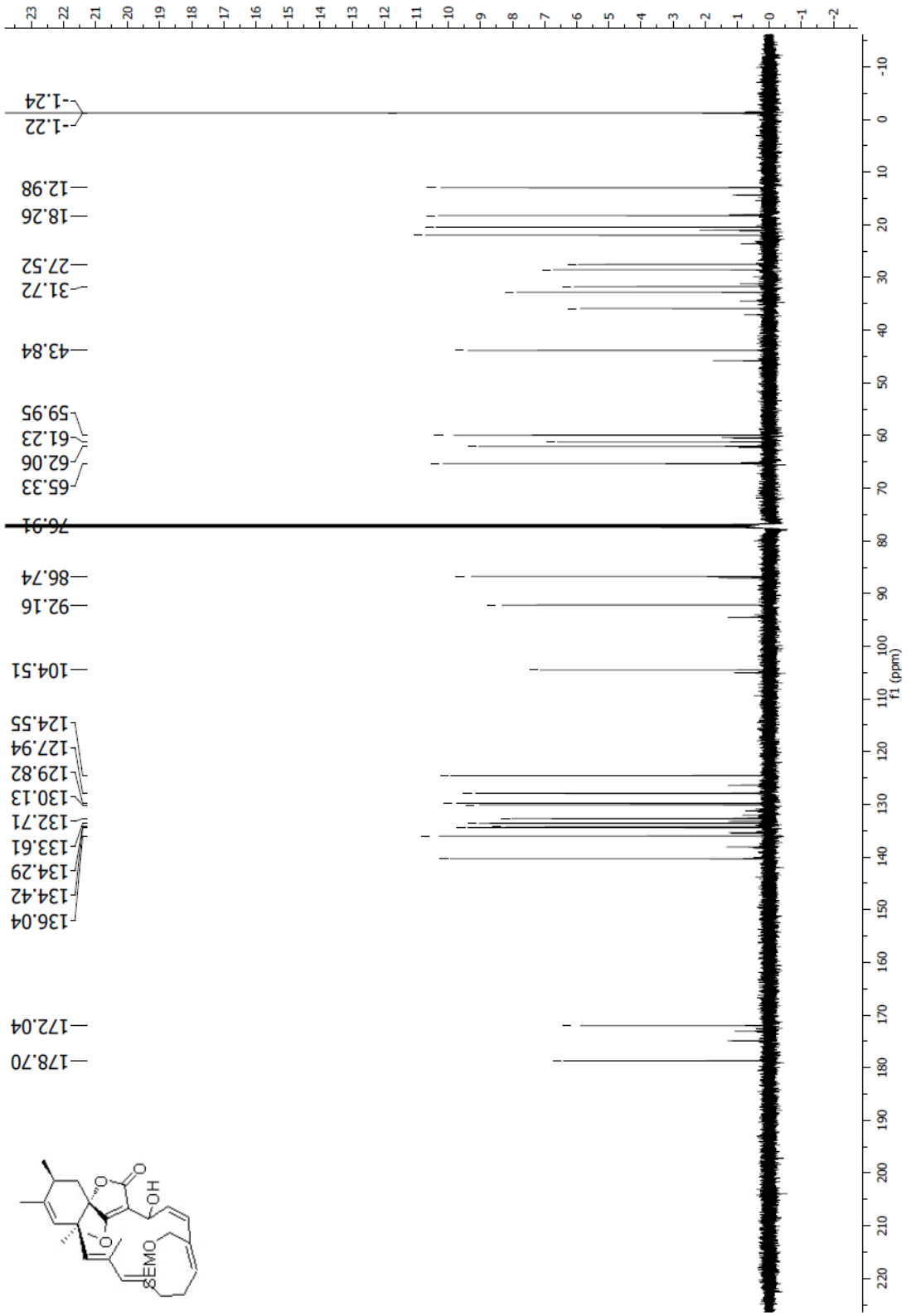

Spectrum 2.174 ^{13}C NMR ($CDCl_3$, 125 MHz) of compound **280**

REFERENCES

1. Sekiasano, M.; Okazaki, T.; Yamagishi, M.; Sakai, N.; Takayama, Y.; Hanada, K.; Morimoto, S.; Takatsuki, A.; Mizoue, K., Isolation and Characterization of a New 12-Membered Macrolide FD-895. *J. Antibiot.* **1994,** 47, (12), 1395-1401.

2. Sakai, T.; Sameshima, T.; Matsufuji, M.; Kawamura, N.; Dobashi, K.; Mizui, Y., Pladienolides, New Substances from Culture of Streptomyces Platensis Mer-11107 I. Taxonomy, Fermentation, Isolation and Screening. *J. Antibiot.* **2004,** 57, (3), 173-179.

3. Semenza, G. L., Targeting HIF-1 for Cancer Therapy. *Nat. Rev. Cancer* **2003,** 3, (10), 721-732.

4. Sakai, T.; Asai, N.; Okuda, A.; Kawamura, N.; Mizui, Y., Pladienolides, New Substances from Culture of Streptomyces Platensis Mer-11107 II. Physico-Chemical Properties and Structure Elucidation. *J. Antibiot.* **2004,** 57, (3), 180-187.

5. Boyd, M. R.; Pauli, K. D., Some Practical Considerations and Applications of the National-Cancer-Institute in-Vitro Anticancer Drug Discovery Screen. *Drug Development Research* **1995,** 34, (2), 91-109.

6. Shoemaker, R. H., The NCI60 Human Tumour Cell Line Anticancer Drug Screen. *Nat. Rev. Cancer* **2006,** 6, (10), 813-823.

7. Mizui, Y.; Sakai, T.; Iwata, M.; Uenaka, T.; Okamoto, K.; Shimizu, H.; Yamori, T.; Yoshimatsu, K.; Asada, M., Pladienolides, New Substances from Culture of Streptomyces Platensis Mer-11107 III. In Vitro and in Vivo Antitumor Activities. *J. Antibiot.* **2004,** 57, (3), 188-196.

8. Kotake, Y.; Niijima, J.; Nagai, M.; Okano, K.; Sakai, T.; Yoshida, M.; Tsuchida, T.; Nakashima, T.; Dobashi, K.; Mizui, Y.; Shimizu, H.; Uenaka, T.; Iwata, M.; Asada, M.; Yoshimatsu, K., Enhanced in Vivo Activity of Pladienolide B; Synthesis, in Vitro and in Vivo Activities of 7-Urethane Derivatives of Pladienolide B. *Clin. Cancer Res.* **2003,** 9, (16), 6208S-6208S.

9. Kanada, R. M.; Itoh, D.; Nagai, M.; Niijima, J.; Asai, N.; Mizui, Y.; Abe, S.; Kotake, Y., Total Synthesis of the Potent Antitumor Macrolides Pladienolide B and D. *Angew. Chem.-Int. Edit.* **2007,** 46, (23), 4350-4355.

10. Kotake, Y.; Sagane, K.; Owa, T.; Mimori-Kiyosue, Y.; Shimizu, H.; Uesugi, M.; Ishihama, Y.; Iwata, M.; Mizui, Y., Splicing Factor SF3b as a Target of the Antitumor Natural Product Pladienolide. *Nat. Chem. Biol.* **2007,** 3, (9), 570-575.

11. Kaida, D.; Motoyoshi, H.; Tashiro, E.; Nojima, T.; Hagiwara, M.; Ishigami, K.; Watanabe, H.; Kitahara, T.; Yoshida, T.; Nakajima, H.; Tani, T.; Horinouchi, S.; Yoshida, M., Spliceostatin A Targets SF3b and Inhibits Both Splicing and Nuclear Retention of Pre-mRNA. *Nat. Chem. Biol.* **2007,** 3, (9), 576-583.

12. Rymond, B., Targeting the Spliceosome. *Nat. Chem. Biol.* **2007,** 3, (9), 533-535.

13. van Alphen, R. J.; Wiemer, E. A. C.; Burger, H.; Eskens, F., The Spliceosome as Target for Anticancer Treatment. *British Journal of Cancer* **2009,** 100, (2), 228-232.

14. Thompson, C. F.; Jamison, T. F.; Jacobsen, E. N., FR901464: Total Synthesis, Proof of Structure, and Evaluation of Synthetic Analogues. *J. Am. Chem. Soc.* **2001,** 123, (41), 9974-9983.

15. Motoyoshi, H.; Horigome, M.; Ishigami, K.; Yoshida, T.; Horinouchi, S.; Yoshida, M.; Watanabe, H.; Kitahara, T., Structure-Activity Relationship for FR901464: A Versatile Method Tor the Conversion and Preparation of Biologically Active Biotinylated Probes. *Biosci. Biotechnol. Biochem.* **2004,** 68, (10), 2178-2182.

16. Albert, B. J.; Sivaramakrishnan, A.; Naka, T.; Czaicki, N. L.; Koide, K., Total Syntheses, Fragmentation Studies, and Antitumor/Antiproliferative Activities of FR901464 and Its Low Picomolar Analogue. *J. Am. Chem. Soc.* **2007,** 129, (9), 2648-2659.

17. Lagisetti, C.; Pourpak, A.; Jiang, Q.; Cui, X. L.; Goronga, T.; Morris, S. W.; Webb, T. R., Antitumor Compounds Based on a Natural Product Consensus Pharmacophore. *J. Med. Chem.* **2008,** 51, (19), 6220-6224.

18. Tsuchida, T. Y., Masashi; Ohta, Kazuo; Kaneko, Katsura; Kominato, Kaichiro. Process for Producing Macrolides and Intermediates Therefor. WO 2009008492, 01-15-2009, 2009.

19. Machida, K.; Aritoku, Y.; Nakashima, T.; Arisawa, A.; Tsuchida, T., Increase in Pladienolide D Production Rate Using a Streptomyces Strain Overexpressing a Cytochrome P450 Gene. *J. Biosci. Bioeng.* **2008,** 105, (6), 649-654.

20. Regina Mikie Kanada, D. I., Takashi Sakai, Naoki Asai, Yoshihiko Kotake, Jun Niijima Process for Total Synthesis of Pladienolide B and Pladienolide D. US20080021226A1, Jan. 24, 2008, 2008.

21. Asai, N.; Kotake, Y.; Niijima, J.; Fukuda, Y.; Uehara, T.; Sakai, T., Stereochemistry of Pladienolide B. *J. Antibiot.* **2007,** 60, (6), 364-369.

22. Sarandeses, L. A.; Mourino, A.; Luche, J. L., Cleavage of 2,3-Epoxyalkylhalides by the Sonochemical Zinc Copper Couple. *J. Chem. Soc.-Chem. Commun.* **1991**, (12), 818-820.

23. Nicolaou, K. C.; Bulger, P. G.; Sarlah, D., Metathesis Reactions in Total Synthesis. *Angew. Chem.-Int. Edit.* **2005,** 44, (29), 4490-4527.

24. Gaul, C.; Njardarson, J. T.; Danishefsky, S. J., The Total Synthesis of (+)-Migrastatin. *J. Am. Chem. Soc.* **2003,** 125, (20), 6042-6043.

25. Paterson, I.; Wallace, D. J.; Cowden, C. J., Polyketide Synthesis Using the Boron-Mediated, Anti-Aldol Reactions of Lactate-Derived Ketones: Total Synthesis of (-)-ACRL, Toxin IIIB. *Synthesis* **1998**, 639-652.

26. Fukuzawa, S.; Matsuzawa, H.; Yoshimitsu, S., Asymmetric Samarium-Reformatsky Reaction of Chiral Alpha-Bromoacetyl-2-Oxazolidinones with Aldehydes. *J. Org. Chem.* **2000,** 65, (6), 1702-1706.

27. Ohtani, I.; Kusumi, T.; Kashman, Y.; Kakisawa, H., High-Field FT NMR Application of Mosher Method - the Absolute-Configurations of Marine Terpenoids. *J. Am. Chem. Soc.* **1991,** 113, (11), 4092-4096.

28. Skaanderup, P. R.; Jensen, T., Synthesis of the Macrocyclic Core of (-)-Pladienolide B. *Org. Lett.* **2008,** 10, (13), 2821-2824.

29. Kolb, H. C.; Vannieuwenhze, M. S.; Sharpless, K. B., Catalytic Asymmetric Dihydroxylation. *Chem. Rev.* **1994,** 94, (8), 2483-2547.

30. Mandel, A. L., Burkart, M.D. In *Stereo-Divergent Synthesis as a Tool for the Stereochemical Evaluation of the Pladienolide B Sidechain*, 232nd ACS National Meeting, San Francisco, CA, United States, Sept. 10-14, 2006, 2006; American Chemical Society: San Francisco, CA, United States, 2006.

31. Mandel, A. L.; Jones, B. D.; La Clair, J. J.; Burkart, M. D., A Synthetic Entry to Pladienolide B and FD-895. *Bioorg. Med. Chem. Lett.* **2007,** 17, (18), 5159-5164.

32. Mandel, A. L., Jones, B.D., La Clair, J.J., Burkart, M.D. In *Studies on the Syntheses of the Pladienolides and FD-895*, 234th ACS National Meeting, Boston, MA, United States, August 19-23, 2007, 2007; American Chemical Society: Boston, MA, United States, 2007.

33. Mandel, A. L. Synthetic Studies Applied to Polyketide Natural Products. Dissertation, University of California, San Diego, San Diego, 2007.

34. Bifulco, G.; Dambruoso, P.; Gomez-Paloma, L.; Riccio, R., Determination of Relative Configuration in Organic Compounds by NMR Spectroscopy and Computational Methods. *Chem. Rev.* **2007,** 107, (9), 3744-3779.

35. Marquez, B. L.; Gerwick, W. H.; Williamson, R. T., Survey of NMR Experiments for the Determination of (N)J(C,H) Heteronuclear Coupling Constants in Small Molecules. *Magn. Reson. Chem.* **2001,** 39, (9), 499-530.

36. Kawauchi, N.; Hashimoto, H., Reaction of Enohexopyranoside Acetates with Lithium Dimethylcuprate(I) and Its Application to Synthesis of Prelog-Djerassi Lactone. *Bull. Chem. Soc. Jpn.* **1987,** 60, (4), 1441-1447.

37. Defina, G. M.; Varela, O.; Delederkremer, R. M., Convenient Synthesis of Chiral Pyranones from Carbohydrates. *Synthesis* **1988**, (11), 891-894.

38. Meng, D. F.; Bertinato, P.; Balog, A.; Su, D. S.; Kamenecka, T.; Sorensen, E. J.; Danishefsky, S. J., Total Syntheses of Epothilones A and B. *J. Am. Chem. Soc.* **1997,** 119, (42), 10073-10092.

39. Inghardt, T.; Frejd, T., Organoaluminum Induced Ring-Opening of Epoxypyranosides .5. Formal Total Synthesis of Antimycin-A3 and Synthesis of (+)-Blastmycinone. *Tetrahedron* **1991,** 47, (32), 6483-6492.

40. Weitz, D. J.; Bednarski, M. D., Synthesis of Acyclic Sugar Aldehydes by Ozonolysis of Oximes. *J. Org. Chem.* **1989,** 54, (20), 4957-4959.

41. Grigg, R.; Markandu, J.; Surendrakumar, S.; Thorntonpett, M.; Warnock, W. J., X=Y-Zh Systems as Potential 1,3-Dipoles .37. Generation of Nitrones from Oximes - Tandem Intramolecular 1,3-Azaprotio Cyclotransfer Intramolecular 1,3-Dipolar Cycloaddition Reactions - Class-4 Processes. *Tetrahedron* **1992,** 48, (47), 10399-10422.

42. Cook, F. L.; Bowers, C. W.; Liotta, C. L., Chemistry of Naked Anions .3. Reactions of 18-Crown-6 Complex of Potassium Cyanide with Organic Substrates in Aprotic Organic-Solvents. *J. Org. Chem.* **1974,** 39, (23), 3416-3418.

43. Reetz, M. T., Chelation or Non-Chelation Control in Addition-Reactions of Chiral Alpha-Alkoxy and Beta-Alkoxy Carbonyl-Compounds. *Angew. Chem.-Int. Edit. Engl.* **1984,** 23, (8), 556-569.

44. Horton, D.; Norris, P.; Berrang, B., Characterization and Interconversions of 2-S-Ethyl-2-Thio-D-Mannose Diethyl Dithioacetal and the Facile Epimerization of 2-Thio-D-Mannopyranose Derivatives. *Carbohydr. Res.* **1996,** 283, 53-71.

45. Vedejs, E.; Daugulis, O., Dual Activation in the Esterification of Hindered Alcohols with Anhydrides Using MgBr2 and a Tertiary Amine. *J. Org. Chem.* **1996,** 61, (17), 5702-5703.

46. Manthorpe, J. M.; Szpilman, A. M.; Carreira, E. M., Scalable Synthesis of a Mycosamine Donor. Overcoming Difficult Reactivity in Allose Systems. *Synthesis* **2005**, (19), 3380-3388.

47. Sakamoto, T.; Kikugawa, Y., Synthesis of Aldehydes from Carboxylic-Acids Via N-Methoxyimidoyl Bromides - Deoximation of O-Methyloximes. *Synthesis* **1993**, (6), 563-564.

48. Bashiardes, G.; Cano, C.; Mauze, B., Regio- and Enantioselective Synthesis of Novel Functionalized Pyranopyrrolidines by 1,3-Dipolar Cycloaddition of Carbohydrates. *Synlett* **2005**, (4), 587-590.

49. Bondar, D.; Liu, J.; Muller, T.; Paquette, L. A., Pectenotoxin-2 Synthetic Studies. 2. Construction and Conjoining of ABC and DE Eastern Hemisphere Subtargets. *Org. Lett.* **2005,** 7, (9), 1813-1816.

50. Tan, H. S.; Espenson, J. H., Regioselective Hydroxylactonization of Gamma,Delta-Unsaturated Carboxylic Acids with Hydrogen Peroxide Catalyzed by Methyltrioxorhenium. *Journal of Molecular Catalysis a-Chemical* **1999,** 142, (3), 333-338.

51. Smith, M. B.; Dembofsky, B. T.; Son, Y. C., 5(R)-Methyl-1-(Chloromethyl)-2-Pyrrolidinone - A New Reagent for the Determination of Enantiomeric Composition of Alcohols. *J. Org. Chem.* **1994,** 59, (7), 1719-1725.

52. Hammarst.S; Hamberg, M., Steric Analysis of 3-Hydroxy Acids, Omega-4-Hydroxy Acids, Omega-3-Hydroxy Acids and Omega-2-Hydroxy Acids and Various Alkanols by Gas-Liquid Chromatography. *Anal. Biochem.* **1973,** 52, (1), 169-179.

53. Fukuda, Y.; Sasaki, H.; Shindo, M.; Shishido, K., Diastereoselective Ring-Closing Metathesis for the Construction of a Quaternary Carbon Stereogenic Center. *Tetrahedron Lett.* **2002,** 43, (11), 2047-2049.

54. Touchard, F. P., Phosphonate Modification for a Highly (Z)-Selective Synthesis of Unsaturated Esters by Horner-Wadsworth-Emmons Olefination. *Eur. J. Org. Chem.* **2005**, (9), 1790-1794.

55. Still, W. C.; Gennari, C., Direct Synthesis of Z-Unsaturated Esters - A Useful Modification of the Horner-Emmons Olefination. *Tetrahedron Lett.* **1983,** 24, (41), 4405-4408.

56. Mandel, A. L.; La Clair, J. J.; Burkart, M. D., Modular Synthesis of Pantetheine and Phosphopantetheine. *Org. Lett.* **2004,** 6, (26), 4801-4803.

57. White, J. D.; Takabe, K.; Prisbylla, M. P., Stereoselective Synthesis of Trisporic Acid-A and Acid-B Their Methyl-Esters, and Trisporol-A and Trisporol-B,

Hormones and Prohormones of Mucoraceous Fungi. *J. Org. Chem.* **1985,** 50, (25), 5233-5244.

58. Fouque, E.; Rousseau, G.; Seydenpenne, J., Iterative Synthesis of Selectively Substituted Alpha,Beta-Unsaturated and Saturated Medium-Ring Lactones. *J. Org. Chem.* **1990,** 55, (16), 4807-4817.

59. Maier, M. E., Synthesis of Medium-Sized Rings by the Ring-Closing Metathesis Reaction. *Angew. Chem.-Int. Edit.* **2000,** 39, (12), 2073-2077.

60. Trnka, T. M.; Grubbs, R. H., The Development of L2X2Ru = CHR Olefin Metathesis Catalysts: An Organometallic Success Story. *Accounts Chem. Res.* **2001,** 34, (1), 18-29.

61. Chatterjee, A. K.; Morgan, J. P.; Scholl, M.; Grubbs, R. H., Synthesis of Functionalized Olefins by Cross and Ring-Closing Metatheses. *J. Am. Chem. Soc.* **2000,** 122, (15), 3783-3784.

62. Alam, M. M.; Varala, R.; Adapa, S. R., Bi(OTf)(3)-Catalyzed Baeyer-Villiger Oxidation of Carbonyl Compounds with m-CPBA. *Synth. Commun.* **2003,** 33, (17), 3035-3040.

63. Hirano, M.; Yakabe, S.; Satoh, A.; Clark, J. H.; Morimoto, T., MMPP (Magnesium Monoperoxyphthalate) in Acetonitrile; A New Approach to the Synthesis of Lactones Via Baeyer-Villiger Oxidation of Cyclic Ketones. *Synth. Commun.* **1996,** 26, (24), 4591-4596.

64. Inokuchi, T.; Kanazaki, M.; Sugimoto, T.; Torii, S., Baeyer-Villiger Type Oxidation in A Dioxygen-Arenecarbaldehyde-Ruthenium Dioxide or Manganese-Dioxide System. *Synlett* **1994**, (12), 1037-1038.

65. Crimmins, M. T.; King, B. W.; Tabet, E. A.; Chaudhary, K., Asymmetric Aldol Additions: Use of Titanium Tetrachloride and (-)-Sparteine for the Soft Enolization of N-Acyl Oxazolidinones, Oxazolidinethiones, and Thiazolidinethiones. *J. Org. Chem.* **2001,** 66, (3), 894-902.

66. Gao, Y.; Hanson, R. M.; Klunder, J. M.; Ko, S. Y.; Masamune, H.; Sharpless, K. B., Catalytic Asymmetric Epoxidation and Kinetic Resolution - Modified Procedures Including Insitu Derivatization. *J. Am. Chem. Soc.* **1987,** 109, (19), 5765-5780.

67. Zhang, W.; Basak, A.; Kosugi, Y.; Hoshino, Y.; Yamamoto, H., Enantioselective Epoxidation of Allylic Alcohols by a Chiral Complex of Vanadium: An Effective Controller System and a Rational Mechanistic Model. *Angew. Chem.-Int. Edit.* **2005,** 44, (28), 4389-4391.

68. Brown, H. C.; Bhat, K. S., Enantiomeric (Z)-Crotyldiisopinocampheylborane and (E)-Crotyldiisopinocampheylborane - Synthesis in High Optical Purity of All 4 Possible Stereoisomers of Beta-Methylhomoallyl Alcohols. *J. Am. Chem. Soc.* **1986,** 108, (2), 293-294.

69. Brown, H. C.; Ramachandran, P. V., Versatile Alpha-Pinene-Based Borane Reagents for Asymmetric Syntheses. *J. Organomet. Chem.* **1995,** 500, (1-2), 1-19.

70. Marshall, J. A., Chiral Allylic and Allenic Stannanes as Reagents for Asymmetric Synthesis. *Chem. Rev.* **1996,** 96, (1), 31-47.

71. Marshall, J. A.; Wang, X. J., Highly Diastereoselective Se' Additions of Enantioenriched Allenylstannanes to (S)-2-(Benzyloxy)Propanal. *J. Org. Chem.* **1991,** 56, (10), 3211-3213.

72. Marshall, J. A.; Wang, X. J., Synthesis of Enantioenriched Homopropargylic Alcohols through Diastereoselective-Se' Additions of Chiral Allenylstannanes to Aldehydes. *J. Org. Chem.* **1992,** 57, (4), 1242-1252.

73. Righi, G.; Pescatore, G.; Bonadies, F.; Bonini, C., A Study on the Chelation Control in the Regioselective Opening of 2,3-Bifunctionalized Epoxides. *Tetrahedron* **2001,** 57, (26), 5649-5656.

74. Wang, S. M.; Howe, G. P.; Mahal, R. S.; Procter, G., Stereoselective Reactions of Alpha,Beta-Epoxy-Aldehydes - the Formation of Chelation Controlled Products. *Tetrahedron Lett.* **1992,** 33, (23), 3351-3354.

75. Yamamoto, Y.; Asao, N., Selective Reactions Using Allylic Metals. *Chem. Rev.* **1993,** 93, (6), 2207-2293.

76. Marshall, J. A.; Schaaf, G. M., Synthesis of Stereopentad Analogues of the C14-C22 Segment of Callystatin A through Additions of Chiral Allenylzinc Reagents to Stereotriads. *J. Org. Chem.* **2001,** 66, (23), 7825-7831.

77. Marshall, J. A.; Ellis, K. C., Total Synthesis of (-)- and (+)-Membrenone C. *Org. Lett.* **2003,** 5, (10), 1729-1732.

78. Zhang, Y. C.; Phillips, A. J.; Sammakia, T., Highly Selective Asymmetric Acetate Aldol Reactions of an N-Acetyl Thiazolidinethione Reagent. *Org. Lett.* **2004,** 6, (1), 23-25.

79. Marshall, J. A.; Adams, N. D., Total Synthesis of Bafilomycin V-1: A Methanolysis Product of the Macrolide Bafilomycin C-2. *J. Org. Chem.* **2002,** 67, (3), 733-740.

80. Pangborn, A. B.; Giardello, M. A.; Grubbs, R. H.; Rosen, R. K.; Timmers, F. J., Safe and Convenient Procedure for Solvent Purification. *Organometallics* **1996,** 15, (5), 1518-1520.

81. Still, W. C.; Kahn, M.; Mitra, A., Rapid Chromatographic Technique for Preparative Separations with Moderate Resolution. *J. Org. Chem.* **1978,** 43, (14), 2923-2925.

82. Gottlieb, H. E.; Kotlyar, V.; Nudelman, A., NMR Chemical Shifts of Common Laboratory Solvents as Trace Impurities. *J. Org. Chem.* **1997,** 62, (21), 7512-7515.

83. Tresner, H. D.; Backus, E. J., A Broadened Concept of the Characteristics of Streptomyces-Hygroscopicus. *Applied Microbiology* **1956,** 4, (5), 243-250.

84. Hochlowski, J. E.; Whittern, D. N.; Hill, P.; McAlpine, J. B., Dorrigocins - Novel Antifungal Antibiotics That Change the Morphology of Ras-Transformed NIH/3T3 Cells to That of Normal-Cells .2. Isolation and Elucidation of Structures. *J. Antibiot.* **1994,** 47, (8), 870-874.

85. Karwowski, J. P.; Jackson, M.; Sunga, G.; Sheldon, P.; Poddig, J. B.; Kohl, W. L.; Kadam, S., Dorrigocins - Novel Antifungal Antibiotics That Change the Morphology of Ras-Transformed NIH/3T3 Cells to That of Normal-Cells .1. Taxonomy of the Producing Organism, Fermentation and Biological-Activity. *J. Antibiot.* **1994,** 47, (8), 862-869.

86. Woo, E. J.; Starks, C. M.; Carney, J. R.; Arslanian, R.; Cadapan, L.; Zavala, S.; Licari, P., Migrastatin and a New Compound, Isomigrastatin, from Streptomyces Platensis. *J. Antibiot.* **2002,** 55, (2), 141-146.

87. Ju, J. H.; Lim, S. K.; Jiang, H.; Shen, B., Migrastatin and Dorrigocins Are Shunt Metabolites of Iso-Migrastatin. *J. Am. Chem. Soc.* **2005,** 127, (6), 1622-1623.

88. Gaul, C.; Njardarson, J. T.; Shan, D.; Dorn, D. C.; Wu, K. D.; Tong, W. P.; Huang, X. Y.; Moore, M. A. S.; Danishefsky, S. J., The Migrastatin Family: Discovery of Potent Cell Migration Inhibitors by Chemical Synthesis. *J. Am. Chem. Soc.* **2004,** 126, (36), 11326-11337.

89. Kohama, T.; Maeda, H.; Sakai, J. I.; Shiraishi, A.; Yamashita, K., Leustroducsin B, a New Cytokine Inducer Derived from an Actinomycetes, Induces Thrombocytosis in Mice. *J. Antibiot.* **1996,** 49, (1), 91-94.

90. Furumai, T.; Eto, K.; Sasaki, T.; Higuchi, H.; Onaka, H.; Saito, N.; Fujita, T.; Naoki, H.; Igarashi, Y., TPU-0037-A, B, C and D, Novel Lydicamycin Congeners with Anti-MRSA Activity from Streptomyes Platensis TP-A0598. *J. Antibiot.* **2002,** 55, (10), 873-880.

91. Herath, K. B.; Zhang, C.; Jayasuriya, H.; Ondeyka, J. G.; Zink, D. L.; Burgess, B.; Wang, J.; Singh, S. B., Structure and Semisynthesis of Platensimide A, Produced by Streptomyces Platensis. *Org. Lett.* **2008,** 10, (9), 1699-1702.

92. Wang, J.; Soisson, S. M.; Young, K.; Shoop, W.; Kodali, S.; Galgoci, A.; Painter, R.; Parthasarathy, G.; Tang, Y. S.; Cummings, R.; Ha, S.; Dorso, K.; Motyl, M.; Jayasuriya, H.; Ondeyka, J.; Herath, K.; Zhang, C. W.; Hernandez, L.; Allocco, J.; Basilio, A.; Tormo, J. R.; Genilloud, O.; Vicente, F.; Pelaez, F.; Colwell, L.; Lee, S. H.; Michael, B.; Felcetto, T.; Gill, C.; Silver, L. L.; Hermes, J. D.; Bartizal, K.; Barrett, J.; Schmatz, D.; Becker, J. W.; Cully, D.; Singh, S. B., Platensimycin Is a Selective FabF Inhibitor with Potent Antibiotic Properties. *Nature* **2006,** 441, (7091), 358-361.

93. Ju, J. H.; Rajski, S. R.; Lim, S. K.; Seo, J. W.; Peters, N. R.; Hoffmann, F. M.; Shen, B., Evaluation of New Migrastatin and Dorrigocin Congeners Unveils Cell Migration Inhibitors with Dramatically Improved Potency. *Bioorg. Med. Chem. Lett.* **2008,** 18, (22), 5951-5954.

94. Metaferia, B. B.; Chen, L.; Baker, H. L.; Huang, X. Y.; Bewley, C. A., Synthetic Macrolides That Inhibit Breast Cancer Cell Migration in Vitro. *J. Am. Chem. Soc.* **2007,** 129, (9), 2434-2435.

95. Li, M. H. T.; Ung, P. M. U.; Zajkowski, J.; Garneau-Tsodikova, S.; Sherman, D. H., Automated Genome Mining for Natural Products. *BMC Bioinformatics* **2009,** 10, 10.

96. Gulder, T. A. M.; Moore, B. S., Chasing the Treasures of the Sea - Bacterial Marine Natural Products. *Curr. Opin. Microbiol.* **2009,** 12, (3), 252-260.

97. Jones, A. C.; Gu, L. C.; Sorrels, C. M.; Sherman, D. H.; Gerwick, W. H., New Tricks from Ancient Algae: Natural Products Biosynthesis in Marine Cyanobacteria. *Curr. Opin. Chem. Biol.* **2009,** 13, (2), 216-223.

98. Udwary, D. W.; Zeigler, L.; Asolkar, R. N.; Singan, V.; Lapidus, A.; Fenical, W.; Jensen, P. R.; Moore, B. S., Genome Sequencing Reveals Complex Secondary Metabolome in the Marine Actinomycete Salinispora Tropica. *Proc. Natl. Acad. Sci. U. S. A.* **2007,** 104, (25), 10376-10381.

99. Gust, B., Cloning and Analysis of Natural Product Pathways. In *Complex Enzymes in Microbial Natural Product Biosynthesis, Part A: Overview Articles and Peptides*, Elsevier Academic Press Inc: San Diego, 2009; Vol. 458, pp 159-180.

100. Baltz, R. H., Genetic Methods and Strategies for Secondary Metabolite Yield Improvement in Actinomycetes. *Antonie Van Leeuwenhoek* **2001,** 79, (3-4), 251-259.

101. van Wezel, G. P.; Krabben, P.; Traag, B. A.; Keijser, B. J. F.; Kerste, R.; Vijgenboom, E.; Heijnen, J. J.; Kraal, B., Unlocking Streptomyces Spp. For Use as Sustainable Industrial Production Platforms by Morphological Engineering. *Appl. Environ. Microbiol.* **2006,** 72, (8), 5283-5288.

102. Poele, E. M. T.; Bolhuis, H.; Dijkhuizen, L., Actinomycete Integrative and Conjugative Elements. *Antonie Van Leeuwenhoek* **2008,** 94, (1), 127-143.

103. Demain, A. L., Induction of Microbial Secondary Metabolism. *International Microbiology* **1998,** 1, (4), 259-264.

104. Hopwood, D. A., Antibiotics - Opportunities for Genetic Manipulation. *Philos. Trans. R. Soc. Lond. Ser. B-Biol. Sci.* **1989,** 324, (1224), 549-562.

105. Wang, L. Y.; Yun, B. S.; George, N. P.; Wendt-Pienkowski, E.; Galm, U.; Oh, T. J.; Coughlin, J. M.; Zhang, G. D.; Tao, M. F.; Shen, B., Glycopeptide Antitumor Antibiotic Zorbamycin from Streptomyces Flavoviridis ATCC 21892: Strain Improvement and Structure Elucidation. *J. Nat. Prod.* **2007,** 70, (3), 402-406.

106. Malina, H.; Tempete, C.; Robertgero, M., Enhanced Sinefungin Production by Medium Improvement, Mutagenesis, and Protoplast Regeneration of Streptomyces-Incarnatus NRRL 8089. *J. Antibiot.* **1985,** 38, (9), 1204-1210.

107. Lee, S. D.; Park, S. W.; Oh, K. K.; Hong, S. I.; Kim, S. W., Improvement for the Production of Clavulanic Acid by Mutant Streptomyces Clavuligerus. *Lett. Appl. Microbiol.* **2002,** 34, (5), 370-375.

108. Lyutskanova, D. G.; Stoilova-Disheva, M. A.; Peltekova, V. T., Increase in Tylosin Production by a Commercial Strain of Streptomyces Fradiae. *Appl. Biochem. Microbiol.* **2005,** 41, (2), 165-168.

109. Kieser, T. B., Mervyn J.; Buttner, Mark J.; Chater, Keith F.; Hopwood, David A. , *Practical Streptomyces Genetics*. The John Innes Foundation: Norwich, UK, 2000; p 613.

110. Lal, R.; Khanna, R.; Kaur, H.; Khanna, M.; Dhingra, N.; Lal, S.; Gartemann, K. H.; Eichenlaub, R.; Ghosh, P. K., Engineering Antibiotic Producers to Overcome the Limitations of Classical Strain Improvement Programs. *Crit. Rev. Microbiol.* **1996,** 22, (4), 201-255.

111. Hopwood, D. A.; Chater, K. F., Fresh Approaches to Antibiotic Production. *Philos. Trans. R. Soc. Lond. Ser. B-Biol. Sci.* **1980,** 290, (1040), 313-328.

112. Schindle.Pw; Zahner, H., Mode of Action of Macrolide-Type Antibiotic, Chlorothricin - Kinetic Study of Inhibition of Pyruvate Carboxylase from Bacillus-Stearothermophilus. *Eur. J. Biochem.* **1973,** 39, (2), 591-600.

113. Gary, N. D.; Bard, R. C., Effect of Nutrition on the Growth and Metabolism of Bacillus Subtilis. *J. Bacteriol.* **1952,** 64, (4), 501-512.

114. Sundaram, T. K.; Cazzulo, J. J.; Kornberg, H. L., Anaplerotic CO2 Fixation in Mesophilic and Thermophilic Bacilli. *Biochimica Et Biophysica Acta* **1969,** 192, (2), 355-&.

115. Pang, X. H.; Aigle, B.; Girardet, J. M.; Mangenot, S.; Pernodet, J. L.; Decaris, B.; Leblond, P., Functional Angucycline-Like Antibiotic Gene Cluster in the Terminal Inverted Repeats of the Streptomyces Ambofaciens Linear Chromosome. *Antimicrob. Agents Chemother.* **2004,** 48, (2), 575-588.

116. Shirling, E. B.; Gottlieb, D., Cooperative Description of Type Cultures of Streptomyces III. Additional Species Descriptions from First and Second Studies. *Int J Syst Bacteriol* **1968,** 18, (4), 279-392.

117. Kumar, Y.; Goodfellow, M., Five New Members of the Streptomyces Violaceusniger 16s rRNA Gene Clade: Streptomyces Castelarensis sp. Nov., Comb. Nov., Streptomyces Himastatinicus sp. Nov., Streptomyces Mordarskii sp. Nov., Streptomyces Rapamycinicus sp. Nov. And Streptomyces Ruanii sp. Nov. *Int J Syst Evol Microbiol* **2008,** 58, (6), 1369-1378.

118. Skerman, V. B. D.; McGowan, V.; Sneath, P. H. A., Approved Lists of Bacterial Names. *Int J Syst Bacteriol* **1980,** 30, (1), 225-420.

119. Validation of the Publication of New Names and New Combinations Previously Effectively Published Outside the Ijsb: List No. 22. *Int J Syst Bacteriol* **1986,** 36, (4), 573-576.

120. Flack, H. D., On Enantiomorph-Polarity Estimation. *Acta Crystallogr. Sect. A* **1983,** 39, (NOV), 876-881.

121. Niu, X. M.; Li, S. H.; Gorls, H.; Schollmeyer, D.; Hilliger, M.; Grabley, S.; Sattler, I., Abyssomicin E, a Highly Functionalized Polycyclic Metabolite from Streptomyces Species. *Org. Lett.* **2007,** 9, (13), 2437-2440.

122. Dale, J. A.; Mosher, H. S., Nuclear Magnetic-Resonance Enantiomer Reagents - Configurational Correlations Via Nuclear Magnetic-Resonance Chemical-Shifts of Diastereomeric Mandelate, O-Methylmandelate, and Alpha-Methoxy-Alpha-Trifluoromethylphenylacetate (MTPA) Esters. *J. Am. Chem. Soc.* **1973,** 95, (2), 512-519.

123. Lemieux, B.; Percival, M. D.; Falgueyret, J. P., Quantitation of the Lysosomotropic Character of Cationic Amphiphilic Drugs Using the Fluorescent Basic Amine Red Dnd-99. *Anal. Biochem.* **2004,** 327, (2), 247-251.

124. Bonjouklian, R., Chemistry of the Microbial Metabolite A88696F, A New 2-(Alpha-Hydroxyalkyl) Tetronic Acid. *Tetrahedron Lett.* **1993,** 34, (49), 7861-7864.

125. Bister, B.; Bischoff, D.; Strobele, M.; Riedlinger, J.; Reicke, A.; Wolter, F.; Bull, A. T.; Zahner, H.; Fiedler, H. P.; Sussmuth, R. D., Abyssomicin C - A Polycyclic Antibiotic from a Marine Verrucosispora Strain as an Inhibitor of the P-Aminobenzoic Acid/Tetrahydrofolate Biosynthesis Pathway. *Angew. Chem.-Int. Edit.* **2004,** 43, (19), 2574-2576.

126. Brufani, M.; Cerrini, S.; Muntwyle.R; Fedeli, W.; Mazza, F., Metabolites of Microorganisms .108. Crystal-Structure Analysis of Chlorothricolide Methyl-Ester. *Helv. Chim. Acta* **1972,** 55, (6), 2094-2102.

127. Momose, I.; Hirosawa, S.; Nakamura, H.; Naganawa, H.; Iinuma, H.; Ikeda, D.; Takeuchi, T., Decatromicins A and B, New Antibiotics Produced by Actinomadura sp. MK73-NF4 - II. Structure Determination. *J. Antibiot.* **1999,** 52, (9), 787-796.

128. Schroeder, D. R.; Colson, K. L.; Klohr, S. E.; Lee, M. S.; Matson, J. A.; Brinen, L. S.; Clardy, J., Pyrrolosporin A, a New Antitumor Antibiotic from Micromonospora sp. C39217-R109-7 .2. Isolation, Physico-Chemical Properties, Spectroscopic Study and X-Ray Analysis. *J. Antibiot.* **1996,** 49, (9), 865-872.

129. Matsumoto, M.; Kawamura, Y.; Yoshimura, Y.; Terui, Y.; Nakai, H.; Yoshida, T.; Shoji, J., Isolation, Characterization and Structures of PA-46101-A and PA-46101-B. *J. Antibiot.* **1990,** 43, (7), 739-747.

130. Kellerjuslen, C.; King, H. D.; Kuhn, M.; Loosli, H. R.; Pache, W.; Petcher, T. J.; Weber, H. P.; Vonwartburg, A., Tetronomycin, a Novel Polyether of Unusual Structure. *J. Antibiot.* **1982,** 35, (2), 142-150.

131. Park, H. R.; Chijiwa, S.; Furihata, K.; Hayakawa, Y.; Shin-Ya, K., Relative and Absolute Configuration of Versipelostatin, a Down-Regulator of Molecular Chaperone GRP78 Expression. *Org. Lett.* **2007,** 9, (8), 1457-1460.

132. Clutterbuck, P. W.; Raistrick, H.; Reuter, F., Studies in the Biochemistry of Micro-Organisms. XLI. The Metabolic Products of Penicillium Charlesii G. Smith. II. The Molecular Constitution of Carolic and Carolinic Acids. *Biochem. J.* **1935,** 29, 300-321.

133. Zapf, C. W.; Harrison, B. A.; Drahl, C.; Sorensen, E. J., A Diels-Alder Macrocyclization Enables an Efficient Asymmetric Synthesis of the Antibacterial Natural Product Abyssomicin C. *Angew. Chem.-Int. Edit.* **2005,** 44, (40), 6533-6537.

134. Takeda, K.; Igarashi, Y.; Okazaki, K.; Yoshii, E.; Yamaguchi, K., An Intramolecular Diels-Alder Approach to the Synthesis of Chlorothricolide - Synthesis of (+/-)-24-O-Methylchlorothricolide. *J. Org. Chem.* **1990,** 55, (11), 3431-3434.

135. Jia, X. Y.; Tian, Z. H.; Shao, L.; Qu, X. D.; Zhao, Q. F.; Tang, J.; Tang, G. L.; Liu, W., Genetic Characterization of the Chlorothricin Gene Cluster as a Model for Spirotetronate Antibiotic Biosynthesis. *Chem. Biol.* **2006,** 13, (6), 575-585.

136. Zhang, H.; White-Phillip, J. A.; Melancon, C. E.; Kwon, H. J.; Yu, W. L.; Liu, H. W., Elucidation of the Kijanimicin Gene Cluster: Insights into the Biosynthesis of Spirotetronate Antibiotics and Nitrosugars. *J. Am. Chem. Soc.* **2007,** 129, (47), 14670-14683.

137. Demydchuk, Y.; Sun, Y. H.; Hong, H.; Staunton, J.; Spencer, J. B.; Leadlay, P. F., Analysis of the Tetronomycin Gene Cluster: Insights into the Biosynthesis of a Polyether Tetronate Antibiotic. *ChemBioChem* **2008,** 9, (7), 1136-1145.

138. Fang, J.; Zhang, Y. P.; Huang, L. J.; Jia, X. Y.; Zhang, Q.; Zhang, X.; Tang, G. L.; Liu, W., Cloning and Characterization of the Tetrocarcin a Gene Cluster from Micromonospora Chalcea NRRL 11289 Reveals a Highly Conserved Strategy for Tetronate Biosynthesis in Spirotetronate Antibiotics. *J. Bacteriol.* **2008,** 190, (17), 6014-6025.

139. Machida, K.; Aritoku, Y.; Tsuchida, T., One-Pot Fermentation of Pladienolide D by Streptomyces Platensis Expressing a Heterologous Cytochrome P450 Gene. *J. Biosci. Bioeng.* **2009,** 107, (6), 596-598.

140. Lin, X.; Cane, D. E., Biosynthesis of the Sesquiterpene Antibiotic Albaflavenone in Streptomyces Coelicolor. Mechanism and Stereochemistry of the Enzymatic Formation of Epi-Isozizaene. *J. Am. Chem. Soc.* **2009,** 131, (18), 6332-6333.

141. Henry, K. M.; Townsend, C. A., Ordering the Reductive and Cytochrome P450 Oxidative Steps in Demethylsterigmatocystin Formation Yields General Insights into the Biosynthesis of Aflatoxin and Related Fungal Metabolites. *J. Am. Chem. Soc.* **2005,** 127, (11), 3724-3733.

142. Bode, H. B.; Bethe, B.; Hofs, R.; Zeeck, A., Big Effects from Small Changes: Possible Ways to Explore Nature's Chemical Diversity. *ChemBioChem* **2002,** 3, (7), 619-627.

143. Hughes, C. C.; MacMillan, J. B.; Gaudencio, S. P.; Fenical, W.; La Clair, J. J., Ammosamides A and B Target Myosin. *Angew. Chem.-Int. Edit.* **2009,** 48, (4), 728-732.

144. Leslie, B. J.; Hergenrother, P. J., Identification of the Cellular Targets of Bioactive Small Organic Molecules Using Affinity Reagents. *Chem. Soc. Rev.* **2008,** 37, (7), 1347-1360.

145. Alexander, M. D.; Burkart, M. D.; Leonard, M. S.; Portonovo, P.; Liang, B.; Ding, X. B.; Joullie, M. M.; Gulledge, B. M.; Aggen, J. B.; Chamberlin, A. R.; Sandler, J.; Fenical, W.; Cui, J.; Gharpure, S. J.; Polosukhin, A.; Zhang, H. R.; Evans, P. A.; Richardson, A. D.; Harper, M. K.; Ireland, C. M.; Vong, B. G.; Brady, T. P.; Theodorakis, E. A.; La Clair, J. J., A Central Strategy for Converting Natural Products into Fluorescent Probes. *ChemBioChem* **2006,** 7, (3), 409-416.

146. Holzbach, R.; Pape, H.; Hook, D.; Kreutzer, E. F.; Chang, C.; Floss, H. G., Biosynthesis of Macrolide Antibiotic Chlorothricin - Basic Building-Blocks. *Biochemistry* **1978,** 17, (3), 556-560.

147. Mascaretti, O. A.; Chang, C. J.; Hook, D.; Otsuka, H.; Kreutzer, E. F.; Floss, H. G., Biosynthesis of the Macrolide Antibiotic Chlorothricin. *Biochemistry* **1981,** 20, (4), 919-924.

148. Lee, J. J.; Lee, J. P.; Keller, P. J.; Cottrell, C. E.; Chang, C. J.; Zahner, H.; Floss, H. G., Further-Studies on the Biosynthesis of Chlorothricin. *J. Antibiot.* **1986,** 39, (8), 1123-1134.

149. Rawlings, B. J., Biosynthesis of Polyketides. *Nat. Prod. Rep.* **1997,** 14, (5), 523-556.

150. Oikawa, H.; Tokiwano, T., Enzymatic Catalysis of the Diels-Alder Reaction in the Biosynthesis of Natural Products. *Nat. Prod. Rep.* **2004,** 21, (3), 321-352.

151. Kelly, W. L., Intramolecular Cyclizations of Polyketide Biosynthesis: Mining for A "Diels-Alderase"? *Org. Biomol. Chem.* **2008,** 6, (24), 4483-4493.

152. Nicolaou, K. C.; Harrison, S. T., Total Synthesis of Abyssomicin C, Atrop-Abyssomicin C, and Abyssomicin D: Implications for Natural Origins of Atrop-Abyssomicin C. *J. Am. Chem. Soc.* **2007,** 129, (2), 429-440.

153. Zografos, A. L.; Georgiadis, D., Synthetic Strategies Towards Naturally Occurring Tetronic Acids. *Synthesis* **2006**, (19), 3157-3188.

154. Takeda, K.; Yano, S.; Sato, M.; Yoshii, E., Synthesis of the Upper Spirotetronic Acid Fragment of Kijanolide. *J. Org. Chem.* **1987,** 52, (18), 4135-4137.

155. Zhang, Y. C.; Sammakia, T., Synthesis of a New N-Acetyl Thiazolidinethione Reagent and Its Application to a Highly Selective Asymmetric Acetate Aldol Reaction. *Org. Lett.* **2004,** 6, (18), 3139-3141.

156. Crimmins, M. T.; She, J., An Improved Procedure for Asymmetric Aldol Additions with N-Acyl Oxazolidinones, Oxazolidinethiones and Thiazolidinethiones. *Synlett* **2004**, (8), 1371-1374.

157. Ainswort.At; Kirby, G. W., Stereochemistry of Beta-Carboxy-and Beta-Hydroxymethyl-Muconic Derivatives. *Journal of the Chemical Society C-Organic* **1968**, (12), 1483-&.

158. Jaroszewski, J. W., Oxidation of Some 2-Methoxyphenols with Chlorous Acid. *J. Org. Chem.* **1982,** 47, (11), 2013-2018.

159. Jaroszewski, J. W.; Ettlinger, M. G., Medium Effects on Formation of Cyclic Enolates from (2E,4Z)-3-Formyl-2,4-Hexadienedioates, A Novel Ring-Chain Equilibrium - Importance of Hydrogen-Bonding, Solvent Dipolarity-Polarizability, and Ion-Pairing Effects - Stereoisomerism of 3-Formyl-2,4-Hexadienedioates. *J. Org. Chem.* **1989,** 54, (7), 1506-1518.

160. Dence C.W., G. M. K., Sarkanen K.V., Studies on Oxidative Delignification Mechanisms Part II. Reactions of Vanillyl Alcohol with Chlorine Dioxide and Sodium Chlorite. *Tappi* **1962,** 45, (1), 29-38.

161. Isobe, K.; Mohri, K.; Tokoro, K.; Fukushima, C.; Higuchi, F.; Taga, J.; Tsuda, Y., Selective Cleavage of Aromatic Rings by Ozonolysis .1. Application to Ortho-Dimethoxybenzene Derivatives. *Chem. Pharm. Bull.* **1988,** 36, (4), 1275-1282.

162. Fukuyama, T.; Lin, S. C.; Li, L. P., Facile Reduction of Ethyl Thiol Esters to Aldehydes - Application to A Total Synthesis of (+)-Neothramycin-A Methyl-Ether. *J. Am. Chem. Soc.* **1990,** 112, (19), 7050-7051.

163. Wright, S. W.; Hageman, D. L.; Wright, A. S.; McClure, L. D., Convenient Preparations of T-Butyl Esters and Ethers from T-Butanol. *Tetrahedron Lett.* **1997,** 38, (42), 7345-7348.

164. Colombo, M. I.; Zinczuk, J.; Bohn, M. L.; Ruveda, E. A., Detours En Route to a Total Synthesis of (+)-Cassiol. *Tetrahedron: Asymmetry* **2003,** 14, (6), 717-725.

165. Moses, J. E.; Baldwin, J. E.; Bruckner, S.; Eade, S. J.; Adlington, R. M., Biomimetic Studies on Polyenes. *Org. Biomol. Chem.* **2003,** 1, (21), 3670-3684.

166. Roush, W. R.; Sciotti, R. J., Enantioselective Total Synthesis of (-)-Chlorothricolide Via the Tandem Inter- and Intramolecular Diels-Alder Reaction of a Hexaenoate Intermediate. *J. Am. Chem. Soc.* **1998,** 120, (30), 7411-7419.

167. Gustafsson, T.; Schou, M.; Almqvist, F.; Kihlberg, J., A Total Synthesis of Hydroxylysine in Protected Form and Investigations of the Reductive Opening of P-Methoxybenzylidene Acetals. *J. Org. Chem.* **2004,** 69, (25), 8694-8701.

168. Marshall, J. A.; Bourbeau, M. P., Directed Pd(0)-Catalyzed Hydrostannations of Internal Alkynes. *Tetrahedron Lett.* **2003,** 44, (5), 1087-1089.

169. Roth, G. J.; Liepold, B.; Muller, S. G.; Bestmann, H. J., Further Improvements of the Synthesis of Alkynes from Aldehydes. *Synthesis* **2004**, (1), 59-62.

170. Frantz, D. E.; Fassler, R.; Carreira, E. M., Facile Enantioselective Synthesis of Propargylic Alcohols by Direct Addition of Terminal Alkynes to Aldehydes. *J. Am. Chem. Soc.* **2000,** 122, (8), 1806-1807.

171. Flohr, A., Stille Coupling Versus Cine Substitution. Electronic Effects Also Influence Coupling Sterically Hindered Stannanes. *Tetrahedron Lett.* **1998,** 39, (29), 5177-5180.

172. Franci, X.; Martina, S. L. X.; McGrady, J. E.; Webb, M. R.; Donald, C.; Taylor, R. J. K., A Comparison of the Still-Gennari and Ando HWE-Methodologies with Alpha,Beta-Unsaturated Aldehydes; Unexpected Results with Stannyl Substituted Systems. *Tetrahedron Lett.* **2003,** 44, (42), 7735-7740.

173. Zografos, A. L.; Yiotakis, A.; Georgiadis, D., Rapid Access to the Tricyclic Spirotetronic Core of Abyssomicins. *Org. Lett.* **2005,** 7, (20), 4515-4518.

174. Roush, W. R.; Limberakis, C.; Kunz, R. K.; Barda, D. A., Diastereoselective Synthesis Endo- and Exo-Spirotetronate of the Quartromicins. The First Enantioselective Diels-Alder Reaction of an Acyclic (Z)-1,3-Diene. *Org. Lett.* **2002,** 4, (9), 1543-1546.

175. Roush, W. R.; Barda, D. A., Highly Selective Lewis Acid Catalyzed Diels-Alder Reactions of Acyclic (Z)-1,3-Dienes. *J. Am. Chem. Soc.* **1997,** 119, (31), 7402-7403.

176. Funel, J. A.; Prunet, J., Enyne Versus Diene RCM in the Synthesis of Cyclopentene Derivatives toward the a Ring of FR182877. *J. Org. Chem.* **2004,** 69, (13), 4555-4558.

177. Williams, D. R.; Nishitani, K., A Mild Oxidation of Aldehydes to Alpha,Beta-Unsaturated Aldehydes. *Tetrahedron Lett.* **1980,** 21, (46), 4417-4420.

178. Wender, P. A.; Christy, J. P., Rhodium(I)-Catalyzed [4+2+2] Cycloadditions of 1,3-Dienes, Alkenes, and Alkynes for the Synthesis of Cyclooctadienes. *J. Am. Chem. Soc.* **2006,** 128, (16), 5354-5355.

179. Marshall, J. A.; Xie, S. P., An Enantioselective Synthesis of the Spirotetronate Subunit of Kijanolide. *J. Org. Chem.* **1992,** 57, (11), 2987-2989.

180. Yamada, S.; Morizono, D.; Yamamoto, K., Mild Oxidation of Aldehydes to the Corresponding Carboxylic-Acids and Esters - Alkaline Iodine Oxidation Revisited. *Tetrahedron Lett.* **1992,** 33, (30), 4329-4332.

181. Trullinger, T. K.; Qi, J.; Roush, W. R., Studies on the Synthesis of Quartromicins A(3) and D-3: Synthesis of the Vertical and Horizontal Bis-Spirotetronate Fragments. *J. Org. Chem.* **2006,** 71, (18), 6915-6922.

182. Yamaguchi, M.; Nobayashi, Y.; Hirao, I., A Ring-Opening Reaction of Oxetanes with Lithium Acetylides Promoted by Boron-Trifluoride Etherate. *Tetrahedron* **1984,** 40, (21), 4261-4266.